Zoophysiology Volume 26

Zoophysiology

Volumes already published in the series:

Volume 1: *P. J. Bentley*
Endocrines and Osmoregulation (1971)

Volume 2: *L. Irving*
Arctic Life of Birds and Mammals Including Man (1972)

Volume 3: *A. E. Needham*
The Significance of Zoochromes (1974)

Volume 4/5: *A. C. Neville*
Biology of the Arthropod Cuticle (1975)

Volume 6: *K. Schmidt-Koenig*
Migration and Homing in Animals (1975)

Volume 7: *E. Curio*
The Ethology of Predation (1976)

Volume 8: *W. Leuthold*
African Ungulates (1977)

Volume 9: *E. B. Edney*
Water Balance in Land Arthropods (1977)

Volume 10: *H.-U. Thiele*
Carabid Beetles in Their Environments (1977)

Volume 11: *M. H. A. Keenleyside*
Diversity and Adaptation in Fish Behaviour (1979)

Volume 12: *E. Skadhauge*
Osmoregulation in Birds (1981)

Volume 13: *S. Nilsson*
Autonomic Nerve Function in the Vertrebrates (1983)

Volume 14: *A. D. Hasler*
Olfactory Imprinting and Homing in Salmon (1983)

Volume 15: *T. Mann*
Spermatophores (1984)

Volume 16: *P. Bouverot*
Adaption to Altitude-Hypoxia in Vertebrates (1985)

Volume 17: *R. J. F. Smith*
The Control of Fish Migration (1985)

Volume 18: *E. Gwinner*
Circannual Rhythms (1986)

Volume 19: *J. C. Rüegg*
Calcium in Muscle Activation (1986)

Volume 20: *J.-R. Truchot*
Comparative Aspects of Extracellular Acid-Base Balance (1987)

Volume 21: *A. Epple* and *J. E. Brinn*
The Comparative Physiology of the Pancreatic Islets (1987)

Volume 22: *W. H. Dantzler*
Comparative Physiology of the Vertrebrate Kindney (1988)

Volume 23: *G. L. Kooyman*
Diverse Divers (1989)

Volume 24: *S. S. Guraya*
Ovarain Follicles in Reptiles and Birds (1989)

Volume 25: *G. D. Pollak* and *J. H. Casseday*
The Neural Basis of Echolocation in Bats (1989)

Volume 26: *G. A. Manley*
Peripheral Hearing Mechanisms in Reptiles and Birds (1990)

Volume 27: *U. M. Norberg*
Vertebrate Flight (1990)

Geoffrey A. Manley

Peripheral Hearing Mechanisms in Reptiles and Birds

With 187 Figures

Springer-Verlag
Berlin Heidelberg New York
London Paris Tokyo
Hong Kong Barcelona

Prof. Dr. GEOFFREY A. MANLEY
Institut für Zoologie der
Technischen Universität München
Lichtenbergstraße 4
D-8046 Garching

ISBN-13:978-3-642-83617-6 e-ISBN-13:978-3-642-83615-2
DOI: 10.1007/978-3-642-83615-2

Library of Congress Cataloging-in-Publication Data. Manley, Geoffrey A., 1945–
Peripheral hearing mechanisms in reptiles and birds. (Zoophysiology; v. 26) Bibliography: p. Includes index. 1. Hearing. 2. Reptiles – Physiology. 3. Birds – Physiology. I.Title. II. Series. QP461.M35 1989 598.21'825 89-11315
ISBN-13:978-3-642-83617-6 (U.S.)

2131/3145-543210 – Printed on acid-free paper

For my children,
Rebecca and David

Preface

To date, there is no comprehensive review of the hearing of reptiles and birds. Although there has been an increasing effort to understand the function of the hearing organ in individual species, little effort has been made to integrate the findings into a conceptual framework of the evolution and function of the non-mammalian ear. One reason for this is to be found in the great diversity of scientific approaches to hearing, not only from the zoological and medical fields, but also from the psychological, psychoacoustical and bioengineering aspects. This fact has led to a wide scattering of the appropriate literature and a disturbing lack of uniformity in the approaches to data collection and quantification.

The great diversity of the hearing organs of the vertebrates (Lewis et. al, 1985) makes it impossible to describe the structure and function of all types in a book of this size. Although it may seem curious to write a book about the hearing systems of birds and reptiles and ignore the other vertebrate groups, the more complex reasoning behind this decision will perhaps become clear in the course of reading this book.

There are three basic structural types of vertebrate hearing organ, only one of which will be described. The fish will not be considered, as their hearing is mediated by different end-organs, which contain otoliths. The amphibian hearing papillae, unlike those of other land vertebrates, do not rest on a basilar membrane and may not even be homologous to the papillae of other tetrapods, so that they, also, will not be described. Reptiles, birds and mammals have a basilar membrane underlying at least most of the basilar papilla. There already exists a quite large literature on the hearing of mammals and their inclusion in this book would impose an unacceptable degree of superficiality. Readers wishing to find more information on the hearing of mammals are referred to recent reviews and conference proceedings which will provide further reference material (e.g., Duifhuis et al., 1988; Klinke and Hartmann, 1983; Lewis et al., 1985; Moore and Patterson, 1986; Pickles, 1982, 1985; Popper and Fay, 1980; Syka, 1988). This book describes the peripheral hearing mechanisms in those species or groups of reptiles and birds for which both anatomical and physiological data are available.

I have tried to bring together information culled from a great variety of sources and to present my understanding of the function of these hearing systems which has gradually emerged from 20 years of work with reptiles, birds and mammals. During this time, there has been a huge increase of information available on the hearing of reptiles, information which is in great need of being summarized and integrated. I have attempted to do his in the last chapter of this book.

I also hope to awaken in the reader an impression of the dynamic of the evolution of a great diversity of structure and function and of the value for our

understanding of the function of the mammalian (and therefore our own) ear of the comparative approach (work with non-mammals). For the latter, I shall occasionally refer to data from mammals without, however, providing much detail.

Due to the limitations of space, it has not been possible to include any consideration of the neural processing of the acoustical information from the hearing organ in the auditory pathway of the brain of reptiles and birds. This is very unfortunate, but unavoidable. Thus the title of the book only refers to "peripheral" mechanisms, that is, those preceding the synapse between the primary auditory nerve fibres and the cells of the cochlear nucleus in the medulla oblongata of the hindbrain. In recent years, many extremely interesting articles have appeared on, for example, the processing of bird song in the avian brain (e.g., Leppelsack, 1978) or the neural activity underlying sound localization by the barn owl (e.g. Konishi, 1986). The present book is only concerned with the mechanisms in the inner ear, mechanisms which, with the exception of the efferent fibres, are independent of neural interactions.

I have attempted to include sufficient information to interest and provide a source of reference for the specialist on hearing and, on the other hand, tried to keep most of the discussion at a level understandable to the generalist. Those who consider this approach a bad compromise must bear with me. I first deal with selected general topics as an introduction to the evolutionary and physiological problems underlying hearing research, and then discuss the structure and function in individual, selected reptile species, beginning with the primitive turtles and then discussing the lizard papillae, starting from the smallest and going through to the most developed. Following this, the hearing organ of Crocodilia and birds is discussed and, finally, an attempt is made to integrate the findings into a consistent picture of the peripheral hearing mechanisms in these animals.

Many colleagues have contributed to the completion of this book. Christine Köppl, Malcolm Miller, Jim Pickles and Ruth Anne Eatock read and commented on all or much of earlier versions. Robert Fettiplace, Rainer Klinke and Jean Smolders commented on individual chapters. I am very grateful for the many helpful suggestions, which have improved the book greatly. I am also very grateful to Christine Köppl for permission to use a lot of her own and of our joint unpublished data and for her support and patience during the months spent writing this book. The editor responsible for this book, Gerhard Neuweiler, provided both encouragement and critical comments on the contents. Thanks are also due to the many authors and publishers who have allowed me to reproduce figures. I also thank my mother for her support during my years as a student, and last, but not least, my friend and teacher Mark Konishi, whose rigorous approach and excitement for research was an inspiration to me as a doctoral student.

Munich, 30th June 1988 GEOFFREY A. MANLEY

Contents

Chapter 1

Introduction

1.1 The Phylogeny of Reptiles and Birds

As is well known, the Mesozoic period of earth history was characterized, among other things, by an extensive adaptive radiation of the reptiles. The evolution of a variety of new structural features, such as a tough, dry skin and the amniotic egg, fitted the reptiles supremely to life on land. Within the relatively short time period of 25 million years at the beginning of the Permian period (285 million years ago), an immense diversity of reptilian forms emerged on land, in the sea and in the air. The reptiles extant today are only the modest survivors of once mighty races (Carroll, 1987).

The many groups of reptiles are classified on the basis of their skull structure, especially the presence and number of openings in the temporal region of the bony skull. Although there is some controversy here, it is generally agreed that the modern group of turtles and tortoises (Chelonia) are the only survivors of the earliest group, the Anapsida, whose skull bore no openings in the temporal region (Fig. 1.1). Of the other types of skull structure, only two more have modern survivors. One group of reptiles, the Synapsida, have a single temporal opening and gave rise to the mammal-like reptiles or therapsids, the ancestors of modern mammals. The transition between the therapsids and true mammals was gradual, not all characteristics of mammals being attained simultaneously. As the classification of fossil animals is necessarily based on those characteristics preserved in their skeletal remains, the mammals and mammal-like reptiles are generally distinguished by such features as the presence of a secondary jaw articulation and three middle-ear ossicles.

The other group with modern survivors is the Diapsida. With the exception of the Chelonia, this book is concerned with animals derived from diapsid ancestors. However, the diapsid group is quite diverse and certainly represents parallel evolution in more than one group. For the purposes of this book, we can regard the diapsids as giving rise to two modern lines, the Lepidosauria and the Archosauria. The Lepidosauria are represented today by the following groups: the Squamata (lizards and snakes), the amphisbaenids, and the ‚living fossil' *Sphenodon* (Rhynchocephalia; the Tuatara of New Zealand; Fig. 1.2). This latter species had an independent origin from the Squamata at the beginning of the adaptive radiation of the diapsids in the Permian period (250 million years ago).

The other line of diapsid reptiles is that of the Archosauria, represented not only by the extinct Dinosauria and Pterosauria but also by the crocodiles and their relatives (Crocodilia) and another extremely important group – the birds (Avia).

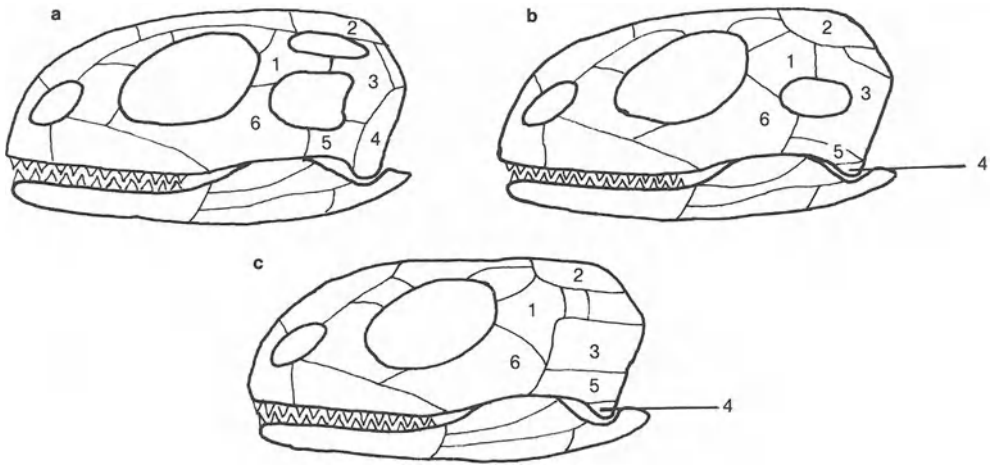

Fig. 1.1 a–c. The configuration of the dermal skull provides a useful way of classifying fossil and living reptiles. The original condition of the temporal openings of the dermal skull is shown for the *a* diapsid; *b* synapsid; and *c* anapsid condition. In many modern species, the skull has been strongly modified through loss and fusion of bones. Homologous individual bones have the same number (After Starck, 1979)

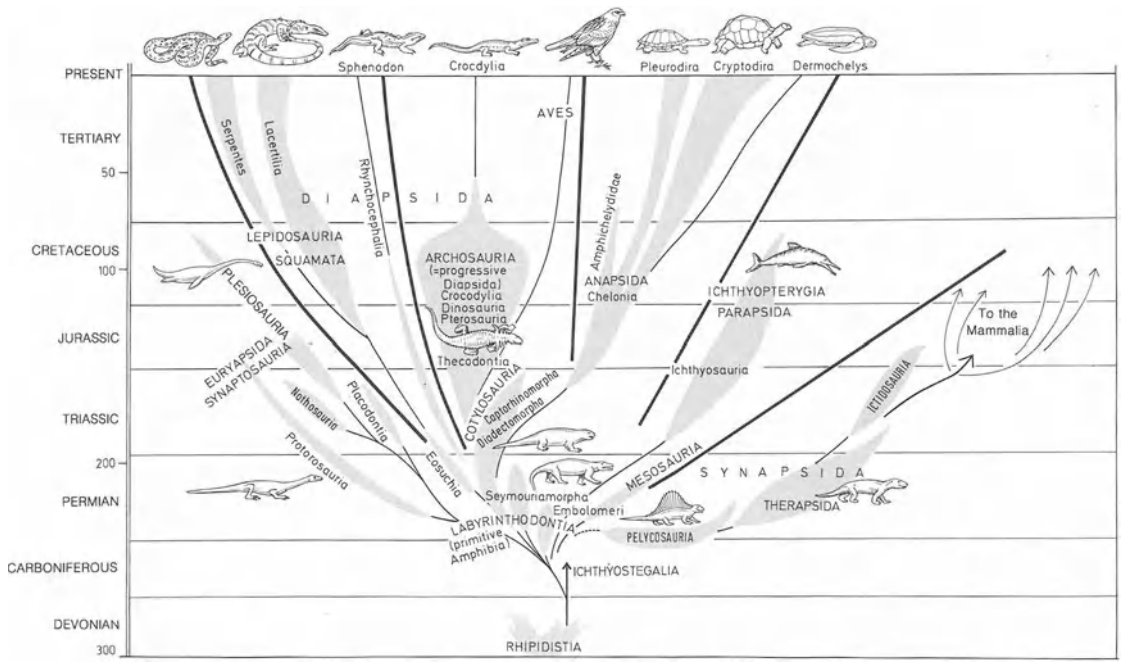

Fig. 1.2. Phylogenetic tree of the reptiles and their descendents. The approximate time of divergence is given by the scale on the *left* (in million years). As can be seen, the major groupings (separated by *thick lines*) all diverged from each other early in the Permian period. The two major groups of diapsid reptiles (*top left*), the archosaurs and the lediposaurs, are drawn separately. Most of the classical dinosaurs of the Mesozoic were archosaurs (*centre left,* Dinosauria; after Starck, 1978)

The systematic divisions described above are also reflected in clear structural differences in the inner ear of modern representatives of the various groups. The modern reptiles and birds can be classified (highly simplified after Starck, 1978) as follows:

Subclass ANAPSIDA

Order Testudines, (Chelonia) -Turtles, tortoises

DIAPSIDA: Subclass Lepidosauria

Order Rhynchocephalia: The Tuatara, *Sphenodon*

Order Squamata: Suborder Amphisbaenia – amphisbaenids
Suborder Serpentes – snakes
Suborder Lacertilia – lizards

DIAPSIDA: Subclass Archosauria, Order Crocodilia – crocodiles, alligators, gavials

DIAPSIDA: Class Aves, Subclass Neornithes – birds

It is not my intention to go into detail about the systematics of modern reptiles and birds, a field covered by many excellent books (e.g., Carroll, 1987; Romer and Parsons, 1977; Starck, 1978; Young, 1981). However, knowledge of these relationships in broad terms is needed to understand the evolution, the diversity of structure and the function of the ears of modern reptiles and birds.

It is believed that the birds are derived from a group of primitive archosaurs, the Thecodontia (Fig. 1.2). These ancestral forms developed feathers, homologous to reptilian scales, and the ability to fly actively. This activity places so many constraints on the morphology that structurally, the birds form a very uniform group compared to other groups of vertebrates. The structure of the inner ear is extremely similar to that of the other group of surviving archosaurs, the crocodiles and their relatives.

In some groups, there is evidence for a slow pace of evolution in inner-ear structure. A comparison of the hearing organs of chelonians (turtles and their relatives) and the Tuatara reveals that, although these two groups diverged from each other early in the great reptile radiation (Fig. 1.2), their hearing organs are quite similar and undoubtedly represent a very primitive stage of development. It is likely that the evolution of the hearing organ was not much advanced on this condition at the time of the origin of the archosaurs, squamates and mammal-like reptiles.

Within the Lepidosauria, later evolution has brought great structural diversity. Whereas the hearing organs of snakes all appear to be fairly uniform and primitive in structure, the hearing organs of lizards show a diversity which is manifested in an almost species-specific structure of the basilar papilla. In some cases, even closely-related species may be distinguished on this basis. However, the structure is sufficiently stable to enable the demarcation of families according to structural features of their hearing organs (Miller, 1980; Wever, 1978).

1.2 Systematics and the Inner Ear of Lizards

Studies over the last few decades have shown that a comparison of lizard families with respect to the structure of their hearing organs leads to a classification of family groups which usually parallels that based on other structural features, e.g., of the skeleton or brain (Northcutt, 1978). For example, some time ago the family Xantusiidae (granite night lizards) were classified with the geckos. However, certain structural features, among other things the structure of the sensory epithelium of the hearing organ, made it obvious that they are more closely related to the skinks.

In general, Miller's (1978 b, 1980) and Wever's (1978) classifications of the lizard families based on inner-ear features bear strong resemblances to those based on other systematic grounds. The lizard families are classified by Starck (1978 and Fig. 1.3) as follows (the asterisk indicates families with representatives which are discussed in some detail in this book):

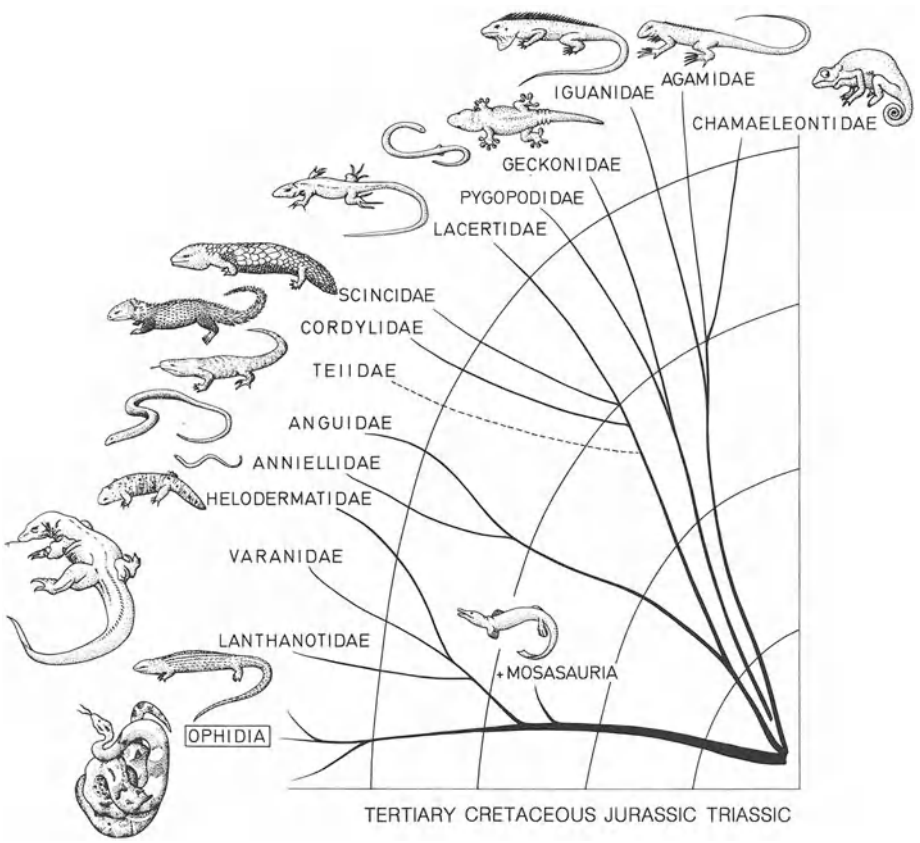

Fig. 1.3. Detailed phylogenetic tree of the lizards and snakes (Lacertilia and Serpentes) during Mesosoic and early Cenozoic times (After Starck, 1978)

Suborder Lacertilia

Infraorder Iguania	Family	*Iguanidae* * (iguanas)
		Agamidae (agamas)
		Chamaeleonidae (chameleons)
Infraorder Gekkota	Family	*Gekkonidae* * (geckos)
		Pygopodidae (snake or flap-footed lizards)
		Dibamidae-Anelytropsidae (flap-legged skinks)
Infraorder Scincomorpha	Family	*Scincidae* * (skinks)
		Teiidae (teiids, tegus)
		Xantusiidae (night lizards)
		Lacertidae * (european lizards)
		Cordylidae (girdle-tails)
Infraorder Diploglossa	Family	*Diploglossinae* (diploglossine lizards)
		Anguidae * (glass „snakes")
		Anniellidae (legless lizards)
		Xenosauridae (xenosaurids)
Infraorder Varanoidae (= Platynota)	Family	*Varanidae* * (monitors)
		Lanthanotidae (earless monitors)
		Helodermatidae (beaded lizards)

The classification given above does not necessarily reflect the opinions of those who use inner-ear structure as a systematic tool. Miller (1980 and personal communication), based on his extensive studies of inner-ear structure, groups the infraorders of the Iguania and Diploglossa together. Miller also feels that the Teiidae, Lacertidae and probably the Varanoidae are closely related. He places on the one hand Scincidae, Xantusiidae and Cordylidae, on the other hand the Gekkonidae and Pygopodidae together. Similarly, Wever (1978) gives a superfamily Lacertoidea, which includes the Teiidae and Lacertidae. These differences of opinion result to some extent from the difficulties involved in deciding whether similar structural features are due to close relationships, to independent evolution, or to the retention of a common ancestral constellation of features (Estes and Pregill, 1988).

1.3 Cochlear Microphonics and the Inner Ear

Historically, the investigation of the function of the inner ear of birds and reptiles began with the recording of cochlear microphonic potentials from the inner ear. The microphonic is a potential of the inner ear which has the same frequency as the stimulus signal and which, though often small in the reptiles (Wever, 1978, measured at a level of 0.1 or 1 μV), can be measured using filtering systems such as wave analyzers. These potentials are the summed electrical fields resulting from the responses of all hair cells that react to the stimulus and, often, potentials

that arise in other locations, such as the auditory nerve. E.G. Wever's book ‚The reptile ear' (1978), contains a detailed description of the wealth of microphonic data that he collected from the ears of many different reptile species. Wever tried carefully to correlate the physiological data with the anatomy of the inner ears of the various species, anatomical data that he also collected himself. The microphonic data were, however, difficult to correlate with the structural variety.

The difficulties associated with using microphonic potentials to study inner-ear responses (Manley, 1981) in the lizards are:

1) At low frequencies (up to about 1 kHz), the responses of nerve fibres tend to phase-lock to the stimulus waveform, so that the summed activity of the nerve cannot be clearly distinguished from the hair-cell microphonic responses.

2) Hair cells have no distinct threshold, so the measurement levels are arbitrary – no absolute threshold can be measured.

3) The size of the potential depends not only on the sensitivity of individual hair cells, but on the total number of hair cells responding and their respective distances from the electrode. Thus, animals with a very large number of hair cells will appear to have a lower threshold than others, although this is artefactual.

4) Perhaps the most important factor making microphonics unsuitable for measuring responses in lizards is the fact that all species have at least one oppositely-oriented hair-cell area (bidirectional orientation pattern, see Sect. 4.3.3). As the oppositely-oriented hair cells respond to opposite phases of motion, they will change their potentials more-or-less out of phase with each other. This introduces a large degree of cancellation of the potentials in the inner-ear fluid spaces before they can be recorded. Perfect interference leaves behind smaller potentials generated partly by nonlinearities in the hair-cell responses, and which are at a multiple of the stimulus frequency. Although the microphonic recordings reported in some cases, especially in geckos (Hepp-Remond and Palin, 1968), contained "very large harmonic contamination", the significance of this phenomenon was never really appreciated and discussed by Wever and his co-workers. The degree of interference will depend on the size of the populations of hair cells and their exact orientations and responses at different frequencies. Under such circumstances, it is not to be expected that the microphonic data would be easily interpretable and comparable between species. It would not even be possible to directly compare the responses of hair-cell areas of different orientation in the same species. The major differences that occur between unidirectionally-oriented and bidirectionally-oriented areas have been illustrated for the Tokay gecko (Manley, 1972 a, see Sect. 10.2.2 and Fig. 14.5). Only where species with purely unidirectional papillae were studied (e.g., turtles) does the form of the microphonic ‚audiogram' resemble neural or behavioural audiograms. However, even here, there is a tendency to overestimate the sensitivity of the lowest and highest frequencies.

In view of these difficulties and the fact that much data are now available using techniques that give absolute thresholds and more comparable values, the microphonic data will not play a great role in the discussions in this book.

Chapter 2

Hair Cells and the Origin of the Hearing Inner Ear

In this chapter, I will introduce hair-cell structural features and stimulus responses by focussing on hair cells of the lateral line and vestibular systems. All or most of these properties undoubtedly have their origin very early in the evolution of the vertebrates. Comparative paleontological, morphological and ontogenic studies all point to part of the lateral line system as the origin of the inner ear.

2.1 Evolutionary Origin of the Inner Ear Sensory Epithelia

The very earliest fossilized vertebrates with well-preserved skulls show that these animals not only possessed a canal system on the body surface, but also a primitive inner ear with one or two semicircular canals (Carroll, 1987). The lateral-line system of modern fish and amphibians may have developed as a simplification of the extensive canal system of the earliest vertebrates. The reduction in complexity to a few main canals or grooves on the body surface probably made the system better able to detect the direction of a disturbance in the water (Denison, 1966).

From studies of modern vertebrates, we know that both the lateral-line system and the inner ear develop from similar ectodermal, dorso-lateral placodes; both systems have similar receptor cells and both are innervated by nerves terminating in the acoustico-lateral area of the brain, nerves whose cells also originate in the placodes (Fig. 2.1; Denison, 1966; Northcutt, 1980; Starck, 1982). There is a tendency for the sensory cells of the lateral line, as seen in most modern bony fish, to sink somewhat below the body surface, contact being maintained at least through canal pores to the surface (Fig. 2.2). It is apparent that in that part of the lateral-line system at the back of the head, some of the canals sank deeply into the head very early in vertebrate evolution and formed a canal system almost cut off from the outside world. The same event can be observed in the ontogeny of modern vertebrates, when the middle part of the dorsolateral head placode sinks into the head of the developing embryo to form the inner ear. Only in the modern elasmobranch fishes is a patent canal to the surface still to be seen (ductus endolymphaticus). The functional result of the sinking-in of part of the canal system may have been to isolate the receptors from outside disturbance and to utilize them to detect motion of the canal fluids caused by the animal's own body movement (van Bergeijk, 1966).

The subsequent evolution of the inner-ear labyrinth system (see Sect. 4.1) is accompanied by an increase in the number of semicircular canals from one to two

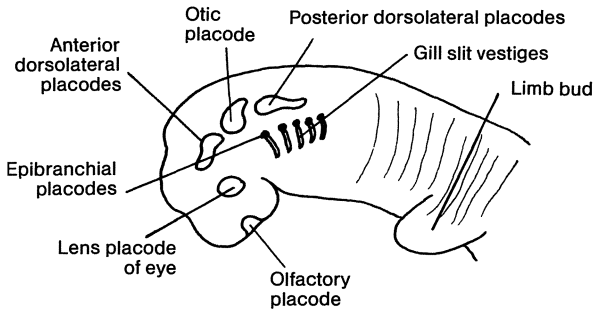

Fig. 2.1. Diagram of the early embryo of an amniote seen in lateral view, showing the location of the three lateral ectodermal placodes, dorsal to the gill slits, which give rise to the inner ear and the lateral-line organs (After Northcutt, 1980)

to three and the development of several other areas of sensory cells specialized for various functions. Hearing is an additional function of the vertebrate ear which entailed the development of a system for the detection of so-called far-field sound waves (those waves which are present only as disturbances of pressure and which do not, as does near-field sound, produce net particle displacement).

As will become evident below, the vertebrate hair cell does not, however, respond to pressure *per se*, but is a detector of mechanical stretching of its specialized membrane. Sound in the water could thus only be detected when it produced a displacement of the fluid over the hair cells. The first system for the transformation from pressure to motion probably developed at the surface of the fish swimbladder, as the pressure of the gas within it could be affected by the sound wave and the surface of the bladder presents an interface between two different densities of material (see Sect. 3.1). This idea is supported by the finding in some fish of special connections between the air bladder and the ear region (e.g., the Weberian ossicles). A gas bubble near the ear would be better placed to carry out this function, and there are indications of the presence of anterior extensions of the spiracular cavity in the Rhipidistian ancestors of the land vertebrates, cavities which were in the same location as the middle ear of the land vertebrates (van Bergeijk, 1966; Thompson, 1966).

Whereas the function of hearing in modern fish seems to involve the two sensory surfaces of the sacculus, the saccular and lagenar maculae (Fay and Popper, 1980), this function in most land vertebrates is assumed by a newly-developed sensory surface, the basilar papilla. More recent evidence has indicated the possibility that the basilar papilla was present in the Rhipidistian ancestors of the land vertebrates. In the related ‚living fossil' coelacanth fish *Latimeria*, Fritzsch (1987) found a structure which may be homologous to the basilar papilla. He also produced evidence that the early phylogenetic differentiation of the basilar papilla was linked to developments of the perilymphatic system and not to middle-ear formation. The structural arrangement of the sensory epithelia in modern amphibians is complex and author opinions differ with respect to their being homologous to that of the reptiles and their derivatives (Fritzsch and Wake, 1988; Lombard, 1980; Lombard and Bolt, 1979).

2.2 An Introduction to Hair Cells

In order to acquaint the reader with some of the fundamental properties of the epithelial receptor cells known as hair cells, I shall briefly discuss their structure and function both in the lateral-line organ, where their arrangement and function is simpler and has been studied for a longer time, and in part of the vestibular portion of the inner ear (sacculus).

The sensory cells of the lateral line tend to be collected into groups, known as neuromasts. These may be directly on the body surface, as in some fish and some amphibians, or in a groove or canal on the body surface (Fig. 2.2). Each neuromast organ is made up of a group of sensory or hair cells and various supporting cells (Fig. 2.3).

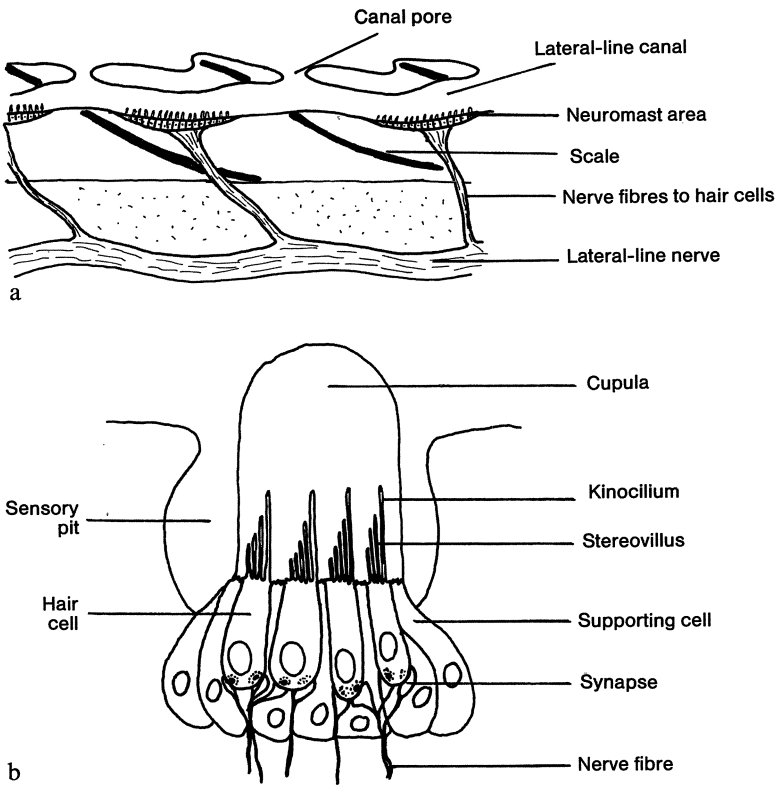

Fig. 2.2 a, b. Schematic diagrams to illustrate the location and structure of neuromast lateral-line organs in aquatic vertebrates. *a* Longitudinal section through the skin of a fish, showing the location of a lateral-line canal beneath the scales; also shown are the canal pores and the innervation of the neuromasts. *b* Schematic view of a cross-section of a neuromast organ lying in a pit on the body surface, showing the tectorial structure (cupula), the hair cells and their innervation and the supporting cells (After Kämpfe et al., 1970; Hildebrand, 1974)

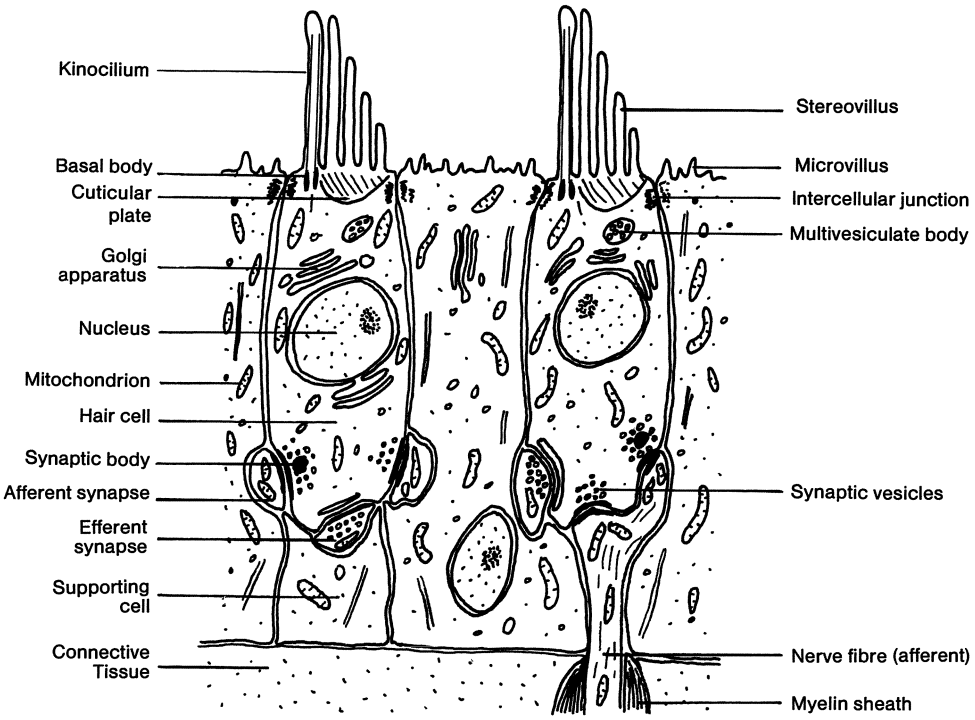

Fig. 2.3. More detailed schematic drawing of generalized hair cells, showing their relationships to the supporting cells and nerve fibres, and illustrating the position of the kinocilium and the stereovilli on the cuticular plate (After Baird, 1974)

2.2.1 The Hair Cell

Hair cells of vertebrates are secondary (epithelial) receptor cells. That is, they are not modified nerve cells but develop locally from the ectoderm. Hair cells are generally columnar in shape and are always found in clusters whose names vary with their location in the body. Thus we speak of neuromasts of the lateral line, maculae and cristae of the vestibular system and papillae of the auditory system.

Hair cells derive their name from a tuft of so-called sensory ‚hairs' projecting from their upper surface (Fig. 2.4). Deflection of this tuft evokes an electrical

Fig. 2.4 A–C. Hair-cell structure as illustrated by the saccular macula of the bullfrog. *A* Transmission electron micrograph of a vertical section through a typical hair cell. The hair cells and the surrounding supporting cells (*SC*) rest in the form of a thin tissue sheet on the basal lamina (*BL*). The tectorial structure is known here as the otolithic membrane (*OM*). The round structure at the top of the stereovillar bundle is the tip of the kinocilium. *B* A light micrograph of a single, isolated hair cell. The position of the nucleus is indicated (*N*). The apical cuticular plate (*CP*) supports the hair bundle (*HB*), to the top right of which the bulbous tip of the kinocilium is just visible. In this hair cell, the tallest stereovilli are about 10 μm long. *C* View of the top of a similar hair cell using the scanning electron microscope to illustrate the tight packing of the tips of the stereovilli in the bundle. There are fewer microvilli on the free hair-cell surface than on the surrounding supporting cells (*A, B* from Hudspeth, 1985; *C* Hudspeth, 1982)

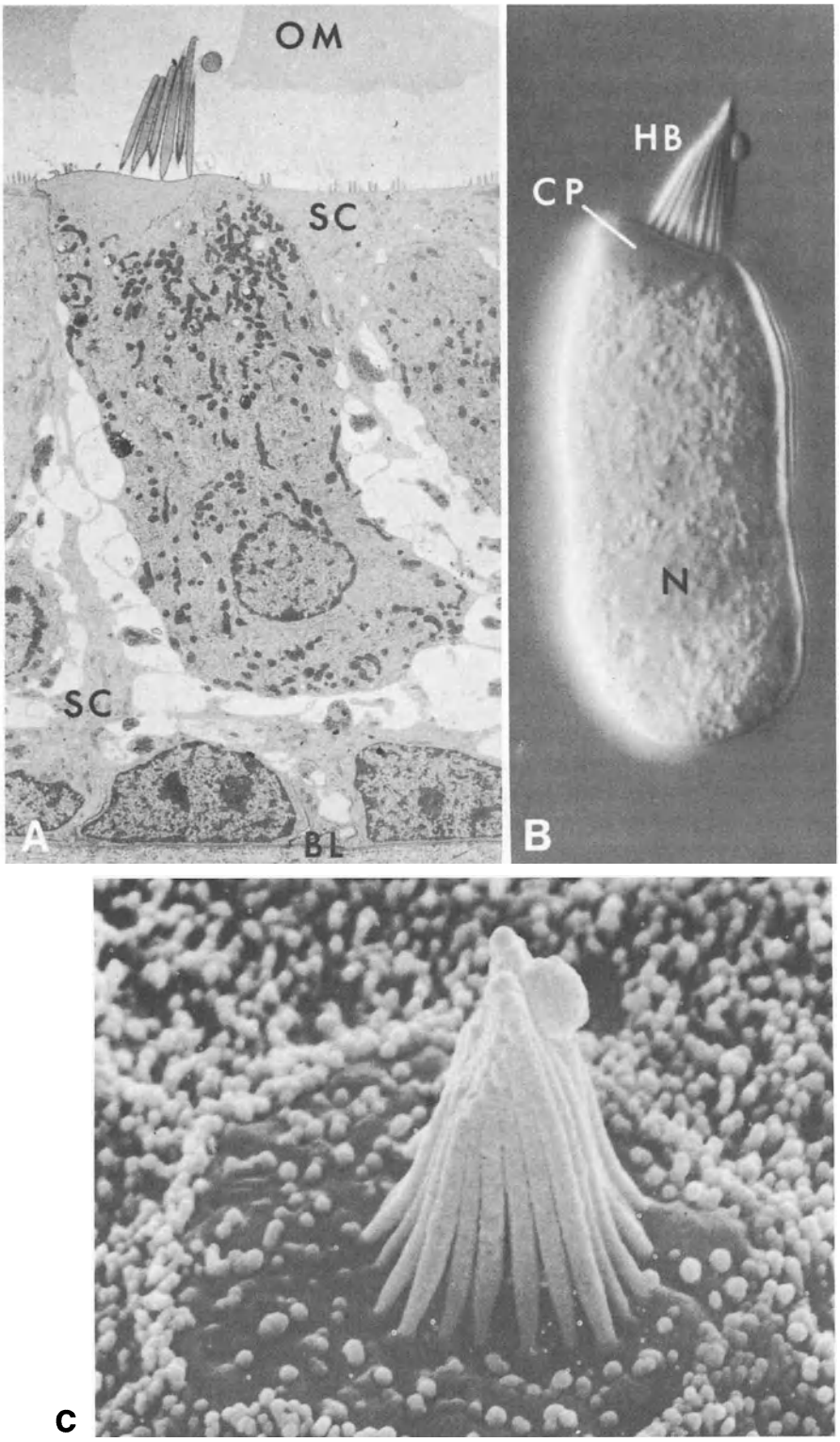
OM
SC
SC
A
BL
HB
CP
N
B
C

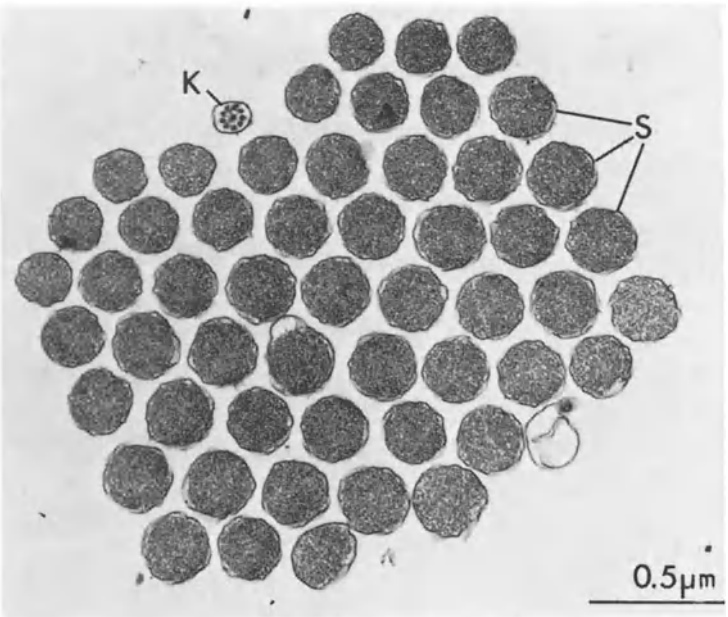

Fig. 2.5. Cross-section near the base of the stereovillar bundle of a hair cell from the basilar papilla of the lizard *Calotes* to illustrate the hexagonal packing of the stereovilli (*S*); *K* kinocilium (Bagger-Sjöbäck and Wersäll, 1973)

response in the cell. The hair bundle actually consists of many stereovilli and, usually, a single, asymmetrically-placed cilium, the kinocilium. The term stereocilia is more commonly used than the term stereovilli, but these structures are not true cilia; I follow the nomenclature of Schmidt and Thurm (1984). In the mammalian cochlea and in some hair cells of the bird cochlea, the kinocilium is absent (its basal body remains, however; Smith, 1981). In the ampulla of the vestibular system of young eels, Rüsch and Thurm (1986) showed that the kinocilium moves actively as a response to a change in the voltage across the epithelium. Such movements of the kinocilium have not been reported from other hair-cell systems.

The diameter of the stereovilli (from below 0.2 up to 1 µm) and length (up to 100 µm) varies with the organ and location in that organ. The length of the stereovilli in one bundle increases towards the kinocilium, which may be much longer than or shorter than the longest stereovilli. The stereovilli are arranged regularly, often in a hexagonal pattern (Fig. 2.5), are connected to each other and to the kinocilium and are well rooted via actin filaments in a dense area of cytoplasm called the cuticular plate (Flock et al. 1981). The entire bundle can be roughly circular in cross-section, but often forms a band across part of the surface of the receptor cell. The number of stereovilli varies in different cells from about 30 up to a few hundred (Lewis et al, 1985). At least under some experimental conditions, the stereovilli are quite stiff (Flock et al, 1977; Hudspeth and Corey, 1977). Further details with regard to the structure of the hair cell, its

stereovilli, the polarization in its stimulus response, etc. will be given in subsequent sections and chapters.

2.2.2 Tectorial Membrane and Hair Cell Environment

The neuromasts of the lateral line are invariably covered with a gelatinous mass, the cupula, which is sometimes very large (Fig. 2.2). ‚Cupula' is one of many terms used for the non-cellular gels which almost invariably cover hair cells in the lateral line and in the vestibular and hearing portions of the inner ear. Because these structures touch the hair bundle and transmit motion to it, they are commonly referred to as ‚tectorial' structures. Although the exact nature of the cupular material is still somewhat unclear, it is apparently connected at least to the kinocilium and perhaps also to the longest stereovilli. The cupula effectively forms an extension of the surface of the hair cells and thus amplifies their sensitivity to water motion. It often almost closes the canal over the hair cells and is moved by the slightest water motion. Recordings from the cupula with ion-sensitive electrodes have demonstrated that it has a positive potential of 15 to 50 mV with reference to the surrounding water and that it contains a higher concentration of potassium and chloride ions than the water. Since these conditions depended upon active secretion from the surrounding tissue, it was concluded that the positive potential and the high concentration of potassium are the result of an electrogenic potassium pump, probably in the supporting cells of the neuromast organs (Russell and Sellick, 1976).

The generation of an ion-rich microenvironment above the hair cells is also typical of the inner ear, although there the entire otic labyrinth (in contrast to the periotic labyrinth) is filled with a special fluid of high potassium concentration, the endolymph (Peterson et al., 1978). In mammals, there is a high positive potential in the endolymphatic space over the hearing organ. Of the groups of interest in this book, only the birds show a medium-sized positive potential in the endolymphatic space of the cochlear duct (up to 20 mV; Runhaar and Schedler, 1988; Schmidt, 1963). This fluid is, in all cases, potentially only in contact with the *apical* (upper, stereovillus-bearing) surface of the hair cells. At least on their sides and lower surface, they are exposed to a fluid which, like most intercellular fluids, is rich in sodium ions. The hair cells maintain a negative membrane potential against the extracellular space, as do nerve and muscle cells and, indeed, as do most cells of the body. The actual function of the high potassium levels and any positive potential which is present is still the subject of debate. One possibility is that the high potassium concentration in the endolymph allows this ion to enter the apical surface of the hair cell and exit the basolateral surface, in both cases down its electrochemical gradient. Although it has often been assumed that they are necessary for normal hair-cell function, several investigations of hair cells have demonstrated an apparently healthy functioning without the tectorial material and with high-sodium solutions over the hair cells (e.g. Hudspeth and Corey, 1977). Another possibility is that Davis' (1968) suggestion is correct, i.e. that the high potassium levels are necessary to maintain the physical properties of the tectorial material. Investigations in mammals have demonstrated that tec-

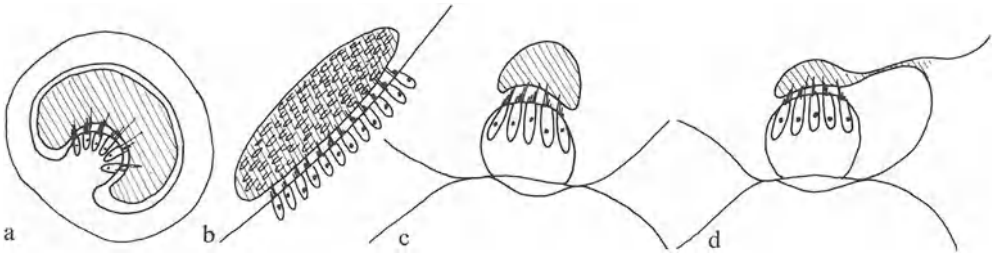

Fig. 2.6 a–d. Highly simplified schematic diagram to illustrate the relationships between hair cells and otolithic-tectorial structures in the various hair-cell receptor systems of land vertebrates (see also Fig. 2.2). In each case, the tectorial structure is *shaded. a* Cross-section of the crista of a semicircular canal; *b* vestibular macula (with otoliths embedded in the tectorial structure); *c* auditory papilla resting on the basilar membrane and with the overlying tectorial structure not attached to the limbus; *d* auditory papilla with attached tectorial membrane

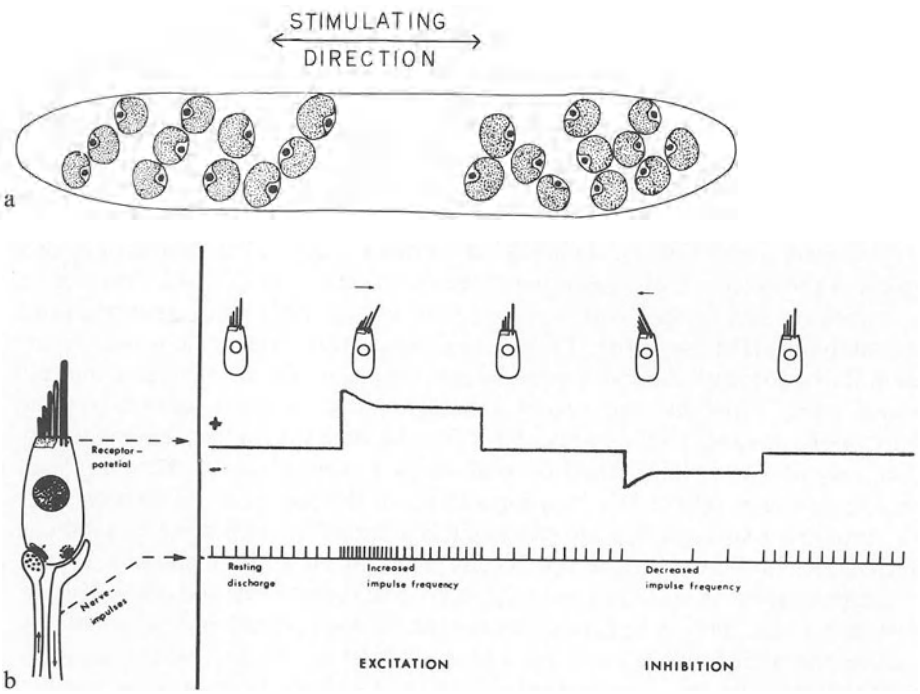

Fig. 2.7 a, b. Diagram illustrating the polarization of the stimulus direction in hair cells. *a* Schematic drawing of hair cells in a neuromast organ of the clawed toad as seen from above, showing that all hair cells are oriented fairly closely along the plane of water motions normally experienced by this organ. The *black dot* on the cell periphery represents the kinocilium in each case. *b* Distortion of the stereovillar bundle towards the kinocilium leads to a depolarization (+, excitation) of the cell and increased activity in the afferent fibre (*left*). Distortion in the other direction hyperpolarizes the cell (*upper line*) and suppresses the nerve-fibre activity below the spontaneous level (*lower line,* "inhibition") (Flock, 1965)

torial material is highly sensitive to its ionic environment and shrinks irreversibly in high sodium-ion solutions (Kronester-Frei, 1979).

With a few exceptions (e.g., in parts of the basilar papilla of a few lizard families), material similar to the cupula is present over all hair cells in lateral-line, vestibular and hearing organs (Fig. 2.6). In auditory receptors, it is called the tectorial membrane. In some maculae, such as the saccular, utricular and lagenar maculae, numerous small calcite crystals, called otoliths, are embedded in the gelatinous matrix of the otolithic membrane. In other cases, as in teleost fish, the entire structure is a solid otolith. Such otolithic receptor systems respond to linear accelerations, such as the force of gravity and/or to substrate vibration; some also detect low-frequency sounds (Lewis et al., 1985).

2.2.3 Polarization of the Hair Cell

The asymmetrical placement of the kinocilium correlates with a polarization of the hair cell's response behaviour. In the lateral line, the hair cells are usually oriented with the kinocilium either facing the head or the tail of the animal (Fig. 2.7a). A group of hair cells having opposite orientation is said to be *bidirectionally oriented.* These orientations correspond with the predominant directions of motion of the cupula. Hair cells, like other secondary receptor cells, make chemical synapses on their basal (inner) surface with afferent and efferent nerve fibres (Figs. 2.7b, 2.8). The transmitter output at the afferent synapse is regulated by the membrane potential of the hair cell. Even in the resting state, some release of transmitter is typical, so that spontaneous activity is generally present in the afferent fibres (Fig. 2.7b; e.g., Flock and Russell, 1976).

The directional sensitivity of the hair cell to motion is such that a deflection of the stereovillar bundle towards the kinocilium depolarizes, and a movement away from the kinocilium hyperpolarizes the hair cell (Fig. 2.7b; Flock, 1971). Motions from other angles cause depolarizations whose magnitude is proportional to the cosine of the angle to the most sensitive direction. Depolarization causes an increase, hyperpolarization a decrease in transmitter output. Hair cells with spontaneous activity can code motion in both directions and oppositely-oriented hair cells show opposite responses to the same stimulus (Flock, 1967, 1971; Flock and Russell, 1976; Harris et al., 1970; Sand et al., 1975; Shotwell et al., 1981). Similar changes in transmitter output can also be evoked in response to artificial de- and hyperpolarization, i. e., via an intracellular electrode.

2.2.4 Hair Cell Innervation

There are two kinds of nerve fibres associated with hair cells in the lateral line system, which can form synapses of different sizes (Fig. 2.8). The first kind is that of the afferent fibre system, which responds to transmitter released from the hair cells and transmits action potentials to groups of nerve cells in the brain. In the auditory system, these brain cells are in the cochlear nuclei of the medulla oblongata. The second group of fibres belongs to the efferent system, whose

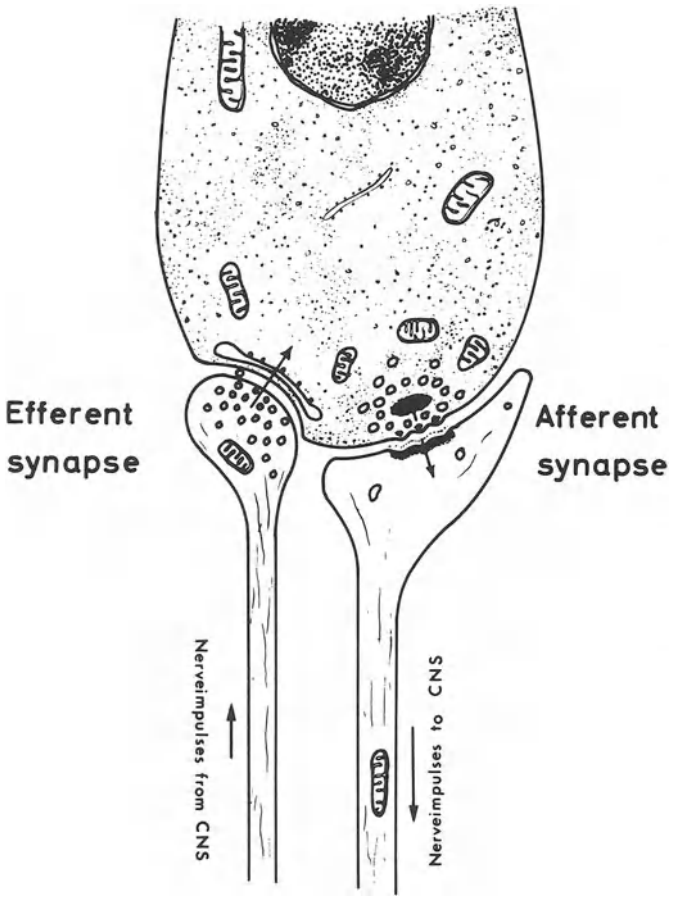

Fig. 2.8. Enlarged schematic drawing of the basal half of a lateral-line hair cell to illustrate the two kinds of nerve fibres contacting the hair-cell and the direction of information flow. The efferent synapse contains transmitter vesicles and there is a subsynaptic cisterna on the hair-cell side of the synapse. The afferent synapse often has a darkly-staining synaptic body surrounded by synaptic vesicles within the hair cell and a thickened post-synaptic membrane. The number of contacts per hair cell is highly variable between different hair-cell systems. Some lizard auditory hair cells only receive afferent contacts (Flock, 1967)

fibres in the auditory system originate in the superior olive of the brainstem and affect the hair cells with their transmitter. There is evidence for the presence of a chemical synapse (e.g., latency) in the responses of the afferent fibres following hair-cell stimulation (Flock and Russell, 1976; Furukawa, 1978). At the present time, there are no definitive indicators for afferent transmitter substances common to all hair cells, but the pharmacological experiments do not yet allow firm conclusions (Klinke, 1986).

Activity in the efferent fibres to lateral-line hair cells causes a slow hyperpolarization of the hair cell, resulting in a decrease or loss of spontaneous activity in the afferent fibres and an inhibition or reduction of the stimulus-induced ac-

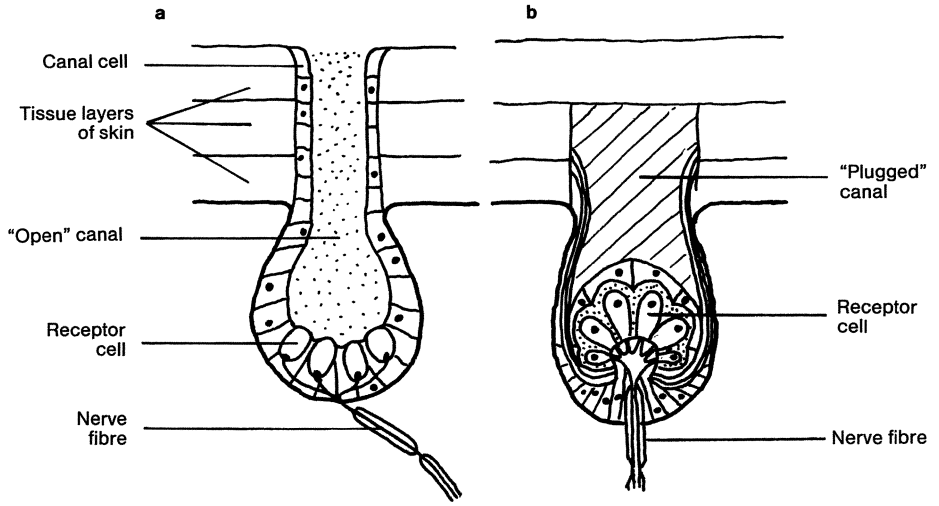

Fig. 2.9 a, b. Highly schematic illustration of the structure of different electroreceptor organs. *a* Ampullary (DC, tonic) receptor cells at the base of an "open" (gel-filled) canal. *b* Tuberous (AC, phasic) receptor cells at the bottom of a plugged canal (After Scheich, 1983)

tivity (Flock et al., 1973; Flock and Russell, 1976). Lateral-line organs of the perch respond as critically-damped low-frequency resonators to the velocity of the stimulus and efferent stimulation alters the damping of this resonance, perhaps by altering the mechanical properties of the stereovillar bundle (Russell and Lowe, 1983). Although there is evidence that acetylcholine is the transmitter at some efferent synapses, the question is not definitely settled (Ashmore and Russell, 1983; Klinke, 1986). Such efferent fibres are active just prior to locomotion of the animal and presumably serve to depress responses at the body surface to self-induced water motion.

Many hair cells are, however, not simply responsive to mechanical stimuli, but also to some extent to electrical stimuli, although the sensitivities to these two stimulus modalities vary widely (Münz et al, 1984; Strelioff and Honrubia, 1978; Suga, 1967). The electroreceptive cells of fish, including the ampullae of Lorenzini, are specialized epithelial cells with the same origin as the neuromasts (Bennett, 1970); that is, they are homologous to hair cells and are innervated by the lateralis nerve. Indeed, the evidence points to both mechano- and electroreceptivity being primitive functional capabilities of these secondary receptor cells. In the course of evolution, many have become more or less specialized for one modality, but some retain a fair measure of sensitivity to both. There is good evidence that one kind of electrical sensitivity is retained in auditory hair cells and contributes to their frequency tuning (Manley, 1986; see Sects. 6.1.3.2, 10.2.1, 13.4.1, 14.3, 14.9.1). It is thus interesting to compare the properties of hair cells with those of electroreceptors.

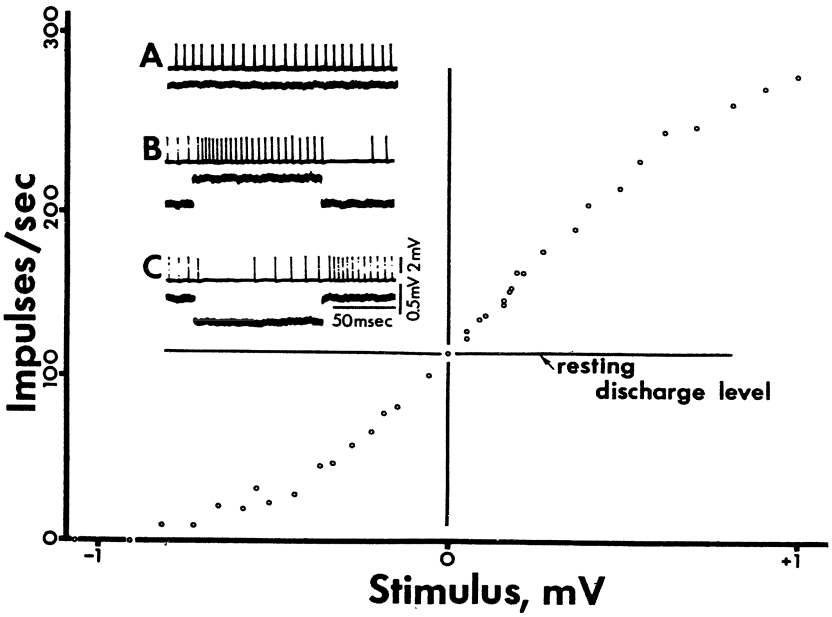

Fig. 2.10 a–c. Response properties of a tonic receptor cell of a weakly-electric fish. In the sets of traces at the *upper left,* the *bottom line* represents in each case the voltage stimulus, the *top line* the activity in an afferent fibre. *A* Spontaneous rate of impulses in the afferent fibre. *B* Increased discharge level during a positive DC stimulus in the canal. *C* Discharge suppression by a negative stimulus. In both *B* and *C,* the cessation of the stimulus is accompanied by a brief response of the opposite kind ("off" suppression or excitation). The diagram illustrates for the same cell the quantitative relationship between the magnitude and polarity of the stimulation and the average discharge rate during a stimulus of 100 ms. It can be seen that the cell discharges in the absence of stimuli at a rate of over 100 spikes/s. Both negative and positive stimuli can be coded by this cell, but only within a total range of ± 1 mV (Bennett, 1971)

2.3 Electroreceptors

A number of different types of electroreceptor cells are found in fish, both in those with and those without special organs for generating electrical pulses into the water, although the ‚tuberous' receptors are only found in the so-called weakly-electric fish (Fig. 2.9; Bennett, 1970; Scheich, 1983). The widespread *ampullary* receptors are groups of receptor cells with smooth membranes, and found at the bottom of ‚open' gel-filled canals in the skin (these canals are very long in the ampullae of Lorenzini of elasmobranch fishes such as sharks and rays). These cells respond optimally to DC or very-low-frequency AC stimuli in the water (Fig. 2.10). Their sensitivity is as high as 1 μV/cm, or the voltage of a normal torch battery over a distance of 15 km! Such receptors are, among other things, capable of detecting the small electric fields generated by prey organisms buried in sand.

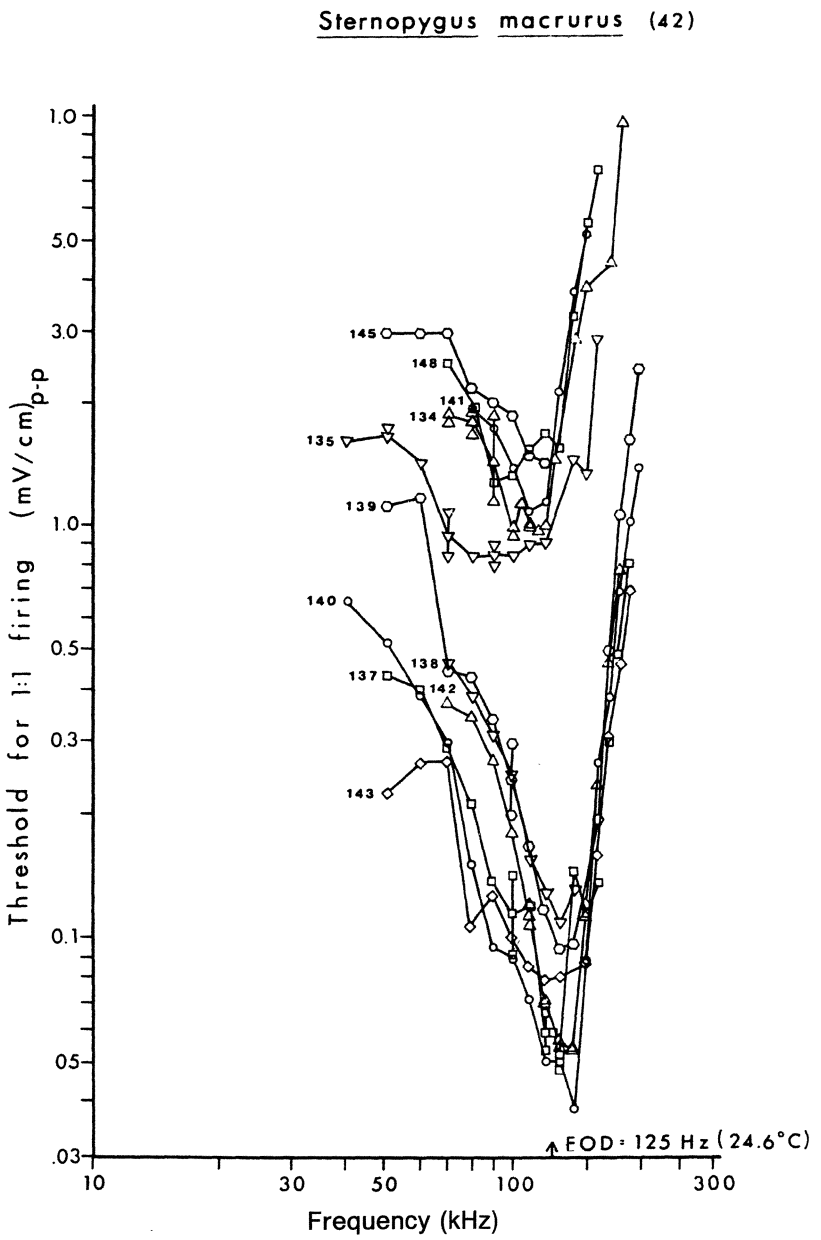

Fig. 2.11. Frequency selectivity of tuberous (phasic) electroreceptors of a weakly-electric fish. Each *line* is the tuning curve for a single afferent fibre and indicates the voltage amplitude at different frequencies necessary to evoke a standard response from the fibre (one spike per period for the sinusoidal stimulus). The *arrow* at the bottom indicates the frequency of the fish's own electric organ discharge (*EOD*). There are two populations of cells, with different thresholds, tuned to frequencies near the EOD. Compare tuning curves from primary auditory nerve fibres in later chapters (Hopkins, 1976)

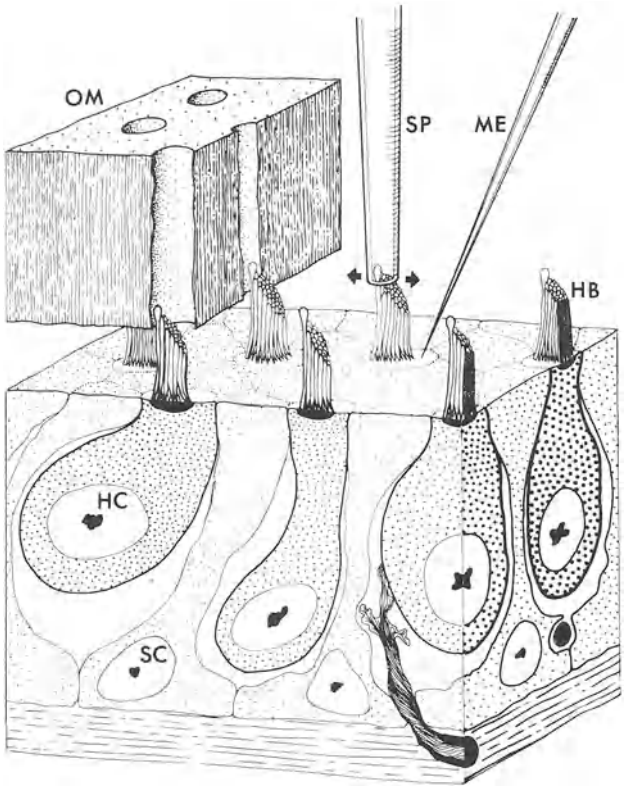

Fig. 2.12. Schematic cut-away drawing of an experimental system used to study the responses of hair cells in the bullfrog sacculus. The otolithic membrane (*OM*) has been partially removed and a microelectrode (*ME*) is used to penetrate a hair cell to record its responses to vibration of the stereovillar bundle (*HB*) induced by a stimulus probe (*SP*); *HC* hair cell; *SC* supporting cell (Hudspeth and Corey, 1977)

Tuberous receptors are found at the bottom of canals which are plugged with cells (Fig. 2.9). Their surface membrane is covered with large, irregularly-shaped microvilli, which increases the membrane capacitance. These cells thus only respond to higher a.c. frequencies (50 to 5000 Hz). This type of receptor cell thus has special relevance to the study of auditory receptor cells. There is good evidence that calcium ions are essential for the normal electrical sensitivity of these phasic electroreceptors (Bennett and Clusin, 1979; Viancour, 1979). In species that communicate via electrical signals, tuberous receptor cells have been shown to have filter properties closely matched to the spectral content of the electrical signals generated by the species' own electric-organ discharge (Hopkins, 1976). These cells respond to an increasingly broad range of frequencies when the strength of the stimulus is increased. Their ‚V'-shaped frequency-threshold, ‚tuning curves' strongly resemble those found in the hair cells of the auditory system of all vertebrates in response to different frequencies of sound (Fig. 2.11). The frequency to which these electroreceptive cells are most sensitive is also

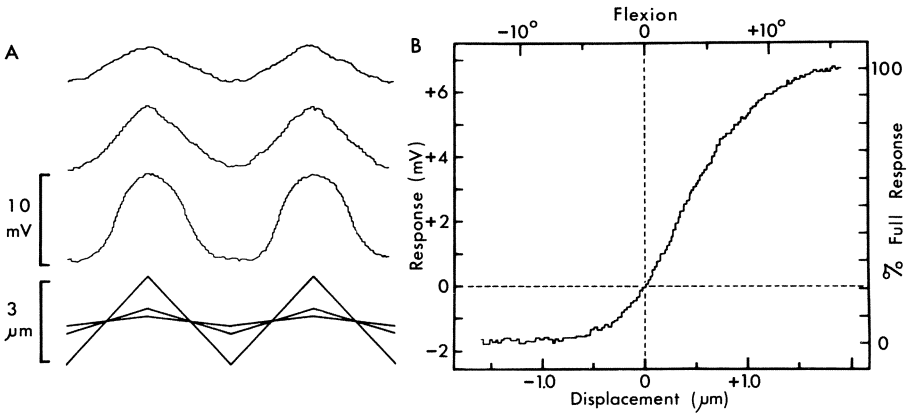

Fig. 2.13 A, B. Response activity of a single saccular macula hair cell. *A* Receptor potentials recorded intracellularly during direct stimulation of the stereovillar bundle. The lower of the four traces shows the triangular waveform of the stimulus at three amplitudes. The response to weak stimuli resembles the stimulus waveform (*top trace*), whereas at higher amplitudes of stimuli, the waveform becomes strongly distorted (*lowest* of the three traces). *B* Graph of the relationship between the displacement of the tip of the stimulating probe and the response of the cell in terms of the potential change from the resting potential (=0 mV). The *upper abscissa* shows the estimated displacement angle of the tip of the stereovillar bundle (cf. Fig. 2.10) (Hudspeth and Corey, 1977)

temperature dependent, being higher at higher temperatures (Hopkins, 1976). This same effect will be discussed in later chapters for the tuning curves of reptilian and avian hearing systems.

2.4 Properties of Hair Cells of the Frog Sacculus

There are a number of detailed investigations of the properties of hair cells in the vestibular system (that part of the inner ear not responsible for hearing), especially hair cells of the saccular macula of frogs (Fig. 2.12). This macula lends itself to such investigations partly because it is large and robust and the otolithic membrane can be relatively easily removed. These investigations have concentrated on the origin of the mechanical sensitivity of the hair cells and on the ionic basis of the transduction currents and receptor potential; they are thus also of great significance for our understanding of hair cells of the auditory system.

2.4.1 Resting Potential and Transduction Currents

Hair cells of the frog sacculus have a resting potential of about −60 mV. A movement of the hair-cell bundle in a stimulatory direction is accompanied by an

increased permeability of the apical cell surface, resulting in an influx of positive ions. The cell can be depolarized in this way to a potential of −40 mV. In contrast, a stimulus in the other direction closes the few channels that are open in the resting state, hyperpolarizing the cell up to about one-quarter of the largest depolarizing response (i.e., to −65 mV, Fig. 2.13; Hudspeth and Corey, 1977). Using voltage-clamped cells, Corey and Hudspeth (1979 a) showed that under the specific ionic conditions of their experiment, the transduction current had a reversal potential near 0 mV. This current could be carried by most positive ions whose diameter did not exceed 0.6 nm.

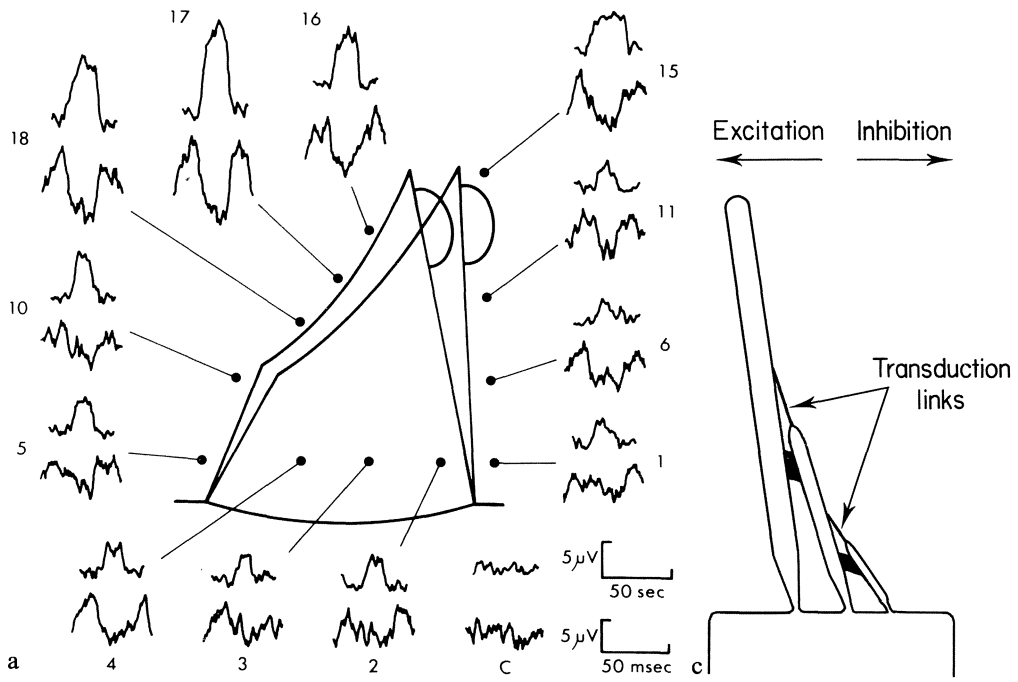

Fig. 2.14 a–c. The transduction channels appear to be near the top of the stereovillar bundle. *a* Responses to a 1 μm, 25 Hz deflection of the hair bundle of a saccular hair cell (the outline of the bundle is drawn for the two extreme positions), as recorded by an extracellular electrode with the tip located at the points shown around the bundle. In each case, the *lower record* is the average of samples of the electrode output for 5 s, the *upper trace* the output of a lock-in amplifier locked to the stimulus signal. The largest responses occur near the tops of the stereovilli, especially on the sloping portion of the bundle. The control records (*C*) indicate the noise level in upper and lower traces. *b* Transmission electron micrograph of a vertical section of the stereovillar bundle of an outer hair cell of a mammal, showing the thin "tip links" running from the tips of smaller stereovilli to the side of the next tallest stereovillus (*arrows*). *c* The model of Pickles et al. (1984), which suggests that the tip links are intimately related to the transduction channels. Shearing of the stereovillar bundle in the direction of the tallest villi (in non-mammals this is also in the direction of the kinocilium) tends to stretch the tip links (and open transduction channels?), shear in the other direction does not. This can explain the well-known polarization of response direction in hair cells (*a* from Hudspeth, 1982; *b* and *c* from Pickles et al. 1984)

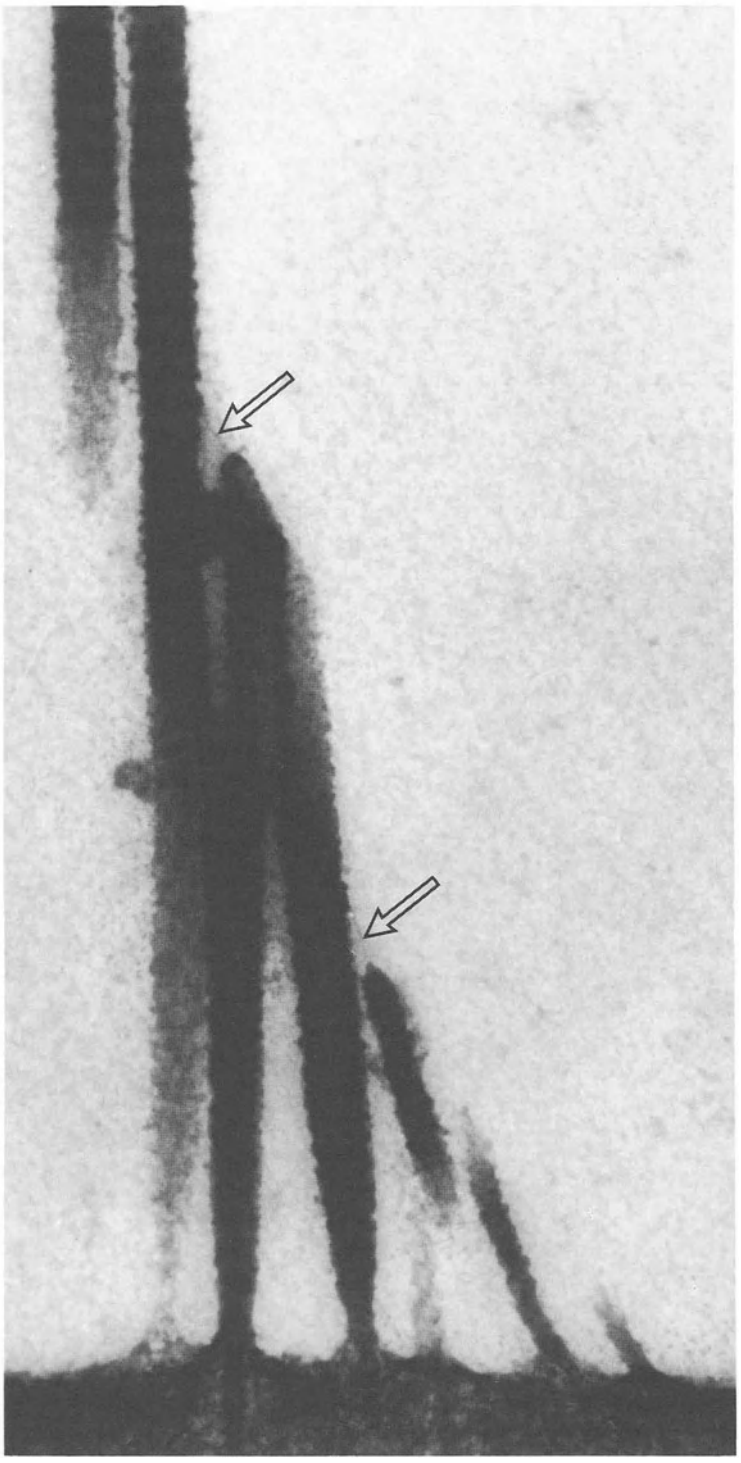

Fig. 2.14b

In the voltage-clamp situation, a saturating stimulus to a saccular hair cell produced a transducer current of 150 pA. Assuming a channel conductance of 25 pS, Corey and Hudspeth (1979 a) calculated that each hair cell has about 100 transducer channels, or about one per stereovillus. In a later study, Hudspeth and Holton (1986) measured the conductance of the transducer channel of saccular hair cells as 13 ± 3 pS at 10 °C and estimated the number of channels to be nearer 280, or a few per stereovillus. By dissecting away some of the stereovilli, Hudspeth and Jacobs (1979) showed that the receptor potential fell according to the proportion of removed stereovilli. This suggests a regular distribution of the transduction channels across the stereovillar bundle. In this bullfrog saccular organ, removal of the kinocilium from the hair cell has no effect on its sensitivity.

Measurements of the current density in the extracellular space around the stereovilli (Hudspeth, 1982) indicated that the transduction channels (membrane channels that open as a direct result of the absorption of stimulus energy) are probably in the upper parts of the stereovilli (Fig. 2.14a). Osborne et al. (1984) and Pickles et al. (1984) have suggested for the guinea-pig cochlea that the connection between the tip of a stereovillus and the adjacent taller stereovillus would exert the most strain on the membrane under normal stimulus conditions (Fig. 2.14b). It may be reasonable to conclude that the transduction channels are near these points of strain. More specifically, Pickles et al. (1984) suggest that the fine strands of material connecting the tips (‚tip links') of the shorter stereovillus to the next tallest villus are suitable candidates for placing strain on a nearby transduction channel in the membrane. Such tip links have also been found in both lizard and bird hair cells (Pickles et al., 1988 a,b). These tip links are always oriented along the anticipated direction of maximal strain between stereovilli during stimulation (Fig. 2.14c). The response latency of the transduction channels (about 40 μs at 22 °C, Corey and Hudspeth, 1979 b) is so short that it is likely that the mechanical strain acts directly on the transduction channel, increasing the probability of it opening.

The dynamic range of the mechanical response is small in saccular hair cells, a saturated receptor potential being reached by a displacement of the stereovillar bundle through 1 μm, or an angle of less than 10 ° (Hudspeth and Corey, 1977). More recent estimates show a saturation near 0.2 μm (Corey and Hudspeth, 1983). As will be discussed in a later chapter, auditory receptors are somewhat more sensitive than this (Sect. 6.1.4). At extreme angles, the saccular hair cell is not very sensitive to small displacements. However, the cells adapt to a constant displacement with a time constant of 20–50 ms, so that the sensitivity to small displacements in the new position is restored, even for displacements of more than 30 ° (Corey and Hudspeth, 1983; Eatock et al., 1979; 1987).

2.4.2 An Electrical Resonance in Saccular Hair Cells

Recent experiments have demonstrated the presence of several different ion-channel types in the saccular hair cell, in addition to, and probably in other parts of the membrane than, the transduction channel. There is evidence for the existence of at least three other channel types: the early potassium channel, a

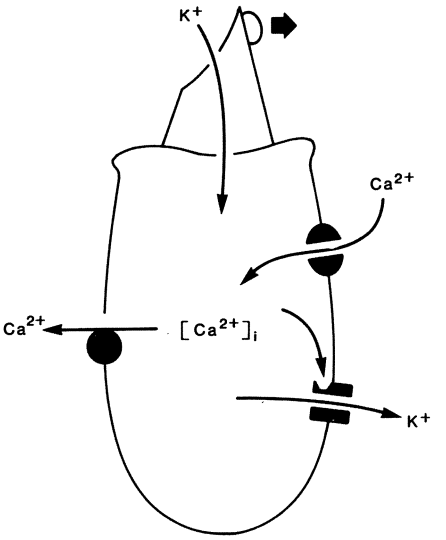

Fig. 2.15. Hair-cell channels involved in an electrical resonance of saccular hair cells. Deflection of the stereovillar bundle in the excitatory direction (*arrow*) opens transduction channels and allows positive ions (here K^+) to enter the cell. The depolarization thus produced opens voltage-sensitive Ca^{2+} channels (*right*), whose inflow increases the depolarization. The higher Ca^{2+} concentration in the cell, however, activates Ca^{2+} sensitive K^+ channels (*lower right*), leading to a loss of K^+ out of the cell. The cell repolarizes, which reduces the activation of Ca^{2+} channels. In addition, the Ca^{2+} concentration is reduced by specific ion pumps in the membrane (*left*). At this low concentration, the Ca^{2+} sensitive K^+ channels close, the cell reverts to near its original potential, and another cycle of the electrical resonance can begin (Hudspeth, 1985)

voltage-sensitive calcium channel and a calcium-sensitive potassium channel (Fig. 2.15). In some cases, it is obvious that these channels work together to endow the membrane with a preferred sensitivity to certain frequencies of stimulation. This frequency often varies systematically from cell to cell, from one end of the organ to the other. In the isolated frog saccule, these electrical ‚resonant' frequencies of the hair cells vary from 11 to 160 Hz (Fig. 2.16; Ashmore, 1983; Lewis and Hudspeth, 1983 a). In the amphibian papilla of a frog, Pitchford and Ashmore (1987) found a range of resonant frequencies in the area from which they could record (rostral and mid-regions of the papilla) of near 60

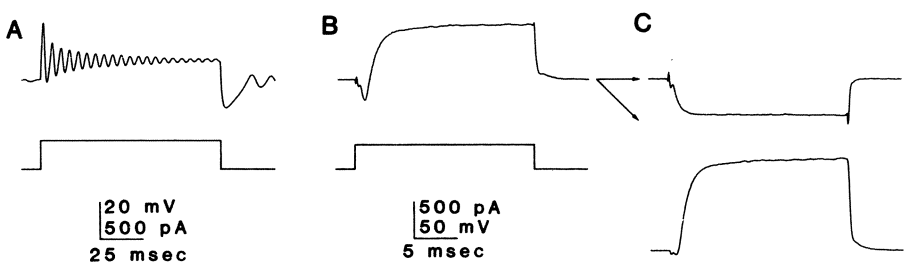

Fig. 2.16 A–C. The ionic basis of electrical hair-cell tuning can be investigated using voltage clamp and channel-blocking techniques. *A* A square-wave current pulse injected intracellularly (stimulus in lower trace) results in a membrane potential which shows a strong, damped oscillation at the beginning and at the end (beginning: 203 Hz). *B* If the cell's resting potential is clamped at −85 mV instead of −40 mV, a biphasic current flow can be measured in response to the injected pulse. There is an early, inward component (deflection down) followed by a larger outward component. *C* If this late component is blocked by 10 mM tetraethylammonium ion (blocks certain K^+ channels), a voltage-sensitive Ca^{2+} inward current is unmasked (*upper trace*). Subtracting the *top trace* in *C* from that in *B* reveals the Ca^{2+} sensitive K^+ current (*lower trace* in C) (Hudspeth, 1985)

to 330 Hz. The membrane-potential resonance apparently arises through the interaction of the kinetics of the fast inward calcium current (voltage activated) and a calcium-activated outward potassium current (Fig. 2.15; Lewis and Hudspeth, 1983 b; Hudspeth and Lewis, 1986; Roberts et al., 1986). There is strong evidence that similar channel kinetics are primarily responsible for the range of tuning frequencies observed in the turtle cochlea (see Ch. 6; Art et al., 1986; Fettiplace, 1987). It may be that the differences in frequency selectivity between individual saccular cells can be explained by differences in the number and kinetics of the ionic channels. Similar findings in the basilar papillae of reptiles will be discussed in later chapters. Fuchs and Mann (1986) and Fuchs et al. (1988) recently describe the involvement of a similar mechanism in frequency-selective responses of hair cells from the apical half of the chick basilar papilla. Further details on similar ionic channels and on the transducer channel of avian hair cells are available for vestibular hair cells of the chick (Ohmori, 1984, 1985).

Chapter 3

The Middle Ear

3.1 Origin of the Middle Ear

The middle ear of land vertebrates presents one of the most remarkable and best documented examples of functional transformation in vertebrate evolution (Carroll, 1987; Lombard and Bolt, 1979). The essentially single ear ossicle of the nonmammals (with two sub-components, the columella and extracolumella), is ultimately derived from a series of cartilaginous rods which were part of an extensive system of gill-support arches in the earliest vertebrates. The acquisition of jaws by later fish led to these particular components of the gill-arch system (the hyomandibular arch, which lay immediately behind the arch giving rise to the jaws) being utilized as structures strengthening the jaw articulation. A later change in the articulation of the jaw produced a redundancy of function, so that these rods became free in the region behind the jaw joint. The various components of the hyomandibular arch can be traced today in the ontogeny of various land vertebrates and be seen to build different parts of the ear ossicle of the nonmammals (Fig. 3.1). The two most important parts of this ossicle are the columella (origin in the pharyngobranchial) and extracolumella (origin in the epibranchial of the hyomandibular arch), which together make up the sound-conducting ossicle. Other hyomandibular components make up, for example, the dorsal process of the columella and intercalary cartilage.

3.2 Pathways of Sound to the Inner Ear

There seems to be little doubt that the columella of many primitive reptiles, especially the Pelycosaurs and Captorhinomorphs, (Carroll, 1977; Hopson, 1966; Watson, 1953) was a rather massive bone and that these animals had inherited from their ancestors an inner ear containing certain areas of sensory cells, such as the saccular macula, which responded to vibration and low-frequency sounds. Unlike in a fish, these sounds could not enter the body over the entire surface. While the acoustic impedance of the body is similar to that of water, it is very much higher than that of air, so that almost all the energy of oncoming sound waves would be reflected from the surface. Thus, in the early land vertebrates (both amphibians and reptiles), most of the vibrational and sound energy reaching the inner ear would have done so through those parts of the body in contact

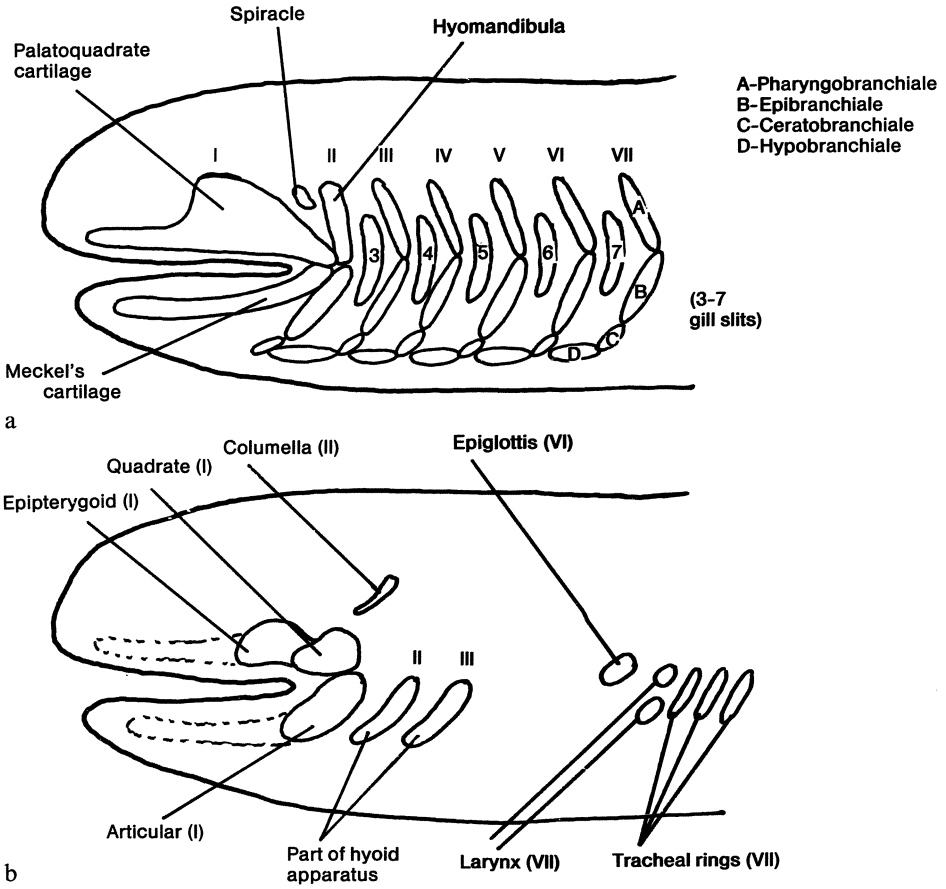

Fig. 3.1 a, b. Highly simplified schematic diagram of the evolutionary derivation of the columella, the middle ear ossicle of amphibians, reptiles and birds, from the hyomandibula of ancient fish. *a* The splanchnocranium of sharks; *b* the situation as in reptiles. The first gill arch (*I*) of fish gave rise to the primitive jaw and later to the quadrate and articular bones of the reptilian jaw joint (*b*). The upper part of the second gill arch (*II*), the hyomandibula, acted initially as a support for the jaw articulation (*a*). As a result of the stabilization of the primary jaw joint, the hyomandibula was free to fulfill other functions and formed the middle-ear ossicle (*b:* columella). In land vertebrates, the gill slits (*a: 3–7*) are lost and parts of the gill arches *II* to *VII* assume other functions (*b*) (After H. M. Smith, 1960 and Remane et al., 1985)

with the ground. Since the most primitive reptiles only had relatively weak limbs splayed out to the side of the body (Reisz, 1975, 1977), in a resting animal this contact area included most of the underside of the body. It was nevertheless necessary, for the detection of these stimuli, that pressure waves generate fluid motion in the inner ear. Thus, the inner-ear capsule could not have been fully closed, but must have had softer ‚windows' which allowed the incompressible fluid to move. It is likely that these fluid motions were made larger by contact between the inner ear and components of the hyomandibular arch. If the hyomandibula (columella) was relatively large and suspended freely, it would

tend to vibrate out of phase with the rest of the head, producing a relative motion between itself and the inner ear.

During the water-land transition period in vertebrate evolution the hyoid arch was relegated to a position within a forward extension of a gill pouch behind the jaw, a pouch which was closed to the outside world by a skin covering. The thin covering was advantageous for the new function of the hyoid, allowing a relatively free motion of this bone at the body surface. Such a scheme seems to me to be the most likely explanation for the massive size of the hyomandibular bone of many early tetrapods (where it is called the columella or stapes) – it certainly could not have functioned like the middle ear of most present-day reptiles and birds. Although there is some evidence (Thompson, 1966) that Rhipidistian fish, the ancestors of the tetrapods, possessed a kind of eardrum, it is very difficult to draw any conclusions as to its function. Whereas it has often been suggested that the earliest land vertebrates inherited a well-functioning middle ear sensitive to air-borne sound (e.g., Watson, 1953), it is difficult to imagine why this should have been abandoned in so many major groups through the adoption of a massive stapes and, often, no tympanic membrane. More recently, the idea that the presence of a tympanic membrane and sensitive hearing is a primitive characteristic of land vertebrates has been strongly challenged (Lombard and Bolt, 1979). These authors propose that a tympanic membrane necessary for sensitive hearing in air is not homologous in terrestrial vertebrates but was developed independently at least three times in evolution, once by the amphibia, once by reptiles ancestral to archosaurs and lepidosaurs and once by the ancestors of mammals. These ideas are strongly supported by important features of the embryological and anatomical relationships between the tympanic membrane, chorda tympani branch of the seventh nerve and the surrounding structures. Within the modern reptiles and birds, however, there is agreement that the only major differences in the middle-ear region concern the developmental state of various processes of the columella-extracolumella complex. According to different views of the evolution of the middle ear, the primitive columella of reptiles had either four or five processes. The otic process connected to the inner ear at the oval window, the other processes were connected to various bones in the middle-ear region. In different evolutionary lines, different combinations of these processes (except the otic) were lost (Lombard and Bolt, 1979). Lombard and Bolt consider that the tympanic process (connection to the tympanum, or eardrum) was not present in primitive ancestors of modern reptiles and birds.

The evolution of the reptiles was accompanied by a number of changes in the body structures which they had inherited from their aquatic ancestors. At least in some groups, these changes had important consequences for middle-ear function (Carroll, 1987). The splayed-out limbs were drawn up to the side of the body and the elbow and knee joints turned, so that with less exertion, the entire body could be lifted and held off the ground. At the same time, the head became smaller and a flexible neck developed, enabling the now more mobile creatures to capture their prey, such as insects, more easily. These and other changes were, however, not without consequence for the ear. The head became more and more isolated from the ground and the path for vibrations to the ear became very long. This may have been the most important selective pressure which, in some lines, led

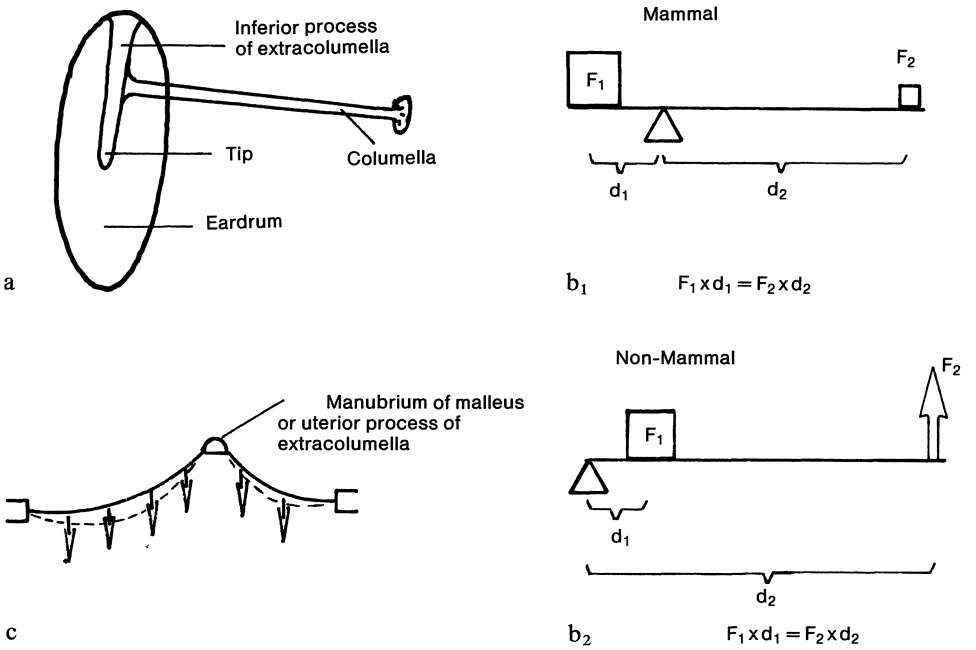

Fig. 3.2 a–c. The three principle methods by which the middle ear achieves its relatively high impedance-matching values. *a* The area of the eardrum is much greater than that of the columellar footplate (large area ratio). *b* The lever ratio produced either as in non-mammals (b_2, with a secondary lever system constructed out of the extracolumella and columella) or as in mammals (b_1, with a primary lever system made up of two ossicles, the hammer or malleus and anvil or incus). *F* force; *d* distance. *c* The curved membrane principle as applied to the tympanic membrane of a nonmammal, shown in section. For the purpose of illustration, all displacement amplitudes are highly exaggerated. The membrane displacement (*solid to dotted line*) is much larger on the free membrane than at the point of attachment of the extracolumella. For further explanation see text (Partly after Tonndorf and Khanna, 1970)

progressively to a dramatic reduction in the mass of the columella. This reduction made it possible for air-borne pressure waves impinging on the thin covering of the old gill pouch to actually move the columella. Most authors assume a cartilaginous ‚extracolumella' to have existed, connecting efficiently the columella and the skin covering the newly-formed middle ear cavity, a skin covering we now call the eardrum. The massive appearance of the columella of some ancestral reptiles, such as captorhinomorphs, pelycosaurs and primitive eosuchians (where the small size of the tympanum and even the position of the columella make it very unlikely that the middle ear functioned as in most modern lizards), can be contrasted with the situation in early lizards, where a large tympanum was obviously present (Carroll, 1977, 1987; Reisz, 1977). Selection pressures affecting feeding mechanisms (e.g. changes in the quadrate bone associated with a more rapid jaw closing on agile prey) apparently ran parallel to changes improving the suitability of the middle ear for detecting air-borne sound.

Hotton (1959) drew a model of the mode of stimulation of the ear of primitive reptiles, in which the motion of the columella at the inner ear was larger than its motion at the eardrum – exactly the reverse of the present-day situation. This kind of motion would have made the middle ear very insensitive to air-borne sound. With a large stapes and small eardrum, it seems more likely that this middle ear was in fact not a middle ear at all – that is, not a structure designed as an impedance-matching device for the air/body interface. It would rather have been an inertial system assisting in the detection of substrate-borne vibrations, vibrating out-of-phase with the rest of the body and thus increasing the stimulus to the inner ear. Another possibility would be to imagine this large columella as being connected to an extensive network of extracolumellar branches or in some other way in contact with the head surface as in modern snakes and amphisbaenids. Thus some sensitivity, albeit a poor one, to air-borne sound might have existed.

With the development of a lighter columella and a larger eardrum supported by a bony ring, the sensitivity to sound – at least low-frequency sound – would have become greater; a true middle ear would have been developed. We can only speculate as to the selective pressures which furthered this. This process probably occurred independently several times (Lombard and Bolt, 1979), providing modern amphibians, reptiles, birds and mammals with a middle ear quite sensitive to sound. Perhaps acoustic communication was present; perhaps the isolation of the ear from the ground made substrate-vibration detection almost impossible. At least in some later reptilian groups, the advantages of such a middle ear were obviously not very great, for the middle ear has frequently been highly reduced. This is true, for example, in burrowing forms (as in the presumed ancestors of the snakes) and in forms where it made way for a more efficient feeding mechanism (Olson, 1966). In other cases, it is possible that a true ‚tympanic' ear was never developed, e.g. as in some modern groups of amphibians (Lombard and Bolt, 1979).

In reptiles which have lost or reduced their middle ear, Miller (1966, 1968, 1978 a) observed a concomitant (relative) reduction in the size of the basilar papilla. Modern snakes, where there is no tympanum and the columella articulates with the quadrate bone, have, in general, small papillae. However, the size of the papilla varies with the nature of the bodily contact to the substrate, burrowing snakes having the longest papillae and tree-living forms the shortest. Ground-dwelling snakes have papillae of intermediate length (Miller, 1968, 1978 a). This may indicate that sound and vibration pick-up from the animal's surroundings are important enough in snakes to influence the evolution of the inner ear. Similar thinking could be applied to the question of the input to the inner ear of many fossil species of reptile. Hartline (1971 a) was able to show that the lung of snakes plays an important role in picking up airborne sound, which is then transmitted through tissue vibration to the inner ear. As a result of these different adaptations, some snakes have a good sensitivity at low frequencies to airborne sound (thresholds of 35 dB SPL at 200 Hz, Hartline, 1971 a,b; see Sect. 6.2).

3.3 General Functional Considerations

3.3.1 Factors Involved in Impedance Matching

The energy involved in producing pressure waves in water is much higher than that involved in moving air. Without an amplification system, more than 95 % of the energy of a sound wave in air is reflected at an air/water interface. The middle ear amplifies the energy arriving at the body surface in three ways.

1) The eardrum itself – the collector of the air-borne sound energy – has a larger area than that of the footplate of the columella which transfers the sound energy to the inner ear (Fig. 3.2a). The energy impinging on the eardrum causes it to move, pushing and pulling on the extracolumella. Of course, the eardrum is fixed all around, so that during sound stimulation, amplitude gradients are set up on the eardrum. These gradients and other factors, such as coupling of the tympanum to the auditory ossicle(s) produce complex motion patterns, depending on the stimulation frequency (see Fig. 3.10). Because of these complex patterns, it is difficult to calculate how much the area-difference between eardrum and columellar footplate contributes to the amplifying effect of the middle ear. It would be necessary to integrate the different amplitudes of the various areas at a given frequency and to know how effective the contribution of different parts of the eardrum are at the extracolumella.

2) We know that the eardrum does not vibrate like a stiff plate, for the amplitudes of the membrane to the sides of the extracolumella are often higher that those of the extracolumella itself. In this case, the curved-membrane lever proposed by Helmholtz almost certainly operates in these middle ears (Fig. 3.2c; see Tonndorf and Khanna, 1970, for a discussion of this theory). Those of us familiar with the great increase in pull which can be obtained on a rope when, instead of directly pulling, the free end of the rope is attached to a tree and we push the rope sideways, can appreciate the effectiveness of a curved membrane on the ossicle. In this case, the membrane pulls both on the ossicle and its (fixed) outer edge.

3) The middle ear of nonmammals also contains a lever system in the ossicle itself. Although it was long thought a unique advantage of the mammalian middle ear that a lever system exists, such a system has been demonstrated in lizard ears (Fig. 3.2b). Thus it is wrong to regard the evolution of the mammalian middle ear as adding "... a lever system to the primitive tetrapod piston" (Hopson, 1966). As an example, we shall look at the measurements of motion amplitudes in different parts of the middle ear of the tokay gecko, *Gekko gecko* (see below, Figs. 3.10, 3.11). As in most nonmammals, the columella inserts on the extracolumella not near the tip at the centre of the eardrum, but nearer the edge of the eardrum (see Figs. 3.2a, 3.5 and 3.12b). Thus, this insertion point is not at the site of greatest displacement amplitude of the drum. Assuming that the energy of the membrane is coupled to the extracolumella along its length proportionally to the area and amplitude of motion of the surrounding drum, then the greatest amplitudes will be found at the tip of the extracolumella. This is the case. The amplitude of motion of the columella is, at low frequencies, actually less than a third that of the tip of the extracolumella, proportional to the length of the lever arms involved (Figs. 3.2b, 3.12b). The amplitude reduction in this (second-

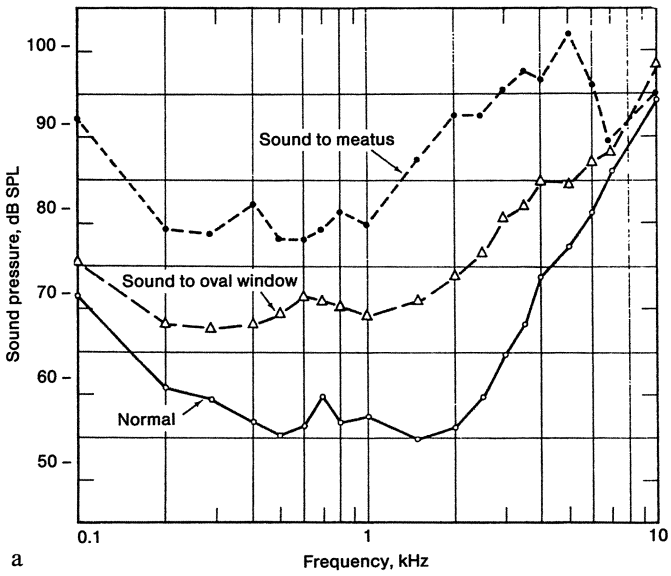

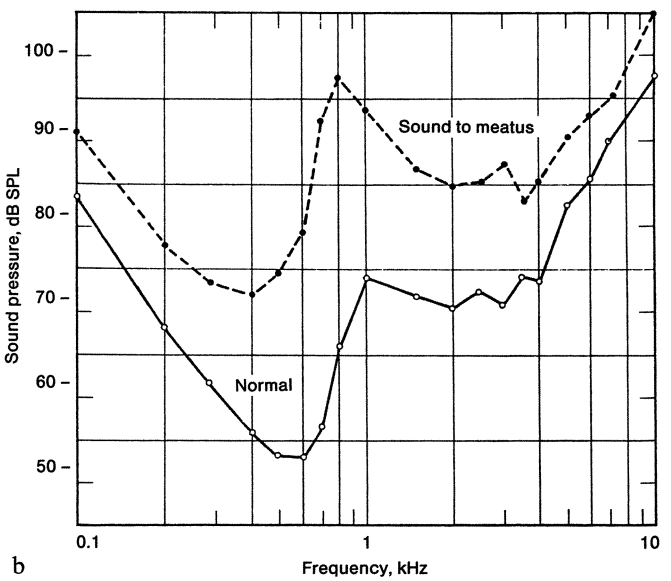

Fig. 3.3 a, b. Diagrams illustrating two experiments in which the amplifying effect of the middle ear was measured. The *continuous curves* illustrate for the two species *a Crotaphytus collaris* and *b Gekko gecko* the sound pressure level (SPL re: 20 μPa) necessary to produce a cochlear microphonic potential of 0.1 μV. The *long-dashed line* indicates the SPL necessary to produce the same criterion voltage after removal of the middle ear and with the sound delivered directly to the oval window. The maximal loss in the iguanid *Crotaphytus* is near 35 dB, in *Gekko,* however, it is near 60 dB. These values indicate the approximate effectiveness of the middle ear in impedance matching. In both cases, the middle ear is most effective in the mid-frequency range (*a* from Wever and Werner, 1970; *b* Werner and Wever, 1972)

order) lever produces a proportional increase in the energy which is transmitted to the columellar footplate.

Thus, the middle ear of most modern nonmammals is an extremely efficient system for transmitting energy from the eardrum surface to the small opening in the inner ear. After removal of the middle ear in lizards, Wever and Werner (1970) and Werner and Wever (1972) report losses in sensitivity of between 35 and 57 dB at low frequencies (Fig. 3.3 a,b). These values are directly comparable with equivalent values for mammals. The middle ear of nonmammals is thus a highly efficient impedance-matching device, at least at relatively low frequencies.

3.3.2 Disadvantage of the Second-order Lever System

The repeated use of the qualifier "at low frequencies" above is, however, important, for at higher frequencies (above 4 to 6 kHz), the lever system breaks down (see below, Fig. 3.12). While it is true that the motion of the eardrum becomes smaller in displacement amplitude and complex in form at high frequencies, this is not unexpected – exactly the same happens in mammalian eardrums of this size. This is partly because the *displacement* amplitude of the air particles also falls with frequency (at a constant sound pressure, the *velocity* of air particles is constant at all frequencies). The problem with the nonmammalian middle ear lies in the incorporation of the joint of the lever system within the extracolumella (Fig. 3.5) and not, as in mammals, between separate bones. In order to transform the swinging motion of the inferior process of the extracolumella into the piston-like motion of the columella, the junction must be flexible. This is normally provided for by the low grade of ossification of the extracolumella compared, for example to that of the columella. At high frequencies, however, when the input impedance of the inner ear is rising, the eardrum motion is only poorly transmitted to the columella. Instead, the inferior process flexes strongly with the eardrum and absorbs much of the energy itself. This may on the surface seem to be no particular disadvantage for the modern nonmammal, as this limitation is strongly correlated with a poor performance at high frequencies by the inner ear anyway. However, this is a typical ‚chicken – and – egg' case, where it is difficult to know which factors are ultimately limiting.

Did the inner ear of nonmammals not develop high-frequency sensitivity because these frequencies were not transmitted efficiently through the middle ear? Or did the lack of inner-ear sensitivity to high frequencies result in the absence of any selective pressures to improve the middle ear? A number of factors speak in favour of the first explanation.

1) The middle ear can be improved somewhat, through additional partial ossification, resulting in a somewhat improved high-frequency hearing, e.g., in the barn owl up to 12 kHz.

2) This kind of improvement is limited, as a full ossification of the extracolumella would severely diminish or destroy the lever action.

3) There is good evidence from the mammals that the removal of the constraints imposed by the middle ear permits an expansion of the hearing range to higher frequencies. This is obvious if we remember that in land mammals, the size and

therefore the physical properties of the middle ear are, to a first approximation, a direct result of the species size. Thus, the larger mammals, such as the apes, ungulates, etc. do not have such high-frequency hearing as smaller mammals, such as rodents, cats, etc. A person can hear an ultrasonic transducer only when it is pressed onto the skull, that is, by direct bone conduction. Large mammals such as whales and dolphins, which have returned to the sea and have given up the type of middle ear suited for impedance matching have, despite their large size, extremely good high-frequency hearing (Manley, 1973). The release of the constraints of the middle ear seems to be responsible for this dramatic difference.
4) There are good reasons for believing that the origin of the two kinds of lever system in the middle ear had nothing to do with their potential high-frequency efficiency. All that we now know indicates that low-frequency hearing in land vertebrates is a primitive condition and that the cochleae of the reptilian ancestors of mammals were not particularly well developed over and above the condition in other reptile groups. Thus, the mammalian middle ear almost certainly developed before the cochlea of mammals or mammal-like reptiles had developed the ability to process high frequencies.

The incorporation of the quadrate and articular bones from the primary jaw joint into the middle ear of mammal-like reptiles as the incus and malleus, respectively, must thus be traced to some other factor, such as an improved absolute sensitivity. Indeed, the columella of pelycosaurs, the direct ancestors of the therapsid or mammal-like reptiles, was massive (Carroll, 1977; Watson, 1953) and the form of the quadrate gives no indication of the presence of a tympanic membrane (Lombard and Bolt, 1979; Olson, 1966). This situation is rather far removed from that of most modern tetrapods, and Olson regards it as being the basic state in all primitive reptiles. Improvements came in the diapsid reptiles (the ancestors of almost all modern reptiles and all birds) through an enlargement of the tympanic membrane and a considerable lightening of the columella (see above). In the therapsids (the ancestors of mammals), improvements came quite independently as a by-product of the development of the secondary jaw articulation, which released the quadrate and articular bones out of the jaw joint (Fig. 3.1) and made possible the three-ossicle linkage we now see in mammals (Lombard and Bolt, 1979; Watson, 1953). Thus it seems most likely that the middle ear of modern mammals did not develop as an ‚improvement' on a single-ossicle middle ear as known from modern reptiles and birds, but during the establishment of a good sensitivity to air-borne sound in a system where this did not exist. The middle ears of modern mammals and those of modern reptiles and birds can thus be regarded as completely independent developments.

That the first-order lever system between the two additional ossicles of mammals would later be of greater advantage in the transmission of very high frequencies must be regarded as one of the most interesting fortuitous developments in evolution. Without it there would have been, for example, no development of the high-frequency hearing typical of mammals (man is a large mammal and thus has a limited high-frequency hearing range) and certainly no echolocating bats! The essential point of this discussion is, however, that the ability of the mammalian middle ear to transmit higher frequencies than the columella ear probably played no role in its selection during the evolution of the mammals. This view is

in contrast to a number of published notions of the functional evolution of the mammalian ear (e.g., Fleischer, 1978).

3.3.3 The Middle Ear of Modern Reptiles and Birds: Structure

The middle ear of reptiles and birds is fairly diverse in its structure, but rather uniform in function and almost certainly made up of homologous components (Lombard and Bolt, 1979). There are a number of morphological types and extensive accounts are given by Olson (1966) and Wever (1978). Most of the differences in form relate to the presence or absence of processes to the side of the extracolumella-columella pair.

In many reptiles, the eardrum is a rather superficial structure, often being almost flush with the surrounding skin (Fig. 3.4). In a few lizard groups, e.g., the geckos and skinks, the eardrum lies relatively deep and a true external ear canal, the external meatus, exists. In this way, the eardrum is given a greater degree of protection from mechanical damage. In geckos, the external meatus is soft and muscular and can be closed off by a muscle. Both the Crocodilia and the birds have an external meatus, which in the Crocodilia is covered and protected by a closeable ear flap. Many reptiles show only a modified or even no eardrum. Chameleons, agamid lizards and especially chelonians (turtles and their relatives) often have eardrums which are covered by a scaly skin and can thus be quite thick. In the Tuatara, the eardrum is also covered by thick connective tissue.

In many burrowing forms, such as many anguid lizards, the external meatus is reduced to an extremely small hole. The amphisbaenids and the snakes have no

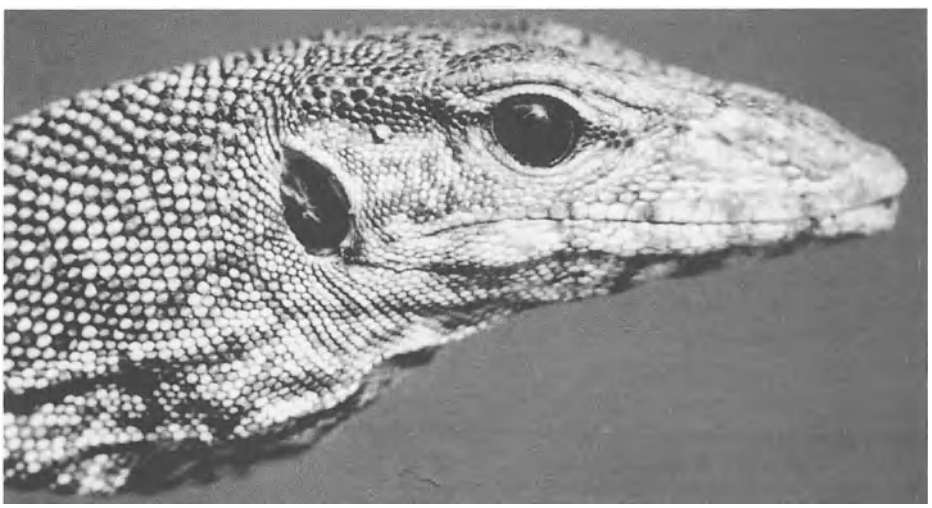

Fig. 3.4. Photograph of the head of *Varanus bengalensis* to illustrate the fact that the tympanic membrane is relatively large and very close to the body surface, a situation typical for reptiles. The inferior process (pars inferior) of the extracolumella can be seen through the eardrum, extending from the dorso-caudal margin to the middle of the eardrum.

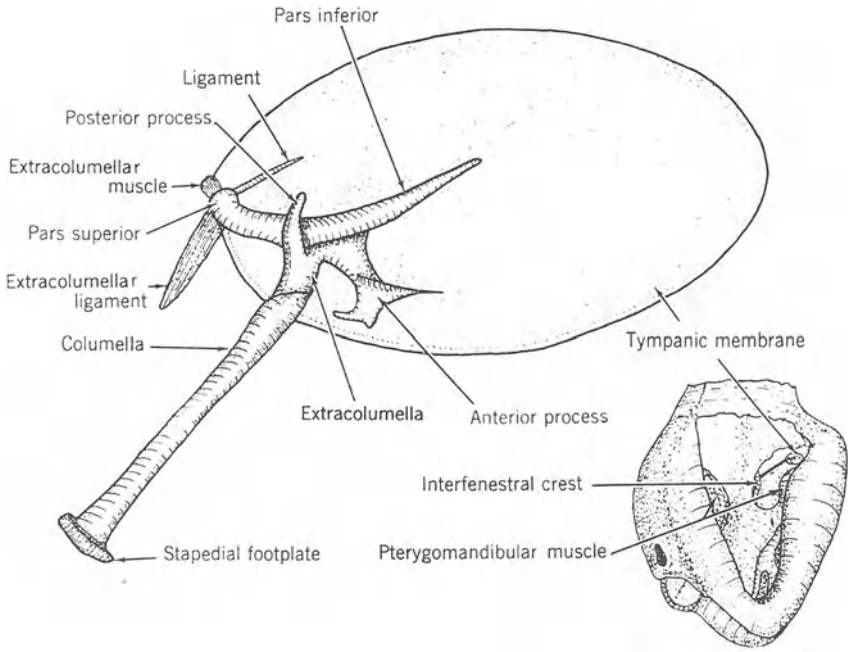

Fig. 3.5. The middle ear of the tokay gecko as seen from inside the mouth, showing the tympanic membrane, various processes of the extracolumella, the columella, and columellar (= "stapedial") footplate, to illustrate the insertion of the extracolumella on the eardrum. The extracolumellar muscle shown here is only found in gekkonid lizards. The *inset* illustrates that the angle of view of the drawing is from a medial, ventral and anterior position (Werner and Wever, 1972)

eardrum and, indeed, no middle-ear cavity, there being thick layers of muscle and skin outside the otic capsule. In contrast to the situation in most lizards, where the middle-ear cavity opens extremely widely into the mouth (buccal) cavity, the middle-ear cavity of Chelonia is small, almost completely enclosed in bone and joined by a short eustachian tube to the mouth cavity. In Crocodilia and birds, the eustachian tube is longer and the tubes from left and right meet in the midline where they have a common opening to the mouth. Indeed, there are two tubes connecting the middle ears to the mouth in Crocodilia, and a prominent tube which connects the middle ears directly and runs dorsally over the brain capsule. In birds, this dorsal connection is not prominent, but may be present via the joined cavities of the spongy bone. Nevertheless, even in these latter groups, the connections to the mouth are larger than would be necessary to ensure pressure equalization of the middle ear with the air outside, and may play an important role in hearing (see below, section 3.4).

The eardrum in most forms is not flat, but is pushed into a convex form. This is in contrast to the concave form (pointing inwards) of mammals. The tympanum is usually transparent enough so that the inferior process of the extracolumella can be seen from outside, sloping from the posterio-dorsal edge of

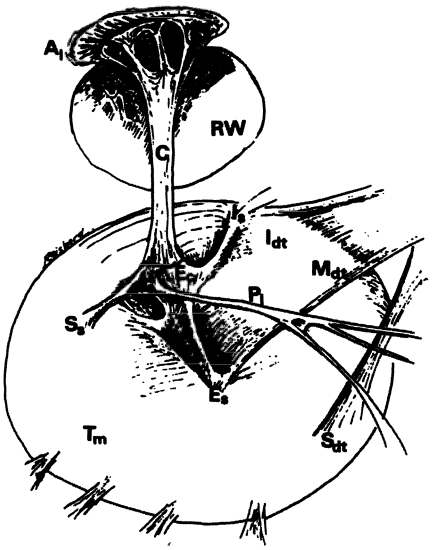

Fig. 3.6. A line drawing of the middle ear of a bird (the parakeet), as seen from within the middle-ear cavity. *Tm* Tympanic membrane; *C* columella; *Ec* extracolumella; *Al* annular ligament of the columellar footplate; *RW* round window; *Idt, Mdt* and *Sdt* inferior, medial and superior drum-tubal ligaments; *Is, Es* and *Ss* infra-, extra- and suprastapedius (= pars superior, pars inferior and pars anterior of the extracolumella respectively); *Pl* Platner's ligament. The columella is 1.35 mm long (Saunders, 1985)

the tympanum to near its centre (Fig. 3.4). The tympanum consists of three layers, a thin epidermal epithelium outside and mucous membrane inside, with fibrous connective tissue between, all of which are stretched between the quadrate bone anteriorly and skin, muscle and connective tissue posteriorly. It is firmly connected to up to four processes of the cartilaginous extracolumella, the pars inferior, pars superior and anterior and posterior processes (Figs. 3.5, 3.6). In addition, in some forms, internal and dorsal processes may be present further down the shaft near the connection to the columella and support the columella from the side through their connections to e.g., the quadrate. In lizards, one or two ligaments underlie the extracolumella on the eardrum and connect internally to cartilage or bone near the edge of the eardrum. In birds, there are ligaments intrinsic to the tympanum and Platner's ligament, which connects the columella (near its synchondrosis to the extracolumella) to the quadrate and squamosal bones in the wall of the middle-ear cavity (Fig. 3.6; Saunders, 1985).

In geckos and pygopodids, there is a middle-ear muscle which joins the pars superior to nearby hyoid cartilage (extracolumellar muscle, Fig. 3.5; Wever and Werner, 1970). The Crocodilia also have an extracolumellar muscle, but it appears to attach to the rim of the eardrum rather than on the extracolumella. The same muscle exists in birds (M. tensor tympani) and pulls both on the eardrum and the extracolumella. In birds, experimental study of the function of this muscle has shown that, at least in owls, it shows reflex contractions to loud sounds. Using pure-tone stimulation, Oeckinghaus and Schwartzkopff (1983) showed that contraction of this muscle reduced the sensitivity of the starling ear to sounds by up to 10 dB, the smallest loss (4 dB) being incurred in the region of greatest sensitivity (2 to 3 kHz in the starling, Fig. 3.7). No data exist on the function of the middle-ear muscle of geckos and Crocodilia.

Modern birds and reptiles usually possess a slender extracolumella and columella, the former generally not being strongly ossified. The medial end of the columella is expanded into a footplate, which is inserted into the oval window of

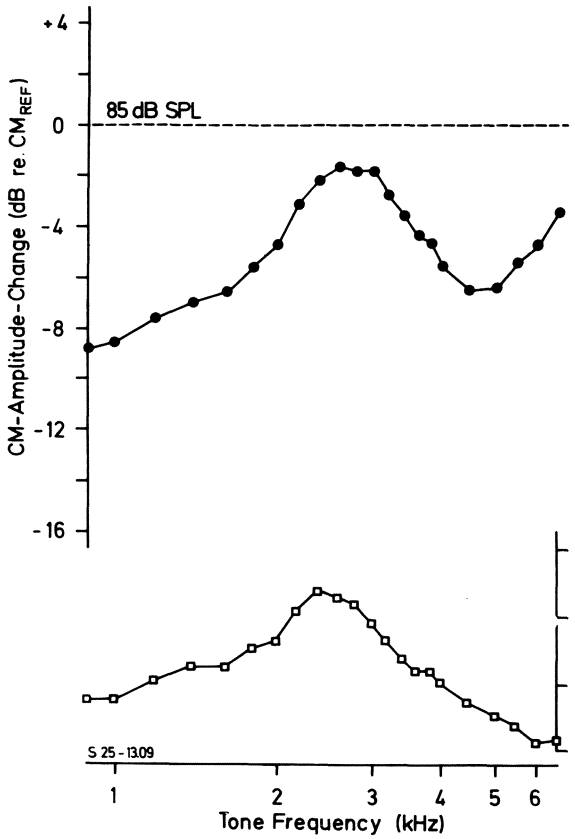

Fig. 3.7. The effect of an electrically-elicited middle-ear muscle contraction in the starling *Sturnus vulgaris* on the amplitude of cochlear microphonics (*CM*) measured in response to tones of 85 dB SPL over a range of frequencies. The figure illustrates the change in CM amplitude in dB (*top*), and the absolute amplitude of the control CM without muscle contraction (*bottom*). The muscle contraction causes a reduction in CM amplitude at all frequencies, the smallest effect being in the mid-frequency range (Oeckinghaus and Schwartzkopff, 1983)

the inner ear and firmly connected by an annular ligament (Figs. 3.8, 4.2). The ratio of the area of the eardrum to the area of the columella footplate varies in birds from about 20 to 30, quite comparable to values given for mammals (Saunders, 1985). The actual length of these structures depends on the depth of the eardrum and the size of the head. In many birds, the pars superior and dorsal process are joined into a ring-like structure. In reptiles with broad heads, the brain cavity is not proportionately broader, so the columella is often quite long. In birds, it tends to be short, due to the large amount of space in the head occupied by the brain. Gaudin (1968) states that the columella is always 3–4 times longer than the width of the footplate in birds. However, in the data of Saunders (1985), it appears that the footplate is more usually about half as wide as the columella is long. In birds, both the eardrum and the columellar footplate are

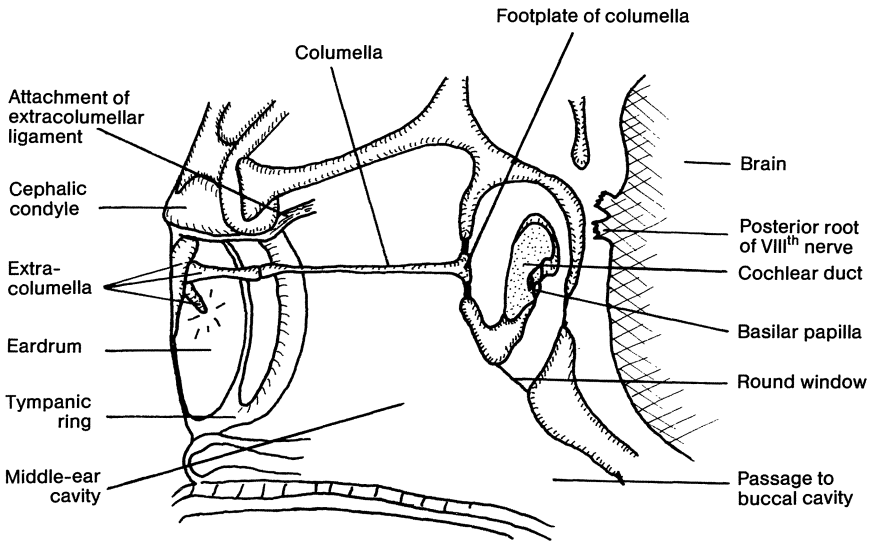

Fig. 3.8. Schematic drawing of a cross-section through the middle ear of a lizard to illustrate the normal reptilian condition, where the middle ear opens widely to the buccal cavity (see also *inset* to Fig. 3.5) (Partly after Wever, 1978)

oval and it has been suggested that under stimulation, the footplate would show a rocking motion with the anterior edge having the greatest displacement (Saunders, 1985). Whether this is true and whether this may also apply to reptiles remains to be investigated.

Chelonia have a simplified extracolumella, and in amphisbaenids it does not connect to an eardrum, but is very long and prolonged into the region of the lower jaw. In snakes, the extracolumella is missing (as is the eardrum) and the columella articulates with the quadrate. The columellar footplate is usually very much smaller than the eardrum, but in snakes it is large. In both snakes and turtles, the footplate is not visible from the middle-ear cavity, but the shaft of the columella disappears through a hole in an extra bony covering of the ear capsule (Fig. 4.4 b,c). The space between the ear capsule proper and this extra bony layer is called the pericapsular sinus and is filled with perilymph. The functional significance of this arrangement is obscure. The eardrum is also lacking in some families of lizards, such as the Anniellidae, Chamaeleonidae and Dibamidae, a condition which is also occasionally found in members of other families, such as Agamidae, Iguanidae and Scincidae.

3.3.4 The Middle Ear of Modern Reptiles and Birds: Function

3.3.4.1 The Amplifying Effect of the Middle Ear

Wever (1978) has reported studies of the function of the middle ear in many reptiles, using the technique of recording cochlear microphonics. Although the

cochlear microphonics seldom give a good estimate of inner-ear sensitivity in reptiles (Sect. 1.3), due to the ease of measurement, this technique lends itself well to relative measurements such as the effect of the removal of the columella on ear sensitivity.

Wever and his collaborators measured the cochlear microphonic sensitivity in certain iguanids, geckos and skinks, then clipped the columella and measured the sensitivity again, this time delivering the sound directly to the footplate in the oval window of the inner ear. In all cases, the loss of the eardrum, extracolumella and columella produced a substantial loss of sensitivity, especially in the mid-frequency range near 1 kHz. The magnitude of the loss was larger in geckos (*Gekko gecko* and *Eublepharis macularius*, up to 60 dB; Fig. 3.3 b) than in skinks (*Mabuya carinata* and *Eumeces gilberti*, up to 50 dB) and in an iguanid (*Crotaphytus collaris*, up to 30 dB; Fig. 3.3 a). However, even in the latter case, the middle ear provides good impedance matching for the inner ear. A more detailed treatment of the complexities of impedance matching by the mammalian middle ear can be found in Rosowski et al. (1986). The mechanics of the different types of middle ear are so complex that as yet no adequate comparative analysis has been published.

In those lizards which have no eardrum and a reduced extracolumella, and in snakes, Wever (1978) showed that the ear has a considerably reduced sensitivity. Clipping the columella in snakes and applying the sound directly to the oval window only brought about a small loss of sensitivity to air-borne sound (about 10 dB) and this only for the mid-frequency range. In contrast, a turtle, with its thick eardrum, still shows a loss of 40 dB in sensitivity upon clipping the columella. Using vibrational stimuli, Wever could show in snakes that, not unexpectedly, the ear responds best to vibration applied to the head surface near the quadrate bone. These animals thus have a much less sensitive ear for sound to the side of the head but, due to the embedding in or attachment of the columella to tissue or bone, a good sensitivity to vibration impinging on the head surface. Far from being deaf, as is commonly believed, snakes are only 20 to 40 dB less sensitive than lizards to sound, the greatest sensitivity being to sound waves impinging on the body surface near the lungs (see Sect. 6.2).

In amphisbaenids, the ear is not particularly sensitive to air-borne sound. However, it becomes much less sensitive (up to 40 dB less) if the columella is sectioned. As mentioned above, the extracolumella in these animals is very large and embedded in tissue of the jaw region. Frequently, there are large sheets of connective tissue attached to the extracolumella. Thus, the entire area of the head forward of the ear region becomes a kind of giant, but relatively insensitive, eardrum.

3.3.4.2 Transfer Characteristics of Bird and Reptile Middle Ear

Direct measurements of the motion of various parts of the middle-ear apparatus exist for reptiles and birds and give a good idea of the actual function of this system. Moffat and Capranica (1978) investigated the middle-ear response in the red-eared turtle *Chrysemys scripta elegans*, using a light-scattering spectroscopy

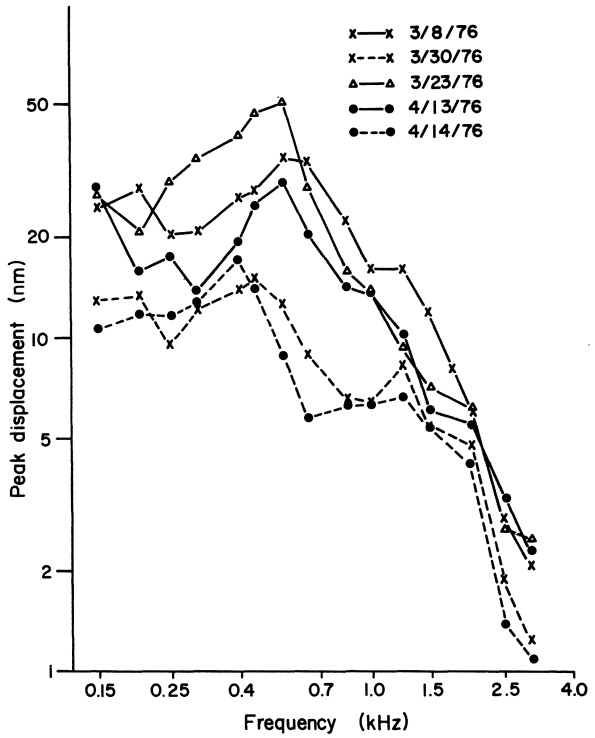

Fig. 3.9. Displacement amplitude of the centre of the tympanum as a function of frequency at 90 dB SPL for five red-eared turtles, *Chrysemys scripta*. In general, the displacement increases little up to a frequency of about 0.5 kHz, then falls off steadily to higher frequencies at a rate of about 9 dB/octave (Moffatt and Capranica, 1978)

technique. They found that the displacement of the centre of the tympanum remained relatively constant over the frequency range 0.15 to about 0.8 kHz, and fell off at higher frequencies at a rate of near 12 dB/octave, becoming immeasurably small above about 3 kHz (Fig. 3.9). Thus, the transfer function resembles that of a low-pass filter, at least for the displacement response. The reduction of the displacement at higher frequencies is partly due to the loss of displacement of air particles with rising frequency (6 dB/octave).

A constant sound pressure means a constant velocity of air particles. The middle ear transfer function for velocity for the red-eared turtle is in fact a band-pass function. It rises at 6 dB/octave up to its resonance frequency near 500 Hz

Fig. 3.10. Isoamplitude contours of the eardrum of the tokay gecko at 12 frequencies (0.25 to 10 kHz) and an SPL of 100 dB, as measured using the Mössbauer technique. These contours are estimates based on interpolations between actual measurement series at the eight points indicated by *dots*. No relative phase information is shown. The *small numbers* adjacent to the contour lines indicate the displacement amplitude in micrometres. As can be seen, the pattern of motion is generally simpler at lower frequencies and the coupling of the extracolumella into the motion of the eardrum is frequency dependent (Manley, 1972a)

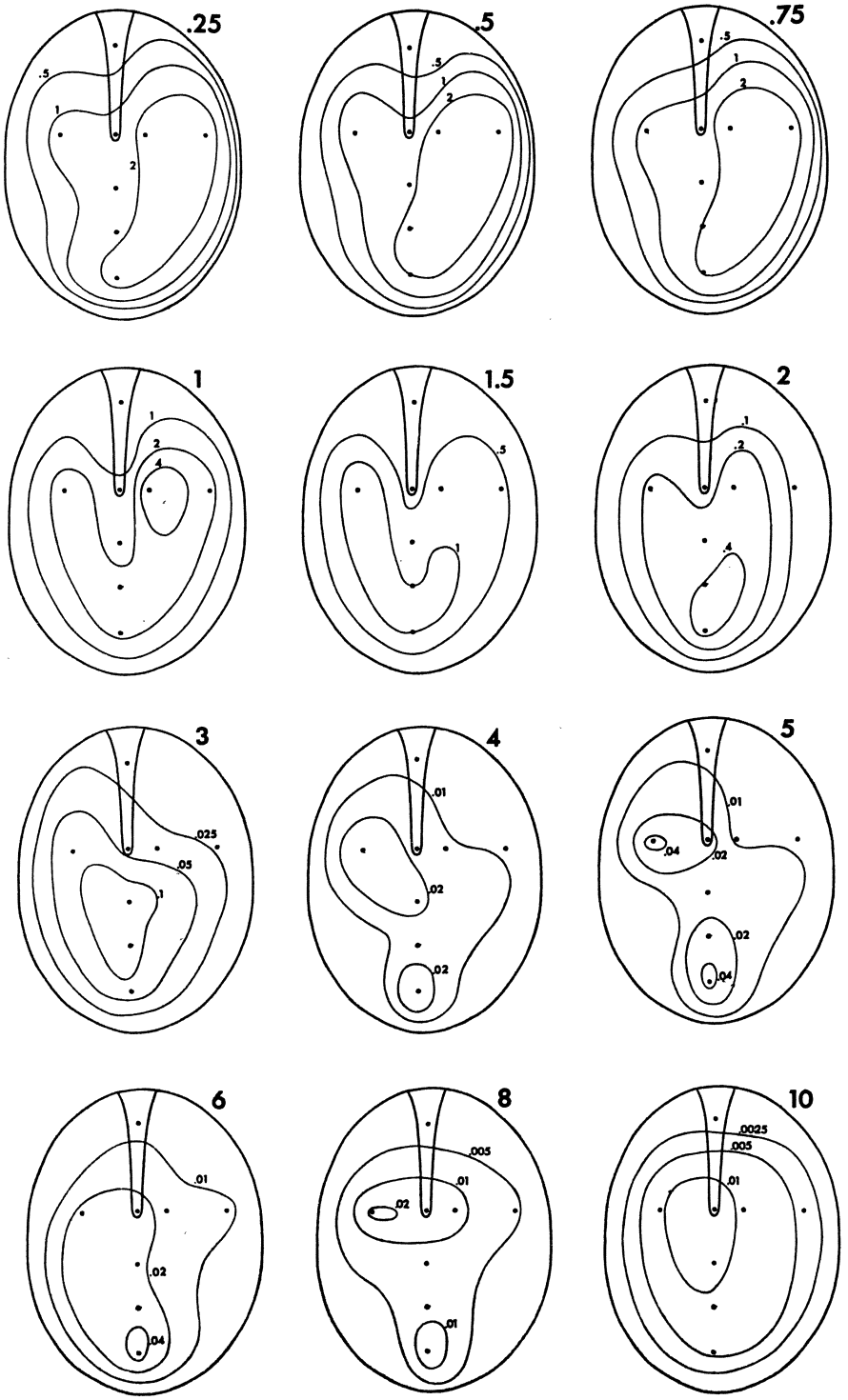
.25
.5
1
2
.5
.5
1
2
.75
.5
1
2
1
1
2
4
1.5
.5
1
2
.1
.2
.4
3
.025
.05
.1
4
.01
.02
.02
5
.01
.04
.02
.02
.04
6
.01
.02
.04
8
.005
.01
.02
.01
10
.0025
.005
.01

and falls with a rate of 6 dB/octave above this. This range corresponds very well with the known low-frequency hearing of this species (see Ch. 6). In lizards and birds, a sound pressure of 100 dB SPL produces an eardrum displacement amplitude of about 1 μm at low frequencies. The corresponding value for the turtle eardrum in Moffat and Capranica's data would be 0.09 μm, less than one tenth. Thus, at the level of the thick turtle eardrum, and contrary to the suggestion of Moffat and Capranica, there is a loss of amplitude of 20 dB compared to nonmammals with a thin eardrum.

Using the Mössbauer technique (Sect. 5.4), I recorded the transfer function of the middle ear of two gecko species, *Gekko gecko* and *Gehyra variegata* (Manley, 1972 a,b,c). Measurements were made at different locations in the transmission pathway, at several places on the tympanum and after various manipulations, so that a fairly comprehensive picture of function emerged. To measure the vibration patterns of the eardrum, eight measurement points on the surface of the eardrum were used, two of which overlie the extracolumella. The data show that below a frequency of about 3 kHz, the free area of the drum always vibrates with a higher amplitude than anywhere on the extracolumella (Fig. 3.10). Similar

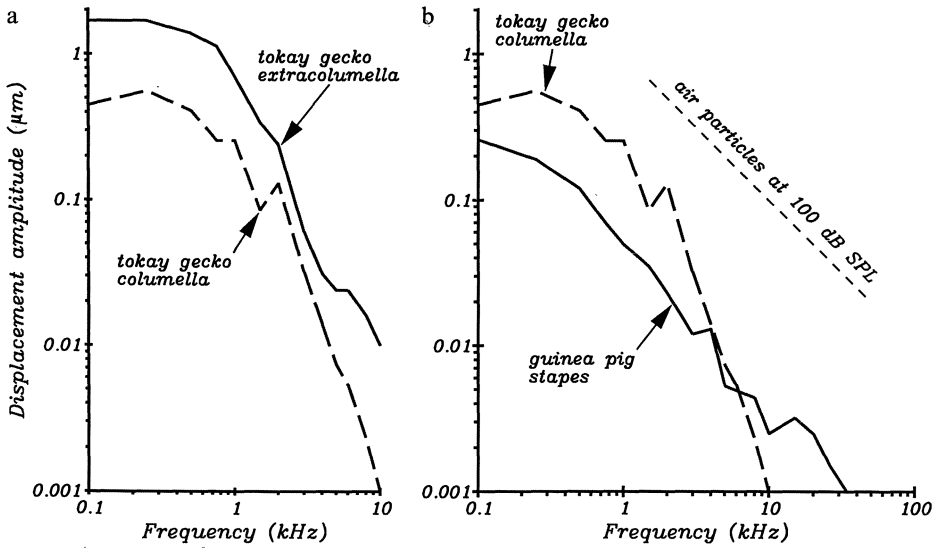

Fig. 3.11 a, b. Middle-ear transfer functions in the tokay gecko (*Gekko*) and the guinea pig (*Cavia*). *a* Displacement amplitude in micrometres of two points on the middle-ear ossicle of *Gekko* at 100 dB SPL, as a function of frequency, measured with the Mössbauer technique. *Continuous line:* tip of the inferior process of the extracolumella on the tympanic membrane (approximately the midpoint of the eardrum); *broken line* columella. The displacement amplitude falls off rapidly above a frequency of about 1 kHz; the displacement amplitude of the columella falls off more rapidly (After Manley, 1972 b). *b* Displacement amplitude of the columella in *Gekko* (*long-dashed line*) as compared to the stapes footplate in *Cavia* (*continuous line*) at 100 dB SPL, to illustrate the difference in the transmission of frequencies above a few kHz. Both curves are average measurements on several animals. Although the guinea-pig middle ear shows a greater resistive loss at low frequencies (in spite of an opened bulla), it is better able to follow the motion of the air particles (*short-dashed line*) up to high frequencies (After Manley, 1972 b; Manley and Johnstone, 1974)

results for one point on the free tympanic membrane of the chicken middle ear are shown by Saunders (1985). We are reminded here of the effectiveness of the curved membrane according to Helmholtz's theory. Above 3 kHz, the membrane amplitude is lower than or equal to that of the tip of the inferior process, depending on just where the measurement was taken on the free membrane. Interpolating between data points allowed an estimation of the vibrational patterns of the entire eardrum at different frequencies (Fig. 3.10). Similar patterns have been measured on the eardrum of the cat; these patterns break up into several nodes and become more complex at higher frequencies (Khanna and Tonndorf, 1972). This complex pattern, with segments vibrating out of phase to one another, points to a breakdown of the efficiency of the tympanic membrane as a sound collector coupled to a middle-ear ossicle or ossicles. Khanna and Tonndorf suggest that above 3 kHz in the cat, the sound stimulates the manubrium of the malleus directly, the eardrum acting only as a protective baffle for the rear side of the manubrium. It is conceivable that a similar conclusion should be brought for the non-mammalian middle ear.

In terms of the velocity, the gecko middle ear also shows a band-pass characteristic, with a resonance peak somewhere between 1 and 2 kHz (Fig. 3.11 a). At low frequencies, the middle-ear response of non-mammals is thus very similar to that of mammals (Fig. 3.11 b; Johnstone and Taylor, 1971). Above 4 kHz, there is a more rapid fall-off in the response in non-mammals, resulting at 10 kHz in up to 20 dB difference between the mammalian and non-mammalian transfer characteristics. In fact, if we take into account the bending of the extracolumella described below, that is, if we compare the motion of the footplate of the columella to that of the mammalian stapes, the difference at high frequencies is even greater.

Measurements of the vibration of the columella compared to those of the tip of the inferior process show that the extracolumella is not a rigid structure. At low frequencies (up to 2 kHz), the vibrational amplitude of the columella is about one-third (−10 dB) of that of the tip of the inferior process (Fig. 3.12 a). This is what would be expected from a comparison of the length of the inferior process on the eardrum to the distance from the fulcrum or pivoting point of the extracolumellar lever system (at the edge of the eardrum) to the point of insertion of the columella itself. If these ossicular components functioned in a frequency-independent fashion, this ratio should be the same at all frequencies. Above 2 kHz, however, the amplitude difference is reduced to 4–5 dB, only to increase very rapidly again at higher frequencies. At 10 kHz, the columella has only one-tenth of the amplitude of vibration of the tip of the inferior process (−20 dB; Fig. 3.12 a,b). A measurement at more than one location on the inferior process showed that at low frequencies, it acts like a stiff rod. At very high frequencies, however, the increasing difference in amplitude to the columella does not indicate an increased lever ratio, but rather that the vibrational energy of the tip of the inferior process is being absorbed in the bending of this process and therefore does not reach the columella (Fig. 3.12 b). Thus at about 4 kHz, this transmission system begins to break down.

Removal of most of the columella uncoupled the eardrum from the inner ear and had two interesting consequences for the motion of the inferior process.

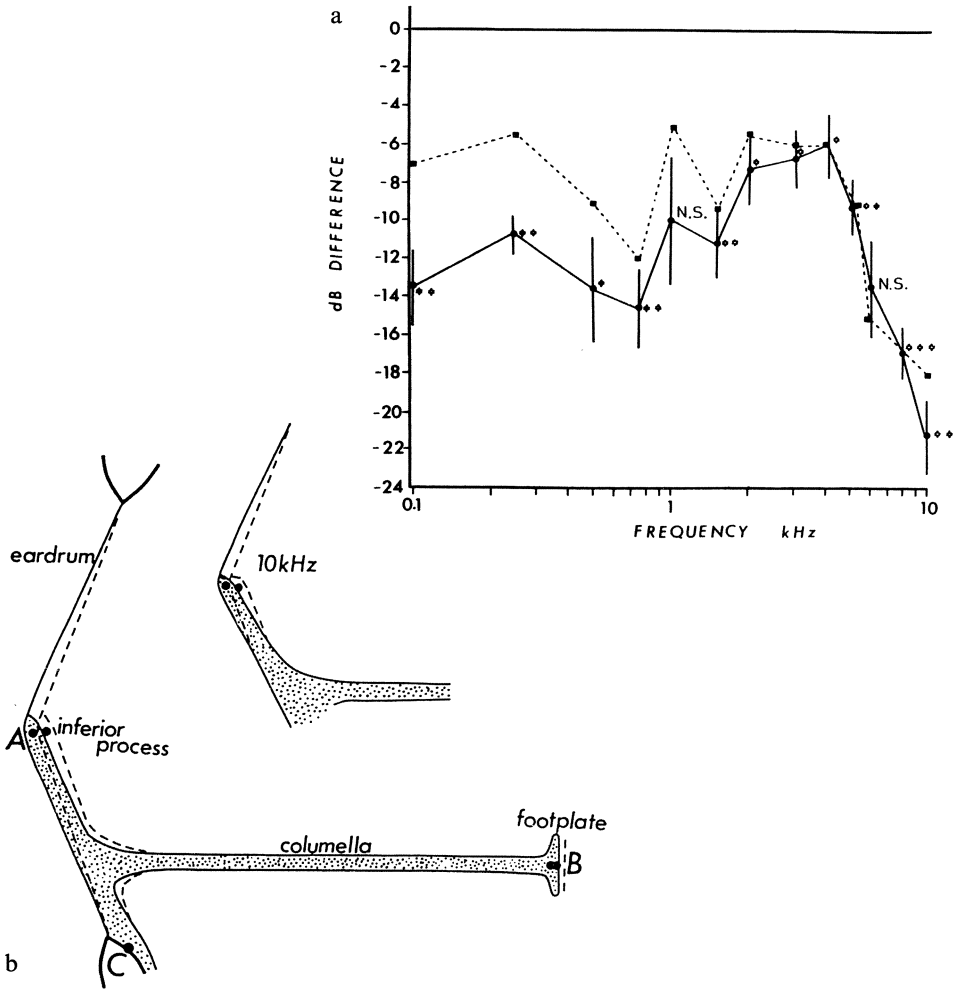

Fig. 3.12 a, b. Function of the lizard middle ear. *a* Measurements of the relative displacement amplitude of different parts of the middle ear of the small Australian gecko *Gehyra*, using the Mössbauer technique. The amplitude of the tip of the inferior process is taken as the reference value (= 0 dB). The amplitude of the columella (*continuous line, bars* are 2 standard errors) and a point half-way down the inferior process of the extracolumella (i.e. half-way between the points *A* and *C* in *b, dashed line*) are given in dB relative to the 0 line. All data points are the mean of four measurements; *asterisks* indicate which points are significantly different from the 0 line ($*p=0.05$, $**p=0.01$, $***p=0.001$). At frequencies below about 3–4 kHz, the extracolumella appears to move as a stiff bar: the half-way point values lie between those of the tip of the extracolumella (0 line) and those of the columella. However, their motion above 4 kHz is essentially identical. This, and the rapid loss of displacement amplitude above this frequency, indicate that the middle-ear transmission efficiency has collapsed. *b* Schematic drawing of the middle ear illustrating the motion of the extracolumella and columella at low and (*inset*) at high frequencies. The *dashed line* shows the highly exaggerated limits of the displacement of the parts of the middle ear. Whereas at low frequencies the inferior process of the extracolumella pivots stiffly around its fulcrum *C* and the columella moves piston-like, at high frequencies the energy of the extracolumella motion is absorbed in bending, so that the columella hardly moves at all (Manley, 1972c)

Firstly, at low frequencies in *Gekko*, there was a considerable loss of damping, resulting in increased amplitudes of the tip of the inferior process. An increase in amplitudes around the resonance frequency of the system (1 to 1.5 kHz) was produced by the same procedure in *Gehyra*. Only some of this effect could be produced by destruction and draining of the inner ear, so that it is probable that the inner ear and the annular ligament of the oval window both effectively damp the resonance of the columellar system. Secondly, after removal of the columella, the bending of the inferior process at high frequencies no longer occurred. It can be concluded that the bending occurs as a result of an increase of the input impedance of the inner ear at higher frequencies, where the inner ear itself ceases to respond to sound.

Using more modern techniques, Rosowski et al. (1984) found that the acoustic admittance of the middle ear of the alligator lizard varied with sound pressure level and with frequency. Nonlinearities appeared with the lowest sound pressure levels near a frequency of 1.6 kHz. As this nonlinear behaviour is greatly reduced when the cochlear partition is destroyed and by other manipulations that affect the integrity of the basilar papilla, the authors suggested that the cochlear partition is the source of nonlinearities. These effects and the gecko data described above indicate that the properties of the inner ear affect the transfer characteristics of the middle ear. The level dependency of the effects complicates the interpretation of results obtained at relatively high levels, such as data of Saunders (1985), Saunders and Johnstone (1972) and Manley (1972 b,c), in spite of the good linearity displayed. It would be useful to repeat some of these measurements at a lower SPL.

As in the red-eared turtle, the gecko eardrum displacement response as measured at the tip of the inferior process and above the resonance frequency falls off at about 12 dB/octave. In contrast to the suggestion of Moffat and Capranica (1978) for the turtle, it is apparent that the audiogram of geckos is not exactly a result of the shape of the transfer function of the middle ear. Whether we take the amplitude or the velocity function of the middle ear into account for correcting the audiogram shape, there is still an additional component attributable to an inner ear sensitivity loss at both low and high frequencies. The difference probably results from the differential response of the basilar membrane to the middle-ear input.

Further data on the transfer characteristic of some nonmammalian middle ears are given by Wilson et al. (1985) for *Caiman*, Gummer et al. (1986) for the pigeon, Johnstone and Taylor (1971) for various species and Manley et al. (1988 d) for the bobtail lizard. All the data from the middle ears of these species conform to the general pattern described above. In addition, Saunders (1985) presented data for the motion of the tympanic membrane of the chick (Fig. 3.13) and the parakeet, where the velocity transfer function shows a 6 dB/octave rise at low frequencies, a resonance peak in the mid-frequency range and a loss of about 16 dB/octave towards higher frequencies. Saunders and Johnstone (1972) show amplitude characteristics of both the eardrum and the columella for the gecko *Phyllurus milii*, the dragon lizard *Amphibolurus reticulatus* and the dove *Streptopelia risoria*. Unfortunately, there are some important inconsistencies between the curves they give and the calculated differences of the displacement of the tip

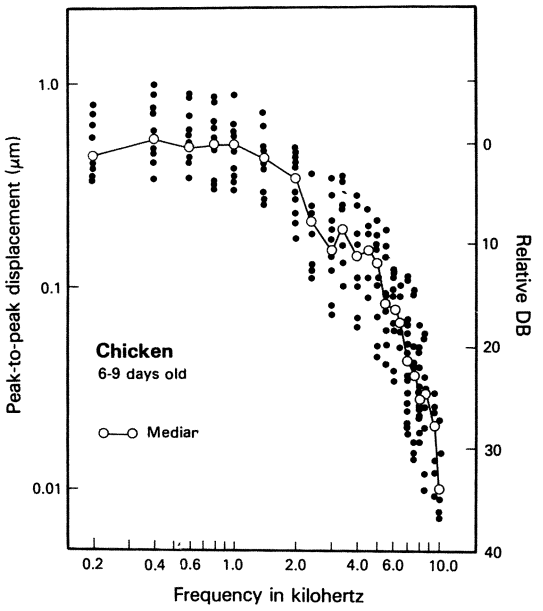

Fig. 3.13. Displacement amplitude of the centre of the tympanic membrane of the young chick as measured by the capacitance-probe method. The *continuous line* gives the median value at each frequency for a series of measurements (*symbols*). As in the reptiles, the displacement amplitude is relatively constant up to a certain frequency (here somewhat higher than in reptiles at 2 kHz), falling off rapidly to higher frequencies at about 12 dB/octave (Saunders, 1985)

of the inferior process (their "manubrium") and of the columella from the data in their paper. The values recalculated from the original data of their figure are compared to other data in Fig. 3.14. It can be seen that in all cases, the greatest differences generally occur at the highest frequencies (6 to 10 kHz). This conforms to the pattern given above for a gecko and implies that poor transmission of high frequencies by the nonmammalian middle ear may generally be due to bending of the inferior process.

It can no longer be concluded, as Saunders and Johnstone speculated, that the large differences at high frequencies indicate a large effective lever ratio. It is probably true, however, as they suggest, and as shown above for *Gehyra*, that the cochlear fluids and membranes load the columella in a way which contributes significantly to the middle-ear transmission characteristic. However, the actual loss of vibrational amplitude of the middle ear compared to that seen in mammals is also seen to a significant degree in the motion of the eardrum and extracolumella.

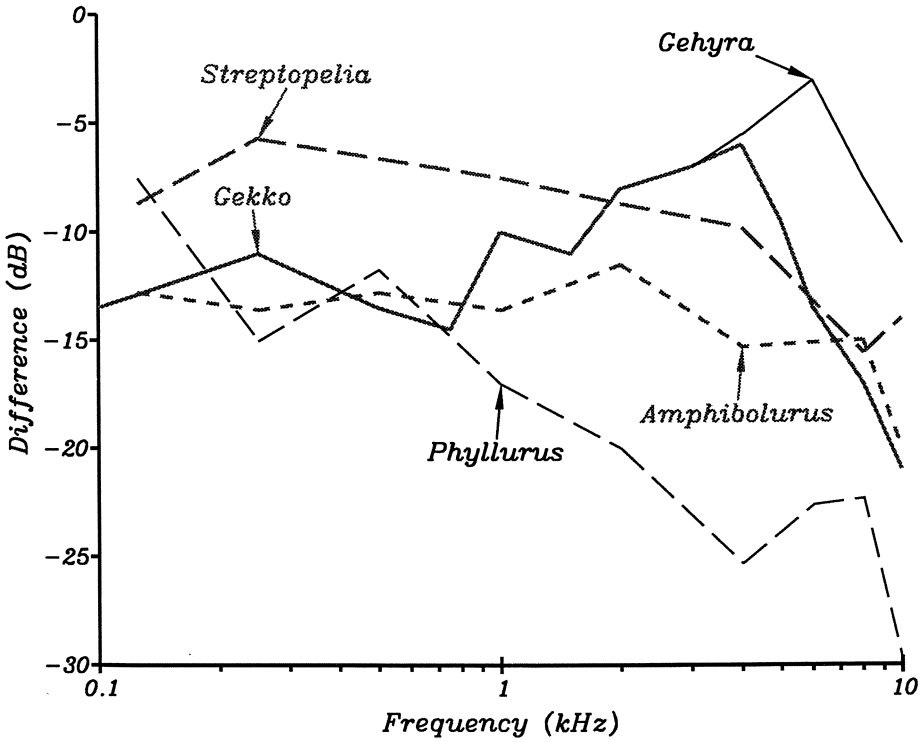

Fig. 3.14. Summary diagram to illustrate the displacement-amplitude difference between the tympanum (tip of the extracolumella) and the columella in some nonmammalian middle ears. There is a distinct loss of transmission of energy at the highest frequencies. *Gekko, Gehyra* and *Phyllurus* are geckos, *Amphibolurus* is an agamid lizard. The dove *Streptopelia* is the only bird represented. The data are re-plotted after Manley (1972 b, c) and Saunders and Johnstone (1972)

3.4 The Middle Ear as a Pressure-gradient Receiver

Sound is localized in space by mammals largely on the basis of differences in sound pressure and time-of-arrival of the sound at the two ears. Birds and reptiles are at a disadvantage compared to mammals, for their head is generally too small to cast a significant sound shadow for the frequencies they can hear and also too small to create large time differences. Useful sound shadows are only cast by a head whose dimensions are similar to or greater than the wavelength of the sound frequencies concerned. Such wavelengths are only found at frequencies higher than nonmammals can perceive. Thus on these criteria, it should be difficult for nonmammals to localize sound.

The middle ear cavities of nonmammals are often widely open to the mouth. Where this is not the case, such as in birds and crocodiles, they are connected via

more-or-less large spaces around the brain cavity. Sound pressure at one eardrum is also present in the middle-ear cavity and can influence the motion of the eardrum on the other side of the head. Because the two tympani are potentially influenced by sound pressure from both sides of the head, the middle ears are often spoken of as being pressure-gradient receivers. The actual motion of each eardrum is the result of a complex interaction of sound pressure and phase arriving from the two sides, decreasing the motion through cancellation or increasing it through addition. Such interactions are highly directional, which can help overcome the disadvantage of operating at low frequencies (Lewis and Coles, 1980). At the present time, however, there are contradictory data and quite divergent viewpoints on this matter, so that only a brief summary of the ideas and potential importance of this phenomenon will be given here.

There are very few data on reptiles regarding this question. In some lizards and *Caiman*, Wever (1978) observed that sound stimuli (closed acoustic system) to one eardrum were present in the middle-ear cavity of the contralateral side with almost undiminished pressure. Rosowski and Saunders (1980) found that a significant amount of sound energy was transmitted through the avian interaural pathway. In the Japanese quail, Coles et al. (1980) and Lewis (1983) reported that, although the head of this bird provided a maximal sound shadow of only 8 dB at 6.3 kHz, the sensitivity of cochlear microphonics of the two ears showed up to 25 dB difference in sensitivity to a free-field sound source moved around the head. This directionality of the interaction through the middle-ear canal could be abolished by blocking one external ear canal. The pattern of interaction across the head was quite complex and produced large differences between closely-spaced frequencies and nearby locations in space, implying that there are certain frequencies where the quail would have great difficulty localizing sounds. Unfortunately, there are no behavioural data available on the quail.

In the barn owl, which can localize sound better than any other animal (including man and other mammals), there is also a large interaural canal. Moiseff and Konishi (1981) showed that this canal operates like a low-pass filter, so that whereas the interaural attenuation at 3.5 kHz is only 13.5 dB, it increases steadily with frequency up to 63 dB at 7 kHz. There seems little doubt that the difference is too large at these high frequencies for the canal to play an important role in sound localization. At frequencies where the inter-aural canal could operate as a pressure-gradient receiver (below 4 kHz), the barn owl localizes poorly or is even unwilling to try. It localizes extremely well in both the horizontal and vertical axes at higher frequencies (between 5 and 9 kHz; Konishi, 1973 b, 1986). This would suggest that the barn owl in fact avoids using the potentially useful interaural canal in sound localization. It has extended its hearing range above that of normal birds, and the various brainstem nuclei involved in processing sound-localization cues contain very few cells which respond to frequencies below 4 kHz (Konishi, 1986; Manley et al., 1988 c). It may be that the inherent complexity of the interaction patterns produced by pressure-gradient receivers strongly reduces its usefulness for an animal whose existence depends on such accurate sound localization. As Coles and Guppy (1988) point out, however, the data of Moiseff and Konishi (1981) are difficult to assess in terms of the effect on the properties of the middle-ear system of the sealing of the sound source into the external

meatus, even though Moiseff and Konishi only closed one ear at a time (the minimum required to make the measurements possible). It is difficult to devise a test of these ideas using a fully open acoustic stimulus and measurement system.

Chapter 4

General Anatomical Considerations: Inner Ear and Basilar Papilla

There are a number of fairly detailed reviews of the anatomy of the ear of reptiles and birds, so that this chapter will serve only as an overview for those relatively unfamiliar with this field. I shall then include in later chapters details of the anatomy of the basilar papilla of the individual species for which the physiological data are described. Readers wishing for more comprehensive formation are referred to the reviews of Baird (1960, 1970), Hamilton (1964), Miller (1966, 1968, 1980, 1985), Smith (1981) and Wever (1978).

4.1 Otic Labyrinth and Cochlear Duct

As is typical in vertebrates, the bony otic capsule is enclosed by the prootic and opisthotic bones and contains two fluid-filled membranous systems, the otic and periotic labyrinths (Fig. 4.1). The inner, endolymph-filled otic labyrinth (the membranous labyrinth or vestibule) is derived embryologically from the otic placode and develops on its walls the various sensory-cell areas of the inner ear. It is mostly surrounded by the periotic labyrinth, which sometimes forms large spaces between the bony capsule and the otic labyrinth. These spaces contain perilymph, a fluid resembling the normal body fluids of the extracellular spaces. The sound input and exit from the inner ear, via the oval and ‚round' windows, is through the perilymphatic spaces (Fig. 4.2). Over most of the non-auditory regions of the otic labyrinth, however, the periotic labyrinth contains mesenchyme-like, loosely-packed cell groups or trabeculae with small perilymphatic spaces.

The otic labyrinth is conventionally divided into superior and inferior portions, which are joined by a short duct (Fig. 4.1). The former is made up of the utricle, a large sac containing two sensory areas, the macula utriculi and the macula neglecta. It also gives rise to the three semicircular canals with their sensory areas, the cristae of the ampullae. The inferior portion of the labyrinth is made up of three compartments, the endolymphatic sac within the braincase, the saccule with its macula sacculi, and the cochlear duct. The cochlear duct (sometimes called the lagena) contains anteriorly or anterio-ventrally the macula lagenae and, nearer the ductus reuniens or sacculo-cochlear duct, the area of sensory cells known as the basilar papilla, which forms the main hearing organ in terrestrial vertebrates (Fig. 4.3). The basilar papilla and the cristae of the semicircular canals are the only sensory areas whose cupular or tectorial covering does not contain otoliths. The lagenar and basilar portions of the cochlear duct

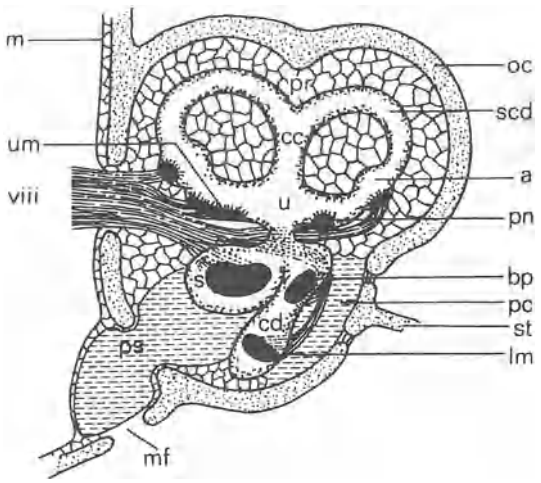

Fig. 4.1. Schematic drawing of the inner ear of a generalized reptile to illustrate the relationship between the otic and periotic labyrinths. The entire structure is enclosed in the otic capsule (*oc;* bone is shown *stippled*). Whereas the superior portion of the otic labyrinth (the semicircular canals, *scd* and utriculus *u*) are surrounded by a periotic reticulum (*pr*), the inferior portion is specialized, in that part of the sacculus (*s*) and the cochlear duct (*cd*) are surrounded by open fluid spaces called the periotic sac (*ps*) and periotic cistern (*pc*). These are partly equivalent to the scala tympani and scala vestibuli respectively. *a* Ampulla of semicircular canal; *bp* basilar papilla; *cc* cruc communis of semicircular canals; *lm* lagena macula; *m* wall of braincase; *mf* secondary tympanic membrane; *pn* papilla neglecta; *st* columella; *um* utricular macula; *viii* eighth cranial nerve (Baird, 1974)

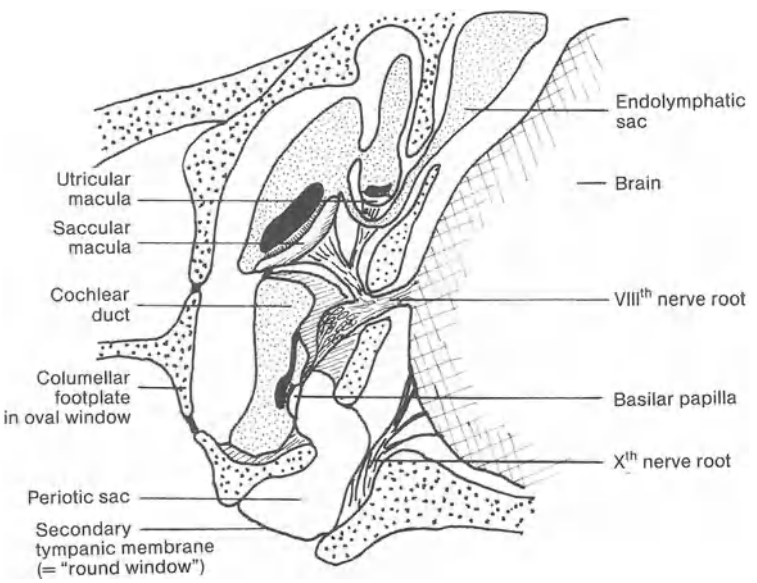

Fig. 4.2. Diagrammatic cross-section of part of a lizard head to illustrate the relationships between the middle ear, some inner ear receptor-cell areas (maculae, papillae) and the eighth nerve. Cut bone is shown *heavily stippled,* the endolymphatic spaces are *lightly stippled,* limbic material is *shaded,* tectorial material is *black* and the edge of the brain is *cross-hatched.* Within the course of the posterior branch of the eighth nerve, but still within the inner ear, are shown some cells of the cochlear ganglion (Partly after Baird, 1970)

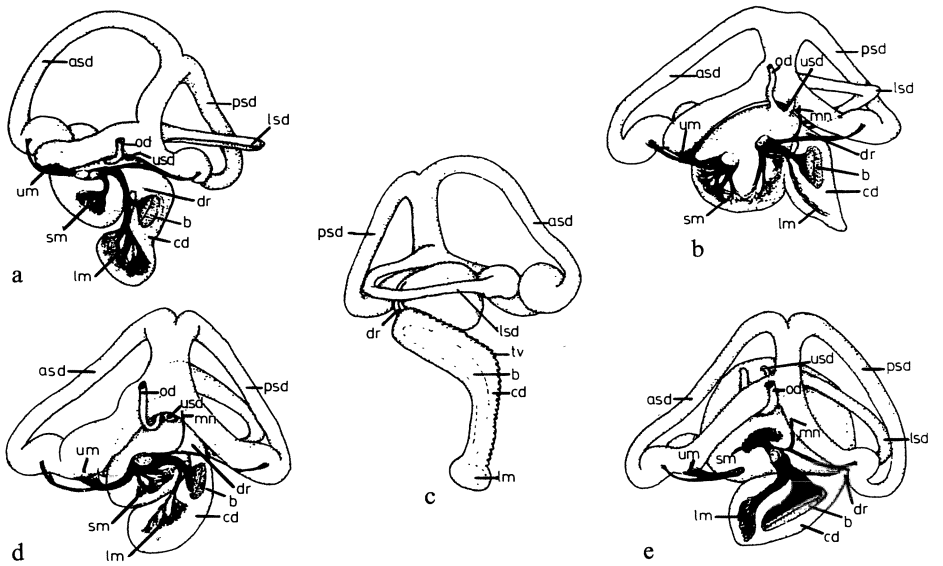

Fig. 4.3 a–e. Schematic representation of the otic labyrinth of five types of reptile: *a Sphenodon, b* a turtle, *c* a crocodylid, lateral aspect, *d* a snake, *e* a lizard (skink). As can be seen, the cochlear duct (*cd*) contains two receptor epithelia in all cases: the basilar papilla (*b*) and the lagena macula (*lm*). The basilar papilla is well developed in scincid lizards and even more so in the crocodylids. *asd* Anterior and *psd* posterior semicircular canals; *lsd* lateral semicircular canal; *od* endolymphatic duct; *usd* utriculosaccular duct; *um, sm* utricular and saccular maculae; *dr* ductus reuniens (= sacculo-cochlear duct); *mn* macula neglecta; *tv* tegmentum vasculosum (After Baird 1974 and E. R. Lewis et al. 1985)

are more or less separate portions of the endolymphatic space in the Tuatara *Sphenodon*, in Chelonia and in snakes. In lizards and in the Crocodilia and birds, there is no obvious division between these areas. The cochlear duct is equivalent to the scala media of mammals.

Among the various differences from the mammalian hearing organ is the frequent absence of a true round window. The pressure of the sound waves arriving from the columellar footplate in the oval window are released in primitive reptiles via periotic spaces in contact with the brain cavity (Fig. 4.4 a). In lizards and crocodilians there is a membrane near the oval window which releases pressure into the middle-ear cavity. This secondary tympanic membrane (Fig. 4.4, STM)

Fig. 4.5. Detail of the relationships between the perilymphatic space and the endolymphatic space of the cochlear duct, to illustrate their close apposition in the region of the basilar papilla (papilla basilaris). From this anterior view of the left cochlear duct of a lizard, the point of access of the sound to the inner ear (oval window) and its exit ("round window") are illustrated. The perilymph spaces are extended around the basilar papilla in the area of the limbic recess (Miller, 1966)

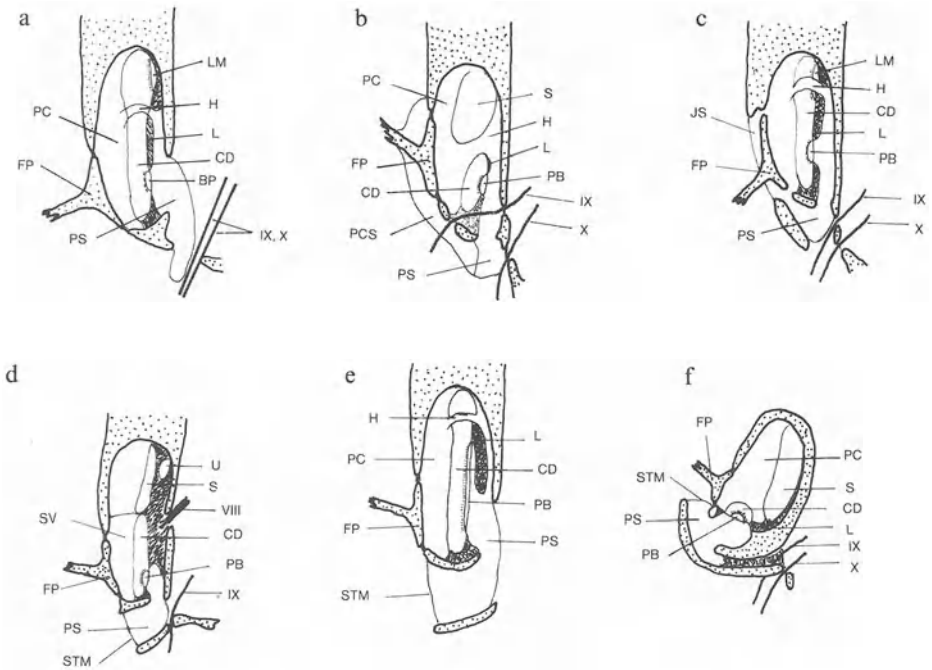

Fig. 4.4 a–f. Drawings representing schematic sections through the cochlear duct area of the inner ear of various reptiles to illustrate the relationships between the oval window (in which the columella footplate is seated), "round window" (= secondary tympanic membrane, *STM*), and the perilymphatic and endolymphatic spaces. *a Sphenodon; b* turtle; *c* snake; *d* lacertid lizard; *e* scincid lizard (the basilar papilla is cut obliquely); *f* crocodylid in transverse section. *BP, PB* basilar papilla; *CD* cochlear duct; *FP* columellar footplate; *H* helicotrema; *JS* juxtastapedial sinus; *L* limbus; *LM* lagena macula; *PC* periotic cistern; *PCS* paracapsular sinus; *PS* periotic sac; *S* sacculus; *U* utriculus; *VIII, IX, X* eighth, ninth and tenth cranial nerves (After Baird, 1960, 1970)

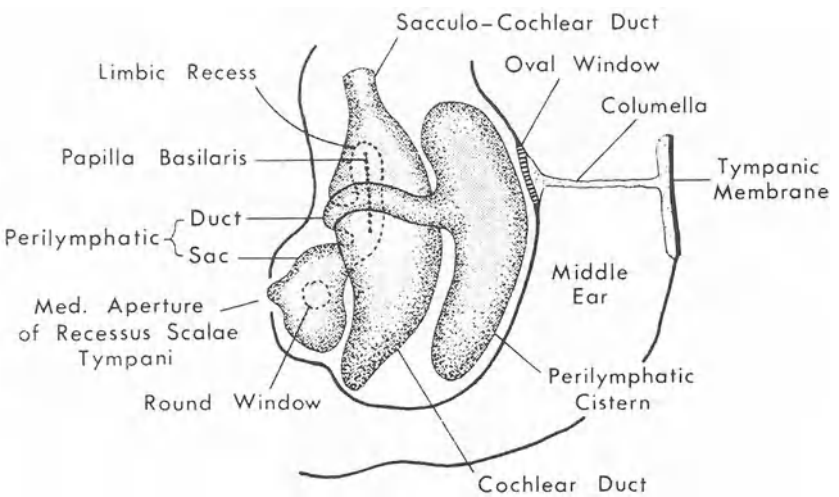

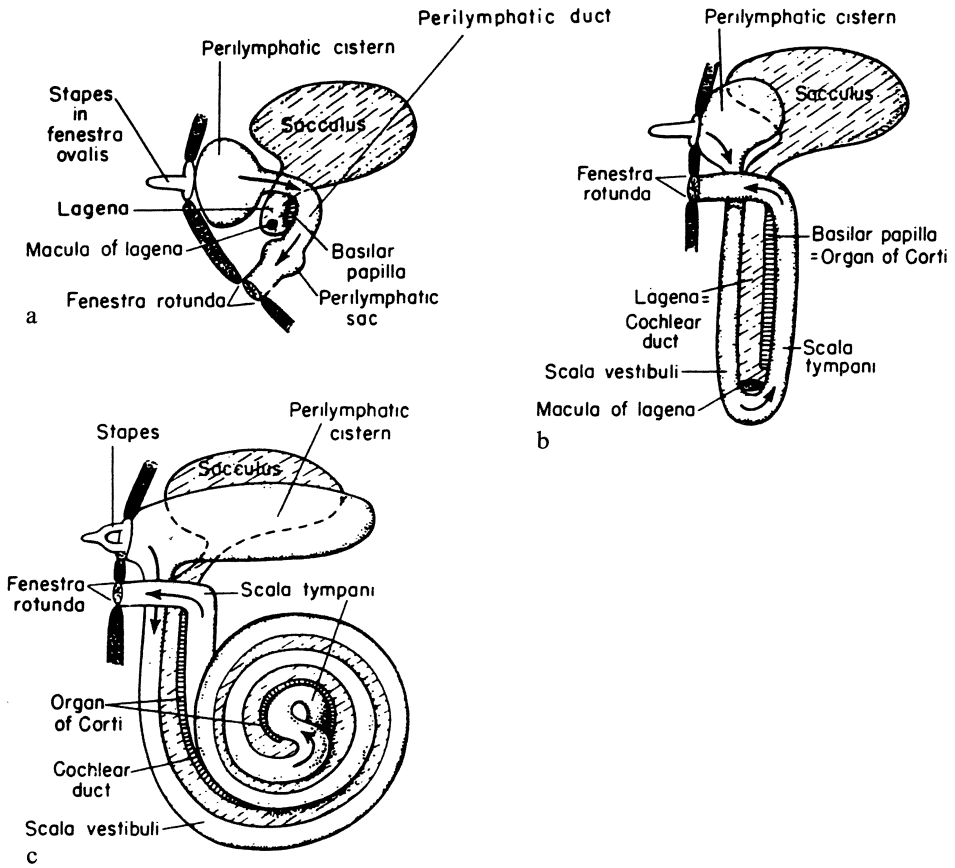

Fig. 4.6 a–c. Schematic representation of the perilymphatic spaces and cochlear duct (*shaded* with the sacculus) in *a* a primitive reptile; *b* a bird or crocodylid and *c* a mammal, to illustrate the elongation of the perilymphatic spaces together with the cochlear duct during the evolution of the inner ear (Romer and Parsons, 1977)

lies distal to the position of the round window of mammals, often at the end of a large recessus scala tympani. It is only analogous to the round window.

Unlike all the other areas of sensory cells of the vestibule, which have their basal membranes attached to relatively immovable parts of the wall of the otic labyrinth, the basilar papilla is situated completely or mostly on the basilar membrane, which is a free area of membrane separating the otic from the periotic spaces (Figs. 4.5, 4.6). The dimensions of this free membrane have been increased in most evolutionary lines (Fig. 4.6). The basilar membrane is supported on all sides by thickened portions of connective tissue called the limbus, which superficially resembles cartilage (Fig. 4.7). As the basilar membrane varies in shape from oval to very elongated, the limbus is also appropriately formed (Fig. 4.8).

Beneath the basilar membrane, the limbus may completely enclose part of the periotic space, which then extends along the basilar membrane like the finger of a

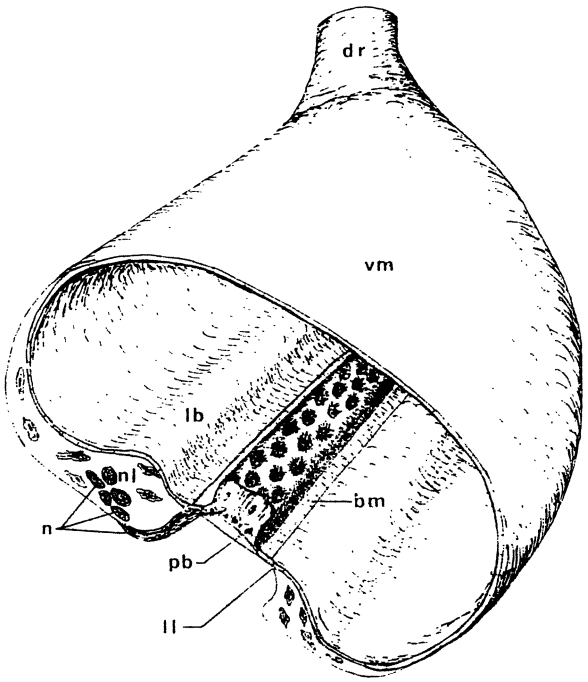

Fig. 4.7. Diagrammatic section through the cochlear duct in the region of the basilar papilla in a lizard in a hair-cell area without a tectorial membrane, to illustrate the three-dimensional structure of the basal half of the duct. *dr* Ductus reuniens (sacculo-cochlear duct); *vm* vestibular membrane; *lb* limbic bulge or ridge; *nl* neural limbus with nerve-fibre bundles (*n*) running to the basilar papilla (*pb*) which lies over the basilar membrane (*bm*); *ll* abneural edge of the limbus (Baird, 1970)

glove. The wall of the cochlear duct opposite the basilar papilla is generally thin, but may be thickened and folded, and is called the vestibular membrane (Fig. 4.7) or, if thick, the tegmentum vasculosum (see Chs. 12, 13). The extension of the periotic space above this vestibular membrane is called the scala vestibuli and connects to the scala tympani below the basilar membrane by a short channel, the helicotrema. This channel is in different locations in different reptile groups and not necessarily homologous to each other (Fig. 4.4). The periotic spaces of the reptiles also vary considerably from group to group and the homologies between the different spaces are in many cases uncertain (Baird, 1960, 1970, 1974).

Some confusion has arisen from the usage of different anatomical terms to describe the position and orientation of structures and papillae in the inner ear. Following the usage of Miller (1973 a, 1978 b, 1980), I shall only use the term *apical* for the end of the cochlear duct anatomically distant from the sacculo-cochlear duct (Fig. 4.9 a). This end of the duct has also been referred to as the ventral or distal end. Similarly, I shall refer to the *basal* end, or to the basal sub-

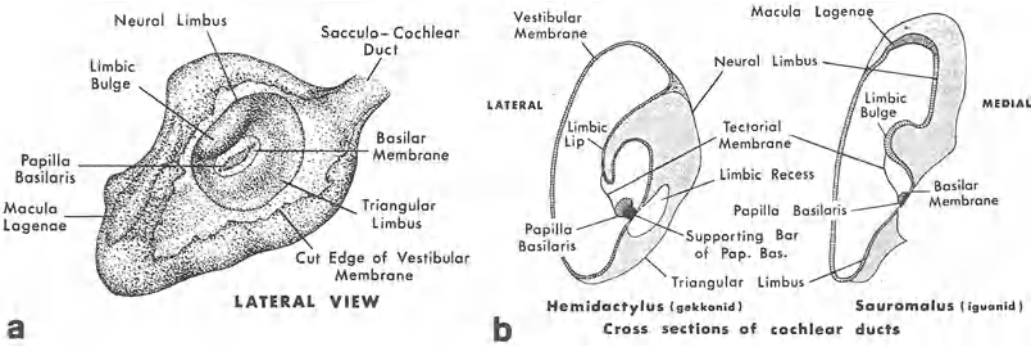

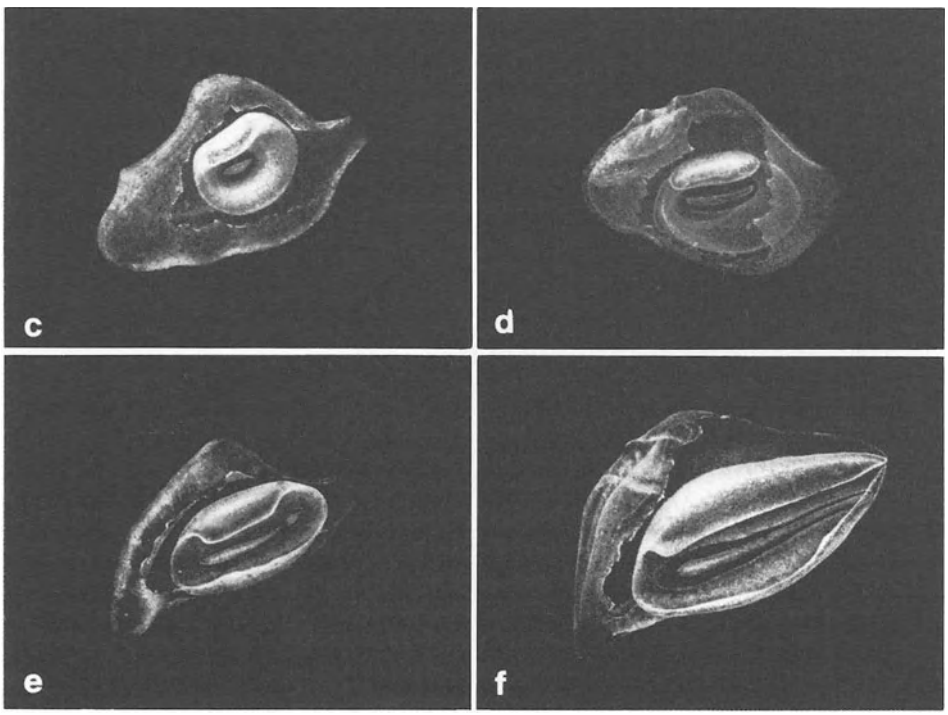

Fig. 4.8 a–f. Three-dimensional structure of various lizard cochlear ducts. *a* A drawing of a lateral view of the cochlear duct of an iguanid lizard showing the main features of cochlear-duct anatomy. The vestibular membrane has been opened. *b* Schematic drawings of cross-sections through the cochlear duct of a gekkonid (*left*) and an iguanid lizard (*right*) to illustrate the way in which the limbus supports the basilar membrane and basilar papilla and showing the connection of the tectorial membrane to the neural limbus. The form of the limbus, which supports the basilar membrane, varies from family to family in lizards. In the gekkonid, the neural limbus arches over the basilar papilla as the so-called limbic lip. *c-f* Four three-dimensional drawings of the cochlear duct in: *c,* an iguanid lizard, shown schematically in *a; d,* an anguid lizard; *e,* a teiid lizard and *f,* a gekkonid lizard, all seen in lateral view, that is, with the vestibular membrane opened (Miller, 1966)

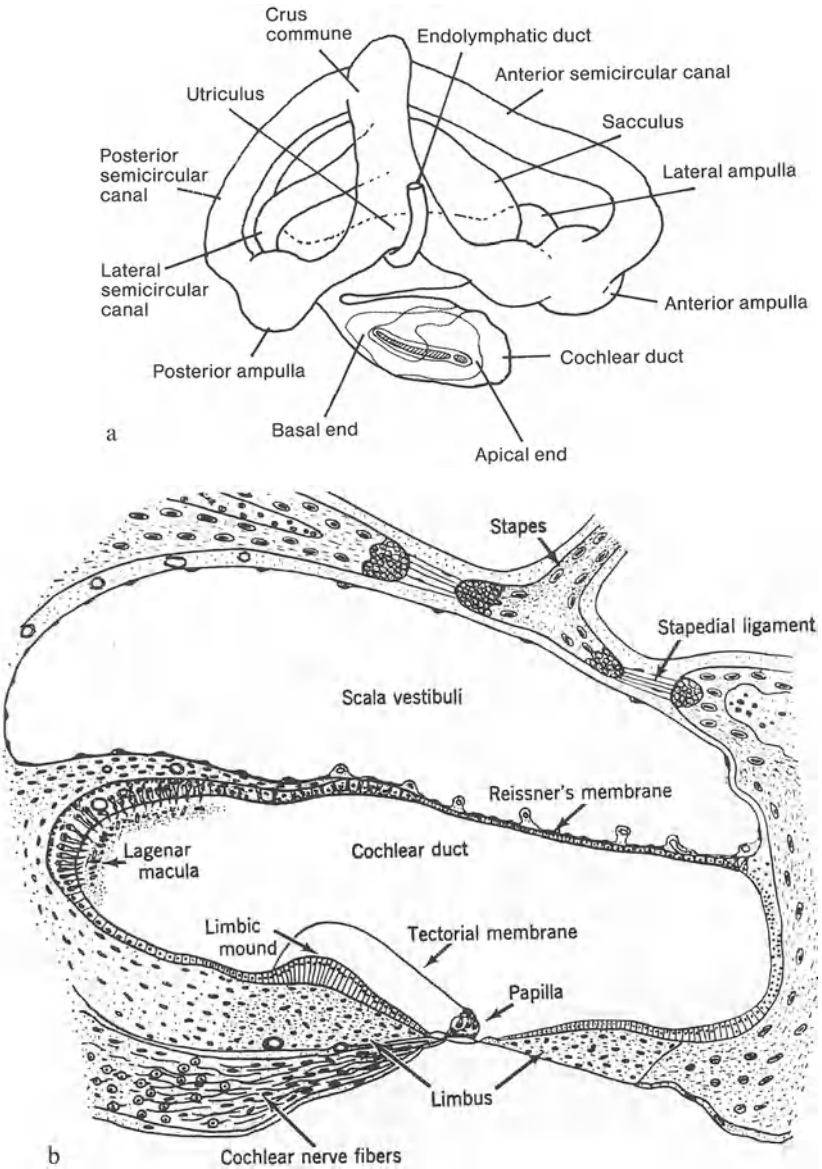

Fig. 4.9 a. Diagrammatic drawing of a medial view of the left membranous labyrinth of a lizard to illustrate the meaning of the anatomical terms "basal" and "apical" with regard to the basilar papilla (After Miller, 1966). *b* Transverse section of the cochlear duct of the iguanid lizard *Uma* to show details of the neural (*left*) and abneural limbus. Stapes = columella; Reissner's membrane = vestibular membrane (Wever 1967 a)

papilla (when the papilla is divided) instead of the dorsal or proximal end or sub-papilla. The side of the basilar membrane where the nerve-fibre bundles enter the papilla is referred to as the neural (superior or anterior) side, the opposite side as abneural (inferior or posterior). These terms are unambiguous and, in only referring to positions within the duct itself, are independent of variations of the position within the head between species of different groups.

4.2 The Tectorial Membrane

A tectorial membrane, consisting of a macromolecular matrix in gel form, is typically supported by the thicker neural limbus and extends to cover the sensory cells of the basilar papilla (Figs. 4.9b, 4.10). In snakes, chelonians and crocodilians and in some cases in lizards, the tectorial membrane contains ‚pockets' on its lower face, into which the hair-cell bundles individually fit. The supporting-cell microvilli often have a fine meshwork of tectorial-like fibrils on their surface, which in life probably connect to the overlying tectorial membrane proper (Fig. 4.11; Miller, 1978 a). This fine meshwork is probably also present even in those hair-cell areas of some lizard papillae (e.g., iguanids, anguids) which have free-standing stereovillar bundles (Bagger-Sjöbäck and Wersäll, 1973). In the agamid lizard *Calotes versicolor* studied by Bagger-Sjöbäck and Wersäll, the network of thin, interconnecting filaments was so thick around hair cells with a tectorial membrane that it totally enclosed the hair bundles. The kinocilial tip of lizard hair cells is often expanded, even bulb-like, and appears to

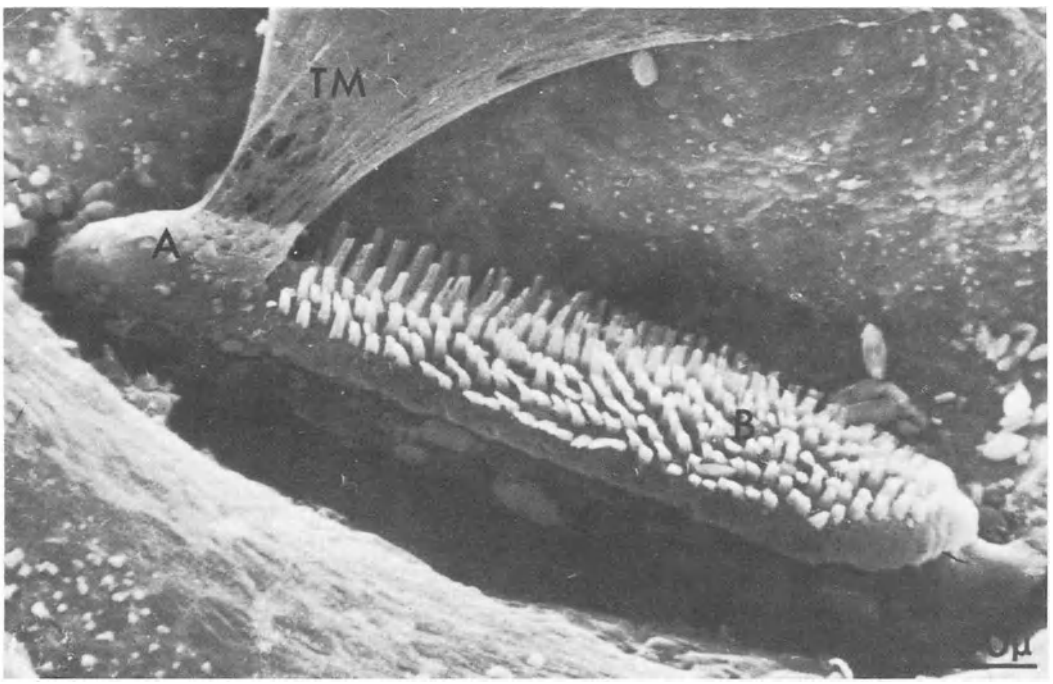

Fig. 4.10. The tectorial membrane does not cover all hair cells in some lizards. The connection of the tectorial membrane (*TM*) to the neural limbus (*top*) and one group of hair cells (*A*) is illustrated for the agamid lizard *Calotes* in this scanning electron micrograph. The white structures in area *B* are the stereovillar bundles of hair cells which do not have a tectorial membrane ("free-standing"). This papilla is about 400 µm long (Bagger-Sjöbäck and Wersäll, 1976)

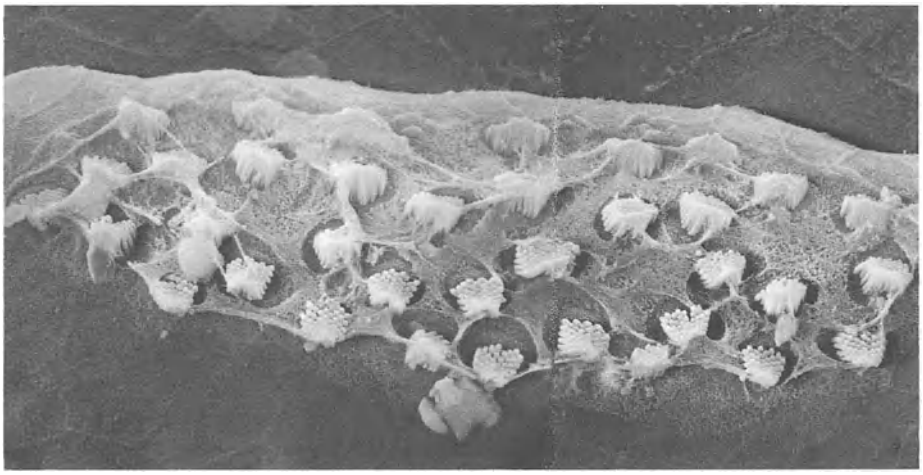

Fig. 4.11. Scanning electron micrograph of the apical area of the papilla of the anguid lizard *Gerrhonotus* (alligator lizard), where the tectorial cap has been removed. Beneath the tectorial cap, there is a meshwork of tectorial fibres around and between the hair-cell stereovillar bundles (Miller, 1973 a)

serve as a connecting surface between the longest 5 or 6 stereovilli and the tectorial membrane when present (Fig. 4.12). It is sometimes so firmly attached to the tectorial membrane that it tears off during preparation of the papilla basilaris (Miller, 1978 a).

Wever (1978) distinguished a large number of types of tectorial structure, based on their appearance in histological sections (Fig. 4.13). We now know that histological preparations can alter the appearance of the tectorial membrane almost beyond recognition, so that great caution is necessary in interpreting the condition in the living animal and the differences between species (Kronester-Frei, 1979; Runhaar, 1988). Thus it is difficult to judge the appropriateness in the living animal of the distinction made by Wever (1978) between direct tectorial connections, tectorial plates, simple fiber connections, connections by fibrous strands and by "finger processes". It is probably safe to assume that we are dealing here with a continuum of structure, from a fairly thick tectorial structure to a much thinner one. The degree of shrinkage increases with thinness, so that after fixation and embedding, the thinner tectorial structures appear only as thin fibrous strands. Thus we have a great range of mass, from the thick tectorial structures of the turtles, the Crocodilia and birds and of parts of some lizard papillae, through to the fine strands of some lizard tectorial processes. They are probably all, as Miller (1978 b) implies, connected via the kinocilium to the tallest group of stereovilli.

In parts of some lizard papillae, as already noted, there is no tectorial membrane. In lizards, many tectorial masses are not connected to the limbus, at least in the mature ear. These Wever classified as inertial and inertia-like restraints. As

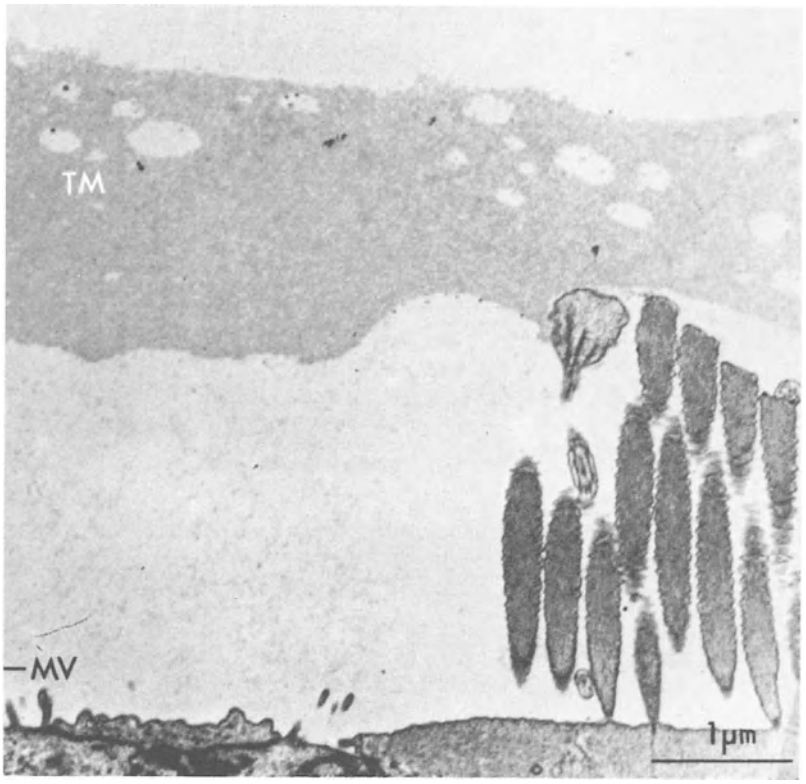

Fig. 4.12 a

Fig. 4.12 a, b. The kinocilium is attached to the tallest stereovilli and to the tectorial membrane. *a* Cross-section; *b* longitudinal section through the stereovillar bundle of a hair cell from the basilar papilla of the agamid lizard *Calotes,* to illustrate the connection of the longest stereovilli (*S*) to the kinocilium (*K*), which, in turn, is connected to the tectorial membrane (*TM*); MV = Mikrovilli (Bagger-Sjöbäck and Wersäll, 1973)

yet, there is no evidence for the existence of a functional difference between these tectorial masses and those affixed to the limbus, a functional difference which prompted Wever to name them "inertial bodies". It is premature to draw conclusions, as it is still not clear to what extent the differences in physiology described in the following chapters between iguanid, anguid, scincid, varanid and gekkonid lizards may be attributable to the wide variety of tectorial structures present.

Under the heading of ‚inertial' structures, Wever (1978) described the sallets (Fig. 4.13, type 6), so called because when fixed and viewed in cross-section, they resemble an ancient French helmet of that name. I will distinguish between the sallets found in e.g., the geckos and skinks (see Chs. 10, 11), which resemble more a connected chain of ‚helmets' and the ‚sallets' of lacertids, which appear more like a smooth worm when seen in the scanning electron microscope (see Ch. 8). Some lizard papillae (e.g., of skinks) have, over some of the hair cells, relatively huge tectorial bodies not connected to the limbus (see Ch. 11). These resemble giant sallets and I shall use the term culmen, as introduced by Wever (1978).

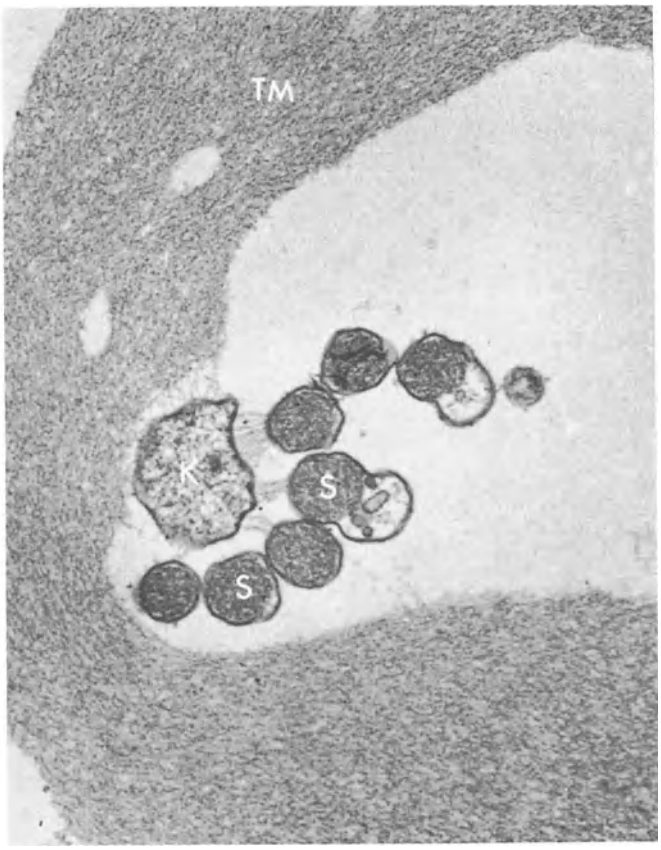

Fig. 4.12b

4.3 The Basilar Papilla

4.3.1 The Primitive Basilar Papilla

The basilar papilla is found on the endolymphatic side of the basilar membrane and, appropriate to the shape of this membrane, is short or elongated. In some primitive forms such as the chelonians and snakes, the sensory epithelium covers only a relatively small area of the basilar membrane. In Chelonia and in the Tuatara *Sphenodon*, some cells at the ends of the papilla are resting on limbic material (Fig. 6.1a). In some advanced forms, such as the Crocodilia and birds, a substantial part of the basilar papilla lies over the neural limbus, on the so-called superior cartilaginous plate (Figs. 12.1 b, 13.2). In the varanid and lacertid families of lizards and in isolated cases in other families, the basilar papilla is almost or completely divided into two hair-cell areas or sub-papillae by a connection between the neural and abneural sides of the limbus (Figs. 8.1, 9.1).

The cochlear duct of *Sphenodon* is universally regarded as being among the most primitive ducts of living reptiles and is described here to represent the con-

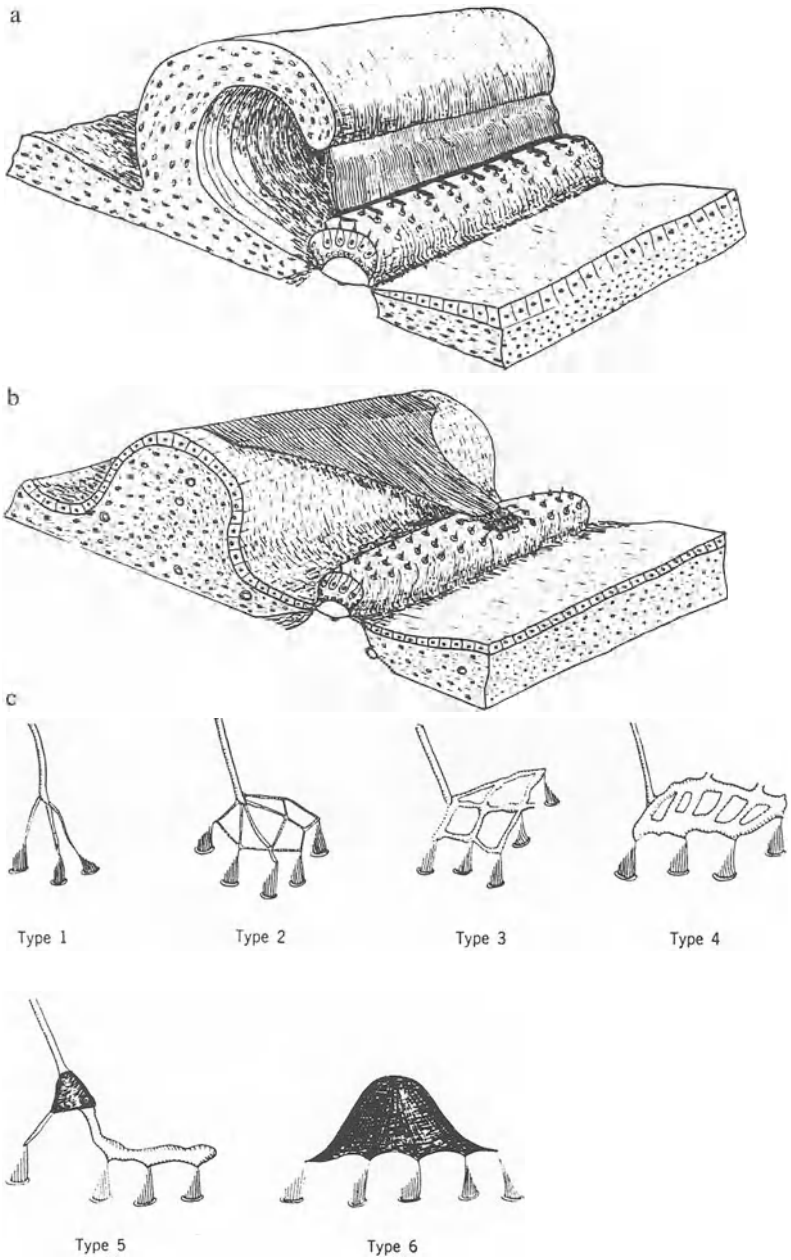

Fig. 4.13 a–c. Types of tectorial structure found in lizards. *a* Schematic representation of a tectorial membrane which is connected to the limbus and covers much of the papilla (*Gekko;* see *type 5* in cross-section in *c*). *b* Schematic drawing of the tectorial membrane of an iguanid lizard (*Iguana*), where the area of hair cells covered by the tectorial plate or cap (*type 4* in *c*) is very small. *c* Types of tectorial structures in lizards as classified by Wever. *Types 1* to *4* form a series of increasing density. *Type 5* is a "finger process"; *type 6* a "sallett". *Types 5* and *6* are shown in cross-section (Wever, 1967 a, b)

dition of the hearing organ in the earliest reptiles (see e.g., Miller, 1980, 1985). There are, unfortunately, no figures available of the whole papilla of *Sphenodon*; however, it resembles that of snakes (Fig. 6.21b). In *Sphenodon*, the size of the basilar papilla in relation to the size of the lagenar and saccular maculae is less than in other reptiles and the limbus is not as thick and specialized. The basilar membrane is not elongated, but oval in shape, being between 725 μm and 1.2 mm long and 350 μm wide in the centre (Miller, 1980; Wever, 1978). A plate-like tectorial membrane connected to the limbus covers all of the approximately 225 hair cells.

Interesting is the question of the hair-cell orientation. As mentioned in chapter 2, the kinocilium of the hair cell is positioned on one side of the stereovillar bundle. Whereas in the auditory receptor of all birds and mammals the kinocilium almost always lies on the side of the hair cell oriented away from the neural limbus (that is, the hair-cell areas are generally *unidirectionally* and *abneurally* oriented), the situation in reptiles varies greatly from species to species. In *Sphenodon*, the Chelonia, Crocodilia and snakes, the same orientation pattern is found as in birds and mammals, that is, generally abneural. The lizards, however, almost always show one unidirectionally-, abneurally-oriented hair-cell area and one or two areas which are bidirectionally oriented (i.e., with different groups of neurally- and abneurally-oriented hair cells; Fig. 4.14). These patterns are family- and to some extent genus-specific (Fig. 4.15).

The question arises as to which of these conditions is primitive. On the one hand, we see that primitive papillae such as those of *Sphenodon*, snakes and chelonians are almost completely unidirectional. On the other hand, it is typical of vestibular maculae, which undoubtedly provided the evolutionary raw material for the basilar papilla, that the hair-cell areas are not unidirectionally oriented. This makes it unlikely that the basilar papilla was purely unidirectional to begin with. In birds, the ‚unidirectional' orientation is in fact only a tendency for the mean orientation of the cells to be abneural – there is substantial variation, albeit systematically organized (see Ch. 13). A number of evolutionary schemes are possible, but at this time there are no convincing arguments either for assuming that the primitive papilla was unidirectional or for assuming that it was bidirectional. An examination of the basilar papilla of the coelacanth fish *Latimeria* (Fritzsch, 1987) in this regard would be rewarding.

Within reptiles, a number of features of auditory papillae have been suggested to be primitive (see e.g., Miller, 1978 a, 1980, 1985). These are:

(1) a low density of hair cells. There is a low number of hair cells per unit area of papilla because the apical portions of the supporting cells are not reduced in diameter between the hair cells. In chelonians and snakes, the hair-cell density lies below 250/10000 μm^2; in the lizards tested, it was 300–400/10000 μm^2 (Miller, 1980).
(2) entirely unidirectional hair-cell orientation, such as in turtles and *Sphenodon*.
(3) innervation of all hair cells by both afferent and efferent nerve fibres.
(4) only one type of cytologically unspecialized hair cell.
(5) a large number of stereovilli per hair cell. In reptiles, a ‚large' number is more than about 75. In some lizards, there are fewer than 40 on some hair cells. (In birds and mammals, however, more than 100 is not uncommon.)

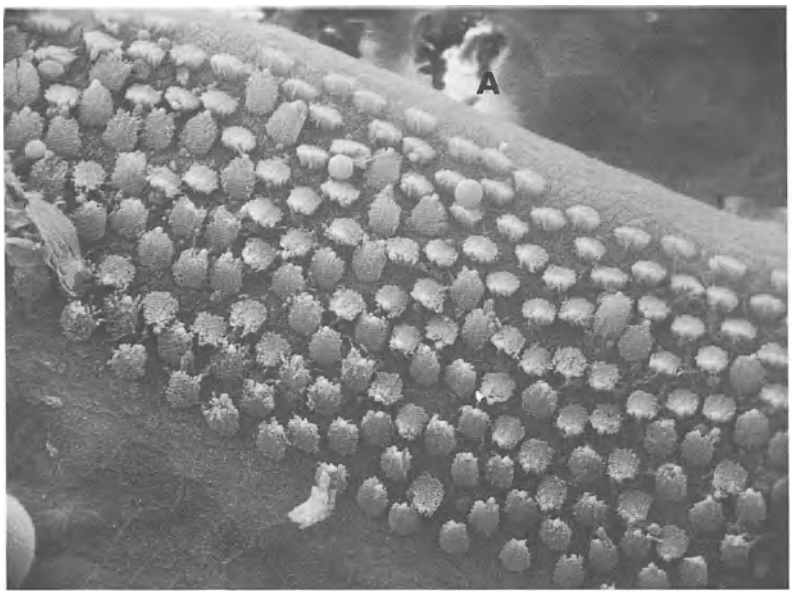

a

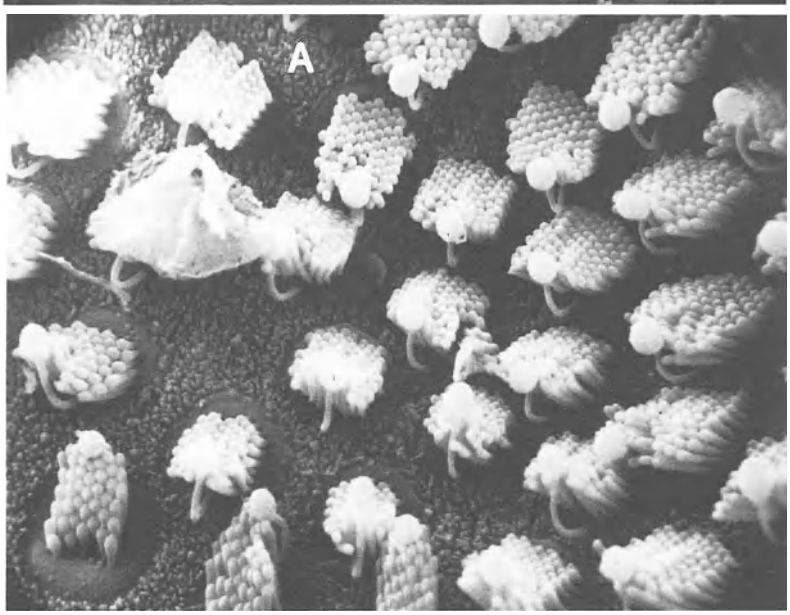

b

Fig. 4.14 a–d. Hair-cell arrangement and orientation in lizard papillae. *a* Scanning electron microscope (SEM) picture of an area of the basilar papilla of the teiid lizard *Tupinambis,* showing a large number of tightly-packed hair cells with a fairly random distribution of neurally and abneurally-oriented cells (*A* = abneural edge of the papilla). *b* A higher magnification of part of the papilla of the teiid lizard *Ameiva,* where all the hair cells in the top two-thirds of the picture are oriented in the same direction (*A* = abneural). *c* and *d* Cross-sections through the papilla of the agamid lizard *Calotes,* showing *c* an area of unidirectionally-oriented hair cells (the stereovilli all become taller towards the kinocilium on the *left*) and *d* a bidirectionally-oriented area (*a* and *b* from Miller, 1973 a; *c* and *d* from Bagger-Sjöbäck, 1976)

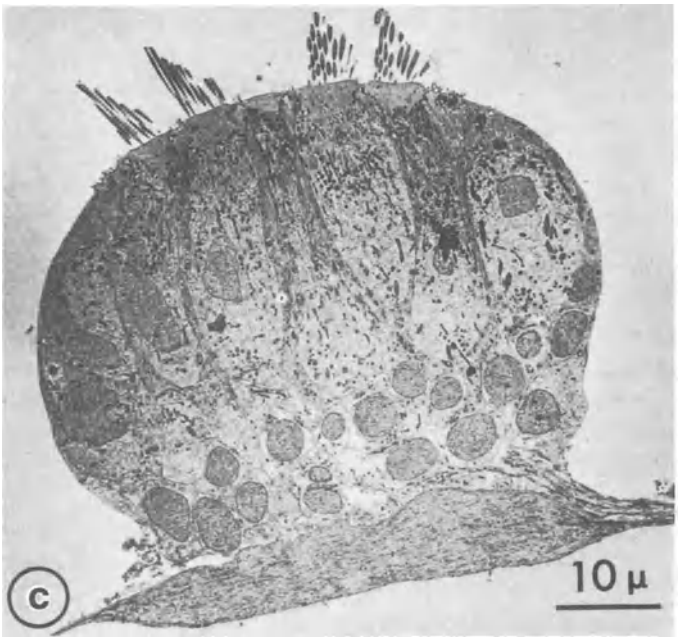
c
10 µ

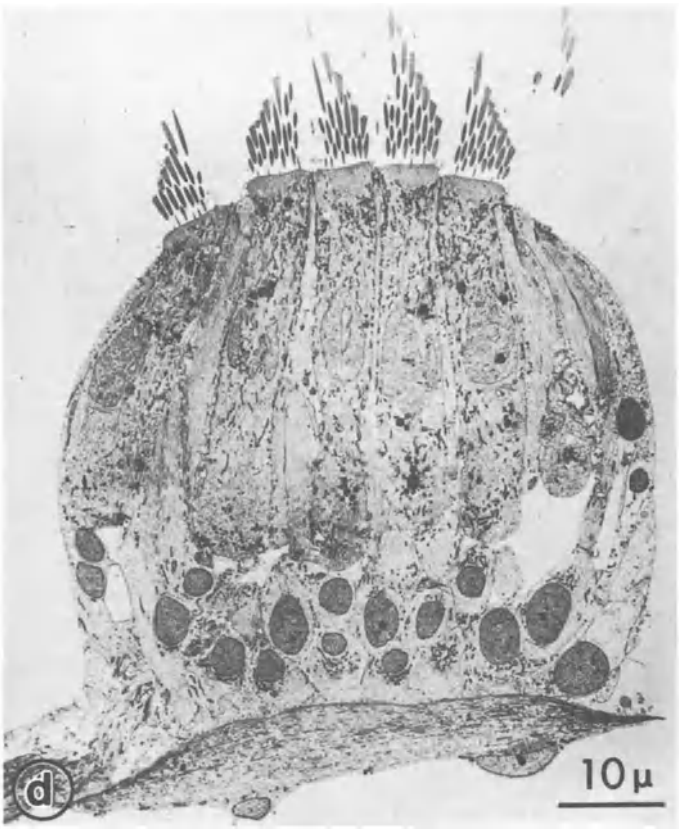
d
10 µ

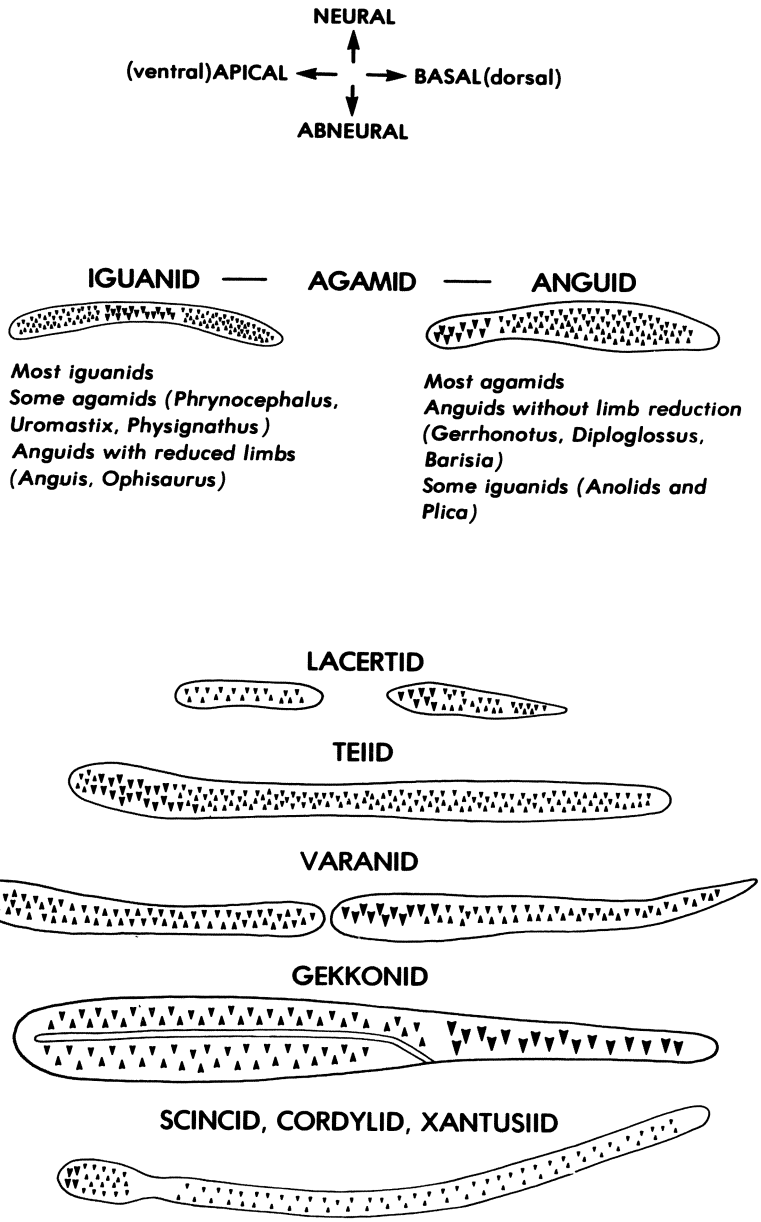

Fig. 4.15. Hair-cell orientation patterns in the papilla basilaris of different lizard families drawn onto a papilla in the shape typical for each family, but not drawn to scale. *Small arrowheads* indicate the orientation of hair cells (not individual cells) in bidirectional areas, *large arrowheads* are used in unidirectionally-oriented areas. The teiid represented in this figure is *Tupinambis*, in which the orientation differs strongly from other teiids such as *Ameiva* and *Cnemidophorus*. More detail on the orientation patterns in lacertid and scincid lizards is given in Chapters 8 and 11 (Miller, 1980 and personal communication)

(6) the presence of an unspecialized tectorial membrane (sheet-like and connected to the limbus).
(7) an irregular arrangement of hair cells, rather than a highly organized arrangement.
(8) a partial separation of the lagenar and papillar portions of the cochlear duct.
(9) a basilar membrane which is much wider than the papilla itself, as in chelonians, snakes and *Sphenodon*.

4.3.2 The Evolution of the Basilar Papilla

During the course of evolution from the most primitive forms, changes in the relative size and structural pattern in the basilar papilla occurred along three broad lines. These led (1) to the Chelonia, (2) to the Crocodilia and birds and (3) to the Squamata. Whereas in most snakes, in amphisbaenids and in some lizard families (e.g. Iguanidae, Agamidae and Anguidae) the basilar papilla is relatively short or even oval-shaped, most lizard families (e.g., Teiidae, Varanidae, Scincidae, Gekkonidae) have an elongated basilar papilla, whose length can be more than 20 times the width. In such papillae, Miller (1978 a) showed that an increase in length of 100 μm is accompanied by an additional 100 hair cells in the papilla.

The chelonian papilla is also somewhat elongated, although it is situated on a broad, oval basilar membrane. The papilla of crocodilians and birds is very elongated (but also broader than in lizards), being at least several mm, in extreme cases in some birds (owls) up to 10 mm or more in length. Thus, there are also great differences in the absolute number of hair cells, ranging from less than 100 to about 2000 in some lizards, to 10000 or more in Crocodilia and some birds. Within the lizards, the range of the numbers of hair cells varies systematically from family to family (Miller, 1985). The variation in hair-cell numbers between individuals of the same species (for one standard deviation or 66% of the population) is about 15%, and is comparable to the figures from other vertebrate groups (Miller, 1985).

4.3.3 The Variety and Evolution of the Lizard Papilla

The lizards have by far the greatest variety of structural variation of the basilar papilla and therefore offer an extremely interesting series of natural experiments for investigating the relationship between structure and function in the auditory periphery of land vertebrates. It was recognized quite early that the structural types seen in the inner ear of lizards offer useful data for the consideration of systematic relationships within the suborder Lacertilia (Baird 1970; Miller, 1966, 1980). Within the lizards, variations in a number of structural components are observed (Fig. 4.15). Leake (1977), Manley (1981) and Miller (1980) list as evolutionary ‚experiments':
- the variations in the orientation patterns of hair-cell areas,
- the division into two sub-papillae through limbal constriction,

– the generation of new types of tectorial membrane structure,
– variety in the bulb-like expansion of the kinocilial tip and
– variations in stereovillar-bundle length (especially in the absence of a tectorial membrane).

I will add here:

– the presence and development of a thickening within the basilar membrane, which can vary systematically in thickness along the papilla (Miller's "papillary bar", Wever's "fundus").

The great variation in stereovillar bundle length in the absence of a tectorial membrane has been interpreted as indicating that the lizards have two hair-cell types, one with a short stereovillar bundle and longer kinocilium attached to the tectorial membrane and a second type without a tectorial membrane, where the stereovillar bundle is long to very long and the kinocilium much shorter (Miller, 1978 a). This difference, which is attributable solely to the presence or absence of a tectorial membrane, does not justify the definition of different hair-cell types. The variation in stereovillar bundle length has, however, important consequences for the micromechanical properties related to frequency tuning (see Sects. 7.4, 11.3).

More recently, Miller and Beck (1988) have derived a new and more comprehensive typology of hair cells in lizards. Their recent studies of the innervation patterns of hair cells indicated that it is possible to define two groups using a number of *cytological* features and not, as in previous attempts, the orientation pattern or presence of a tectorial membrane. It struck these authors that the following features characterize one group of cells:
– a greater basal diameter of the hair cell,
– the presence of an efferent innervation,
– large numbers of, and larger afferent nerve fibres and
– a larger number of afferent synapses per fibre.

In most, but not all, lizard papillae, these cells are in an area where all hair cells are abneurally-oriented, commonly called a "unidirectionally-oriented area". They propose calling such hair cells the "unidirectional type" (which I will abbreviate as UDT hair cells). Functionally, these cells are always responsible for low-frequency responses (see later chapters).

The second hair-cell type is the "bidirectional type" (BDT). These cells respond to higher sound frequencies. Although most BDT regions are also bidirectionally oriented, the characteristic features of the cells are their small size, the lack of an efferent innervation and the smaller and fewer afferents with small synaptic areas.

Miller (1985) has also offered a new viewpoint on the evolution of the basilar papilla of lizards, based on his recent studies of the hair-cell and innervation patterns of the various families. This is different to the ‚classical' view expressed by Baird (1960, 1970), Miller (1980) and Wever (1978), which regards the papillae of iguanid and agamid lizards as primitive (due to their small papillae with few hair cells and the primitiveness of the lizard families themselves). It appears as if the evolution of the ear may to an unexpected extent be independent of the evolution of the rest of the body. Other lizards which are considered in some ways to have a

primitive structure have very advanced and complex basilar papillae (e.g., the geckos). Instead, Miller proposes that those lizard papillae which have predominantly unidirectionally-oriented hair-cell areas, innervation patterns similar to those of chelonians and an unspecialized tectorial membrane (such as in *Sphenodon* and chelonians) should be regarded as primitive. This description applies especially to the teiid lizards, a family for which, unfortunately, there exist no data on the auditory physiology. Using this family as his starting point, Miller derives the other types of lizard papilla, e.g., the iguanid-agamid-anguid type through a better ordering of the bidirectional area and the loss of its tectorial membrane. The gekkonid and scincid types are derived through a clearer arrangement of the hair cells of the bidirectional area and a specialization of the tectorial membrane (see Ch. 14). In addition, Miller and Beck's (1988) more recent redefinition of the hair-cell types in lizards (see above) also contributes to clearing up past dilemmas with regard to the evolution of the papilla. Thus, although the teiid lizards have a large unidirectionally-oriented hair-cell area, much of this area in fact consists *cytologically* of BDT hair cells.

In many cases, the ears of more advanced reptiles tend to show a mixture of primitive and advanced features. In the inner ear of crocodilians and birds, for example, which has evolved independently of the squamate inner ear for a very long time, the tectorial membrane, the number of stereovilli and the hair-cell orientation patterns are of the primitive type. However, the hair-cell density and specialization, the innervation patterns etc. are advanced features.

The detailed anatomy of the various species which have been studied using neurophysiological methods will be described in each group in the following chapters. Based on these anatomical and physiological data, an attempt will be made to create a general scheme of the structure-function relationships in the basilar papillae of reptiles and birds (Ch. 14).

4.3.4 Innervation Patterns of the Basilar Papilla

It is a curious fact that, although the number of hair cells varies greatly between very small lizard papillae (about 100 hair cells) and large papillae (near 2000 hair cells), the number of nerve fibres varies by less than a factor of three. This implies that the innervational patterns of the hair cells in large and small papillae are quite different, a fact which could have important functional consequences. The ratio of the total number of nerve fibres to the number of hair cells has been studied in detail in lizards by Miller (1985; Fig. 4.16). Whereas in some lizard families this ratio is about one (e.g., Varanidae, Gekkonidae, Scincidae), in many families with smaller papillae (e.g., Anguidae, Iguanidae, Agamidae, Lacetidae), the ratio is substantially higher than one, e.g., 3.7 to 7.4 (Fig. 4.17). That this is not purely a question of the number of hair cells or papillar size can be seen in a comparison of the ratio for Teiidae with a mean number of 575 hair cells (ratio 2.6) with the Cordylidae, which have a mean hair-cell number of about 590 (ratio 0.8; Fig. 4.17). However, a tendency does exist towards a lower ratio in the larger

papillae, which is also borne out by a glance at the ratio for a bird (pigeon, 0.5). Ratios for mammals, where only the inner hair cells receive a dense innervation, are from about 2 (in man) through 3 or 4 (for cat and rodents) up to 15 in a bat.

In a detailed study of the small papilla of the iguanid lizard *Sceloporus occidentalis*, Teresi (see Ch. 7) found that each individual nerve fibre only innervated a single hair cell. However, each hair cell in such papillae is innervated by at least three afferent nerve fibres which do not contact other hair cells (*exclusive* innervation). Miller and Beck (1988) report a similar innervation pattern in the iguanid lizard *Crotaphytus wislizeni*. Here, both UDT and BDT types of hair cells are exclusively innervated. The low ratios of the longer papillae do not, however, indicate that each hair cell is innervated by only one fibre, but rather that each fibre innervates several hair cells (*non-exclusive* innervation; Miller, 1985).

In an extensive study of lizards of different families, Miller and Beck (1988) gathered sufficient data on innervation patterns to make the following generalizations:

1) In the iguanid-agamid-anguid type of papilla, the innervational pattern is largely exclusive, with some non-exclusive innervation of BDT hair cells of anguids (such as the alligator lizard, see Ch. 7).

2) ln lacertid-teiid type papillae, the afferent innervation of the BDT hair cells is exclusive, with each fibre usually making only one synapse. The afferent innervation of the UDT hair cells is mixed exclusive/non-exclusive (see Ch. 8).

3) In the gekkonid-type papilla, it is the UDT hair cells whose innervation is exclusive; that of the BDT is non-exclusive (see Ch. 10).

4) Finally, in the scincid papilla, all hair cells are non-exclusively innervated (see Ch. 11).

Miller and Beck (1988) also note that in all lizard species studied to date, the number of afferent *synapses* is greater on UDT hair cells than on BDT hair cells. The ratio varies from over 50:1 in *Ameiva*, a teiid lizard, to almost 1:1 in *Mabuya*, a scincid lizard. In *Sceloporus*, Teresi (1985) studied the afferent innervation pattern of the entire papilla and reported that there is a gradual decrease in the number of afferent synapses per hair cell in the BDT area when going from the central papillar region (near the UDT hair cells) to the papillar extremity.

From these data, we would be justified in expecting some rather dramatic functional differences in the behaviour of nerve fibres in ears of these various groups. The differences are, at least superficially, much smaller than expected. The fact that UDT hair-cell areas respond to low frequencies has nothing to do with the innervation patterns. Miller and Beck (1988) note that in all the papillae of the 6 different families they studied, the UDT hair cells are supplied by a larger number of synapses than the BDT hair cells. It might be expected that the discharge patterns of cells in different areas may be different. Unfortunately, the physiological data have, to date, not been extensively analyzed in this respect (but see Sect. 14.6). What little data is available will be discussed later for individual species.

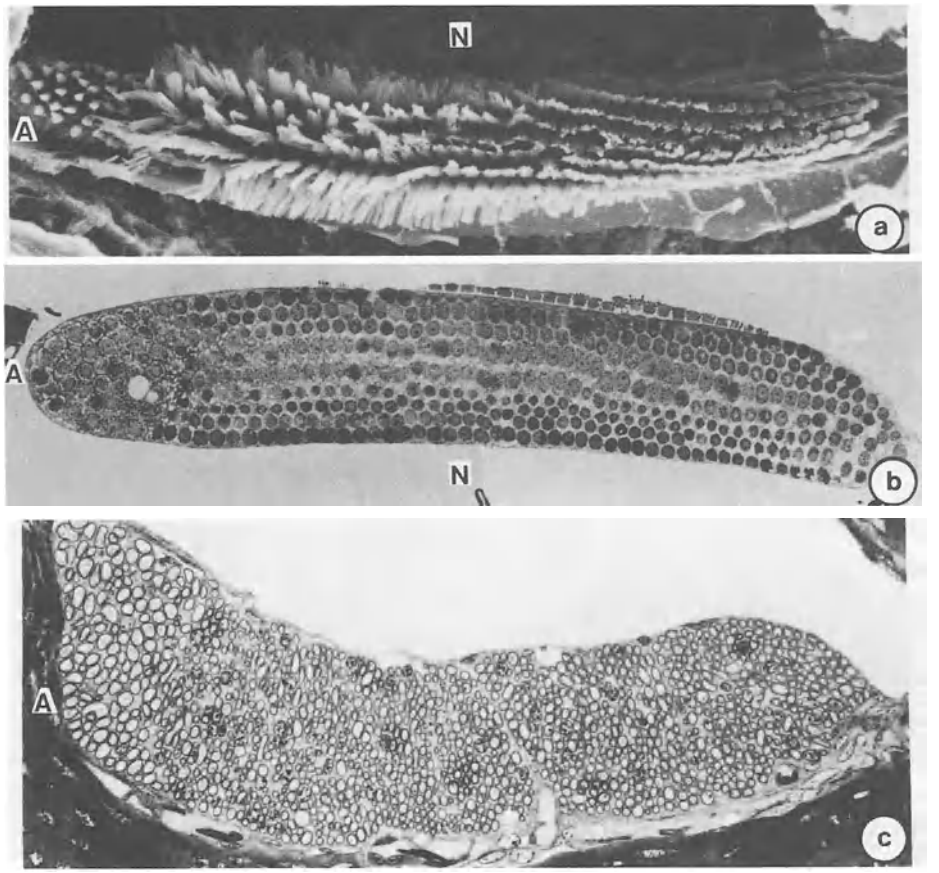

Fig. 4.16 a–c. Hair-cell patterns and innervation in the anguid lizard *Celestus*. *a* SEM of a left papilla, showing a short apical region of unidirectionally-oriented hair cells to the *left* (*A*), where the tectorial membrane has been removed. The stereovilli of the bidirectionally-oriented hair cells (*right* three-quarters of the picture) are longest near the apical area and become progressively shorter basally (*N* = neural limbus). This papilla is about 250 μm long. *b* Frontal section through the hair cells of the papilla of *Celestus*, showing that the unidirectionally-oriented hair cells (*left*) are larger (*N* = neural limbus). *c* Cross-section of the left papillary nerve of the same species, showing the pronounced difference in average size of the nerve fibres to the apical area (*left*) and the smaller fibres to the basal, bidirectionally-oriented area (*right*) (Miller, 1985)

There is also good evidence that efferent nerve fibres in lizards, which are present in almost all species studied, are only found in contact with UDT and not with BDT hair cells. Miller and Beck (1988) report that in *Ameiva*, efferent fibres also contact afferent nerve terminals. Such contacts are also found in the turtle *Chrysemys* (Sneary, 1987) and in *Caiman* (von Düring et al., 1974).

Miller (1985) studied the distribution of nerve-fibre diameters in the auditory nerve of a large number of lizard species. In 35 species of different families, the

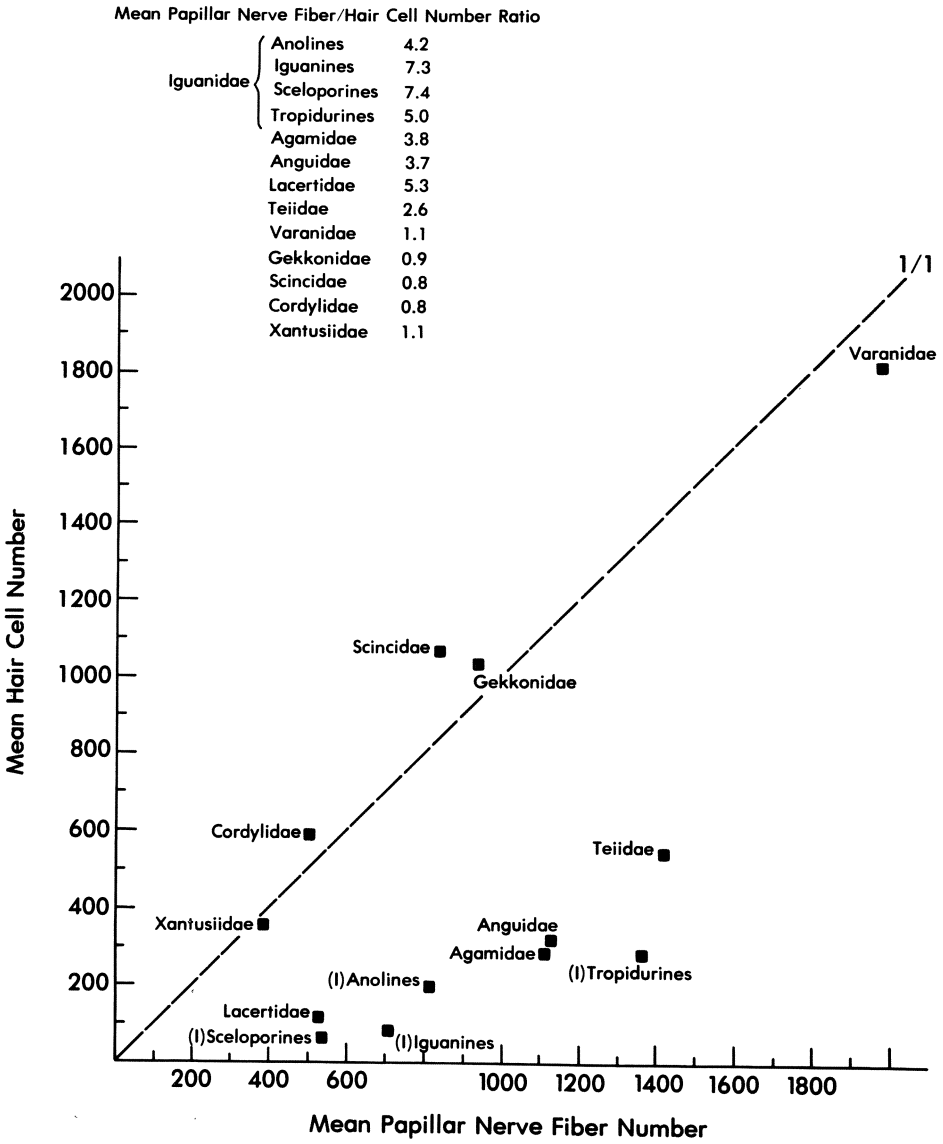

Fig. 4.17. Graphical representation of the relationship between basilar papilla nerve-fibre number and the hair-cell number in the same species for different lizard families. The *black squares* are the mean values of nerve-fibre and hair-cell numbers in each family or subfamily. The *dashed line* indicates a 1 : 1 ratio. Smaller papillae (e.g., Iguanidae, Agamidae) tend to have more nerve fibres than hair cells (Miller, 1985)

distribution of diameters is unimodal and more than 99% of the nerve fibres had diameters between 0.8 and 6.0 μm. The larger nerve fibres were found to supply UDT hair-cells areas (Fig. 4.16c, left side). Thus those species with a larger unidirectionally-oriented area (e.g., teiids, varanids, scincids, etc.) had a larger mean nerve-fibre diameter than those with few hair cells in such areas (e.g., anolines). In *Anolis carolinensis*, only 13% of nerve fibres had a diameter greater than 3 μm, whereas the figure for a species of *Varanus* was 87%. According to Boord (1969, cited in Miller, 1985), in the pigeon auditory nerve, the largest number of fibres have a diameter of 1 to 2 μm.

Chapter 5

Some Techniques Used in Hearing Research

It is not my intention in this chapter to give a detailed exposé of the various techniques used to obtain the data described in this book. Some of the techniques may, however, be of special interest to some readers, as they are either new or specialized for work with reptiles and birds. This chapter will also serve to illustrate that auditory research is a highly technical field, many rapid advances being dependent on the development of new techniques. More detail about specific techniques can be found in the papers quoted in each chapter and in various technique books (e.g., Beagley, 1979). This chapter serves to give the reader a brief introduction to the rationale behind some of the techniques described in later chapters.

5.1 Obtaining Reptiles

Those of us working with reptiles have a responsibility, when planning an experimental series, to chose an experimental animal which is not a species in danger of extinction, even though scientific research has never been an important factor leading to the decimation of reptilian species. In the course of the last 20 years, the situation for a number of reptiles has become quite critical. It is easy to forget that some reptiles need about 10 years before they become sexually mature, so that it takes a very long time before a decimated population can recover. The methods used to catch, hold and transport some reptile species are not seldom illegal and are so unsuitable, that many die before they reach their goal. A scientist can have no part in such practices, even though they may not have a very significant effect on the population compared to other factors, such as habitat destruction or poaching for skins or food, and even though they may be tolerated or condoned by local officials.

Those animals we have caught in the field have been caught in locations where they are abundant and, where necessary, with permission of local authorities. A number of reptiles are so slow in their movements that they can simply be taken in the hand, others such as night-active geckos can be caught under stones in the early morning when they are still cold and do not move so quickly. For fast-moving smaller lizards, we use a sling. For this, we pass a 1 mm nylon thread through a thin aluminium tube 1 m long and fix the front end firmly to the outside of the tube. Such a tube is light enough and short enough to hold at arms' length for long periods of time. A loop whose diameter is at least double that of the animal's head is formed in the thread. Having spotted a lizard, the trick is to approach as slowly as possible with no sudden movements, to bring the loop near

the animal's head, slip it over to the neck and pull the other end of the thread just tight enough to hold the animal until it can quickly be grasped with the other hand and freed from the loop. We have found that lizards tend to ignore the thread, but may get curious and attempt to bite the end of the tube. Experience will quickly help to know when the animals have a need to warm themselves and, even if frightened into their hiding place, will return quickly to expose themselves to the sun. Some individuals are very wary and exceed our patience, others will be caught at the first attempt.

Fortunately, there are now many reference works on keeping reptiles in terraria, so that it is not difficult to hold them, feed them adequately and in some cases even breed them. We always free the freshly-caught animals from ectoparasites, such as ticks, and treat them with an external anti-mite preparation, to reduce the chance of an outbreak of infestations and infections in the colony.

5.2 Anaesthesia and Surgery

Over the years, we have collected a fair amount of experience with anaesthetizing reptiles. One considerable difference to mammals and birds lies in the slow reaction to the anaesthetic. Whereas a bird may close its eyes within seconds of an injection into the pectoral muscle, reptiles respond much more slowly to our intraperitoneal injections. Here, one must be patient and wait at least 15 to 30 minutes between doses, and not simply quickly give additional doses which, after a time, will prove to be an overdose. With turtles, I used to give an injection of pentobarbital sodium on the evening before an experiment, in order to have them anaesthetized the next morning! Using both urethane (ethyl carbamide) and pentobarbital sodium, we have found it very important, once the total initial dose is established, not to give all the dose at once. Such a single dose can lead to a state of the animal where the auditory nerve is completely inactive. The initial dose (in *Podarcis* and *Tiliqua*, we used 35 mg/kg and about 60 mg/kg body weight Nembutal, respectively) should be spread out as two or three partial doses over 45 to 90 minutes. Even then, individual animals may show some adverse effects of the anaesthetic, such as a reduced spontaneous activity in the auditory-nerve fibres. In the case of the bobtail skink, we demonstrated that the dose necessary to induce surgical anaesthesia varies considerably with the season of the year (Ch. 11). While it is likely that other species also show some such effect, there are no systematic data available. Atropine given after the initial dosage seems to help stabilize heart and breathing activity. It should be remembered that the heart beat of reptiles is a very poor indicator of condition. The heart may beat for hours after the nervous system is ‚clinically dead'.

In birds, a number of different anaesthetics have been used without, however, extensive tests to look for anaesthetic-dependent effects (see refs. in Ch. 13). Otoacoustic emissions in the starling are strongly anaesthesia dependent (Ch. 13) and we traced the putative seasonal effects on hearing in the bobtail skink of

Australia to a variation in the anaesthetic requirements with season (Ch. 11). A recent paper describes a powerful influence of anaesthesia on the spontaneous activity of single vestibular-nerve fibres in the pigeon (Anastasio et al., 1985).

Following the establishment of anaesthesia, there are a number of surgical approaches to the papilla and nerve of reptiles and birds, all of which are adequately described in the various publications listed in each chapter. It should, however, be noted that the auditory nerve of reptiles is often very small (e.g., 500 fibres of average diameter 3 μm gives a nerve with the dimensions of about 30 by 150 μm). If a microelectrode does not readily penetrate the surface, the pressure it exerts may do considerable damage to the nerve. Further peripherally, near the papilla, the nerve may only be a few fibres thick, but it is not covered by anything which significantly interferes with electrode penetration. While an approach to the peripheral part of the nerve (peripheral to the ganglion) has some advantages, such as the relative ease of mapping the tonotopic organization, it involves more radical surgery. Thus, it is generally necessary to remove the secondary tympanic membrane (usually erroneously called the round window) and its surrounding bone (see Weiss et al. 1974), or, having penetrated the brain cavity, to remove the medial bony wall which separates the brain cavity from the cochlear duct. In both cases there is a danger of bleeding which, if blood enters the cochlear duct, can both damage the papilla and obscure the view. With care, however, all or part of the papilla can in many cases be exposed with remarkably little or no effect on gross potentials (e.g., compound action potential). In some cases, the peripheral part of the auditory nerve can be exposed by simply removing the secondary tympanic membrane.

In general, we have found that larger animals withstand the surgery much better than smaller animals. To expose the trunk of the auditory nerve in lizards, we almost always use a surgical approach through the floor of the mouth. Once the skin, thin muscle and mucous membrane layers have been opened, it is possible to see the middle ear on both sides from inside and the bony ridges over the secondary tympanic membranes. Depending on how hard the bone is, it is then necessary to use a scalpel or a drill to remove bone in the appropriate places. Once the underside of the *medulla oblongata* has been exposed, it is *gently* pushed *a little* to one side and held there with rolled paper tips, to expose to view the auditory nerve as it runs from the otic capsule to the dorsal part of the medulla.

For our work with birds, we developed a new method of exposing the auditory ganglion, which lies fully within the cochlear duct near the central area of the papilla (see Ch. 13). In order to reach this area, skin and thin muscle layers are pushed aside from the dorso-lateral aspect of the rear of the skull. Using landmarks, it is then possible to remove the thin bone layers of the skull which lie above the middle-ear cavity. This exposes the thin bone overlying the recessus scala tympani, which is partly removed while exercising great care not to break small blood vessels (Manley et al., 1985).

In the turtle, a method has been developed to isolate the papilla of one side while maintaining the surrounding and supporting bone and the middle ear (see Ch. 6). This preparation takes advantage of the immense physiological robustness of turtle organs and gives much easier access to the nerve and hair cells than if the papilla was left in the whole skull.

5.3 Acoustic Stimulation

In modern bioacoustical laboratories, closed acoustic stimulation systems are generally used for peripheral auditory physiology. Thus, either two condenser microphones (one to measure the sound pressure, the other driven in reverse as an earphone) or a microphone and an earphone are enclosed in an airtight holder which is connected by a closed tube to the external auditory meatus. Generally, the microphone for measuring the sound pressure level (SPL) is coupled through a probe tube to within a small distance (<1 mm) of the eardrum. The earphone is driven by appropriate oscillators, tone gates and amplifiers. These should have a very small total harmonic distortion (preferably below -60 to -70 dB), in order to present the ear with relatively pure, well-defined signals. This latter precaution is necessary whenever measurements are to be made over a dynamic range of more than 40 dB, which is almost always the case. In addition, the onset and offset of the sound stimuli are made to be gradual, over 1 to 5 ms, depending on the frequency of the signal. Without these ‚rise/fall' times, the stimulus would produce broad-band transients at the beginning and the end.

5.4 Measuring the Motion of Middle- and Inner Ear Structures

The incredibly small amplitudes of motion of the middle- and inner-ear structures is often cause for wonder to the uninitiated and, indeed, to the expert. Ever since the time when von Békésy (1960) made his measurements of the motion of the basilar membrane and discussed dimensions in the range of the diameter of hydrogen atoms, a controversy has raged over whether the ear can really be so sensitive. In fact, newer studies of basilar-membrane motion in mammals have shown that von Békésy's interpretation was wrong. He measured basilar-membrane motion in a variety of mammals and chicken cadavers under a microscope with the aid of stroboscopic illumination. In order to create visible motions, it was necessary for him to use SPLs up to 130 dB. His estimates of motion at threshold were extrapolations from these measurements. We now know that in mammals, at least, active processes involving hair cells serve to increase the amplitude of displacement of the basilar membrane at low levels. Thus, the estimates he made were too small. What we have also learned in the meantime, however, is that the basilar-membrane motion exceeds that of the middle ear, and that methods to measure middle-ear motions have to be sensitive in the nanometer range.

There have been a number of technical developments which have made possible the measurement of the velocity or the displacement of ear structures – the Mössbauer effect, the capacitative probe, ‚fuzziness' detection using laser light (little used) and sensitive differential photodiodes. All of these methods have their own advantages and disadvantages (Yates and Johnstone, 1979).

The Mössbauer effect is the oldest and is a velocity-sensitive effect (see e.g., Johnstone et al., 1970; and Ch. 3). It is based on the fact that radioactive metal

isotope atoms (e.g., of cobalt) embedded in a crystal lattice cannot recoil when they emit gamma radiation. This means that the radiation is of a very pure frequency and can be absorbed easily with thin sheets of a specific metal. When the radiation source is moving, however, the frequency shifts due to the Doppler effect and penetrates through the absorber. The amount of radiation which can be measured behind the absorber film is thus an indicator of the velocity of the source. This method is sensitive to movements of fractions of mm/sec but, being velocity-sensitive, is not very sensitive to low frequencies.

The capacitative probe is a displacement-sensitive device (Wilson and Johnstone, 1975; and Ch. 3). It is based on the idea that, if the moving structure is made to be one pole of a condensor and a fine metal probe the other pole, then it is possible with an appropriate electrical circuit to detect changes of capacitance between the poles. This requires, however, that the poles be very close together (a matter of micrometers) and separated either by air or an insulating fluid (see e.g., Fig. 12.4). This latter requirement is, for inner-ear measurements, difficult to fulfill, actually causes changes in the motion patterns and makes measurements under normal conditions impossible.

A more recent technique is to project the enlarged image of a structure, with or without an attached reflector, onto differential photodiodes (Yates, 1982 and in preparation). With appropriate circuitry and signal extraction techniques (e.g., lock-in amplifiers), these methods, which are sensitive to displacements in the nanometer range, can enable measurements at SPLs close to threshold. In this respect they are very much better than the older methods, with which it was necessary to measure at higher levels and assume linearity down to levels 40 to 80 dB below the measurement level.

5.5 Recording the Electrical Activity of the Ear

Gross potentials from the ear can be recorded simply by placing a wire electrode on the secondary tympanic membrane or on nearby bone. An averager, spectrum analyzer or lock-in amplifier is of great advantage since, in most species, the signals may be small compared to the noise (e.g. a few μV). In this way, cochlear microphonics, summating and compound action potential can be measured. These, especially the latter, may then serve as a control to monitor the success of further surgery. If the papilla has been exposed, it is then possible to measure the motion of the basilar papilla to different stimuli using different techniques (see Chs. 7, 11, 12 and 13).

A number of experiments have been carried out recording from single hair cells of reptiles and birds (see Chs. 2, 6, 7 and 13). In many cases, the hearing organ was removed and a number of hair cells isolated for recording *in vitro*. The hair cells can be separated from the basilar membrane and supporting cells either mechanically (i.e., with a fine needle) or by using proteolytic enzymes or both. For recording *in vivo*, it is necessary to push the recording electrode through the basilar membrane which, being often thick, it not easy to accomplish without

damage. The *in vivo* method has the advantage of leaving the hair cells surrounded by the normal fluids and connected to the tectorial membrane, if present. It also permits the normal route to be used for acoustic stimulation, through the middle ear. More recently, it has proved possible to stimulate the bundles of hair cells with piezo-electric devices and to record the mechanical motion of individual hair bundles. The isolated hair cells are of course more easily visualized and are accessible on all sides for recording. In addition, they can be more easily studied using voltage-clamp or patch-clamp techniques, in combination with changing the ionic constituents of the fluids around the hair cell, for determination of the properties of their membrane ion channels (see e.g., Chs. 2, 6, 13).

The nerve fibres of the papilla of birds and reptiles are large enough to permit ease of recording with normal glass micropipettes. The time of contact varies with the size of the fibre and the stability of the recording situation, but can exceed 1 h. In this time, it is possible to examine the spontaneous activity and the response activity to a wide variety of stimuli. In order to analyze this vast number of action potentials and their temporal relationships, it is necessary either to use an on-line computer system to do immediate data reduction and/or to tape-record the data for off-line analysis. The latter also allows analysis of the data in several different ways. The action potentials from the individual nerve fibres are fed to the computer via a Schmitt-trigger device, which produces a TTL-pulse (computer-compatible, brief 5 V positive pulse) when the signal voltage exceeds a pre-set, adjustable level. The adjustment of the threshold of the trigger is greatly facilitated by using an extended TTL pulse to flash the Z-axis (brightness) of the oscilloscope beam where the action potentials are being displayed. In this way, even relatively small potentials can be reliably triggered above the noise level.

The spontaneous activity of a nerve fibre can be described in terms of its rate, but also as the pattern of the distribution of all time intervals during recording period as displayed in the time-interval (TIH) or the joint-interval histogram. The former quantifies the frequency of occurrence of interspike intervals of different time duration and, for auditory-nerve fibres of vertebrates, typically shows a Poisson distribution (modified by the refractory period of the fibre) almost certainly attributable to the random release of transmitter 'packets' at the hair-cell synapse. The joint-interval histogram reveals whether inter-spike intervals of a certain length are, as expected, followed randomly by intervals of other lengths. This procedure can help expose injured cells, which tend to show a 'bursting' discharge activity.

The tuning characteristics of a cell can be measured by exposing the ear to pure tones of different frequencies and measuring the lowest SPLs for a response at different frequencies. This response may be a phase-locking to the stimulus without a rate increase; that is, the cell begins to fire non-randomly at preferred phases of the sound stimulus. The response may also be a decrease or an increase in the firing rate during the stimulus. These responses can be investigated by changing settings of the apparatus by hand, or, more commonly, under computer control. Experienced operators of the equipment can, by hand, repeat a threshold measurement to within 1 dB. The computer is, however, a more objective instrument: it does not grow tired, can cope better with high spontaneous activity of

cells and can be programmed to use specific threshold criteria which can vary with e.g., the spontaneous rate or be an increase of a certain percentage above that rate. Nevertheless, it is important that the experimenter continuously monitor the electrical threshold of the Schmitt-trigger mechanism which transforms the action potentials into TTL pulses for the computer, to make sure that only these and no electrical noise or other disturbances are accepted as data. Occasionally, other techniques such as reverse correlation have been used to find the frequency selectivity of nerve fibres.

We generally use a computer program which randomly presents a matrix of different frequencies and SPLs, each point up to 9 times. We prefer this to threshold-hunting routines (in which the SPL at a specific frequency is varied until a specific response criterion is exceeded), since the use of the latter assumes that the fibres have, as in mammals, simple excitatory responses to all sounds or none at all. That this is not the case has, among other things, been shown by the demonstration of single-tone suppression of spontaneous activity in birds and some reptiles (Sects. 11.2.3, 13.4.5.3). From the data collected in the matrix, it is possible to extract intensity functions for different frequencies, or tuning curves derived for different rate-response criteria. The addition of a second, steady tone to the matrix of stimuli also gives a reliable way of detecting two-tone rate suppression (TTRS) and allows the study of suppression contours. In addition, we tape data in response to tones in order to examine the time patterns in the responses both during and after the stimuli (e.g., through the use of peristimulus-time histograms) and the phase responses.

5.6 Marking of Hair Cells and Nerve Fibres

Intracellular injection of dyes (e.g., alcian blue or lucifer yellow) has been used to identify hair cells or other cells of the auditory papilla from which electrical activity has been obtained. Lucifer yellow also can be used to mark avian nerve fibres, but the small quantity injected fades rapidly when exposed to the ultraviolet light necessary for its fluorescence. We have used the standard horseradish peroxidase (HRP) method for marking identified nerve fibres in the bird auditory nerve or ganglion (see Ch. 13), but this method involves the use of unpleasant, toxic and carcinogenic chemicals.

In an attempt to find a better method for staining single fibres in the lizard auditory nerve, a technique which for years has been used successfully in insects was modified for use with inner ears of reptiles and birds. This method involves injecting cobalt hexamminchloride into or near the fibre, allowing time for its diffusion and transport in the axons, deposition of cobalt sulphide before fixation of the nerve and, finally, an intensification process (Köppl and Gleich, 1988). Apart from the unpleasant 'rotten eggs' odour of the ammonium sulphide, this method is less toxic than the HRP technique and is very reliable (success rates up to 100%). Nerve fibres so treated showed dark staining not only into the fine branches of their peripheral synaptic regions but often also up to their synaptic con-

tacts with cells of the cochlear nuclei of the medulla; that is, both anterograde and retrograde transport occurs. Such techniques make it possible to collect integrated information on the peripheral origin and central connectivity of fibres whose physiological activity has been examined in detail. As an alternative, it is possible to stain many fibres in the auditory nerve simultaneously, in order to investigate their innervation patterns (e.g., Mulroy and Oblak, 1985).

5.7 Measuring Otoacoustic Emissions

One of the more important discoveries in the field of auditory research in recent years was Kemp's (1978) demonstration of the existence of what were initially called "echos" from the ear. That is, the ear was shown not only to absorb sound, but to produce it, too. It was quickly recognized that the sounds which could be measured in the ear canal were not echos in the classical sense, for their energy content sometimes exceeded that of the stimulus and they often were produced spontaneously, that is, with no external source of stimulus.

In mammals, it has become well established that these otoacoustic emissions are a result of the activity of hair cells, in all probability the outer hair cells. They can be identified using certain criteria (see, e.g., Zwicker and Manley, 1981) and have provided an immensely useful non-invasive technique for the study of the inner ear. They are either present spontaneously, or can be elicited by short stimuli (appearing as a short-latency sound response after the stimulus) or by continuous low-level tones (where they appear as interference dips and peaks in the SPL measured in the external ear canal). Although there is speculation that these phenomena are, in mammals, only produced by the outer hair cells, the finding of otoacoustic emissions from the frog ear and from the caiman (Ch. 12) and bird ear (Ch. 13) would rather tend to indicate that all hair cell groups are capable of some sort of reverse, that is, electro-mechanical transduction.

5.8 Anatomical Studies of the Papilla

A great variety of light- and electron-microscope techniques have been applied to the study of the reptilian inner ear (Ch. 4). Here, I will simply point out that, just as much as the physiological responses of nerve fibres or hair cells can be strongly influenced and altered by the experimental conditions, the structures of the inner ear are not easy to preserve in their normal state. Techniques of fixation, staining and dehydration of the tissues produce shrinkage, probably differentially between different tissues. The tectorial membrane is especially affected by the sodium ions in the buffer solutions, but also shrinks strongly during histological preparation. It often changes its dimensions and detaches from some or all of the

hair cells. The network of tectorial fibrils under the tectorial membrane vanishes under most preparation techniques. Thus, although it is possible to obtain, for example, clean, beautiful scanning electron microscope pictures of a papilla, caution must be exercised in the interpretation of its appearance in the living state.

Chapter 6

Turtles and Snakes

6.1 The Hearing Organ of the Red-eared Turtle *Pseudemys (Chrysemys) scripta*

It is very fortunate that detailed anatomical and physiological investigations of this turtle hearing organ have been carried out. As stated in earlier chapters, this allows us to try to reconstruct the capabilities of a primitive basilar papilla and to examine the fundamental principles underlying its function. Most of these data come from a series of elegant investigations carried out by a team in Cambridge University, England (Art and Fettiplace, 1984; Art et al. 1982, 1984, 1985; Crawford and Fettiplace, 1980, 1981 a,b, 1983, 1985; Fettiplace and Crawford, 1978, 1980; Fuchs et al. 1983). The red-eared turtle is a handsome, medium-sized terrapin closely related to the painted turtles of North America. These relatively active animals are common in shallow fresh water, eating both plant and animal material (insects, snails, tadpoles and fishes). The name comes from the bright red strip of scales behind the eyes.

6.1.1 The Turtle as an Experimental Preparation

A recent paper (Lutz et al, 1985) has highlighted some of the reasons why the organs of the Chelonia are suitable for some physiological investigations. Their metabolism is, to a large extent, not dependent on a continuous supply of oxygen, a fact which can be seen in the duration of the underwater dives made by some species. This metabolic robustness and independence from oxygen made it possible for Crawford and Fettiplace to work with only that part of the head surrounding the inner ear. Thus they could circumvent the difficult problems involved in exposing a basilar papilla enough to be able to make good recordings, while also trying to maintain the animal under optimal conditions. The semi-isolated basilar papillae remained in good condition for hours after losing their connection to a functioning blood system. These workers were thus able to carry out a series of interesting experiments, recording from the nerve fibres and from individual hair cells responses to sound stimuli and to direct stimulation of the stereovillar bundle. Such experiments have revealed that many of the functional principles previously observed in other, more advanced species are already present in the primitive papilla of the red-eared turtle. As outlined in Chapter 2, some of these hair-cell properties were 'inherited' from the cells of the lateral line and electroreceptors of the ancestors of the land vertebrates.

6.1.2 Anatomy of the Papilla Basilaris

The hearing organ of the red-eared turtle consists of a thin, oval basilar membrane, about 1.1 mm in length and 300 μm in width, with four or more irregular rows making up a total of about 1,100 hair cells (Fig. 6.1 a). They are all covered by a thick tectorial membrane (Fig. 6.1 b; Miller, 1978 a; Wever, 1978). Most of the hair cells are in a long, thin band (about 130 μm wide and 700 μm long) nearer the neural side of the basilar membrane, but some (more than 400), especially at the apical end, are present in terminal 'hook' portions, which lie on the limbus and have a less substantial tectorial membrane (Fig. 6.1 a). At the basal

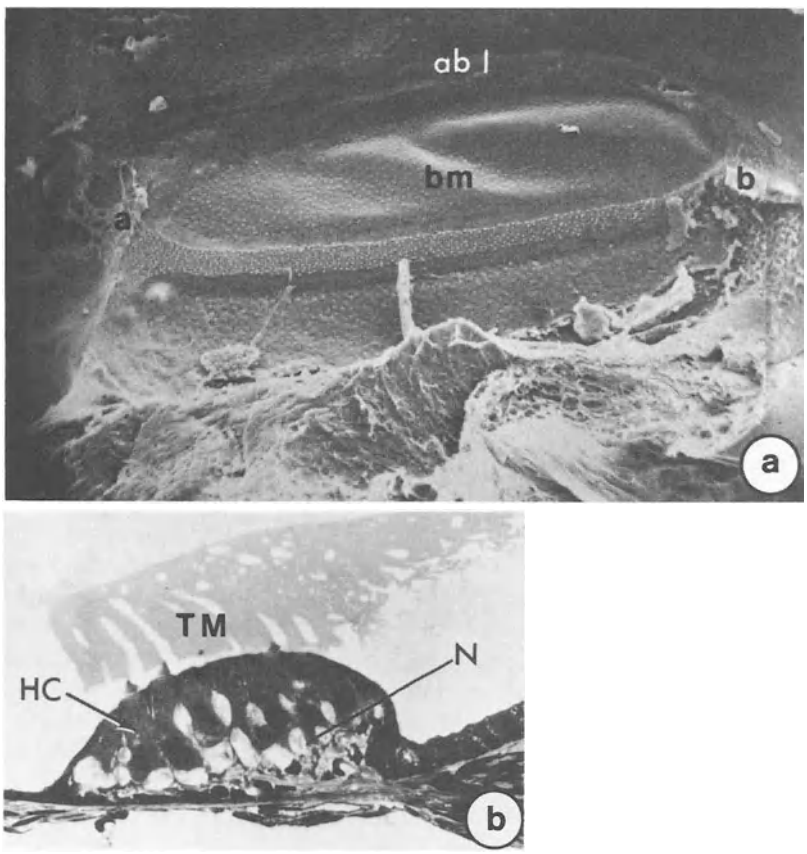

Fig. 6.1 a–d. Anatomical features of turtle basilar papillae. *a* A scanning electron micrograph (SEM) of the upper surface of the basilar papilla of *Pseudemys scripta* without its tectorial membrane, showing that the basilar membrane (*bm*) is much wider than the papilla and that some hair cells are located off the membrane at the basal (*b*) and apical (*a*) ends; *abl* abneural limbus. *b* Light micrograph of a cross-section through the basilar papilla of *Pseudemys scripta,* showing the thick tectorial membrane (*TM*) overlying the hair cells (*HC*). The neural limbus is to the right. *N* afferent nerve ending. The papilla is about 130 μm wide. (*c, d* s. p. 87)

Fig. 6.1 c Magnified view of a small section of an SEM of the basilar papilla of the turtle *Kinosternon* sp. without the tectorial membrane, to show the low packing density of the hair cells. A mat of tectorial material overlies the supporting cells. All hair cells are abneurally oriented (neural limbus, *n*, is at *top*). This section is about 50 µm wide. *d* High-power SEM of a single hair cell in the basilar papilla of the turtle *Kinosternon* sp., to show the microvilli (*mv*) on the neural side of the hair-cell surface. Note the mat of tectorial-like material (*t-l-m*) covering the supporting cell surfaces: The kinocilial shaft is thicker than the stereovilli and the bulb (*kb*) at its tip is connected to adjacent stereovilli (*arrowhead*) (Miller, 1978 a)

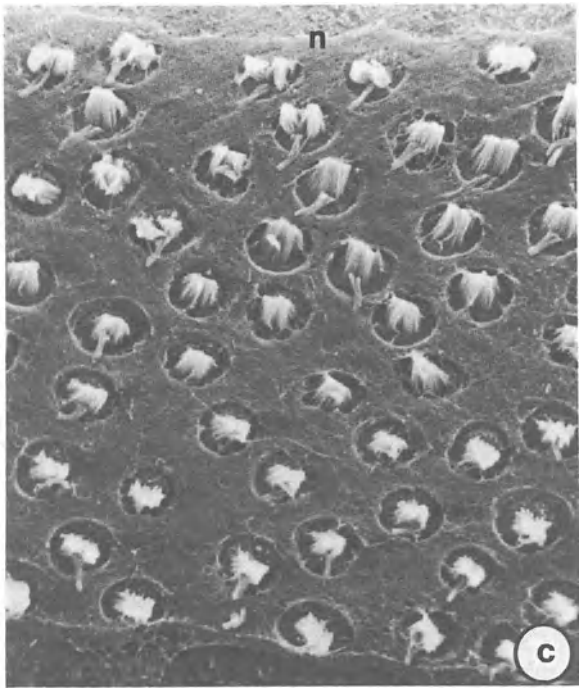

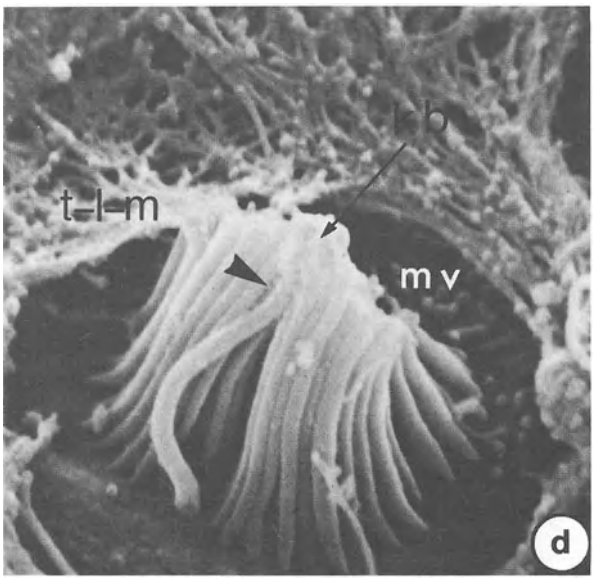

end, Wever (1978) states that the hair cells on the limbus are smaller, forming up to 30 rows, and closer together than other hair cells. In this region, he distinguished an anterior group of smaller hair cells from a posterior group of larger hair cells continuous with those on the basilar membrane. Apically, this band of hair cells spreads out widely on to the limbus again.

Miller (1978 a) found a much thinner tectorial membrane on the limbic hair cells, as distinguished from the limbus-attached, thick, plate-like tectorial membrane over the hair cells on the basilar membrane (Fig. 6.1 b). Almost all hair cells are abneurally oriented and widely separated (Fig. 6.1 c). The cuticular plate measures about 6 μm in the apical-basal axis and 4 μm in the neural-abneural axis. As in some other reptiles, there are a small number of microvilli on the neural side of the cuticular plate (Fig. 6.1 d; Miller, 1978 a). There are about 90 stereovilli. They are narrow at the base and about 0.25 μm thick throughout most of their length. The tallest at the apex are 9 μm long, and at the base 6 μm long (Sneary, 1987). The kinocilium is about 0.5 μm thick, except at the tip, where it expands to a width of 0.75 μm for the last 1 μm, making the kinocilial 'bulb' (Fig. 6.1 d). Its stalk is long and curved (Miller, 1978 a).

A recent study of the innervational patterns of this species (Sneary, 1986, 1987) has provided some important details. The papilla has a low ratio of afferent nerve fibre-to-hair cell numbers (1.5; 900 hair cells and 1350 afferents, Sneary, 1986) and different modes of innervation of the hair cells over the basilar membrane and those on the limbus. Fibres to basal (high frequency) hair cells branch less than those to apical (low frequency) hair cells (1.3 hair cells per afferent fibre as against 1.8), but most hair cells are non-exclusively innervated. They also show more synapses than do apical fibres (51 synapses per fibre as against 24). Sneary (1986, 1987) suggests that the sharper tuning and greater sensitivity of high frequency fibres may be explained by these differences. However, similar changes are seen in lizard species which have different innervational patterns. Fibres to the limbic hair cells innervate several hair cells (Miller, 1985). Apparently all cells also receive efferent fibres (Fig. 6.2). The afferent nerve-fibre diameters are relatively large (mean of 3.7 μm, Sneary, 1986).

6.1.3 Electrical Activity of Hair Cells

According to Schmidt and Fernandez (1962) and Schmidt (1963), the endolymph of turtles has an electrical potential near 0 mV with reference to the perilymph. Crawford and Fettiplace (1980) found a potential of a few mV (positive) in the endolymph of the cochlear duct of the red-eared turtle. The physiological data from the hair cells of this species will be summarized from the following papers: Art and Fettiplace (1984); Art et al. (1982, 1984, 1985, 1986); Crawford and Fettiplace (1980, 1981 a,b, 1983, 1985); Fettiplace and Crawford (1978, 1980).

Three types of intracellular recording were obtained, attributable to hair cells, supporting cells or to nerve-fibre terminals. The sites of recordings were often verified through the injection of a fluorescent dye through the electrode. Hair cells had DC resting potentials as negative as −55 mV and a.c. receptor potentials at the stimulus frequency up to 45 mV peak-to-peak (Fig. 6.3). The receptor

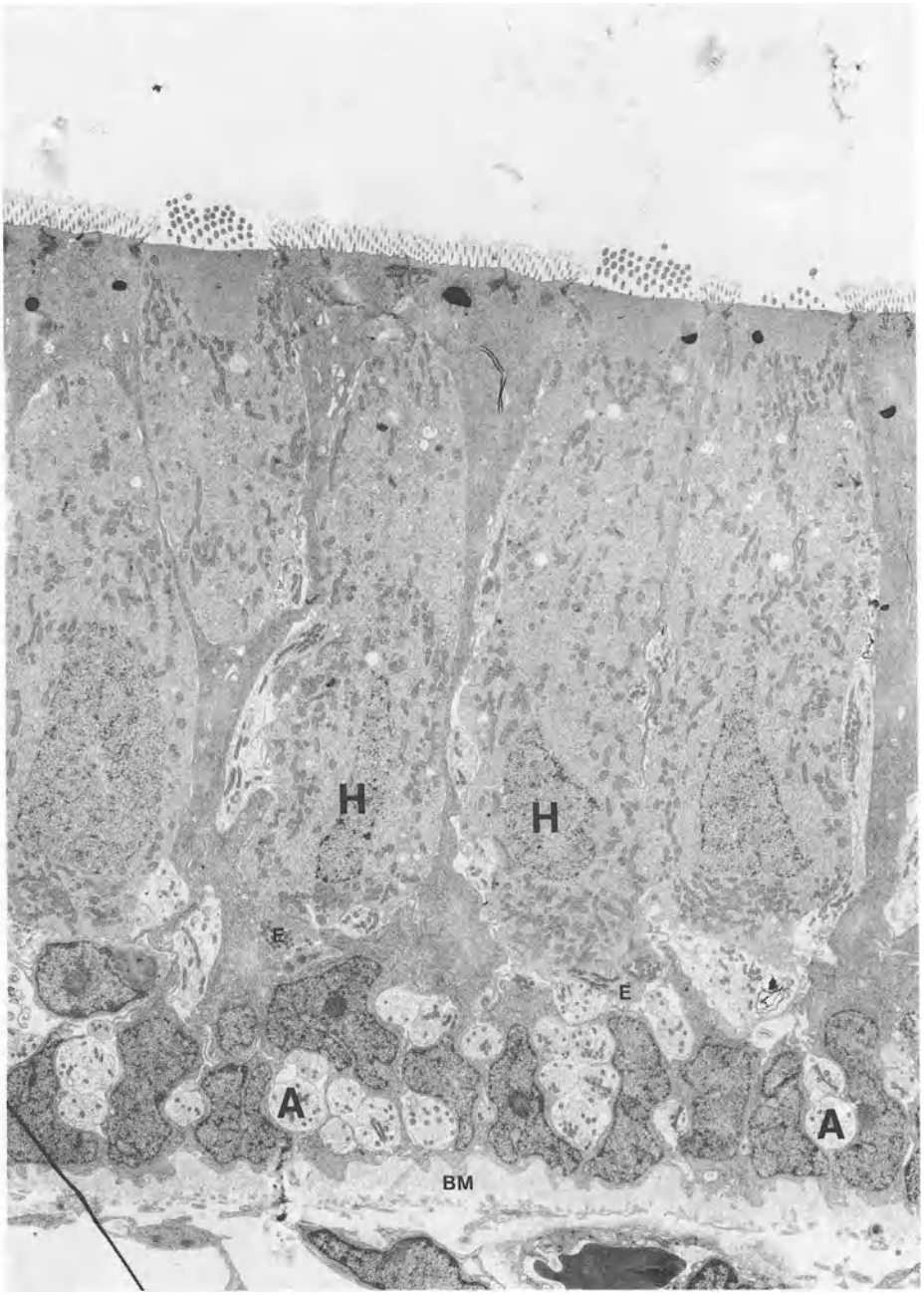

Fig. 6.2. Transmission electron micrograph of several hair cells (*H*) of the turtle *Chrysemys scripta,* to show the presence of afferent fibres (*A*) and terminals and efferent terminals (*E*) on the base of hair cells; *BM* basilar membrane. At the *top* can be seen many obliquely-cut stereovilli, the kinocilium of three hair cells and the (thinner) microvilli of the supporting cells, the latter being embedded in the tectorial-like mat. Each hair cell is 40–50 μm tall (Sneary, 1986)

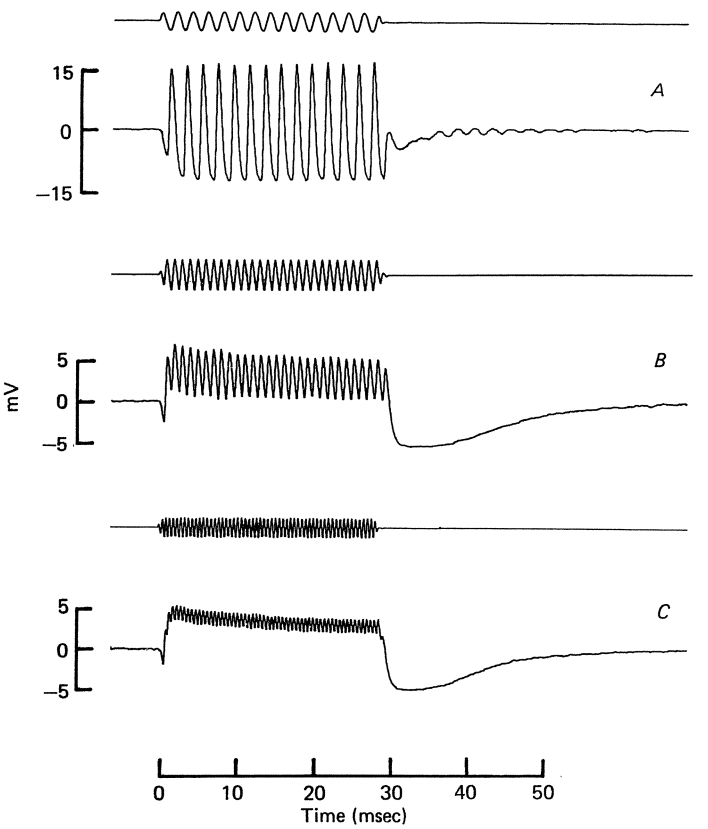

Fig. 6.3. Averaged (n = 32) receptor potentials of a hair cell with CF 425 Hz from the turtle *Chrysemys* to high-intensity tones at different frequencies (*A* 500 Hz, 120 dB SPL; *B* 1 kHz, 122.5 dB; *C* 2 kHz, 125 dB). The *upper trace* in each case is the sound monitor, the *lower trace* gives the hair-cell voltage with respect to its resting potential (−46 mV). Measurements taken at 25 °C (Crawford and Fettiplace, 1980)

potentials contained only relatively small DC components, a nonlinearity which was, however, larger at higher frequencies (up to 4–5 mV). These DC components for high-frequency stimulation (above 1 kHz) adapted with a time constant of about 10 ms, with consequent after-hyperpolarizations following stimulus offset. Probable nerve-fibre terminals had resting potentials of −60 mV and showed spontaneous synaptic potentials of up to 10 mV in amplitude, which could trigger action potentials. Supporting cells had large resting potentials (−80 mV) and no response to sound.

6.1.3.1 Tuning Properties of Hair Cells

To stimuli of frequencies below 1 kHz, hair cells gave essentially nonadapting graded responses which were highly nonlinear, saturating at higher sound-

pressure levels (SPLs), and restricted for each cell to a certain range of frequency (Fig. 6.4). At the onset and offset of the tones, the receptor potentials grew and decayed exponentially, a response pattern not unlike that observed in artificial tuned resonators. At higher SPLs, the frequency response range was wider, the iso-amplitude (receptor potential) 'tuning' curves being 'V'-shaped, as discussed in Chapter 2 for the electroreceptors of fish. Each hair cell had one frequency, the characteristic frequency (CF), to which it responded at the lowest SPL. The highest CF was about 670 Hz (Fig. 6.5). It was proposed that the responses of the hair cells in the frequency domain are the result of two filters, a sharply-tuned filter due to an electrical resonance of the hair-cell membrane and different for each cell, and a broader filter with similar characteristics for all cells and possibly reflecting the tuning of the entire basilar membrane (Fig. 6.6). The electrical resonance has properties closely resembling those already described for saccular hair cells (Sect. 2.4.2).

Loud, low-frequency stimulation of the hair cells below their CF produced damped oscillations on the waveform of the receptor potential (Fig. 6.7). This 'ringing' occurred on the depolarizing and hyperpolarizing phases and could also be produced by the injection of square-wave current pulses. The oscillation frequency for small current pulses corresponded very well to the acoustic CF, so that the 'ringing' frequency varied with the CF of the cell (Fig. 6.11 b). The ringing effect is due to the presence in the cell membrane of voltage-sensitive conductances in addition to the simply passive components of resistance and capacitance, as explained in Section 2.4.2. The inductive properties of the hair-cell membrane producing this effect could be responsible for the resonance of the sharply-tuned hair-cell filter whose phase responses are shown in Fig. 6.8. The fact that the oscillation frequency to small current steps and the acoustic CF of the cells are strongly correlated can be interpreted to mean that the receptor current in response to natural stimulation is filtered by the electrical properties of the hair-cell membrane in the same way as are the injected current pulses. This would imply that the filter takes effect after the production of the receptor current.

From the decay times of the ringing responses, tuning quality factors were calculated for individual hair cells. These Q-factors are reasonably similar to the tuning-curve sharpness measured during acoustic frequency sweeps, and are quantified as a measure of the frequency selectivity by measuring the response bandwidth 3 or 10 dB above the CF. The ratio of the CF to the bandwidth is then given as the 'Q' or quality factor of the tuning. In this case, $Q_{3\ dB}$ was in the range of 5 to 10, $Q_{10\ dB}$ was up to 3.5. The Q factor was independent of the criterion level of receptor potentials used to generate the tuning curves (1 mV, 10 mV, etc.) except at higher levels, where the tuning curves became blunter. Similarly, the tuning quality indicated for large current injections is poor.

From the responses to clicks, it was observed that hair cells depolarize as a result of a displacement of the basilar membrane up, towards scala vestibuli, and hyperpolarize for motion down, towards scala tympani (Crawford and Fettiplace, 1980). A similar conclusion was reached by subtracting the calculated phase shift of the electrical resonance circuit of each hair cell, which is responsible for a sharp phase transition in swept-frequency responses near the CF, from the total phase shift with frequency (Fig. 6.8).

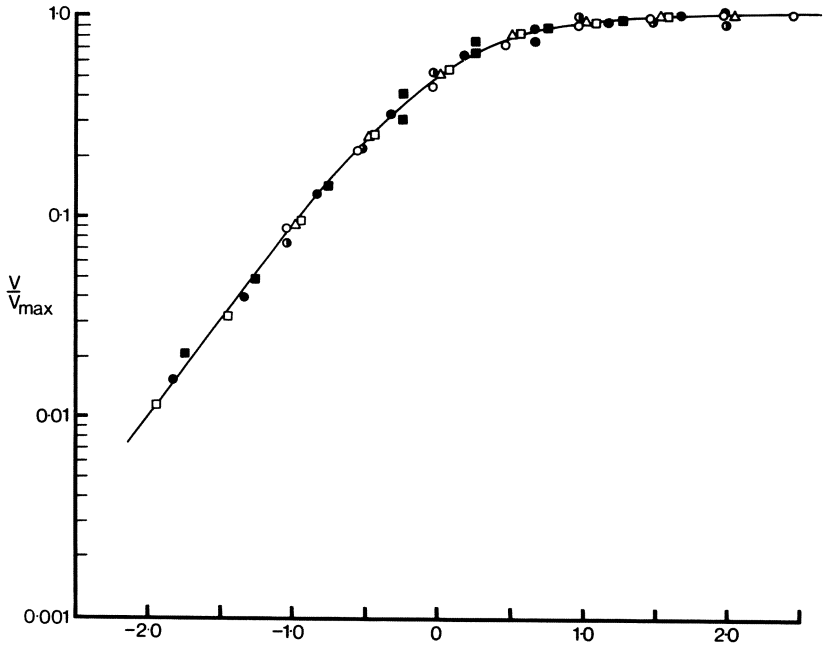
1·0
0·1
0·01
0·001
V/Vmax
-2·0
-1·0
0
1·0
2·0
log(P/P̄)

a

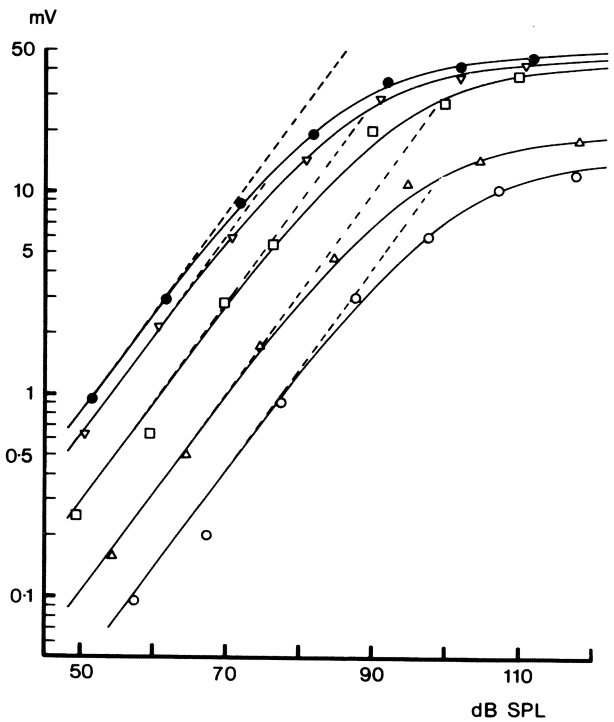
mV
50
10
5
1
0·5
0·1
50
70
90
110
dB SPL

b

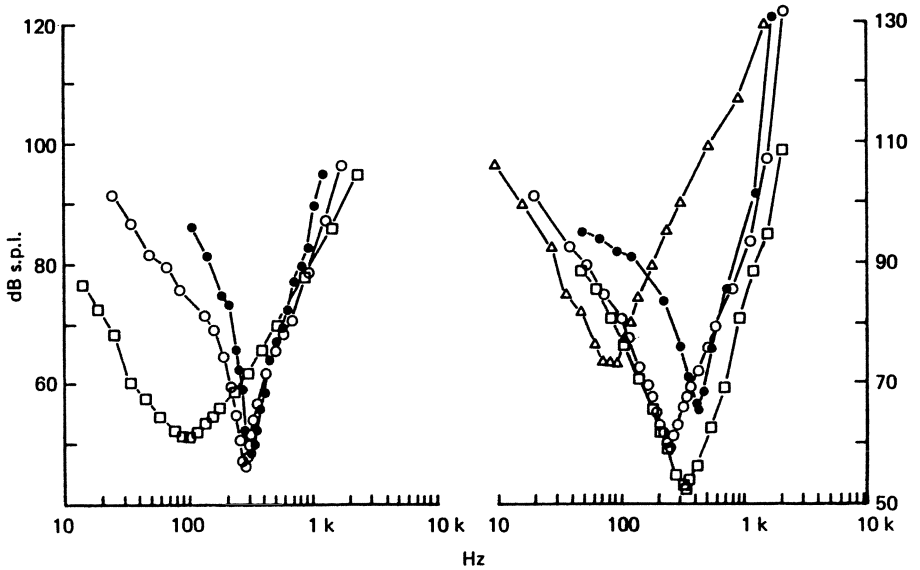

Fig. 6.5. Tuning curves for seven hair cells of the turtle *Chrysemys*, representing the SPL necessary to produce an AC response amplitude of 1 mV peak-to-peak, as a function of frequency. The SPL axis on the *right* is shifted 10 dB downwards relative to that on the *left* (Crawford and Fettiplace, 1980)

The CF of the individual hair cells was specific to the location within the papilla, with apical cells (only those on the free basilar membrane were measured) having low CFs, basal cells high CFs, and with a systematic trend between the two extremes (Fig. 6.9). When the distribution of CFs along the papilla was quantified, it was seen that the rate of CF increase with distance was up to 170 μm/octave (a doubling of frequency) in adult animals (Fettiplace, personal communication). For sharply-tuned cells, the 3 dB bandwidth of the tuning curve occupies a distance on the papilla of about one hair-cell width. Since it is unlikely that this kind of tuning is present in the mechanical response of the basilar membrane, these considerations strengthen the idea described below that electrical filtering contributes a substantial part of the hair-cell filter mechanism.

Fig. 6.4 a, b. A Intensity functions for six hair cells of the turtle *Chrysemys*. For each cell, the peak-to-peak amplitude of the AC response as a function of SPL is given for tone bursts at or near the CF. The plots are normalized, in that the ordinate gives the response as a fraction of the maximum response, and the abscissa is normalized to that sound pressure (=0) which produced a half-maximum response. The smooth curve is an empirical fit based on an equation for a rectangular hyperbola. *B* Intensity functions for one hair cell of *Chrysemys* at different stimulating frequencies, given as peak-to-peak response plotted against SPL. The frequencies are (*top to bottom* curve): 100, 58, 33.5, 500 and 840 Hz. The curves are empirical fits as in *A*. The *dashed lines* indicate a linear relationship between response and SPL. Resting potential of this cell was −55 mV, the temperature 21 °C (Crawford and Fettiplace, 1980)

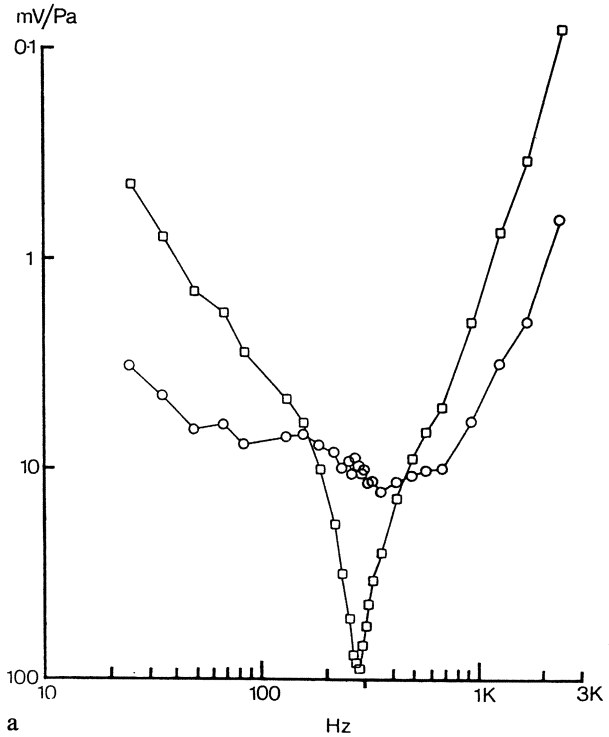

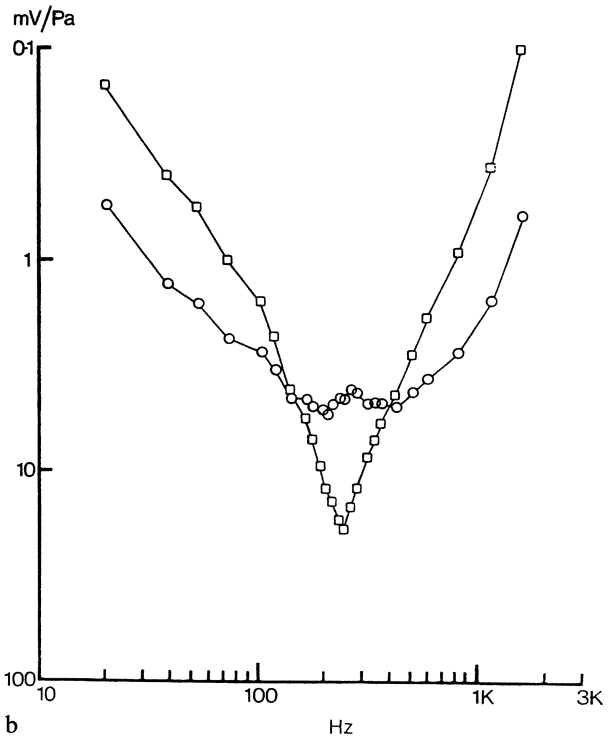

Fig. 6.6 a, b. Graphical representation of the tuning of two turtle hair cells (*A* and *B*) with (*open squares*) and without (*open circles*) electrical tuning of the cell membrane. Each sharply-tuned curve (*open squares*) is derived from an acoustical isointensity frequency sweep at low SPL. The response without electrical tuning (residual curve, *open circles*) was derived by dividing the sharply-tuned curve data by the normalized impedance of the electrical resonance calculated according to equations derived in the source paper using values for CF and Q of 274 Hz, 9.0 and 248 Hz, 4.0, respectively. The relative position of the residual curve on the ordinate is subject to certain assumptions (Crawford and Fettiplace, 1981 a)

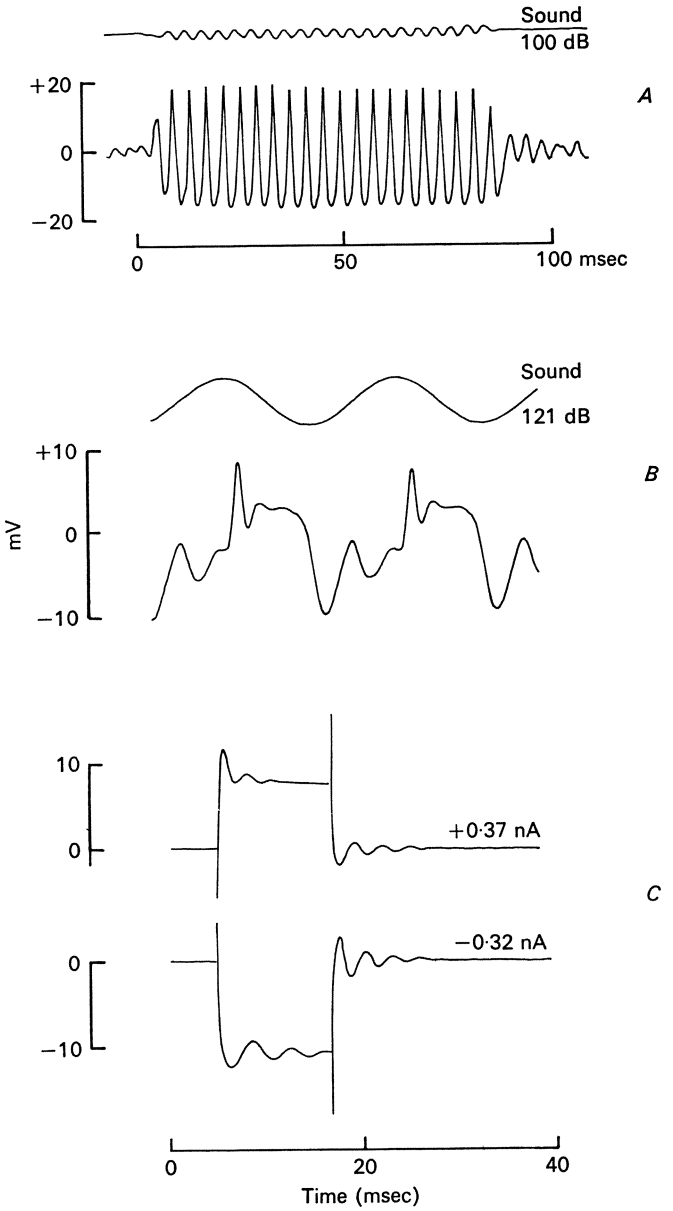

Fig. 6.7 A–C. Averaged intracellular responses to sound and injected electrical current in turtle hair cells, in terms of the voltage change from the resting potential (in these two cases −48 mV). *A* Response to a tone burst at the cell's CF (250 Hz) and 100 dB SPL. The *top trace* is the sound monitor. *B* Ringing' response to a low frequency (50 Hz), high-SPL tone burst in a cell of CF 340 Hz. *C* Responses in the same cell as in *B* to injected current pulses whose polarity and amplitude is indicated. The ringing frequency is higher for positive-going changes in cell potential than for negative-going changes (Crawford and Fettiplace, 1978)

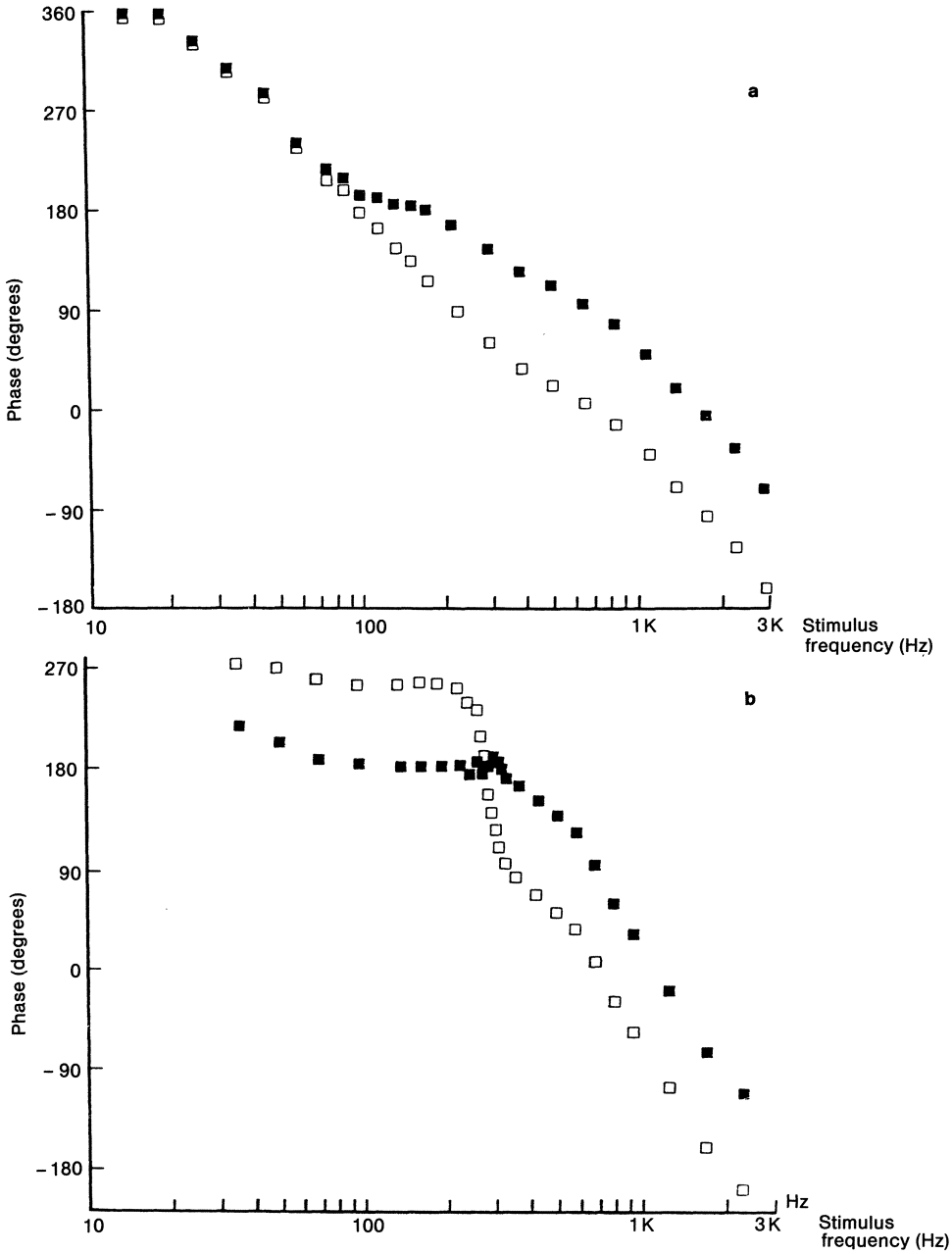

Fig. 6.8 a, b. Contribution of the hair-cell electrical resonance in the turtle *Chrysemys* to the linear phase behaviour of two hair cells. For each cell, the measured phase characteristic to a range of stimulus frequencies (*open symbols*) has been corrected by substraction of the expected contribution of the electrical resonance (calculated as given in source paper) to give the residual phase characteristic (*filled symbols*). Values of CF and Q assumed in the calculations were *A* 134 Hz, 1.07 and *B* 274 Hz, 9.0. All measurements corrected for the sound measuring and recording systems (Crawford and Fettiplace, 1981 a)

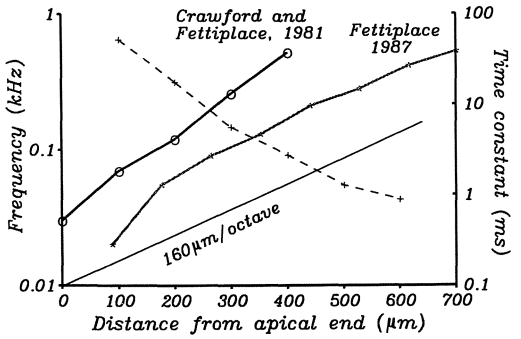

Fig. 6.9. Tonotopic organization of the basilar papilla of the red-eared turtle *Chrysemys scripta,* plotted as a function of distance from the apical end of the basilar membrane. The data are normalized to a papillar length of 700 μm. The *thin black line* represents a frequency distribution of 160 μm/octave. The measurements were made by determining the position of the tip of the electrode at the end of each recording. The data are after Crawford and Fettiplace, 1980 (*continuous line, open circles*) and Fettiplace, 1987 (*grey line, asterisks*). The *dashed line with crosses* shows the average time constants for hair cells at the various positions in the papilla and refers to the right ordinate (also after Fettiplace, 1987)

Response nonlinearity of the hair cells was also indicated by the presence of two-tone suppression, manifesting itself as the suppression of a CF response by a simultaneously-added second tone. At low SPLs, the tuning curves of the suppressive effect (on a constant response to a CF tone) are centred on and resemble the normal tuning curve, but are broader at higher sound-pressure levels (Fig. 6.10).

6.1.3.2 Ionic Basis of Electrical Tuning

The frequency of ringing varies with membrane voltage: increasing depolarization increases ringing frequency, while increasing hyperpolarization decreases ringing frequency, especially at the onset of the current pulse (Fig. 6.11). Since the ringing disappears at hyperpolarization levels of −80 mV, the reversal potential for potassium ions, it was proposed that a voltage-sensitive potassium conductance could be responsible. In more detailed later experiments, a large outward K^+ current and a smaller, more rapid inward Ca^{2+} current were found to be activated by a small depolarization of the cell from its resting potential. The addition of Cd^{2+} ions, which block the Ca^{2+} current, also blocked the K^+ current, suggesting that, as in the bullfrog sacculus (Sect. 2.4.2), the K^+ conductance is $[Ca^{2+}]$-dependent.

The relaxation time constant of the K^+ current is inversely proportional to the square of the resonant frequency, varying from 150 ms in the cells with the lowest CF to less than 1 ms in the highest. It was argued that the measured variation in the size and kinetics of the K^+ and Ca^{2+} currents is the main factor determining the electrical resonance frequency (Art et al., 1986; Art and Fettiplace, 1987). The magnitude of the Ca^{2+} conductance increases with resonant

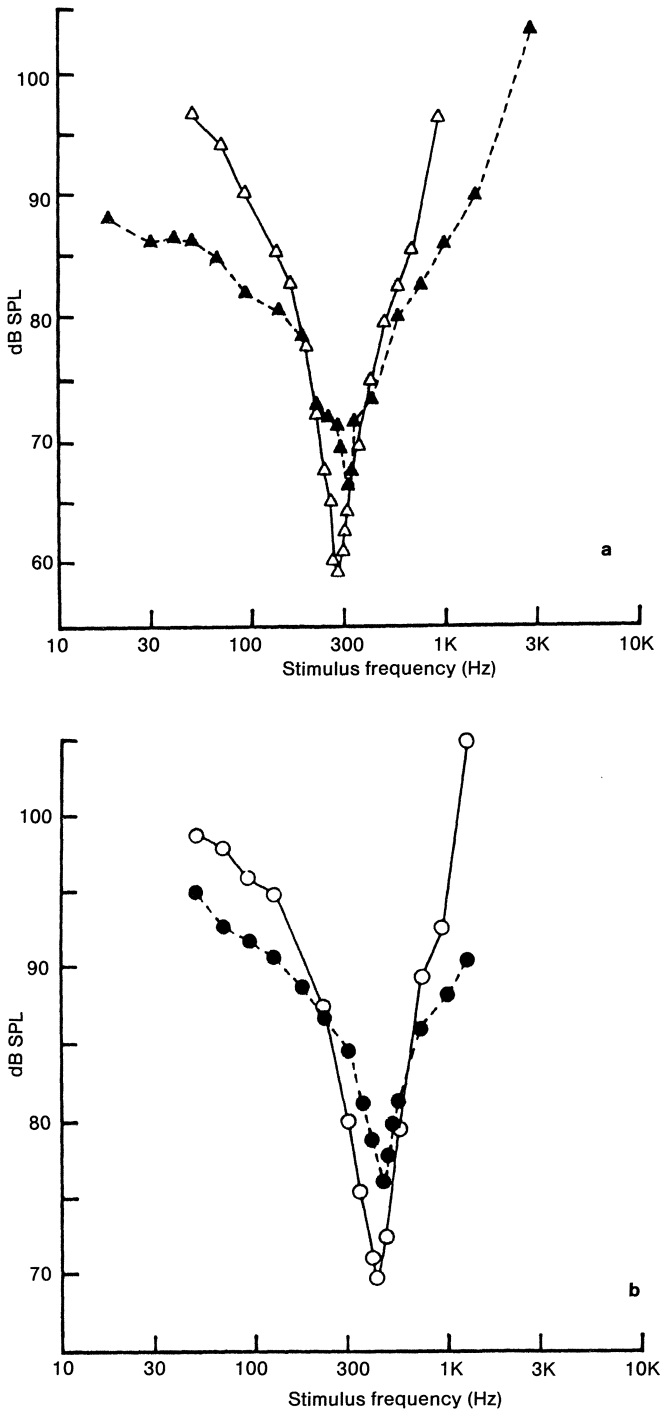

Fig. 6.10 a–b. Isoamplitude contours for intracellular responses of two different hair cells of the turtle *Chrysemys,* both in two stimulus situations; with single tones (*open symbols*) and under two-tone suppression (*filled symbols*). For the two-tone suppression curves, the *ordinate* represents the SPL of the suppressor tone required to produce a 20% reduction in the amplitude of the response to a test tone, the *abscissa* is the frequency of the suppressor tone. For cell *a* (CF = 275 Hz), the frequency and SPL of the test tone and response criterion voltage were 275 Hz, 60 dB and 4 mV. For the second cell *b* (CF = 425 Hz), the values are: 450 Hz, 79 dB and 2.7 mV (Crawford and Fettiplace, 1981 b)

Fig. 6.11 a, b. Frequency of the voltage oscillations (*ordinate*, in Hz) produced by rectangular current injections in hair cells of the red-eared turtle *Chrysemys scripta* as a function of current strength (*abscissa*, in nA). *a* A cell with CF 353 Hz. *Filled circles:* oscillations at current "on"; *open circles:* oscillations at current "off". The *open circles* show that after current injections of different strength, the oscillation frequency returned to about the same baseline value. Smooth curves are derived from equations derived in the source paper. *b* Correlation between the acoustical CF and the electrical CF (oscillation frequency resulting from turning *off* small current injections as in *a*) for different hair cells. The *line* has a slope of 1.0 (Crawford and Fettiplace, 1981 a)

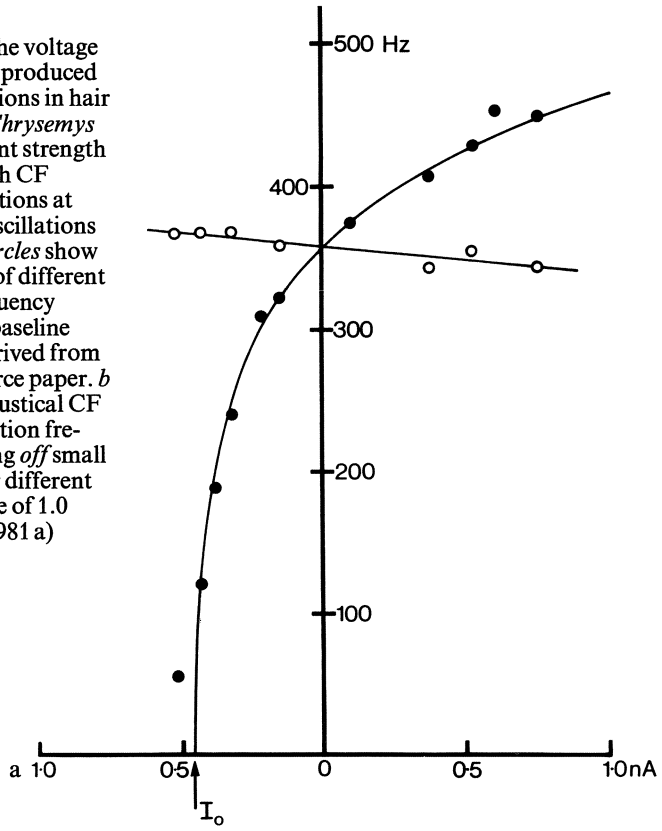

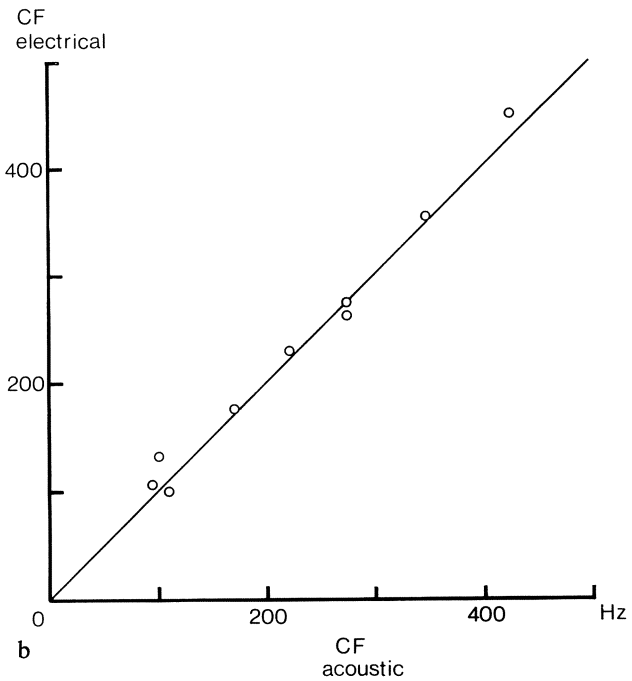

frequency, whereas the K^+ conductance shows faster kinetics and a smaller increase in size in higher-CF cells. Similar findings were discussed for the frog saccular hair cells in Section 2.4.2. The fact that these properties are graded monotonically with distance along the basilar papilla (Art and Fettiplace, 1987) make it reasonable to assume that the electrical tuning of hair cells is the major determinant of the frequency response properties of this hearing organ (Fettiplace, 1987). Interestingly, the electrical filter manifested itself even in the absence of acoustic stimulation. In the unstimulated state, the hair-cell membrane potential fluctuated constantly (amplitude 5–10 mV, several times larger than the near-threshold hair-cell responses; Fig. 6.12). Spectral analysis of this membrane noise indicated principal frequency components near the cell's CF. As the oscillations did not correlate with random acoustic noise at the tympanum, it was concluded that they arise within the hair cells themselves.

Detailed studies of the hair-cell current-voltage relationships indicate that the transduction current is due to the sound modulating the hair-cell permeability to an ion or ions with an equilibrium potential of near zero (Fig. 6.13). This could be a potassium and/or chloride current exchanged with the endolymph or a non-selective conductance change to ions of the perilymphatic space. At the condensation peaks of sound pressure, the opening of transduction channels reduces the cell membrane resistance and time constant to half their original value (e.g., 100 MΩ to 50 MΩ, 2 ms to 1 ms).

6.1.3.3 Efferent Effects on Hair Cells

Electrical stimulation of efferent axons to the hair cells produced slow, long-lasting, hyperpolarizing synaptic potentials (IPSP). The IPSPs are up to 30 mV in size. They reduce the receptor potential amplitude by up to 95% and also reduce the sharpness of tuning of the hair cell (Figs. 6.14 and 6.15a; Fuchs et al. 1983). Single shocks to the efferent-fibre bundle generate a hyperpolarization of about 1 mV for 100 ms. The effect of a hyperpolarization is large (Fig. 6.15b), an IPSP of 2.6 mV reduced the amplitude of a 9 mV receptor potential by half. Threshold depression of the hair cell resulting from large efferent discharge bursts could be more than 70 dB. The reversal potential of the synaptic hyperpolarization was near -80 mV. Evidence from experiments involving changing the potassium concentration of the perilymph or introducing the potassium-channel blocker TEA indicates that the current is carried by potassium ions leaving the cell. These data are very similar to results of experiments on lateral-line efferent effects (Flock and Russell, 1976).

There is evidence that the efferent effect is mediated only via the hair cells and that there are no direct effects on afferent fibres. As adding acetylcholine to the perilymph causes a transient hyperpolarization, and the efferent effects were reversibly blocked by curare or atropine, it is likely that the efferent transmitter is acetylcholine. The efferent effect seems to be due both to a reduction in the size of the receptor potential as well as a hyperpolarization of the hair cell, at least for frequencies near the CF.

6.1.4 Direct Stimulation of the Stereovillar Bundle

In preparations in which the papilla was excised, the stereovillar bundles of single hair cells were deflected directly using a piezo-driven, fine glass fibre pushed against the bundle while recording intracellularly from the cell (Crawford and Fettiplace, 1985; Art et al., 1986). Measurements of the stiffness of the bundle at different positions indicated that the stereovilli rotate stiffly about an axis near the apical pole of the cell. Displacements of the bundle towards the kinocilium produced depolarization. The mechanical sensitivity was estimated to be better than 0.1 mV/nm, and the depolarization saturated for displacements near 80 nm.

A step displacement of the glass fibre caused not only a step displacement of the bundle, but also a damped oscillation of both the bundle and the membrane potential (Fig. 6.16). The oscillations of the bundle resembled strongly the membrane oscillations. The mechanical oscillations of the bundle were graded with step size up to 20 nm peak-to-peak and were reduced by those current injections into the cell that reduced the oscillations of the receptor potential. The resonant frequencies were different for different cells and varied systematically along the papilla, as in CF measurements of receptor potentials in the more intact preparation. It was concluded that opening the cochlear duct and removing the tectorial membrane for these experiments did not seriously affect the frequency organization of the basilar papilla.

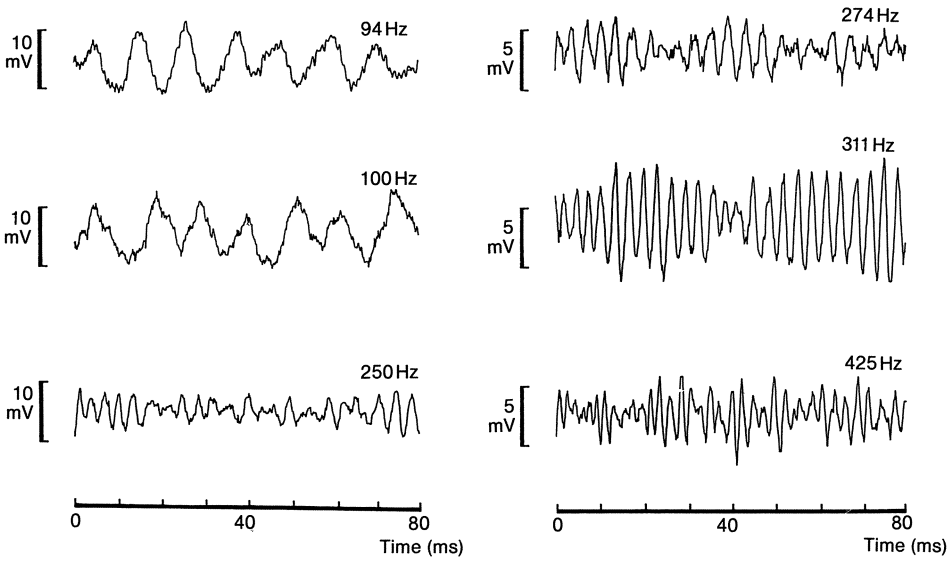

Fig. 6.12. Voltage fluctuations in intracellular recordings from six different turtle hair cells in the absence of sound stimulation. Beside each trace is given the cell's CF and a voltage scale. The major frequency components in the voltage noise are correlated with the CF of the individual cells, the authors give data for three cells indicating that the peak frequency of the noise was within 10% of the cell's acoustic CF (Crawford and Fettiplace, 1980)

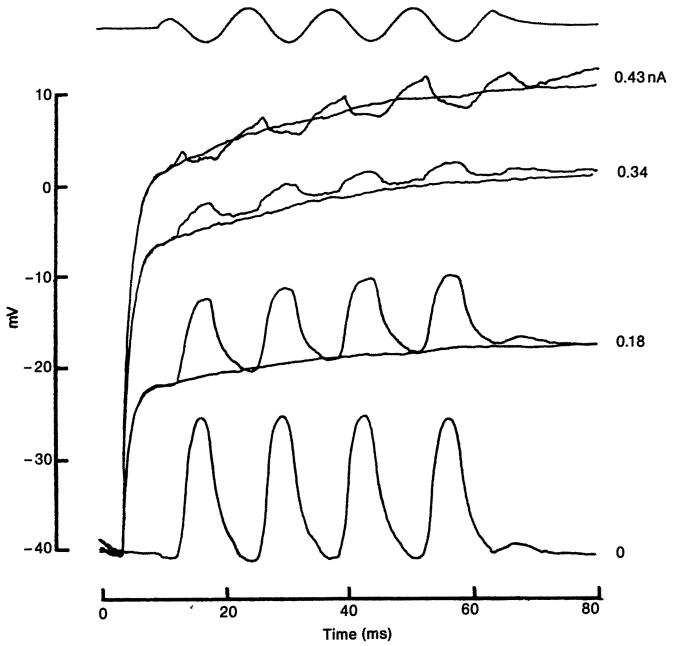

Fig. 6.13. Averaged hair-cell responses to a 77 Hz, 122 dB SPL tone burst showing the phase reversal induced by the injection of steady, positive current. *Top trace* is the sound monitor, other averaged traces give the responses during injections of different current strengths as indicated on the *right* of each trace. The *ordinate* is the intracellular voltage. The receptor potential reverses phase in the 0.43 nA trace, the reversal potential is near 0 mV. The three middle traces also give the time course of the current injection in the absence of sound stimulation. Cell CF was near 100 Hz (Crawford and Fettiplace, 1981 b)

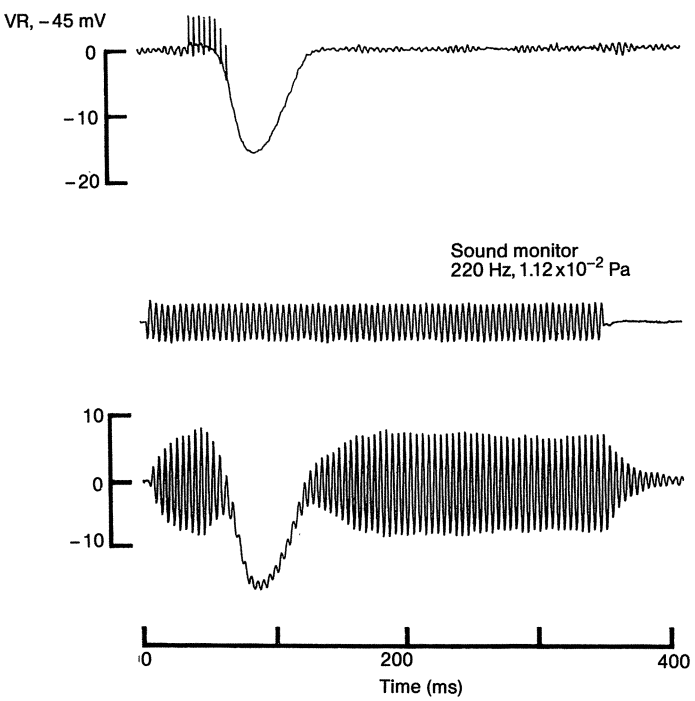

Fig. 6.14. Top trace: a large inhibitory postsynaptic potential (IPSP) in a hair cell of the turtle *Chrysemys*, resulting from 8 shocks to the efferent fibre bundle supplying the basilar papilla. The timing of the stimulation is given by the upward-going artefacts in the trace. The averaged (55 times) potential change is shown relative to the resting potential (−45 mV). The *lower trace* shows the efferent effect in combination with a tone burst (sound monitor in *middle trace*). The efferent stimulation strongly reduces the amplitude of the cell's response to sound (Fuchs et al., 1983)

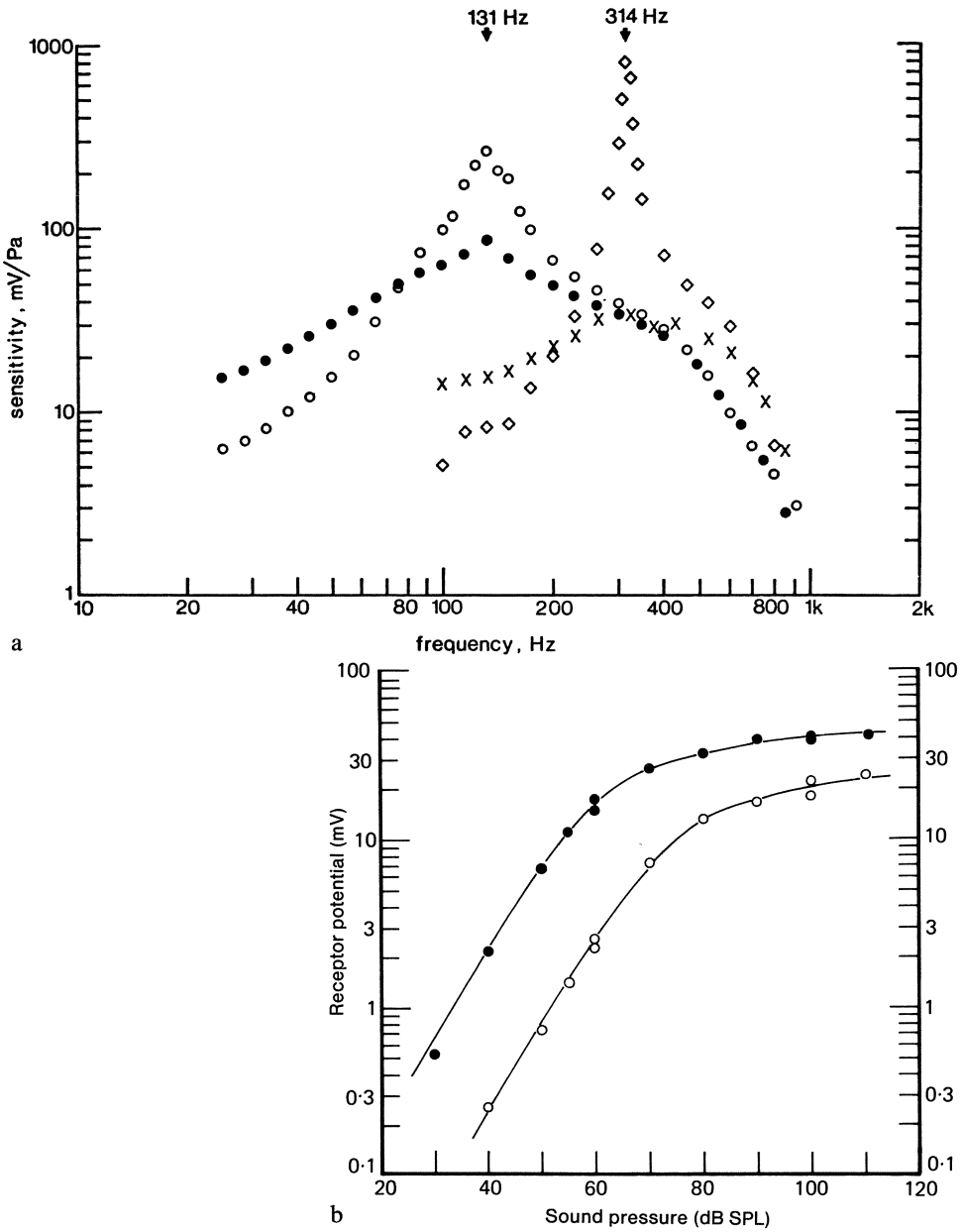

Fig. 6.15 a, b. Effects of efferent-fibre stimulation on sound-evoked responses of hair cells of the red-eared turtle *Chrysemys scripta*. *a* Isointensity hair-cell frequency-response curves in the absence and presence of continuous efferent stimulation at 50/s. Sensitivity for both cells (r.m.s voltage divided by sound pressure) is plotted as a function of frequency for sweeps at 45 dB SPL and 55 dB SPL (*open symbols*, without efferent stimulation); *closed symbols* and *crosses*, with efferent stimulation). The IPSP magnitude was 5 mV and 8 mV for the lower- and higher-CF cells, respectively (Fuchs et al., 1983) *b* Intensity functions for the hair-cell receptor potential as a function of SPL with (*open symbols*) and without (*closed symbols*) efferent stimulation during tone bursts at 204 Hz (near CF). The *upper curve* was drawn by eye through the control points and then displaced to the right and down to overlie the experimental curve. Efferent stimulation both shifts the curve to higher SPLs and reduces the magnitude of the saturation response (Art et al., 1984)

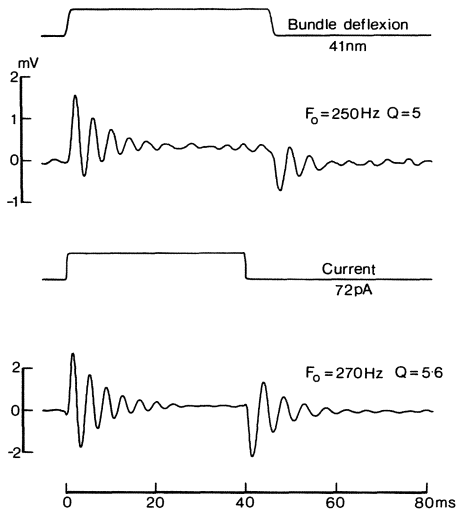

Fig. 6.16. A comparison of the averaged responses of a hair cell of the red-eared turtle *Chrysemys scripta* to mechanical deflections of the stereovillar bundle of 41 nm (*top*, time course of bundle deflection is indicated; upwards is towards the kinocilium) and to the injection of rectangular depolarizing currents of 72 pA through the intracellular electrode (*bottom*, upwards is depolarizing). *Ordinates* are membrane potentials relative to the resting potential (−44 mV). Values for the resonant frequency (*Fo*) and quality factor of the tuning (*Q*) for the onset oscillations are shown in each case (Art et al., 1986)

Small, injected currents into the hair cell could cause the same kind of oscillating motion of the stereovillar bundle, with a displacement amplitude of up to 10 nm (Crawford and Fettiplace, 1985). Movements occurred towards the kinocilium for depolarizing currents and away from the kinocilium for hyperpolarizing currents. If the force driving the bundle can stimulate transduction, and transduction currents then influence the cell's mechanical response, these electrically-induced bundle deflections would operate as a feedback system. The mechanical feedback from the cell is of the correct polarity to be a positive feedback (Art et al., 1986). The oscillating motion of the bundle is not a prerequisite for the production of an oscillating voltage, as the cell potential shows oscillation even when a very stiff fibre is used to produce a step response of the bundle. Thus, Art et al. suggest that the cell-membrane properties are the primary determinants of the oscillation frequency. The general problem of the significance of electro-mechanical behaviour in hair cells and its possible importance in augmenting passive mechanical processes is briefly discussed in Section 14.9.

Interestingly, the stereovillar bundles showed spontaneous mechanical oscillations which had spectral components within a narrow band of frequencies specific to each cell. The spontaneous mechanical oscillations correlated very well in time and spectral content with the oscillations of membrane potential of the cell (Fig. 6.17). As described above, the electrical filter properties of the cell membrane restrict the oscillations in the potential to a narrow band of frequencies. It was suggested that the hair-cell bundle is being driven by the oscillations in the cell-membrane potential, and that the hair cell contains a force-generating mechanism (Crawford and Fettiplace, 1985). This effect may be a factor influencing the extremely low resonant frequencies of these very tiny bundles (below 1 kHz). The calculated torque behind such spontaneous oscillations is about one tenth of that generated by a motile cilium, the force being about the same as that generated by a single skeletal-muscle cross-bridge. The elucidation of the con-

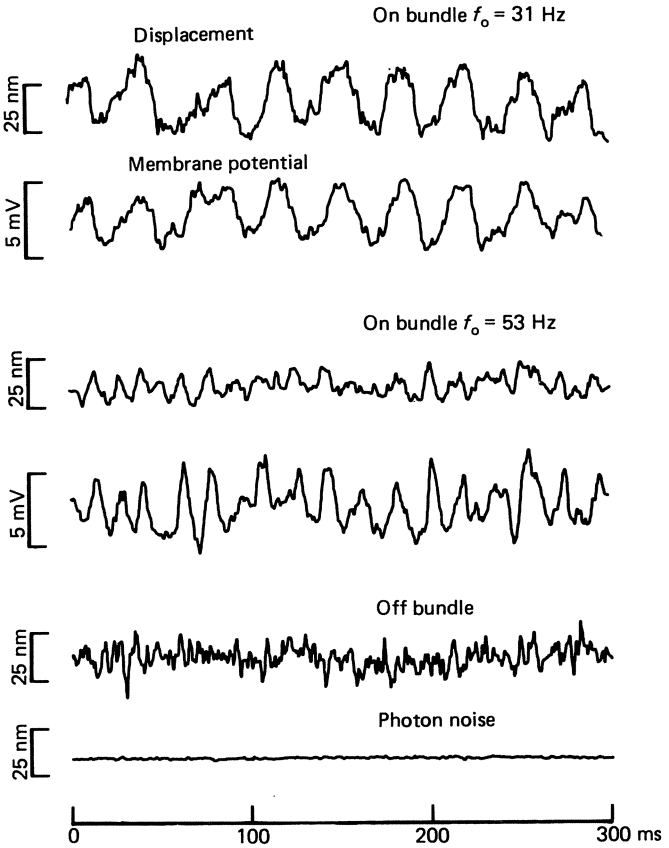

Fig. 6.17. Correlation between spontaneous mechanical and electrical activity in hair cells of the red-eared turtle *Chrysemys scripta*. The top two pairs of traces are single sweeps of simultaneously-recorded stereovillar bundle displacement and cell membrane potential of two different hair cells, the displacement being measured via the motion of a flexible fibre attached to the bundle. A sample of the motion of this fibre not attached to a bundle is shown in the lower part of the figure, together with the noise of the photodetector when the fibre was not in the light beam. The r.m.s. displacement for the cell with CF 31 Hz was 11.2 nm, that of the 53 Hz cell was 6.0 nm, off-bundle was 5.7 nm (Crawford and Fettiplace, 1985)

tributions of the various factors involved in the hair-cell response to sound is thus complicated by the presence of an *intracellular feedback* mechanism.

6.1.5 The Activity of Auditory-nerve Fibres

Not surprisingly, the activity of the afferent nerve fibres innervating these hair cells accurately reflects the hair-cell activity described above. The shape and sharpness of the tuning curves and the rate functions can so be accurately predicted. The tuning curves are approximately symmetrical when plotted on a logarithmic frequency scale (Fig. 6.18a; Crawford and Fettiplace, 1980). The nerve fibres are tonotopically organized according to the place-dependent hair-cell tuning; the CF range is 30 to 700 Hz. The best sensitivity of the fibres is about 30 dB SPL and the sharpness of tuning ($Q_{10\ dB}$; for definition see Fig. 6.18) increases with increasing CF from a mean value near 1 at CF 100 Hz to 5 near CF 600 Hz (Fig. 6.18b). Similar data were reported by Paton et al (1976) from the auditory nerve of this species. Neighbouring nerve fibres of similar CF had $Q_{10\ dB}$ differing by a factor of 2.

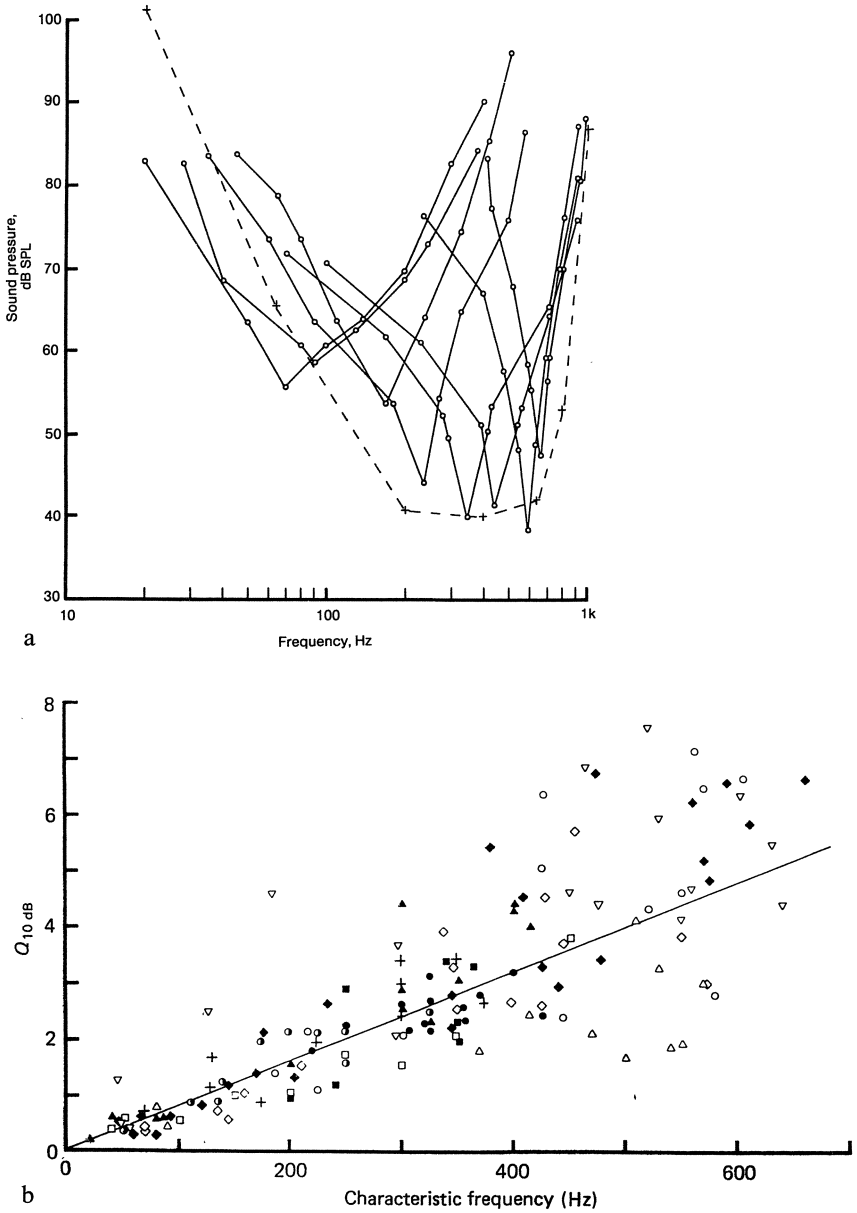

Fig. 6.18 a, b. Shape and sharpness of tuning curves of the red-eared turtle *Chrysemys scripta*. *a* Rate-threshold tuning curves for eight single auditory-nerve fibres as a function of stimulus frequency. The *ordinate* gives the SPL necessary at different frequencies to produce a threshold response of the fibre. Temperature was 22 °C. The *crosses* joined by the *dashed curve* are the mean auditory thresholds derived from behavioural experiments of Patterson (1966). *b* Sharpness of tuning of single auditory-nerve fibres, given as the quality factor Q_{10dB} (CF divided by bandwidth 10 dB above threshold at CF) and plotted against the CF of the fibre in each case. The different *symbols* represent data from 11 different animals. The *line* was drawn by eye and represents a constant 10 dB bandwidth of 125 Hz (linear frequency axis) (Crawford and Fettiplace, 1980)

The spontaneous activity of the fibres varied from several to about 70 spikes/s, although details about spontaneous activity are lacking. In 33 of 40 fibres examined, a clear periodicity in the interval histograms of the spontaneous activity was found. These 'preferred intervals' presumably reflect the spontaneous oscillations in membrane potential of the innervated hair cells (Fig. 6.19; Crawford and Fettiplace, 1980).

In response to stimuli at low sound levels, the spikes were synchronized to the sound waves and, in general, the responses of the nerve fibres to tonal stimulation were very well phase-locked. Above threshold level (defined as a just-noticeable rate increase), the firing rate of afferent nerve fibres to CF-stimuli increased over a dynamic range of about 25-40 dB. Using a piezo-electric probe to drive the basilar membrane, it was shown that the r.m.s. basilar-membrane displacement equivalent to a threshold response of auditory-nerve fibres was near 0.1 nm (Crawford and Fettiplace, 1983).

To a large extent, the effects of the stimulation of efferent nerve fibres on the activity of afferent fibres can also be predicted from their known effects on hair cells. Nerve fibres ceased to respond to sound for a relatively long period following shocks to efferent fibres (Fig. 6.20 a; Art and Fettiplace, 1984). Tuning curves of afferent fibres become broadened and their threshold elevated (up to 80 dB; Fig. 6.20 b). For small inhibitory effects, this threshold elevation is largely due to the loss of the sharply-tuned area of the tuning curve near the CF. The tuning curves of fibres initially having very different $Q_{10\ db}$ values each had about the same tuning-curve shape and Q-value during efferent activity ($Q_{10\ dB} = 0.8$; Fig. 6.20 b). The slope of the rate functions of the afferent fibres and their maximal firing rates were both reduced by efferent stimulation and the functions shifted to higher SPLs (Art et al., 1985). The dynamic ranges of a sample of fibres were increased from 23 dB to 36 dB for 4 to 11 shocks to the efferents (Art and Fettiplace, 1984).

The activation of the efferents, parallel to raising threshold, leads to an improved dynamic range and temporal resolution of the responses of the afferent nerve fibres. However, it is not possible at this stage to delimit the function of these inhibitory fibres, as it is not known under what conditions they are normally active.

6.1.6 A Behavioural Audiogram for the Red-eared Turtle

It is a remarkable fact that there is only one single behavioural audiogram for a reptile species – that determined by Patterson (1966) for *Pseudemys (Chrysemys) scripta* (see Fig. 6.18 a). This is to some extent due to the difficulty of finding a paradigm appropriate to the behaviour of individual species, although there have been a number of clever but unsuccessful (and unpublished!) attempts. Using a negative-reinforcement conditioning procedure, Patterson was able to determine clear behavioural thresholds to seven frequencies, ranging from 20 Hz to 1 kHz. The data are in good agreement with the lowest thresholds of primary auditory-nerve-fibre thresholds of this species (see above, Crawford and Fettiplace, 1980).

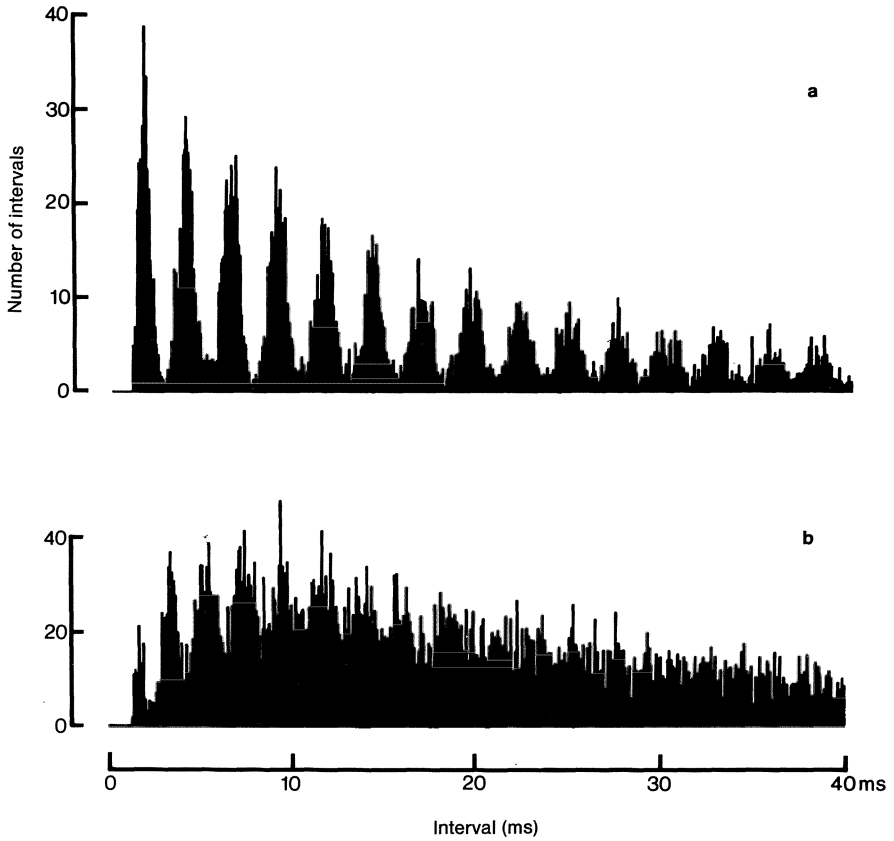

Fig. 6.19 a, b. Interspike-interval histograms for the spontaneous activity of two auditory-nerve fibres in the red-eared turtle *Chrysemys scripta. a* CF 380 Hz, threshold 43.5 dB SPL, spontaneous rate 43 spikes/s. *b* CF 480 Hz, threshold 44.6 dB SPL, rate 33 spikes/s. Bin width was 80 μs. The periods of the preferred intervals correlate with the CFs (Crawford and Fettiplace, 1980)

Fig. 6.20 a, b. Effect of the stimulation of efferent fibres on the activity of afferent fibres in the turtle *Chrysemys. a* Effect of efferent stimulation on the response activity of a single auditory-nerve fibre to a CF tone, 20 dB above threshold. The *top trace* is the sound monitor and also indicates the time of shocks to the efferent fibres; the *middle trace* is a single sweep showing the extracellularly-recorded spikes of the fibre. At the *bottom* is a histogram of 90 superimposed responses (bin width 2 ms). Efferent stimulation results in a long-lasting inhibition of activity. *b* Frequency-threshold tuning curves for two auditory-nerve fibres of the turtle *Chrysemys* without (*open symbols*) and with efferent stimulation (six shocks, *closed symbols*). On the left, the middle curve is with only a five-shock train to the efferents, which mainly produces an effect at frequencies near the cell's CF. Temperature was 26.5 °C (Art and Fettiplace, 1984)

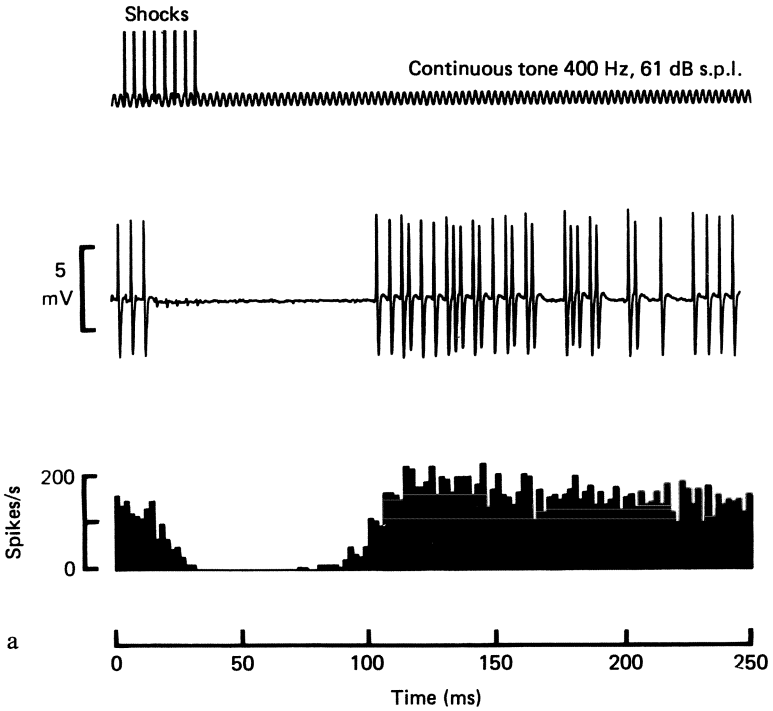
Shocks
Continuous tone 400 Hz, 61 dB s.p.l.
5
mV
200
Spikes/s
0
a
0
50
100
150
200
250
Time (ms)

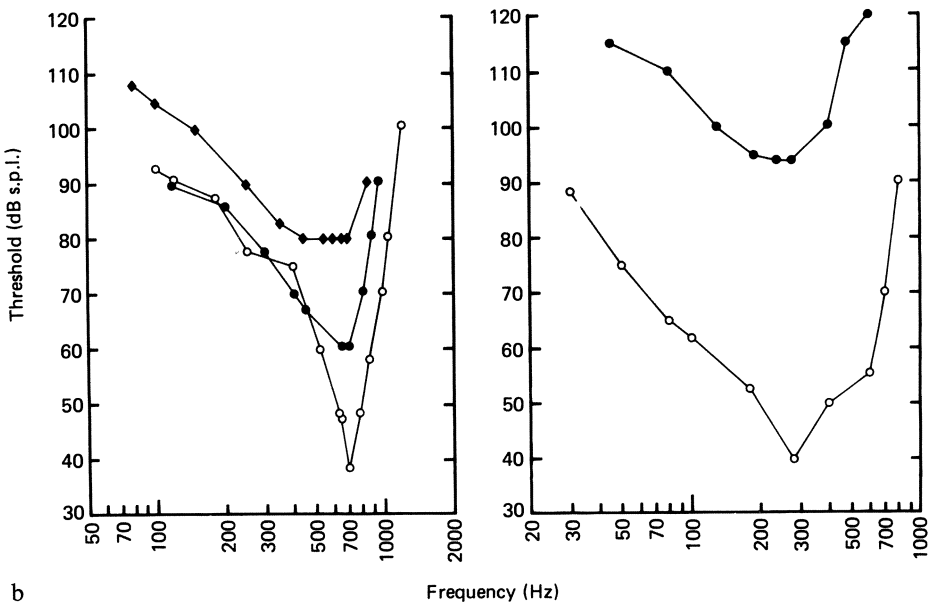
Threshold (dB s.p.l.)
120
110
100
90
80
70
60
50
40
30
50
70
100
200
300
500
700
1000
2000
20
30
50
70
100
200
300
500
700
1000
b
Frequency (Hz)

6.2 The Hearing of Snakes

The fallacy that snakes are deaf is one of the most obstinate rumours about hearing in vertebrates. One of those responsible for this fairy tale is certainly W. von Buddenbrock (cited in Hartline and Campbell, 1969), who concluded (translated) "According to all that we now know, the snakes must be regarded as totally deaf." Of course, as with the lizards, it is extremely difficult to make casual and

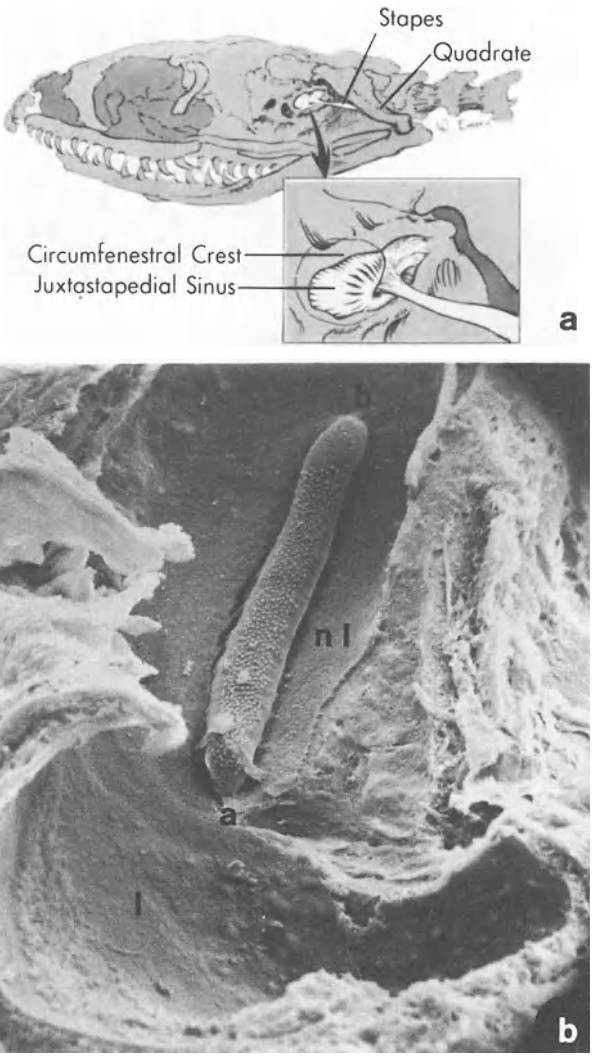

Fig. 6.21 a. Drawing of the lateral aspect of the skull of a snake to show the relationship between the columella (here, labelled *stapes*) and the quadrate bone. *b* Scanning electron micrograph of the papilla of the boid snake *Epicrates cenchris* (rainbow boa). *l* Lagena; *a* apical; *b* basal; *nl* neural limbus. The tectorial membrane has been removed. The papilla is about 500 μm long (Miller, 1978 a)

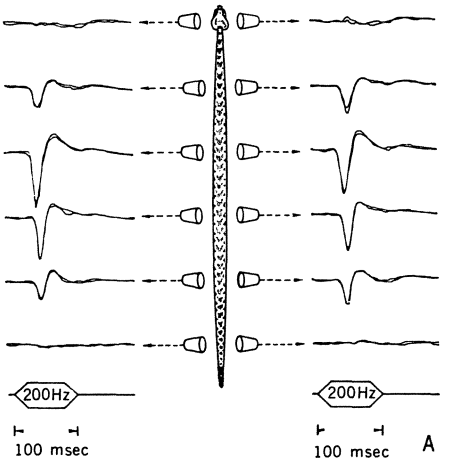

Fig. 6.22. Averaged responses (n = 20) of the neural elements in the mid-brain of the rattlesnake *Crotalus viridis* to localized sound (200 Hz, 70 dB SPL), shown for different positions of the loudspeaker along the length of the body. The largest responses are evoked with the loudspeaker near the lungs (Hartline and Campbell, 1969)

even scientific observations which would indicate any kind of reaction to sound in snakes. The observations sometimes mentioned in books can all be attributed to inadvertent visual cues.

As noted in Chapter 4, the papilla of snakes (Fig. 6.21 b) is similar to that of *Sphenodon*, being relatively small and having only unidirectionally-oriented hair-cell areas. In this respect, it is similar to that of the red-eared turtle. That the snake inner ear generates cochlear microphonics was established by Wever and Vernon (1960), who found a good sensitivity in the range of 80 to 700 Hz. These authors concluded that the fact that the quadrate plays a role in sound transmission points to a significant input to the ear through the tissues of the body (Fig. 6.21 a).

In a careful study of evoked and single-unit potentials in the midbrain of species of three families of snakes, Hartline and Campbell (1969) and Hartline (1971 a,b) established beyond doubt that sounds evoke electrical activity in the brain of snakes. While it is not the purpose of this book to discuss neural information processing in the auditory pathway of the brain of reptiles, I will briefly outline their results, as we have no information on neural activity in the auditory nerve of these animals.

Using both air-borne sound and substrate vibration and carefully controlling the acoustic pathways to the ear, these authors demonstrated responses to sound and to vibration in neighbouring areas of the midbrain. The responses to sound were, for the low frequencies involved, relatively sensitive, being 35 dB SPL at the peak sensitivity near 200 Hz. Above 500 Hz, however, the responses rapidly became less sensitive, so that at 1 kHz, more than 100 dB SPL was necessary to elicit a response. During investigations of sound transmission to the inner ear, it was noted that hearing was most sensitive when the loudspeaker was near the animal's lung area. It was even more sensitive over the lung than over the ear (Fig. 6.22). The sound apparently causes larger tissue motions near the lung, which transmit to the head and stimulate the ear. As Miller (1968) noted, the inner ear is better developed (or less reduced) in burrowing than in ground-living snakes, and better developed in the latter than in tree-living snakes. These differences point to definite functions of the ear in the life of the animal.

Chapter 7

The Alligator Lizard and Granite Spiny Lizard

Anguid lizards are found on most continents and most have strongly reduced limbs. The alligator lizard of western North America is exceptional, in that it has relatively well-developed limbs and moves in a similar way to most other lizards. Since 1974, an extensive series of reports has been published on the structure and response activity of the hearing organ of the alligator lizard, *Gerrhonotus multicarinatus*, a member of the Anguidae. This is mainly work from the laboratory of T.F. Weiss, Massachusetts Institute of Technology. More recently, interesting parallels to the data from the alligator lizards have been described in the (not very closely related) iguanid granite spiny lizard, *Sceloporus orcutti*. Iguanids are, with very few exceptions, restricted to the new world. *Sceloporus* and similar lizards are typical insect catchers of warm, dry regions of N. America. As mentioned in Chapters 1 and 4, there are strong anatomical similarities between the ears of iguanid, agamid and anguid lizards. The present chapter also describes similarities in the physiological data.

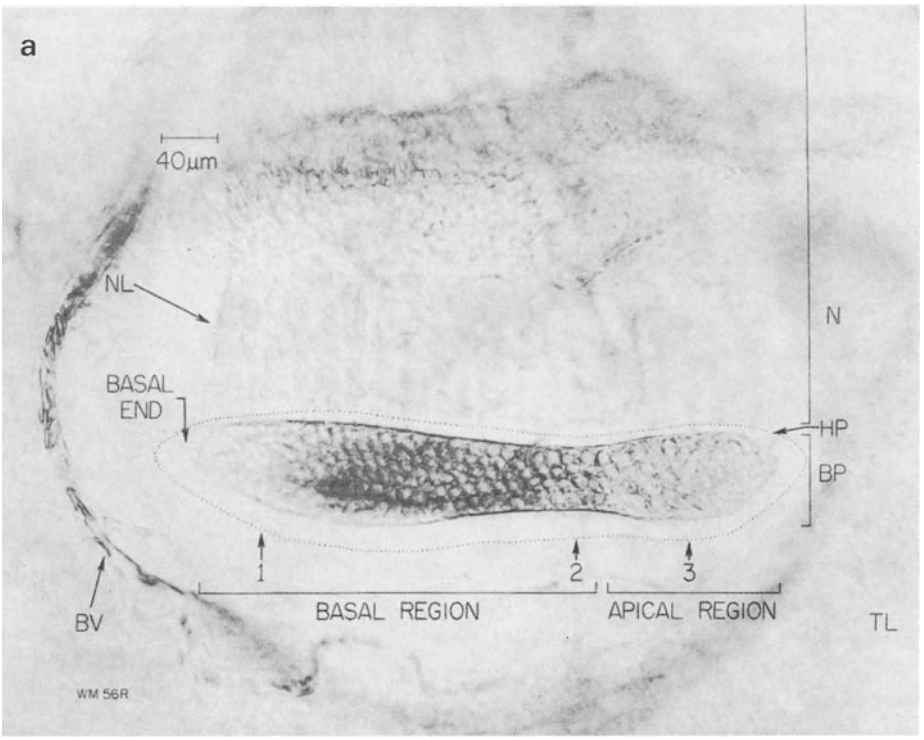

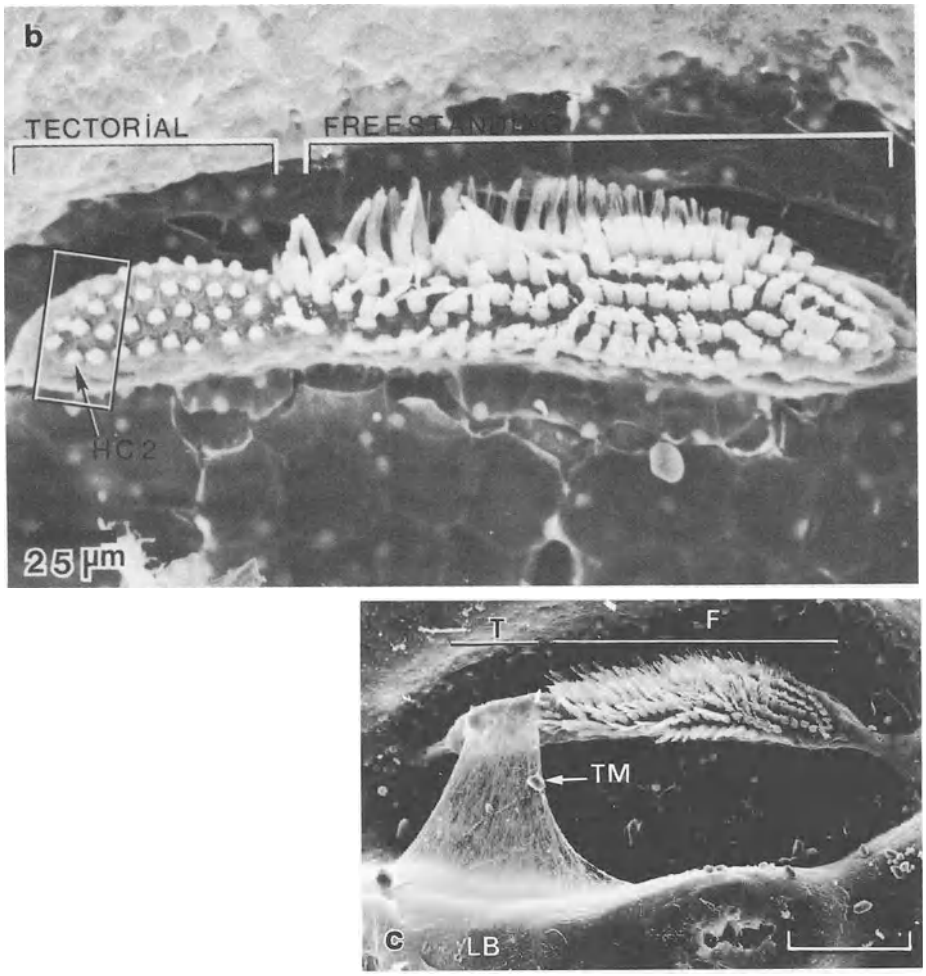

Fig. 7.1 a–c. The basilar papilla of the alligator lizard *Gerrhonotus*. *a* The right basilar papilla of *Gerrhonotus,* photographed from the lateral (scala vestibuli) side, to illustrate the general size and position of the parts. At the "habenula perforata" (*HP*), which is present along the neural side of the papilla, the nerve fibres from the nerve fan (*N*) leave the neural limbus (*NL*), lose their myelin sheath and enter the basilar papilla (*BP*). *BV* blood vessel; *TL* triangular (abneural) limbus; positions *2* and *3* correspond roughly to the planes of section shown in Fig. 7.2 *A* and *B* respectively. *b* Scanning electron micrograph (SEM) of the papilla of *Gerrhonotus* as seen from above, to illustrate the position of hair cells with different heights of the stereovillar bundle. In this picture, the apical region (tectorial) is to the *left,* the tectorial membrane is missing. In the apical region, the stereovilli are relatively short. In the basal (free-standing) region, the height of the bundles decreases systematically towards the basal end on the *right*. The cell marked with an *arrow* is reconstructed in Fig. 7.5. *c* SEM from the same viewpoint, but with the tectorial membrane in place over the apical (*T,* tectorial) region on the *left*. The tectorial plate is joined by a wide netlike membrane (*TM*) to the neural limbus (*LB*); *F* free-standing (basal) region. The scale *bar* in *c* represents 100 µm (*a* from Mulroy, 1974; *b,* Mulroy 1986; *c,* Mulroy and Williams, 1987)

7.1 Anatomy of the Papilla Basilaris

7.1.1 The Papilla of the Alligator Lizard

The cochlear duct of these lizards is moderate in size and contains a small basilar papilla (Miller, 1966, 1973 a, 1980; Mulroy, 1974; Wever, 1978). In *Gerrhonotus*, the papilla is 0.4 mm in length and 60 μm wide (Fig. 7.1 a,b). A shorter apical area (about one quarter or 120 μm) is separated by a slight constriction from the longer basal area. This is a pattern typical of anguids with normal limbs; those with reduced limbs have a basilar papilla more like that of iguanids (Miller, 1980). The connective tissue below the basilar membrane is thickened to form a so-called papillary bar, which is thickest apically (Fig. 7.2 b).

There are between 150 and 200 hair cells, 80% of which are in the basal area (Miller, 1973 a; Mulroy and Oblak, 1985). The apical area of the basilar papilla has a unidirectional hair-cell orientation and is covered by a relatively dense tectorial membrane, which is connected by a delicate membrane to the limbic lip (Figs. 7.1 c, 7.2 b). In this apical area, the stereovillar bundles of the hair cells are all short (7 ± 2 μm; Figs. 7.1 b, 7.3). There is a tendency for the height of the stereovillar bundles to increase across the *width* of the papilla, being shortest on

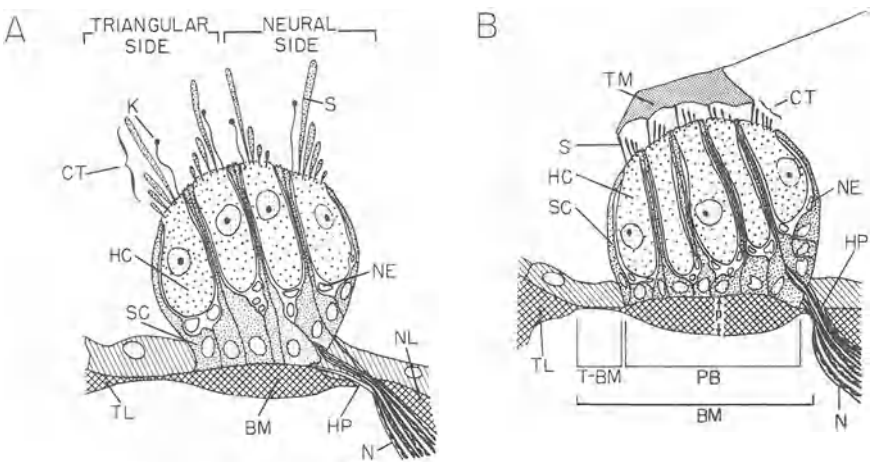

Fig. 7.2. Schematic cross-sections through the basilar papilla of *Gerrhonotus*, to show the differences between *A* the basal and *B* the apical region. In *B*, the hair cells (*HC*) are surrounded by supporting cells (*SC*) and the longest stereovilli (*s*) of their bundles (*CT* = "ciliary tuft") are in contact with the plate-like tectorial membrane (*TM*). All hair cells have the same orientation (abneural). In *A*, the hair cells on the abneural (triangular) side are oppositely oriented to the hair cells on the neural side. The dimensions of various structures indicated in *B* are given in Fig. 7.3. *S* maximum height of stereovillar tufts; *BM* width of basilar membrane; *p* maximum thickness of papillary bar (*PB*); *NE* nerve ending; *K* kinocilium; *NL* neural limbus; *N* nerve fibres; *HP* habenula perforata; *TL* triangular (abneural) limbus (Mulroy, 1974)

A The distribution of hair cells with neural (towards nerve on the triangular side) and abneural (away from nerve on the neural side) orientation.

B The number of hair cells of different orientations along the papilla.

C Whereas the maximum height of the stereovillar bundles in the basal region increases systematically towards the apex, up to 31 μm, those of the apical region are short.

D The total width of the basilar membrane and that of its thin region.

E The maximum thickness of the papillary bar as a function of position in the basilar papilla. *BM* in *E* represents the total length of the basilar membrane (Mulroy, 1974)

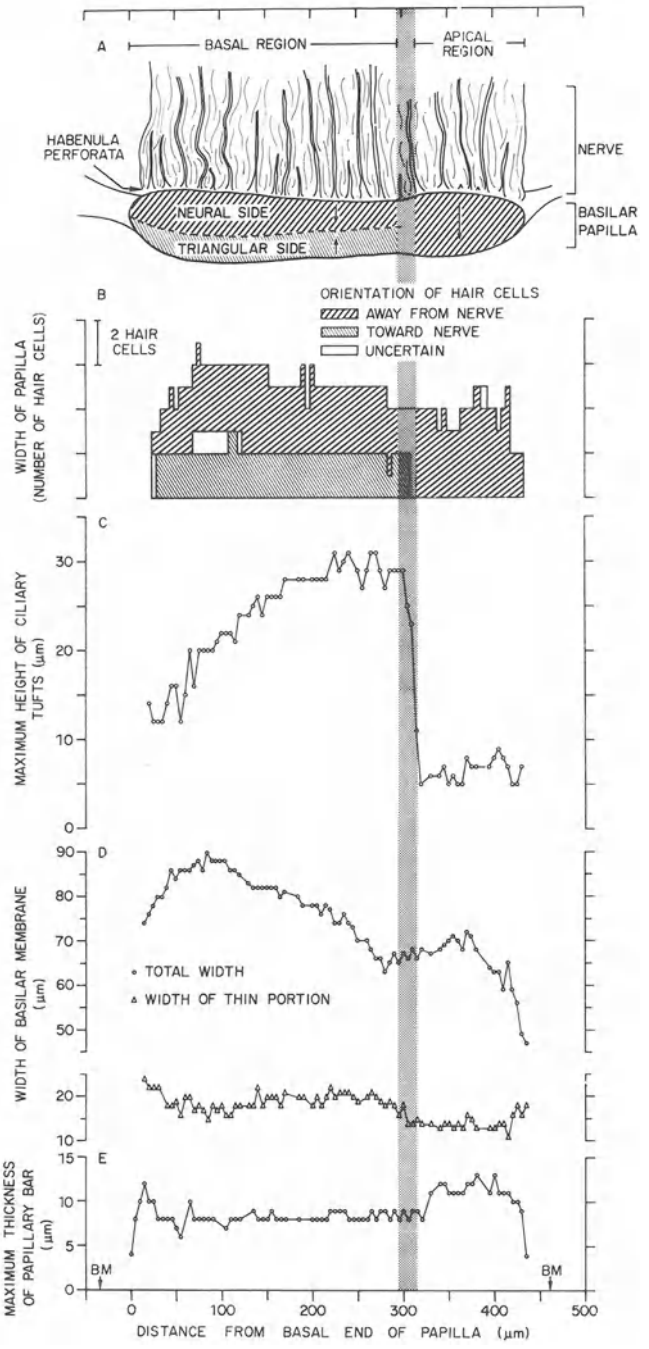

Fig. 7.3 A–E. Diagram summarizing the dimensions of different aspects of the structure of the basilar papilla of *Gerrhonotus*. The *vertical grey stripe* indicates the position of the border between apical and basal regions in all parts of this figure.

the neural side (6 μm compared to 9.2 μm abneurally, Mulroy and Williams, 1987). At the same time, the number of stereovilli per bundle decreases from 55 neurally to 44 abneurally.

In contrast, the orientation of the basal area is bidirectional (Fig. 7.4c) and there is no true tectorial membrane, although possibly a fine network of fibrils among the stereovillar bundles of the hair cells. Along the length of this area, there is a systematic difference in height of the tallest stereovilli, from 12 μm basally to 37 μm near the border of the apical area (Figs. 7.1 b, 7.3). The number of stereovilli remains fairly constant from the base to the apical part of this area (Mulroy and Williams, 1987). As there is no tectorial membrane to connect to the stereovilli via the kinocilium, the kinocilium of each hair cell in this basal area is much shorter than the tallest of the stereovilli (Fig. 7.4a).

In the distal auditory nerve of one papilla of *Gerrhonotus*, Mulroy and Oblak (1985) found 891 nerve fibres. Of these nerve fibres, 29% innervate the apical region (the mean fibre diameter was 1.03 μm) and 71% the basal region (mean diameter 0.67 μm). With a total of 193 hair cells (151 basal, 42 apical), this means a ratio of 6.1 fibres per hair cell apically and 4.2 basally. Of the nerve fibres, 99% are myelinated up to the *habenula perforata*. The innervation pattern of the two hair-cell areas differs considerably (Mulroy and Oblak, 1985). Basal fibres terminate on hair cells in the immediate area where they enter, whereas some apical fibres send branches along the papilla. In addition, hair cells of the apical area synapse with both afferent and efferent fibres. Efferents were not seen in the basal area (this is the general pattern in lizards, see Ch. 4).

Mulroy (1986) describes in detail the innervation of some individual hair cells. The afferent innervation of all the apical hair cells appears exclusive, whereas only about 80% of the afferents to basal hair cells innervate only 1 hair cell (17% innervate 2 adjacent hair cells). However, as Mulroy could only detect nearest-neighbour contacts with his technique, he could not follow all branches of apical fibres to their synapses. Although all hair cells are innervated by four or five afferents, the apical hair cells apparently have on average a larger number of synapses than do basal hair cells. This is because apical (‚tectorial') fibres make more synapses per fibre (the range was 4 to 34 for apical fibres, 1 to 11 for basal fibres; Fig. 7.5). Thus, whereas the apical region showed an average of more than 60 afferent synapses per hair cell, the basal region has only 15 synapses per cell.

7.1.2 The Papilla of the Granite Spiny Lizard

Although a few exceptional iguanids show a papilla similar to the anguid *Gerrhonotus* (Miller, 1980), in most iguanid papillae, the unidirectional hair-cell area is located centrally and there are two bidirectional areas located apically and basally. These two bidirectionally-oriented areas are a mirror-image of each other. The papilla of the granite spiny lizard *Sceloporus* is relatively small (0.3 mm), with 21 hair cells in the unidirectionally-oriented area and 30 to 33 cells in each of the two bidirectionally-oriented areas (Turner, 1987; Fig. 7.6). As in anguids, the unidirectional area is covered by a tectorial plate (torn off in Fig. 7.6) connected to the limbus. The 'sceloporine' lizard papilla (as in

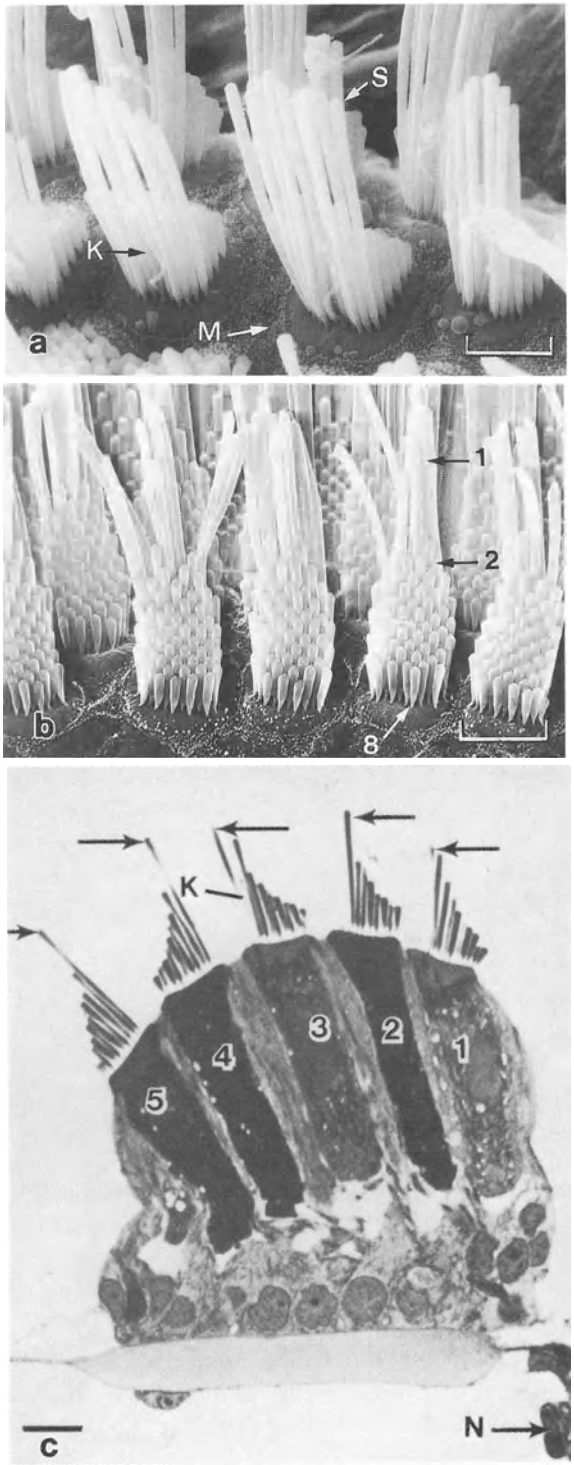

Fig. 7.4 a–c. SEM of basal (free-standing) stereovillar bundles, to illustrate the non-uniform increase in height of the villi across the bundle. *a* As seen from the front of the bundle, showing the short kinocilium (*K*) and the tallest stereovilli (*S*), as well as microvilli (*M*) of the supporting cell surface. *b* As seen from the opposite side. Whereas the stereovilli gradually get taller from the eighth (*8*) to the second (*2*) row, the first row (*1*) is twice as tall as the second row. The scale *bar* in *a* and *b* is 5 μm. *c* Light micrograph of a cross-section through the basal region, illustrating the opposite orientation of the hair-cell bundles and the height of the tallest stereovilli (*arrows*) and kinocilium (*K*); *N* bundle of nerve fibres. Scale *bar* in *c* is 10 μm. Over much of the basal region, the bundles of row-*1* cells are somewhat shorter than those of row-*5* cells (Mulroy and Williams, 1987)

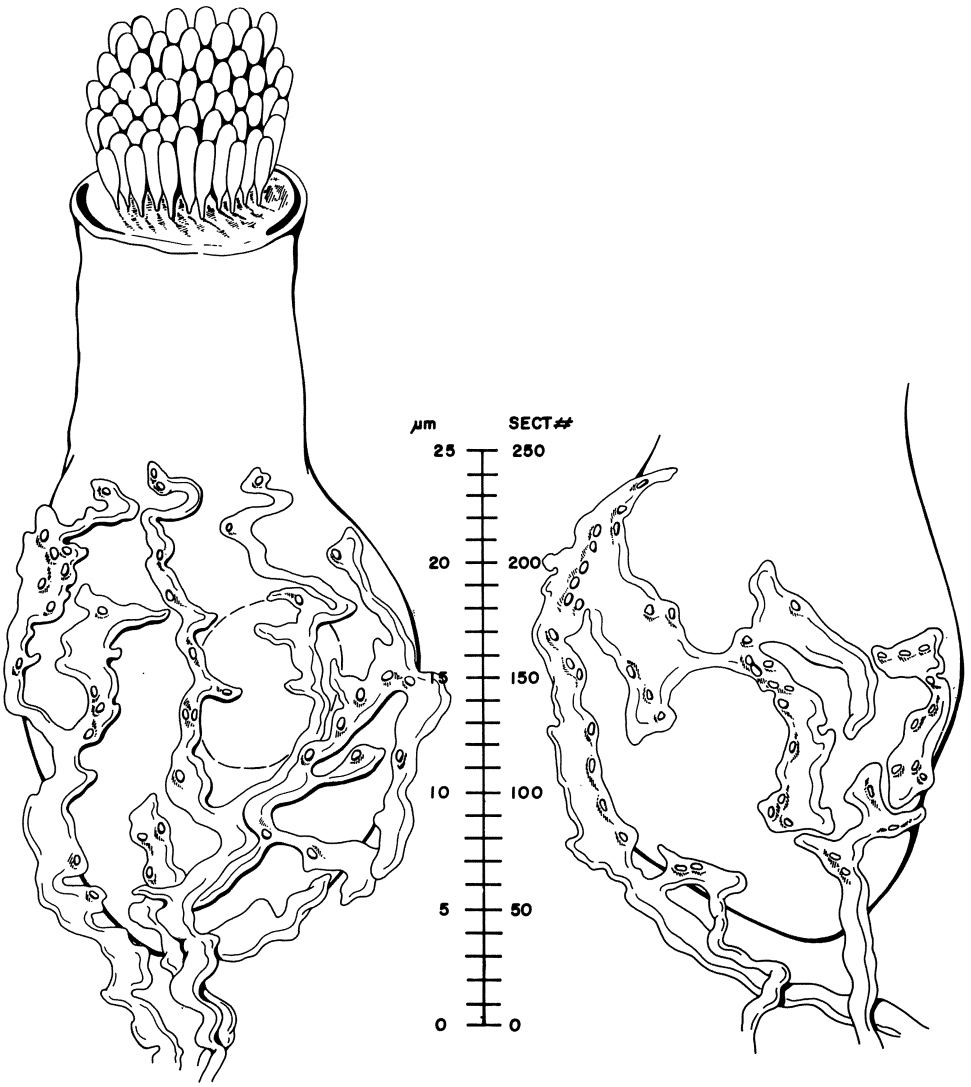

Fig. 7.5. A scale reconstruction from serial sections of an apical hair cell of *Gerrhonotus,* to show the afferent innervation pattern as seen from the neural side (*left*) and abneural side (*right*). The position of this cell in the papilla is marked with an *arrow* in Fig. 7.1 *b*. Three afferent fibres branch and form many synapses on the neural side, two others synapse on the abneural side, making a total of five fibres and 88 synapses. These hair cells are exclusively innervated (Mulroy, 1986)

Sceloporus) differs from that of other iguanid-lizard groups in that the number of hair-cell rows of the bidirectional areas is reduced to two (Miller, 1981).

The longest stereovillar bundles are located on hair cells next to the central unidirectional area. From these cells, with stereovillar lengths of 23 μm, the bundles get shorter towards the base and apex (to 5 μm). In the unidirectional hair-cell area, there is, as in the alligator lizard, a tendency for the stereovillar

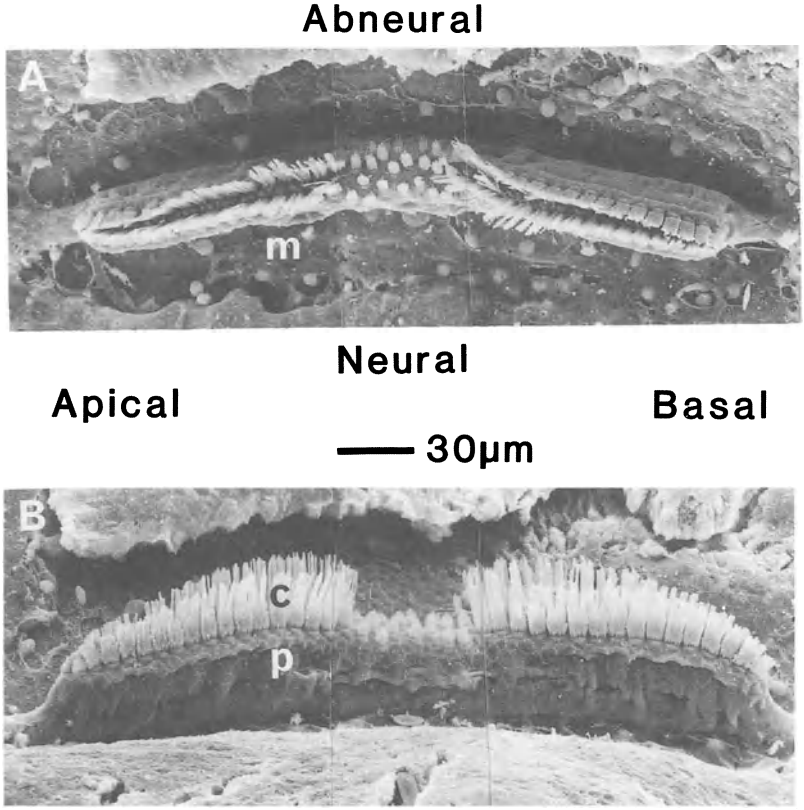

Fig. 7.6 A, B. SEM of the right papilla of *Sceloporus,* seen from above (*A*) and from the neural side (*B*). Here, there are three distinct populations of hair cells, with a small group of abneurally-oriented hair cells in the centre which are normally covered by a tectorial membrane. Basally and apically to this region, there are two mirror-image groups of hair cells without a tectorial membrane. *c* Stereovillar bundles of hair cells; *m* basilar membrane; *p* basilar papilla (Turner, 1987)

bundles to be shorter (4 μm) on the neural side and longest (9 μm) abneurally (Turner, 1987).

Although we have no information on details of the innervational pattern of the granite spiny lizard papilla, Teresi (1985) has studied the innervation of the papilla of the related blue-bellied fence lizard *Sceloporus occidentalis.* There are significant differences between the innervation of *Sceloporus* and *Gerrhonotus.* In *Sceloporus*, all hair cells are exclusively innervated, each afferent or efferent fibre is unbranched and contacts only one hair cell. In the unidirectional area, each hair cell synapses with 4 to 17 afferent (mean of 10) and 0 to 5 efferent fibres (mean of 2.7). In the bidirectional area, only afferents are present (5 to 13 endings, mean of 10). The number of afferent fibres supplying a single hair cell also varies with the location of the hair cell on the papilla, being greatest for hair cells lying most neurally. Hair cells of the unidirectional area had, however, twice

as many synapses per fibre (range of 1 to 10, mean of 3.6) as those of the bidirectional area (range of 1 to 5, mean of 1.8). Within the bidirectional areas, there is a gradual decrease in the number of afferent *synapses* per hair cell when going from the central papillar region to the ends of the papilla. Thus the innervational pattern in these iguanid lizards is relatively simple.

7.2 Recordings from Hair Cells

The endolymph of the scala media of the alligator lizard is at a positive potential of about +16 mV compared to the perilymphatic space (Weiss et al., 1978 a). Baden-Kristensen and Weiss (1983), Holton and Weiss (1983 a,b), Mulroy et al. (1974) and Weiss et al (1974, 1978 b) report data from intracellular recordings from hair cells of the papilla of the alligator lizard. Intracellular resting potentials of identified hair cells were about −70 mV.

To determine their frequency selectivity, cells were acoustically stimulated with tone bursts or with clicks. Hair-cell responses (greater than 2 mV peak-to-peak) were fast; the delay from pressure onset at the eardrum to the response was only 200 μs (most of this delay is probably due to the middle ear). The initial polarity of the hair cell's electrical response was correlated with the orientation of the hair-cell area. The steady-state response to tones consisted not only of AC

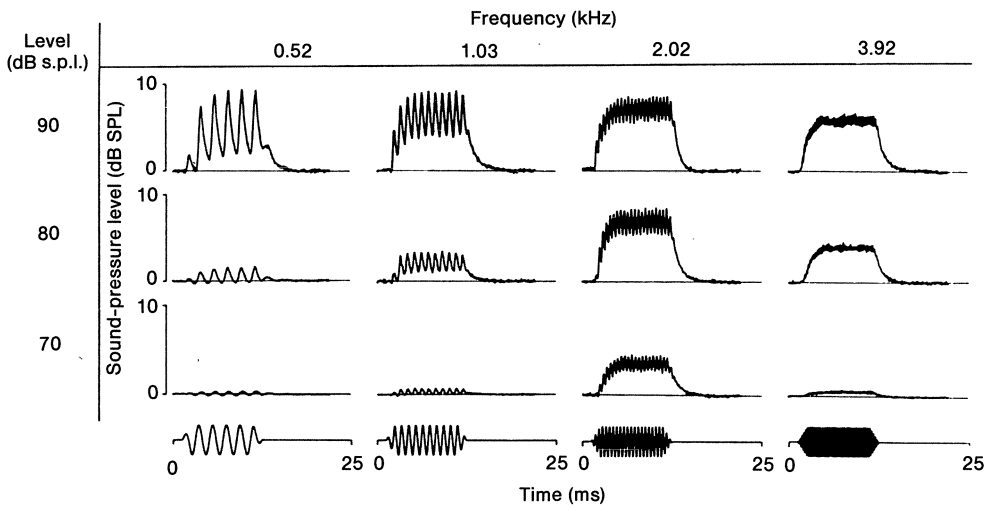

Fig. 7.7. Intracellular responses of a hair cell from the basal region of the papilla of *Gerrhonotus* to pure tones of differing frequency and SPL. In the *bottom row* are shown the sound monitor traces and time axes. The responses are frequency-dependent, the best DC response at 70 dB SPL being at 2 kHz. The responses consist of an AC and DC component, which saturate at high levels (see 2 kHz at 80 and 90 dB SPL). The AC component becomes smaller towards higher frequencies, illustrating low-pass filtering in the hair cell (Holton and Weiss, 1983 a)

components which showed frequency selectivity, non-linearity and low-pass filtering, but also of a depolarizing DC component (Holton and Weiss, 1983 a; Fig. 7.7). At any one SPL, the AC component becomes smaller relative to the DC component towards higher frequencies. The best response frequencies could be divided into a low- and a high-frequency group (0.35 to 0.58 and 1.3 to 2.6 kHz) and there was some indication that the high-frequency responses came from the basal, the low-frequency responses from the apical area. Although the hair-cell responses did not produce detailed information regarding the tonotopic organization of the papilla, they are consistent with a more detailed map obtained from afferent nerve-fibre recordings.

No evidence of electrical ringing, as seen in the hair cells of the turtle (see Ch. 6) was observed, a fact which may indicate that electrical tuning phenomena do not play an important role in hair cells of this species. The tuning curves of the hair cells' DC and AC-fundamental component were 'V'-shaped (Fig. 7.8), the tip of the AC tuning curve around the CF being, however, sharper when the

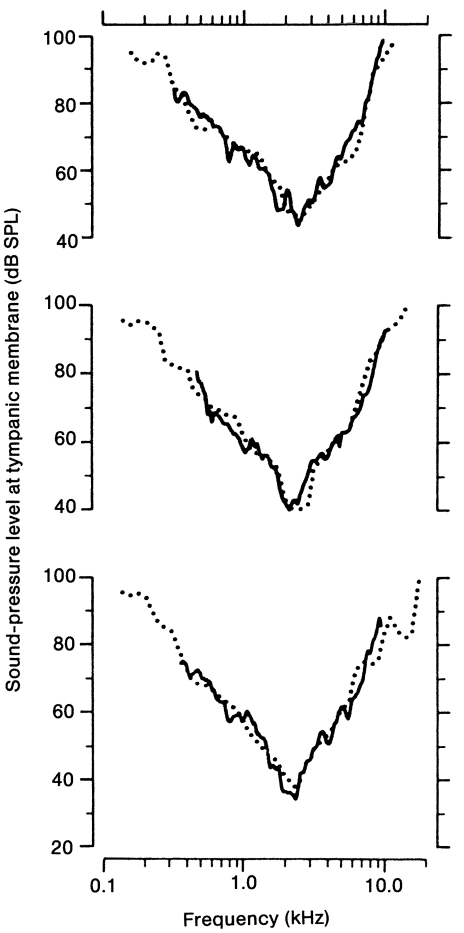

Fig. 7.8. A comparison of DC tuning curves of *hair cells* of the basal region of *Gerrhonotus* (*dotted lines*) and tuning curves of *single nerve fibres* (*continuous lines*). The figure shows the respective thresholds in terms of the sound pressure at the tympanic membrane (Holton and Weiss, 1983 b)

curve was measured with a lower voltage criterion. The relationship between DC and AC tuning curves was complex and level-dependent. The hair cells (AC and DC responses measured separately) showed increased intracellular potential with increasing SPL up to a saturation level 30 dB or more above the lowest threshold. The slopes of these level functions were similar for all frequencies, except near the CF for the AC function, where the slope was much lower. This indicates the presence of a compressive non-linearity, which has the effect of making the AC tuning curve sharper than the DC curve near the CF.

7.3 Activity of Primary Auditory-nerve Fibres

7.3.1 Auditory-nerve Fibres of the Alligator Lizard

The primary nerve fibres in *Gerrhonotus* are irregularly spontaneously active, with discharge rates up to 80 spikes/s (temperature near 20–22 °C). Most rates

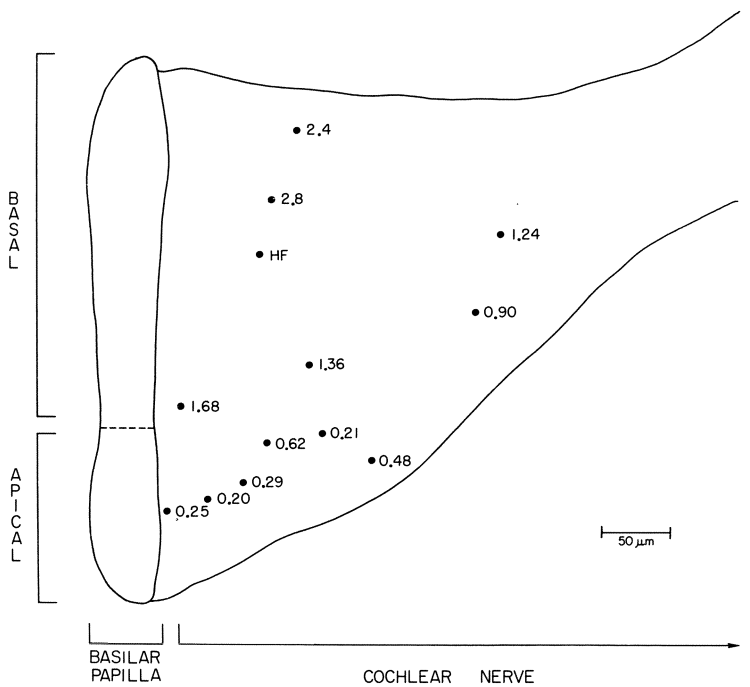

Fig. 7.9. Distribution of nerve-fibre responses with different characteristic frequencies (CF in kHz) in the nerve fan near the basilar papilla of *Gerrhonotus*. Low-CF responses originate in the apical, high-CF responses in the basal area of the papilla. The location of the recording sites was determined by spots of dye ejected from the electrode. *HF* marks the location of a penetration in which three high-CF units were encountered (Weiss et al., 1976)

are below 50/s (Weiss et al., 1976). Frezza (1976) states that low-CF fibres had spontaneous rates below 20/s, whereas the high-CF fibres had rates across the whole range. For most units, the interval histograms showed an approximately exponential decay.

Primary auditory-nerve fibres respond at 100 dB SPL to tonal stimuli covering a range up to 12 kHz. The best threshold sensitivities over the frequency range 0.3 to 3 kHz lie between about 15 and 25 dB SPL. The CFs of the nerve fibres are tonotopically arranged. As the fibres tend to leave the papilla and run in fascicles in a more-or-less straight path as a sheet across the limbus, it is possible, through measurement of the location of the electrode tip, to localize a fibre with reference to the papillar region it innervates. The low-CF fibres (0.2 to 0.8 kHz) originate in the apical, tectorial region. In the basal region, the lowest-CF fibres (0.9 kHz) innervate the hair cells nearest the apical area and the highest-CF fibres (4.0 kHz) run to the extreme basal end of the papilla (Fig. 7.9). Systematic differences between the activity patterns shown by nerve fibres innervating the basal and the apical regions of the papilla of *Gerrhonotus* are described below (Holton, 1980; Holton and Weiss, 1978, 1983 b; Weiss et al., 1976).

The shapes of the tuning curves and the slopes of the tuning-curve flanks vary with CF (Fig. 7.10). For fibres from the high-CF area, it is striking that the low-frequency flanks of the curves lie further apart in the frequency axis than do the high-frequency flanks (Fig. 7.11). Very similar data are shown for the skink *Tiliqua* (see below, Ch. 11). Tuning curves of the low-CF units are more sharply tuned, especially on the high-frequency slope. Whereas their mean low-frequency slope was only about double that of the high-CF fibres (-30 vs. -15 dB/octave), the high-frequency slope was substantially higher (mean near 200 dB/octave vs. about 22 dB/octave). This difference may be related to the absence of the effect on tuning of a tectorial membrane in the high-CF area (see section 14.4). The difference in the tip regions of the tuning curves was much smaller. It was not possible to determine whether near the CF the fibre tuning curve was more correlated to the hair-cell DC curve or to the hair-cell AC curve. However, the fibre tuning curve has a higher mean $Q_{10\ dB}$ value (2.34 as compared to 1.2 for the hair-cell DC tuning curve). Higher-criterion sharpness measures for fibres and hair cells were more similar (e.g., $Q_{30\ dB}$ was 0.53 vs. 0.4; Fig. 7.8).

Holton (1980) reports that for some apical fibres (low CF), the low-frequency side of the tuning curve does not show a smooth slope, but has 'notches' of higher threshold in it. The number of these notches is CF-dependent, increasing with CF. Fibres with CF >400 Hz have two or more notches, whose frequencies vary systematically with CF. The high-frequency slope of the tuning curve can be divided into a lower slope near the CF and a high-slope segment at higher frequencies. The break frequency between these slopes increases with CF. The notches in the tuning curves are related to the presence of two-tone rate suppression (TTRS; Holton, 1980; Holton and Weiss, 1978). This phenomenon describes the suppressing effect of a second tone on the discharge-rate response to a steady first tone (usually at the cell's CF, see Ch. 5). TTRS was not found for any basal fibres, but did occur for apical fibres in a broad 'U'-shaped area above the CF and in the region of the notches on the low-frequency slopes of the tuning curves

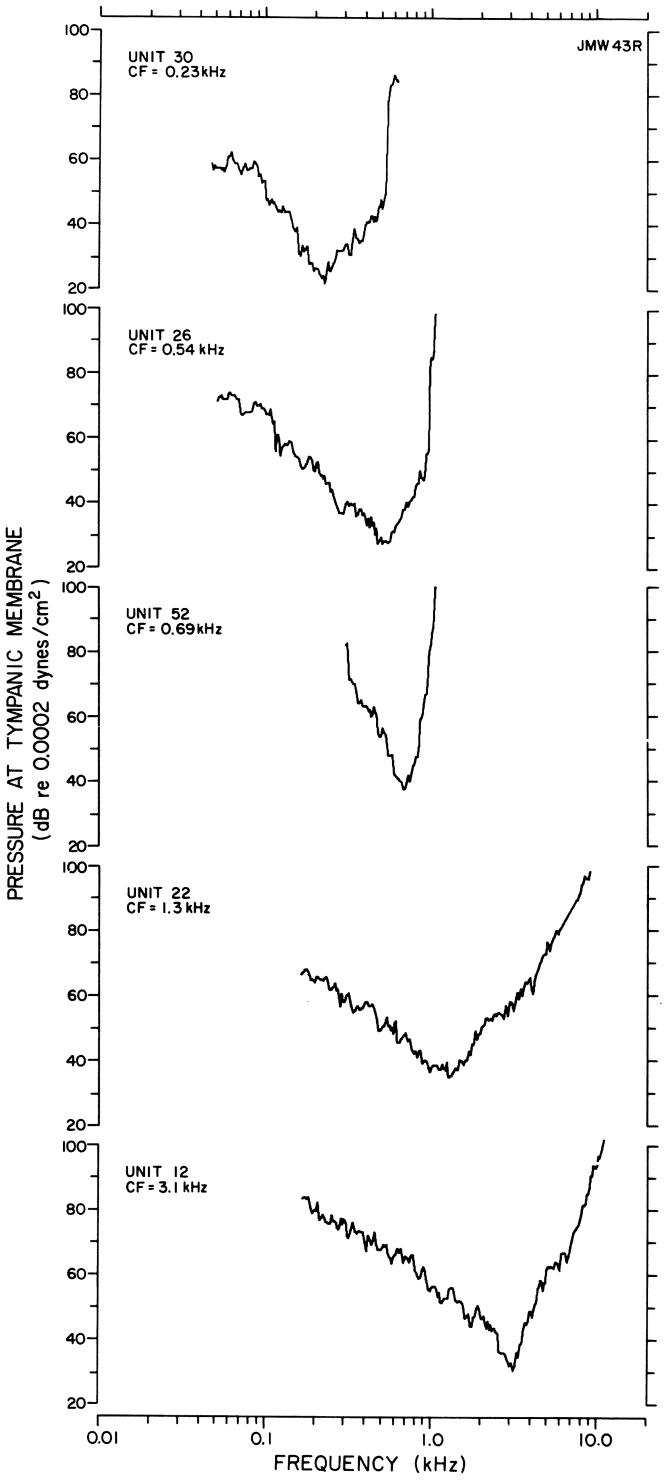

Fig. 7.10. Tuning curves belonging to different CF groups in the nerve of *Gerrhonotus*. The *upper three curves* are low-CF, the lower two high-CF units. The low-CF units have much steeper slopes on the high-frequency side (Weiss et al. 1976)

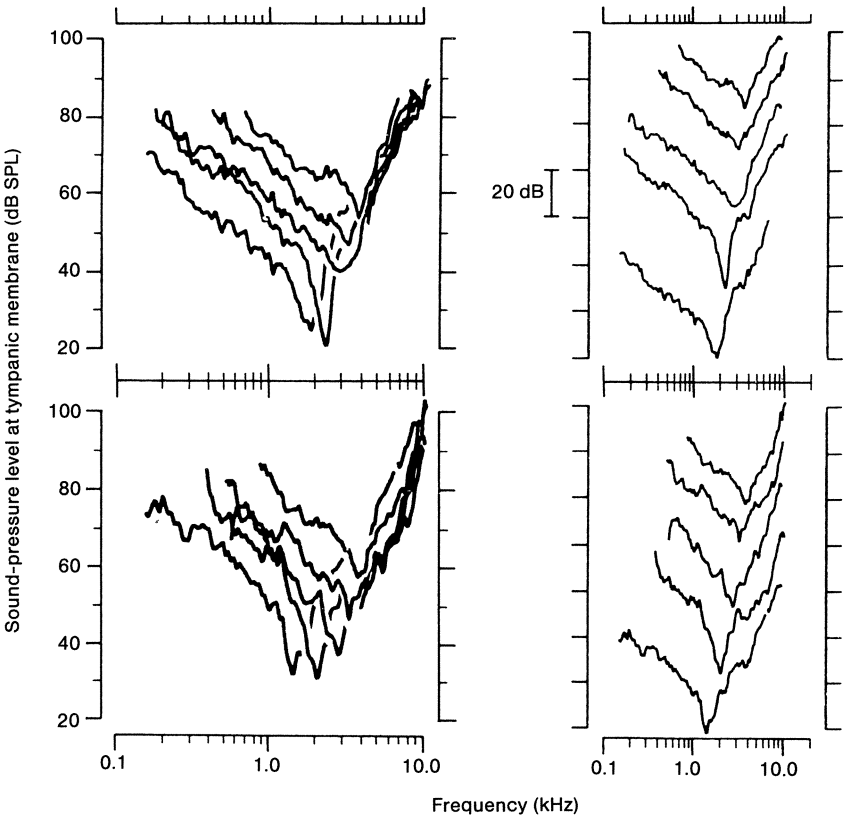

Fig. 7.11. Superimposed (*left*) and staggered (*right*) plotting of high-CF tuning curves from two specimens of *Gerrhonotus* (*top* and *bottom*). This figure illustrates the variation in shape of high-CF tuning curves, and the fact that the high-frequency slopes run close together at levels above about 60 dB, whereas the low-frequency slopes run separated but parallel to each other (Holton and Weiss, 1983 b)

(Fig. 7.12 a,b). Plotting all the measured 'U' contours for the low-CF fibres together showed that the suppression curves for all fibres are similar. There is a steep low-frequency slope, whose position depends on the CF, and a shallow (about 26 dB/octave) high-frequency slope (Fig. 7.12 c), whose position is largely independent of CF. Thus, the 'CF' of the TTRS-curve increases with CF of the fibre's tuning curve. The data suggest a relationship between the sharp tuning characteristic of apical fibres and the presence of TTRS. Both phenomena may result from properties of the micromechanics of stereovillar excitation in this species. One possible candidate for producing these differences between the responses of apical and basal fibres is the tectorial membrane, which is only present apically. These TTRS data are strongly reminiscent of data from *Tiliqua* (see Ch. 11).

The rate-level functions for tonal stimulation of nerve fibres innervating the apical and basal areas differ (Eatock and Weiss, 1986). Apical fibres have a

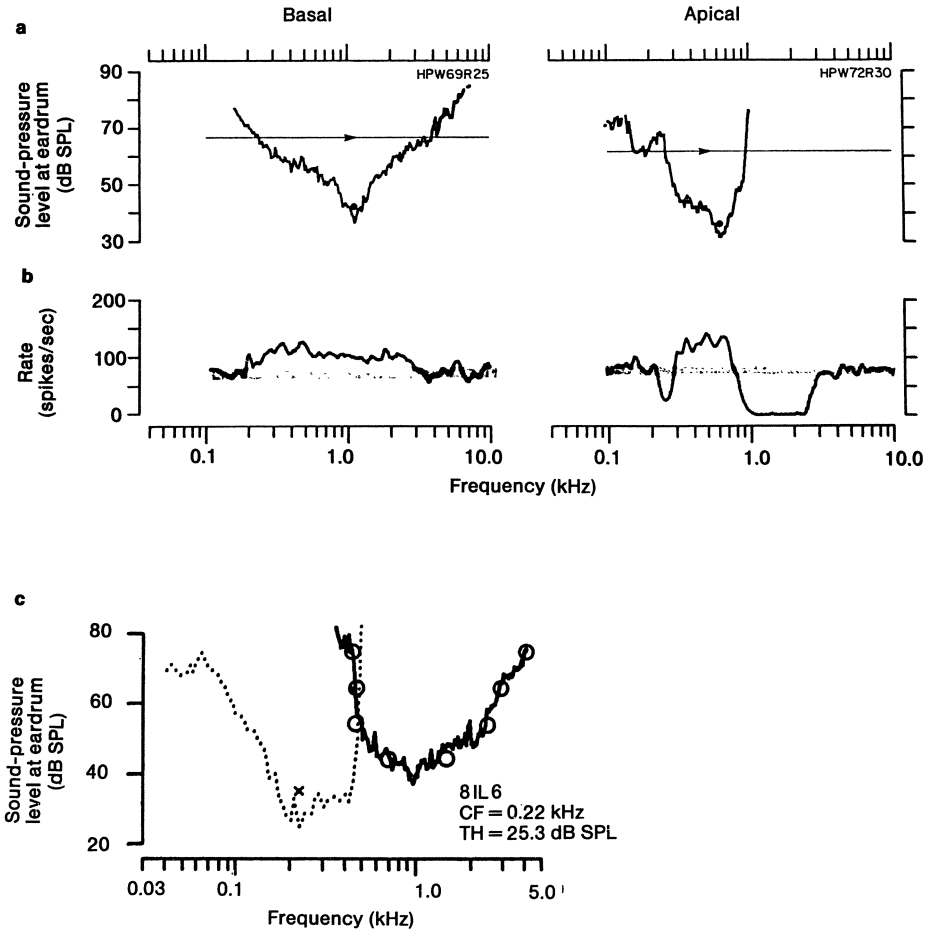

Fig. 7.12 a–c. Two-tone suppressive effects as measured in the responses of tuning curves of nerve fibres of *Gerrhonotus*. *a* The tuning curves of a basal (free-standing, *left*) and an apical (tectorial, *right*) cell are shown together with the levels of the tones used in the two-tone situation: a fixed tone at the respective CF, 5 dB above threshold (*dot* in middle of curve) and a second, swept tone (*line with arrow*) at 30 dB above threshold (0.1 to 10 kHz). *b* Discharge rate of the cells in response to the two tones. The basal cell (CF near 1 kHz) only raises its discharge rate (*continuous line*) above the rate to the CF tone alone (*stippled band*), whereas the low-CF fibre (*right*) shows two frequency bands below and above CF where the rate is strongly suppressed by the second tone. *c* Excitatory tuning curve (*dotted line*) of a low-CF nerve fibre and the two-tone rate suppression (TTRS) threshold for frequencies above CF (*thick line*), suppressing the response to the CF tone (level marked with an *x*) near 200 Hz. These TTRS contours for all low-CF cells are very similar in shape, their lower-frequency flank shifting with the cell CF (*a* and *b* from Holton and Weiss, 1978; *c*, Holton, 1980)

steeper growth slope (narrower dynamic range) and the discharge rate saturates at lower rates for frequencies above CF. The steeper rate of growth of discharge rate with increasing sound-pressure level may be related to the fact that apical fibres make about three times as many afferent synapses than do basal fibres. Basal-fibre saturation rates appear to be independent of frequency, which is similar to the response of the DC component of basal hair cells. At the same time, the average rate in the basal fibres saturates at lower SPL levels than does the receptor potential of the basal hair cells. Thus saturation of nerve fibres results from the saturation of a process between the receptor potential and action potential discharge in the nerve, i.e., a synaptic process or the process of generating action potentials from postsynaptic potentials.

Rose and Weiss (1988) and Weiss and Rose (1988) investigated the phase-locking behaviour in single primary nerve fibres of *Gerrhonotus*. Fibres of both the low- and high-CF populations showed phase locking only to frequencies below 1 kHz. In general, low-CF (apical) fibres showed better synchronization and a higher corner frequency than basal fibres, although the average firing rates to tones of basal fibres were higher (38 vs. 25 spikes/s during 12.5 ms tone bursts). The low-CF population of fibres shows phase-locking over most of the range of frequencies within their tuning curves, whereas the high-CF fibres do not. The AC component of the electrical responses of hair cells of the high-CF area follow the stimulus oscillations up to higher frequencies than present as phase-locked responses in their fibres. This may be related to the fact that apical (low CF) fibres make more synapses per fibre on the hair cell than basal (high CF) fibres. It has already been noted above that the apical fibres have steeper rate-level functions, possibly for the same reason. We do not, however, have any other information about possible correlates of the differences in innervational patterns in the two regions and the activity of the auditory nerve. Rose and Weiss (1988) suggest that the low-CF fibres subserve the function of transmitting information requiring the measurement of temporal synchronization at low sound levels ("timing pathway"), such as the localization of low-frequency sounds (see Sects. 11.2.3 and 14.10).

Similarities between the responses of the compound action potential (CAP) of the alligator lizard and those of mammals have been demonstrated (Turner and Shepard, 1986). Recording with a wire electrode near the inner ear, they measured this summed activity of the entire nerve (CAP) under masking conditions. Using *forward* masking of specific tonal responses (a masker tone is presented before the test tone), they found CAP tuning curves which resembled single-fibre tuning curves, even to the extent of having identical slopes and tuning sharpness ($Q_{40\ dB}$). With *simultaneous* masking (the masker and test tones are presented simultaneously), the tuning curves resemble the boundaries of single-fibre TTRS.

7.3.2 Auditory-nerve Fibres of the Granite Spiny Lizard

In *Sceloporus*, single-fibre CFs vary from 0.25 to 4.3 kHz. There is a low-CF population originating from the unidirectional area, with CFs up to 0.9 kHz and

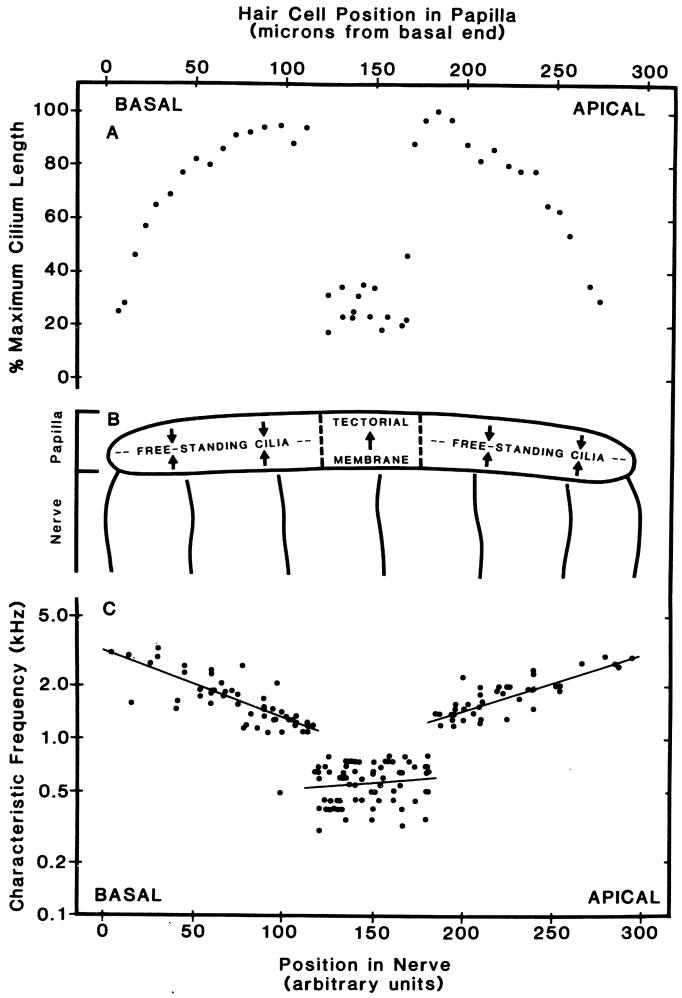

Fig. 7.13.A–C. Correlation between the CF of nerve fibres in different locations along the length of the papilla and the maximum height of the stereovillar bundles of the hair cells at the corresponding papillar locations in *Sceloporus*. *A* The heights of stereovillar bundles of hair cells as a function of the position in the papilla as measured from the basal end and as a percentage of the maximum length. *B* Schematic diagram of the three hair-cell areas drawn to the same scale. *C* CF of nerve fibres encountered in different locations in the nerve, drawn from maps in eight animals. The diagram is normalized to the size of the nerve in individual animals, so that the positions given on the abscissa are in arbitary units. The *solid lines* are simple regression lines for each fibre group, the correlation coefficients are +0.82 (apical), +0.15 (central) and −0.80 (basal) (Turner et al., 1981)

a high-CF population originating in both bidirectional areas, both of which have CFs from 0.9 to 4.3 kHz (Turner, 1987; Fig. 7.13). The best thresholds were near 15 dB SPL. Details of the shape of tuning curves, $Q_{40\ dB}$ sharpness coefficients etc. are remarkably similar to the data described above for the alligator lizard.

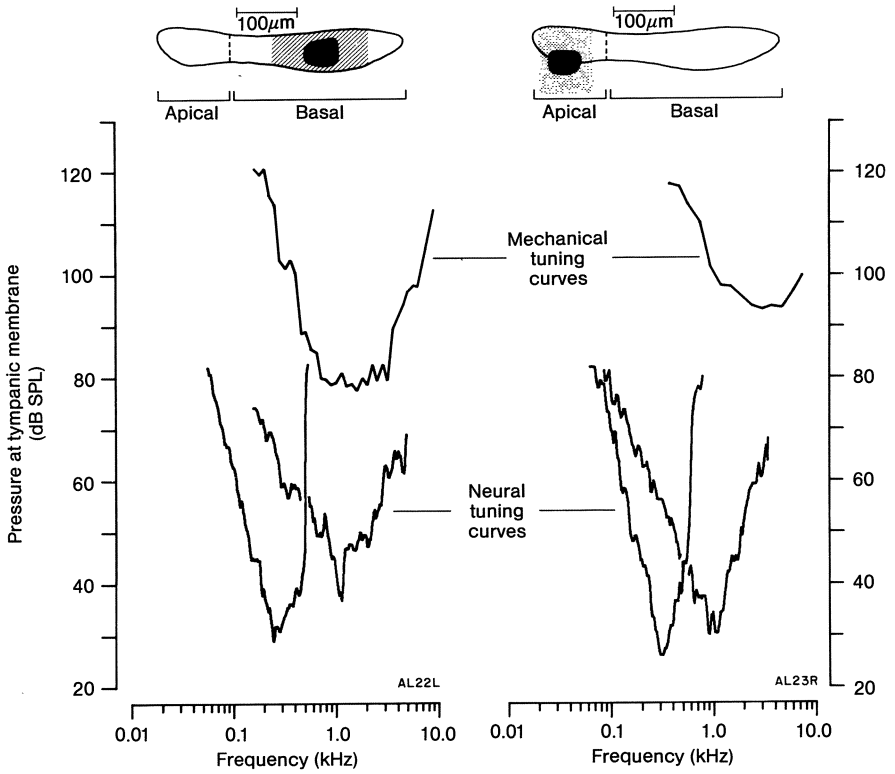

Fig. 7.14. Basilar-membrane tuning curves for the basal (*left*) and apical (*right*) areas of the papilla of *Gerrhonotus,* represented as the SPL necessary at different frequencies to produce a velocity of 0.8 mm s^{-1} of the basilar membrane. The *black spot* on the papillae shown at the *top* indicates the location of the Mössbauer source for the mechanical measurements. Below the mechanical tuning curves are shown two neural tuning curves in each case obtained during mechanical measurements, to illustrate that the papillae were in good physiological condition and that the tonotopicity in the neural responses is not seen in the mechanical responses (Weiss et al., 1978 b)

7.4 Mechanics of the Basilar Papilla and Micromechanics of the Hair Cell Bundles

Using the Mössbauer effect (see Sect. 5.4), Peake and Ling (1980) have measured the motion of the two areas of the basilar membrane of *Gerrhonotus* in response to sounds of different frequencies. They found no systematic variation in the frequency dependence of the motion of the basilar membrane along its length (Fig. 7.14). The velocity of the basilar membrane is about equal to that of the extracolumella over the frequency range 500 Hz to 6 kHz; the tuning of the basilar membrane motion is thus dominated by the tuning of the middle ear.

Frishkopf and DeRosier (1983) and Holton and Hudspeth (1983) used stroboscopic light techniques to follow the motion of the tall stereovillar bundles

of the basal hair cells in isolated preparations of the papilla of *Gerrhonotus*. Although it is difficult to know how the stimulation techniques used for isolated papillae compare to natural stimulation, it is likely that they induced motions at the high end of the physiological range. Rocking motions of the basilar membrane were observed, which pivoted about the neural limbus. In the basal area, this motion was in phase for all frequencies, except that at high frequencies the most basal region had the largest relative displacement between stereovillar bundles and hair-cell bodies. Under these conditions, the stereovilli were found to pivot about their base; tip displacements were less than 2.3 °. Each stereovillar bundle behaved as a nearly critically-damped mechanical resonator. At relatively low frequencies (1.2 kHz), the bundles of the hair cells with the longest stereovilli (apical end of basal area) moved out of phase with the motion of the cell body, which presumably stimulates these cells. In contrast, such low-frequency stimuli produced no relative motion between bundle and cell body for the shorter bundles of the bidirectional region. Similarly, high-frequency stimuli (3.8 kHz) caused relative motion between cell and bundle only in cells with short bundles (Fig. 7.15). Bundle resonant frequencies varied inversely along the papilla with a power between 3/2 and 2 of bundle height and were similar to the CFs of auditory-nerve fibres measured *in vivo* at corresponding locations in the nerve. The hair cells of the apical, tectorial region were not tested.

These data indicate that there is a tonotopic organization of the micromechanical frequency responses along the basal part of this papilla. This is presumably based on the frequency-selective motion of the stereovillar bundles. The data presented do not, however, allow us to determine to what extent the effect determines the frequency selectivity of the individual hair cell or nerve fibre. The fact that the tuning of the bundles appears to be broader than that of nerve fibres could be real or be due to a number of factors, including the high SPLs necessary to measure the motions in the papilla (as noted earlier, sharpness of tuning varies inversely with criterion response level in the basal nerve fibres and hair cells). It is interesting to note, however, that the relationship between length and resonant frequency in bundles lacking a tectorial membrane (basal) must be different from that determining the responses of apical hair cells. The latter cells, although they have the lowest CFs, have the shortest bundles. The tectorial membrane presumably plays a very important role in determining the resonant frequencies of the low-CF region. As yet, perhaps due to its small size, it has not proved possible to demonstrate a tonotopic organization of the apical area (Weiss et al., 1976). As the height of the stereovillar bundles of the apical area in both species varies across the papilla, however, it is probable that there is a tonotopic organization running at right angles to the length of the papilla.

Although there have been no measurements of stereovillar motion in the papilla of *Sceloporus*, the correlation between bundle length and CF is similar in the two bidirectionally-oriented, tectorial-membrane-free areas. This suggests that the micromechanical response patterns will resemble those of *Gerrhonotus* (Turner et al., 1981). There is, however, a difference in the range of the bundle lengths in the two species (5 to 23 μm in *Sceloporus*, compared to 12 to 31 μm in *Gerrhonotus*), although the frequency ranges given (0.9 to 4.3 kHz as compared to 0.8 to 4.2 kHz) are virtually the same (Holton and Weiss, 1983 b; Turner et al.,

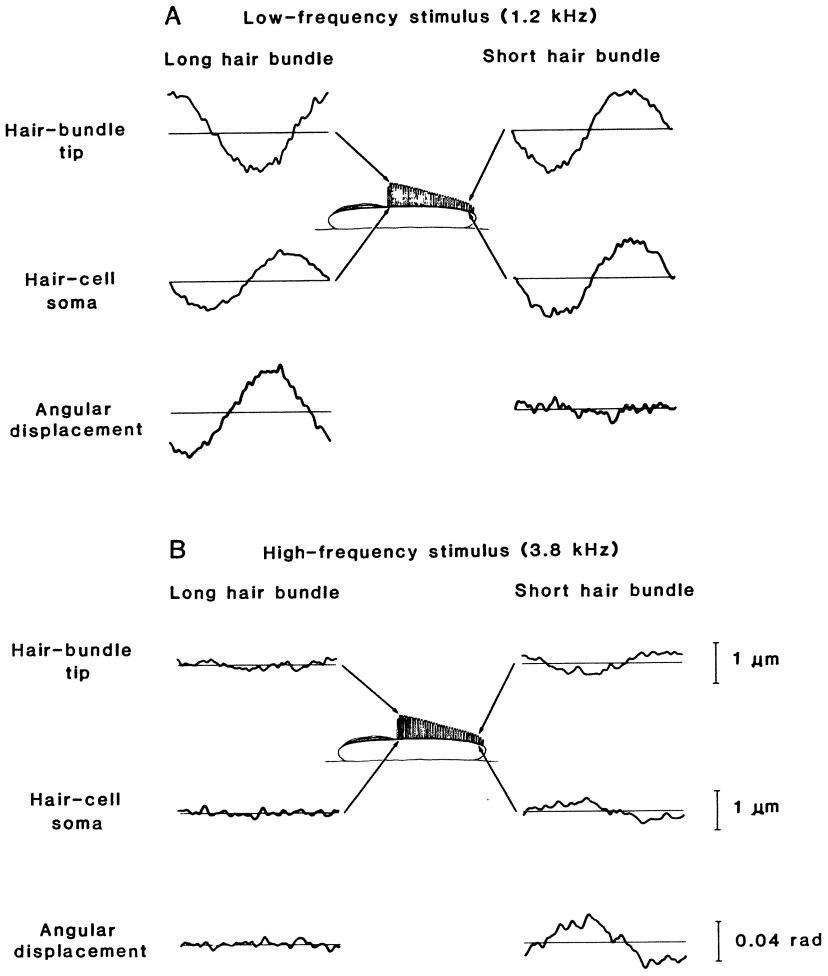

Fig. 7.15 A, B. Measurements of the motion of basal (free-standing) stereovillar bundles of hair cells in in vitro preparations of the basilar papilla of *Gerrhonotus*. The waveform of the motion of the hair-cell soma (*middle traces*) and bundles (*top traces*) of more apical (taller bundle) and more basal (shorter bundle) cells is illustrated for *A* low-frequency stimuli (1.2 kHz) and *B* high-frequency stimuli (3.8 kHz). The *lower traces* give the angular displacement of the bundles relative to the soma for the different stimuli. At low frequency, the taller bundles are displaced out-of-phase to the cell soma, the same is true for short bundles at high frequency. This produces large relative displacements at low and high frequency, respectively (Holton and Hudspeth, 1983)

1981). Thus there may be other species-specific factors determining the response parameters. For *Gerrhonotus*, Weiss and Leong (1985 a) show that a model of the stereovillar-bundle micromechanics in the basal area can account both for most features of the frequency selectivity and for the range of frequencies and tonotopic organization of the basal hair cells. The question of tuning mechanisms is dealt with in a more general way in Chapter 14.

Chapter 8

The European Lizards, Lacertidae: *Podarcis sicula* and *Podarcis muralis*

Lizards of the family Lacertidae are often called 'typical' lizards. They are long-tailed and very agile and are found on the European, Asian and African continents in a great variety of habitats, even in regions where it is extremely cold in winter. During their active season, they emerge from holes in the ground or between rocks to warm themselves in the sun and hunt for insects, spiders, snails, etc. The species described in this chapter are small lizards of central and southern Europe. The ruin lizard *Podarcis sicula* may be found in the same habitat as the wall lizard *P. muralis*, but the wall lizard is generally found in or on walls whereas the ruin lizard spends more time on the ground. They are known in the older literature as *Lacerta sicula* and *muralis*. The European lizards were the subjects of one of the first documented, scientific attempts to assess behaviourally whether reptiles can hear. Although she only had crude instruments available, Berger (1924) produced very good evidence that *Lacerta agilis* (the sand lizard) reacts to air-borne sounds, with an upper frequency limit near 8 kHz. The data described below are from Köppl (in preparation) and Köppl and Manley (in preparation).

8.1 Anatomy of the Hearing Organ

The lacertids are especially interesting, as they are the only family of lizards where the papilla basilaris is always completely divided into two sub-papillae. A papilla more or less divided into two is also seen in most varanids and a few other isolated species. The arrangement of sub-papillae seen in the Lacertidae could easily be derived from the type of papilla show by some iguanids, which have two bidirectional areas flanking a unidirectional area (see Sect. 7.1), by inserting a limbic bridge between the apical bidirectional hair-cell area and the unidirectional area (see also Fig. 14.1).

In lacertids, the apical and basal sub-papillae are small, each being between 100 and 300 μm long, and separated by a bridge of limbic material up to 100 μm long. There is a total of only 90 to 160 hair cells (Köppl, in preparation; Miller, 1980; Wever, 1978). According to Wever (1978), the basilar membrane is, as in many other lizard families, mostly strongly thickened by a papillary bar (his 'fundus') which varies in shape and thickness along the sub-papillae.

In the species under discussion here, *Podarcis sicula* and *Podarcis muralis*, the limbic enclosure is a total of 550 μm long. The sub-papillae are each 160 μm long, separated by a 70 μm bridge (all values in the fixed state, Fig. 8.1). An additional peculiarity (not entirely unique to lacertids) is the fact that the hair cells are not

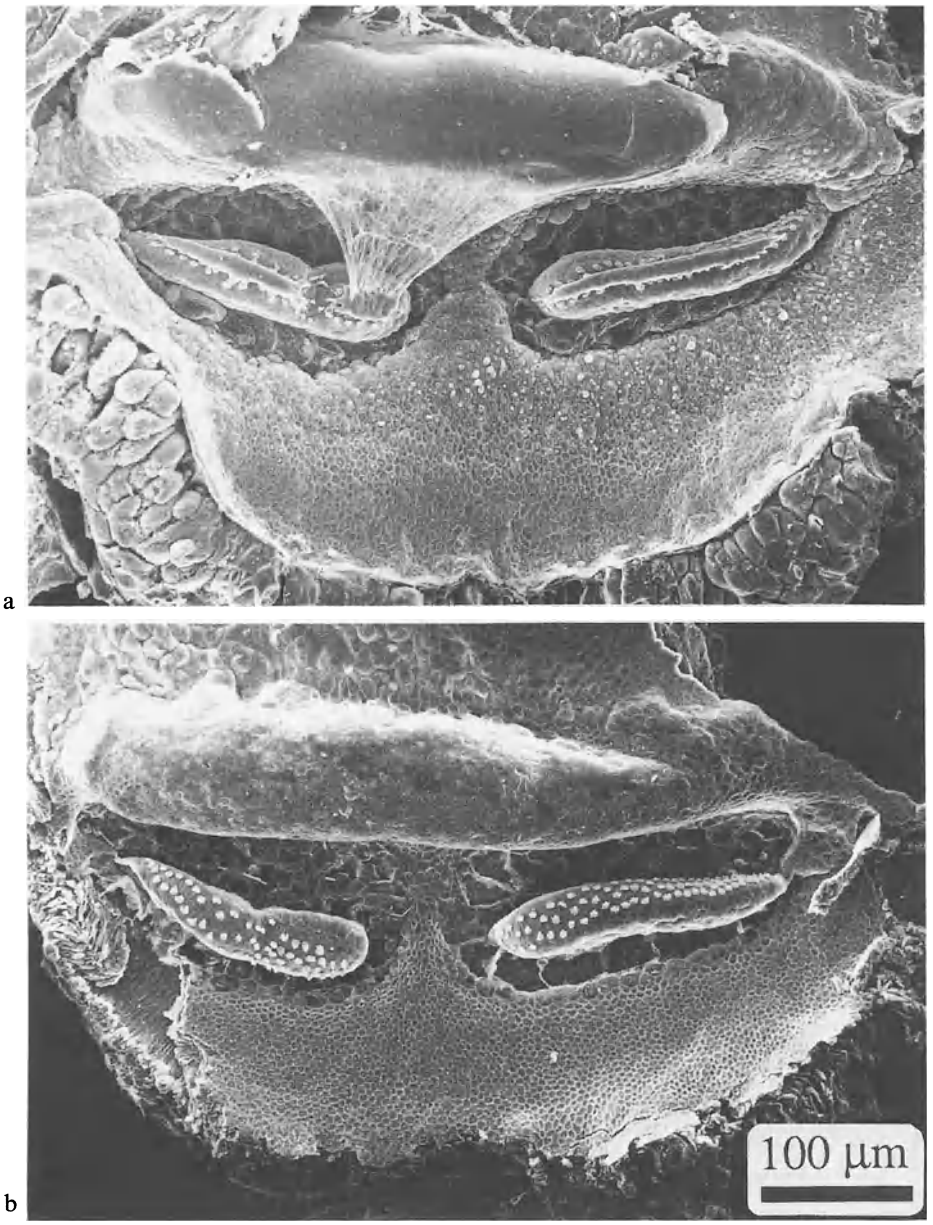

Fig. 8.1 a, b. Scanning electron micrographs (SEM) of the hearing organ of the European lizard *Podarcis muralis* in lateral view. The cochlear duct has been opened laterally to expose the basilar papilla, which is completely divided into two sub-papillae. The upper part of the figure shows the papillae with the tectorial structures preserved, in the lower part, they have been surgically removed. Apical is to the *right*, neural to the *top* (Courtesy of C. Köppl)

all upright in the papillae, but some are tipped to the side (Fig. 8.2). Whereas in the ends near the separating bridge, the hair cell axes are slightly tipped towards the abneural side, there is a gradual change of position towards both ends, such

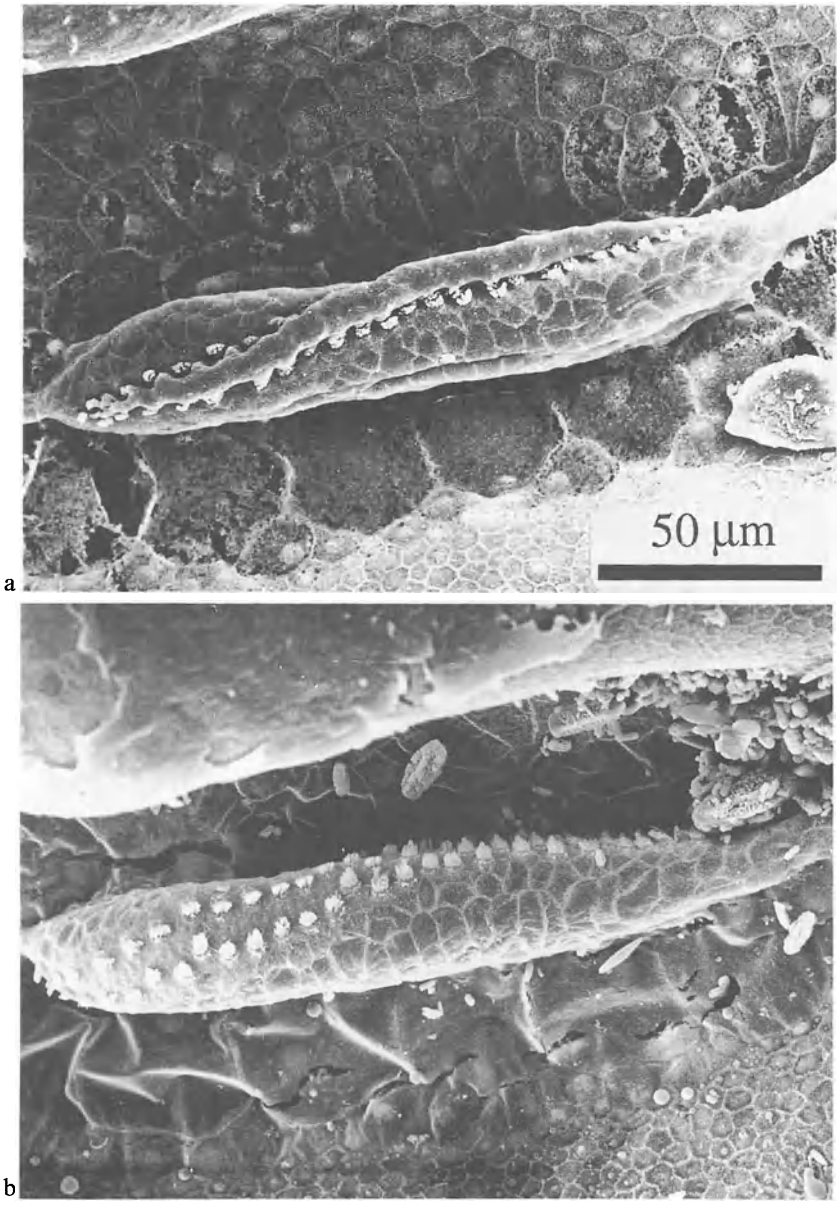

Fig. 8.2 a, b. SEM of the apical sub-papilla in the European lizard *Podarcis sicula,* with (top) and without (bottom) the tectorial membrane overlying it. Note the gradually changing position of the hair cells from abneural to neural, giving the impression of a twisted papilla. Apical is to the *right,* neural to the *top* (Courtesy of C. Köppl)

that the most apical and most basal hair cells are strongly tipped to the neural side. This effect, which has been observed in many species of lacertids, results in a positional difference of approximately 90° between the two ends of each sub-papilla, the difference being greater in the apical papilla (Köppl, in preparation).

The basal sub-papilla of *P. muralis* has, on average, 60, that of *P. sicula* 58 hair cells. There are, however, relatively large differences between individuals (ranges 52 to 67, 51 to 68, respectively). This subpapilla has two types of tectorial membrane (Fig. 8.1). The apical third of the sub-papilla is somewhat wider and is covered by a plate-like tectorial membrane which is connected to the relatively large limbic lip by a thin sheet or network of fibrils (Köppl, in preparation). The hair cells under the tectorial plate have, on average, a somewhat larger surface area and conform to the unidirectional-type (UDT) hair cells of Miller and Beck (1988). In the apical portion of this tectorial-plate area, the hair cells are predominantly unidirectionally oriented (Fig. 8.3). The rest of this subpapilla contains cells conforming to Miller and Beck's bidirectional type (BDT).

In the area of transition between the area with a tectorial plate and the rest of this sub-papilla, Wever (1978) thought that there are a few hair cells with free-standing stereovilli. While these cells are indeed unique in this papilla, in that their stereovilli are exceptionally long and few in number (see below), they are in fact all connected to one or the other tectorial membrane. In the scanning electron microscope, it is obvious that both tectorial structures shrink strongly during fixation, pulling the two types of tectorial structure apart and either freeing the bundles of those hair cells lying between or at least pulling strongly on the attached kinocilia and stereovilli (Fig. 8.4). In transverse section, such bundles might appear to be unattached. Under the tectorial plate, the hair cells have fewer and longer stereovilli than elsewhere on the papilla.

The entire apical sub-papilla is occupied by about 71 hair cells in *P. muralis* (range 62 to 84) and probably less in *P. sicula* (57 in the only specimen measured); this area is bidirectionally-oriented and contains hair cells of the BDT type (Fig. 8.3). In both apical and basal BDT areas, the hair cells are covered with tectorial material which is not connected to the limbic lip. This was described by Miller (1978b) as a "thick, shell-like tectorial cap" or "caterpillar-like" and by Wever (1978) simply as sallets. It does not, however, show the obvious subdivisions of the chain sallets of, e.g., the geckos and skinks (Köppl, 1988; Wever, 1978). The tectorial structure follows the stereovillar bundles as they tip to the side, so that it appears twisted (Fig. 8.2).

The hair cells are irregularly arranged and do not show a particularly high packing density. The kinocilia have a terminal bulb (Fig. 8.5), and the hair cells all have rather short stereovillar bundles, although a trend of length does exist in the two sub-papillae. The hair cells of the apical end of the basal sub-papilla tend to have fewer stereovilli than those of the basal end. The lowest numbers of villi (38) occur consistently in the (UDT) apicalmost area of the basal papilla, and in the transitional area between the tectorial structures (43 stereovilli). Towards the basal end of the basal papilla, the number rises to near 55. Although the absolute values and the gradients in length differ between individual papillae, a consistent trend is also seen in the apical sub-papilla. The stereovillar number increases from base to apex of this sub-papilla from, on average, about 50 to 86.

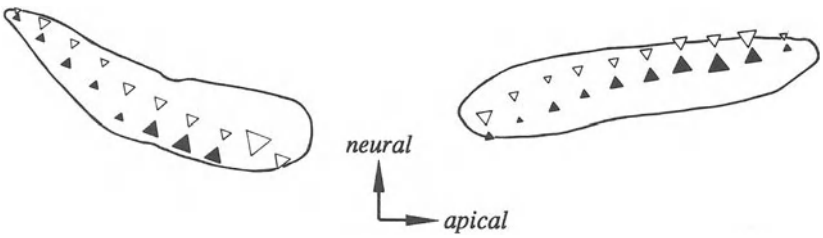

Fig. 8.3. Schematic drawing of the hair-cell orientation pattern on the two sub-papillae of *Podarcis muralis*. *Filled triangles* represent neural, *open triangles,* abneural orientation. The size of the triangles corresponds to the average percentage of cells with the one or the other orientation of the total hair-cell number found in each of 10 equally wide strips on each sub-papilla (mean of 5 specimens for the basal, 4 for the apical sub-papilla) (Courtesy of C. Köppl)

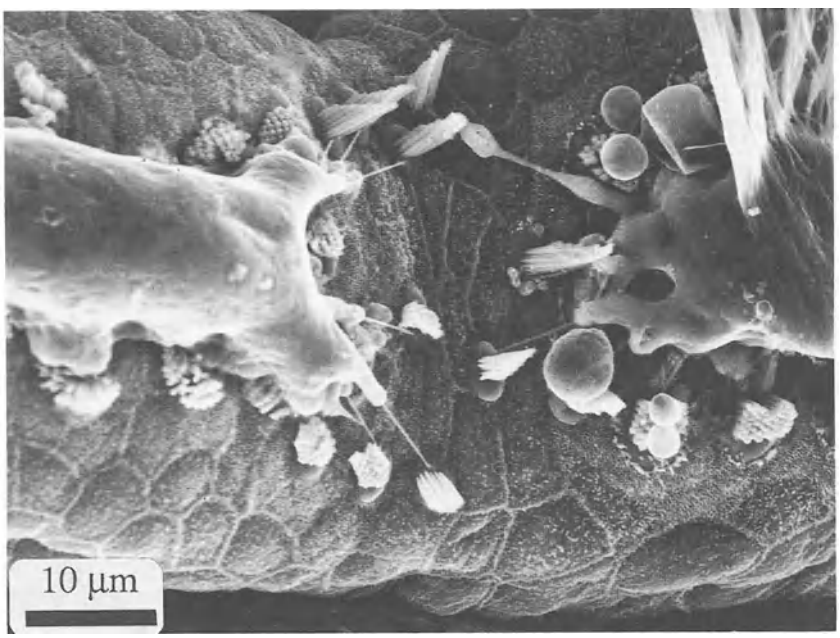

Fig. 8.4. SEM of the transition zone between the two different types of tectorial structures on the basal sub-papilla basilaris of *Podarcis muralis*. Note that every hair cell visible has contact to one or the other type. Both tectorial structures appear greatly shrunken due to the histological procedures and are certainly much closer to each other in the living organ. The shrinkage has caused the kinocilia of some hair cells to be torn from its contact with the stereovilli and be pulled tight. Apical is to the *right,* neural to the *top* (Courtesy of C. Köppl)

The heights of the longest stereovilli do not show great changes over the different areas of the papilla. They are longer in the transitional area (over 5 µm) than in the unidirectional area (3.5 to 4.5 µm; Fig 8.6). However, over the rest of the basal sub-papilla and the whole apical sub-papilla, the stereovilli are very short (2.5 to 3.5 µm).

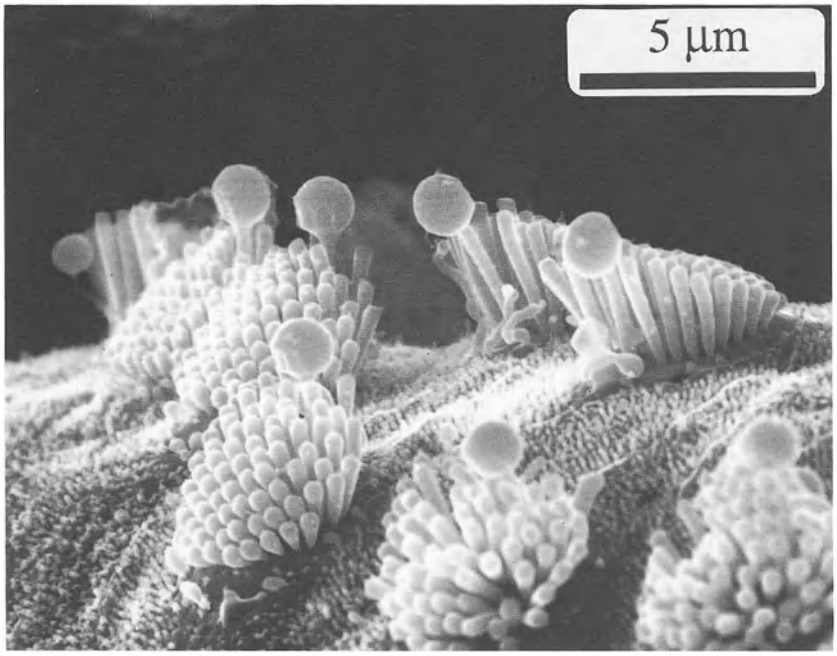

Fig. 8.5. SEM of a group of hair cells near the basal end of the basal subpapilla basilaris of *Podarcis muralis*, with the tectorial membrane removed. There are two rows of oppositely-oriented hair cells. Their kinocilia end in a spherical bulb which shows indentations from the tallest stereovilli (Courtesy of C. Köppl)

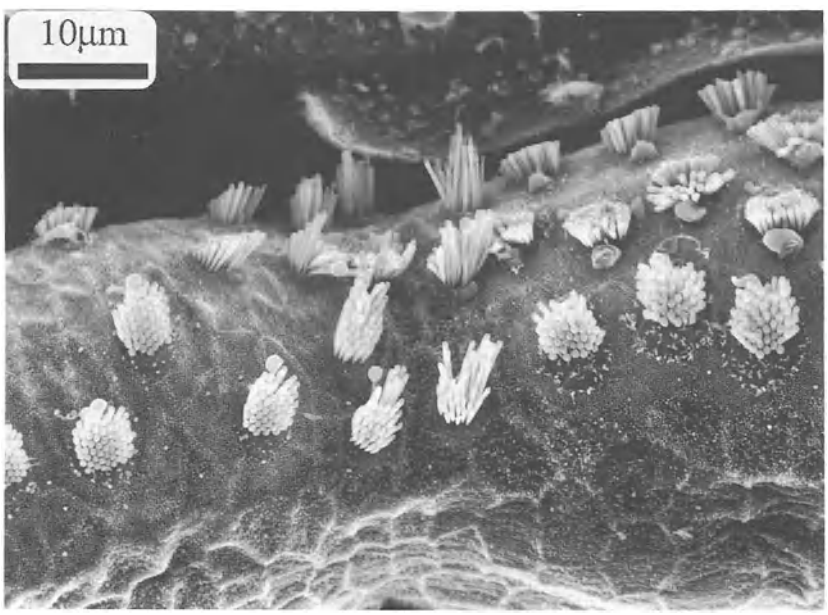

Fig. 8.6. SEM of part of the basal subpapilla of *Podarcis muralis*. In this area, the papilla is slightly constricted and there is a transition between two types of tectorial structures (see Fig. 8.4), which have been removed in this specimen. A few hair cells right at the border between the different tectorial structures always have much longer stereovillar bundles than their neighbours in either direction. Apical is to the *right*, neural to the *top* (Courtesy of C. Köppl)

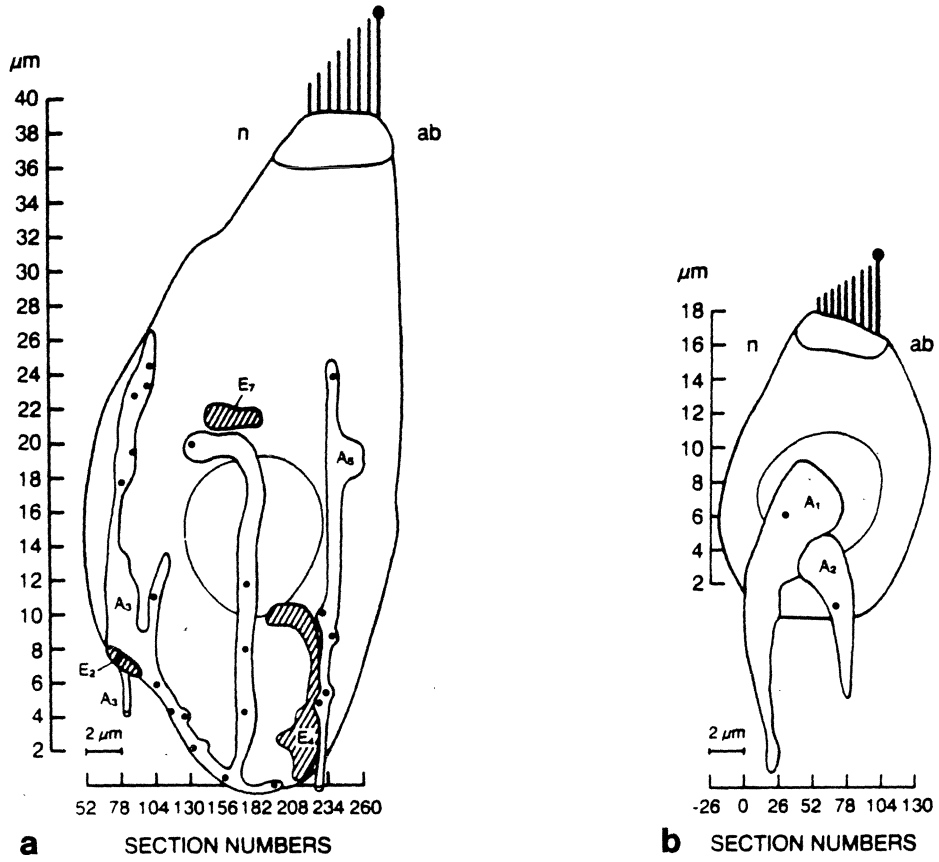

Fig. 8.7 a, b. Schematic drawings of the positions of afferent (*A*) and efferent (*E*) synapses on one side of hair cells of *Podarcis*, reconstructed from ultrathin sections. *a* UDT hair cell, connecting with two afferent (numbered *A3* and *A5*) and three efferent fibres (*E2,4,7; cross-hatched*) on the side shown. Not shown are three other afferent and five efferent fibres supplying the other side and the base of the hair cell. One of the afferents and several efferent fibres also supplied other hair cells. *b* BDT hair cell exclusively innervated each with one synapse by two unbranched afferent fibres (*A1,2;* no efferent fibres) on the side shown and two on the other side. Only one side of the hair cell is shown, as the two sides are similar. Synaptic sites within the afferent terminals are shown as *black dots; n* neural side; *ab* abneural side of cuticular plate (Miller and Beck, personal communication)

The innervational pattern of the papilla of *P. sicula* has been studied by Miller and Beck (1988). There are between 479 and 601 nerve fibres in the auditory nerve and the ratio of nerve-fibre number to hair cells is 5.3:1 (Miller, 1985). Only the hair cells of the apical end of the basal sub-papilla (UDT hair cells) receive efferent synapses (Fig. 8.7). Whereas the BDT hair cells are exclusively innervated, the UDT hair cells have a mixed type of afferent innervation from the larger nerve fibres which enter the papilla in this area, only some UDT hair cells being exclusively innervated. The number of afferent fibres supplying each UDT and BDT hair cell is similar, but the number of afferent *synapses* on the UDT cells is 12 times greater than on the BDT cells (Fig. 8.7). Afferent fibres supplying BDT hair cells rarely make more than one synapse, whereas those to UDT hair cells make, on average, 12.

8.2 Activity Patterns of Auditory-nerve Fibres

8.2.1 Spontaneous Activity

Spontaneous activity, if present, was always irregular: The time-interval histograms (TIH; see Sect. 5.4) were, in most cases, unremarkable. Spontaneous discharge rates ranged from 0 to 71 spikes/s. Almost all of the higher rates were found for cells with higher CFs. Preferred intervals were only found in four of 11 low-CF fibres for which enough data were available; these intervals corresponded very well to the period of the CF in each case. As hair cells of the unidirectionally-oriented area can be either exclusively or non-exclusively innervated, some variation in activity patterns in these low-CF fibres is not unexpected.

8.2.2 Activity in Response to Tones

Not surprisingly, no differences in the neurophysiological data from nerve fibres emanating from the very similar papillae of the two species were found. Even between the anatomically-different papillae of the alligator lizard (Anguidae) and the granite spiny lizard (Iguanidae), no essential differences in the behaviour of the nerve fibres could be documented (see Sects. 7.3.1, 7.3.2; Turner, 1980, 1987; Weiss et al., 1976). Thus the data from *P. sicula* and *P. muralis* will be considered together. We (Köppl and Manley, in preparation) recorded from single primary nerve fibres of *P. sicula* and *P. muralis* both in the brain cavity and within the inner ear. While the latter approach made it possible to optically distinguish the two nerve branches innervating the two sub-papillae and to record separately from these branches, the surgical opening of the inner ear is a technique which can influence the response behaviour of the fibres and, of course, produce damage to the papilla. Findings with regard to the tonotopic localization of fibres of different CFs according to this method were confirmed and extended through the staining of fibres between the internal meatus and the brain. Such cobalt-stained fibres could be followed to their end terminations in the papilla. In this way, not only was the localization of CFs possible, but also some details of the innervation pattern became clear.

Low-CF fibres (up to about 800 Hz) emanate from the apical portion of the basal papilla, from hair cells covered by tectorial material connected to the limbus. The mid-frequency range from about 1 kHz up to about 2.7 kHz is located in the basal part of the basal sub-papilla. CFs above about 2.7 kHz emanate from the apical sub-papilla, with the highest CFs (roughly 5 kHz) being localized in the extreme apical area (Fig. 8.8). The mapping constants of the two sub-papillae are quite different. Whereas the basal subpapilla accommodates more than two octaves (less than 90 μm/octave), the apical papilla has less than one octave (more than 300 μm/octave). The distribution varies even within the basal sub-papilla, for CFs in the UDT area (below about 800 Hz) map at about

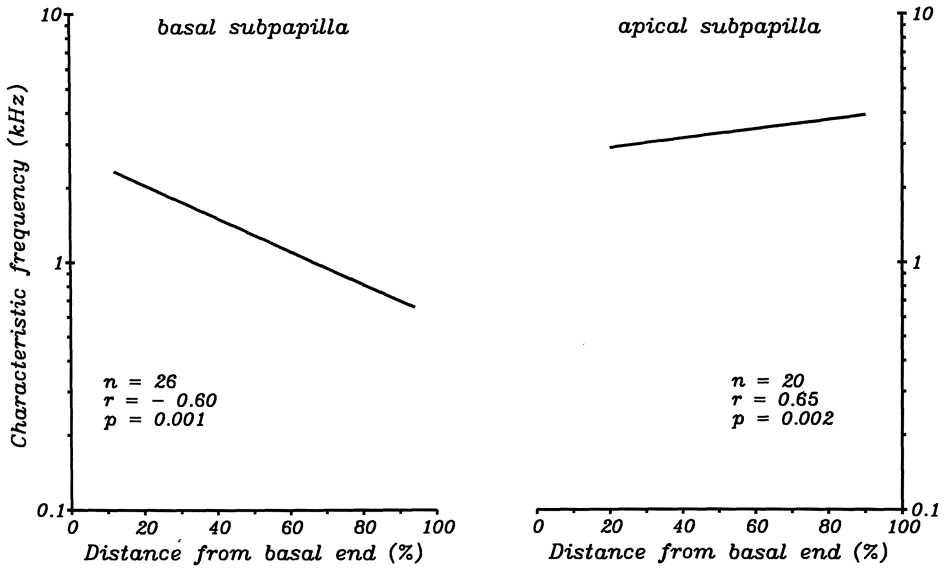

Fig. 8.8. Map of characteristic frequencies in the two sub-papillae of *P. sicula* and *P. muralis*. Shown are regression lines representing exponential fits to data points given by the innervation positions of many cobalt-stained auditory-nerve fibres of known CF. Statistical data for each regression line are shown in each case. The difference in the mapping constants for the two sub-papillae is obvious (Courtesy of C. Köppl)

60 μm/octave. As discussed in Section 14.10, a difference in mapping constants between low- and high-CF areas is almost universal among land vertebrates.

Due to the probability that individual animals differ somewhat in the characteristics of the papillae, it is not possible to state whether the frequency ranges of apical and basal papillae actually overlap a little in individual animals. However, the similarities between the tonotopic organization of this papilla and that of the granite spiny lizard (see Sects. 7.2, 7.3, 7.4) and the monitor lizard (Sect. 9.2) are striking, in that a low-CF area is bordered on both sides by cells responding to higher frequencies. In both the lacertid and monitor lizards, however, these high-CF areas are not mirror-images of each other as they are in the iguanid lizard. Rather, there are in both cases essentially non-overlapping high-CF ranges. It is reasonable to conclude that the presence of a physical division between the two subpapillae has allowed the reduction of redundancy of frequency responses at the hair-cell level, presumably yielding a more efficient analysis of the higher frequency range by increasing the amount of space and therefore the number of hair cells devoted to each octave.

There is an obvious correlation between the number of stereovilli per hair cell and the preferred response frequency. Thus the highest CFs originate in cells with over 80 stereovilli, intermediate frequencies from cells with 50 to 60 stereovilli and low frequencies from cells with about 40 or less stereovilli. The number of stereovilli and their length are important factors influencing the stiffness of the stereovillar bundles.

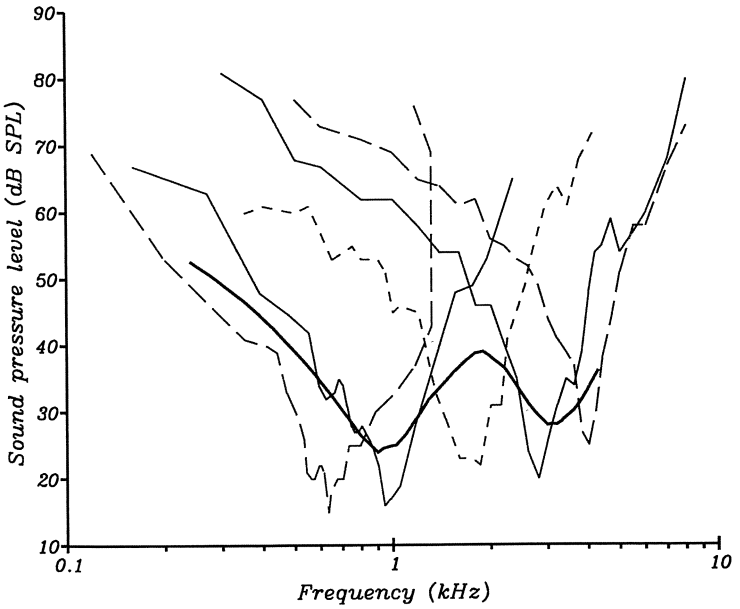

Fig. 8.9. Tuning curves of five single auditory-nerve fibres in *Podarcis*. The *thicker line* represents a locally-weighted regression for thresholds at the CF for all fibres recorded without opening the inner ear (Courtesy of C. Köppl)

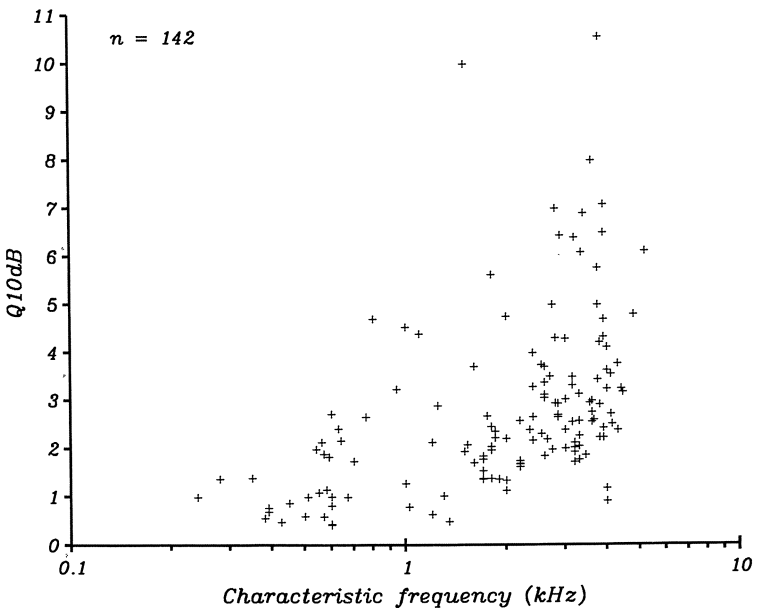

Fig. 8.10. Scatter plot of the Q_{10dB} (frequency-selectivity coefficient) for 142 single auditory-nerve fibres in *Podarcis*. The data are derived from recordings from the nerve in both the opened and closed inner ear. However, the distributions in these two situations show only minor differences (Courtesy of C. Köppl)

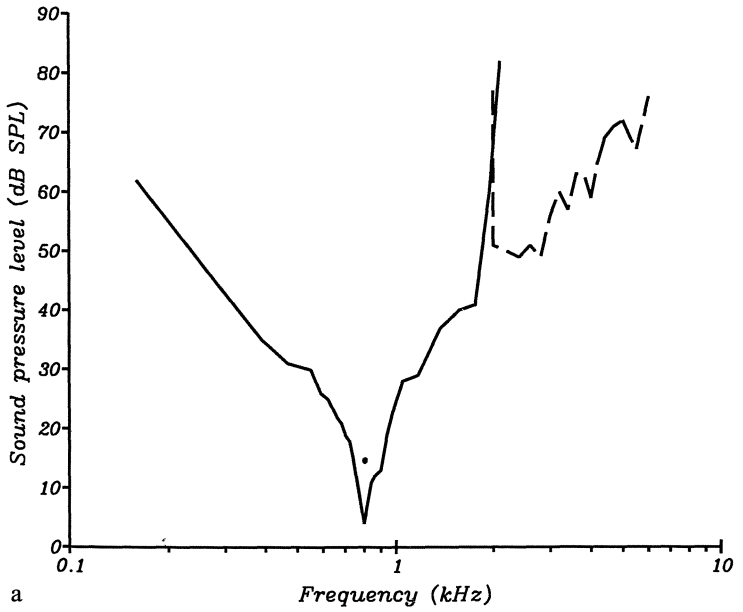

a

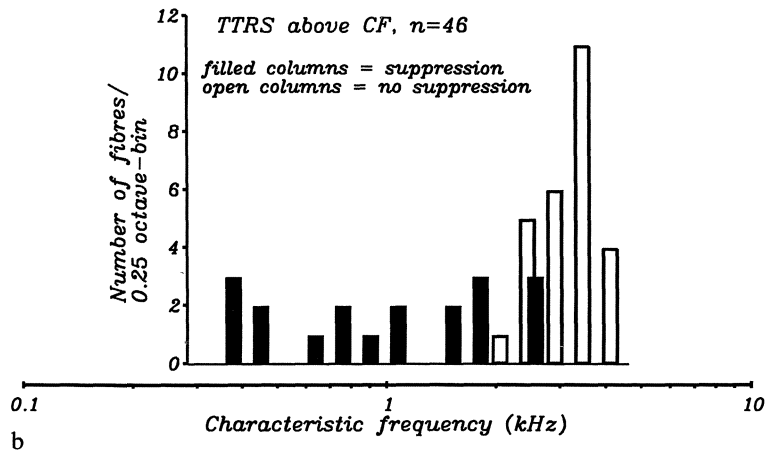

b

Fig. 8.11 a, b. Two-tone rate suppression (TTRS) in auditory-nerve fibres of *Podarcis*. *a* Excitatory tuning curve (*continuous line*) and two-tone rate suppression curve (*dashed line*) for a single auditory-nerve fibre of CF 800 Hz. The *dashed curve* represents the sound pressures necessary to reduce the discharge rate in response to a simultaneously-presented tone pulse at the CF and 10 dB above threshold (*dot* within the excitatory tuning curve). *b* Histogram showing the presence (*filled columns*) and absence (*open columns*) of TTRS in fibres of different CF. TTRS was only found in a low-CF group of fibres, and here only by using second-tones of frequencies above the high-frequency flanks of the excitatory tuning curves (Courtesy of C. Köppl)

The tuning curves are 'V'-shaped and usually strongly asymmetrical, being sharper on the high-frequency side (Fig. 8.9). Some fibres responded with a threshold near 5 dB SPL, with mean best values between 20 and 30 dB SPL. The threshold was somewhat higher for fibres with CFs around 2 kHz, which may be due to the division into two sub-papillae (Fig. 8.9). The $Q_{10\ dB}$ sharpness coefficient of individual tuning curves increases systematically with CF, from a mean of 0.9 up to 4 (Fig. 8.10).

A comparison of the peri-stimulus-time histograms (PST) for different frequencies within one cell's response range showed that the tonic component of the responses was strong at lower frequencies, but that towards higher frequencies, the phasic component became progressively more important. Concomitant with the loss of the tonic component is a fall in the discharge rates (averaged over the entire tone presentation), so that the slope of the intensity function is lower for higher-frequency stimuli. Maximal discharge rates (averaged over the 50 ms tonal stimulus) ranged from 63 to over 450 spikes/s. In a comparison of cells of different CF, phasic PST response types are more common for cells of higher CF. A similar distribution of PST types has also been found in the monitor lizard and tokay gecko (see Sects. 9.2 and 10.2.2). The dynamic ranges of different fibres ranged from 14 to 40 dB.

Fibres were also tested for two-tone rate suppression (TTRS) by simultaneous presentation of a tone burst of the CF and at about 10 dB above threshold and a second tone burst of varying frequency and SPL (Fig. 8.11 a). A reduction of the discharge rate to the CF-tone was never found for second-tone frequencies lower than the CF, but only for second tones above CF (Fig. 8.11 b). In addition, only low- and mid-frequency fibres (CF up to 2.5 kHz) showed TTRS at all (Fig. 8.11 b). According to the CF map (Fig. 8.8), these frequencies emanate from the basal sub-papilla.

Chapter 9

The Monitor Lizard, *Varanus bengalensis*

The monitor lizards (family Varanidae, genus *Varanus*) are relatively large animals, ranging in length up to more than 2 m. They occur in the warmer areas of the African, Asian and Australian continents. They have long necks and long, forked tongues. Being large, their prey tends not to consist of insect-sized animals, but rather other lizards, snakes, fish, frogs, birds and their eggs, and mammals. The Komodo dragon of the Sundra islands of Indonesia, *Varanus komodoensis*, grows to 3 m in length and kills and eats young deer and pigs. The long tail of all monitors can be used as an effective weapon and is flattened in the species which spend a lot of time in water.

As noted in Chapter 4, the monitor lizards show a strong tendency towards constriction of the basilar papilla at a point about one-third of the distance from the apical end. In some cases, the division of the papilla by the constriction is essentially complete, there being no hair cells in the thin bridge between sub-papillae. This is the case with the bengal monitor, *Varanus bengalensis*, which is the subject of this chapter.

9.1 Anatomy of the Basilar Papilla

In *V. bengalensis*, the apical sub-papilla is about 0.6 mm, the basal subpapilla 1.2 mm long (fixed and dried, Miller, 1978 b) or 0.7 mm and 1.45 m (fixed and embedded, Wever, 1978) and up to 125 μm wide (Fig. 9.1 a,b). All hair cells are covered by a relatively heavy tectorial membrane, which is attached to the limbus along the entire length of the papilla (Fig. 9.1 c). Its thickness and structure varies along the length of the papilla (Wever, 1978). Miller (1978 b) gives the hair-cell numbers for the apical and basal segments as 786 and 1006 respectively (total 1792).

The apical sub-papilla has a higher hair-cell density, with up to ten hair cells across the width. The orientation is irregularly bidirectional and 55% of hair cells are oriented abneurally (Fig. 9.2). The hair cells have an average of 45 stereovilli, but no data on possible systematic trends in this number are available. The longer basal sub-papilla is divisible into an apical quarter, where the orientation is unidirectional (abneural) and the basal three-quarters, which shows the same irregular, bidirectional orientation as the apical segment (Fig. 9.2). Here, 60% of the hair cells, which have an average of 50 stereovilli, are abneurally oriented.

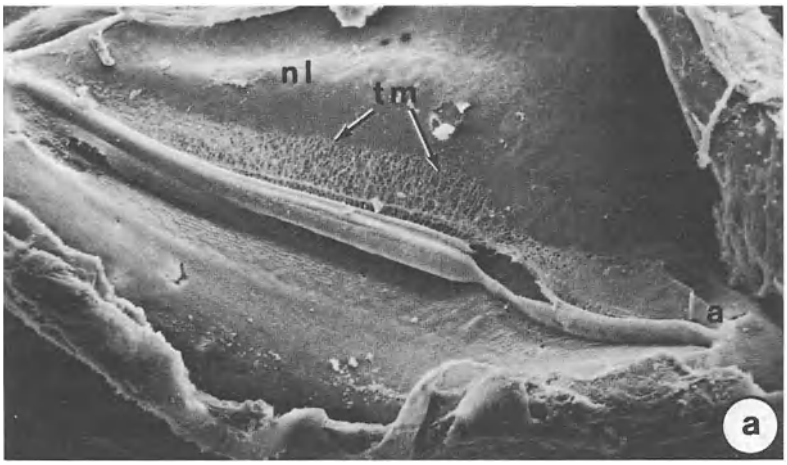

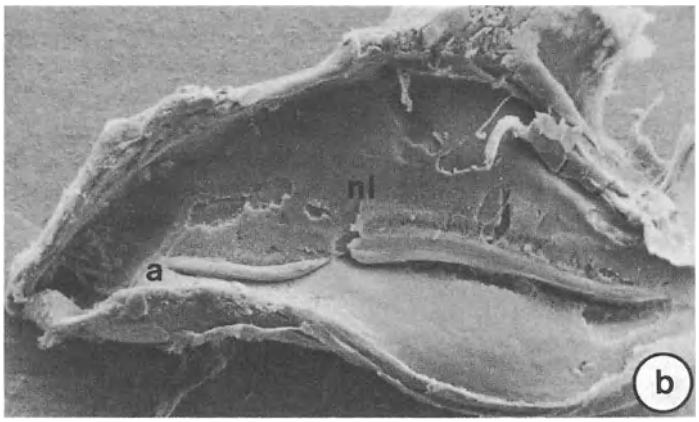

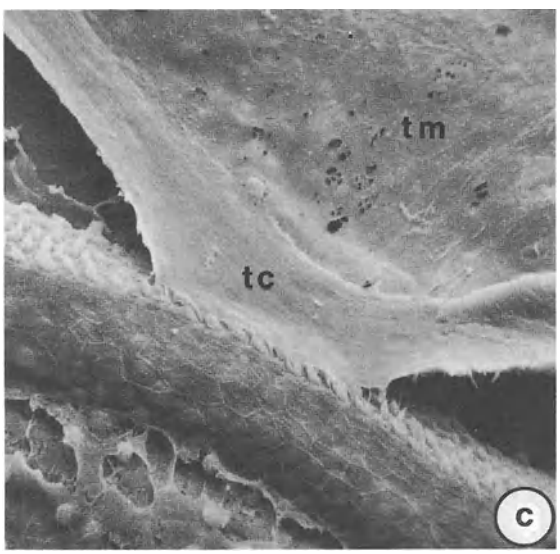

Fig. 9.1 a–c. Morphology of the basilar papilla of monitor lizards. *a* Scanning electron micrograph (SEM) of the basilar papilla of the monitor lizard *Varanus exanthematicus* as seen from the scala media side, showing that the papilla is strongly constricted about a third of the length from the apical end (i.e., from the *right*). Also seen is the connection of the tectorial membrane (*tm*) to the neural limbus (*nl*). *b* SEM of the papilla of *Varanus bengalensis*, showing the complete division of the papilla into a shorter, apical sub-papilla (*left*) and the longer, basal sub-papilla (*right*). *c* Portion of the papilla of *Varanus bengalensis*, to show the tectorial cap (*tc*) of the hair cells being torn off by shrinkage of the tectorial membrane (*tm*) network connecting it to the neural limbus (Miller, 1978 b)

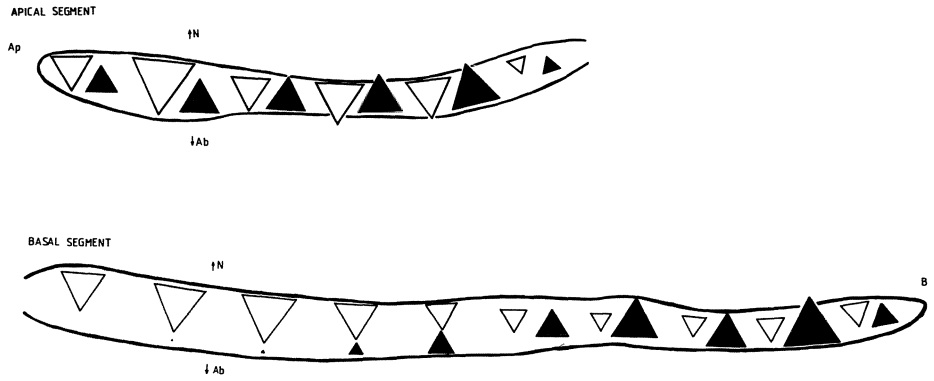

Fig. 9.2. Scale drawing of the basilar papilla of *Varanus bengalensis,* showing the orientation of hair cells in both apical (*above*) and basal (*below*) sub-papillae. *Filled triangles* represent neural, *open triangles,* abneural orientation. The size of the triangles corresponds to the average percentage of the total hair cell number with the one or the other orientation found in each 100-μm-wide strip along the whole papilla. Thus, the size of each triangle represents both the local weighting of orientations and the density of the hair cells. As can be seen, the apical part of the basal segment is essentially unidirectionally, abneurally-oriented. In the bidirectionally-oriented areas, cells of opposite orientation are not systematically arranged, but are mixed in an irregular pattern. *Ap* apical; *B* basal; *N* neural; *Ab* abneural (Redrawn by B. Böhm from data of Miller, 1978 b)

There is also no information available on any changes in stereovillar length with position on the papilla.

Miller's studies of the lizard auditory papilla indicate that in *V. exanthematicus*, a closely similar species, the larger nerve fibres project to the unidirectional hair-cell area. The hair cell-to-nerve fibre ratio is 1.1, most of the nerve fibres being larger than 3 μm in diameter (Miller, 1985; Miller and Beck, 1988).

9.2 Activity Patterns of Primary Auditory Fibres

Wever (1978) reported a high degree of sensitivity to the low and medium frequencies in his cochlear microphonic studies of two specimens of this species. Curiously, one of the microphonic sensitivity curves showed only one maximum of sensitivity, the other two. Some single-cell recordings have been made in the trunk of the auditory nerve of *V. bengalensis* as it leaves the ear capsule and courses to the brain (Manley, 1977). This involved exposing the brain case through a hole in the skin of the lower jaw and opening the brain case at a position just ventral to the eighth nerve. This technique does not damage the inner ear, but also does not allow visualization of the hearing organ.

Using a modified approach in four cases, I opened the ventro-medial aspect of the *recessus scala tympani.* This procedure involves removing bone very close

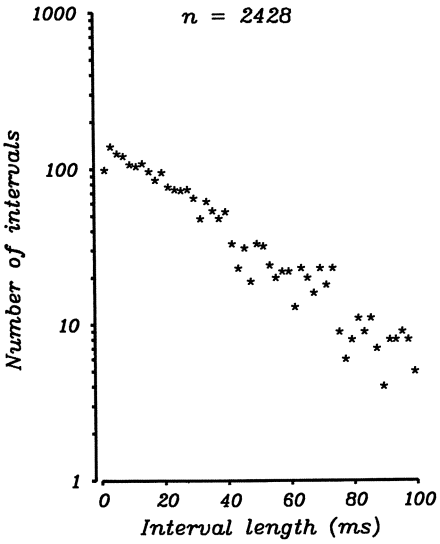

Fig. 9.3. A time-interval histogram of spontaneous activity of a primary nerve fibre of the monitor lizard *Varanus bengalensis*. The histogram shows the relative frequency of intervals of different lengths in a series of 2428 intervals, with a bin width of 2 ms

to the papilla and can result in damage to all or part of it. The exposure does, however, permit visualization of almost all of the apical and more than half of the basal papilla. It was possible to place recording electrodes in the distal portion of the acoustic branch of the eighth nerve, in the sheet of nerve fibres emanating from the neural side of the papilla.

Primary fibres are spontaneously active, with discharge rates between 0.65 and 52.1 spikes/s. The firing patterns are irregular, producing the exponential decay of the time-interval histogram of spontaneous activity typical for vertebrate primary auditory fibres (Fig. 9.3). Although the data sample is too small to be sure, clear preferred intervals were not found in the spontaneous activity. The lowest threshold to sound was shown by a cell responding at its CF of 700 Hz and 19 dB SPL. A cell with a CF of 800 Hz in the cochlear nucleus (the first relay nucleus in the medulla oblongata) of another animal had a threshold of 8 dB SPL (Manley, 1976). Since the cochlear nucleus recordings were made via a dorsal surgical approach, the 10 dB poorer sensitivity in the peripheral recordings could be due to the opening of the buccal cavity – middle ear space (see also Ch. 10) while stimulating with an open sound system.

Threshold responses to tonal stimulation of all fibres showed typical 'V'-shaped tuning curves, with CFs between 0.25 and 2.8 kHz (at 32 °C; Fig. 9.4). In the peripheral responses, the cells could be divided into two groups. Such a division had been previously observed in the responses of cochlear nucleus units (Manley, 1976). One population is more sensitive, with CFs from 0.25 to 1.1 kHz. The other is a less-sensitive population, with CFs from 1.3 to 2.8 kHz (Fig. 9.4). Just as in the cochlear nucleus data, the high-CF fibre group made up about 20% of the population of nerve fibres. On average, the tuning curves did not show any particular symmetry, for at any CF there were as many tuning curves which have a steeper high- than low-frequency slope as *vice versa*. The sharpness quotient for

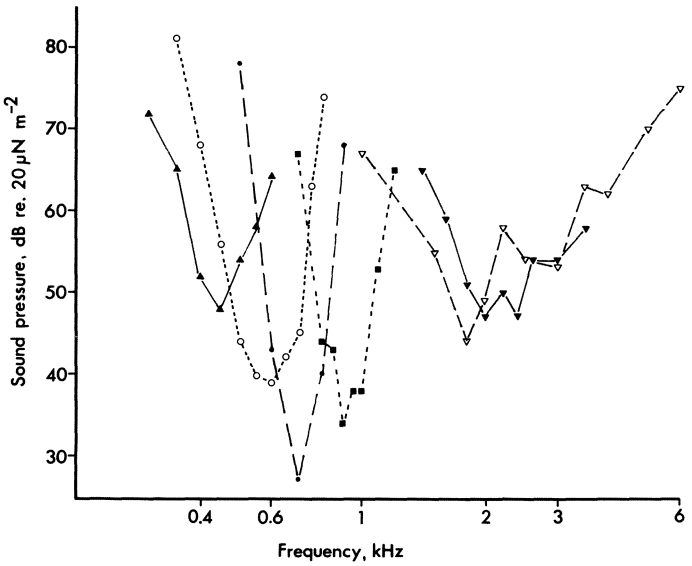

Fig. 9.4. Representative tuning curves from primary auditory neurones in *Varanus bengalensis*. Four units in the low-CF group and two units in the high-CF group are shown, not all from the same animal. The high-frequency slopes of the high-CF group may be somewhat shallower than normal due to damage incurred through the opening of scala tympani. The sound-pressure scale is equivalent to dB SPL (Manley, 1977)

the tuning curves of the monitor lizard ($Q_{10\ dB}$) did not increase with increasing CF. The lower-CF population of cells had, on average, higher values and a greater spread of $Q_{10\ dB}$ (Fig. 9.5).

The recordings from the distal nerve sheet were interpreted on the assumption that the nerve fibres leave the papilla at or near the hair-cell area they innervate and run straight towards the brain. This has been shown to be justified by new anatomical data on the auditory nerve of other lizard species (Chs. 7, 8, 11). Recording sites as close to 50 μm from the edge of the basilar membrane were possible over most of the apical and over more than half of the basal sub-papilla. This method allowed the localization of the lowest frequencies at the apical end of the basal sub-papilla and revealed a clear tonotopic organization of this sub-papilla, where the CF increases up to about 0.9 kHz towards the basal end (Fig. 9.6). The extreme basal end was not accessible.

The CFs of units innervating the apical sub-papilla were clearly those of the high-CF group. Here, CFs from 1.4 to 2.2 kHz were recorded, although in the small number of recordings, no clear tonotopic arrangement was observed. Due to the difficulties of the technique, however, it cannot be excluded that a regular arrangement of CFs is present. In order to ascertain the CFs of the inaccessible basal portion of the basal papilla, the entire accessible portions of both papillae were destroyed with a blunt electrode following the peripheral recordings. It was still possible to record from some fibres in the nerve trunk, which had CFs between 700 Hz and 1.1 kHz. I interpreted this to mean that the entire basal sub-

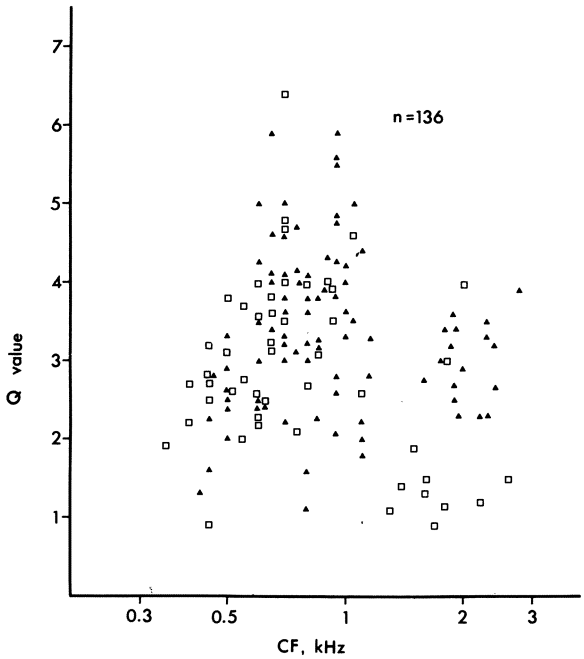

Fig. 9.5. The sharpness of tuning of single-fibre tuning curves in the auditory nerve (*open squares*) and cochlear nucleus (*filled triangles*) of *Varanus bengalensis*. The sharpness of tuning is given in terms of the Q_{10dB}. The apparent discrepancy between high-CF cells of the nerve and nucleus may be due to surgical damage during the opening of scale tympani for the nerve recordings (Manley, 1977)

Auditory Nerve Fibers in the Monitor Lizard

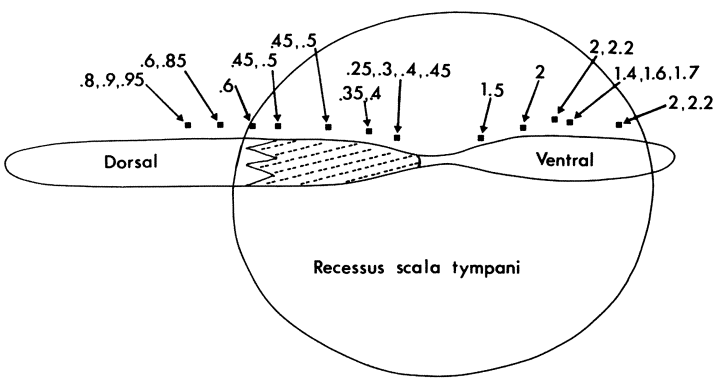

Fig. 9.6. Schematic drawing of the basilar papilla of *Varanus bengalensis* showing the area (*large circle*) of the papilla which is visible through the *recessus scala tympani*. *Dots* on the neural limbus indicate ink spots deposited by the recording electrode. The *adjacent numbers* are the CF, in kHz, of units recorded in each location. The data are a composite from four animals. The two most dorsal (basal) ink spots represent estimates as to the recording location. Physiological data from these recordings suggest that the hatched area is unidirectionally oriented (cf. Fig. 9.2) (Manley, 1977)

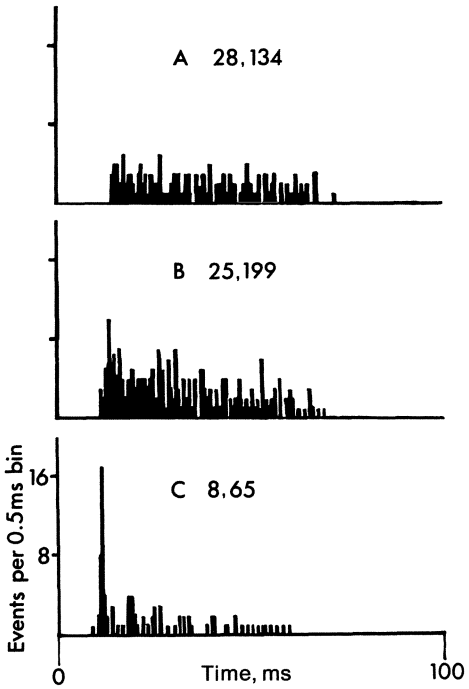

Fig. 9.7 a–c. Sample peri-stimulus-time histograms to illustrate the three basic patterns of pure-tone responses to 50 ms pure-tone bursts in three auditory nerve fibres of the monitor lizard. *A* Tonic ("filled") type from low-CF units. *Numbers* indicate dB above threshold (28) and total number of spikes to 30 repeated tone bursts (134). *B* Phasic-tonic ("intermediate") type. *C* Phasic ("peaked") type. These patterns do not change fundamentally with intensity (Manley, 1977)

papilla is tonotopically organized, with CFs from 0.25 kHz apically to 1.1 kHz basally.

In responses to CF tones, particularly as expressed in the form of the peri-stimulus-time histogram (PSTH) at 20 dB above threshold, there was also a trend in the activity pattern from low to high CF. Cells with CF below 600 Hz showed tonic discharge patterns and high discharge rates. This type of histogram was gradually replaced up to CF 900 Hz by a PSTH with a more phasic appearance, and a lower discharge rate (Fig. 9.7). Above CF 900 Hz, all cells showed the latter type of PSTH. This spectrum of activity patterns was correlated with a gradual fall in the saturation discharge rates. At high CFs, such PSTH are associated with shallow rate-intensity functions.

Interestingly, only cells with CF below about 0.6 kHz showed a shift in the response-peak latency for a reversal of the polarity of a click stimulus. This was interpreted to mean that above this CF, the nerve fibres innervate hair cells of both orientations. Thus it was predicted that the hair-cell area of the lowest CFs would be unidirectional in orientation (Manley, 1977). Even though this prediction proved to be very accurate (Miller, 1978 b), it remains to be seen whether the assumptions regarding the innervation patterns were correct.

Chapter 10

The Hearing of Geckos

Geckos are found world wide in almost all regions which are relatively warm. The largest grow to a length of about 34 cm. Most are nocturnal and are able to climb on vertical surfaces and even upside down, thanks to their specialized finger-tip pads. Geckos form one of the most interesting families of lizards from the point of view of their hearing, for they are the only lizards that use strong vocalizations. These are chirps, croaks or barks that are used in intraspecific communication and as aggressive warning sounds (Frankenberg, 1975; Marcellini, 1977; Werner et al., 1978). Their signals have a pronounced time structure, which forms an optimal stimulus for the gecko inner ear (see below). It is possible that this usage of the auditory system developed in combination with their predominantly nocturnal or crepuscular way of life. The geckos also represent the only case in which we know of another clear usage of the auditory system in the life of lizards. Sakaluk and Belwood (1984) report that Mediterranean house geckos (*Hemidactylus tursicus*) exhibit positive phonotaxis to a loudspeaker broadcasting cricket calling song. In the field, these geckos are found close to the burrows of calling male crickets, a behaviour which enables them to intercept female crickets attracted by the male's call.

10.1 The Basilar Papilla of the Tokay Gecko, *Gekko gecko*

Wever (1978) noted that the ear structure in geckos correlates with the systematic division into four subfamilies. The papilla of geckos is elongated (0.7 to 2.5 mm) and highly organized, with many hair cells (435 to 2500, Miller, 1985). As the tokay gecko has been studied the most, the structure of its basilar papilla will be discussed as an example. Its papilla is about 2 mm long unfixed, is wider at the apical end (130 μm compared to 50 μm basally) and contains over 2000 hair cells. The basilar membrane supports a rather thick papillary bar or fundus (Fig. 10.1 c). Each hair-cell surface is ovoid, 4 μm in the basal-apical axis and 6 μm in the other (Miller, 1973 b). The kinocilium is about as long as the tallest stereovilli (7 μm), although it is not known if all cells have bundles of the same length; in view of what we now know about other papillae, this is very unlikely. On average, there are 42 stereovilli per hair cell, each 0.5 μm thick except at the (thinner) base. The kinocilium is only 0.25 μm thick, except for the large, bulb-like tip (1.4 μm), where it attaches to the tectorial membrane.

As in almost all geckos, there is a basal, unidirectionally-oriented hair-cell area. The apical region, which is two-thirds of the papilla, consists of two strips

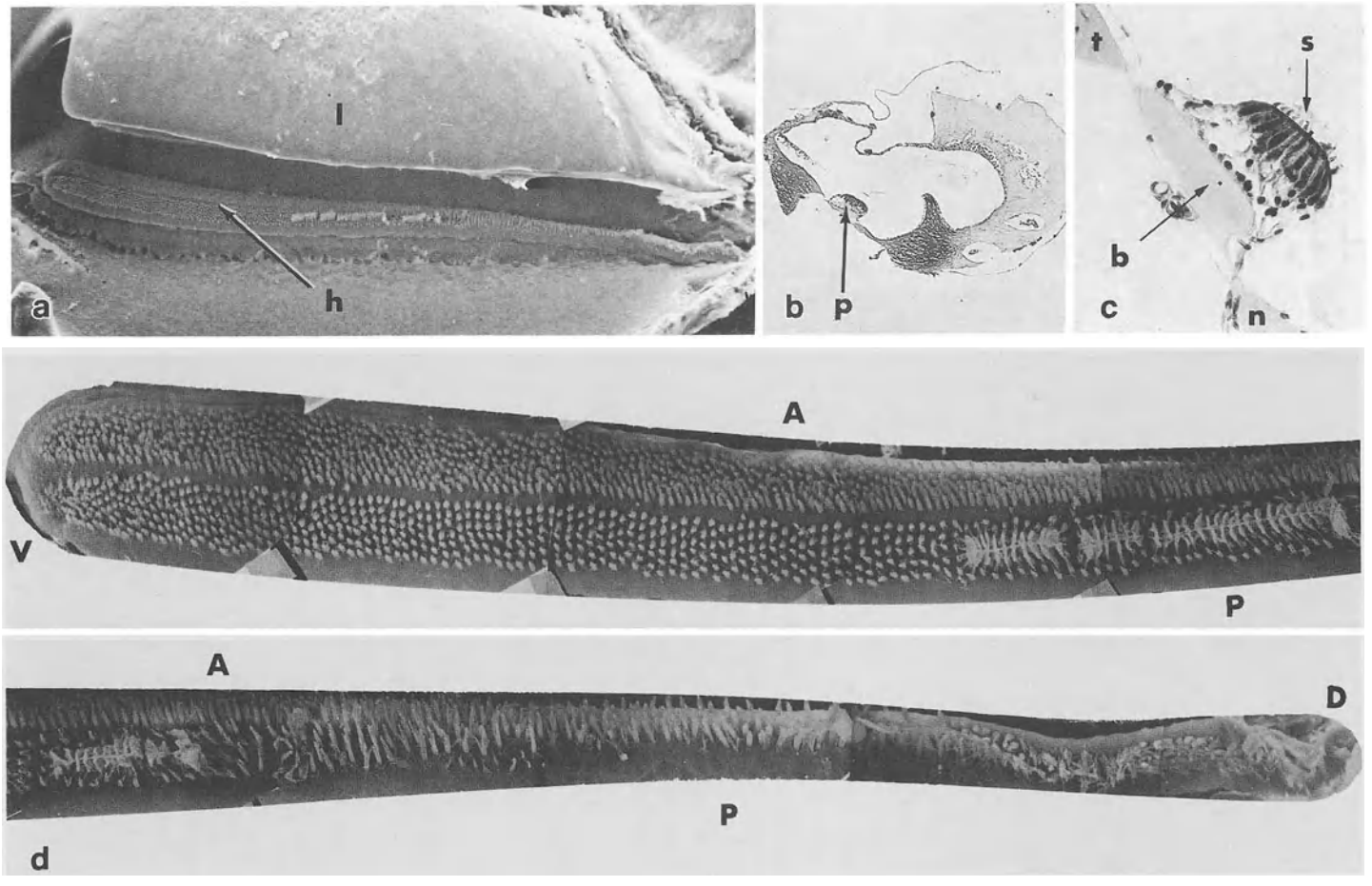
l
h
a
b
P
t
s
b
c
n
A
V
P
A
D
P
d

of bidirectionally-oriented hair-cell areas, separated by a longitudinal hiatus (Fig. 10.1 a,d). It should be noted that, in contrast to all other lizard families with two hair-cell areas (except the related pygopodids), the unidirectionally-oriented area lies *basal* on the papilla. The bidirectionally-oriented hair-cell strips are both highly organized. The respective neural sides of the strips consist of abneurally-oriented cell rows, the abneural sides of neurally-oriented rows (Miller, 1973 b). Thus, Miller speaks of the apical two-thirds of the papilla as being doubly bidirectional and names the hair cells on the neural side the pre-axial group, those on the abneural side post-axial.

In this gecko, the ratio of hair cells to nerve fibres is 0.9. Almost 82% of the nerve fibres have a diameter greater than 3 μm (Miller, 1985). The nerve fibres innervating the bidirectional regions are thinner than those to the basal unidirectionally-oriented area. Although there is no information available on the papilla of *Gekko*, Miller and Beck (1988) report details of the innervation pattern in the gecko *Coleonyx variegatus*, whose papilla resembles that of *Gekko*. Hair cells of the unidirectional area of *Coleonyx* are exclusively innervated by 4–5 afferents (mean of 13 synapses each fibre) and non-exclusively innervated by 8–9 efferents. There are no efferents to the hair cells of the bidirectionally-oriented area and the afferent innervation (six fibres per hair cell with a mean of about 6 synapses per fibre) is non-exclusive.

This papilla displays three different types of tectorial structure in the hair-cell areas. From the extremely prominent, overhanging limbic lip (Fig. 10.1 b) typical of the family, a thin tectorial membrane covers the unidirectional area. A thicker membrane with finger-like processes (in the fixed state) covers the neural (pre-axial) area of bidirectionally-oriented cells (Fig. 10.2). The abneural (post-axial) bidirectional area is covered by about 170 chain sallets (Figs. 10.2, 10.3; Miller, 1973 b; Wever, 1978). These sallets are only connected to each other by a relatively fine strand and each one covers all the hair cells in one single neural-abneural row on the abneural side of the hiatus. Correlated with this arrangement is the fact that the hair cells are not arranged in longitudinal (basal-apical) rows, but in rows across the papilla (Fig. 10.1 d). The tectorial structures attach to the kinocilium and, indirectly, to the five tallest stereovilli (Miller, 1973 b).

Fig. 10.1 a–d. Scanning electron micrographs and light microscope sections through the basilar papilla of the tokay gecko *Gekko gecko*. *a* SEM of the entire papilla, apical is to the *left,* and most of the tectorial materials has been torn off in preparation. *1* is the neural limbus, where most of the tectorial membrane is still attached; *h* shows the hiatus between hair-cell areas in the apical region. *b* Cross-section of the cochlear duct showing the papilla (*p*) on the basilar membrane and the neural limbus arching over the papilla to its left. *c* Higher magnification of the papilla, showing the papillary bar (*b*) beneath the basilar membrane, the neural limbus (*n*) and the sallet (*s*) lying over the stereovillar bundles of the hair cells. *d* Photomontage of an SEM in higher power of (*top*) the apical half and (*bottom*) the basal half of the papilla of *Gekko gecko*. The hiatus and the organization of the hair cells in rows across the papilla in the apical half can be seen, as well as some sallets remaining over the hair cells. In the basal area, most of the tectorial material remains. (Miller, 1973 b)

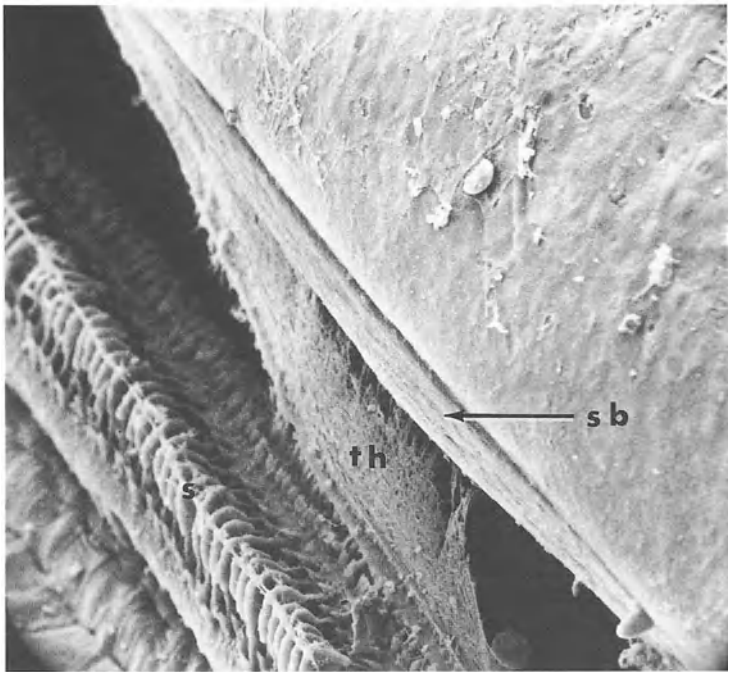

Fig. 10.2. Higher magnification of part of the central area of the papilla of *Gekko gecko,* to show a thickening of the tectorial membrane just below the limbic lip, the spindle body (*sb*), the connecting portion of the tectorial membrane (*th*). The latter is connected to the tectorial tissue (partly torn away) over the pre-axial hair cells. Post-axial hair cells (to the *left* of the picture) are covered by a row of sallets (*s*) (Miller, 1973 b)

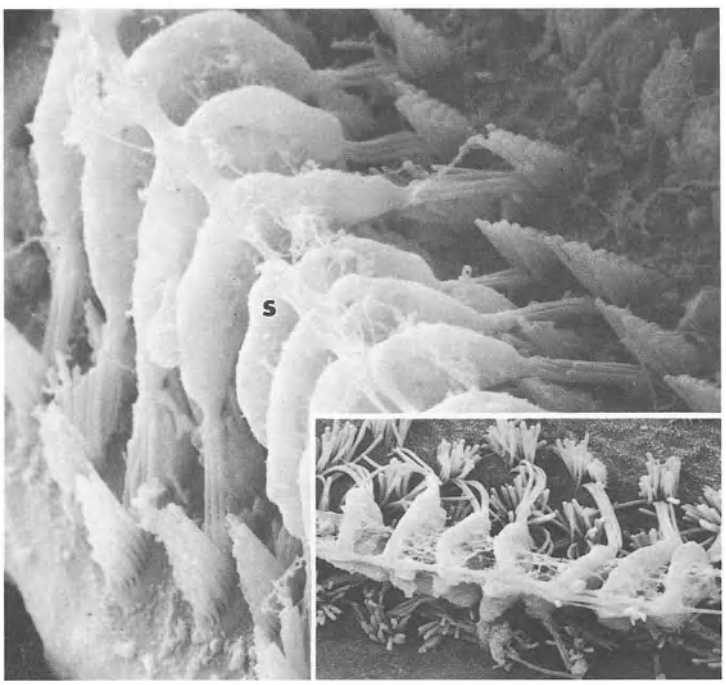

Fig. 10.3

10.2 Activity of Afferent Auditory-nerve Fibres in *Gekko*

10.2.1 Spontaneous Activity

The most information available on the function of the basilar papilla of geckos is derived from a study of the spontaneous and driven activity of 427 primary fibres of *Gekko gecko* (Eatock and Manley, 1981; Eatock et al., 1981). Spontaneous activity consisted of irregularly-occurring action potentials and, with the exception of a few silent units, spontaneous rates were between 1.6 to 40 spikes/sec (64 units). Time-interval histograms (TIHs) of units with CF above 0.5 kHz resembled those seen in birds and mammals; that is, they show a quasi-Poisson interval distribution (Fig. 10.4 A,B).

Fibres with lower CF had a more complex discharge pattern, with preferred intervals (that is, intervals which occurred more often than expected in a Poisson TIH), separated by intervals which seldom occurred (Fig. 10.4 C-F). These preferred intervals appear as more-or-less prominent peaks in the TIH; their duration is at least roughly the same as the reciprocal of the CF frequency, i.e., the period of the CF. There are a number of good reasons for believing that this activity is truly spontaneous. Among other things, some of the cells were not very sensitive to sound and unlikely to have responded to the very low noise in the recording chamber. Also, in at least one case, the interval (5 ms) was quite different from the CF period (3.3 ms) expected in responses to uncontrolled noise. It was suggested that such activity is the result of spontaneous oscillations in the resting potentials of the hair cells, with the most energy usually being at the frequency of the cells' CF (Eatock and Manley, 1981; Manley, 1979). The hair cells were considered to contain an electrical filter system which, under normal conditions, shows oscillation centred on the CF. The fact that preferred intervals are confined to low frequencies may correspond to the fact that only hair cells of the unidirectionally-oriented area of the papilla are exclusively innervated. It is expected that non-exclusive innervation would lead to non-synchronous synaptic input to a fibre from different hair cells, even if the individual hair cells have the same CF and thus oscillation frequency. The idea that preferred intervals are the result of hair-cell electrical oscillations has received a great deal of support for a number of species in more recent papers (see Sect. 14.3).

10.2.2 Responses to Tonal Stimulation

The responses to pure-tone stimulation were quite sensitive and the tuning curves were sharply tuned. An audiogram drawn through the most sensitive points of all

Fig. 10.3. SEM of a row of 8 sallets covering the hair cells in 8 rows running across the post-axial part of the papilla. Individual sallets (*s*) are connected to one another by a thick strand of tectorial material running along the tops of the sallets and by thin strands connecting them lower down. The connecting strands are seen better in the *inset* (Miller, 1973 b)

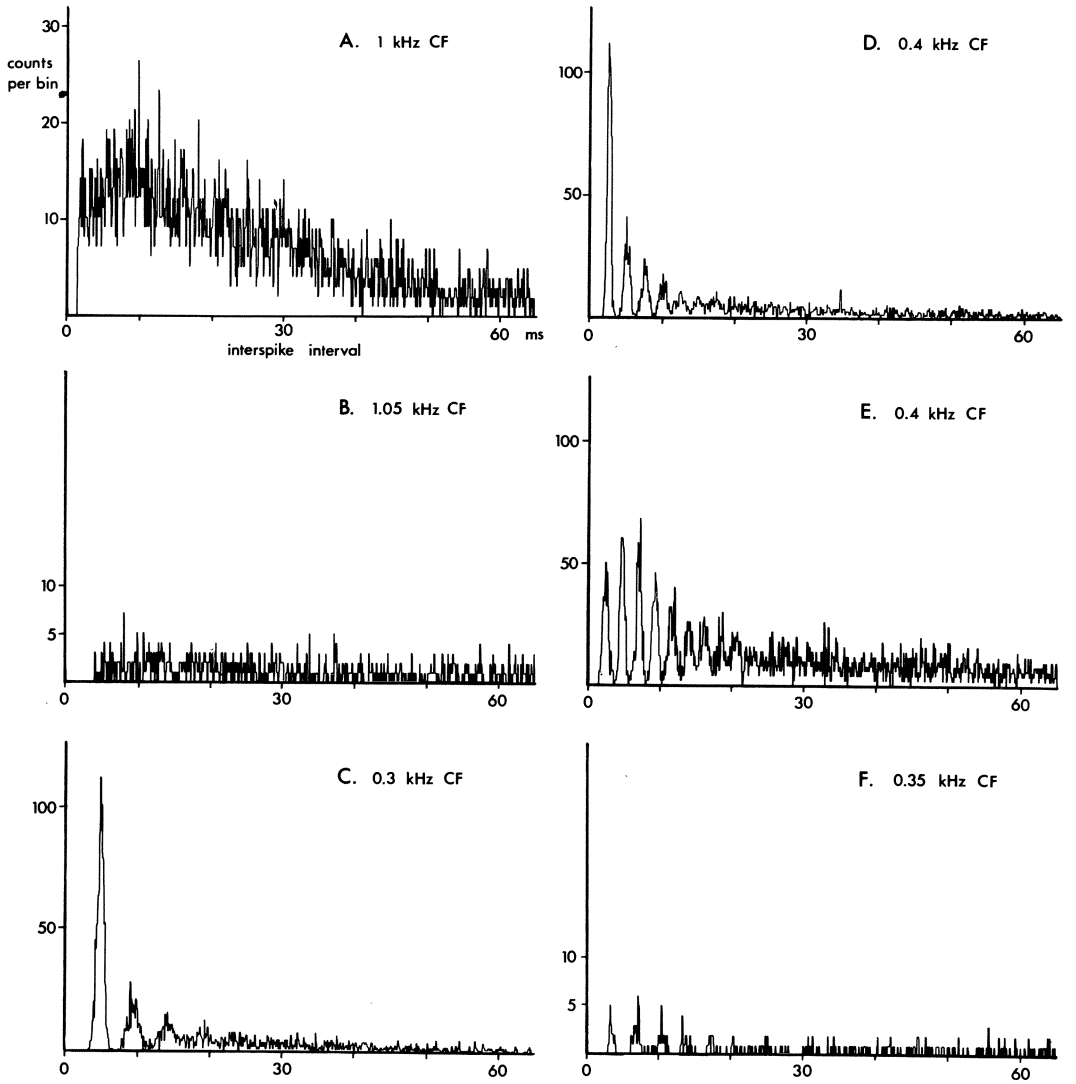

Fig. 10.4 A–F. Representative time-interval histograms (TIH) of spontaneous activity in six auditory-nerve fibres of the tokay gecko. *Abscissa:* interspike interval (ms) with a time resolution of 0.1 ms. *Ordinate:* relative frequency of interspike intervals of different lengths. Ordinate scales vary. In each case, the CF of the fibre is indicated. In the cells *C* to *F*, the TIH show prominent preferred intervals even when very few intervals are analyzed (*F*) (Eatock et al. 1981)

tuning curves indicates that the animal has two sensitivity peaks, at about 0.7 and 2 kHz, both near 17 dB SPL. A comparison of the sensitivity data (Fig. 10.5) to that obtained from the cochlear microphonic response by Hepp-Reymond and Palin (1968) and Werner and Wever (1972) indicates that there are strong similarities in the low-frequency sensitivity peak. The upper peak, however, is ab-

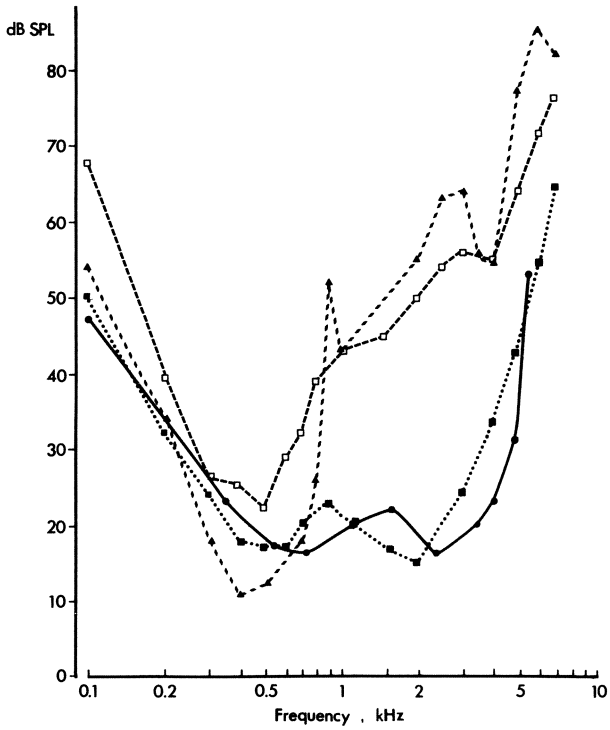

Fig. 10.5. Auditory sensitivity curves or audiograms for the tokay gecko derived from neural and microphonic data. *Open squares* connected by *dashed lines* and *filled triangles* connected by *dashed lines* are cochlear microphonic data from Hepp-Reymond and Palin (1968) and Werner and Wever (1972) respectively. Both curves represent the intensities required at different frequencies to produce 0.1 μV of microphonics at the round window. The sensitivity curves derived from the most sensitive points on tuning curves of cochlear nucleus cells (*filled squares and dotted lines,* Manley 1972a) and of primary nerve fibres (*filled circles, continuous line,* Eatock et al., 1981) show an additional, high-frequency sensitivity not evident in the microphonic data (Eatock et al., 1981)

sent in the microphonic data. Using the arguments already discussed in Section 1.3, it is reasonable to assume that the higher-frequency responses are primarily derived from the bidirectional hair-cell areas. The microphonic responses (fundamental component) would cancel each other so strongly (there are equally large populations with both orientations all along the apical area) that the microphonic potentials measured for the fundamental frequency would be extremely small. They are in fact 30 to 40 dB less sensitive than expected from the neural data. Data derived from evoked potentials from the cochlear nucleus of *Gekko* (Campbell, 1969) and from single units in the cochlear nuclei (Manley, 1972 a) show two-peaked audiograms similar to that of the primary nerve fibres.

The tuning curves of individual nerve fibres are 'V'-shaped (Fig. 10.6), with CFs between 0.15 and 5 kHz (at 24 °C). The low-frequency slopes of the tuning curves ranged from 20 to 240, the high-frequency slopes from 20 to 300 dB/octave (Fig. 10.7a). Overall, the slopes are higher at higher CFs. There is

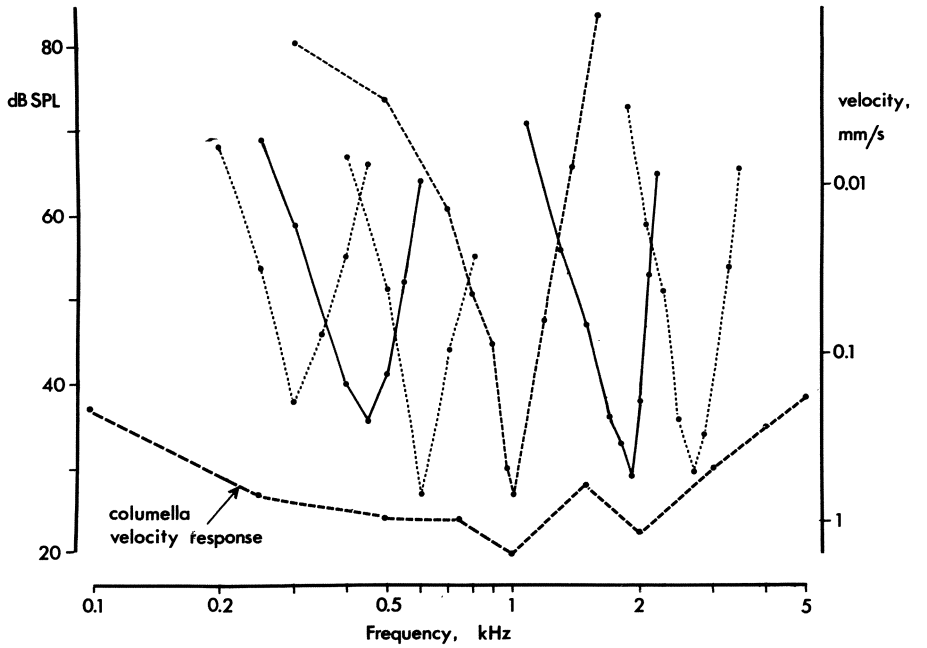

Fig. 10.6. Representative tuning curves of auditory-nerve fibres in the tokay gecko, not all from the same animal. Also shown is the velocity of the columella at 100 dB SPL in this species (inverted scale, ordinate on right) as a function of frequency (average of three animals) (Eatock et al., 1981)

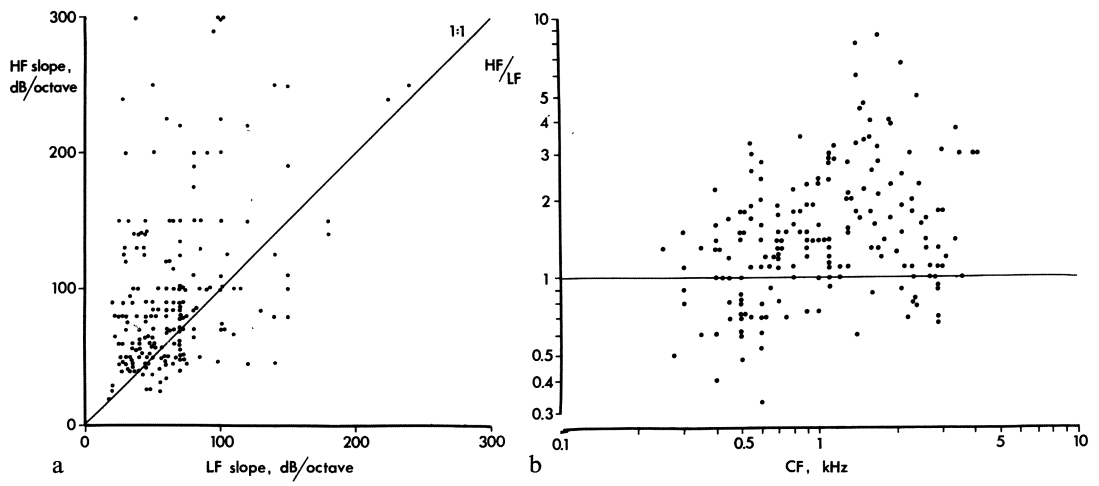

Fig. 10.7 a, b. Tuning-curve parameters for auditory-nerve fibres of *Gekko*. *a* High-frequency slope as a function of low-frequency slope of the tuning curves (slopes measured from 3 to 23 dB above threshold). The majority of tuning curves had steeper high-frequency slopes (*line* indicates a ratio of 1). *b* The ratio of the high-frequency to the low-frequency slope of the tuning curves is CF-dependent. Below CF 700 Hz, almost half the units had steeper low- than high-frequency slopes, above this CF, the high-frequency flanks tend to be steeper. The *line* indicates symmetrical tuning curves (Eatock et al., 1981)

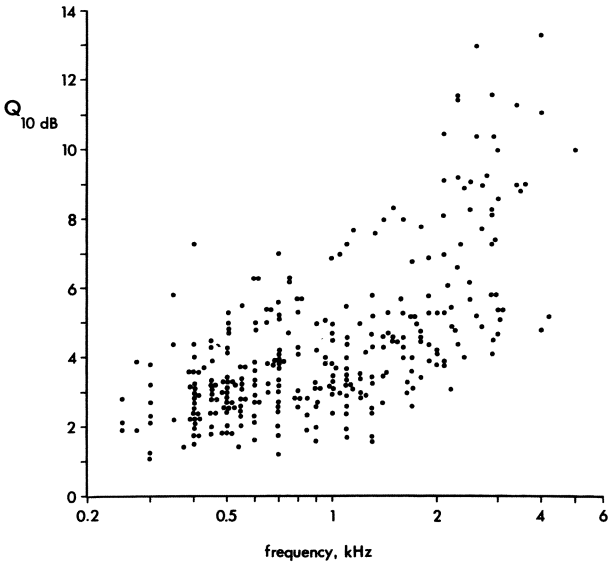

Fig. 10.8. The sharpness of tuning of primary auditory-nerve fibres in the tokay gecko, represented as the Q_{10dB} value, as a function of the CF. On average, the tuning sharpness rises with CF (Eatock et al., 1981)

also a tendency to asymmetrical tuning curves at higher CFs, where the high-frequency slope is steeper (Fig. 10.7b). In addition, the average $Q_{10\ dB}$ increases with CF, from 2–3 at low CFs to near 8 at high CFs (Fig. 10.8). The nerve is tonotopically organized, which is not unexpected, as a tonotopic arrangement has already been demonstrated for the cochlear nuclei of this species (Manley, 1972 a). Low-CF fibres were found at the posterior edge of the posterior branch of the eighth nerve. High CFs lay deep in the anterior edge. Taken together, the above data suggest that the papilla itself is tonotopically organized (with the lowest CFs basal, see below).

Peristimulus-time histograms (PSTH) were computed for the pure-tone responses of 81 fibres, each PSTH being the summed responses to 30 repeated identical tone bursts (not, however, phase constant). The PSTHs were divided according to their shape into three broad categories, tonic, phasic and intermediate (phasic-tonic; Fig. 10.9). The tonic responses adapt very little throughout the 50 ms tone burst (Fig. 10.9 A). In intermediate and phasic responses (Fig. 10.9 B-D), there is an increasing tendency to adaptation, the phasic cells often showing a number of narrow, prominent onset peaks, with more peaks at higher SPLs (Fig. 10.9 D). With increasing SPL, all fibres, regardless of their PSTH pattern at low levels, showed an increasing tendency to adapt. Thus, a cell with an intermediate PSTH at low levels becomes phasic at high levels. If the PSTH form at 20 dB above threshold is taken for classification, the tonic form is shown by cells of CF below 0.7 kHz, the phasic form for cells above 0.7 kHz. The intermediate form is found in an overlapping range, from 0.4 to 2 kHz. The phasic and tonic form are rather independent of the rise time of the stimulus.

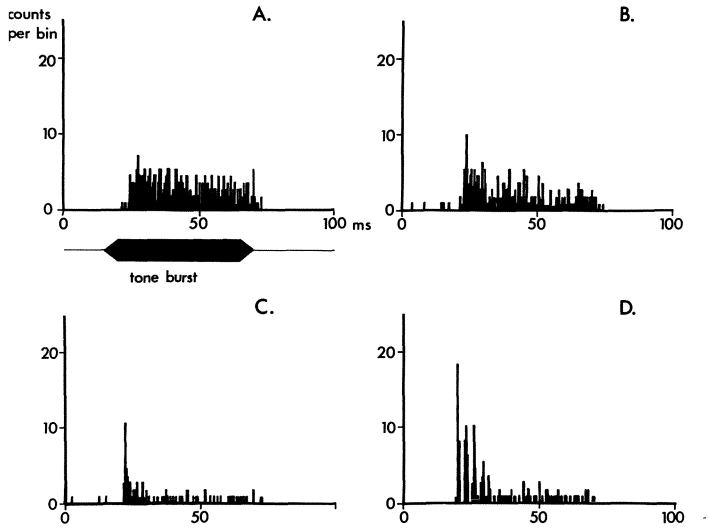

Fig. 10.9 a–d. Illustration of the major types of peri-stimulus-time histogram encountered in the responses of single auditory nerve fibres of *Gekko*. *A* Tonic; *B* intermediate; *C* phasic with a single peak; *D* phasic with multiple peaks. Each PSTH represents the summed response of a different single unit to 30 stimulus presentations of a tone at CF and 30 dB above the respective threshold. The placement of the tone burst in time at the animal's eardrum is shown below histogram *A* (Eatock et al., 1981)

The tonic histogram form is related to the fact that, at low frequencies, the cells respond in a phase-locked manner to every, or every second, cycle of the stimulus. This ability to phase lock falls off at higher frequencies, so that above 0.8 kHz, no phase-locking of any significance is observed. On average, the tonic fibres respond with the highest discharge rates to tonal stimulation, their intensity function having slopes of 12–14 spikes/s/dB and reaching saturated rates of 200 to 300 spikes/s. Most phasic units increase their rates at about 6 spikes/s/dB and have lower saturated rates.

Although two-tone rate suppression (TTRS) was only studied in eight fibres over a range of cell CF of 0.45 to 2 kHz, all showed this phenomenon (Fig. 10.10). The TTRS was demonstrable for second tones both above and below the excitatory tuning curve, with frequencies of the upper suppressive area generally being effective at lower SPL than those of the lower area.

Most experiments on the auditory nerve of the tokay gecko were carried out using free-field stimulation. In view of the fact that the skin of the lower jaw is open in the recording situation, it is possible that the sound entering the mouth and accessing the eardrum from the inside affects the results. In a study of 48 units in one animal using a closed acoustic system, it was shown that one possible effect of free-field stimulation is a drop in sensitivity of the fibres; the fibres in the closed-system experiment were up to 10 dB more sensitive. Thus, the best sensitivity of the tokay gecko actually lies below 10 dB SPL. These experiments confirmed the 10 dB drop in sensitivity seen in the audiogram near 1 kHz and the somewhat lower tuning-curve slopes for fibres in this region (Manley, 1981).

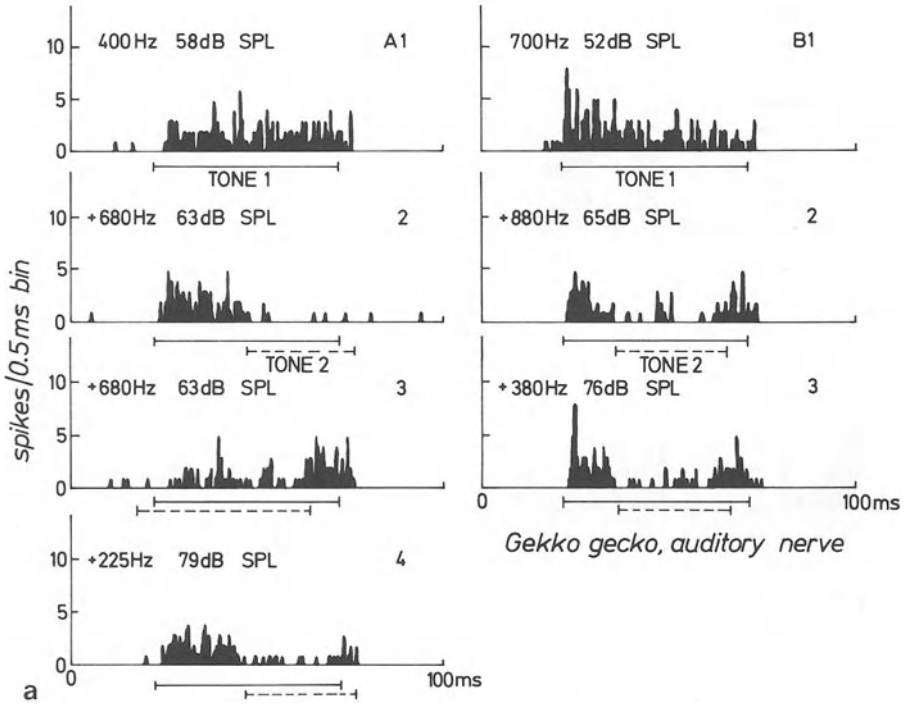

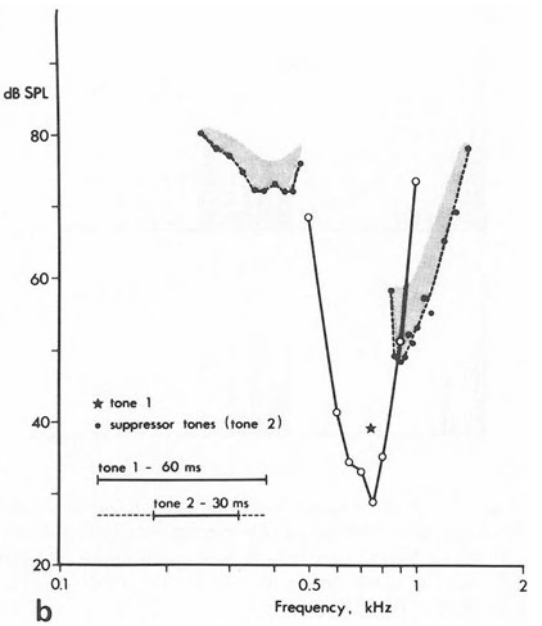

Fig. 10.10 a, b. Two-tone rate suppression (TTRS) in auditory-nerve units in the tokay gecko. *a, A1* A unit with CF 400 Hz stimulated with CF tone alone, 15 dB above threshold (*tone 1*); *A2* same, but with a second, shorter tone added (*tone 2*), at 680 Hz, 63 dB SPL; *A3* same, second tone displaced in time to begin before *tone 1; A4* same cell and first tone, but second tone now 225 Hz, 79 dB SPL. All second tones shown produced TTRS. *B1* A fibre with CF 700 Hz; *tone 1* is 700 Hz, 20 dB above threshold. *B2* Added second tone of 880 Hz, 65 dB SPL. *B3* Second tone now 380 Hz, 76 dB SPL. *b* Excitatory tuning curve (*continuous line*) of a single auditory-nerve fibre. TTRS threshold areas (*shaded*) as a function of frequency of *tone 2* are shown below and above the CF using *filled symbols* and *dashed lines*. The *star* indicates *tone 1*, at CF, 10 dB above threshold. The relative time parameters for the two tones are shown at *lower left* (Eatock et al., 1981)

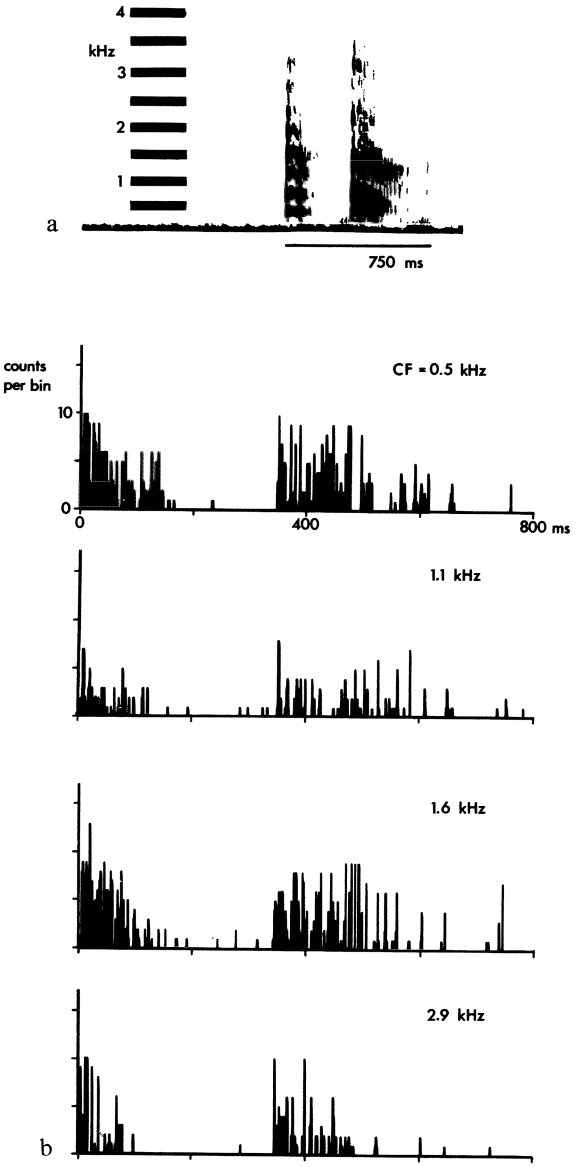

Fig. 10.11 a, b. Auditory-nerve responses to natural stimuli in *Gekko*. *A* A wide-band sonographic analysis of the spectral content of the two-component, advertising "to"-"kay" call of *Gekko gecko,* which was used as an acoustic stimulus for primary auditory nerve fibres. The *dark bands* at 500 Hz intervals are the frequency calibration, time is on the *abscissa*. *B* PSTH of the responses of four nerve fibres with different CFs as shown, each to ten repeated presentations of the call shown in *A*. The time axis is not the same as in *A*. Cells with CF 500 Hz and 1.6 kHz show strong responses, corresponding to the large amount of sound energy in these frequency bands (see *A*). The pulsatile nature of the call (seen well in *A* towards the end of the second component) is well represented in the histograms (Eatock et al., 1981)

On the basis of the microphonic data outlined above and the comparison with responses from species of other families, we can assume that the low-CF responses are derived from the unidirectional, basal area of the papilla. The frequency distribution is thus the *reverse* of that known for birds, mammals and most other reptiles described in this book. However, in view of the fact that the frequency distribution is complex in many lizards (see e.g. the chapters on the alligator, European and monitor lizards), this is not very surprising (see also Sect. 14.8 and Fig. 14.1).

10.2.3 Responses to Species-specific Vocalizations

The responses of primary fibres to playback of tape-recorded species-specific vocalizations were also examined. The two-component 'to-kay' call is about 750 ms long and consists of a short (150 ms) component followed (after a 190 ms pause) by a longer (400 ms) component. Each component is rather broadband, with the main energies at frequencies below 1.7 kHz. However, frequencies up to 3.5 kHz occur in the early part of both components. This vocalization has a very prominent time structure, especially obvious at the end of the second component, where the individual sound pulses can easily be seen in the sonagram (Fig. 10.11 A). All 20 fibres tested (CFs from 0.3 to 3.6 kHz) responded to both components, the discharge PSTH-pattern containing many peaks which reflect the pulsed nature of the call (Fig. 10.11 B). The higher-CF cells only responded to the first part of each component, where there is energy at higher frequencies. When the responses of higher-CF fibres to natural vocalizations are compared to pure-tone responses, it is striking that the firing rate is higher than for pure tones. This is due to the fact that the pulses of the call do not induce adaptation, as compared to a continuous pure tone.

The sharply-defined peaks at the beginning of many PSTH of high-CF units are not easily explained. The interval between peaks was a constant value (between 1.5 and 4 ms) for a given unit. Given the fact that the smallest intervals in TIH for high-CF fibres were generally 2 ms or more, it is possible that the multiple peaks indicate that the stimulus is so intense that the cell is firing as rapidly as it can. Thus, the fixed interval would indicate roughly the duration of the absolute refractory period of the fibre. Such peaks have also been observed in the activity of fibres in the skink *Tiliqua* (see Sect. 11.2.3).

10.3 Temperature Effect on Tuning

Encouraged by the obvious effects of temperature on the sensitivity of microphonics in lizards (e.g., Werner, 1972, 1976), a short pilot series of experiments was carried out, recording the responses of cochlear-nucleus cells of *Gekko* to changes of temperature (Manley and Werner, unpublished). The individual units showed a shift of the entire tuning curve to higher frequencies at higher temperatures. This study was followed up on 75 primary fibres, with the same result

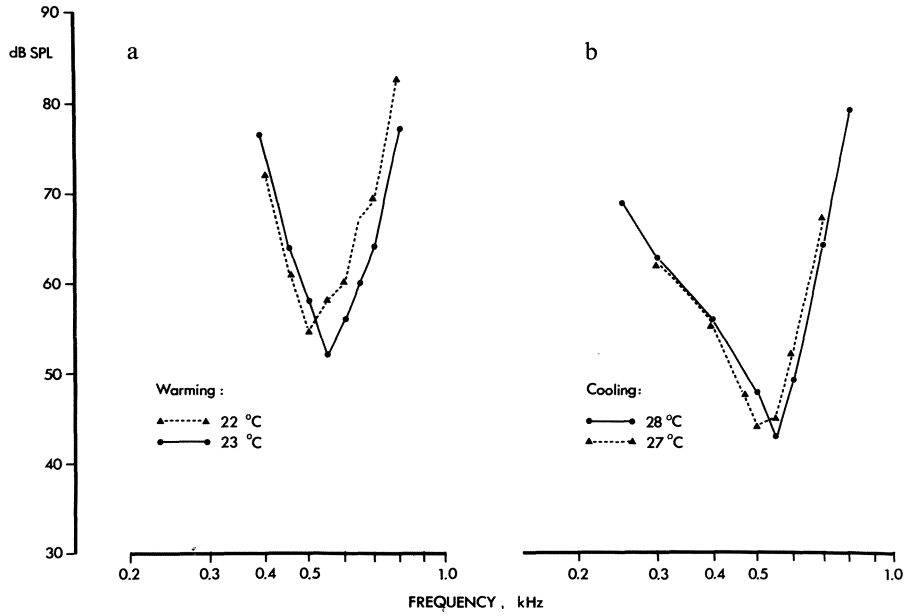

Fig. 10.12 a, b. Tuning curves of two auditory-nerve fibres, each at two temperatures, to illustrate the temperature effect on tuning. Both cells have a CF near 500 Hz. In *A*, the animal was warmed from 22° to 23 °C, shifting the curve up in frequency; in *B* cooled from 28° to 27 °C, which shifted the curve down in frequency. The sensitivity shifts on the flanks of the tuning curves for a difference of 1 °C are quite substantial (Eatock and Manley, 1981)

(Fig. 10.12; Eatock and Manley, 1981). The CF and, indeed, the whole tuning curve, shifts reversibly up in frequency with warming and down with cooling, at a rate of 0.05 to 0.06 octaves/ °C. For a 1 kHz cell at 20 °C, this changes the CF to about 1.55 kHz at 30 °C.

If we take into account the fact that a substantial number of the tuning curves of more than 400 fibres were measured at 24 °C, the CF distribution up to 5 kHz should be revised upwards for optimal behavioural temperatures. Although the optimum for the tokay is not very well defined, it certainly lies above 24 °C. The $Q_{10\ dB}$ value of the tuning of fibres and their absolute sensitivity were not greatly affected by the shifts in temperature over ranges of a few degrees. The shift of CF with temperature has also been observed in *Caiman* (Sect. 12.5) and the pigeon (Sect. 13.4.5.4), and the possible mechanisms are discussed in detail in Section 14.9.1. It is taken to be a further indicator that an electrical tuning mechanism is present in the hair cells of this species, as concluded above.

Chapter 11

The Bobtail Skink, *Tiliqua rugosa*

The skinks are the most widespread of the lizards. The bobtail is a large (generally up to 500 g), live-bearing skink found in almost all of the southern half of Australia. Due to its short, fat tail, it has also been called the two-headed lizard, but is also referred to as the sleepy, stump tail, shingle-back or pine-cone lizard. It is also known in the literature as *Trachysaurus* or *Trachydosaurus rugosus*. Although this animal is omnivorous, it possesses massive jaw muscles; this means that the head is also very wide. As the cranium is small in all lizards, the eardrum in this animal would normally be very far from the inner ear. Due to the presence of an external ear (about 6 to 10 mm deep) however, the columella is not exceptionally long. This external ear offers an ideal site for ticks to attach themselves to the skin at a location where they cannot be sloughed off. Not only is the external meatus normally full of ticks, but the presence of the ticks hinders normal skin moults, so that especially in older animals the meatus is blocked by one or more layers of sloughed skin. It is difficult to judge the significance of this ubiquitous phenomenon for the normal hearing of bobtail skinks. The results of our experiments on the bobtail lizard have been published (Köppl, 1988; Manley et al., 1988 d, 1989 b) or are in preparation as a series of publications.

11.1 Anatomy of the Hearing Organ

As a family, the skinks possess a very well developed basilar papilla and in this respect, the bobtail is no exception. The papilla is about 2.1 mm long in the living state and, as measured from scanning electron microscope pictures, contains a mean number of about 1920 hair cells (Köppl, 1988; mean of 5 specimens). Wever (1978) reports 1400 hair cells for this species, as measured from serial sections. Only part of the difference can be explained by the variability shown in this species. Some of the papillae we examined showed abnormalities (missing part of the papilla, areas without hair cells).

The papilla has a smaller apical segment which is, on average, 254 μm long (=16%) and 110 μm wide and a long basal segment (1800 μm long, gradually changing in width apically to basally from 105 to 125 μm, Fig. 11.1 a,b). The apical and basal segments contain on average 278 and 1645 hair cells, respectively (Köppl, 1988). Along the basal segment, the number of hair cells in a single cross-section grows from 5 to 9 towards the basal end. Their density increases in the same direction. Unlike almost all other lizard papillae, there is no unidirectional hair-cell area. The basal region is bidirectionally oriented, with a higher hair-cell

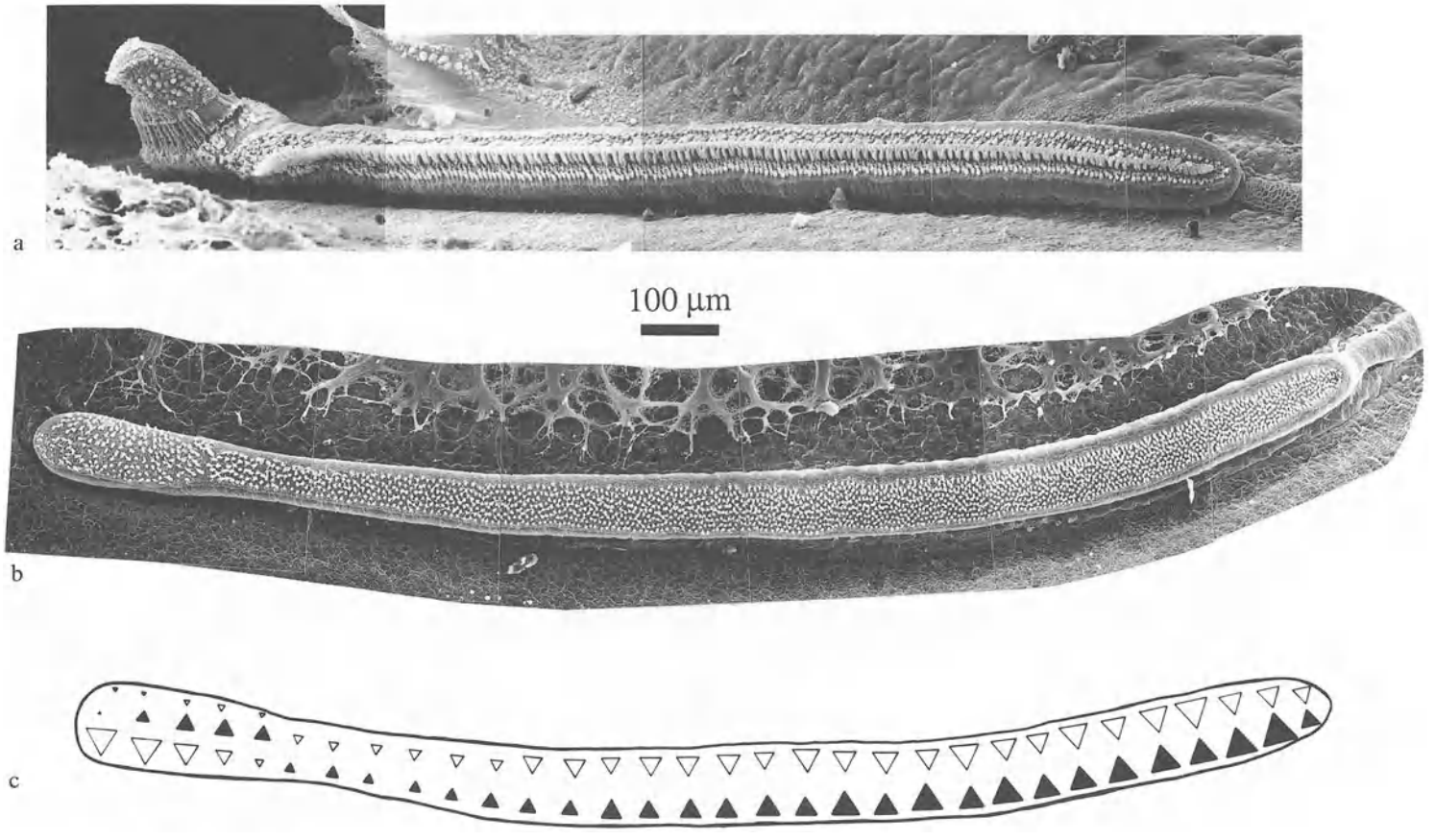
a
100 µm
b
c

density in its basal region (Fig. 11.1 c). The apical area is more complex; the orientation changes twice in one cross-section. The orientation pattern of most of this area differs from the opposing pattern of the basal area, in showing a divergent bidirectionality, that is, the kinocilia are directed towards the edges of the papilla instead of towards the midline. The innervational pattern (see below) and cytological structure of the apical area, however, indicates that divergent bidirectionality in skinks is a later derivation from the unidirectional pattern and that the apical area contains unidirectional-type (UDT) hair cells. According to Miller and Beck (1988), some skinks such as *Scincus scincus* have an apical area which is unidirectionally, abneurally oriented.

All hair cells in *Tiliqua* are attached to tectorial membrane material. None of the tectorial material is attached to the limbus. The apical area has a single, enormous, isolated tectorial structure which Wever (1978) refers to as a "culmen". Near its centre, it reaches a cross-sectional area of nearly 9000 μm^2 even in the fixed state (Fig. 11.2 a). Over the basal hair-cell area, in contrast, there is a long chain of 70–90 much smaller tectorial structures called sallets which are connected by a central, rope-like strand (Köppl, 1988; Wever, 1978; Figs. 11.1 a, 11.4b). Over the basal half of this hair-cell area, the sallets become smaller (Fig. 11.2 a). Due to systematic changes in the size and distance apart of these sallets and in the density of the hair cells, there is a systematic change in the number of hair cells connected to each sallet along the length of the basal segment. If sallets are considered to each cover the whole width of the papilla, then the number of hair cells per sallet increases from about 8 at the apical end of the basal segment up to about 25 at 80% of the distance to the basal end, falling thereafter to 17 at the extreme basal end.

The number of stereovilli per bundle is, in comparison to many other lizard species, quite small. From 40 to 50 in the apical segment (average: 46.5) and 40 to 45 for the apical half of the basal papilla, the number gradually falls to about 30 at the extreme basal end (average for basal segment: 39). With regard to the surface area of the hair cells, there is a more systematic trend. In the apical area, the area is about 27 μm^2. At the apical end of the basal area, the area starts out at 33 μm^2 and falls steadily to the extreme basal end, where the cell surface area is only about 15 μm^2. There is also a trend in the height of the stereovillar bundles of the hair cells of the basal segment: they become much shorter towards the

Fig. 11.1 a–c. Scanning electron micrographs (SEM) of the hearing organ of *Tiliqua rugosa.* The cochlear duct has been opened laterally to expose the upper surface of the basilar papilla. The apical end is to the *left. a* A specimen with the tectorial structures preserved. *b* In a different specimen, and viewed more from above, the tectorial structures have been removed to expose the stereovillar bundles of the hair cells. Apical is to the *left,* neural to the *top. c* Schematic diagram of the hair-cell orientation pattern on the basilar papilla. *Filled triangles* represent neural; *open triangles* abneural orientation. The triangle size corresponds to the percentage of hair cells with the one or other orientation counted in approximately 50-μm-wide strips with reference to the total hair-cell number in the apical or basal segment, respectively (mean of 5 specimens for the apical segment, 2 for most of the basal segment). Thus, the size of each triangle represents both the local weighting of orientations and the density of the hair cells. (*a* and *b* courtesy of C. Köppl; *c* from Köppl, 1988)

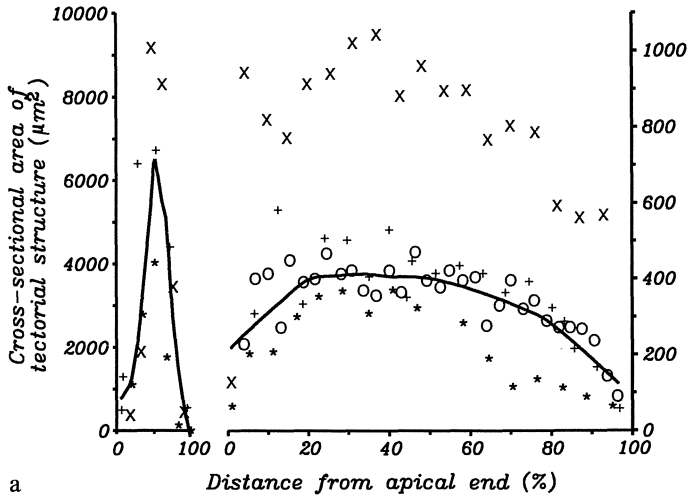

a

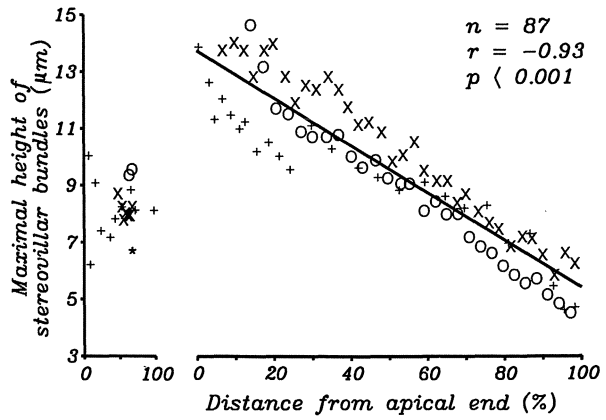

b

Fig. 11.2.a Diagrammatic representation of the size of the tectorial membrane over the length of the papilla of the bobtail skink *Tiliqua rugosa*. The area of the membrane was determined at intervals of 50 or 100 µm from transverse sections of the papilla. Due to the differences between individual animals in the relative lengths of the two papillar segments, the figure is divided into two. In both apical (*left*) and basal (*right*) sections, the length of the respective papillar areas is expressed on the abscissa as 100%. Note that there are two ordinate axes: that on the *left* refers to the apical (different *symbols* refer to different individuals), that on the *right* to the basal papillar segment (four individuals). The area of the tectorial membrane in the apical segment is up to 10 times that of the basal segment. One individual showed larger areas than the others (*x*): this ear was fixed using a high-potassium medium (see text). The *lines* are locally-weighted regressions including all data points. *b* Height of stereovillar bundles of hair cells in different areas of the papilla. The graph is divided into apical and basal areas, as in *a*. The data are measurements from transverse sections of the papilla; different *symbols* refer to different individuals. Each *point* is the mean of 2 to 8 hair cells. The *line* is a linear regression for the data from the basal area (After Köppl, 1988)

end (Fig. 11.2b). The height of the tallest stereovilli in a hair-cell bundle falls over this segment from about 14 μm to near 5.5 μm at the basal end. In the apical hair-cell area, the height is, on average, 8 μm (Köppl, 1988; Fig. 11.2b).

There is little published information on the pattern of the innervation in *Tiliqua*. As the patterns seem to be consistent within families, however, it is probably similar to that of other skinks such as *Mabuya carinata* (Miller and Beck, 1988). Whereas in earlier studies it was thought that lizard efferent nerve fibres are only associated with unidirectionally-oriented hair cell areas, this has been qualified through the recent re-classification of hair-cell types by Miller and Beck (1988; see Sect. 4.3.4). It seems that UDT hair-cell areas usually receive efferent innervation; thus the divergently bidirectional area (the apical part of the papilla) in *Mabuya* receives efferent fibres (Miller and Beck, 1988). For two apical hair cells studied in detail, Miller and Beck found three or four efferent fibres (each also supplying other hair cells) with one synapse each. The afferent innervation is quite dense, these same two hair cells receiving 13 and 14 afferent fibres, respectively, making a total of 50 and 42 afferent synapses. These fibres differed strongly from each other, in that one fibre made more than 10 synapses, three each made more than four and the rest made three, two or only one synapse. It is not clear whether (a) all single fibres make connections of differing complexity with different hair cells or (b) whether there really are some fibres which, for example, make only single synapses with all the hair cells they contact and others which always make stronger connections. The relative uniformity of the physiological data would tend to favour option (a).

The two hair cells studied by Miller and Beck in the basal hair-cell area of *Mabuya* had no efferent synapses. Each had connections with 5 afferent fibres, making a total of 37 and 39 synapses, respectively. Of the five fibres, three made more than 10 synapses each, the others made only minor connections. All afferent fibres apparently were branches from fibres supplying other hair cells, each fibre making synapses with at least 2 or 3 hair cells. Thus in skinks, it appears as if no afferent fibres innervate hair cells exclusively. UDT hair cells contact more than double the number of afferent fibres but only make 1.5 times more afferent synapses than BDT hair cells.

In *Tiliqua*, some information on the innervational pattern is available from cobalt staining of individual, physiologically-characterized nerve fibres (Köppl and Manley, in preparation. It is clear that all nerve fibres innervate more than one hair cell. One fibre was found to innervate at least 8 hair cells (Fig. 11.3). In the apical area, some fibres have very extensive innervational areas but tend to run along the papilla innervating hair cells of only one orientation. In the basal region, it is clear that most afferent fibres innervate hair cells of opposing polarities (Fig. 11.4), which is the first anatomical evidence on this question in lizards. Basal-segment fibres tend to branch across the papilla and have a very limited basal-apical extent. Physiological evidence from the phase-locking responses of fibres (see below) indicates that in many cells, this innervational pattern is also reflected in the discharge patterns to pure tones.

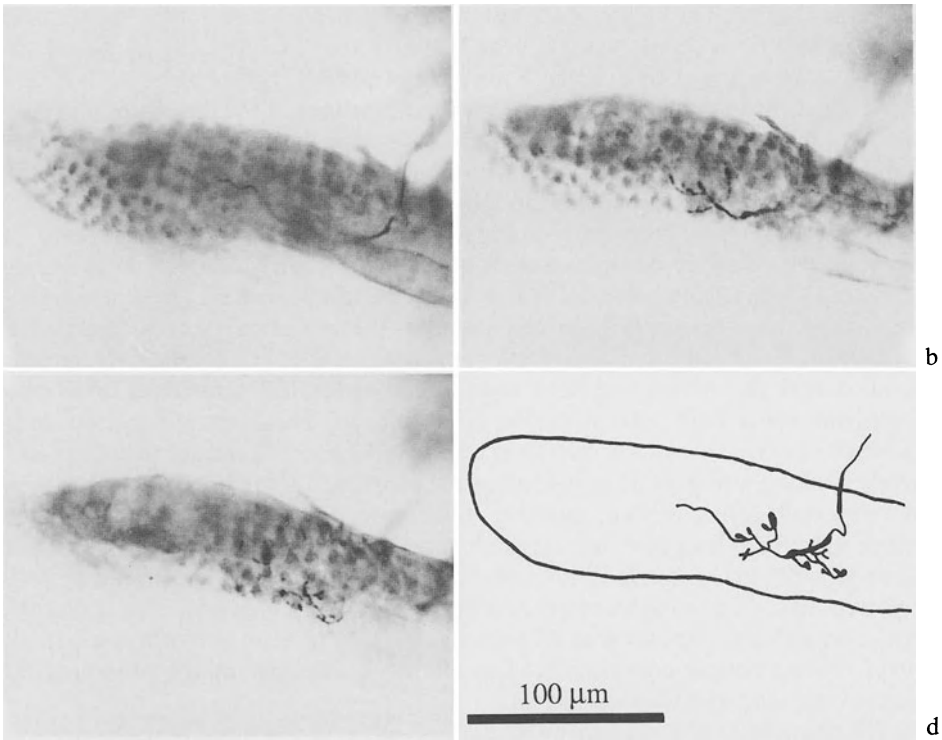

Fig. 11.3 a–d. Whole-mount preparation of the apical end of the basilar papilla of a bobtail skink *Tiliqua rugosa,* showing a single primary auditory-nerve fibre stained with cobalt. *a–c* A series of photographs beginning at the focus level where the fibre enters the apical papillar segment and moving the focus level progressively up to the hair cells. *d Camera lucida* drawing of the same fibre. This fibre makes extensive arborizations over about 100 µm along the length of the apical segment of the basilar papilla. It was estimated to innervate 8–10 hair cells (Courtesy of C. Köppl)

Fig. 11.4.a Whole-mount preparation of a small part of the basal segment of the basilar papilla of a bobtail skink *Tiliqua rugosa,* showing the terminal area of a single, physiologically-characterized, primary auditory-nerve fibre stained with cobalt. The fibre branches several times over almost the full width of the papilla and innervates at least 5 different hair cells on both the neural and abneural sides of the papilla (as estimated from sections). *b* SEM of a part of the basilar papilla that is comparable in location and magnification with that shown in *a,* and showing that the hair cells on the two sides of the papilla are oppositely oriented. The tectorial structure overlying the hair cells is divided into small individual units oriented across the papilla and linked by a central string running along the papilla. Such tectorial structures have been called "sallets" by Wever (1978). Due to the shrinkage of the tectorial material during histological preparation, the sallets pull strongly on the kinocilia of hair cells at the upper and lower edges of the papilla. This tension has pulled the kinocilia from the bundles and disrupted the regularity of the stereovillar bundles. The sallets thus normally overlie the entire width of the hair-cell area. The fibre shown in *a* innervates hair cells of opposing polarity. The calibration *bar* represents 10 µm in both cases (Courtesy of C. Köppl)

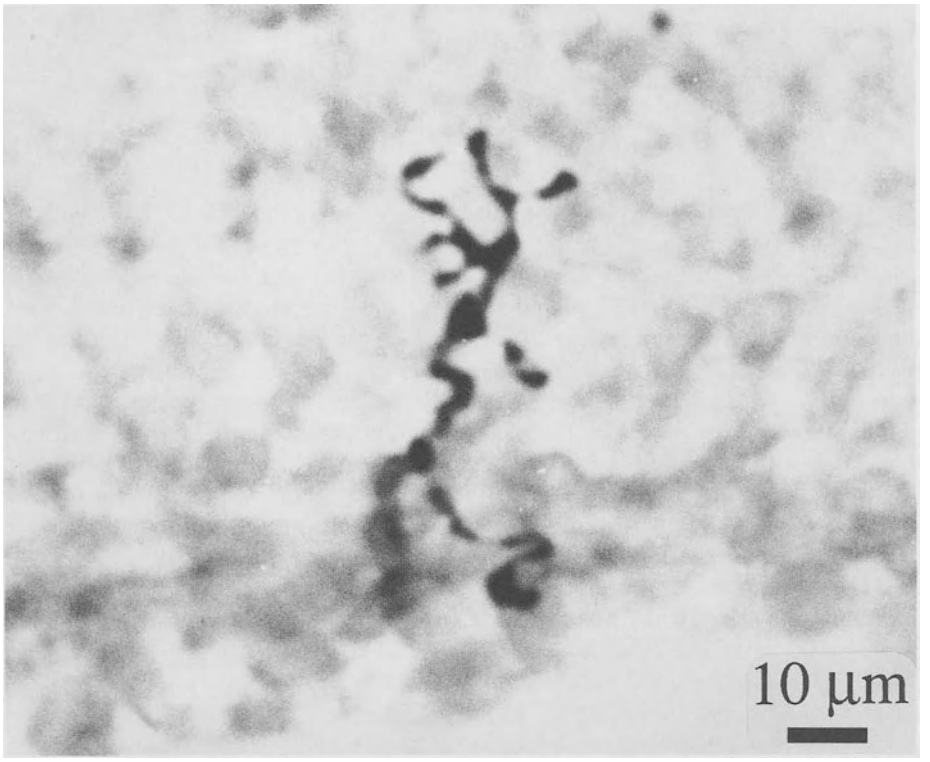

a

b

11.2 Activity Patterns of Auditory-nerve Fibres

11.2.1 Tuning Properties

Single-fibre recordings from the auditory nerve in the bobtail lizard have been made both from the nerve trunk in the brain cavity and from more peripheral locations, where the nerve fibres fan out to innervate the different papillar regions (Fig. 11.5). We (Köppl and Manley, in preparation; Manley and Köppl, in preparation; Manley et al., in preparation) reported data from over 300 nerve fibres. Each fibre is tuned to a certain frequency and has a ‚V'-shaped tuning curve. The characteristic frequencies (CFs) at 30 °C ranged from 200 Hz to 4.5 kHz. If we divide the CF range into roughly four octaves, the distribution of the number of fibres in each CF-octave is unequal. The percentages of fibres in each octave from the lowest to the highest are: 10, 31, 38 and 22%. This may be partly due to an unequal number of hair cells devoted to each octave, for the tonotopic organization indicates that one octave at low frequencies (below 800 Hz) occupies less space (150 µm/octave) than at higher frequencies (750 µm/octave, see below). Sensitivities of individual nerve fibres at their CF are down to below 10 dB SPL; the most sensitive fibres have a CF near 1.3 kHz. The overall shape of the audiogram correlates well with the shape of the basilar-membrane response curve (Fig. 11.6a).

The physiological data described here for the inner ear of *Tiliqua* were collected mainly through the cooperation of the Auditory Research Laboratory of the Department of Physiology (Prof. B. M. Johnstone), but also the Department of Zoology of the University of Western Australia, Perth.

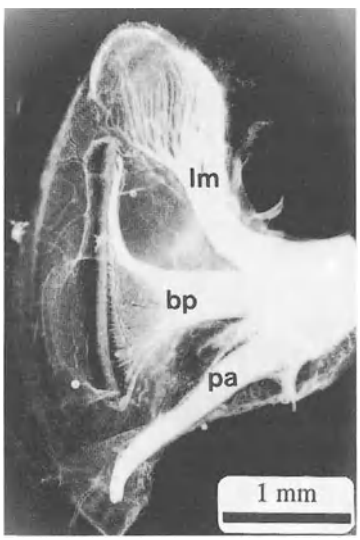

Fig. 11.5. Whole-mount preparation of an isolated cochlear duct of the bobtail skink *Tiliqua rugosa*, as seen from the medial side. Part of the posterior branch of the VIIIth nerve (*white*) enters on the *right* of the picture and divides into three branches to innervate the posterior ampulla (branch labelled, *pa*), the lagenar macula (*lm*) and the basilar papilla. The auditory branch (*bp*) fans out towards the basilar papilla in the basal half (*lower half* in the figure), whereas in the apical half the fibres are forced into a compact bundle by an extension of the limbus that encloses this part of the papilla like the finger of a glove (Courtesy of C. Köppl)

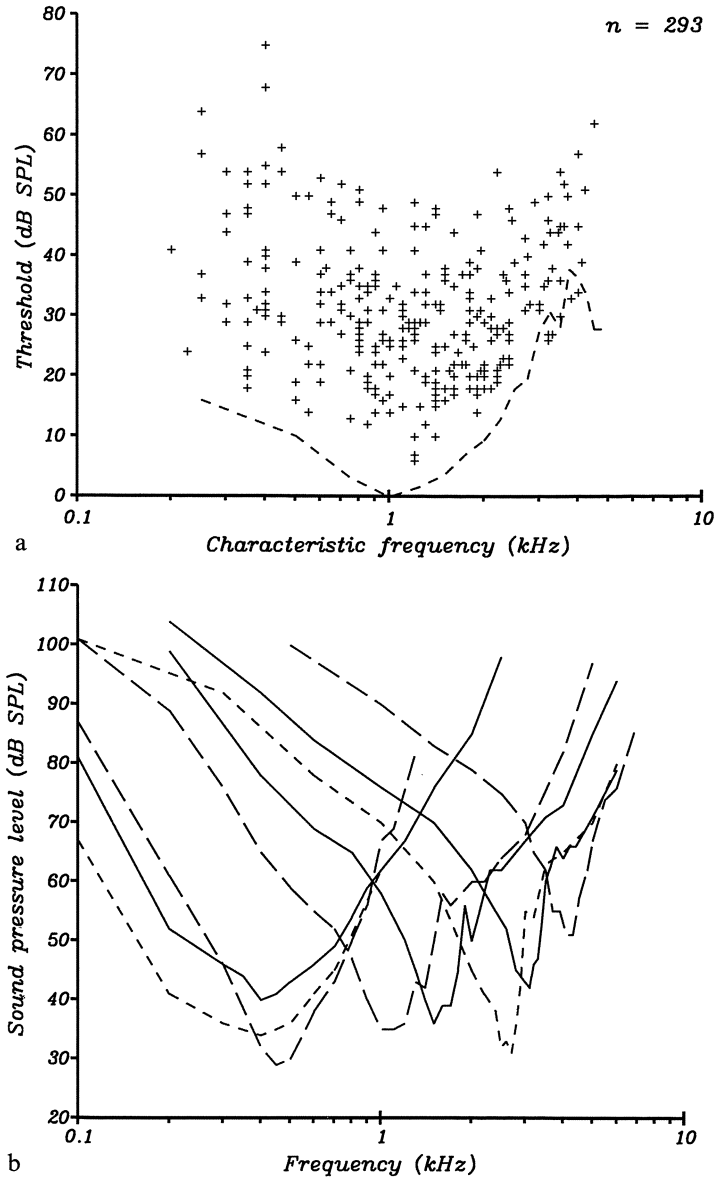

Fig. 11.6 a, b. The hearing range of the bobtail skink *Tiliqua rugosa* as indicated by a scatter plot of the characteristic frequency (CF) and the threshold at CF for 293 primary auditory nerve fibres from many animals. The *dashed curve* shows the shape of the basilar-membrane "threshold" curve for one individual animal placed arbitrarily on the ordinate scale, and illustrates its similarity to the overall shape of the single-cell threshold pattern. The ripples in the high-frequency part of the basilar-membrane curve were not present in all measurements. *b* Representative tuning curves of single primary auditory-nerve fibres from one individual bobtail skink. Note the smooth shape of tuning curves with low CF as compared to those with higher CF (above CF 800 Hz), which show a slope discontinuity on both of their flanks, producing a more or less pronounced "tip" region (Manley et al., in preparation)

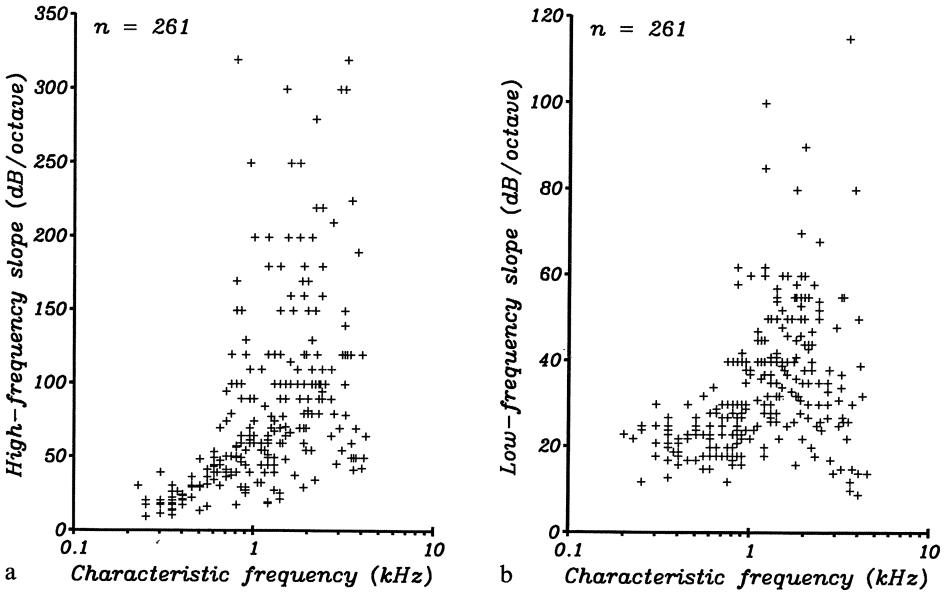

Fig. 11.7 a, b. Comparison of the high- (*a*) and low-frequency (*b*) slopes of the tuning curves of single primary auditory-nerve fibres of the bobtail skink *Tiliqua rugosa*. Slopes on each tuning-curve flank were measured between 3 and 23 dB above the threshold for the characteristic frequency. The high-frequency slope is about 3 times steeper than the low-frequency slope for higher-CF units (note different ordinate scales) (Manley et al., in preparation)

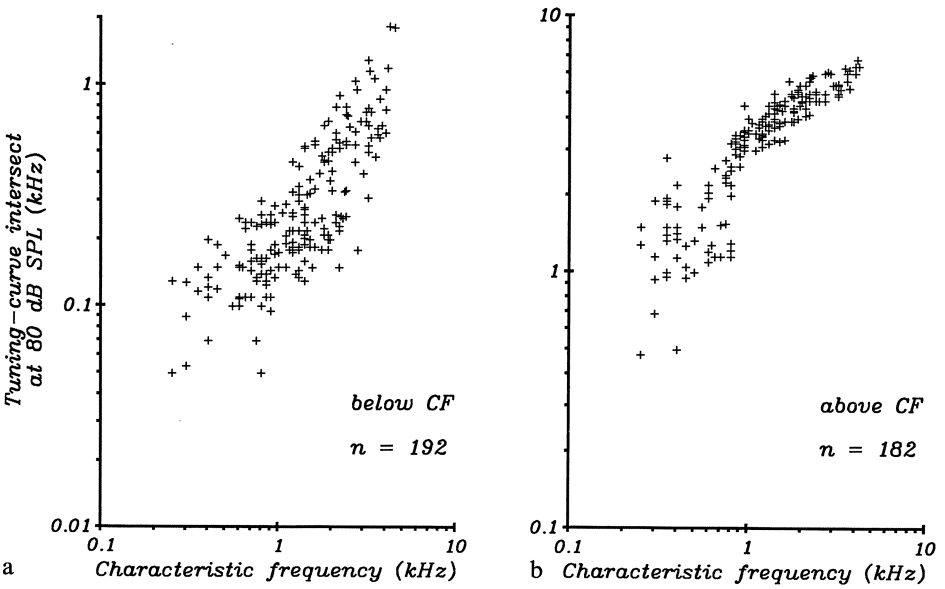

Tuning curves of single auditory-nerve fibres are almost all asymmetrical, with the steeper slope usually on the high-frequency side (Fig. 11.6b). High-frequency slopes sometimes exceed 300 dB/octave, whereas low slopes rarely exceed 80 dB/octave (Fig. 11.7). The shape of the tuning curves is not uniform throughout the whole CF range, however, and permits the division of the fibres into a low (CF below 800 Hz) and a high-CF population. One obvious difference between these groups is in the high-frequency flanks of the tuning curves. Whereas all the high flanks of the curves of fibres with CF over 850 Hz tend to come together at high frequencies, those of the low-CF population do not and show a greater spread. This difference becomes especially obvious in an analysis of the frequencies where the flanks of the different tuning curves intersect the 80 dB SPL level (Fig. 11.8).

This difference in the low-CF population is correlated with their curious variability with respect to two-tone suppression (see below). A difference in shape of the tuning curves from the two populations is also seen in the tendency of high-CF fibres to show a pronounced, sensitive tip to their tuning curve (Fig. 11.6b). Such tips were not seen in low-CF fibres. In general, however, the usual measure of the sharpness of tuning, the $Q_{10\ dB}$, shows a tendency to increase with CF, with a greater spread of values at higher CF. The average 10 dB-bandwidth of the tuning curves is relatively constant at 350–400 Hz for low-frequency CFs up to about 850 Hz. Above this CF, the bandwidth rises steeply, reaching more than 1000 Hz at the highest CFs. Due to the presence of a prominent tip to the tuning curve of high-CF units, the difference between the $Q_{10\ dB}$ values of low- and high-CF fibres is proportionately greater than the difference between their $Q_{40\ dB}$ values (Fig. 11.9). A division of the data points into a low- and a high-CF group is also indicated in Fig. 11.9b.

11.2.2 Tonotopic Organization of the Papilla

The possibility of recording at more peripheral locations permits the direct assessment of the presence of a tonotopicity in this papilla. Unfortunately, only the basal half of the papilla is directly accessible, the apical area within the scala tympani being enclosed within the arched limbus. Recordings from single fibres were made within a distance of 200 μm from the point at which they emanate from the papilla. In this region, the fibres run almost at right angles from the papilla towards the brain, so the region of papilla innervated by a given fibre

Fig. 11.8a, b. Frequencies at which the high- and low-frequency flanks of bobtail lizard (*Tiliqua rugosa*) tuning curves intersect with the 80 dB SPL level as a function of their characteristic frequency (CF). Note that the intersect points for the low-frequency side (*a*) tend, although scattering somewhat, to rise steadily with increasing CF, indicating that the low-frequency flanks run roughly parallel to each other. The intersect points for the high-frequency side (*b*), on the other hand, fall into two groups: one group has CFs above about 800 Hz, and shows a very tight and slowly rising distribution of points, i.e. their high-frequency flanks run closely together. In the second group, with CFs below 800 Hz, the greater scatter indicates that their high-frequency flanks run quite diversely (Manley et al., in preparation)

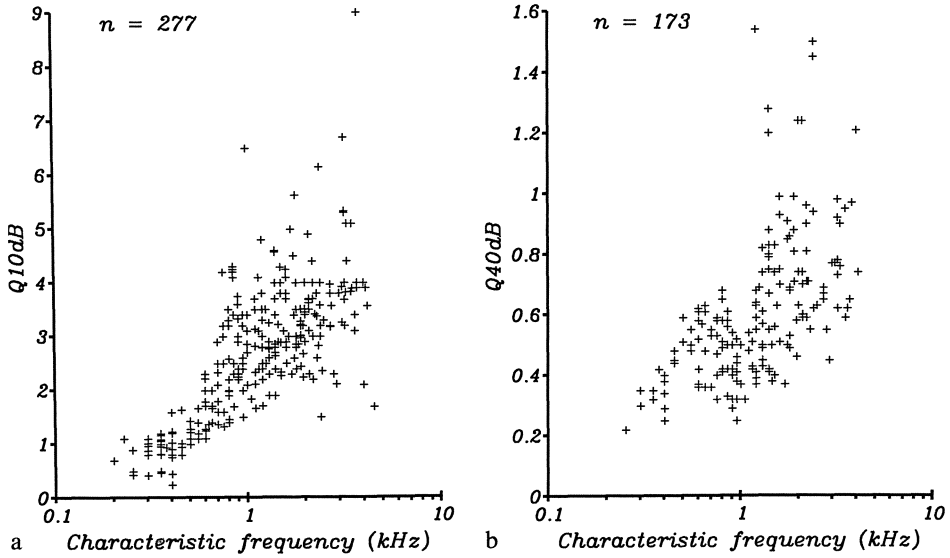

Fig. 11.9 a, b. The frequency selectivity of tuning curves of the bobtail lizard *Tiliqua rugosa,* as a function of the characteristic frequency (CF). As an indicator for the sharpness of tuning, the Q10dB (*a*) and Q40dB values (*b*) were calculated (CF divided by the bandwidth of the tuning curve 10 and 40 dB above the threshold for the CF, respectively). In both cases, there is a trend towards higher Q-values, i.e., higher frequency selectivity, with increasing CF. A suggestion of the presence of a low- and high-frequency population can be seen in *b* (Manley et al., in preparation)

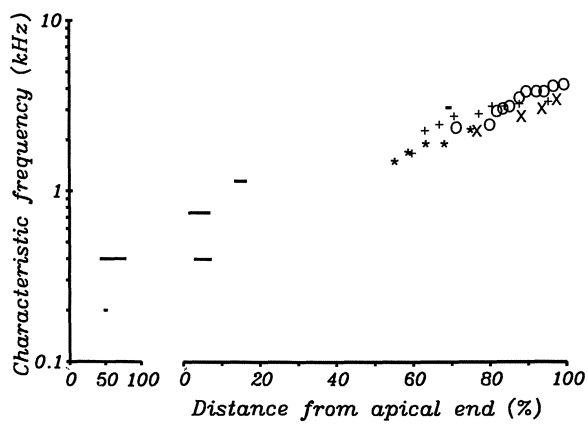

Fig. 11.10. The CF distribution in the basilar papilla of the bobtail skink, *Tiliqua rugosa,* as estimated from systematic electrode penetrations in the basal papillar half and from six stained primary nerve fibres. The *symbols* (different symbols represent four animals, +, *, *o, x*) indicate that there is a clear tonotopic arrangement of characteristic frequencies according to the position where the nerve fibres were recorded, with the highest CFs located at the basal end. The six short *bars,* one of which lies above the symbols at 68% of the length along the basal segment, represent the positions of the terminations of stained single nerve fibres of known CF. Due to the differences between individual animals in the relative lengths of the two papillar areas, the figure is divided into two. In both *left* (apical) and *right* (basal) sections, the length of the respective papillar areas is expressed on the abscissa as 100% (Köppl and Manley, in preparation)

bundle can easily be assessed. Data for four series of recordings from fibres innervating the basal 0.7 to 0.8 mm of the papilla are shown in Fig. 11.10. It can be seen that there is a clear tonotopic organization of the CFs, with 4.2 kHz located most basally and 1.4 kHz at the most apical point of the accessible region. The variability in the data is due in part to the presence of ‚holes' in the thin sheet of nerve fibres, areas where the nerve bundles no longer run close together (cf. Fig. 11.5, basal end). These ‚holes' are bordered on their apical and basal sides by fibres with the same CF.

As is described below, two groups of primary nerve fibres are distinguishable in the physiological data. We suspected that the lower-CF group (CFs up to about 800 Hz) represented fibres which innervated the separate apical group of hair cells. Not being able to access this area directly, we used the cobalt-staining technique (Köppl and Gleich, 1988; Sect. 5.6) to label single, physiologically-characterized fibres of different CFs. In this case, we concentrated on CFs below 1.4 kHz. As well as being able to confirm the origin of the low-CF responses in the apical region, a number of other interesting findings emerged from these staining experiments. Firstly, the tonotopic organization is not regular throughout the papilla; the apical and basal areas not only show a dichotomy in terms of the space devoted to one octave, as described above. The *direction* of the tonotopic organization also differs: whereas in the basal area, the organization is along the papilla, it runs *across* the apical segment. Secondly, it became obvious that some nerve fibres innervated large areas of hair cells. Thirdly, many nerve fibres obviously innervated hair cells of both polarities (Fig. 11.4).

11.2.3 Discharge Patterns of Single Fibres

One-third of primary auditory-nerve fibres show no spontaneous activity. The rates of active fibres rarely exceed 80 spikes/s (Fig. 11.11). In a few cases, the discharge was clearly rhythmic with the heart beat, without any signs of injury discharges. These were low-CF fibres which may have been responding to variations in blood pressure in arterioles which run directly below the basilar membrane. An analysis of the intervals in the spontaneous activity revealed a quasi-Poisson distribution of intervals. Preferred intervals were not obvious in any case (Köppl and Manley, in preparation). However, their absence may be due to the lack of exclusive innervation in this papilla.

Driven activity rates of fibres were often very high. The response patterns as indicated by the shape of peri-stimulus-time histograms (PSTH) vary from tonic to strongly phasic (Fig. 11.12). At least four groups of cells could be distinguished on the basis of their PSTH. Whereas almost all low-CF cells showed more tonic discharge patterns at their CF, higher-CF cells showed strongly phasic or intermediate types. For low-CF cells, the form of the PSTH and the maximal discharge rate varied with stimulus frequency; the highest rates were found at the CF. Below the CF, the cells tended to phase lock to the stimulus, producing lower rates. Above CF, these cells showed phasic histograms resulting partly from the late onset of primary suppression. This often resulted in an average discharge rate during the stimulus which was lower than the spontaneous rate (Fig. 11.12). The PSTH of higher-CF cells were classified into three groups,

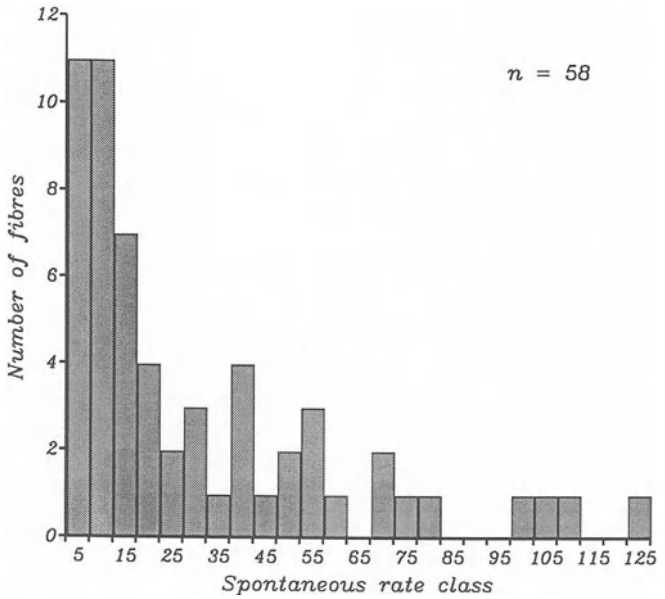

Fig. 11.11. Distribution of spontaneous discharge rates for 58 primary auditory nerve fibres of the bobtail lizard *Tiliqua rugosa*. Only exact rates determined from at least 500 tape-recorded action potentials were considered; thus, cells with no spontaneous discharge are omitted in this diagram. As it takes a long time to record a sufficient number of intervals from very low-rate units, and cells can be lost before the recording is complete, there is a bias in this figure towards higher rates. The data are grouped in rate classes of 5 spikes/s, i.e. up to 5, 6–10, etc. (Köppl and Manley, in preparation)

two highly phasic, one phasic-tonic. In contrast to low-CF cells, their PSTH were similar at all stimulus frequencies. Maximal rates for one group averaged over the 50 ms tone burst sometimes exceeded 500 spikes/s. As in *Gekko*, the highly phasic cells very often showed sharp peaks (1 to 10) at the beginning of the histogram, with a mean separation of about 2 ms. Here, these "chopper" cells are apparently discharging near their highest possible rate. These "chopper" discharge patterns resemble those recorded in certain cell types of the mammalian cochlear nucleus. There, this pattern has been shown to result from the long time constants of the cell membranes of these cells (Oertel, 1985).

A curious suppression phenomenon was seen in some low-CF cells. This is illustrated in a comparison of two tuning curves in Fig. 11.13 and their rate-level

Fig. 11.12 a, b. Rate-level functions and PSTH form at various stimulus frequencies and SPL for two cells (*a, b*) of the low-CF group (apical segment) in the bobtail lizard *Tiliqua rugosa*. The rate-level functions are average rates during a 50 ms stimulus. *a* The cell in Fig. 11.13 a, which shows a separate two-tone suppression (TTRS) area. At higher stimulus frequencies, the PSTH became more phasic and the mean rates very low. *b* The cell of Fig. 11.13 b, where the excitatory tuning curve "overlaps" the TTRS area. At 1200 Hz, the average discharge rate is below the spontaneous rate for all SPL (see text). The inclusion of the upper portion of the curve in the excitatory tuning area is thus very dependent on the criteria chosen and the techniques used (Köppl and Manley, in preparation)

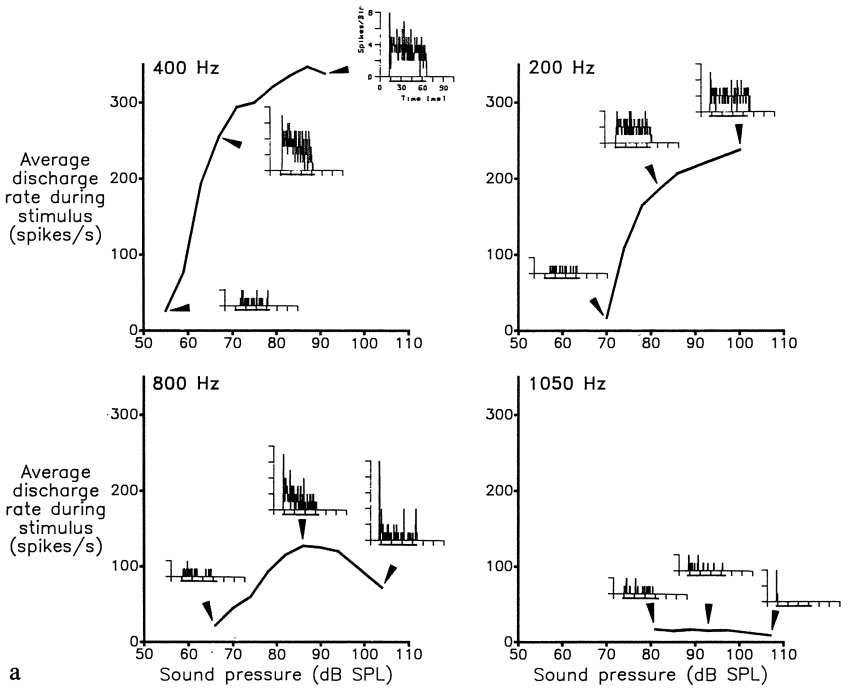
400 Hz
200 Hz
800 Hz
1050 Hz
Average discharge rate during stimulus (spikes/s)
Sound pressure (dB SPL)
a

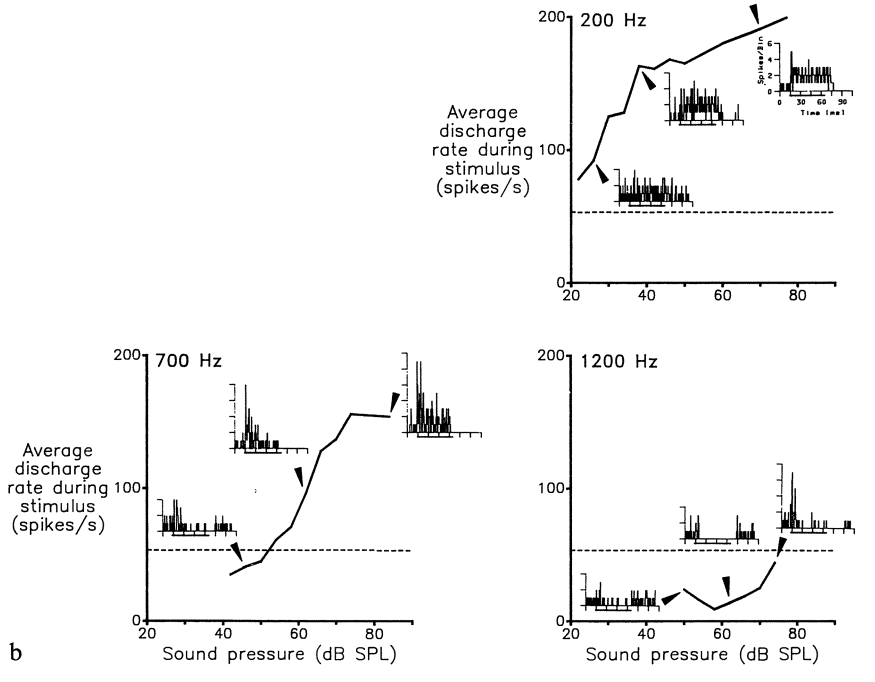
200 Hz
700 Hz
1200 Hz
Average discharge rate during stimulus (spikes/s)
Sound pressure (dB SPL)
b

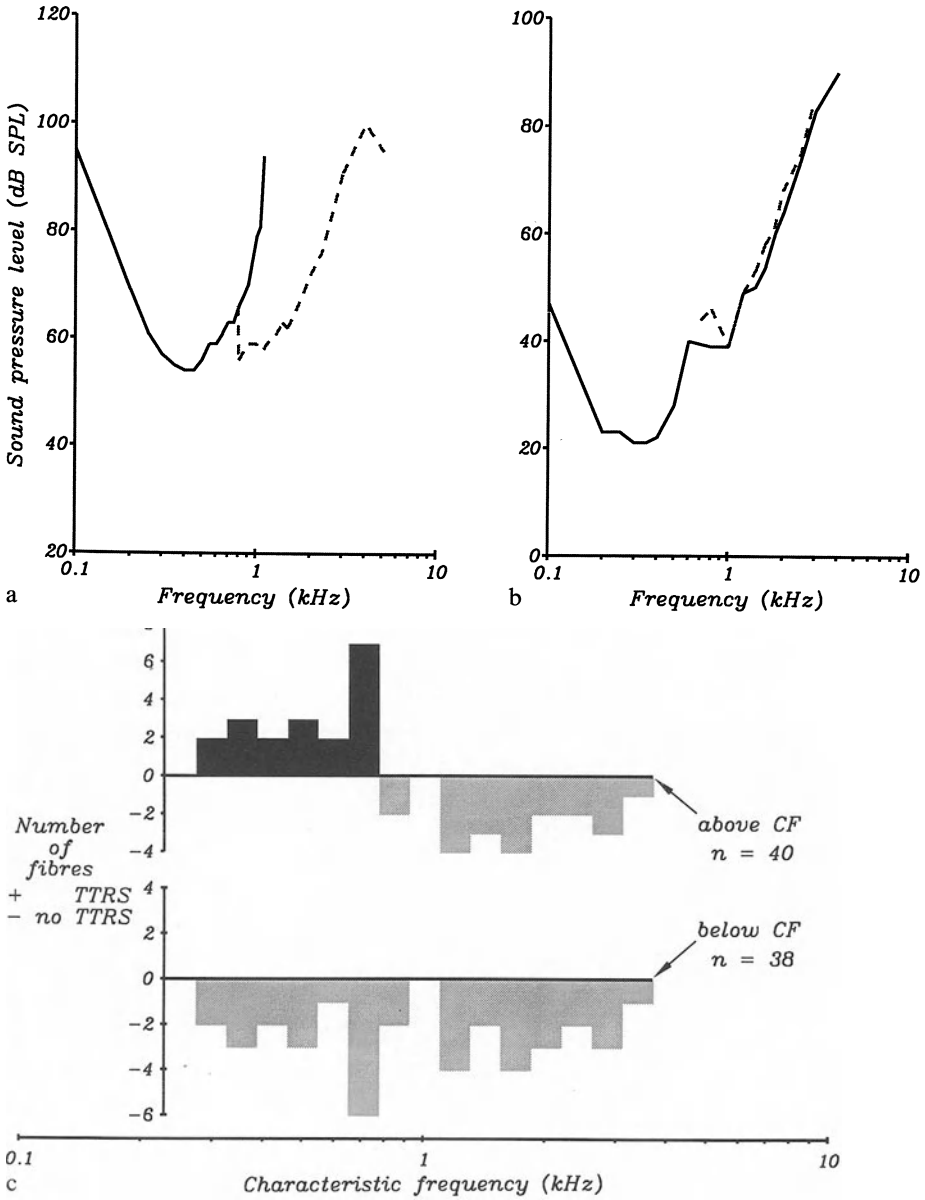

Fig. 11.13 a–c. Excitatory and two-tone suppression response patterns for primary fibres of different CF in the bobtail lizard *Tiliqua rugosa*. *a* A low-CF cell where the excitatory tuning curve (*solid black line*) is flanked on the high-frequency side by a TTRS area (*dashed grey line*). This TTRS area represents the SPL necessary at various frequencies to suppress the cell's response to a CF tone, 10 dB above CF threshold. *b* A low-CF cell where the excitatory tuning curve (*solid black line*) overlaps the TTRS area (*dashed grey line*). This means that in the TTRS area, there is an observable response to single tones, although these responses are, when averaged over the whole 50 ms response time, primary suppression (see Fig. 11.12 *b*). *c* A histogram to illustrate the presence (+, *black columns*) or absence (−, *grey columns*) of TTRS in cells of different CFs using second tones above CF (*upper columns*) and below CF (*lower columns*). Cells are grouped according to their CF in quarter-octave bins. TTRS was observed only in cells of the low-CF group, and in these, only above the high-frequency flank of the tuning curves (Köppl and Manley, in preparation)

functions and PSTH shown in Fig. 11.12. In one cell, there is an area at frequencies higher than the excitatory tuning curve where there is no reaction to single tones, but where a second tone can suppress the activity to a CF tone presented at 10 dB above threshold – this is the classical two-tone rate suppression (TTRS; Fig. 11.13 a). These cells showed steep high-frequency flanks to their excitatory tuning curves. Some other low-CF cells seemed to include the TTRS area in their excitatory tuning curve (Fig. 11.13 b). However, the actual response to single tones in this higher-frequency area differed in pattern to that within the ‚normal' tuning area (Fig. 11.12 b). In this higher-frequency area, single tones elicited a short onset response followed by a more or less complete suppression of spontaneous activity. As these tuning curves were made using audio-visual criteria, this pattern was clearly audible as a response and therefore included in the tuning curve. Only the evaluation of the PSTH data revealed an obvious difference in the discharge pattern. The difference between the two types of cells seems to lie in the latency of the onset of the suppression. In some fibres, it sets in after the onset of response activity; this results in a brief burst of excitation at stimulus onset. The variability in the high-frequency slopes of tuning curves mentioned above (Fig. 11.8 b) is traceable to the differences between low-CF cells in this respect. Although there are similarities between these TTRS data and those presented for the alligator lizard (Ch. 7), the tuning curves for the alligator lizard were all collected using an automated procedure to detect a standard rise in average rate during the presentation and thus may have excluded the response phenomenon described here. TTRS in the bobtail lizard was only observed in cells belonging to the low-CF group, and in these, only near the high-frequency flanks of the tuning curves (Fig. 11.13 c).

As in other vertebrates, all auditory-nerve fibres of *Tiliqua* show phase locking at low frequencies, that is, the neurones discharge on average at a preferred phase of the sound signal (Fig. 11.14; Manley et al., 1988 e). In general, however, phase locking was very weak above 1 kHz, with optimal frequencies near 300-400 Hz. Low-CF cells (CF below 0.9 kHz) show two corner frequencies, one at 300 Hz, the other at 700 Hz, above which phase-locking becomes rapidly poorer. In general, it appears that at their highest response frequency near 1 kHz they phase-lock better than high-CF cells (CF above 0.9 kHz; Fig. 11.15). High-CF cells only show almost as good phase-locking as low-CF cells near 300 Hz, above which their ability to phase lock falls off more rapidly than it does for low-CF cells. It is understandable that high-CF cells phase-lock poorly at low stimulus frequencies, where the stimuli are only marginally above threshold. However, above 700 Hz, most high-CF cells should be in the advantage from the point of view of effective sound-pressure level. However, the low-CF group of fibres still shows on average better phase-locking (Fig. 11.15). The data thus bear a close resemblance to phase responses of fibres of the alligator lizard (Sect. 7.3.1; 14.10). It is interesting to note that if long membrane time constants are responsible for generating the "chopper" discharge patterns described above for mid- and high-frequency cells, then such long time constants would certainly adversely affect the phase-locking ability of these cells at higher frequencies. Perhaps different nerve-fibre time constants can explain the different phase-locking behaviour of low- and high-CF cell populations.

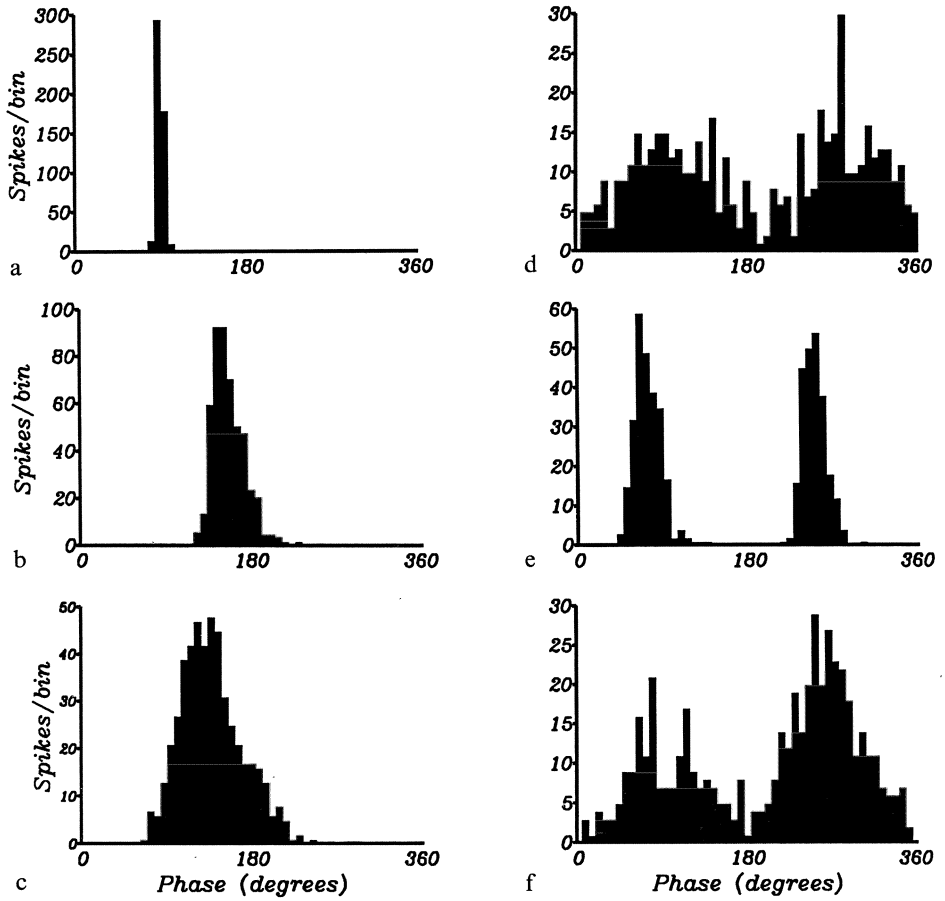

Fig. 11.14 a–f. Cyclic histograms illustrating phase-locked responses of two primary auditory nerve fibres in the bobtail lizard *Tiliqua rugosa*. In each histogram, the *abscissa* represents one cycle (360°) of the stimulus and is divided into 50 bins. Each histogram plots the number of action potentials occurring within each bin until 500 events have been recorded. In all cells, the peaks shift to the right between different frequencies, due to the larger phase lag at higher frequencies. In fact, in both cells of this figure, the response peak(s) shift almost a whole cycle between 100 and 300 Hz and again between 300 and 500 Hz. *a–c* A fibre showing only a single peak within each 360° cycle. *a* 100 Hz; *b* 300 Hz; *c* 500 Hz. *d–f* A fibre which presumably innervated hair cells of opposing polarities and shows double-peaked histograms. Frequencies *d–f* as in *a–c* (Manley et al., in preparation)

In the *Tiliqua* data, about a quarter of the cells showed two phases of the signal which were stimulatory, producing a phase histogram with two prominent peaks which lie 180 ° apart (Fig. 11.14d-f). That the second peak is not due to harmonic distortion is also shown by the fact that the peaks can be equally large down to and even below the audio-visual rate threshold for the cell. The presence of two peaks separated by 180 ° is attributable to the fact that these fibres innervate hair cells of opposing polarities. Each peak is the result of the activity of one group of hair cells with the same orientation. The responses of the hair cells

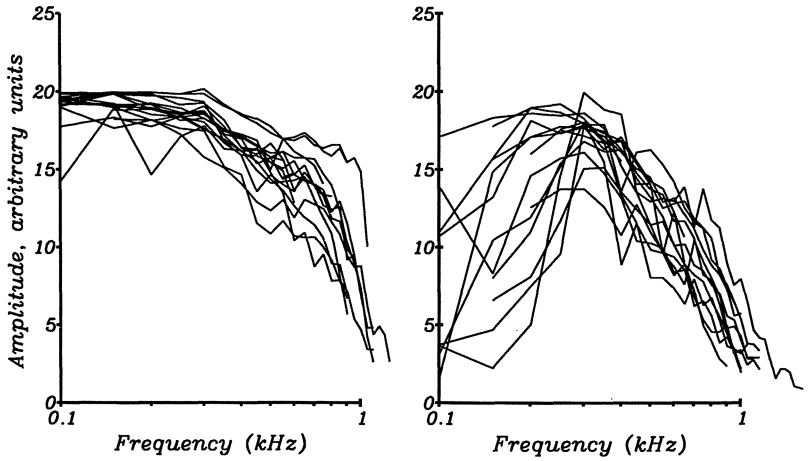

Fig. 11.15. Strength of phase-locking in low- and high-CF fibres of *Tiliqua rugosa*. Each *line* is the phase amplitude at different stimulus frequencies for a single cell. *a* Auditory-nerve fibres of CF below 0.8 kHz. The amplitude of phase locking is steady up to about 0.3 kHz, above which the amplitudes fall with increasing frequency to a second corner frequency at about 0.7 to 0.8 kHz, above which the amplitudes fall rapidly. *b* Auditory-nerve fibres of CF above 0.8 kHz. The highest amplitudes are found at 0.3 kHz; below this, the sound pressure was probably too close to threshold to stimulate adequately. Above 0.3 kHz, the phase-locking amplitudes fall off more rapidly than in the low-CF cells (Manley et al., in preparation)

themselves are likely not to differ from those of other vertebrates. Interestingly, there was a correlation between the innervation patterns of nerve fibres to the apical and basal segments of the papilla and the phase-response patterns. The branching patterns of auditory-nerve fibres in *Tiliqua* indicate that those innervating the high-CF, basal hair-cell area most probably contact hair cells of both polarities. In the low-CF, apical area, in contrast, there is an obvious tendency to avoid innervation of cells of different polarities. Cycle histograms which show two peaks, 180° apart were rare among low-CF units (1 out of 14 fibres), whereas of 19 high-CF fibres, 15 (=80%) showed two-peaked cyclic histograms. These response patterns correspond very well to the fibre distributions revealed by cobalt staining.

After correcting for the phase-delay characteristics of the sound system, the response phase of a nerve fibre shifts with reference to the sound source as the frequency is changed. The amount of this shift depends on the CF of the fibre in a systematic way; the lower-CF fibres show a more rapid change with frequency than do the higher-CF fibres. Specific delays exist between the sound source and the response of cells of different CFs and a delay time can be calculated from the slope of the phase – frequency characteristic for each cell. The delay times strongly resemble those previously reported for other vertebrate auditory-nerve fibres (Manley et al., 1988 e; Fig. 11.16).

In mammals, such delay times have been interpreted as being the result of the delays due to the travel time of the travelling wave along the basilar membrane from higher to lower frequencies. The data have even been used to calculate the

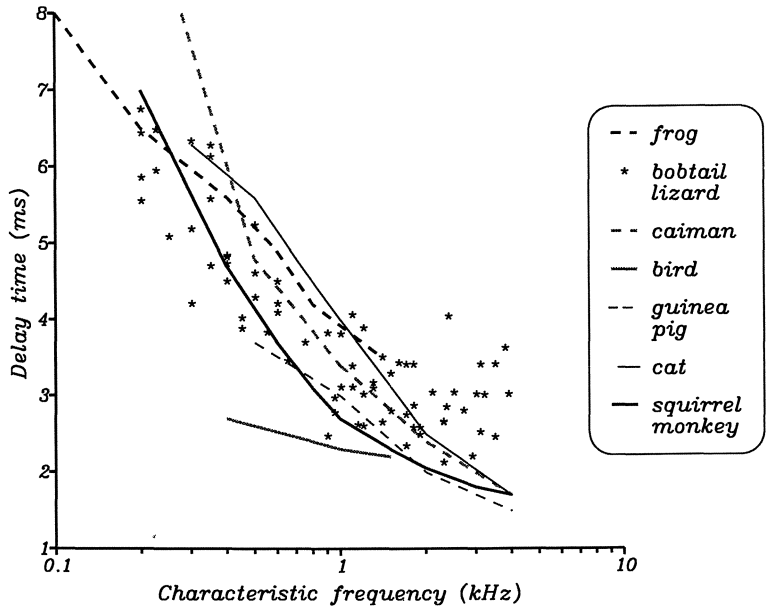

Fig. 11.16. A comparison of the delay times for the responses of auditory-nerve fibres of different CF to pure-tone stimuli, as calculated from the slopes of phase-frequency functions for different vertebrates. The data for 72 fibres in *Tiliqua rugosa* are shown as *stars;* data for other animals are shown as mean values at different CFs estimated from published figures. There appears to be very little difference in the phase-vs-CF delays of auditory-nerve fibres of the frog, reptiles, and mammals. The data for this figure are from Hillery and Narins, 1984 (frog), Manley et al., 1988 g (bobtail lizard), Smolders and Klinke, 1986 (caiman), Gleich and Narins, 1988 (bird), Palmer and Russell, 1986 (guinea pig), Kiang et al., 1965 (cat), Anderson et al., 1971 (squirrel monkey)

wave velocity along different portions of the membrane. The fact is, however, that the phase-delay patterns are very similar to those for the frog (which has no basilar membrane), the bobtail, where the basilar membrane is poorly tuned and does not show a travelling wave with place-determined frequency response (see below) and for the mammals. This is true although the mammals have a much longer basilar membrane and a travelling wave. We have suggested that these facts make it likely that the delay times reported for mammalian auditory-nerve fibres can be attributed to the travelling wave only as a secondary phenomenon (Manley et al., 1988 e).

Hillery and Narins (1984) believe that the presence of these phase-delay patterns in the frog indicate that a travelling wave exists in the tectorial membrane of the amphibian papilla. Such an explanation cannot be true in the bobtail lizard, however, as the tectorial structure is discontinuous and, in addition, is very much more massive at the apical end. Such a sudden change in mass should produce a discontinuity in the delays. Also, the delays change regularly over the CF range, whereas the CFs are not evenly distributed in space over basal and apical areas. A travelling wave, if present in the apical area of the bobtail papilla, would have to have a velocity as low as 0.1 m/s. It seems much more likely that the CF-

dependent delays are due to mechanisms intrinsic to the hair cell(s), perhaps to mechanisms involved in the active response of hair cells to stimulation. This question is important, for it concerns the nature of the filter responsible for the relatively long latencies revealed in the phase data. It has also been discussed by Smolders and Klinke (1986) for the caiman and by Pitchford and Ashmore (1987) for mammals.

11.3 Basilar-membrane Mechanical Response and a Model of Frequency Tuning in *Tiliqua*

We (Manley et al., 1988 d) measured the mechanical response of the middle ear and of the basilar membrane of this species. Using an optical technique (Yates, in preparation; see Ch. 5), it was shown that the middle-ear response is very similar to that of other nonmammals (Yates et al., in preparation; see Ch. 3). The transfer function of the middle ear determines most of the selectivity of the basilar membrane. The most important finding with regard to basilar-membrane mechanics is that there is no systematic, place-dependent frequency selectivity such as that observed in the activity of the nerve fibres innervating the different regions of the papilla. There is thus no selective basilar-membrane contribution to the tuning of local regions of the papilla (Manley et al., 1988 d; Fig. 11.17).

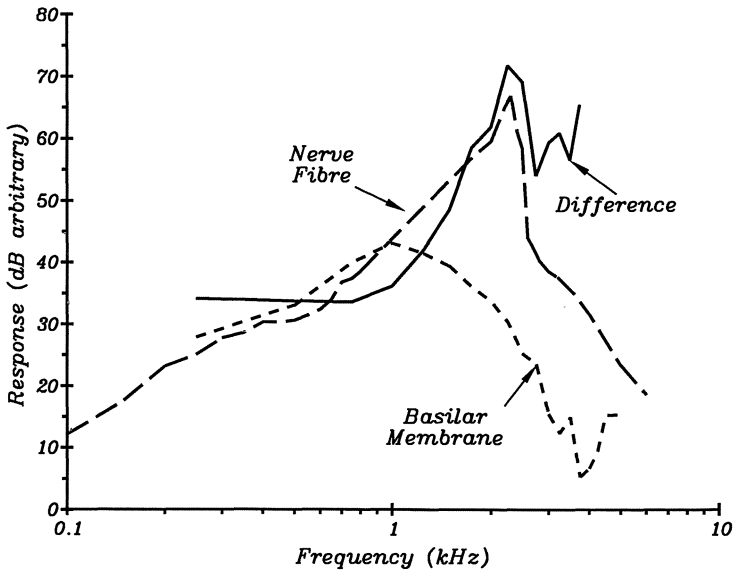

Fig. 11.17. A comparison of the frequency selectivity of the basilar membrane (*short-dashed line*) and a primary nerve fibre (*long-dashed line*), both from the same location in the papilla of an individual bobtail lizard *Tiliqua rugosa*. To compare the curves, the tuning curve of the nerve fibre has been inverted to mimic a response curve. Both this and the measurement of the basilar-membrane motion are placed arbitrarily on a decibel scale, while matching the low-frequency flanks of both curves. The *solid line* represents the difference between the response of the nerve fibre and that of the basilar membrane (After Manley et al., 1988 d)

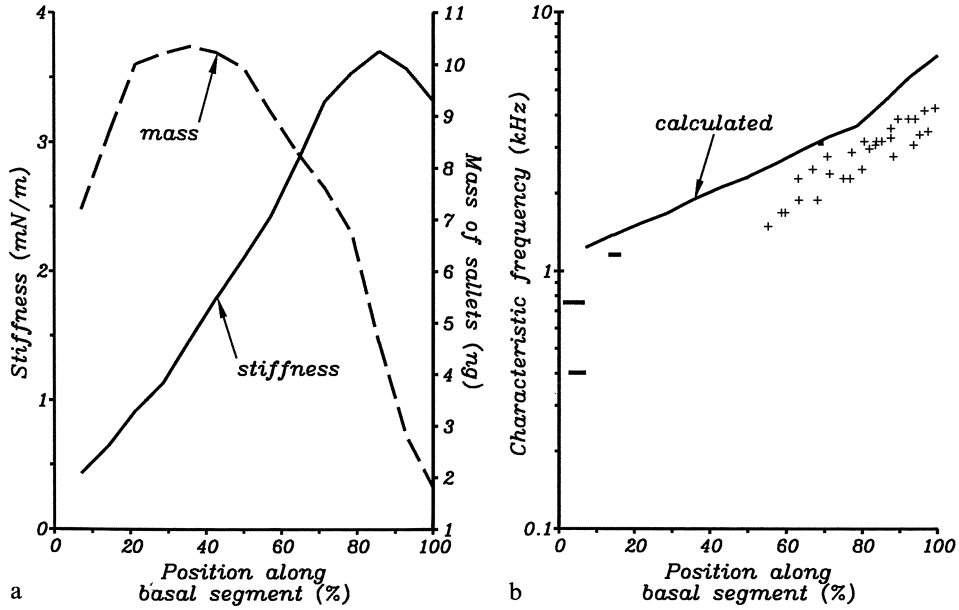

Fig. 11.18 a–c. A model of micromechanical tuning in the basal papillar segment of the bobtail lizard *Tiliqua rugosa*. *a* Change in the estimated mass of individual sallets (*dashed line, right ordinate*) and the total stiffness of all stereovilli connected to each sallet (*solid line, left ordinate*) as a function of position along the basal segment. *b* A comparison of the modelled CFs (*solid line;* for calculation, see text) and measured CFs (*symbols, bars*) as a function of position along the basal segment. The *crosses* represent the CF of individual primary fibres in four different animals as measured by recording with microelectrodes next to the papilla (see also Fig. 11.10). There are four bars (one almost hidden by the model line at 68%) which represent the position of single, cobalt-stained, physiologically-characterized primary fibres in three animals. The mean lowest CF of the basal segment as estimated from physiological data (see text) is about 850 Hz. *c* A family of modelled tuning curves calculated by cascading for each curve an approximation to the basilar-membrane tuning curve with a coupled pair of two-pole filters (which resembles the "difference" curve in Fig. 11.17). The general shape and the depth of the sharply-tuned tip region of the neural tuning curves from the basal segment (see Fig. 11.6 *b*) are well matched by these modelled curves. The Q-factors of the filters used (roughly equivalent to the Q_{3dB}) ranged from 1.25 to 8.5 (*a, b* after Manley et al., 1989 b; *c* after Manley et al., 1988 d)

In a number of experiments, both basilar-membrane tuning and the selectivity of nerve fibres innervating exactly the same regions of the papilla in the same ear were measured, allowing a direct comparison of tuning. As in the case of the recordings from nerve fibres near the papilla to determine the tonotopicity, only the basal half of the papilla was accessible for these measurements. A comparison of the two selectivity curves showed that the nerve fibres were, near their CF, very much more sharply tuned than the basilar membrane. Indeed, it appeared as if the slopes of the upper portion of the neural curves strongly resembled the poor selectivity of the basilar-membrane selectivity. To this, each neural curve added a ‚tip' portion having its own pivate CF. These tip portions had a depth of up to 40 dB. The difference between these two functions resembles the response characteristics of a relatively simple high-pass resonance filter (Fig. 11.17).

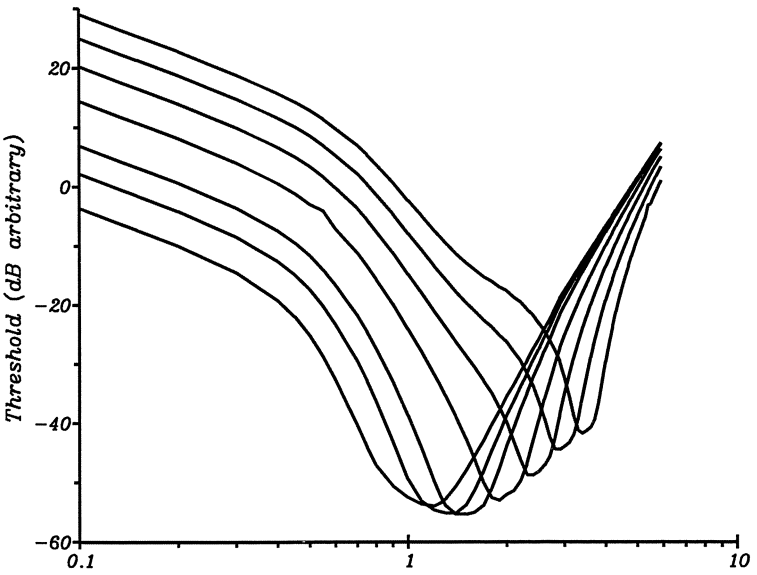

Fig. 11.18c

By adding a standard high-pass filter function of differing centre frequency to an average basilar-membrane tuning function, it was possible to model a series of tuning curves similar to those of the auditory nerve. In order to match the depth and the rounded tips of the neural tuning curves, however, it was necessary to assume that between the response of the basilar membrane and the neural tuning curve, at least two such high-pass filters would work in series. The physical location of these high-pass filters was presumed to be in the coupling of the individual hair cells to the semi-isolated salletal tectorial-membrane structures in this higher-CF region. Under the influence of basilar-membrane motion and the selective responses of hair cells, it was assumed that each group of hair cells with their sallet set up a resonant network with a high degree of frequency selectivity.

If the resonance frequency of local sallet-hair cell groups is simply determined by mechanical factors such as mass and stiffness, then it should be possible using the known values of the anatomical gradients to calculate these frequencies. In doing this, we made the assumption that the local resonance frequency is dependent only on the mass of the sallet and the stiffness of all the stereovillar bundles connected to that sallet (Manley et al., 1988 d). Since tectorial gels are mostly water, the specific gravity of the sallets was assumed to be 1100 kg/m^2. The calculated mass of the sallets varies along the papilla (Fig. 11.18a). The stiffness depends on the number of hair cells connected to each sallet, on the bundle length and on the number of villi in each bundle (Fig 11.18a). We calculated the stiffness of each resonant unit using the data of Crawford and Fettiplace (1985) for the rotational stiffness of single hair-cell bundles in the red-eared turtle (2×10^{-14} N.m/rad) divided by the average number of villi in the turtle bundle (90), taking into account the height of the longest villi in the stereovillar bundles of *Tiliqua* and the total number of villi per sallet. This total number varies along the papilla. The calculations from the morphological data indicate that it is mainly the variation in stereovillar length which determines the gradient of resonance

frequencies. The inverse trends of mass and stiffness together produce a smooth gradient of resonance frequencies (Fig. 11.18 b).

The absolute resonance frequency for each salletal hair-cell unit is given by $1/(2\pi)\sqrt{(\text{stiffness/mass})}$.

The results of this calculation for locations along the basal segment are shown in Fig. 11.18 b. The calculated frequency ranges from 1080 Hz at the apical end of the basal segment to 6800 Hz basally (Manley et al., 1989 b). The actual CF range estimated from neurophysiological experiments and measured for the basal half by recording from fibres next to the papilla and from stained fibres is from 850 to 4500 Hz (at 30°C; Fig. 11.18 b). Considering the uncertainty in the necessary assumptions and that some variables are not taken into account in the calculation (for example, that the slope of the heights of the villar rows in different bundles also varies systematically along the papilla, Köppl, 1988, and the effect of the surrounding fluid), the agreement between the neural data and the calculated resonance frequencies is extremely good, suggesting that the fine tuning in this area is really only due to mechanical resonances. It should, however, not be forgotten that the value for the stiffness of a single bundle taken from Crawford and Fettiplace (1985) almost certainly includes an active component from the hair-cell itself, that is, the model described here does not indicate that the resonance frequencies are reached purely on the basis of passive properties of the stereovillar bundles, in spite of the obvious anatomical gradients present. This implies that the passive micromechanical properties of the bundle reflected in the morphological gradients and the active contribution of the hair-cell body somehow become matched in their frequency response during the development of the hearing organ.

We thus proposed that the tuning of the tip region in high-frequency hair cells in *Tiliqua* is due to the mechanical resonance of local hair-cell groups and their sallet, superimposed on the broad basilar-membrane tuning. Frequency selectivity would be greatest if each resonant unit is only weakly coupled to adjacent units (Manley et al., 1988 d). We assumed that the degree of coupling is optimized by the sub-divided, salletal structure of the tectorial membrane of this basal region. This presumably enables the discrete units to resonate without substantially influencing differently-tuned, more remote regions. The salletal structure could break up the basal area into maximally about 80 possible, independent ‚units', i.e., about 30 per octave. This figure is, given the shape of the individual neural tuning curves, more than adequate to explain the frequency selectivity of the organ. This is also consistent with the assumption in our model of a degree of coupling of hair-cell groups to produce the characteristic tips of the high-CF group of tuning curves (Figs. 11.6 b, 11.18 c). In view of recent suggestions that the tectorial membrane of mammals is not stiff enough to act as a shearing partner for the hair cells but could act as a mass in a resonant circuit (Strelioff et al., 1985; Zwislocki et al., 1988), a model similar to ours could be applied to the mammalian organ of Corti.

The morphological characteristics of the apical segment of the basilar papilla are quite different from those just discussed for the basal segment. There is, for example, no obvious gradient in the height of the stereovillar bundles. Also, the entire hair-cell area is covered with one enormous, undivided tectorial structure.

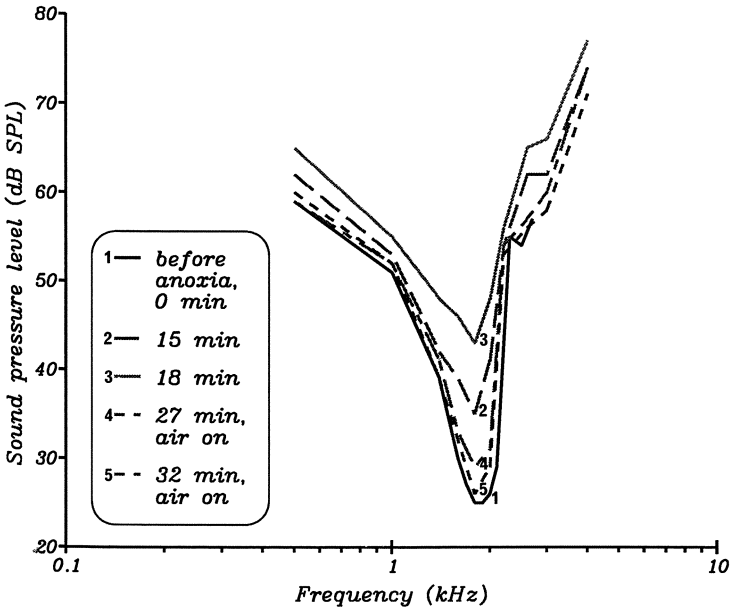

Fig. 11.19. Effects of experimentally induced hypoxia on the tuning curve of a single primary nerve fibre of the bobtail lizard *Tiliqua rugosa*. The *black solid line* (*1*) represents the tuning curve immediately before turning off the artificial ventilation. It took about 9 min for the thresholds to show any change, then the threshold of the sharp tip of the tuning curve gradually shifted up almost 20 dB, leaving the flanks much less affected (*upper solid grey curve, 3*). Upon restoration of the air supply (at 19 min) thresholds were almost fully restored at 32 min (*curve 5*) (Manley et al., in preparation)

As in other reptiles and in birds, significantly less space is devoted to the low-frequency octaves in this apical area (150 μm/octave) than to higher-frequency octaves (750 μm/octave; Manley, 1986; Manley et al., 1988 a,b). Thus, the frequency selectivity of hair cells in this apical segment is most likely not primarily achieved through micromechanical factors but by means of an electrical tuning mechanism such as that described for the red-eared turtle (Crawford and Fettiplace, 1981 a; see Sects. 2.4.2 and 6.1.3). In this apical area, we were able to show that the tonotopic organization is organized across the papilla. Nerve-fibre branching in this area is along the papilla, staying within the same frequency area and apparently innervating hair cells of only one orientation.

The fact that anoxia leads to a reduction in the depth of the tip of the neural tuning curve, hardly affecting the flanks (Fig. 11.19), would speak for an active involvement of the hair cells themselves in generating tuning or at least in maintaining the physical conditions necessary for it to occur (e.g. the stiffness of the stereovillar bundle).

11.4 Seasonal Effects on Hearing

There are several reports in the literature concerning the presence of a strong seasonal effect in the responses of the inner ear of the bobtail lizard. Johnstone

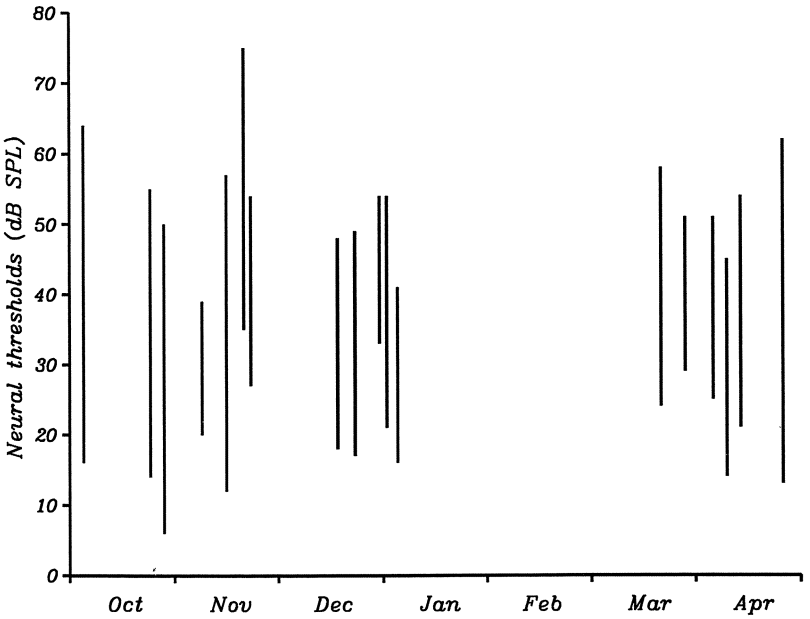

Fig. 11.20. Range of thresholds of all single primary auditory fibres at their CF for 18 individual bobtail lizards, *Tiliqua rugosa,* in relation to the time of year of the experiment. There is no consistent change of thresholds over the time periods investigated. The variation between individuals is probably exaggerated by the fact that representative sampling of thresholds over the entire hearing range was not achieved in all animals. The March-April experimental period (1987) was in fact separated by an additional 12 months from the period October to January (1985–1986) (Köppl et al., in preparation)

and Johnstone (1969 a,b) report that the size of the summating potential in response to sound and the activity of auditory-nerve fibres is low for most of the year but increases dramatically for a few weeks in the austral spring. Whereas for most of the year it was difficult to record active nerve fibres, there were "an unlimited number of active fibres" for 2 weeks in the spring (Johnstone and Johnstone, 1969 b). Holmes and Johnstone (1984) report similar effects for the summating potential and the compound action potential of the eighth nerve (with, however, very large individual variations) and suggest that these effects may be due to changes in the state of the hormonal system and of hydration of the animals.

In contrast to the above findings, we (Köppl et al., 1988) found rather uniform response characteristics for the spring and the autumn. A comparison of the sensitivity of all fibres recorded in individual animals at different times of year reveals no systematic seasonal effect (Fig. 11.20). One possible explanation for this discrepancy may be that there is a seasonal effect on the amount of anaesthetic necessary to produce surgical levels of anaesthesia and that the level of anaesthesia has an influence on the activity of the hair cells and/or auditory-nerve fibres. We found that in the spring, much larger doses were necessary. Although it is difficult to judge from the earlier published work exactly how the anaesthesia was handled, it appears as if standard initial doses were used which could have led to an overdosing of animals outside the spring period (see Ch. 5).

Chapter 12

The Hearing of the Caiman, *Caiman crocodilus*

The caiman is an alligator which, together with the crocodiles and gavials, form the few remaining reptilian descendents of the huge group of ruling diapsid reptiles of the Mesozoic period, the archosaurs (Fig. 1.2). They are closely related to the birds, a relationship which is immediately apparent in a comparison of the structure of the inner ear. When considering these inner ears and their performance in comparison to that of the lizards on the one hand, and the mammals on the other, it should be remembered that the Crocodilia-Aves type of inner ear has evolved independently from those of other groups of reptiles for over 200 million years. Members of the Crocodilia are known to be very vocal, using several different sounds as communication signals (see, e.g., Garrick et al., 1978) both as adults and as young even within the egg.

12.1 Anatomy of the Basilar Papilla

The anatomy of the crocodilian papilla basilaris has been described by Baird (1970), von Düring et al. (1974), Leake (1976, 1977) and Wever (1978). In *Caiman*, the papilla occupies about two-thirds of the cochlear duct, being nearly 4 mm long and thus about twice the length of the longest lizard papilla (Fig. 12.1 A). It is also very broad, being 400 μm wide near the basal end and nearly 600 μm wide at the apical end. Although there is no papillary bar on the basilar membrane, it is thickened quite considerably by connective tissue on the scala tympani side, which Wever (1978) refers to as the tympanic lamella (Fig. 12.2).

The papilla has about 11500 hair cells spread out broadly across the basilar membrane and embedded in supporting cells. All hair cells are reported to be abneurally oriented. A substantial proportion of the hair cells does not lie on the free basilar membrane, but on the presumably firmer substrate of the superior cartilaginous plate on the neural side (Figs. 12.1 B, 12.2). The ganglion cells of the afferent innervation lie below this plate and the nerve-fibre bundles enter the papilla through a *habenula perforata* below the neural area of hair cells (Fig. 12.2).

There are two anatomical types of hair cells, a fact which Retzius (1884) alluded to. Baird (1974) and later authors (von Düring et al., 1974; Leake, 1976, 1977) describe a sharp transition between these hair-cell types (Figs. 12.2, 12.3). One population (3000) of hair cells is columnar in shape and situated over the superior cartilaginous plate. The other hair cells (8500) are more bowl-shaped and

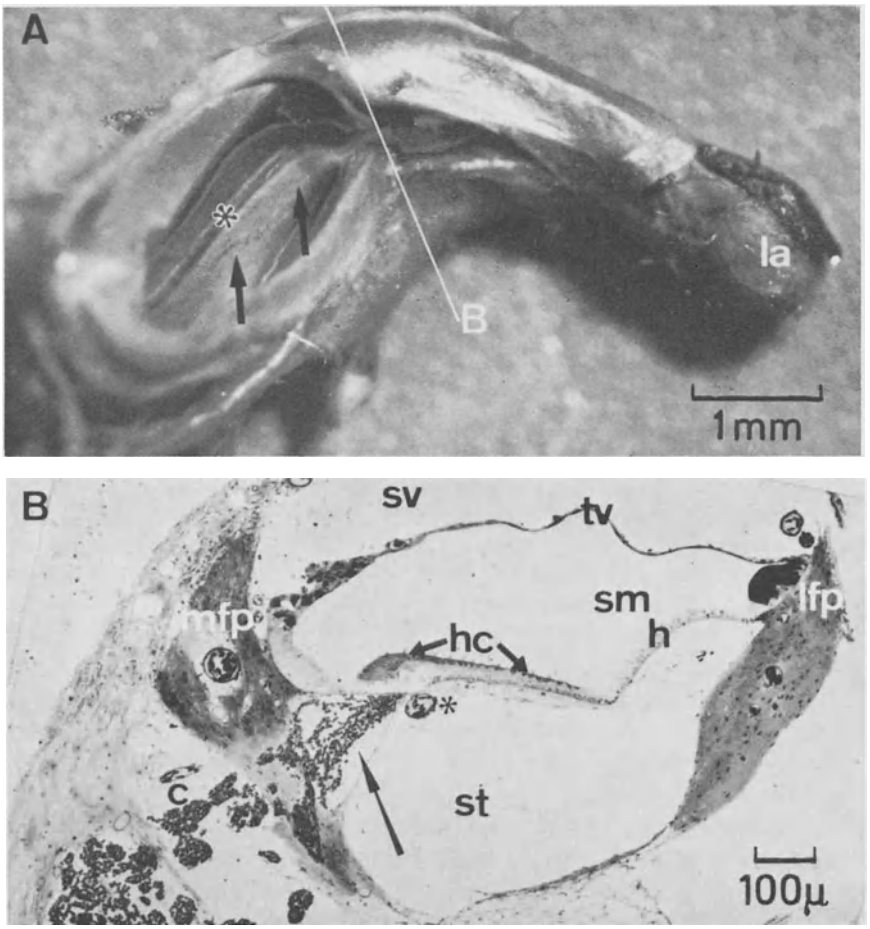

Fig. 12.1 A, B. Structure of the cochlear duct in *Caiman crocodilus*. *A* Photograph of the isolated cochlear duct. On the *right*, the lagena macula (*la*) is within the bulge at the apical end of the duct. On the *left* is the opening in the limbus represented by the *recessus scala tympani*, through which the underside of the basal area of the basilar membrane (*arrows*) is visible, with the adjacent blood vessel (*asterisk*). The *white line* across the duct represents the position of the transverse section shown in *B*. *B* Transverse section through the cochlear duct of *Caiman crocodilus* at the level indicated in *A*. At this level, the scala tympani (*st*) is closed off by the limbus. The tegmentum vasculosum (*tv*, quite thin at this position) separates scala vestibuli (*sv*) from scala media (*sm*). The hearing organ, with the darkly stained hair cells (*hc*) and hyaline cells (*h*) is on the (artefactually crumpled) basilar membrane, which stretches between the lateral (*lfp*) and medial (*mfp*) cartilaginous plates. The tectorial membrane is not visible, probably due to its poor staining. The blood vessel shown in *A* is marked with an *asterisk*, the *arrow* shows the position of the cochlear ganglion; *c* bundles of nerve fibres (von Düring et al., 1974)

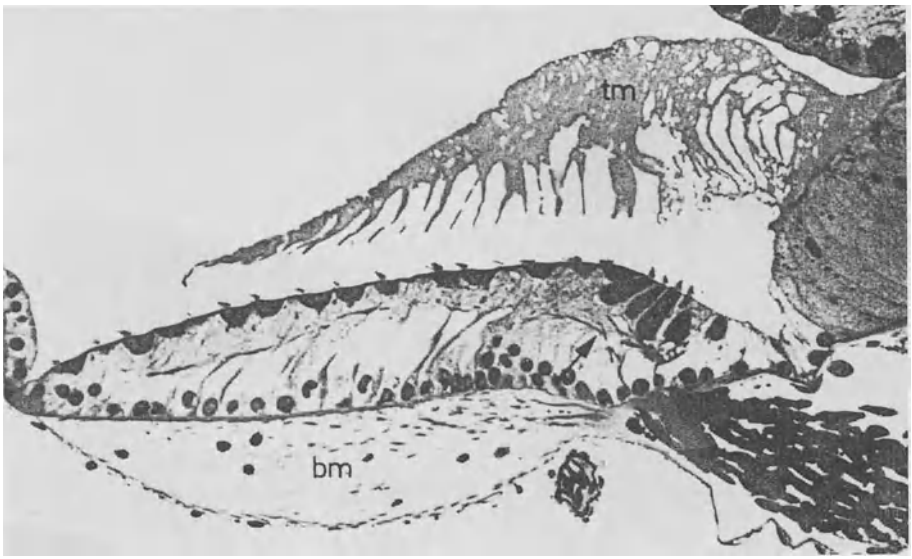

Fig. 12.2. A higher magnification cross-section of the basilar papilla of *Caiman crocodilus*. The neural limbus (medial cartilaginous plate of Fig. 1) is to the *right* in this figure. The basilar membrane (*bm*) is quite thick, the tectorial membrane (*tm*), with many indentations on the lower face, is torn off the epithelium. The papilla itself consists of a thick layer of lightly stained supporting cells and dark hair cells above and between them. To the *left* are the basin-shaped short hair cells, the tall hair cells are on the inner side of the papilla (to which the arrow is pointing), and lie above the neural limbus where the nerve-fibre bundles enter (Baird, 1974)

lie over the free basilar membrane. Many authors assume the same functional division as in mammals to be present and therefore call these groups the inner and outer hair cells, respectively. There are good reasons to be cautious in this regard (see Ch. 14), so I shall refer to them with the terms often used for these cells in the birds, namely tall and short hair cells. From the basal end of the papilla to the apical end, the number of tall hair cells in any one cross-section increases from between 2 and 6 basally to 12 apically, the number of short hair cells from 11 basally to 25 medially, then down to 6 near the apical end. At the extreme apical end, only tall hair cells are found (von Düring et al., 1974). The border between tall and short hair cells is very easy to recognize in a scanning electron microscope picture of the papillar surface (Fig. 12.3). Within their respective areas, the tall and short hair cells are not found in rows, but are distributed mosaically (Leake, 1977).

The tall hair cells have a small, rounded endolymphatic surface, most of which is covered by their stereovillar bundle (Fig. 12.3b). These cells have a length of 25 to 30 μm and an endolymphatic surface diameter of 6 μm apically and 14 μm basally. The stereovillar bundles of these tall hair cells consist of 70 to 90 stereovilli of diameter 0.3 to 0.4 μm, whose greatest height is said to grade systematically from 10 μm basally to 70 μm apically (von Düring et al., 1974). There appears, however, to be an error in these extremely large values for the height of the stereovilli. In the figures given by Leake (1976, 1977), the stereovil-

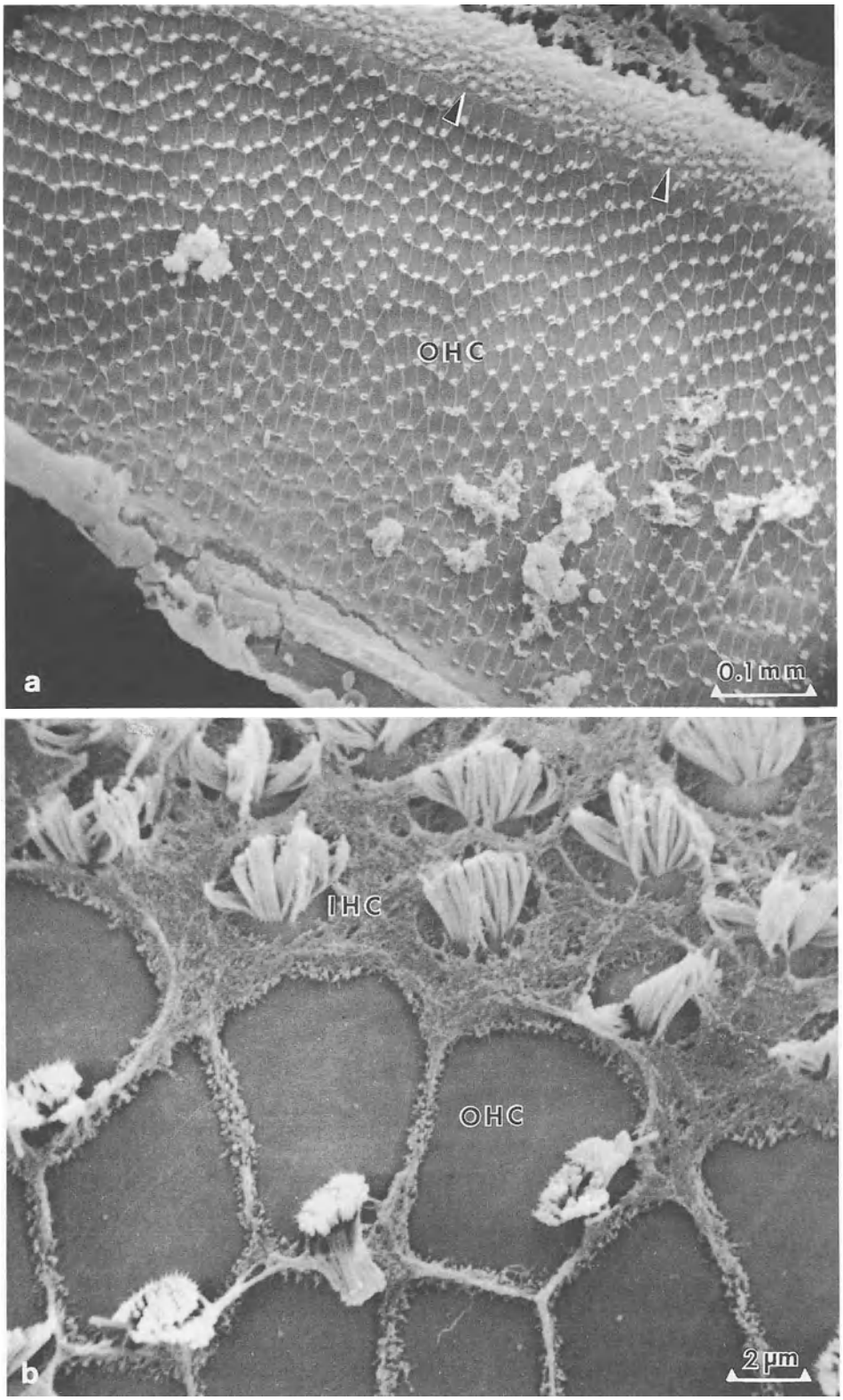
OHC
a
0.1 mm
IHC
OHC
b
2 µm

lar bundles are substantially shorter (e.g. 7–8 μm on short hair cells near the apical end of the papilla, her Fig. 8, 1977). In other vertebrate species, stereovillar bundles below a tectorial membrane rarely exceed 10 μm in height. The kinocilium has the same diameter, but is longer than the tallest stereovilli in juvenile caiman (Leake, 1976) but shorter in older animals (von Düring et al., 1974). It has been assumed that the kinocilium degenerates with age.

The short hair cells have a vertical extent of 6 μm and, from basal to apical, their endolymphatic-surface changes shape from hexagonal to elongate. There are 100 to 150 stereovilli per bundle, with a maximal length of 5 μm basally and 30 μm apically (von Düring et al. 1974; *however*, see above with regard to the height of stereovilli). The stereovillar bundles of short hair cells, in any one cross-section of the papilla, are thus shorter than those of the tall hair cells (Leake, 1977) and are found on the abneural side of the hair cell. Thus, these cells have a much larger free surface (without a cuticular plate) than the tall hair cells (Fig. 12.3 a,b). The supporting cells of the basilar papilla have, as in other tetrapods, microvilli on their endolymphatic surface (Fig. 12.3 b), but are thought to be more specialized than those of other reptiles because their cytoskeleton contains a greater development of clusters of microtubules (Miller, 1980). This may be related to the fact that the microvilli are firmly attached to the tectorial membrane. All hair cells are also attached to the thick tectorial membrane, which originates on the neural limbus (Fig. 12.2). Since the lower face of the tectorial membrane exhibits a honeycomb-like structure in the fixed and dried state and since the depressions correspond in their respective size and position along the papilla with the individual hair cells, it has been suggested that each depression encloses one hair-cell stereovillar bundle.

As is normal in tetrapod papillae, the nerve fibres (about 6000 of average diameter 4 μm, Klinke and Pause, 1980) lose their myelin sheath when they pass through the *habenula perforata*. Within the papilla, von Düring et al. (1974) could distinguish between the afferents (0.8 μm) and efferents (1.3 μm). The efferents make en passant synapses with afferents near the habenula and one or two axosomatic synapses with tall hair cells. They also synapse with short hair cells, with their surrounding supporting cells and also with the hyaline supporting cells lying on the abneural side of the hair-cell area. A tall hair cell typically has synaptic contact (by way of ribbon synapses) with four afferent fibres, each contact having up to four ribbons. Each afferent may contact up to three tall hair cells. Up to three short hair cells may contact one afferent axon, with up to two synaptic ribbons per hair cell (von Düring et al., 1974). According to Klinke and

Fig. 12.3 a, b. Scanning electron micrographs (SEM) of parts of the papilla basilaris of *Caiman crocodilus*. *a* SEM across the entire width of the papilla, showing the large number of short hair cells (*OHC*), each having a relatively large upper surface area. The transition to the (smaller) tall hair cells is indicated by the two *arrowheads*. *b* A higher magnification SEM of the border region between the short (*OHC*) and the tall (*IHC*) hair-cell regions. The surfaces of the supporting cells, with their microvilli and the remnants of tectorial material, are very narrow between short hair cells. The stereovillar bundles occupy a much smaller proportion of the hair-cell surface in the short hair cells than in the tall hair cells. The hair-cell bundles are rather disarrayed in this specimen (Leake, 1977)

Pause (1980), who cite a personal communication from M. von Düring, 40% of the afferent fibres innervate short hair cells. There are no detailed data on the relative distribution of the afferent or of the efferent fibres to the two hair-cell populations.

12.2 Mechanics of the Basilar Membrane

The frequency-response characteristics of the middle ear and the basilar membrane of *Caiman* have been reported by Wilson et al., (1985). The middle ear was described in Chapter 3. The displacement amplitude of different locations on the underside of the basilar membrane for different frequencies of stimulation was measured using a capacitative probe (see Sect. 5.4). The accessible area was from about 0.5 mm to 2 mm from the basal end. Whereas the motion of the limbic material resembled that of the footplate of the columella, the basilar-membrane peak response was 20 to 30 dB higher in its amplitude. The basilar-membrane displacement response to constant SPL at the eardrum resembles a low-pass filter with a slight increase of amplitude (2 dB/octave) at low frequencies up to a cut-off frequency, followed by a rapid roll-off of amplitude above this frequency (30 to 80 dB/octave). The phase response of the basilar membrane displacement shows an increasing lag with frequency up to a maximum of about 1 cycle at 5 kHz. The more basal locations had higher cut-off frequencies, indicating the presence of a tonotopic organization.

After correcting for the middle ear, the basilar-membrane displacement has a band-pass characteristic, with a distinct rounded peak (Fig. 12.4a). Near the peak, the slopes are about 15 dB/octave on the low-frequency side and 15 to 60 dB/ octave on the high-frequency side. These slopes diminish to very low values at frequencies far above the frequency of peak response. The phase response starts with a 0.25-cycle lead at low frequencies and ends with a 0.25-cycle lag at high frequencies (Fig. 12.4b). Unlike the responses of primary auditory-nerve fibres (see below), the recorded mechanical vibration of the basilar membrane was unaffected by a change of temperature. The mapping coefficient of the frequencies on the basilar membrane is 1.4 mm/octave, starting from a frequency near 2.5 kHz at the extreme basal end. The frequencies are to be corrected by about 0.5 octaves for the draining necessary for the capacitative probe (see Fig. 12.4). Both the tuning characteristics and the phase responses of the basilar membrane indicate the presence of a travelling wave, albeit rather rudimentary, with very little phase shift when compared to that of the mammalian basilar membrane. Since the tuning of single fibres is much sharper than that of the basilar membrane and their phase shift is very much greater (see below), it is evident that one or more filter mechanisms intervene between the observed basilar-membrane motion and the nerve-fibre responses. However, since the technique used for these measurements can damage and reduce the sensitivity of the hearing organ, the conclusion that the basilar membrane is not the major tuned element in the inner ear of *Caiman* must be accepted with caution. The con-

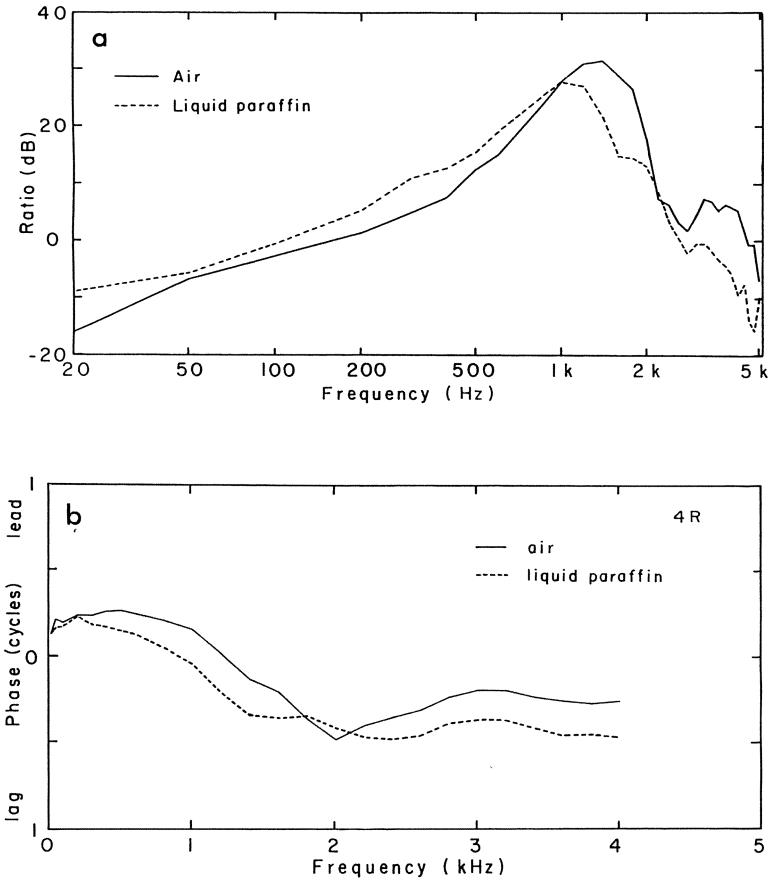

Fig. 12.4 a, b. Mechanical response to sound of the basilar membrane of *Caiman crocodilus* at a position 1.3 mm from the basal end, as measured with the capacitative probe technique. *a* Displacement amplitude of the basilar membrane over a wide frequency range expressed relative to the displacement of the columella of the middle ear (in dB). The relative displacement of 20 dB at about 1 kHz indicates a ten times greater amplitude of the basilar membrane than the columella. The best frequency for this position is roughly 1.3 kHz. *b* Phase of the displacement relative to the columella. Note the linear frequency axis. In both *a* and *b* are shown the measurements both for the scala tympani drained and filled with the insulating fluid liquid paraffin. The latter, while preserving the insulation of the capacitative probe, probably better represents the normal mechanical conditions of the inner ear (Wilson et al., 1985)

clusion would be strengthened by demonstrating that the profound effects of temperature on neural tuning are intact while in the same animal showing that the basilar membrane does not change its response pattern with temperature (Wilson et al., 1985). In addition, it should be remembered that only some of the hair cells lie over the free basilar membrane.

12.3 Otoacoustic Emissions from the Caiman Ear

Brief reports are available indicating that low-level otoacoustic emissions (OAEs) are emitted by the caiman ear (Klinke and Smolders, 1984; Strack et al., 1981; see Sect. 5.7). Whereas delayed OAEs in response to clicks could not be detected, simultaneous OAEs were present as ripples in the waveform of sound-pressure level of a swept tone in the outer ear canal. The emissions were fairly broad-band (with synchronization widths near 200 Hz), non-linear in their growth with increasing SPL and suppressible by second tones. The most effective suppressor tones were near the emission frequency. These data strongly resemble those described for the starling (Manley et al, 1985; Sect. 13.3).

12.4 Discharge Patterns of Primary Auditory-nerve Fibres

Klinke and co-workers have provided us with detailed information on the activity patterns of the primary auditory fibres of *Caiman crocodilus* (Klinke and Pause, 1980; Smolders and Klinke, 1984, 1986). All fibres displayed an irregular spontaneous activity, with rates between 0.5 and 80 spikes/s. The rates showed a bimodal distribution, 30% of fibres belonging to a population with rates below 20 spikes/s. The modes of the interval histograms lay mostly between 2.5 and 6 ms, irrespective of spontaneous rate. In these respects, they resemble mammalian auditory-nerve fibres.

All fibres showed a strong frequency selectivity, when stimulated with pure tones and with clicks. Frequency-threshold tuning curves were, with the exception of very few symmetrical cases, always steeper on the high-frequency side (Fig. 12.5 A,B). Thus the slopes of the high-frequency flanks lay between 30 and 180 dB/octave, whereas the low-frequency slopes were 10–150 dB/octave. The characteristic frequencies lay between 30 Hz and 2.8 kHz, whereby the best sensitivities were shown by cells between 500 Hz and 1.5 kHz. Some of these responded at levels of 5 dB SPL (Fig. 12.6). There was a wide range of thresholds at any one frequency (range about 50 dB; Fig. 12.6). When tuning curves were generated with higher rate criteria, the CF was found to shift to a lower frequency at a rate of up to 10% of CF per 10 dB (Fengler et al., 1978). The $Q_{10\ dB}$ measures of frequency selectivity ranged from near 1 for low-CF cells up to 7 at high CFs (Fig. 12.7). There was, however, considerable scatter between cells; only a small part of this scatter could be explained by a correlation with the different thresholds of the individual cells. In response to clicks, cells of different CF showed latencies of 3 to 4 ms for low-CF cells and near 1 ms for the highest CFs, similar to, but somewhat shorter than, corresponding values for mammalian fibres.

Peri-stimulus-time histograms revealed a phasic-tonic response pattern for higher-level stimuli. The maximal discharge rates during 400 ms tones averaged 120 spikes/s, with a range of 40 to 200 spikes/s. Below CF, cells could reach

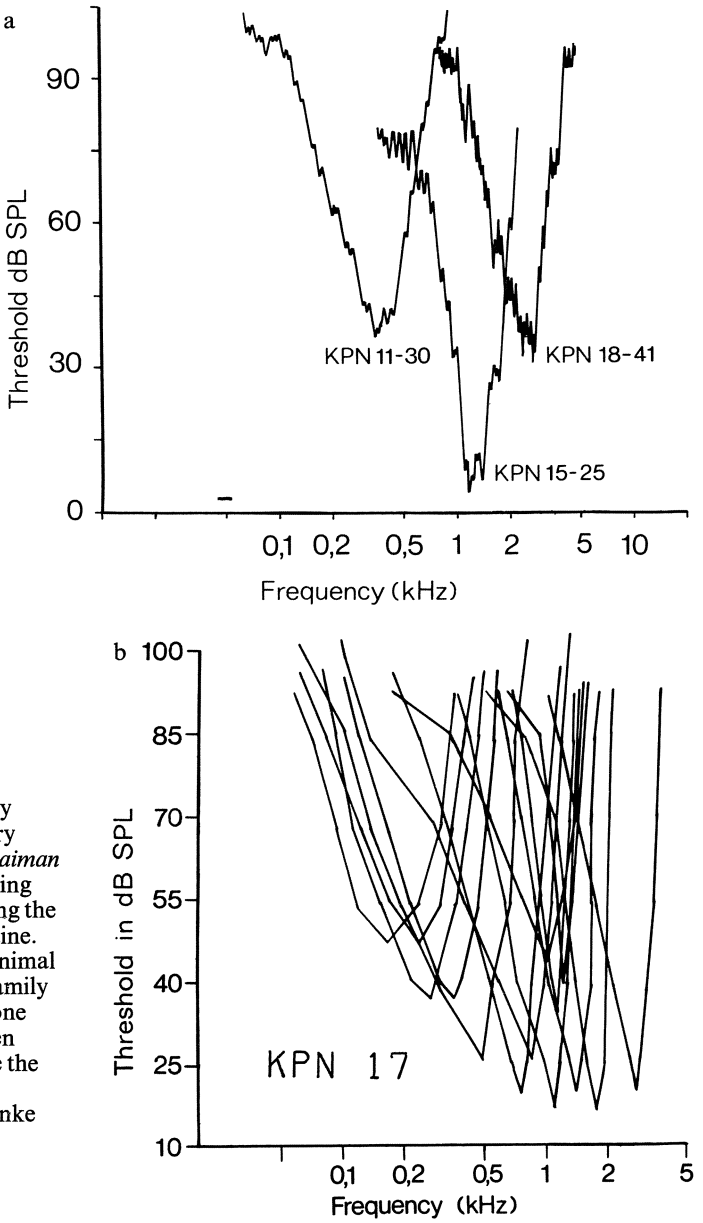

Fig. 12.5 a, b. Frequency tuning curves of primary auditory neurones in *Caiman crocodilus*. *A* Three tuning curves as measured using the threshold-hunting routine. The *numbers* indicate animal and cell number. *B* A family of tuning curves from one animal, which have been simplified to reproduce the slopes derived from threshold-hunting (Klinke and Pause, 1980)

higher rates than at CF. There was no correlation between the maximum rate and the spontaneous rate of individual cells. Near threshold, the rates increased by about 4 spikes/s/dB and dynamic ranges varied between 20 and 40 dB. The intensity functions were, however, nonmonotonic, decreasing again at high levels even down to near the spontaneous rate. Two-tone suppression was clearly present in the units tested, with suppressive side bands on both sides of the CF,

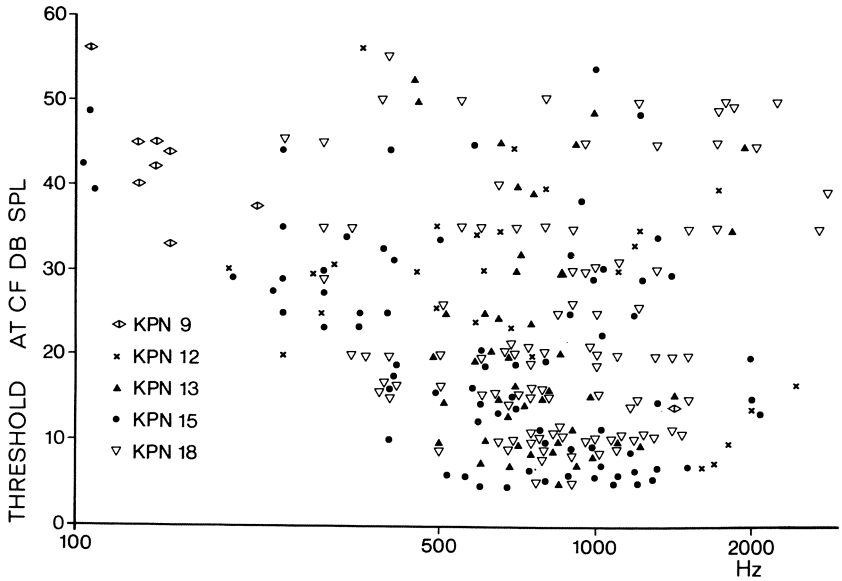

Fig. 12.6. Threshold of auditory-nerve fibres in five caiman (*Caiman crocodilus*), plotted as the threshold of individual fibres at their characteristic frequency (CF). The CFs range from near 100 Hz to 2.8 kHz (Klinke and Pause, 1980)

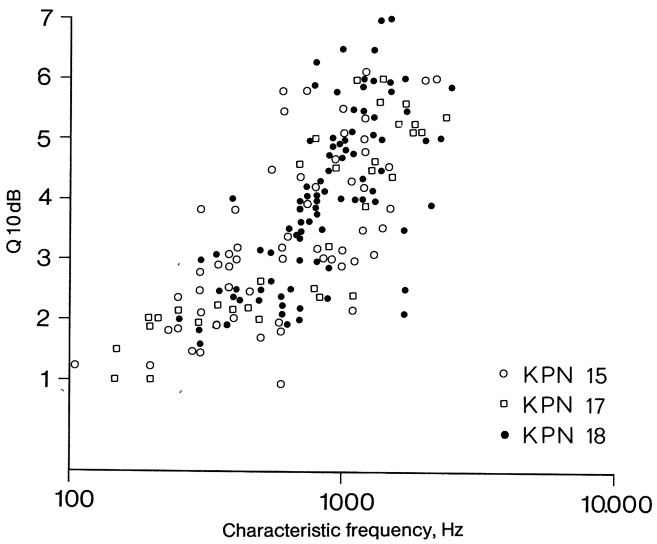

Fig. 12.7. Sharpness of tuning of auditory-nerve fibres from three caiman (*Caiman crocodilus*), represented as the Q_{10dB} of individual fibres. As is found in most auditory systems, the mean Q_{10dB} rises with CF (Klinke and Pause, 1980)

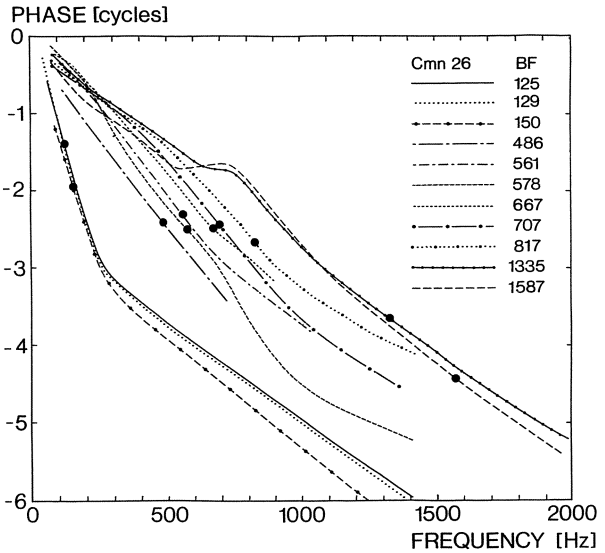

Fig. 12.8. Cumulative phase of the phase-locked response as a function of the frequency of pure tones at 85 dB SPL for 11 auditory-nerve fibres of *Caiman crocodilus* from the same ear and with a wide range of CFs. The *large dots* indicate the fibre CF in each case. It can be seen that the rate of accumulation of phase lag is highly CF-dependent. The rapid accumulation for low CF cells indicates a long time delay between the sound stimulus in the external ear canal and the fibre discharge (Smolders and Klinke, 1986)

being wider on the low-frequency side. However, suppression below the spontaneous level was not demonstrated.

Strong phase-locking behaviour has been reported in the primary auditory fibres of *Caiman* (Smolders and Klinke, 1986). The phase-versus-frequency response characteristics of individual cells are highly CF-dependent (Fig. 12.8). For low-CF cells, the phase roll-off with frequency is faster than for high-CF cells. The characteristics of the phase roll-off permit the calculation of a delay (slope of the phase response) at CF for responses of individual cells. These are more than 10 ms for the lowest-CF cells and 2 ms for high-CF cells (Fig. 12.9). The latencies and delays as observed in response to clicks and from the phase-response data are not only similar to those reported for mammals, but also to those of the treefrog. This fact led Smolders and Klinke (1986) to suggest that, although such delays are consistent with the presence of a travelling wave, it would be equally legitimate to explain them on the basis of the response characteristics of an array of tuned elements which lie between the basilar-membrane motion and the nerve fibre. Their mechanical measurements on the basilar membrane (see above) did indeed indicate the presence of a crude travelling wave, indicating that the travel time of the travelling wave could be partly responsible for these group delays. The estimates of wavelength of the travelling wave from neural data differ, however, from those measured on the basilar membrane. It was not possible for these authors to be sure that, as in the earlier measurements of basilar-membrane motion in mammals, the experimental procedure had not

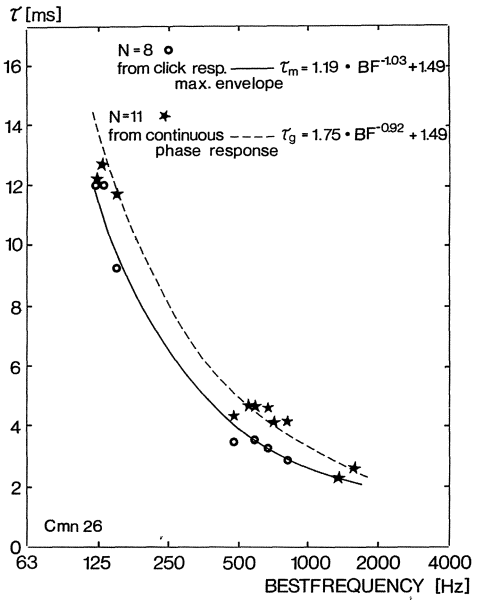

Fig. 12.9. Group delay in auditory-nerve fibres of *Caiman crocodilus*. *Stars* Group delay for 7 of the fibres shown in Fig. 12.8, as a function of their CF ("best frequency") calculated assuming a straight-line fit to the phase-delay curves and correcting for middle ear, synaptic and neural delays (given as 1.49 ms). *Open circles:* Group delay estimates for the same fibres from response delays to click stimuli (estimated mode of the first response peak in the click PSTH). The *solid* and *dashed lines* represent the respective least-squares fits to the data points (Smolders and Klinke, 1986)

damaged a sensitive component of the basilar-membrane motion. Thus, for *Caiman*, the question as to the origin of the long neural group delays remains open. This point is also discussed in Section 14.9.3. Similar neural phase data have been discussed in Section 11.2.3 for the bobtail skink.

In spite of the separation of the afferent innervation of the tall and short hair cells in this species, Klinke and his co-workers could not find any consistent way of separating the primary fibres according to their physiological response properties into more than one population. The two groups of spontaneous rates, for example, could not be correlated with any other differences between these cells. Thus it appears as if the fibres which innervate the short hair cells (near 40% of all fibres) either are not active or respond in all respects like those innervating the tall hair cells. This conclusion had also been reached in the case of mammals and of birds (Ch. 13) and is, at least initially, intuitively unacceptable. In both mammals and birds, however, it has been shown that all acoustically-active primary afferents only contact one hair-cell population (inner and tall hair cells, respectively). This problem is discussed further in Section 14.5.

12.5 Effects of Temperature on Tuning

As in fibres of the amphibian papilla of the frog (Moffat and Capranica, 1976) and in the primary auditory fibres of the Tokay gecko (Eatock and Manley, 1976, 1981, see Ch. 10), the tuning of *Caiman* fibres is temperature-sensitive (Smolders and Klinke, 1977, 1984). These temperature effects are reversible. The frequency-threshold curves of all fibres shift with temperature, the CF increasing nearly linearly with temperature (Figs. 12.10, 12.11 A). The slopes in different fibres of 3 to 90 Hz/ °C translate into shifts of 0.14 octaves/ °C at 15 °C and about 0.06 octaves/ °C at 30 °C, irrespective of the initial CF at a standard temperature. The sharpness of tuning was essentially unaffected by temperature. There was an optimum temperature near 28 °C with regard to the threshold of fibres (Fig. 12.11 B). Below and above this temperature, the thresholds rose by 1.9 dB/°C. Temperature also affects the mean spontaneous firing rate, which increases linearly with increasing temperature at a rate of from 0.2 to 3.5 spikes $s^{-1}\,°C^{-1}$ (Fig. 12.11 C). The distribution of spontaneous rates remains bimodal at all temperatures.

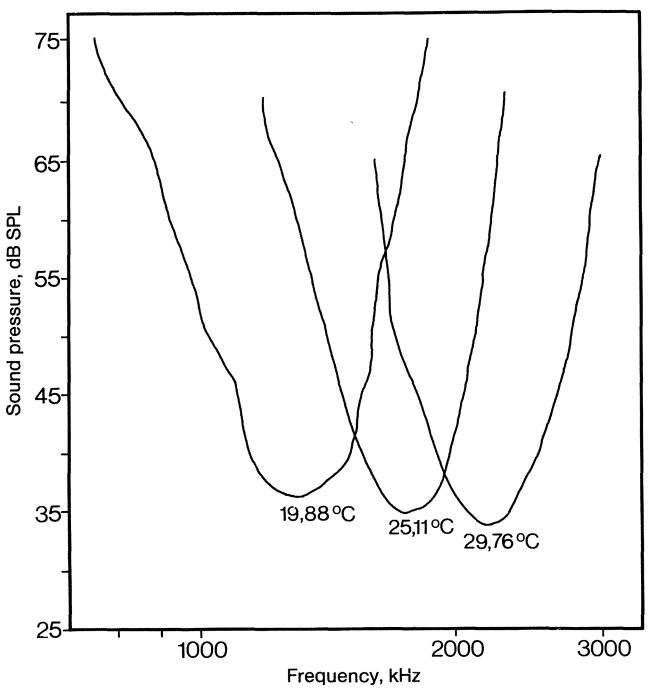

Fig. 12.10. Temperature dependence of the frequency tuning curve of a single primary auditory fibre of *Caiman crocodilus* over a range of almost 10 °C and measured at the three temperatures indicated. The threshold is defined as a 50% increase in discharge rate above the spontaneous rate at each temperature (spontaneous rate also changes with temperature, Fig. 12.11 *c*) (Klinke and Smolders, 1984)

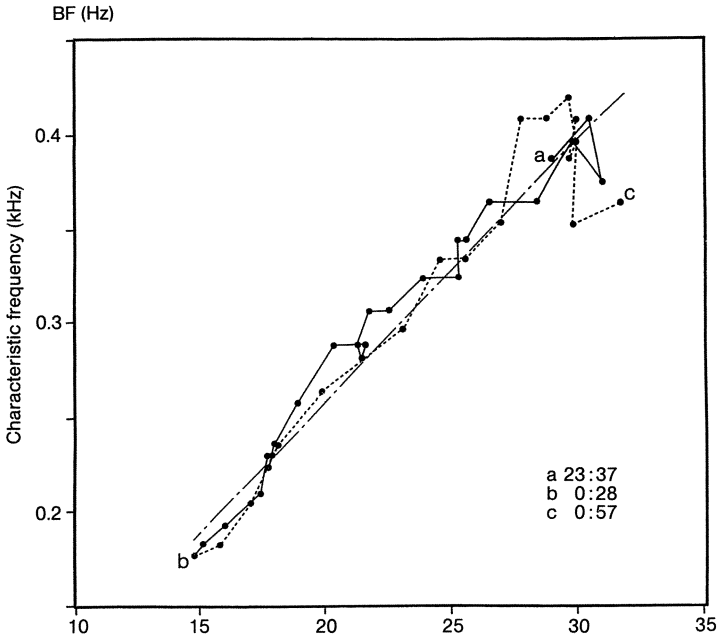
BF (Hz)
Characteristic frequency (kHz)
0.4
0.3
0.2
a
b
c
a 23:37
b 0:28
c 0:57
10
15
20
25
30
35
Temperature (°C)

a

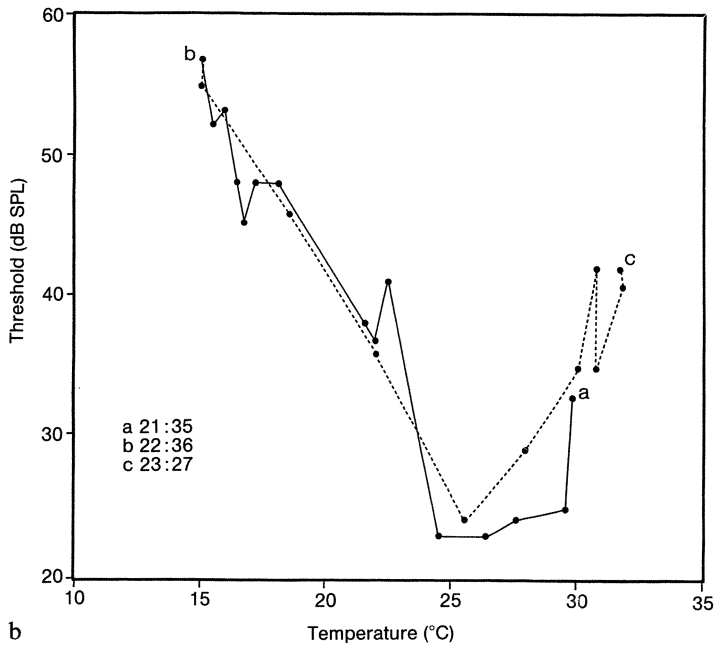
Threshold (dB SPL)
60
50
40
30
20
b
a
c
a 21:35
b 22:36
c 23:27
10
15
20
25
30
35
Temperature (°C)

b

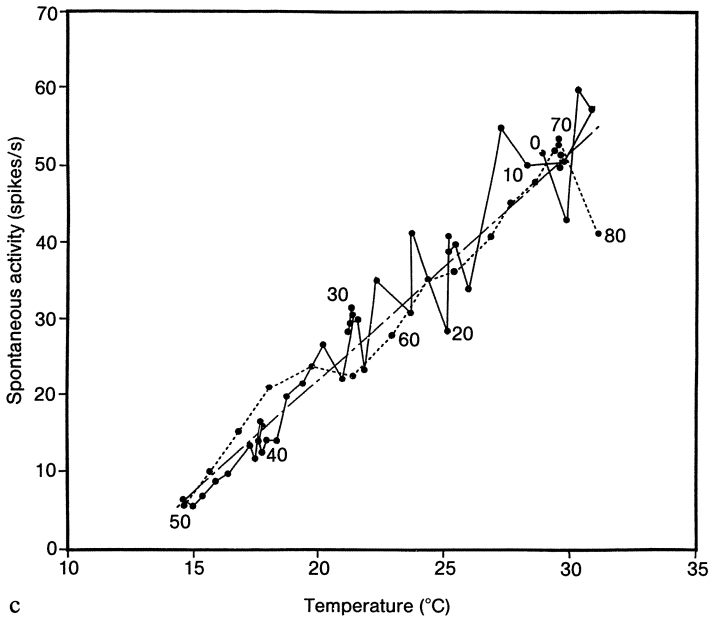

Fig. 12.11 a–c. Temperature effects on the activity patterns of auditory-nerve fibres in *Caiman crocodilus*. *A* Characteristic frequency of a single fibre with temperature changes, during cooling (*solid line*) and rewarming (*dotted line*). The rate of temperature change can be estimated from the times given for the data points at *A–C*. *B* Threshold in dB SPL of a different auditory fibre as a function of inner-ear temperature during cooling (*solid lines*) and rewarming (*dashed lines*). There is a threshold optimum near 26 °C. In both *a* and *b*, the time of starting (24-h system) is given at *a*, start of rewarming at *b*, and the end of the measurement at *c*. *C* Spontaneous firing rate of the same fibre as in *a*, as a function of temperature. The *numbers* next to data points indicate the time in minutes after the start of the measurements. The *dot-dashed lines* in *a* and *c* represent simple linear-regression fits (Smolders and Klinke, 1984)

It is likely that these temperature effects are the result of an electrical tuning of hair cells. Evans and Fuchs (1987) isolated tall hair cells from the apical basilar papilla of the alligator and studied their electrical properties. They found both Ca^{2+} and Ca^{2+}-dependent K^+-currents similar to those reported for the frog saccular-, and red-eared turtle basilar-papilla hair cells (Sects. 2.4.2, 6.1.3) and which are strongly implicated in electrical membrane resonances. However, Evans and Fuchs found in addition Na^+ action-potential activity in hair cells from the most apical region and conclude that such spikes enhance the ability of the hair cell to transmit time-dependent information across the synapse.

Chapter 13

The Peripheral Hearing Organ of Birds

Compared to the reptiles, birds are, in general, highly vocal animals. Although there is thus no problem in delimiting an obvious function for the hearing system, it is somewhat enigmatic that this vocality is not accompanied by large anatomical differences in the inner ear compared to that of the much less vocal Crocodilia, the most closely related group of reptiles. In the past, there have been divergent views on the function of the avian hearing organ. Because the anatomical features were so different to those of mammals, most authors took a cautious approach, assuming that apart from some basic aspects, the function of the bird

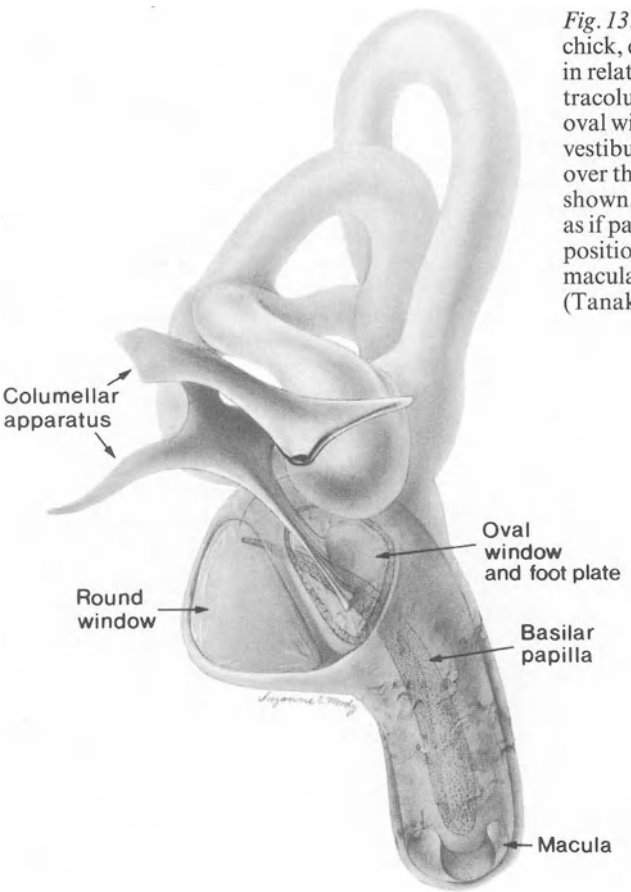

Fig. 13.1. The otic capsule of the chick, drawn in its normal position in relation to the columella and extracolumella of the middle ear. The oval window over the scala vestibuli and the round window over the recessus scala tympani are shown. The cochlear duct is drawn as if partially transparent, and the position of the basilar papilla and macula of the lagena are visible (Tanaka and Smith, 1978)

and mammal cochleae would show substantial differences. In recent years, there has been an increasing interest in the function of the inner ear of birds, especially since some new findings indicate that there may indeed be important functional parallels to the inner ear of mammals. In general, the hearing of birds has received more attention than that of reptiles, so that it has been necessary in this chapter to be more selective in the presentation of data and discussion. For more anatomical detail, the reader is referred to other reviews (Baird, 1974; Lewis et al., 1985; Pumphrey, 1961; Saito, 1980; Schwartzkopff and Winter, 1960; Smith, 1985)

13.1 The Anatomy of the Cochlear Duct

As outlined in Chapter 1, the birds and Crocodilia are closely related, one indication of which is the strong similarity to be found in the structural arrangement of the cochlear duct, with its lagenar macula and basilar papilla (Fig. 13.1, see also Ch. 12). The duct is not coiled, but, especially in the longer ducts like those of owls, twisted in a complex fashion (Schwartzkopff and Winter, 1960).

In both cases, there is a thick *tegmentum vasculosum* (Figs. 13.2 and 13.3), which probably has the same function as the stria vascularis of mammals, giving rise to the endocochlear potential of up to 20 mV between the scala media and the scala vestibuli (Schmidt, 1963) and producing an endolymph high in potassium ions. In the chick, the potassium concentration in scala media is 150 to 160 mM, which is very similar to that of mammals (Runhaar and Schedler, 1988).

As also seen in Crocodilia, there are thousands of hair cells situated on a relatively short (mostly less than 5 mm) basilar membrane. There are at least two (intergrading) types of sensory cells, the tall and short hair cells. Most of the tall hair cells are situated over the neural limbus (superior cartilaginous plate). A thick tectorial membrane covers the entire papilla. As can be seen in a cross-sectional view of the cochlear duct (Fig. 13.2), the scala vestibuli is quite small (Schwartzkopff and Winter, 1960), whereas the scala tympani is, especially towards the basal end, large. Although there are several differences in the arrangement of the scalae and their connections (Schwartzkopff and Winter, 1960), it can be assumed that the fundamental processes of stimulus delivery to the hair cells are essentially the same as in other vertebrates. The cochlear ganglion is not, as in mammals, completely covered by bone. We developed a technique for recording from this ganglion within the recessus of the scala tympani using glass microelectrodes (Manley and Leppelsack, 1977; Manley et al., 1985).

13.1.1 The Sensory Hair Cells

The number of hair cells in the avian basilar papilla ranges from a few thousand in some song birds (e.g. starling, 5800), where the papilla (in the fixed, dried state) is 2.25 mm long, to 9600 in the pigeon papilla. In the papilla of some owls, where

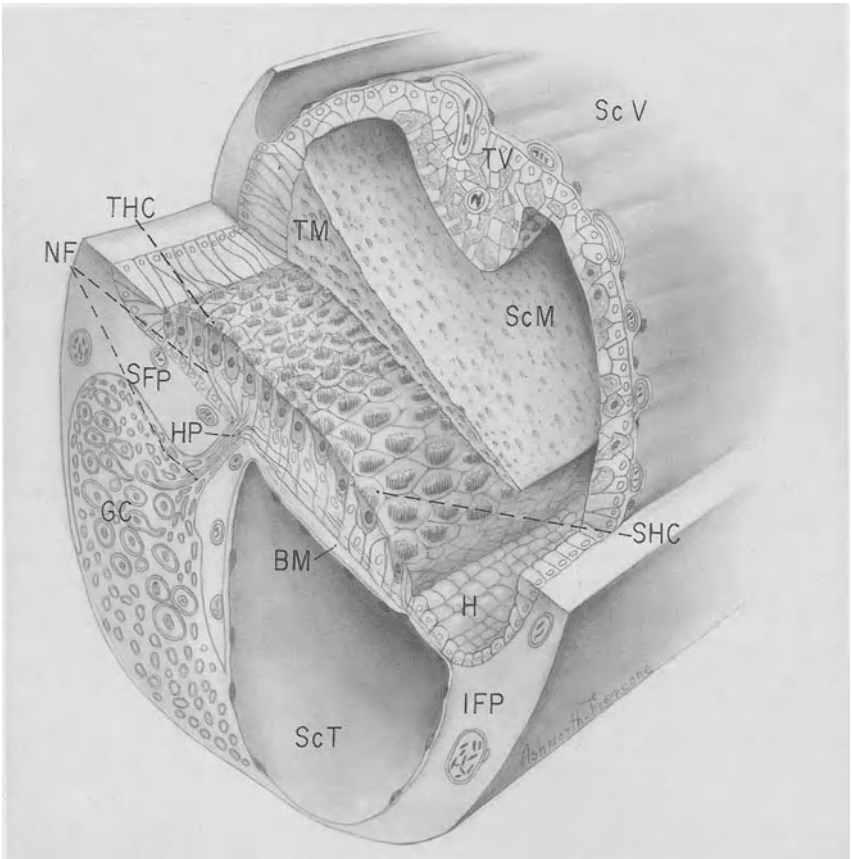

Fig. 13.2. Schematic drawing of a transverse section of the pigeon's cochlear duct, cut such that the upper and lower halves are displaced somewhat along the papilla. The tegmentum vasculosum (*TV*) separates the scala vestibuli (*ScV*) from the endolymphatic cochlear duct (scala media, *ScM*). The thick tectorial membrane (*TM*) overlies both tall (*THC*) and short (*SHC*) hair cells, the *THC* lying over the superior fibrocartilaginous plate (*SFP*, equivalent to the neural limbus), the *SHC* over the free basilar membrane (*BM*). Nerve fibres (*NF*) from the cochlear ganglion (*GC*) enter the papilla at the habenula perforata (*HP*). At the outer edge of the basilar papilla, the hyaline cells (*H*) are continuous with epithelial cells of the inferior fibrocartilaginous plate (*IFP*) (Takasaka and Smith, 1971)

the basilar papilla exceeds 11 mm in length, there are more than 10000 hair cells (Fischer et al., 1988; Gleich and Manley, 1988; Schwartzkopff, 1968). It would be wrong to assume, as Pumphrey (1961) states, that "the basilar membrane of birds is only about one tenth (as long) of that of mammals". His comparison was between a songbird and man, but it would be possible with other examples to prove the reverse (e.g., comparing some owls with some rodents or bats). In general, however, the average bird papilla is shorter and wider than that of a typical mammal. At the widest area of a bird papilla (apical), there can be over 50 hair cells in a single cross-section, compared to 4 to 6 in mammals (Figs. 13.2,

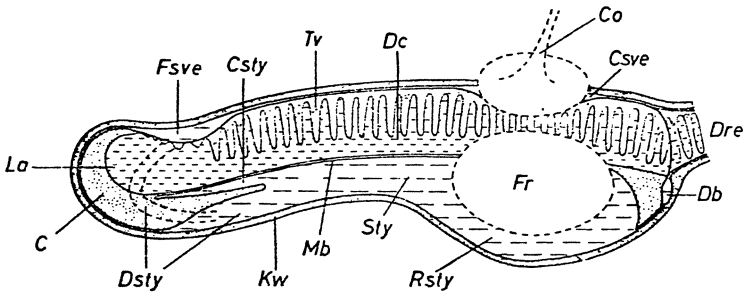

Fig. 13.3. Schematic drawing of a longitudinal section through the cochlea of a bird, to illustrate the relationships between the various fluid spaces within the bony wall (*Kw*). The footplate of the columella (*Co*) abuts on a narrow fluid space of the scala vestibuli (*Csve*), which is otherwise only somewhat widened at the fossa scala vestibuli (*Fsve*). There is a connection to scala tympani (*Sty*) via the basal ductus brevis (*Db*) and the apical ductus scalae tympani (*Dsty*). At the apical end, the scala tympani is also narrow (cavum scala tympani, *Csty*). The round window (*Fr*) covers part of the recessus scala tympani (*Rsty*). Sectioned apical and basal cartilage (*C*) is stippled; *La* lagena; *Tv* tegmentum vasculosum; *Dre* ductus reuniens or cochleo-saccular duct; *Dc* ductus cochlearis, or scala media; *Mb* membrana basilaris (Schwartzkopff and Winter, 1960)

13.4). Thus, the *total* number of hair cells in the papilla is comparable to that of mammals.

Although some authors see no structural justification for distinguishing more than one hair-cell type in avian papillae (Jahnke et al., 1969), others have recognized two to four intergrading hair-cell types, i.e., the tall, intermediate, short and lenticular hair cells (Smith, 1985). Not all types have been recognized in all species and they are, unlike in the very similar papilla of *Caiman*, frequently difficult to distinguish in a surface view (Fig. 13.4). These types grade into each other and the designations are used mainly for descriptive purposes. The hair cells are surrounded by numerous supporting cells.

The tall hair cells are the least specialized and most strongly resemble the typical hair cell of more primitive groups of vertebrates. They are distinguished from the short hair cells by their columnar shape (Figs. 13.2 and 13.5) and the different innervation pattern (see below, Sect. 13.1.3). They are found predominantly supported by the neural limbus and, at the apical end of the basilar papilla, by the basilar membrane. They can be entirely absent from the basal end. In contrast, the short hair cells are wider than they are tall and have large cuticular plates (Fig. 13.6). These cells occupy most of the space over the free basilar membrane. Intermediate cells are intermediate in both shape and position, but have not been described in all species. The actual distribution of these hair-cell types is species-specific, the most striking differences being found at the apical end (Smith, 1985). A few hair cells at the basal end of the chick papilla and many hair cells of the basal 3 mm of the barn owl papilla have been called lenticular hair cells. They are flattened, with a large surface area, only part of which has a cuticular plate (Smith, 1985). In addition, the hair bundle occupies the opposite side of the hair-cell surface than in short hair cells. Our analysis of the surface view of the barn owl papilla, however, indicates that the short hair cells grade into the lenticular

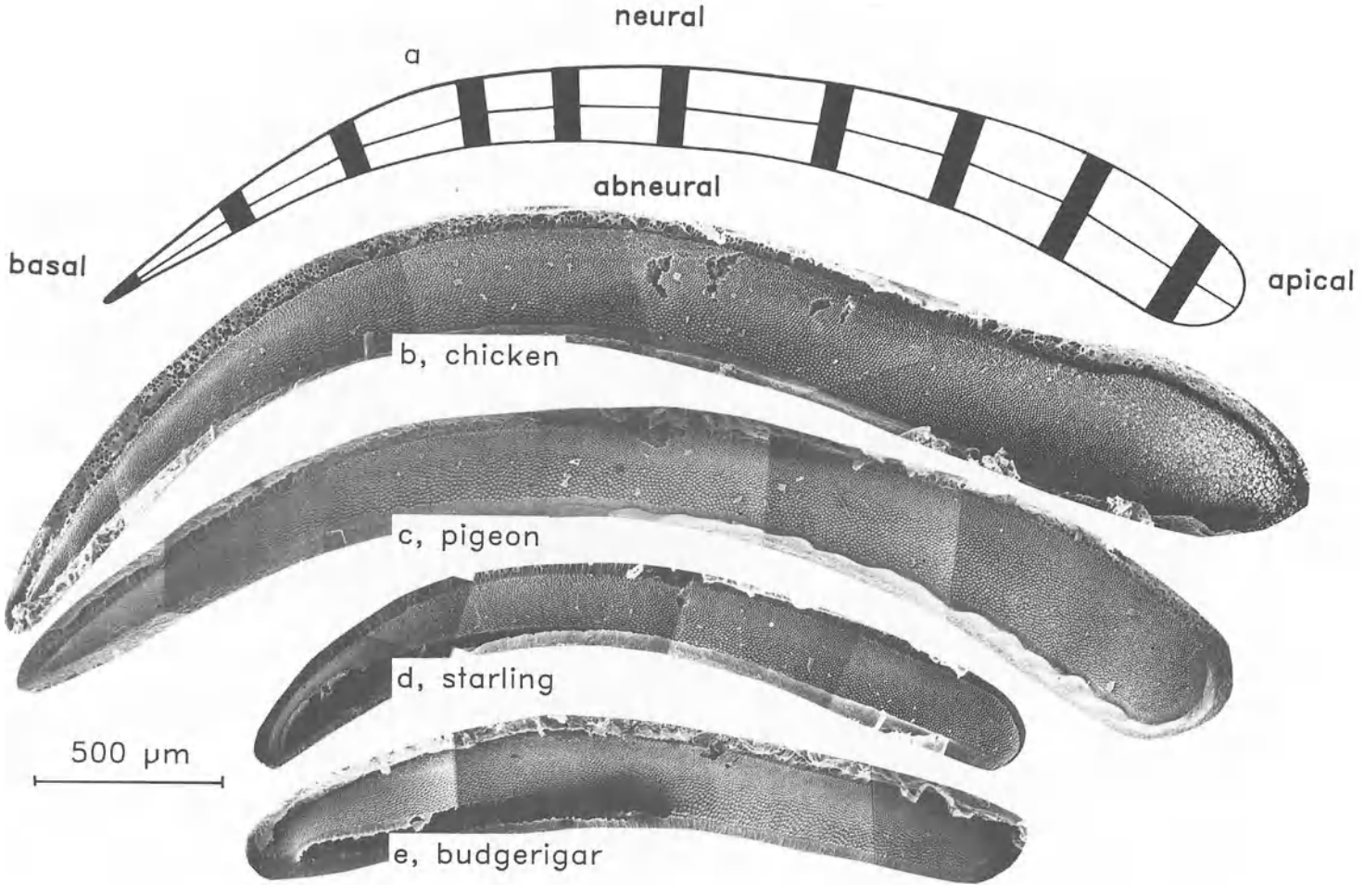
neural
a
abneural
basal
apical
b, chicken
c, pigeon
d, starling
500 μm
e, budgerigar

type and that at any one location, these cell types can be neighbours (Fischer et al., 1988).

All authors since Held (1926) have commented on the massive appearance of the tectorial membrane of birds. The membrane is wedge-shaped, being thickest on the neural side over the tall hair cells and thinning out towards the abneural edge of the hair-cell area (Fig. 13.2). It is connected via a thick surface web on its underside to very small but numerous microvilli of the supporting cells. The underside of the tectorial membrane has a honeycombed appearance, with regularly-placed cavities, presumably for the hair-cell bundles. If a kinocilium is present, both it and the longest stereovilli of the hair cells make a firm connection with the tectorial membrane at the top of this cavity (Smith, 1985; Tanaka and Smith, 1975). Although adult pigeon hair cells possess a kinocilium, it is often missing in the chick and starling cochlea. The kinocilia are not bulbed, as in many reptile hair cells. The stereovilli resemble those of other vertebrate hair cells, containing large numbers of regularly-arranged actin filaments (Tilney and Tilney, 1986). Although it has often been reported that the upper side of the tectorial membrane is also full of holes, this is almost certainly an artefact of fixation. As shown by Kronester-Frei (1979), the tectorial membrane of mammals is sensitive to sodium ions (normally found in fixation buffers) under whose influence it shrinks irreversibly. With some histological preparation methods, the upper surface of the bird tectorial membrane has a very smooth appearance (Fig. 13.7; Runhaar, 1988).

13.1.2 Patterns in the Arrangement of Hair Cell Stereovillar Bundles

In contrast to statements found in many papers, the arrangement of hair-cell orientations in the bird basilar papilla is by no means as regular as that of mammals. Whereas there is no bidirectionality as in reptiles, there are substantial deviations from a purely abneural orientation (Fischer et al., 1988; Gleich and Manley, 1988; Tilney et al., 1987). Thus, the regularly abneural orientation pattern described by Takasaka and Smith (1971, their Fig. 35) for the pigeon's papilla (based on sectioned material) is incorrect. Indeed, some apical hair-cell bundles have an orientation which deviates 90 ° from abneural (Fig. 13.8).

13.1.2.1 The Papilla of Starlings, Pigeons, and Chickens

We (Gleich and Manley, 1988) have described quantitatively the morphological patterns of the papilla of the starling and the pigeon. There are obvious

Fig. 13.4. Photomontages of scanning electron micrographs of the basilar papillae of four bird species, illustrating the size differences between the papillae of the chicken, pigeon, starling and budgerigar. *a* The position of the apical and basal ends, together with the neural and abneural papilla sides. The dark strips in *a* represent the areas in which hair cell morphological features were quantified (see later figures) (Gleich and Manley, 1988)

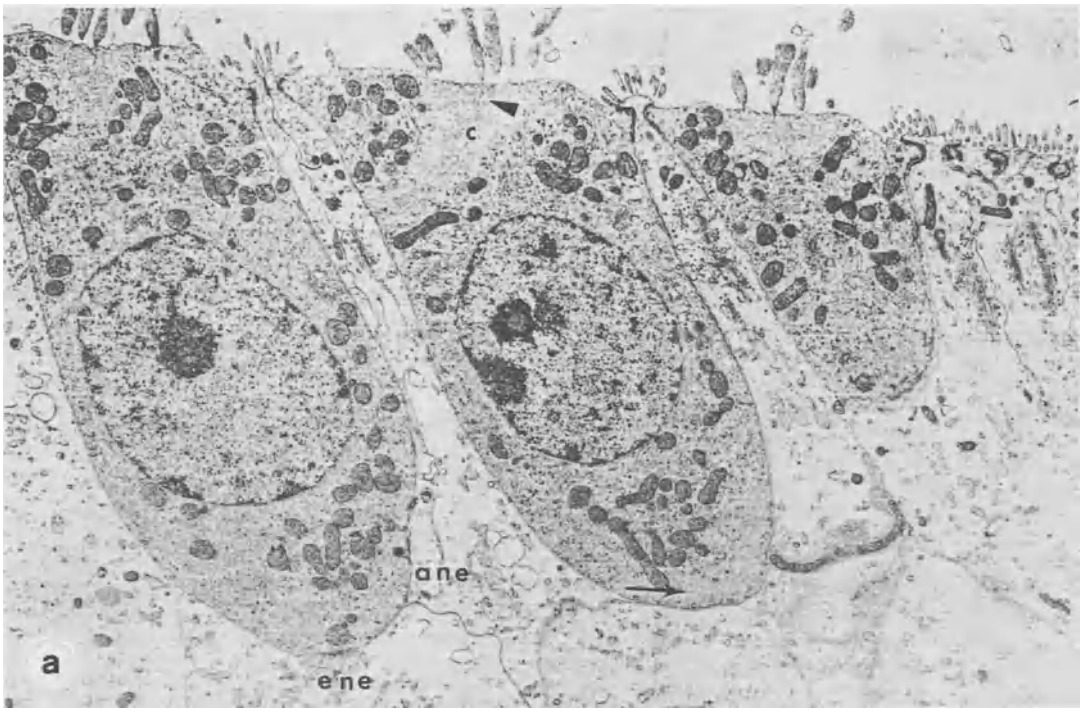

Fig. 13.5 a, b. Morphological features of tall hair cells of birds, illustrated in (*a*) transmission electron micrographs and (*b*) schematic three-dimensional drawings. *a* Three tall hair cells can be seen, sectioned at different levels, only the left cell showing its full length and some afferent (*ane*) and efferent (*ene*) nerve terminals at its base. *b* Supporting cells (*SC*) separate the tall hair cells with narrow strips of microvilli-rich (*MV*) membrane. Each hair cell normally has a kinocilium (*K*) on the abneural side of the stereovillar bundle (*S*). The bundle is embedded in the cuticular plate (*CU*). Cochlear (afferent) nerve fibres (*C*) make large synapses with tall hair cells at levels below the nucleus (*N*), frequently there are synaptic bodies (*SB*). Efferent nerve-fibre endings (*E*) are small and faced on the hair-cell side by subsynaptic cisternae (*SSC*) (*a* from Chandler, 1984; *b*, Takasaka and Smith, 1971)

similarities to the patterns known from the chick (Tilney and Saunders, 1983; Tilney et al., 1987) and the seagull (Counter and Tsao, 1986), so that it is reasonable to regard the data as typical for the avian papilla. Although the basilar papilla has a different length in the various species, it is roughly five times wider at the apical end than at the basal end (starling, 190 to 40 μm). It reaches its widest point about 80–90% of the length from the basal end. The only exception to this rule is the pigeon, where the width increases steadily from 40 to 190 μm at 60% of the length from the basal end and then becomes disproportionally wider to 250 μm at 85%, before tapering somewhat to the apical end (Fig. 13.9 a,b). While in the pigeon and starling the number of hair cells in any one cross-section roughly parallels the width of the basilar membrane (ranging from 8 at the basal end in starling, pigeon and chick, and rising steadily to 30 in the starling and about 40 in the chick), the apical third of the pigeon papilla has more hair cells than expected even from the disproportionate width increase. Between 65% and 88% of the

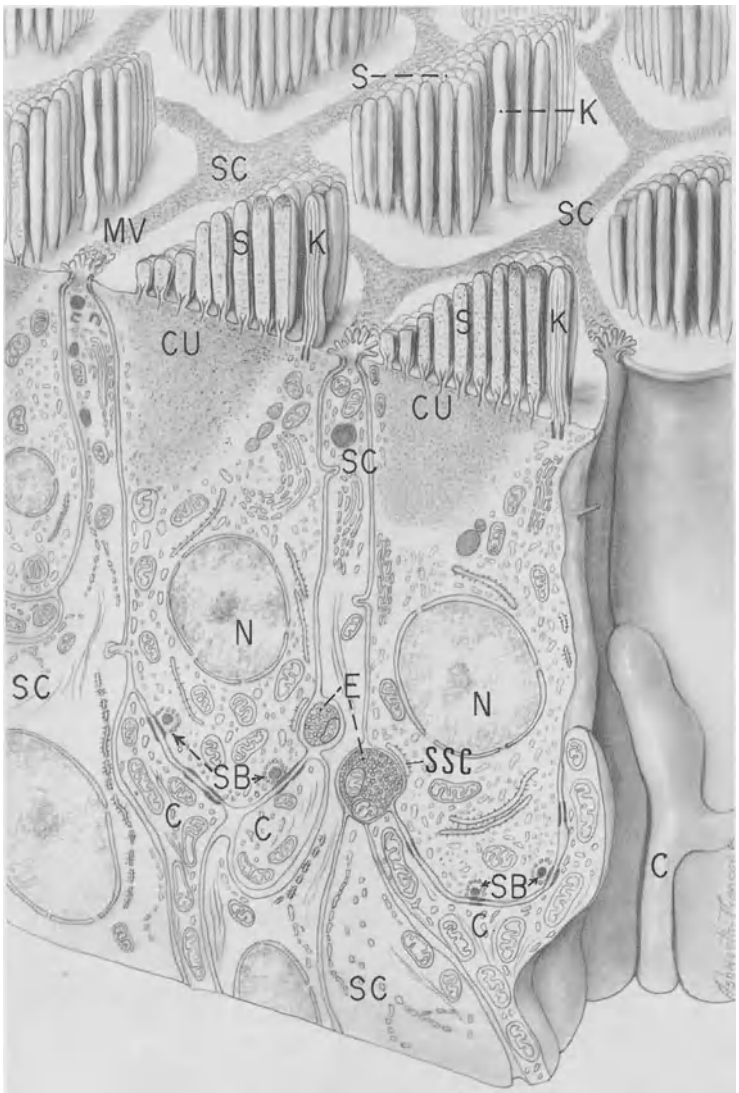

Fig. 13.5b

length, the number of hair cells in a transect rises from 30 to almost 50 (Fig. 13.9c,d). This is accompanied by a dramatic reduction in the surface area of the hair cells of the abneural side of the papilla which, in the pigeon, falls from near 120 μm^2 at 60% of the length from the basal end to less than 40 μm^2 at 85% of the length. A smaller size reduction is seen in hair cells in the middle area of the papilla. Such dramatic dimensional changes are not seen in the starling. Thus there can be morphological specializations in certain areas of the papilla. The specializations in the pigeon are found in the apical area described by Klinke and Schermuly (1986) as giving rise to responses to infrasound stimuli.

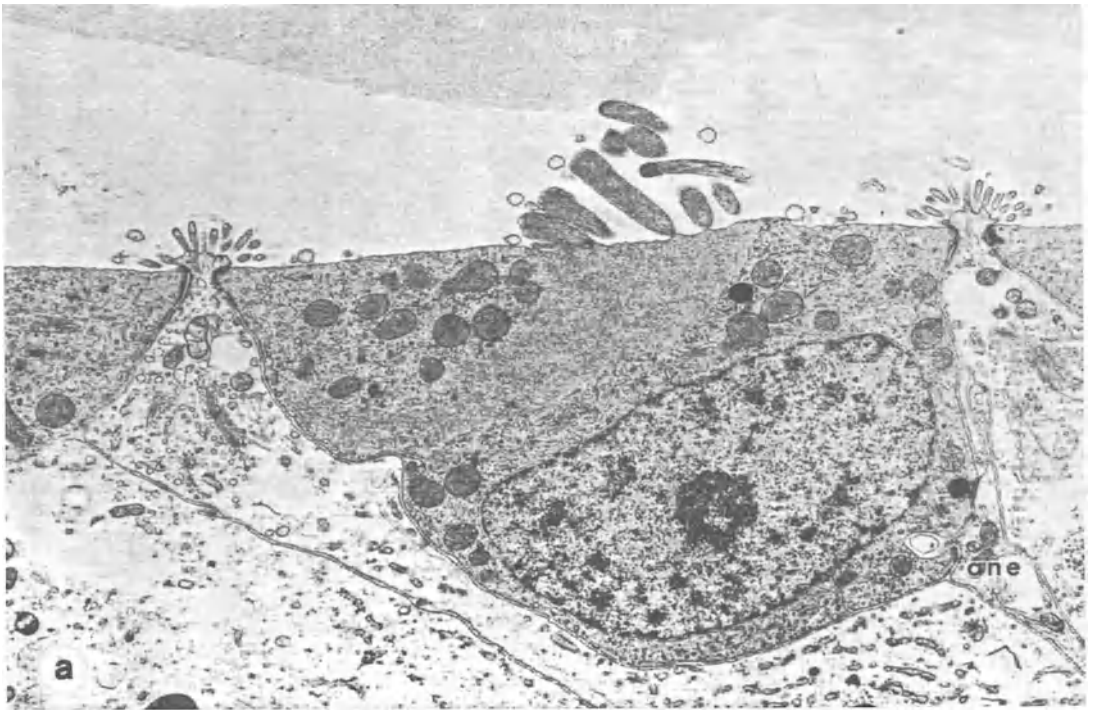

Fig. 13.6 a, b. As in Fig. 13.5, but for short hair cells. Here, the cochlear nerve fibres are few and small, the efferents more numerous and large (*a* from Chandler, 1984; *b*, Takasaka and Smith, 1971)

Despite these differences between the pigeon and starling, their papillae are similar in many other respects. Thus the number of stereovilli per cell falls in both species from near 200 at the basal end to near 50 at the apical end. In general, the neural cells have slightly more stereovilli than the abneural cells. In the chick, the number of stereovilli per cell falls from near 300 to 50 (Tilney and Saunders, 1983). On average, the hair-cell surface occupied by the stereovillar bundle decreases from the base to the apex (starling 11 to 6 μm^2, pigeon 18 to 4 μm^2). Whereas in the starling, the stereovillar bundle occupies roughly 25% of the cell surface over the entire neural and 15 to 20% over the abneural cell area, the abneural cells in the pigeon papilla again show more dramatic changes. Thus, abneural hair cells of the basal end of the pigeon papilla have almost 50% of their surface covered by the stereovillar bundle. This percentage falls to only about 10% for cells near the middle of the papilla and remains constant to the apical end, the cells and their bundles both getting progressively smaller (Fig. 13.10). This change in the relative surface area of cell and bundle occurs in spite of the fact that the number of stereovilli per cell falls quite steadily from base to apex.

With regard to the height and orientation of the stereovilli, the data from the starling, pigeon and the chick are relatively consistent (Gleich and Manley, 1988;

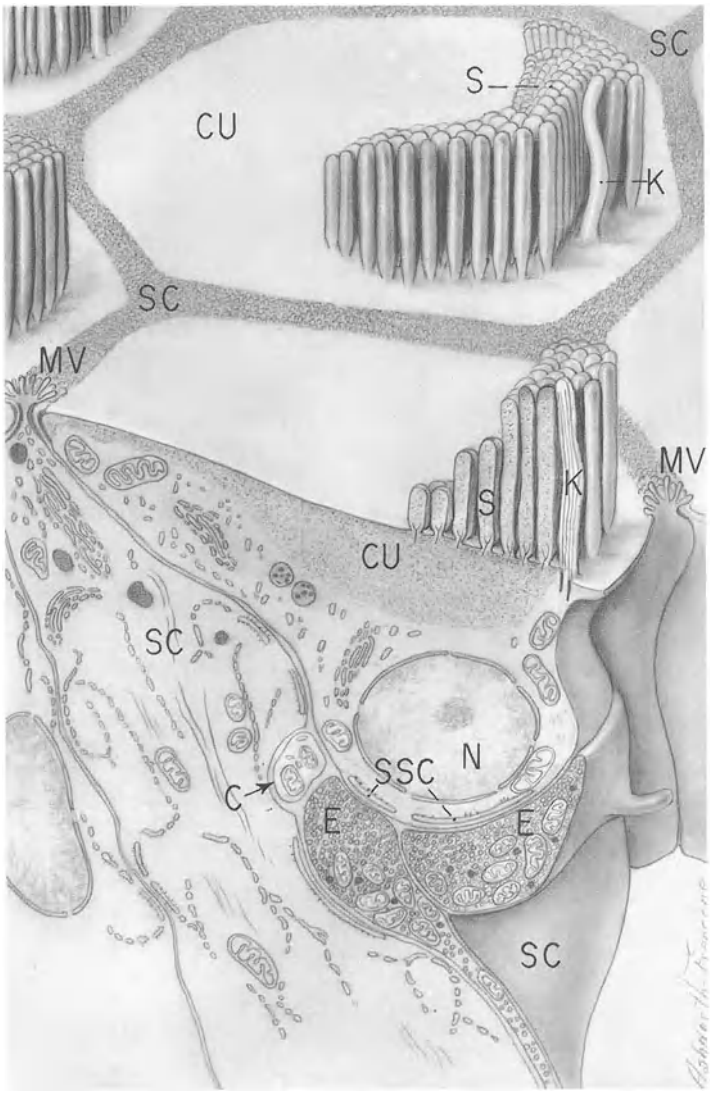

Fig. 13.6b

Tilney and Saunders, 1983; Tilney et al., 1987). The height of the longest stereovilli in the bundles (in the fixed, embedded state) varies in the starling from about 2.7 μm basally to 9.4 μm apically and in the pigeon from 4.0 to 12.7 μm, respectively. This compares to 1.5 to 5.5 μm (Tilney et al., 1987) or up to 8.5 μm (Fuchs, 1988) in the chick. The increase in height is not, however, linear with distance along the starling papilla, but is much faster in the apical third (Fig. 13.11). In the owl, the height of the tallest stereovilli is constant over the basal half of the papilla, and varies only in the apical half. It is difficult to discern if there is any such pattern in the chick papilla (cf. Fig. 4 in Tilney et al., 1987 and Fig. 7 in Tilney and Saunders, 1983). The starling data do not show a consistent difference

Fig. 13.7. SEM of the upper surface of the papilla of the chick, with the tectorial membrane in place (lower edge is abneural). The fixation with potassium (rather than sodium)-based buffers tends to reduce the shrinkage of the tectorial membrane, so that the upper surface is smooth, rather than, as often published, full of holes. The smooth surface was especially obvious where neural and abneural tears in the papilla had reduced the tension on the membrane during fixation. The particles visible on the surface are individual otoliths deliberately disloged from the lagenar macula (Courtesy of G. Runhaar)

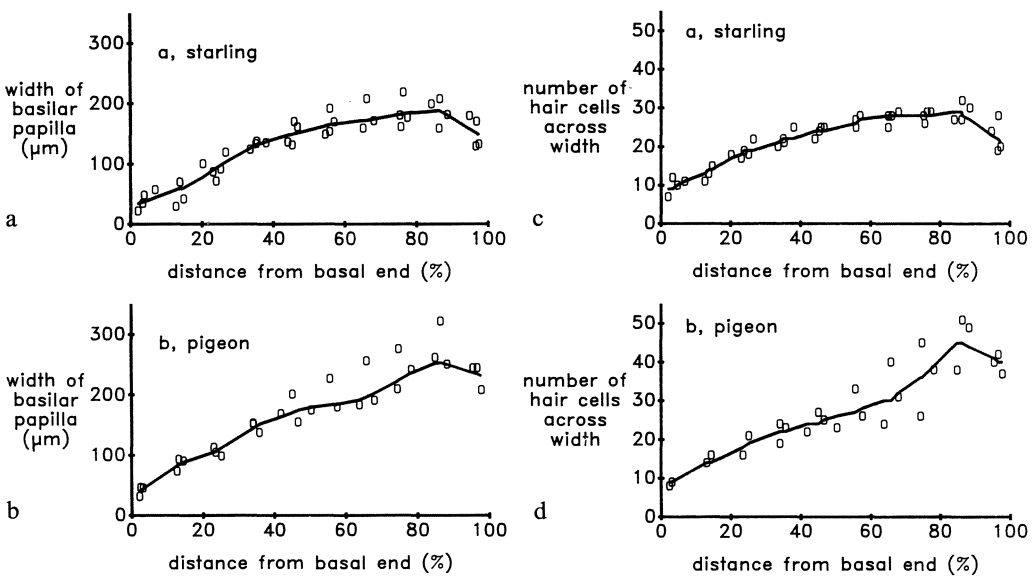

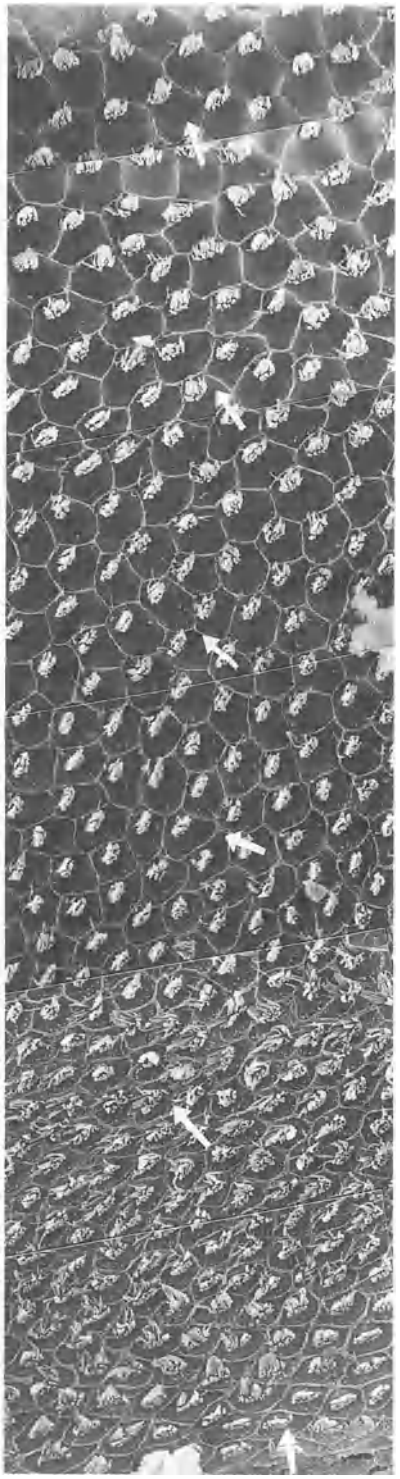

Fig. 13.8. SEM of a strip of hair cells across the basilar papilla of the starling, to illustrate the gradual change of hair cell orientation (*arrows*), so that in the centre of the papilla hair cells have their stereovillar bundles oriented at an angle towards the apex (which is to the *left*). The *top* of the figure is neural, the *bottom* abneural (Courtesy of O. Gleich)

Fig. 13.9. Graphical representation of the width of the basilar papilla and the corresponding number of hair cells across the papilla in *a, c* the starling and *b, d* the pigeon, represented in terms of the relative distance from the basal end in percent. The apical one-third is substantially wider in the pigeon and in this region, the pigeon has a much larger number of hair cells in a given cross- section. Lines are locally- weighted regressions on the data (Gleich and Manley, 1988)

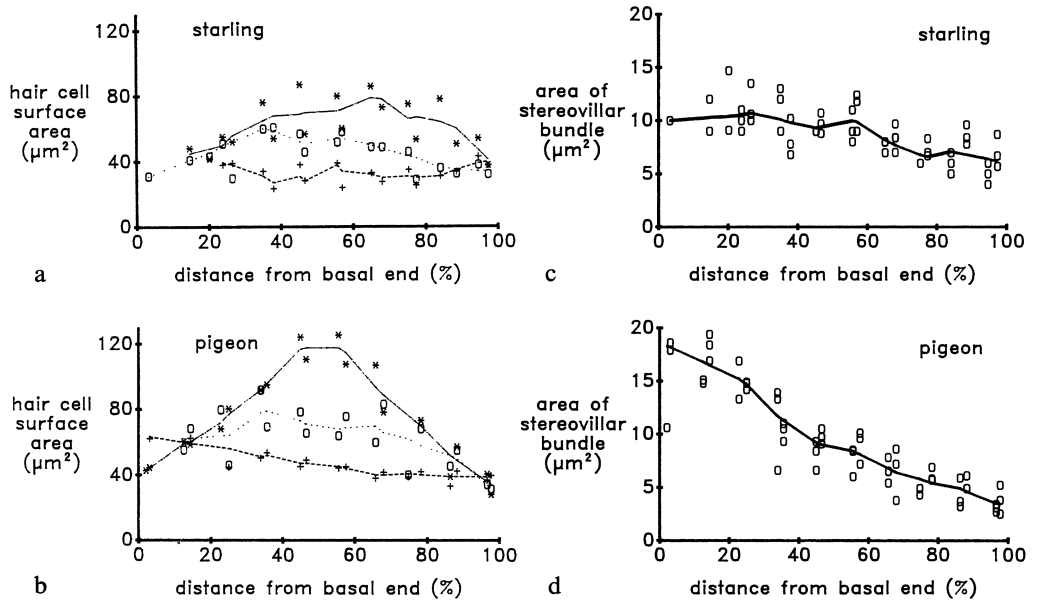

Fig. 13.10. Hair-cell surface area (μm²) of *a* the starling and *b* the pigeon as a function of the distance from the basal end of the papilla. Data are presented separately for neural (*crosses*), central (*open squares*) and abneurally-lying (*asterisks*) cells, in each case with a *line* representing the locally-weighted regression. *c, d* Area of the stereovillar bundle in hair cells of *c* the starling and *d* the pigeon, as a function of the distance from the basal end of the papilla. *Lines* are locally-weighted regressions (Gleich and Manley, 1988)

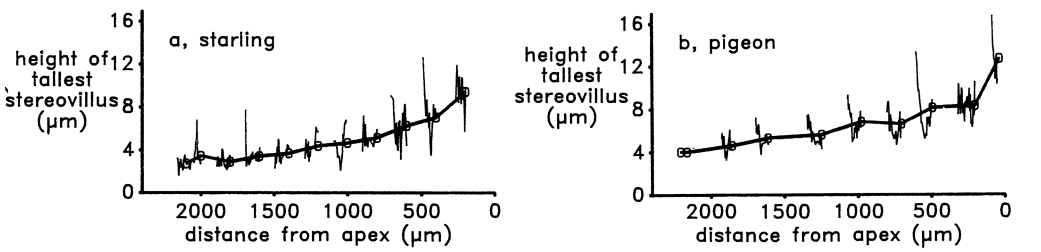

Fig. 13.11. Height of the tallest stereovilli in hair cells of *a* the starling and *b* the pigeon, as a function of the position of the cells relative to the apical end of the papilla, in μm. The abscissa is reversed, so that the basal end is at the *left,* as in the other quantitative figures. The data are presented for 10 (starling) and 9 (pigeon) sub-series from cross-sections of the papilla at the locations shown by *open squares.* In each of these sub-series (*thin lines*), the neural cells are on the *left,* abneural on the *right.* In many cases, it can be seen that the cells near either edge of the papilla have taller stereovillar bundles than the centrally-lying cells. The *thick lines* are locally-weighted regressions on the mean values for each sub-series (Gleich and Manley, 1988)

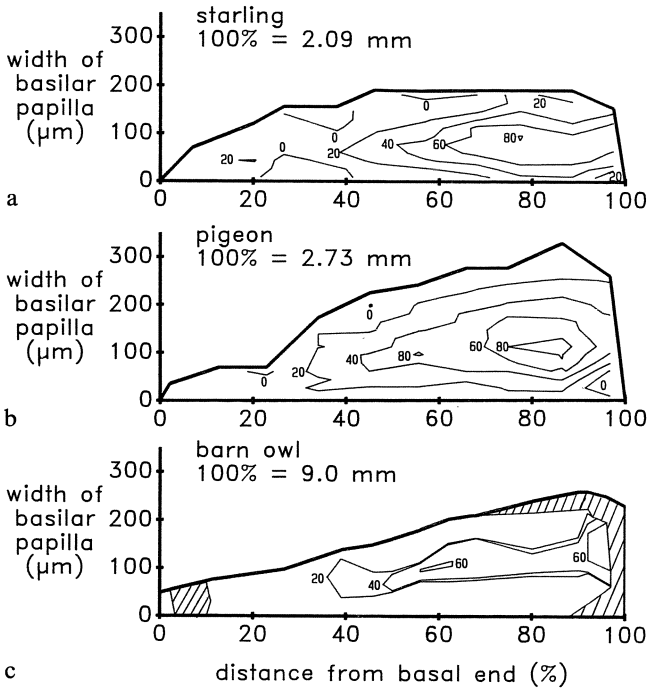

Fig. 13.12. Hair-cell stereovillar bundle orientation in the starling (*a*), pigeon (*b*) and barn owl (*c*). The iso-orientation contours for the hair-cell bundles are plotted within the scaled outlines of the papillae. The papillar lengths given (= 100%) are for fixed, dried specimens. The *numbers* adjacent to the iso-orientation lines give the orientation in degrees of the hair-cell bundles with reference to the abneural papillar edge. *Shaded areas* in the owl were damaged in preparation and not measurable. In the barn owl, there is a sudden shift of orientation (up to 90°) towards the centre of the apical end of the papilla. The same orientation shift is much more gradual in the other two species (After Gleich and Manley, 1988 and Fischer et al., 1988)

between the height of the neural and abneural bundles in each transect, as apparently found in the chick, where the height of bundles on neurally-located hair cells is consistently greater. In the chick, the diameter of the stereovilli varies both across and along the papilla; they are thickest (0.19 μm) on basal short hair cells and thinnest on all cells at the apical end (Tilney and Saunders, 1983).

In all avian papillae, cells lying at the extreme neural and abneural positions on the papilla have their stereovillar bundles all oriented nearly perpendicularly (±20 °) to the edge of the papilla (Fig. 13.8). Cells in the centre of the papilla tend to have their stereovillar bundle turned towards the apex. Although this tendency is hardly noticeable (but generally present) at the base, the orientation angle increases to such an extent that the bundles of centrally-located cells at the apex are rotated up to 90 ° towards the apex. In the starling and the pigeon, the orientation gradually changes in any cross-section towards the middle of the papilla (Fig. 13.12a,b). In the chick, Tilney et al. (1987) report a pattern of orientation which is correlated with the distribution of the different heights of the stereovillar bundles across the papilla. They find that contour lines of constant bundle height

coincide with lines which indicate the direction of morphological polarity for each cell. They thus suggest that the pattern of vibration across the papilla for a given pure tone is not perfectly diagonal, but oblique according to these morphological patterns. This is also consistent with the patterns of noise damage to tall and short hair cell areas in the chick papilla (Tilney et al., 1987). As these morphological patterns differ in the starling and pigeon, it is not yet possible to draw general conclusions in this regard.

13.1.2.2 The Papilla of the Barn Owl

We (Fischer et al., 1988) have recently analyzed the surface morphology of the basilar papilla of the barn owl *Tyto alba*. This papilla is over 11 mm in length in the unfixed state and contains over 16000 hair cells; it is thus one of the best developed of all bird papillae. In the fixed, dried state, the papilla is about 9 mm long, being roughly 250 μm wide at the apical end and gradually reducing to 50 μm at the basal end. The change in hair-cell orientation in the owl papilla is very abrupt. Thus, in a cross-section in the apical two-thirds, the neurally-placed and abneurally-placed hair cells are oriented at right angles to the edge of the papilla. In the centre of the papilla, however, is a region where the orientation suddenly changes to at least 50 ° and up to 90 ° (apical orientation), and, further over the papilla, just as suddenly back again to 0 ° (Figs. 13.12c, 13.13a). This sudden change is in contrast to the gradual change described for the starling and pigeon papilla. On the neural side of middle and apical areas of the barn owl papilla, the sudden change in orientation occurs at the place where Smith et al. (1985) indicate a border between the tall, intermediate and short hair cells. The orientations in the apical tenth of the papilla are irregularly arranged with a mean angle between 0 and 20 ° (±15 °).

The number of stereovilli per bundle rises in the barn owl from as low as 80 at the basal end up to between 150 and 200 at 2 to 3 mm from the base of the papilla, decreasing gradually again to near 50 towards the apex. The number of stereovilli per bundle in any one cross-section is, however, not constant, especially in the middle of the papilla. Here, the sudden change in hair-cell orientation is often accompanied by a sharp rise in the number of stereovilli at exactly the same place, so that a change in orientation angle from 0 ° to 50 ° may e.g., be correlated with a rise in the number of stereovilli from 120 to 180 per hair cell. Similarly, a return to 0 ° orientation is accompanied by a fall in the number of stereovilli (Fig. 13.13b). This pattern is, however, not completely constant from animal to animal.

The height of the tallest stereovilli in any one bundle changes from near 5 μm apically to 1 μm basally, with no particular tendency for differences to appear between tall and short hair cells at any one location. Most of the height reduction occurs, however, in the apical half of the papilla, so that by 4.5 mm towards the base, it has already dropped to about 1.5 μm (Fig. 13.14). The relative stability in bundle height over the basal half is accompanied by only a small change in diameter of the individual stereovilli, which means that the bundle shape and size remains roughly constant (about 10 to 12 μm long and 2 μm wide). At the apex of

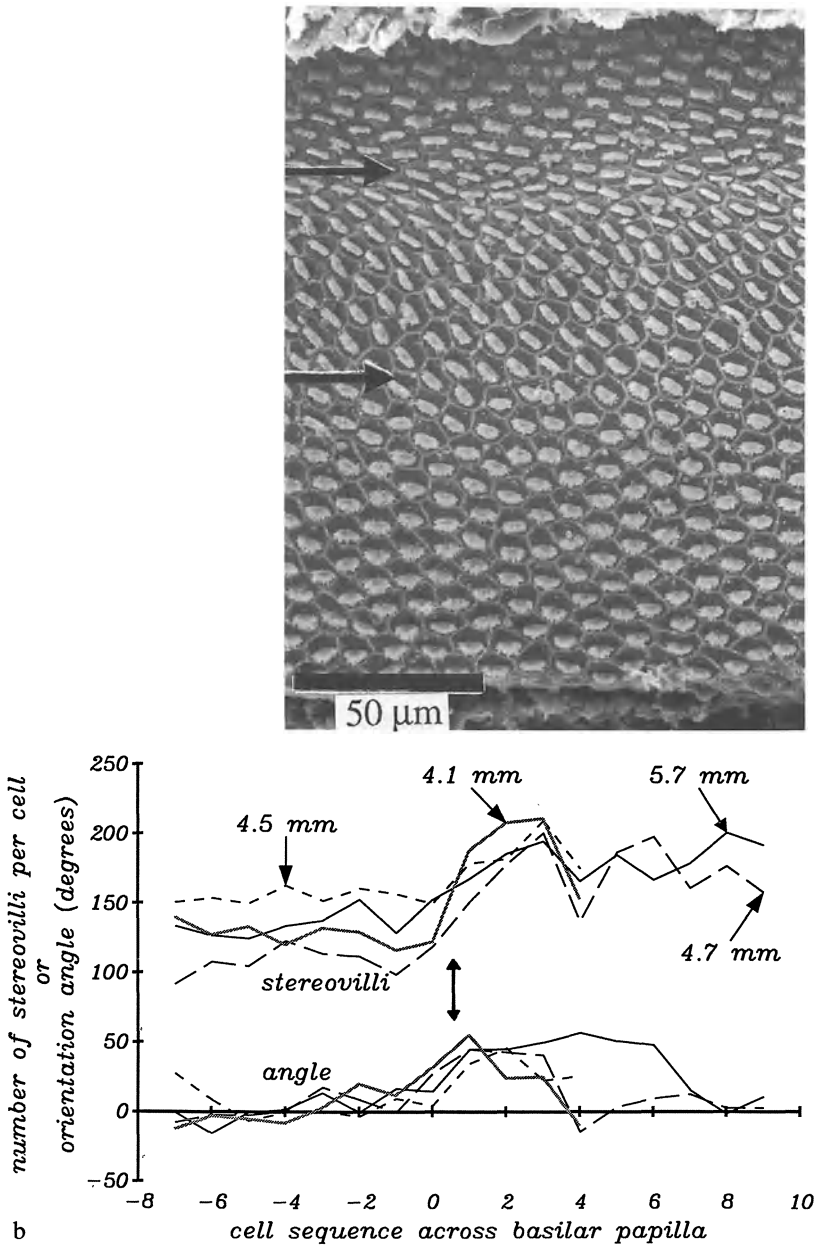

Fig. 13.13 a, b. Orientation angles of hair cells at different locations across the barn owl papilla. *a* SEM of part of the apical end of the papilla of a barn owl to illustrate the rapid change of orientation of the hair-cell bundles (*between arrows*). *b* Correlation between orientation angle and number of stereovilli per hair cell. The rapid change of bundle orientation (*lower curves*) is accompanied (*double arrow*) by a rise of up to 100% in the number of stereovilli in each bundle (*upper curves*). Measurements were made at four locations (4.1 to 5.7 mm from the basal end) across one papilla from neural to abneural edges and the series then normalized for different positions on the papilla, in that the last cell before the orientation shift was designated cell zero. The number of stereovilli remains higher even where the orientation angle has returned to zero degrees (Fischer et al., 1988)

the papilla, the bundles are almost rounded. The individual villi of a bundle have a mean diameter of 0.3 μm at the base, rising to near 0.6 μm at the apex. The changes in these various parameters lead to the typical surface appearance of cells of the whole basal half of the papilla, where the stereovillar bundle occupies only about 25% of the total cell surface area. Towards the apical end, the actual cell surface area becomes smaller, so that the bundle, whose area remains roughly the same, occupies almost half the surface area of apical hair cells (Fischer et al., 1988).

From the above data it can be concluded that whereas the apical half of the barn owl papilla shows structural patterns which resemble those of the entire papillae of other birds, the basal half is different. This is presumably a specialization for processing of the high frequencies (5 to 9 kHz) used by the barn owl for sound localization. Smith et al., (1985) found that this basal end has a marked thickening of the basilar membrane, a feature which has been found in specialized areas of some mammalian (e.g., bat) cochleae.

13.1.2.3 Functional Implications of Variations in Papillar Anatomy

Our understanding of the function of the avian basilar papilla is still relatively poor. It is thus difficult to realize the full implications of the anatomical findings discussed above. There are, however, some features which will be of particular interest to future research into the relationship between structure and function.

It should be noted at first that each of the bird papillae investigated to date is unique and could be recognized as such by an expert. We thus expect that there will be species specificities in the response patterns. Some of the known differences in function are outlined in the sections below, such as the presence of infrasound responses in the unusually wide apical area of the pigeon. In the basal area of the barn owl papilla, where the high-frequency responses presumably originate, there is obviously a specialization of the hair-cell structure and orientation pattern.

In the chick, the pattern of hair-cell orientation led Tilney et al. (1987) to suggest that there is an unexpected pattern of hair-cell stimulation, unexpected that is, when we consider the purely radial shear pattern thought to be present in the mammalian cochlea. Since we found similar morphological patterns in the starling, pigeon and the barn owl, they can probably be considered as typical of birds. In the barn owl, the abruptness of the change in orientation is striking and it appears to correlate in position both with a change in the number of stereovilli on the hair cells and, at least in the neural half of the papilla, with the edge of the neural limbus. That is, hair cells on the two sides of the outer edge of the superior cartilaginous plate have quite different stereovillar-bundle orientations.

In the chick, overstimulation of the papilla leads to a damage pattern which suggests that a simple radial shear pattern is not present (Tilney et al., 1987). We should consider the possibility that hair-cell populations in a given area of the papilla may have different functions or even response frequencies. Some of the fibres of the pigeon which responded to infrasound, which were stained by Klinke and Schermuly (1986) innervate an abneural area of the pigeon papilla

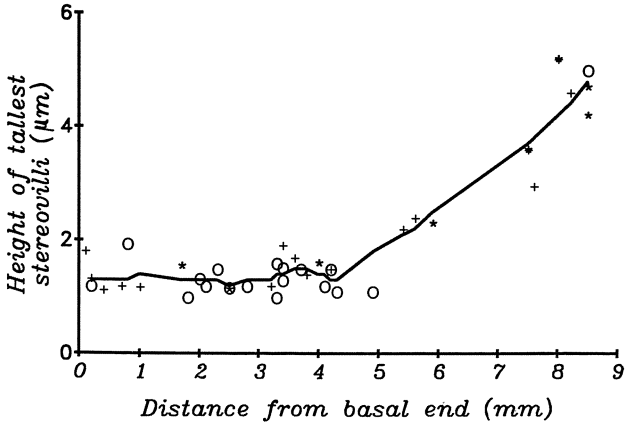

Fig. 13.14. Height of the tallest stereovilli of hair cells in several different papillae of the barn owl (each ear has a different *symbol*), as a function of the distance of the cells from the basal end of the papilla. The stereovillar height is constant over the entire basal half. The *line* is a locally-weighted regression (Fischer et al., 1988)

which almost certainly lies adjacent to an area of neural cells responding to a few hundred Hz. Our finding (Manley et al., 1988 a,b) both in the starling and the young chick that active primary fibres of the auditory nerve only contact tall hair cells would also indicate that there is a division of labour among the different hair-cell populations of the avian papilla (Manley et al., 1989 a).

In order to gain an impression of the frequency-response parameters of the different cells, it is not enough to know, e.g., the height of the stereovillar bundles. This parameter has played an important role in, e.g., the modelling of the frequency responses of the hair cells of some lizards (Sects. 7.4; 11.3). In the basal half of the owl papilla, however, this parameter is constant. At low frequencies, even a knowledge of all bundle parameters will not suffice if electrical tuning plays a dominant role (Sect. 14.9).

13.1.3 Innervation of Avian Hair Cells

Although detailed studies are still lacking, it is possible to make some general statements about the afferent and efferent innervational patterns in the avian auditory papilla. Whereas tall hair cells have large afferent and small efferent synapses (Fig 13.5), the innervation of the short hair cells is just the reverse (Figs. 13.6, 13.15). Short hair cells have small bouton-like afferent terminals occupying the small area of membrane not taken up by the several large efferent synapses. During early development, there is a reduction of the branching of afferent fibres, so that in the adult bird, fibres innervate either tall or short hair cells, but not both (Fig. 13.16). In addition, there is little branching among tall-hair-cell afferents (Rebillard and Pujol, 1983; Whitehead and Morest, 1985 a). The number of afferent fibres is to some extent related to the number of tall hair cells at any given location of the papilla (Fig. 13.17 a,c)

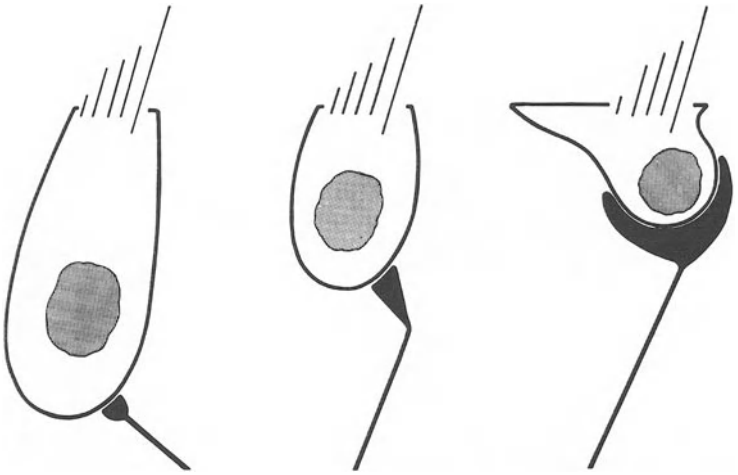

Fig. 13.15. Highly schematic representation of the size and shape of the efferent endings in, from *left to right,* tall, intermediate and short hair cells of the budgerigar basilar papilla (Firbas and Müller, 1983)

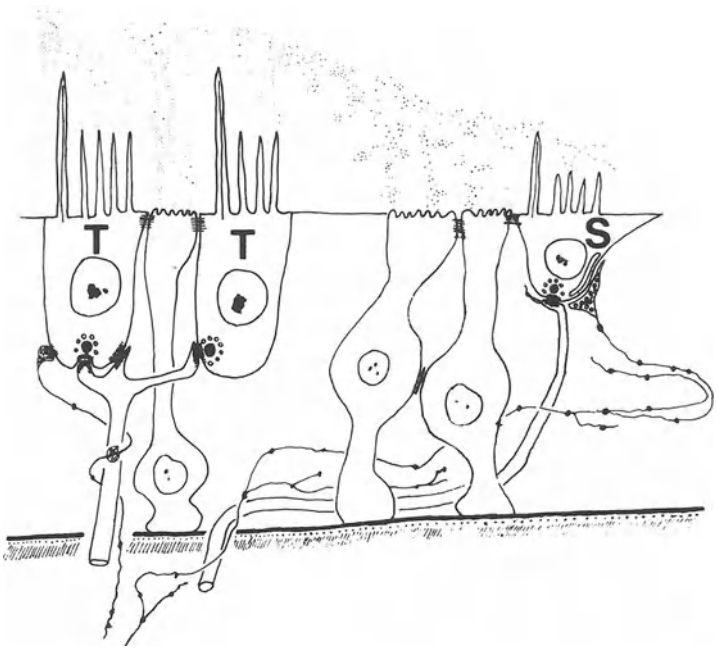

Fig. 13.16. Schematic drawing of some cells in the bird papilla during late synaptogenesis, to illustrate the distribution of afferent and efferent fibres to the tall (*T*) and short (*S*) hair cells. Afferent fibres are drawn as *thick branches,* efferent fibres as *thin lines with dots* along them. Other cells are supporting cells (Whitehead and Morest, 1985 b)

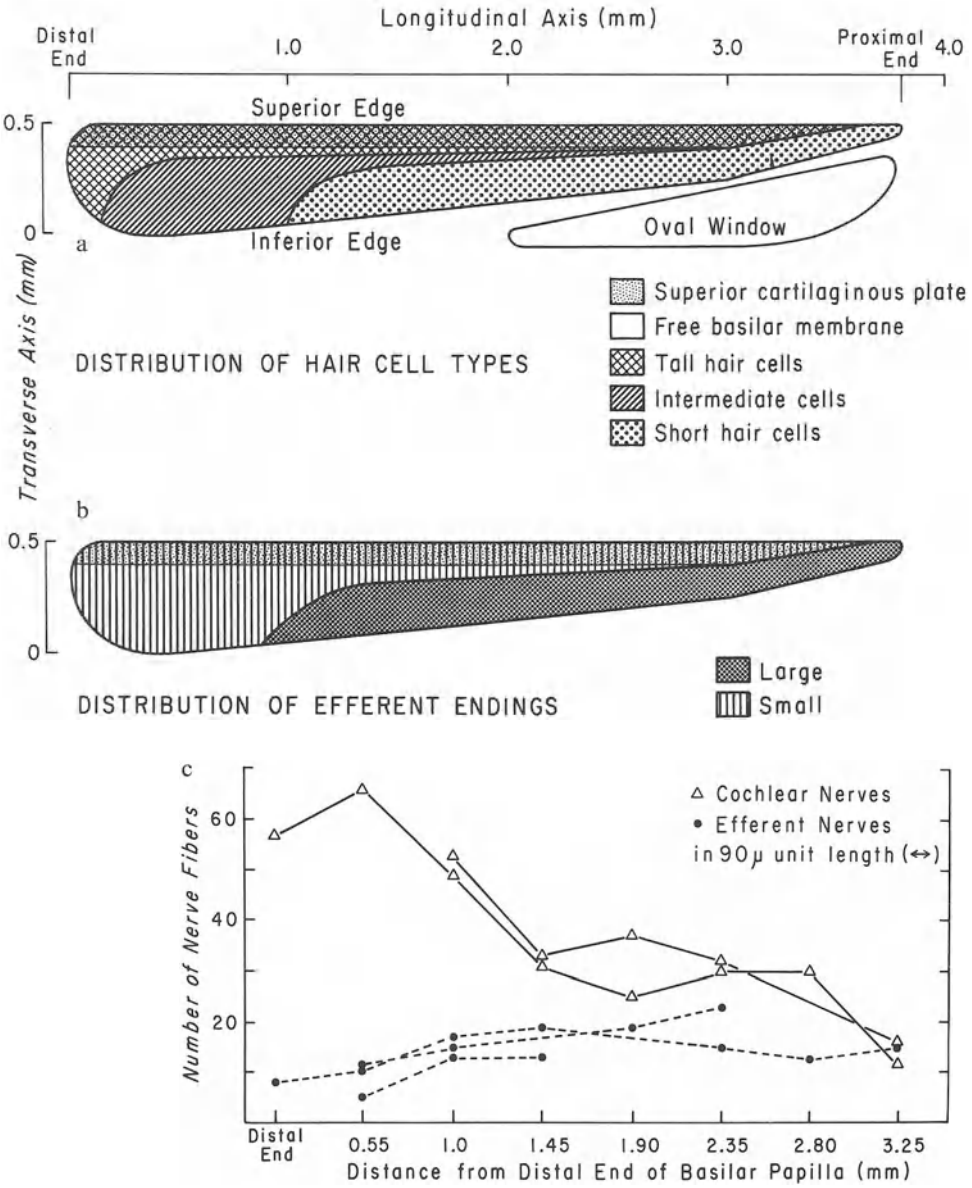

Fig. 13.17 a. Schematic representation of the distribution of hair-cell types on the basilar papilla of the pigeon showing that, except for the apical end, tall hair cells are only found on the neural (= superior) side over the superior cartilaginous ridge; distal = apical, proximal = basal. *b* Schematic drawing of the pigeon's basilar papilla to show that the distribution of large efferent endings corresponds to the location of the short hair cells. *c* Number of afferent (cochlear) nerve fibres (*solid line, open triangles*) and efferent fibres (*dashed line, dots*) as a function of the distance from the apical end of the papilla of the pigeon. In comparison with *b*, it can be seen that the number of nerve fibres corresponds to the number of tall hair cells in a cross-section (Takasaka and Smith, 1971)

Efferents are apparently more dense at the basal end of the pigeon's papilla (Fig. 13.17b; Takasaka and Smith, 1971). Firbas and Müller (1983) report similar patterns of efferent innervation for the budgerigar, where single efferent fibres branch to innervate several hair cells. Apparently, efferent terminals to the short hair cells reach maturity later than those to the tall hair cells (Rebillard and Pujol, 1983) and the efferent innervation of the bird's basilar papilla is primarily direct to the short hair cells. Axoaxonal terminals have been reported to be very rare (Rebillard and Pujol, 1983). Efferents are also found among hyaline cells, apparently without terminals (Takasaka and Smith, 1971). Our own observa-

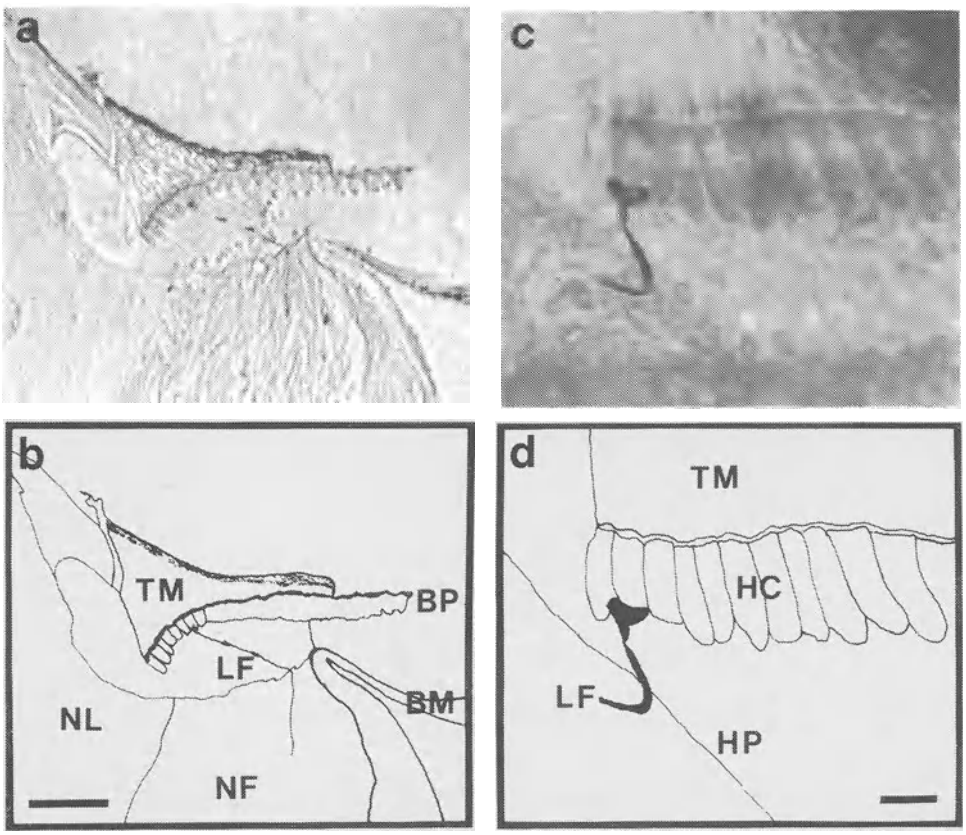

Fig. 13.18 a–d. Localization of terminations of stained single auditory-nerve fibres in the avian papilla. *a* Primary nerve fibre in a cross-section of the papilla of a starling, stained with cobalt. The fibre made a bouton-shaped synapse on one tall hair cell. *b* A drawing of the same section as in *a*. *c* Nerve fibre in a cross-section of the papilla of a young chick, stained with horseradish peroxidase and shown at higher magnification to that in *a*. *d* A drawing of the section shown in *c*. The fibre makes a large synapse on a single tall hair cell on the neural edge of the papilla. *TM* tectorial membrane; *NL* neural limbus; *NF* nerve fibres; *BM* basilar membrane; *BP* basilar papilla (broken); *LF* labelled fibre; *HP* habenula perforata; *HC* hair cells. The scale *bar* in *b* is 50 μm; in *d* it is 10 μm. Both fibres of *a* and *c* were physiologically characterized before staining (Manley et al., 1988b)

tions in the chick indicate that at least some of the fibres (afferents or efferents) to the short hair cells cross the papilla completely before turning back to innervate the short hair cells.

In the pigeon also, afferent fibres of the apical end tend to run directly across the papilla before innervating hair cells. There is a gradual change towards the basal end, such that there, the fibres to the short hair cells run obliquely basally across the papilla (Takasaka and Smith, 1971). According to von Düring et al. (1985), a single tall hair cell in the birds they studied receives between 1 and 4 afferent nerve fibres, the neural portion of the papilla showing the highest innervational density. Tall hair cells near the zone of transition to short hair cells receive only one afferent fibre. A single nerve fibre contacts only one or two neighbouring tall hair cells. In contrast, a single afferent fibre contacts up to 6 short hair cells (on average three). On the basis of innervational densities, von Düring et al. calculated that only 18% of afferent fibres in the starling innervate short hair cells.

One interesting aspect of the innervational pattern of avian hair cells emerged from studies of the tonotopic organization of the basilar papilla of the chick and the starling (Manley et al., 1987 a, 1988 a,b). In those studies, single auditory-nerve fibres which had been characterized according to their frequency responses were marked by the iontophoretic injection of horseradish peroxidase or a cobalt salt, both of which are transported to the terminals of the nerve fibre and can be developed to show a dark-staining reaction product (Köppl and Gleich, 1988). Although in some cases more than one fibre was stained, all cases of single-fibre staining were of fibres which each innervated only one single tall hair cell (Fig. 13.18). Thus, all unambiguously-traced active afferent fibres had synaptic contact with only one single tall hair cell; this indicates among other things that fibres innervating more than one tall hair cell must be rare. These recent data give strong physiological support to the increasing body of evidence that, in spite of the justified reluctance of some authors (including myself) to assume it, some functional equivalence really exists between the tall and short hair cells of birds (and Crocodilians?) and the inner and outer hair cells of mammals, respectively. The evidence to date for this equivalence (Manley et al., 1989 a) is:

1: The relative position of the cell groups with respect to each other is the same.
2: In each case, the cells of the neural side are phylogenetically the more primitive ones.
3: The tall and inner hair cells receive a stronger afferent innervation than the short and outer hair cells. The short and outer hair cells receive a stronger efferent innervation, which also develops later than afferent fibres to these hair cell groups.
4: Outer and short hair cells are more easily damaged by loud sounds.
5: Unambiguously-labelled active afferent fibres connect only to single inner hair cells of the cat (Libernam, 1982 a) or to single tall hair cells in the chick (Manley et al., 1987 a, 1988 b) and starling (Manley et al., 1988 c). In the guinea pig, at least some fibres which innervate outer hair cells are 'silent' (Robertson, 1984).

13.2 Macromechanics of the Avian Cochlea

Von Békésy (1960) described a travelling wave measured on the basilar membrane of the (postmortem) chick papilla. Using a stroboscopic technique, he found a similar kind of mechanical frequency analysis on the bird papilla to that already seen in mammals. However, we now know that his measurements for the mammal cochlea are not very representative for the living state, where the frequency selectivity is very much higher (see Manley, 1983 for refs). Von Békésy's data may, however, be taken as evidence that there is also a mechanical tonotopic organization in the bird cochlea. In addition, noise-damage studies (e.g. Cotanche et al., 1987) have indicated that the location of damage caused is related to the frequency of the damaging sound.

Recently, Gummer et al. (1986) reported measurements of basilar-membrane motion in the pigeon, using the Mössbauer technique (see Sect. 5.4) to investigate travelling-wave motion and frequency selectivity of the avian basilar membrane. Access was surgically restricted to the first 1.4 mm from the basal end (the papilla is about 4 mm long). The basilar-membrane response was shown to be tuned and tonotopically organized, the best frequency shifting down with increasing distance of the Mössbauer source from the basal end. For a given frequency, the phase lag of the mechanical response increased with distance from the base, indicating the presence of a travelling wave. The degree of change of phase with distance was larger in animals with a more sensitive response, i.e., a number of other papillae were obviously not in good condition. In papillae in good condition, there was a good correlation between the logarithm of the CF and distance of the source from the basal end.

The tuning of the mechanical response of the basilar membrane was much less sharp than the tuning observed in single primary fibres with the same CF. The frequencies over the range investigated are so arranged that each octave occupies a specific amount of space, in this case 0.63 mm/octave. This value matches well with that given for the high-frequency area of the chick and starling papilla (0.6 mm; Manley et al., 1987 a, 1988 a). As the displacements of the membrane are more equivalent to those of damaged or off-center frequency responses in mammals, however, Gummer et al. (1986) do not rule out the possibility that the difficult exposure of the papilla prohibited the measurement of basilar-membrane motion under optimal conditions.

13.3 Otoacoustic Emissions from the Starling Cochlea

Work in my laboratory (Manley et al., 1987 b) on the awake starling has demonstrated the presence of otoacoustic emissions (OAEs) from the avian ear, which in their properties are very similar to those reported for the caiman ear (see Ch. 12). No delayed evoked emissions could be detected (the latencies were

probably too short). Emissions were evoked by swept tones (SEOAEs), and appeared as interference peaks and dips in the sound pressure in the external ear canal. SEOAEs were found predominantly in the upper half of the hearing range of the starling (2 to 5.5 kHz), and showed typical nonlinear intensity functions to rising stimulus level. Their sound-pressure levels were calculated from the interference patterns with the stimulus tones and ranged from near 0 dB down to about −40 dB SPL. They were also suppressed by anaesthesia and by second tones (Manley et al., 1987 b).

We had actually wanted to investigate the effect of hypoxia on the SEOAEs, to compare to known effects in mammals (Zwicker and Manley, 1981). However, the anaesthetics used to suppress breathing enough to induce hypoxia were themselves sufficient to reduce the size of the SEOAEs. Using the fast-acting inhalation anaesthetic halothane, we were able to examine the time course of the suppression due to the anaesthetic. Both the rapid suppression and the two time courses of the period of recovery from the anaesthetic (50% recovery within 200 s, full recovery taking more than 500–600 s) were remarkably similar to the time courses seen in *hypoxic* effects on emissions from the guinea-pig cochlea (Zwicker and Manley, 1981).

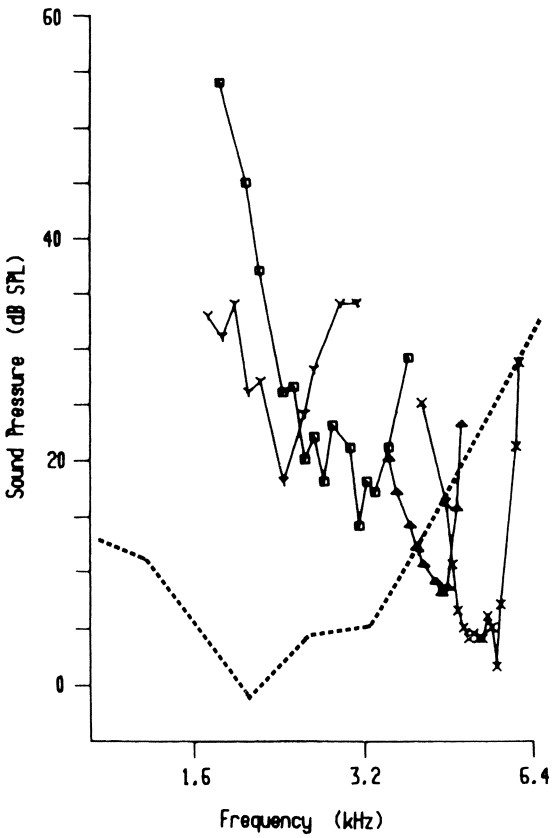

Fig. 13.19. Iso-suppression curves for four oto-acoustic emissions from three different starlings, with swept-tone emission frequencies near 2.2, 2.7, 4.1 and 5,45 kHz, respectively. Each of the four sharply-tuned curves represents the SPL of the second tone (suppressor) necessary at the various frequencies to produce 6 dB of suppression of the level of the respective emission. Not all the curves were measured at the same level on the emission intensity function, so they are not completely comparable in terms of their absolute level. The levels of the swept stimulus tones lay between −3 and 5 dB SPL. The *dashed curve* represents the behavioural audiogram of the starling from Kuhn et al. (1982) (Manley et al., 1987 b)

Fixed tones near the emission frequency most strongly suppressed the emissions to the swept tone. Curves representing the second-tone SPL necessary to suppress the emission by a fixed amount resemble single-fibre tuning curves both in their shape and in their sharpness of tuning (Fig. 13.19; $Q_{10\ dB}$ values between 2.6 and 4.9). Although these emissions from the starling ear had quite broad synchronization widths (about 200 Hz, thus resembling emissions in *Caiman*) and were thus much broader than similar emissions in mammals, they strongly resemble mammalian emissions in other respects (Manley et al., 1987b). Should it be true, as has been often suggested, that emissions in mammals are due to active motions of outer hair cells involved in the tuning mechanisms, then similar considerations should apply to the avian auditory papilla.

13.4 Activity of Auditory-nerve Fibres

As there are very little data on the electrical activity of avian basilar-papilla hair cells (but see Sect. 2.4.2), it will be necessary to use the activity of primary auditory-nerve fibres as indicators of the sensory analysis being carried out in the papilla. Such data are available for the pigeon (Gross and Anderson, 1976; Sachs et al., 1974; Temchin, 1982, 1988) for the starling (Manley, 1979; Manley and Gleich, 1984; Manley and Leppelsack, 1977; Manley et al., 1985) for the redwing blackbird (Sachs et al. 1980) and for the chicken (Manley et al., 1987 a). In the redwing blackbird and pigeon, eighth-nerve fibres were recorded as they entered the brain cavity. In the starling and chick, the recessus of the scala tympani was opened and fibres recorded directly in the cochlear ganglion. In the latter case, the higher-frequency fibres are less easily accessible and more subject to the influence of surgical damage to the cochlea.

13.4.1 Spontaneous Activity

Boord and Rasmussen (1963) demonstrated in the pigeon that cochlear and lagenar nerves run together out of the cochlear duct. Thus, it is not surprising that in the starling and the chick cochlear ganglion, cells are encountered which are unresponsive to sound. Some of these cells have a spontaneous activity with a regular pattern, whereas others have an irregular pattern (Fig. 13.20). It is not possible at this time to definitively distinguish between those non-auditory cells which have an irregular spontaneous activity and those auditory cells which were not adequately stimulated by our test stimuli or which were too insensitive to respond to sound for some other reason (Oeckinghaus, 1985). Both auditory and non-auditory cells with irregular spontaneous activity respond to a middle-ear muscle contraction with a change in their discharge rate, whereas regularly-discharging, non-auditory units were not affected (Oeckinghaus, 1985). Thus, the irregularly-firing, non-auditory units could originate in either the lagena macula or in the apical part of the basilar papilla. Klinke and Schermuly (1986, see

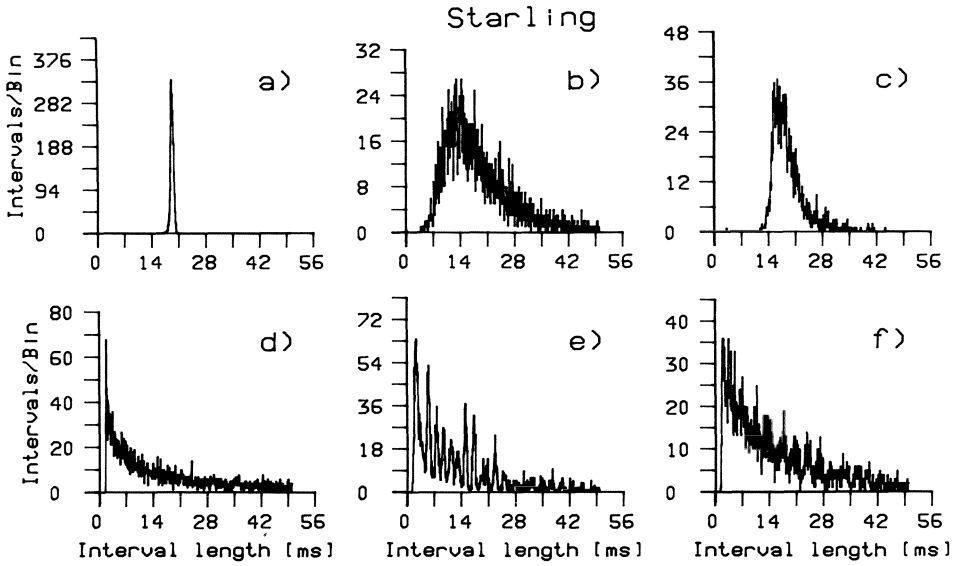

Fig. 13.20 a–f. Typical time-interval histograms (TIH) of spontaneous activity in different primary neurones of the starling cochlear ganglion. *a–c* Non-auditory; *d–f* auditory cells. Non-auditory cells can be either regularly (*a*) or irregularly-firing (*b*) or intermediate (*c*). Some auditory units show prominent (*e*), others less prominent preferred intervals (*f*), yet others exhibit no preferred intervals (*d*). Bin width in all histograms, 0.1 ms. Number of intervals, discharge rate in spikes/s and (only *d–f*) CF in kHz are as follows: *a* 3100, 51.8; *b* 2940, 52.4; *c* 2100, 52.5; *d* 3635, 42.7, 1.8; *e* 3851, 68.1, 0.4; *f* 3763, 55.2, 0.25 (Manley et al., 1985)

below) report finding infrasound-sensitive units in the pigeon eighth nerve which innervated hair cells over the free basilar membrane of the apical 1 mm of the basilar papilla. Unfortunately, they do not say whether they were regularly or irregularly spontaneously active.

All auditory units show an irregular spontaneous activity (Fig 13.20). In general, it has been thought that the level of this activity lies above that typically recorded for mammalian auditory fibres (Manley et al. 1985). There is, however, a discordance in the avian data, for whereas in the starling the mean rate of all fibres was 48 spikes/sec, Sachs et al. (1980) report a rate of 90 spikes/sec for both the pigeon and the redwing blackbird. Temchin (1988) gives an average rate of the spontaneous activity in 26 pigeon units he studied as 78 spikes/sec. It would be unexpected if the rate difference between chick and starling, on the one hand, and pigeon and redwing blackbird, on the other hand, were so large. Sachs et al. (1974) found that the same anaesthetic technique as they used for the pigeon gave 'normal' results for the cat, making it unlikely that the difference in the bird rate data is due to anaesthetic effects. However, some recent studies indicate that these differences between birds may indeed be partly an artefact of different anaesthetic regimes. In a study of the activity of primary afferents of the vestibular system in anaesthetized and unanaesthetized pigeons, Anastasio et al. (1985) found the rates of spontaneous activity to be about 80% higher in the un-

anaesthetized state. Different anaesthetics may produce different degrees of depression of the activity.

The distribution of spontaneous rates in birds is consistently unimodal, whereas it is bimodal in mammals (Sachs et al. 1980; Manley et al. 1985). Oddly enough (in view of the very similar cochlear anatomy), the rates in *Caiman* are also bimodally distributed (Sect. 12.4). The population of mammal and *Caiman* units which have spontaneous rates near zero does not exist in birds. Geisler (1981) offered an explanation for a bimodal distribution of rates, in which some fibres require the simultaneous arrival of two of more transmitter packets at the hair-cell synapse in order to discharge. These form the low-rate population, as such events would not be frequent. In birds, it is conceivable that all fibre thresholds for the transmitter are low, requiring only one transmitter packet to induce discharge. Nonetheless, the typical time-interval histogram (TIH) of the spontaneous activity is very similar to that of mammals, showing a Poisson distribution partly modified by the refractory period of the fibre (Fig. 13.20). The modes in the starling data were typically as short as 1 to 2 ms, the dead times as short as 0.5 ms. The slope of the decay of the frequency of intervals of different duration in the TIH is closely correlated with the absolute spontaneous rate (Fig. 13.21; Manley et al. 1985).

The typical quasi-Poisson distribution of intervals in spontaneous data is, in some cases, strongly modified by the presence of preferred intervals. In such cells, the activity is highly non-random, such that certain intervals occur more often and others less often than expected (Figs. 13.20e,f and 13.22a; Manley, 1979; Manley and Gleich, 1984; Manley et al., 1985; Temchin, 1982, 1988). A number of interesting properties of these preferred intervals have been demonstrated:

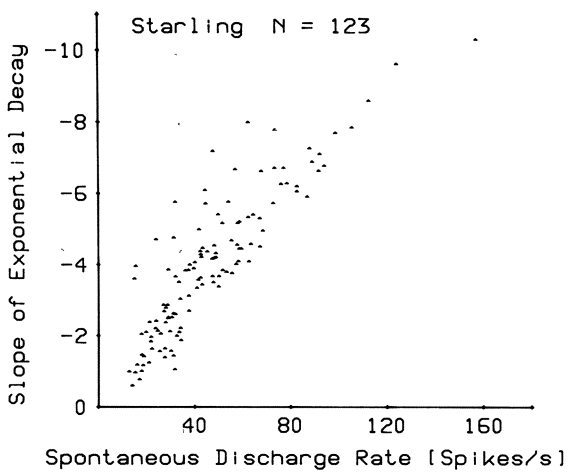

Fig. 13.21. The slope of the exponential decay of interval frequency (from regression lines calculated on the TIH) in the spontaneous activity of 123 auditory neurones of the starling as a function of their spontaneous discharge rate. The slope is in arbitrary units (Manley et al., 1985)

1. They are only found in cells of relatively low CF, mainly below about 1.7 kHz, but only about half of starling fibres in this CF range show the phenomenon. The prominence of the peaks in the interval histogram varies. The limit in frequency could be related to the fact that the nerve fibres and, presumably, the hair cells of the avian hearing organ rapidly lose their ability to phase-lock above about 1 kHz (Gleich and Narins, 1988).
2. These intervals are not the result of inadvertent stimulation of the cells or of background noise (Manley et al., 1985; Temchin, 1988).
3. Within each histogram, the positions of the peaks are highly consistent, variations of inter-peak intervals are almost all smaller than 5% (Manley et al. 1985). The inter-peak intervals are inversely related to the CF of the cell, being on average either at the CF-period (pigeon, Temchin, 1988) or 15% longer (Fig. 13.22e; starling, Manley et al., 1985). The fact that the basic interval (mean of all inter-peak intervals) does not always correspond to the CF-period has also been interpreted as an additional indication that the activity is not the result of inadvertent noise stimulation (Manley et al., 1985).
4. The mode of the histogram (the most frequent interval) is not always at the position of the first peak of the TIH, but may be at a later peak. Even in those low-CF cells of the starling which do not show preferred intervals, the mode itself is highly correlated with the CF (Fig. 13.22d). Here, the interval of the mode is on average slightly longer than the CF-period (see point 3 above); the mode is thus a special case of a preferred interval.

These details presumably indicate that the spontaneous activity of many avian auditory fibres is influenced by a rhythmic behaviour characteristic of individual hair cells. Curiously, this kind of spontaneous activity was not reported by Sachs et al. (1980) in the redwing blackbird or the pigeon, although Temchin (1988) found it to be very prominent in the pigeon. Such behaviour has also been reported for auditory-nerve fibres of some reptiles (see Sects. 2.4.2, 6.1.5 and 10.2.1). The phenomenon has been interpreted as evidence for electrical tuning of many avian and reptilian hair cells, such as that described in previous chapters for frog saccular and turtle auditory hair cells (Manley, 1979; Manley and Gleich, 1984; Manley et al., 1985; Temchin, 1982, 1988). In the phase response characteristics of primary auditory fibres of the starling, Gleich (1987 a,b) found evidence of an electrical tuning whose best frequency was, on average, 20% lower than the acoustic CF of the cell (see Sects. 13.4.5.2). This corresponds extremely well to the discrepancy noted above between preferred intervals and the period of the CF in the starling.

Isolated tall hair cells from the apex of the chick cochlea show slow electrical resonances resembling those of turtle basilar papilla and frog sacculus (Fuchs, 1988; Fuchs and Mann, 1986). Superimposed on the oscillations of very apical tall hair cells were action potentials, as already described for alligator hair cells (Sect. 12.5; Fuchs, 1988). The frequencies of these oscillations depended on the original location of the hair cell and were estimated by Fuchs (1988) to be up to 1 kHz for hair cells from the middle third of the chick papilla at the temperature of the living animal.

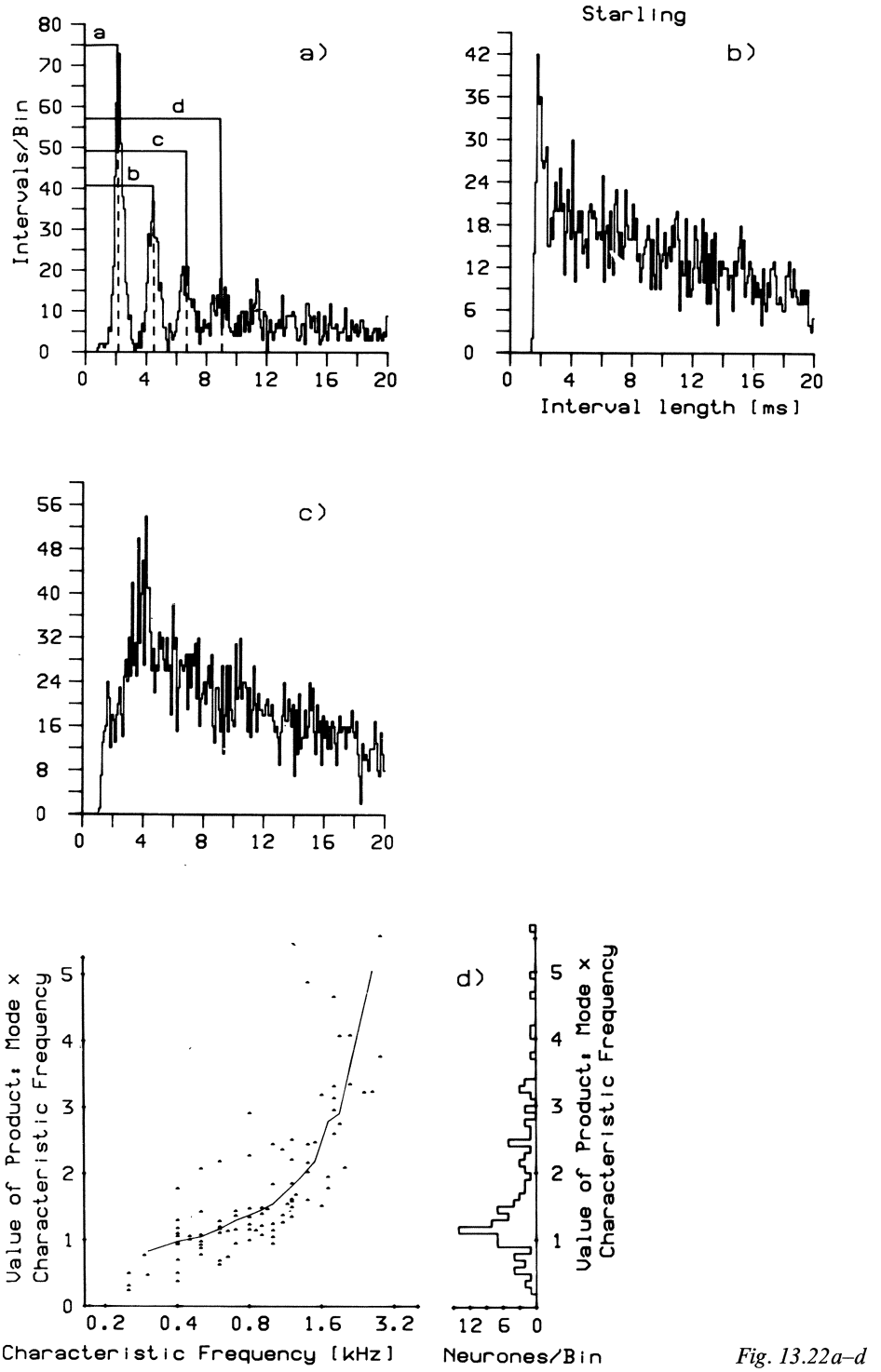
Starling
a)
b)
c)
d)
Intervals/Bin
Interval length [ms]
Value of Product: Mode x Characteristic Frequency
Characteristic Frequency [kHz]
Neurones/Bin
0.2
0.4
0.8
1.6
3.2
12 6 0

Fig. 13.22a–d

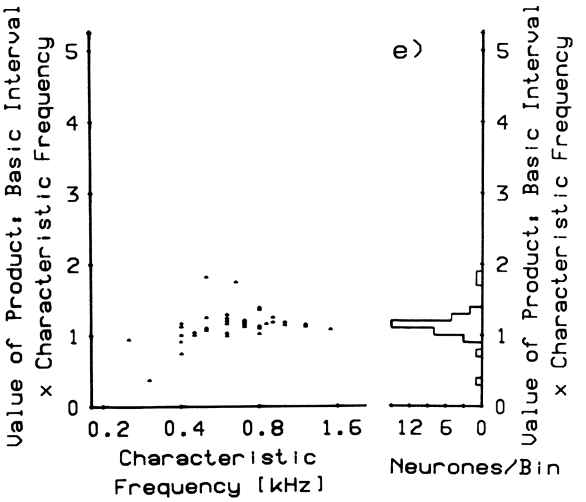

Fig. 13.22 a–e. Preferred intervals in the spontaneous activity of primary auditory fibres in the starling. *a* A TIH showing preferred intervals. The lengths of these intervals were determined as indicated and a "basic" interval was calculated using the formula: length of basic interval = (b/2+c/3+d/4)/3. For each neurone, the product of CF and basic interval was then calculated. A perfect agreement between the basic interval and the CF-period of each neurone would result in the product value of 1. *e* These product values are plotted against the respective CF for 37 neurones. The distribution of product values (*right side* of *e*) shows that they are on average somewhat higher than 1. This is in good agreement with the results of a similar calculation of the product of the mode (tallest peak in the histogram) and CF in TIHs of 108 cells (*d*). The scatter towards higher product values in the distribution shown on the *right side* of *d* results partly from the inclusion of units with long modes in their "shoulder" type of histogram (as shown in *c*) as compared to a "normal" TIH (*b*). The curve in *d* shows a three-point running average of the data of the scatter diagram. Data for individual units are as follows (number of intervals, discharge rates in spikes/s, CF in kHz): *a* 1,873, 48.6, 0.45; *b* 2,621, 51.6, 0.5; *c* 3,832, 57.8, 0.5 (Manley et al., 1985)

13.4.2 Frequency Selectivity of Single Nerve Fibres

In common with all other vertebrate auditory fibres, the single units of the avian auditory nerve are highly frequency selective (Fig. 13.23). The tuning curves are, if anything, more sharply tuned than those of mammals in the equivalent frequency range (Manley et al., 1985; Sachs et al., 1980), at least when measured as the sharpness of the tip region ($Q_{10\ dB}$; Fig. 13.24). When compared to those of a mammal, however, avian tuning curves do not show such a consistent asymmetry. Whereas guinea-pig tuning curves are almost all steeper on the high-frequency side, the starling curves are, on average, almost symmetrical (Fig. 13.25 a–c). The symmetry changes with CF in the starling such that below 1 kHz, twice as many cells show a steeper low-frequency slope of the tuning curve than a steeper high-frequency slope. Above 1 kHz, the reverse is true (Fig. 13.25 d; Manley et al., 1985).

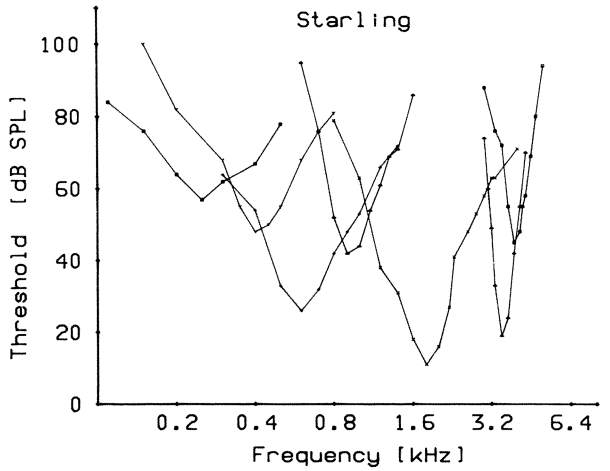

Fig. 13.23. Representative tuning curves of primary auditory neurones over a wide range of CFs in the starling (Manley et al., 1985)

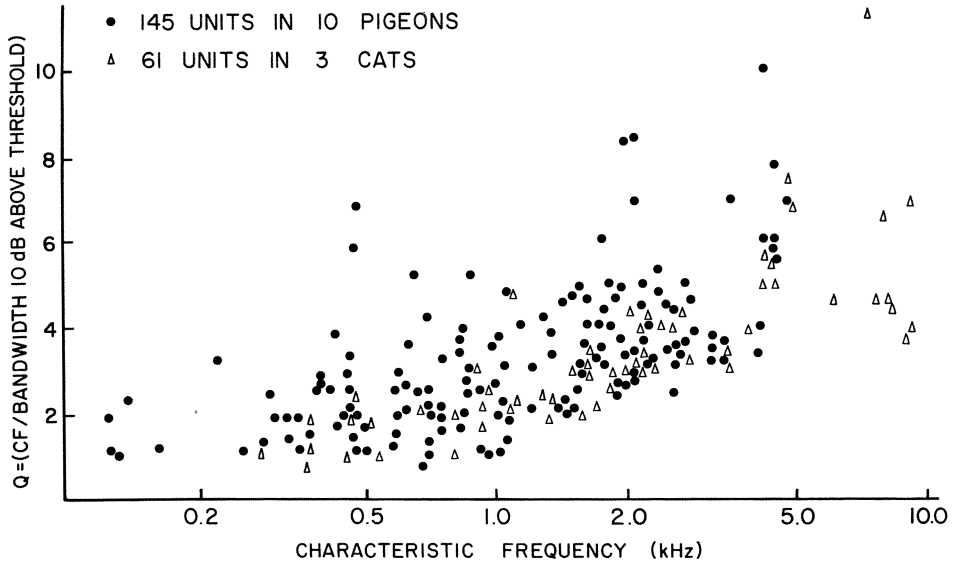

Fig. 13.24. The sharpness of tuning of primary auditory neurones, as measured as the Q_{10dB} in the pigeon (*filled circles*), as compared to the same measure for primary units in the cat (*open triangles*) for the same frequency range (Sachs et al., 1978)

The hearing ranges (measured behaviourally or as the range of CFs of the tuning curves) of most avian species studied so far cover a frequency range from near 100 Hz to about 6 kHz (Fig. 13.26). Konishi (1970), studying the behaviour of units in the cochlear nucleus of a number of passerine birds, noted that smaller birds tended to have higher upper limits of the CF range. Exceptions to the range

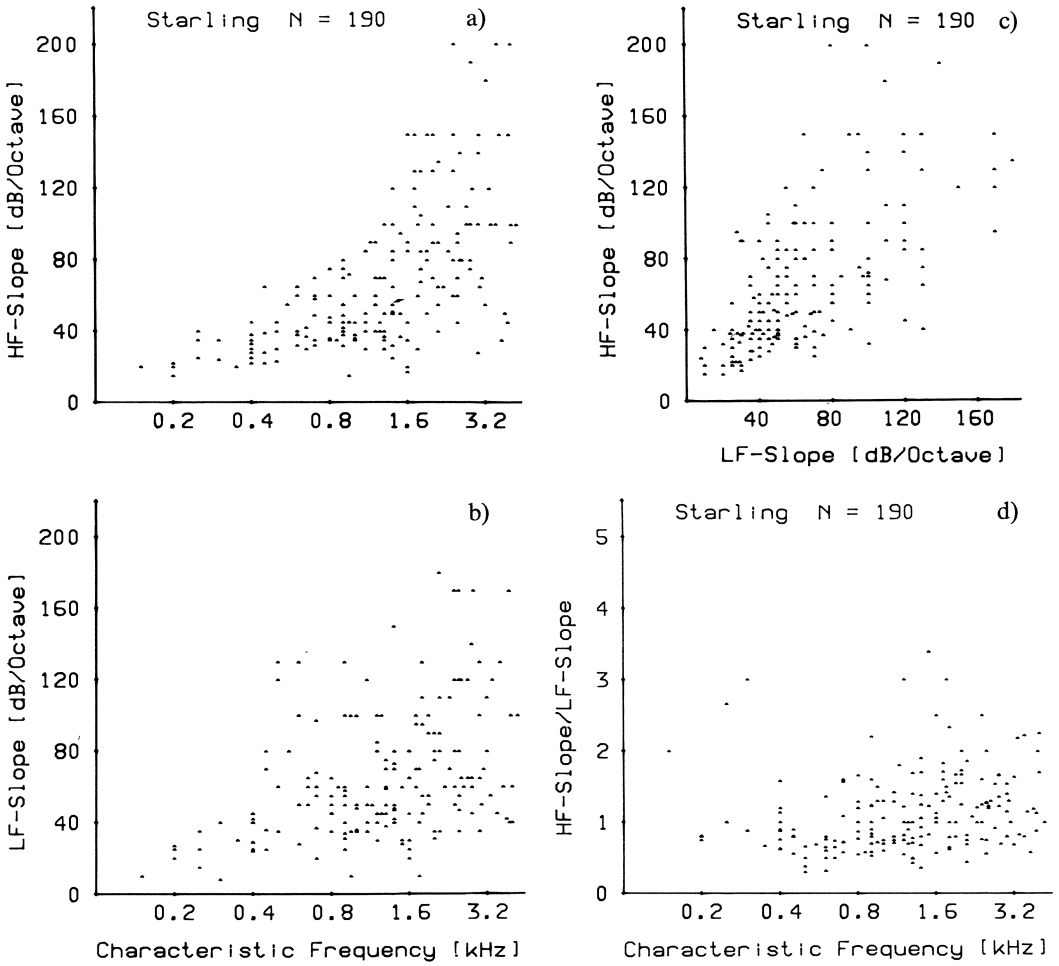

Fig. 13.25 a–d. Slopes of the tuning curves of 190 starling primary fibres, measured from 3 to 23 dB above threshold on *a* the high-frequency and *b* the low-frequency side of the tuning curve. *c* A plot of high- vs. low-frequency slopes of starling tuning curves as a measure of symmetry relationships. The distribution is roughly symmetrical about a 1:1 line. *d* The ratio of high- to low-frequency slope in starling tuning curves. Many tuning curves have a ratio below one, that is they are steeper on the low-frequency side, although the proportion of fibres with this pattern is higher at frequencies below about 1 kHz (Manley et al., 1985)

given above are found. The pigeon is sensitive to very low sound frequencies, a sensitivity which disappears upon removal of the cochlear duct (Fig. 13.27; Kreithen and Quine, 1979). Klinke and Schermuly (1986) report finding very low frequency responses in pigeon auditory-nerve fibres (which phase-locked to the stimulus rather than increasing discharge rate). When stained, these fibres were found to innervate intermediate hair cells in the most apical part of the basilar papilla. At this extreme apical end of the pigeon papilla, there are only tall and intermediate hair cells (Takasaka and Smith, 1971). In most previous experi-

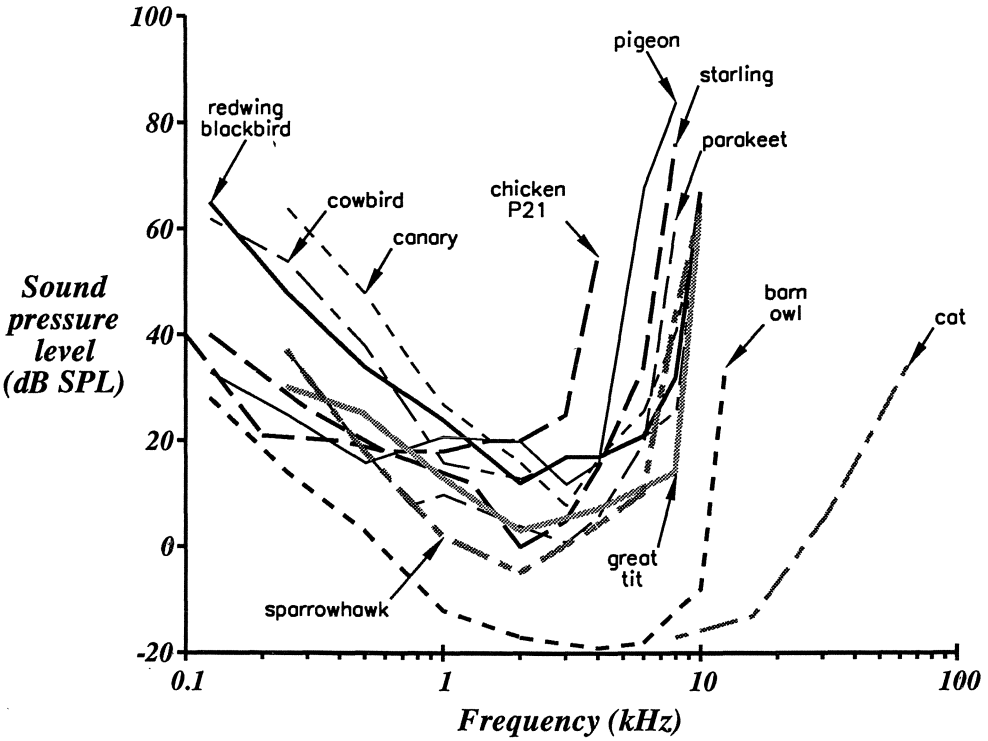

Fig. 13.26. A comparison of the threshold curves of ten bird species. Most of the audiograms are very similar to each other, with the exception of the less sensitive chicken and the highly sensitive barn owl at higher frequencies. The upper end of an audiogram for the cat is shown in order to emphasize the greater high-frequency sensitivity of a mammal. The lower frequency part of the cat audiogram is virtually the same as that of the barn owl (Redrawn from Klump et al., 1986; Konishi, 1973 b; Kuhn et al., 1982; Sachs et al., 1978)

ments, however, the sound systems used were inadequate to stimulate adequately below about 100 Hz, so it is difficult to generalize about the presence or absence of very low frequency responses. Warchol and Dallos (1987) report finding cells in the cochlear nucleus of chicks which responded to low-frequency sound (10 to 500 Hz). About half of the cells responded with equal sensitivity to frequencies between 10 and 100 Hz, the other half having broad, but more classical, auditory tuning curves with CF near 100 Hz. Many of these cells responded to sound only with a modulation of their spontaneous discharge and had more Gaussian than Poisson distributions of intervals in the spontaneous activity.

At the upper end of the frequency range, Sullivan and Konishi (1984) report recordings in the brainstem of the barn owl which, together with the behavioural audiogram (Konishi 1973 b), indicate that in this large bird, the CFs in the nerve reach 9–10 kHz (Fig. 13.26).

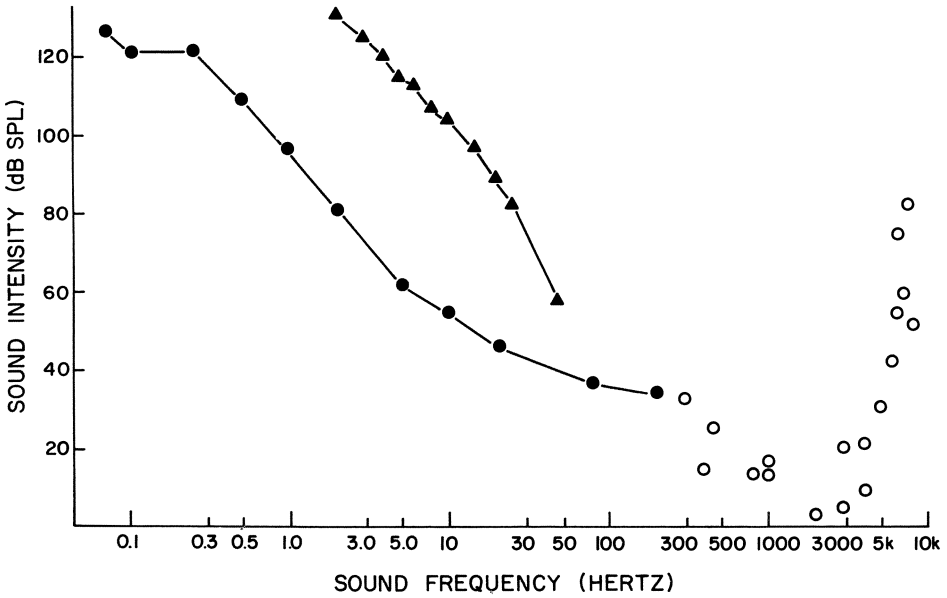

Fig. 13.27. Thresholds for low-frequency and infrasound detection by homing pigeons (*filled circles*) compared to auditory thresholds for man in the same frequency region (*filled triangles*). *Open circles* represent pigeon thresholds at higher frequencies. (After Kreithen and Quine, 1979)

13.4.3 Tonotopicity and the Localization of Active Afferents

The various CFs of the nerve or cochlear ganglion are distributed non-randomly in space, indicating a strong tonotopic organization of the papilla (Manley et al., 1985, 1987 a, 1988 a,b). Recently, the use of single-fibre staining techniques has permitted tracing the origin of responses in different frequency ranges to specific locations in the papilla of the starling and the chick (Gleich, 1988; Manley et al., 1987 a, 1988 a,b). Using horseradish peroxidase and cobalt stains, fibres which had been physiologically characterized were traced to their synaptic contacts. Almost all fibres only synapsed with tall hair cells (see above), and their locations were measured in the papilla to construct for both species partial maps of the distribution of CFs (Fig. 13.28). A strong tonotopic organization was evident, with an indication that the distribution is not best represented by a linear or a purely logarithmic representation (mm/octave), but that much less space is devoted to octaves below 1 kHz than to those above. In the starling, the CF distribution in the low-frequency range is about 0.1 mm/octave, whereas at high frequencies it is near 0.6 mm/octave (Gleich, 1988; Manley et al., 1988 a). This phenomenon is also known, but is not so pronounced, in the cat cochlea (Liberman, 1982 b). In the bobtail lizard and alligator lizard (see Sect. 14.10), a similar difference in space allocation is found. The tonotopic organization observed in the cochlear

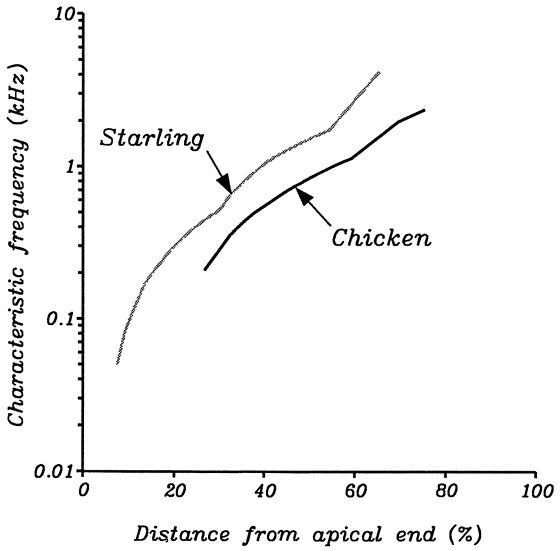

Fig. 13.28. Tonotopic organization of the basilar papillae of the 2-day-old chick (*black line*) and the adult starling (*grey line*). *Lines* are locally-weighted regressions for the frequency distribution for the chick (near 0.06 mm/octave; n = 13) and for the starling (at low CFs about 0.1 mm/octave, at mid- to high frequencies near 0.5 mm/octave; n = 34). Data for the chick from Manley et al. (1987 a); for the starling from Gleich (1988)

ganglion of starling and chick and the single-unit mapping data described above indicate that the low frequencies are analyzed at the apical end of the avian cochlea and the high frequencies at the basal end.

In whole mounts of the starling cochlea, 20 single fibres and 14 small groups of afferents (2–6 fibres), and in the chick cochlea, 21 single afferents or groups of afferents were traced to their synaptic terminations on hair cells (Gleich, 1988; Manley et al. 1987 a, 1989 a). Of these fibres, 24 and 15, respectively, were also successfully localized in transverse sections of the papillae. Those hair cells with a height/width ratio greater than one were designated as THC, as it was not possible to use more sophisticated criteria (such as details of the innervation pattern) for delimiting hair-cell populations. In virtually all cases, each afferent fibre only contacted one single THC (Fig. 13.29 a,b).

To describe the exact position of the hair cells receiving these afferent terminations, the number (= rank) of each innervated hair cell across the row of cells in sections was counted, starting from the neural side of the papilla. Virtually all hair cells (the two exceptions are discussed below) had a rank of less than 15, even though up to 35 hair cells were found in any one cross-section (Fig. 13.29 a). Using the data on the tonotopic organization of the papillae (to represent the position of fibers along the length of the papillae) and the number of hair cells across each papilla at each location, a normalized diagram illustrating the position of the individual innervated hair cells with respect to the length and width of the papilla was drawn (Fig. 13.29 b). It is obvious that in both species, with two exceptions, the innervated hair cells lie on the neural side of a line separating tall from short hair cells (1:1 line), even though the actual position of this line is place- and species-dependent.

Although the SHC afferent innervation is reported to make up about 18% of the fiber population (von Düring, 1985), only two stained fibers (= 3.6%) in-

nervating hair cells lying abneurally were found (Fig. 13.29 a,b). Both were in the apical part of the starling papilla (Gleich, 1988). One innervated about 6 hair cells and was the only branched fiber found. These two fibers had unusual response properties – they not only had high thresholds (> 70 dB SPL) but also extremely flat, low-frequency tuning curves for which it was hardly possible to define a characteristic frequency. They resemble the infrasound fibers stained by Schermuly and Klinke (1988) in the apical abneural area of the pigeon's papilla. These two fibers thus apparently belong to a different group of apical fibers not forming part of the main group representing the 'normal' frequency map of the avian papilla.

Although the fibers stained innervate only THC, this area is much greater than the equivalent area for mammals, which have only a single row of IHC. This difference offered the opportunity of examining their physiological response characteristics to see if there are any differences in the properties of fibers at different positions *across* the papilla (Manley et al., 1989 a). Although the sharpness of tuning and the spontaneous activity of the fibres showed no correlation with position across the papilla, there was a trend in the rate-response threshold of fibers (Fig. 13.29 c), such that the most neurally-lying cells were more sensitive to sound. For this analysis, the data sample was only large enough in the starling (Gleich, 1988). To exclude threshold differences due to the shape of the audiogram, the CF range between 0.6 and 1.8 kHz was selected, where the starling audiogram is quite flat (Kuhn et al., 1982). As can be seen in Fig. 13.29 c, there is a surprisingly strong relationship between threshold and position. According to the linear correlation, there is a threshold shift of almost 6 dB/cell, which is equivalent to 64 dB between the most neurally-lying and the most medially-lying cells whose fibres were stained. Should the trend to increasing threshold continue through to fibers contacting SHC, they would have thresholds above 80 or 90 dB SPL. Large threshold differences between neural and medial fibers would explain why it is not unusual in auditory-nerve recordings in birds to find threshold ranges for any one frequency region in individual animals which exceed 50 dB SPL (Manley et al., 1985).

In birds, almost all of the THC are supported by the superior cartilaginous plate and do not lie over the free basilar membrane. The higher sensitivity of such hair cells is contrary to intuition based on traditional concepts in auditory physiology, which dictate that hair cells lying over the free basilar membrane (with the largest displacement amplitudes to sound) should be more sensitive. However, very little is known about the mechanisms of hair-cell stimulation in birds. The trend of hair-cell bundle orientation across the starling papilla, in which medially-lying apical hair cell bundles are rotated up to 90 ° towards the apex, would reduce the effectiveness of radial stimulation on rotated cells. Even if we assume a purely radial shear motion of the tectorial membrane and a cosine function for the effectiveness of stimulation of the hair-cell bundle, the maximal threshold effect of this rotation of bundles in the frequency region we analyzed would, however, be only about 10 dB.

The high sensitivity of neurally-lying hair cells supports the suggestion that our concepts of the mechanisms of hair cell stimulation need revision. There is now evidence that the tectorial membrane is not stiff enough to act as a shearing

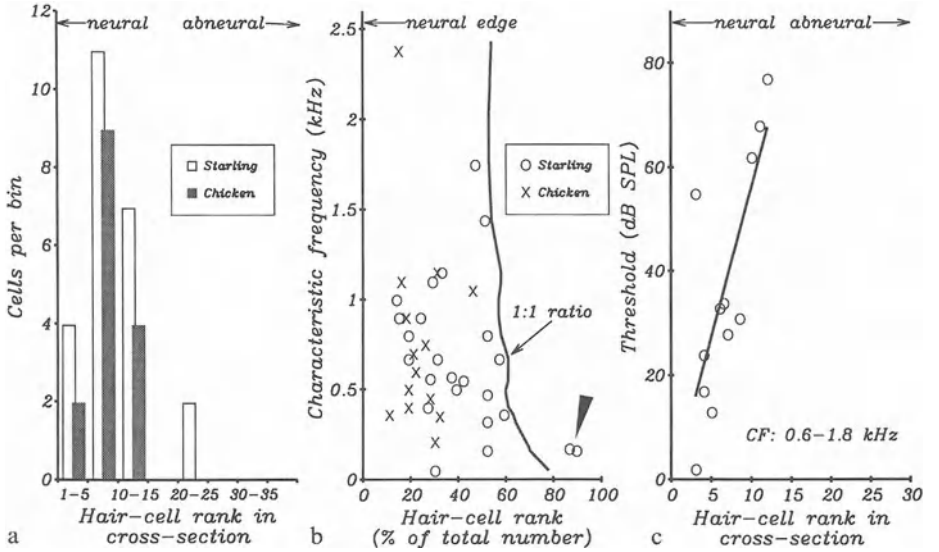

Fig. 13.29 a–c. Characteristics of avian primary auditory fibres as a function of the position of the innervated hair cells within the sensory epithelium. *a* Relative position of hair cells synapsing with labelled fibres in the starling and chicken. The rank indicates the location of the hair cell in cross-sections of the papilla, counting the hair cells from the neural side and placing them into groups of 5 cells. Only two exceptional fibres are found on hair cells with a rank greater than 20. *b* Schematic diagram illustrating the localization of innervated hair cells over the surface of the papilla. The *ordinate* represents the characteristic frequencies of the individual fibres, the *abscissa* indicates their rank in the cross-sections. In order to compare the two species, where the total number of hair cells in one cross-section is different, the rank has been normalized. The *thick line* delineates the border between cells on the neural area, which have a length : width ratio greater than 1, and those on the abneural area, which are shorter than this, in the starling. The 1 : 1 line for the chick has been left off, to avoid confusion: it would lie 5–10% to the left. Only two fibres in the low-frequency, apical area (*arrowhead*) innervated hair cells abneural to this line. We consider only the rank of each hair cell, but not its corresponding width. Thus, because the surface area of THC is much smaller than that of SHC, in an actual surface-area map of the space on the bird papilla, the 1 : 1 line would lie much nearer the neural edge. *c* Correlation between the rate-response threshold (threshold for an increase in discharge rate) for 12 fibres in the starling and their rank across the epithelium. In order to exclude effects due to threshold differences inherent in the form of the audiogram, only cells with CF between 0.6 and 1.8 kHz are included. The *line* represents a simple linear regression. For thresholds vs. position across the papilla, $n = 12$, $r = 0.764$, $p < 0.01$ (Manley et al., 1989 a)

partner for the hair cells during basilar-membrane motion, but that it contributes its mass to a resonance system (bobtail lizard, Manley et al., 1989 b; guinea pig, Zwislocki et al., 1988). If the stimulus to the hair cells depends on a resonance of the tectorial membrane, there is no reason why hair cells over the basilar membrane should be more sensitive. On the other hand, it is also possible that the SHC receive similar mechanical input to that of THC and produce comparable electrical signals, but that their receptor potentials may result in a mechanical response rather than in transmitter output.

13.4.4 Ontogeny of the Tonotopic Organization

An abundant literature exists with respect to the ontogeny of the cochlea and hearing in birds, especially of the chicken. It has long been known that the ability to hear begins at low frequencies and develops within the first few days and weeks after hatching to include the higher frequencies (Fig. 13.30; Konishi, 1973 a; Saunders et al. 1973). This has been interpreted as an enigma, as the actual development of the cochlear tissues appears to be faster near the basal, i.e., high-frequency, end (Rebillard and Rubel, 1981; Rubel and Ryals, 1983). From studies of noise damage in the chick, Ryals and Rubel (1982; Rubel and Ryals, 1982) reported an apparent shift in the position of damaged cells on the papilla for certain test frequencies as the young post-hatching chick developed. They interpreted their data as indicating that the individual hair cells change their frequency responses with time, which would explain the enigma outlined above. As noise-damage experiments are notoriously difficult to interpret, we (Manley et al., 1987 a) studied the development of the tonotopic organization of the chick

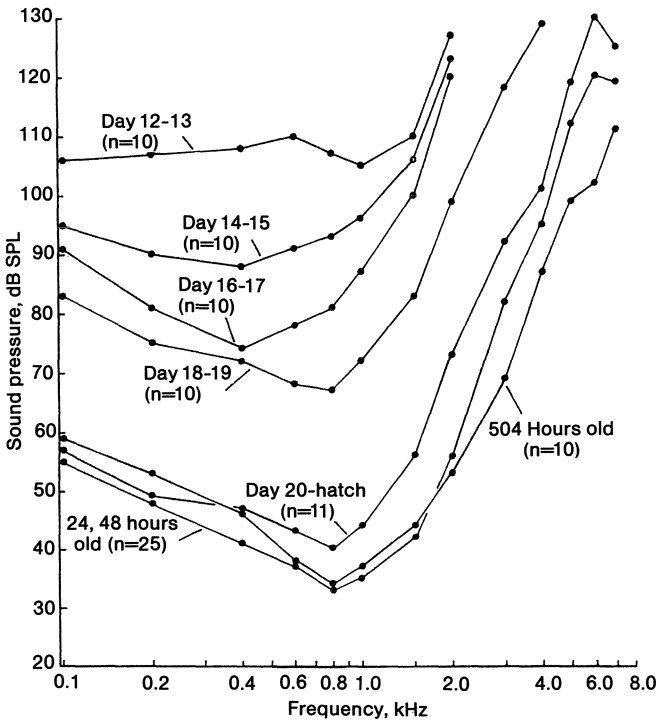

Fig. 13.30. The development of the evoked-response thresholds for the young chick, presented as threshold audiograms of evoked potentials from the cochlear nucleus for different ages, from embryonic day 12 to post-hatching day 21 (504 h); in most cases the mean of 10 animals is given (Saunders et al., 1973)

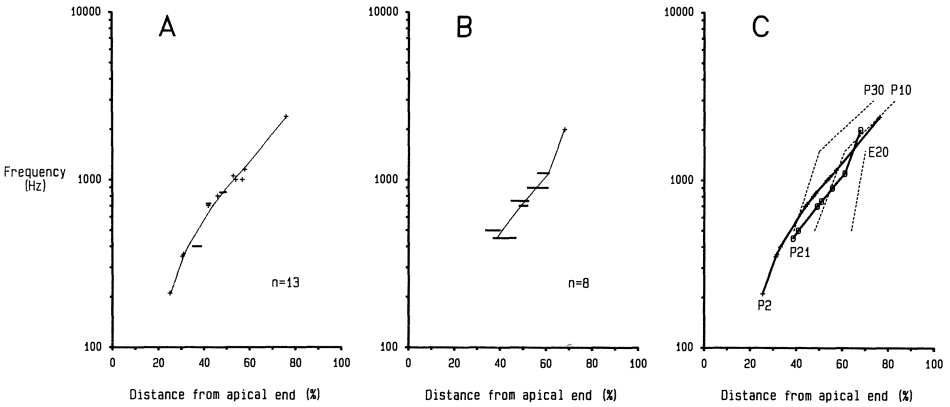

Fig. 13.31 A–C. The distribution of characteristic frequencies of HRP-stained tall hair-cell afferents in the chick papilla at *A:* age 2 days post-hatching and *B* age 21 days post-hatching. The data points represented as *crosses* show the positions of the termination of single fibres of known CF in the papilla. *Short bars* indicate the extent of terminations in cases where more than one fibre was stained. Position is given in terms of the % distance from the apical end. In *B,* two points overlap at 900 Hz. *C* A comparison of the two distributions with the developmental data of Rubel and Ryals (*dashed lines*), who show the position of damage produced by loud noises of three frequencies at days E20 (just prior to hatching), post-hatch 10 and 30 (Manley et al., 1987a)

papilla using the direct method of marking characterized fibres in animals of different ages (post-hatching day 2 and post-hatching day 21). Our data indicate no statistically significant shift of the frequencies on the papilla (Fig. 13.31). The large discrepancy between these two studies can be explained on the basis of two observations:

1). The stained fibres studied in the chick, so far as single-fibre stains were observed, innervated only *tall* hair cells. Cotanche et al. report that noise affects the different hair-cell groups differently, tending to damage *short* hair cells first, so that much of the data of Rubel and Ryals would concern a different hair-cell population to our data.
2). Cotanche et al. (1987) observed that the changes in damage patterns observed with age by Rubel and Ryals are mimicked at one single age by a change in intensity of the damaging sound. They suggest that there is thus no real shift of damage patterns on the papilla with age, but that the middle ear changes its admittance with age, so that the effective damaging intensity of a sound increases with age. The middle ear of the chick is not completely mature at hatching, but takes some days to reach its adult state (Saunders et al., 1973).

The situation is not made clearer by the claim that a change in the position of acoustic trauma occurs, but only over the few days around hatching (Cousillas and Rebillard, 1985). It is still difficult to know how to interpret acoustic trauma studies in terms of the normal function of hair cells at SPLs which are up to 100 dB lower than those used to damage the hair cells. Brix and Kaiser (1988) reported that not only is the tonotopic organization in the chick stable after

hatching, but that other parameters, such as the spontaneous activity, threshold to pure tones and tuning-curve shape and sharpness also do not change between the ages of 2 and 21 days post-hatching.

13.4.5 Discharge Patterns to Pure Tones

13.4.5.1 Firing Rates to Tonal Stimuli

Avian auditory-nerve fibres can respond to a sound stimulus in one of three ways. They can increase their firing rate above the spontaneous level, decrease it below spontaneous level, or phase-lock to a tonal stimulus without changing the rate. The second of these phenomena, also known as primary or single-tone suppression, has not been observed in mammals.

The most common response to a tonal stimulus is a tonic increase in discharge rate. With increasing sound-pressure level, the response includes an increasingly large phasic component, whose time course may exceed that of the stimulus (Fig. 13.32; Manley et al., 1985). That is, the fall in rate has not reached a plateau before the stimulus is terminated. Except for near-threshold stimuli, the tonal response is followed at offset by a period of reduced spontaneous activity, presumably due to a fall in the available transmitter in the synapse. The magnitude and duration of the reduction are related to the strength and duration of the stimulus. For intense sounds, the duration can far exceed that of the stimulus. The details of these interdependencies have, however, not yet been studied.

The discharge rate to a stimulus increases monotonically with increasing sound pressure, often up to rates exceeding 300 spikes/s (mean rate over entire stimulus – the instantaneous rates at onset are much higher). These rates are higher than equivalent rates reported for mammals (Manley, 1983) and correlate with the higher spontaneous rates in birds. Differences in saturation levels were not correlated with other response parameters of the cells (Manley et al., 1985), except that low saturation rates were found in cells with narrow dynamic ranges. Similar rate-level functions were reported for nerve fibres of the redwing blackbird, for which Sachs et al. (1980) describe a range of slopes and saturation characteristics like those found in mammals.

13.4.5.2 Phase-locking to Tonal Stimuli

Gleich and Narins (1988) demonstrated that in the starling, significant phase-locking occurs in most low-CF cells at sound pressures below the mean rate threshold (mean 9 dB below), but a range of behaviours was seen. The ability to phase-lock was similar for all low-CF cells, but no phase locking was observed above about 4 kHz (Fig. 13.33a). In the pigeon, Temchin (1988) observed phase-locking in low-CF cells down to 45 dB below the rate threshold. Similarly, Klinke and Schermuly (1986) describe cells that phase locked to a broad range of infrasound frequencies, but for which a rate-threshold CF below 90 dB SPL could

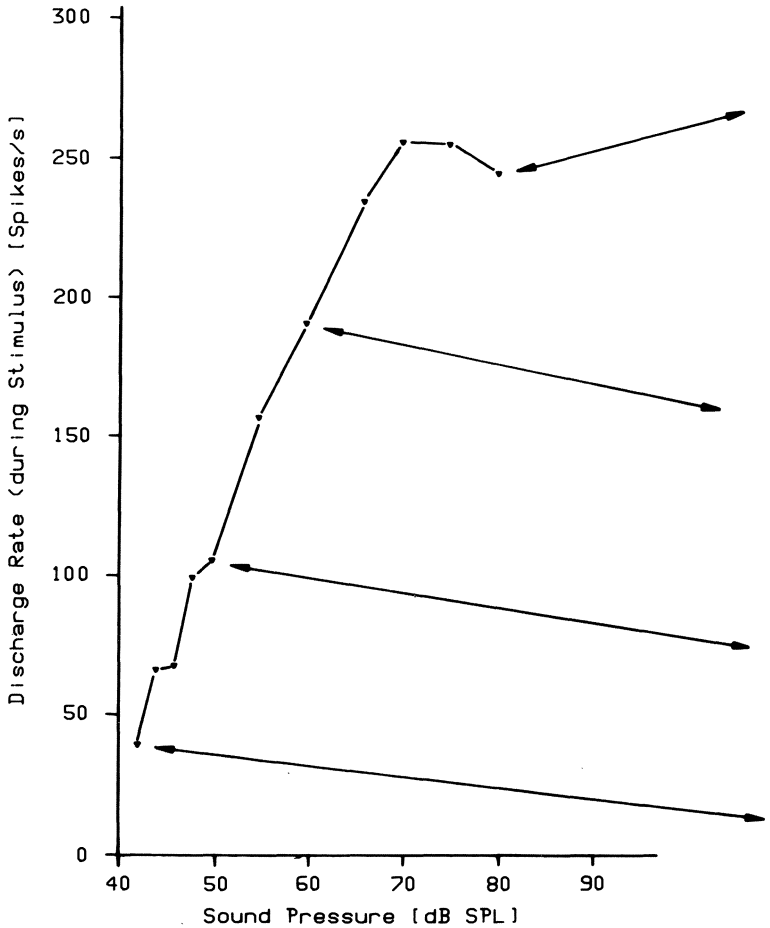

Fig. 13.32a

not be determined. Sachs et al. (1974; 1980) demonstrated that the phase-locking behaviour of redwing blackbird and pigeon nerve fibres is almost the same as that of cat fibres (frequency limit near 5 kHz).

A plot of phase versus frequency for single primary nerve fibres of the starling does not always result in a perfectly straight line. Rather there is, in many cases, a systematic variation such that below CF, the phase lag is more than expected from a straight-line fit and is less than expected for frequencies above CF (Gleich, 1988). Gleich fitted filter functions to the curves which result from subtracting a straight line from the individual phase function. Using an iterative procedure, a putative simple filter function was fitted to these resultant curves for each cell, to give the centre frequency and sharpness of a filter which best matches the resultant curve (Fig. 13.33c). As in the case of the preferred intervals (see above),

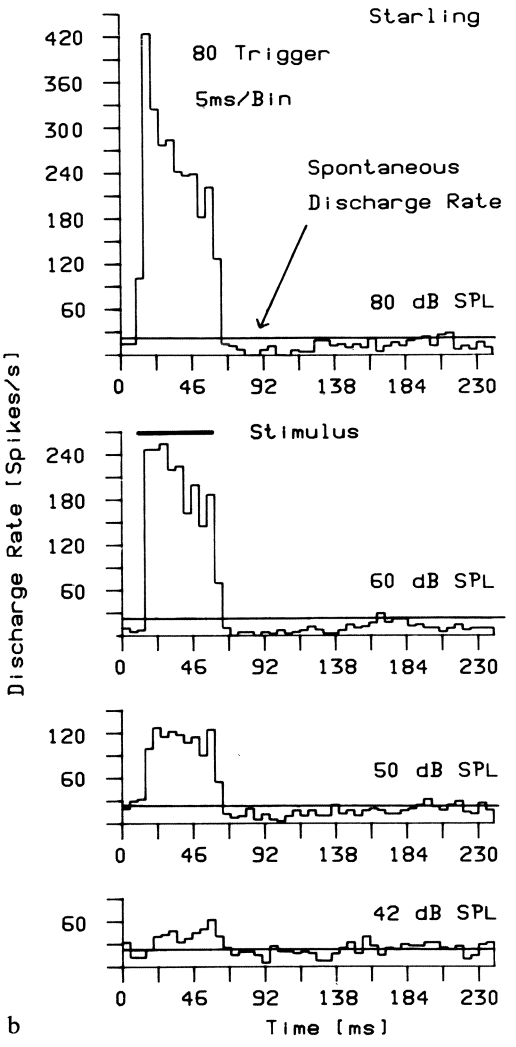

Fig. 13.32 a, b. Rate-level functions at CF of a single primary auditory afferent in the starling, stimulated with 50 ms tone bursts (time course shown below top histogram, "stimulus"). The PST histograms on the *right* illustrate the response patterns at the indicated sound pressures on the curve. The higher-level PSTH show a time course of decay which is longer than the tone burst; they also show the post-stimulus suppression of activity below the spontaneous activity (*horizontal line*) (Manley et al., 1985)

many individual fibres had a best filter match in which the centre frequency was not the same as that of the acoustic CF of the fibre, but was about 20% lower. This indicates the presence of a contribution to the tuning of an electrical filter which is, in most cases, mismatched to the acoustic CF. A few cells in the starling showed unusual phase-locking behaviour, tending to fire at intervals representing their CF (e.g. 900 Hz) when stimulated with much lower frequencies (e.g. 300 Hz). As these response patterns are not a result of distortions in the stimulus, this may be another indicator of the presence of electrical tuning in the hair cells (Gleich and Narins, 1988; Manley et al., 1985). In the pigeon, click latencies are also highly CF-dependent, being near 1 to 1.5 ms for higher-CF cells and near 3 ms for units with CF 400 Hz (Sachs et al., 1974).

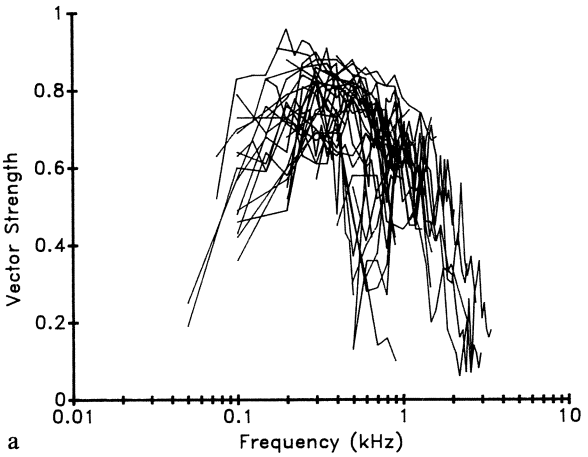
Vector Strength
1
0.8
0.6
0.4
0.2
0
0.01
0.1
1
10
Frequency (kHz)

a

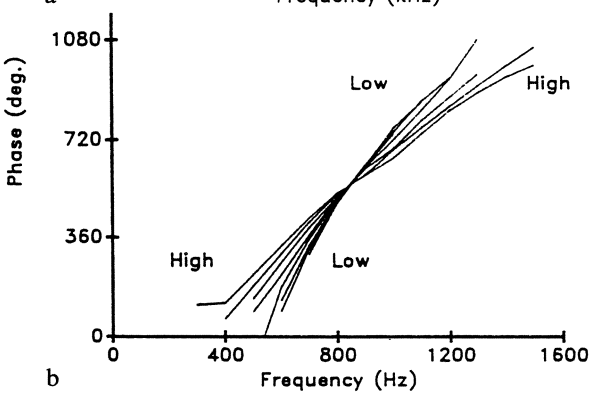
Phase (deg.)
1080
720
360
0
Low
High
High
Low
0
400
800
1200
1600
Frequency (Hz)

b

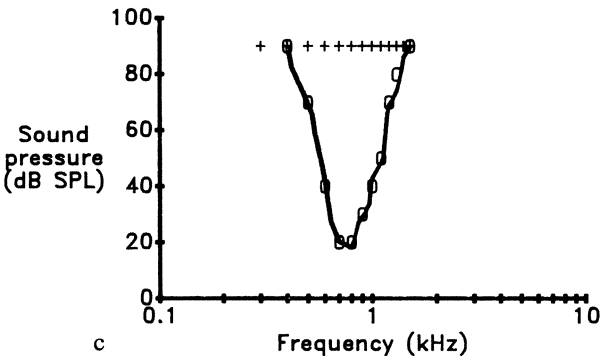
Sound pressure (dB SPL)
100
80
60
40
20
0
0.1
1
10
Frequency (kHz)

c

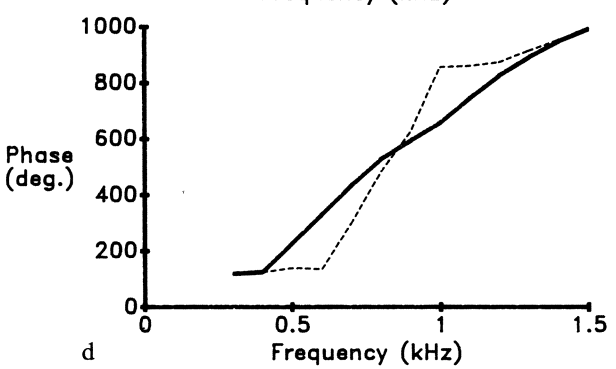
Phase (deg.)
1000
800
600
400
200
0
0
0.5
1
1.5
Frequency (kHz)

d

13.4.5.3 Primary and Two-tone Suppression

In the avian auditory nerve, not only can some tones suppress responses to other tones (two-tone suppression), but spontaneous activity can often be suppressed by single tones which do not themselves excite the cell (single-tone or primary suppression). The phenomenon of primary suppression has only been studied systematically in recent years. Although it is not possible in the case of very sensitive cells to exclude the possibility that the fibres are responding to uncontrolled, low-level noise, many fibres showing this phenomenon are rather insensitive. The observation of non-classical responses to sound from single fibres have been reported, but not extensively studied, by Gross and Anderson (1976), Manley et al. (1985) and Temchin (1988). Using audio-visual criteria or threshold-hunting automatic procedures to examine the tuning properties of nerve fibres has led to the tendency to ignore primary suppressive effects, as they are not readily detected by these techniques. An automated procedure used in my laboratory for examining responses to a large matrix of frequencies and pressure levels, however, readily revealed the presence of such suppressive side bands on tuning curves in the starling and chick (Fig. 13.34; Manley et al. 1985; Gleich, 1988; Manley et al., in preparation). The discharge rate of the cell falls below the spontaneous rate – sometimes even to zero. Such suppression is often accompanied by an 'off' response, where the discharge rate after the stimulus offset briefly rises above the spontaneous level (Fig. 13.35). Of course, such effects can only be seen in cells with a significant spontaneous activity. In the starling and the pigeon, the effect is most often observed at frequencies above the high-frequency flank of the excitatory tuning curve (Gleich, 1988; Temchin, 1988). Curiously, Sachs et al. (1974) report that in the pigeon nerve, "spontaneous activity was never inhibited by acoustic stimuli". This difference may be explained if these authors only refer to stimuli within the excitatory tuning curve. Primary suppression will not be detected by threshold routines which search for a rise in the discharge rate.

We (Manley et al., in preparation) found primary suppression both on the high side and the low side of the tuning curves of young chicks. The sensitivity of these suppressive areas was relatively constant from cell to cell (50 dB SPL $\pm$ 15 dB) and often almost as sensitive as the tuning curve (Fig. 13.34). Such suppressive areas were not, as in the pigeon (Temchin, 1988), only found in cells which showed preferred intervals in their spontaneous activity.

Fig. 13.33 a–d. Phase-locking behaviour of cells in the starling cochlear ganglion. *a* The vector strength of phase-locking vs. stimulus frequency at a constant 90 dB SPL for 38 cells. Only test frequencies within each cells' tuning curves are plotted and connected, always including the CF. *b* Phase vs. frequency functions of a single cell for 8 steps of stimulus SPL from 20 (low) to 90 dB SPL (high). The slopes become shallower with increasing level, but the phase around CF is invariant. *c* The preferred response phase of a cell measured either using a steady 90 dB SPL (*crosses*) or at SPLs near (*open circles*) the cell's thresholds (*continuous line*). *d* The corresponding phase vs. frequency functions; the *solid line* is for 90 dB, the *dashed line* is at threshold. Near threshold, the cell shows a rapid, large phase shift near the CF (Gleich and Narins, 1988)

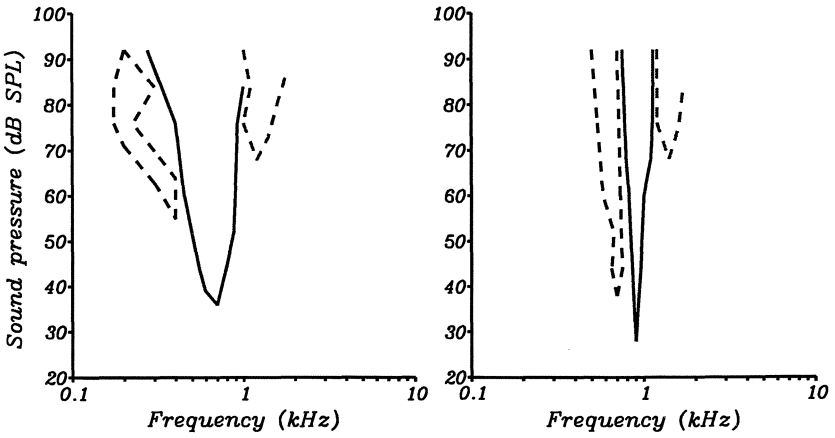

Fig. 13.34. Excitatory tuning curves and areas of primary suppression for two primary fibres in the 2-day-old chick. Each V-shaped tuning curve (*solid lines*) is bounded at higher and lower frequencies by an area where the discharge rate is lower than spontaneous rate (*dashed lines*). The diagrams represent schematically an area of frequency (*abscissa*) and SPL (*ordinate*). The iso-rate contours are drawn by a computer through a matrix of responses to frequency-intensity combinations over the entire area. The computer separates areas whose discharge rate to single tones exceed or go below the spontaneous rate by a given amount (Courtesy of J. Brix)

In many mammals and nonmammals, the phenomenon of two-tone suppression (TTRS) has similar properties to those described here for primary suppression. The threshold for suppression of a CF tone (10 dB above threshold) by a second tone is lower for frequencies of the second tone which lie above the high-frequency side of the tuning curve than for frequencies of the second tone which lie below the low-frequency flank (Sachs and Kiang, 1968; Manley, 1983). TTRS areas with characteristics similar to those of the primary suppression areas were found in young chicks and in the starling (Gleich 1988; Manley et al., in preparation). This phenomenon was also described for the pigeon by Sachs et al. (1974).

That the suppression is not a synaptic (inhibitory) phenomenon is indicated by the fact that its latency does not differ from that of the normal excitatory response of the fibres. There is thus no time for a neural circuit to feed back and inhibit hair-cell activity (estimated minimum time necessary is 6–8 ms). In addition, Temchin (1988) observed its presence even after severance of the eighth nerve in the pigeon. Temchin also observed the suppressive effect almost exclusively in cells having preferred intervals in their spontaneous activity. He termed tuning curves showing suppressive flanks 'complex' tuning curves but observed no difference in the sharpness of tuning of the excitatory areas of cells showing suppression and those not showing it.

Temchin interprets the phenomenon of single-tone suppression as being related to the presence of electrical tuning in the hair cells of birds. If, as in the turtle, the electrical tuning can manifest itself in an active motion of the stereovillar bundles of the hair cells (see Ch. 6), the electrical tuning could itself create a stimulus for the hair cells analogous to that of an external sound stimulus. These

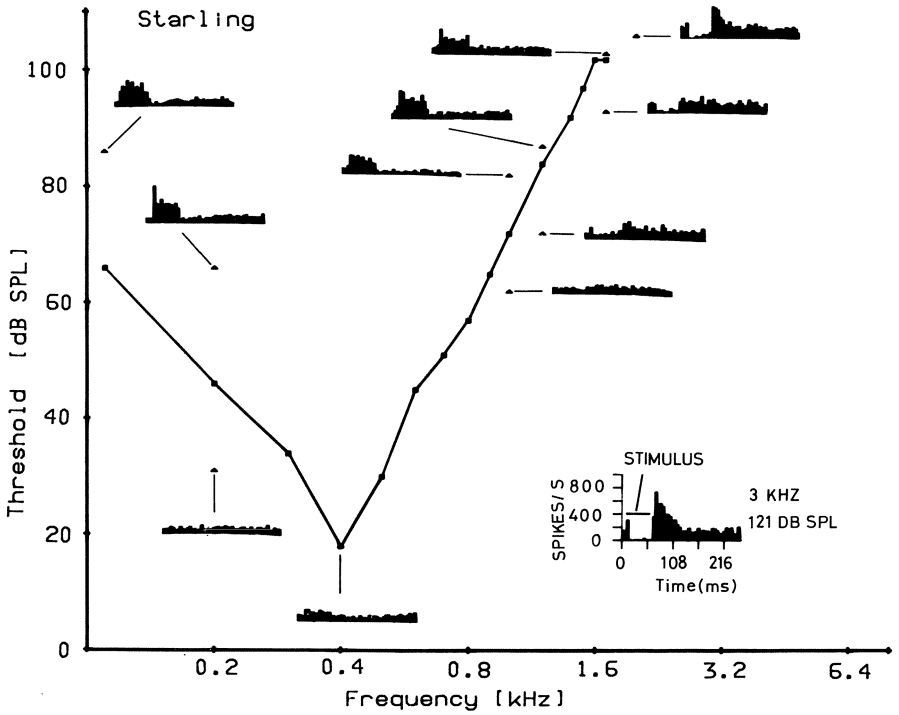

Fig. 13.35. Excitatory tuning curve of a single cochlear ganglion afferent in the starling. For this unit, 12 PST histograms are shown collected at stimulus frequencies and sound pressures as indicated by the *filled triangles*. The PSTH at *lower right* (3 kHz, 121 dB SPL) gives the time scale for the stimulus in all cases. This histogram and the four histograms to the right of the high-frequency flank of the tuning curve show primary suppression of the spontaneous rate during the stimulus and an "off" discharge at higher SPL (Manley et al., 1985)

stimuli, whether internal or external, might be suppressed by a tone, a 'second' tone in the case of external stimulation. Occasional 'on-off' responses (Manley et al., 1985; Temchin, 1988) may also be due to 'ringing' phenomena in hair cells resulting from electrical tuning. We (Manley et al., 1985) suggested that the fact that birds show primary suppression and mammals do not may be related to the absence of a firm connection between the inner hair cells of mammals and the tectorial membrane. Unlike mammalian inner hair cells, all avian hair cells are firmly connected to the tectorial membrane (see above). The participation of the tectorial membrane in two-tone effects has also been suggested for reptiles (see Sect. 14.4). It seems likely that these two phenomena are caused by similar mechanisms.

13.4.5.4 Temperature Effects

As in the Tokay gecko (Sect. 10.3) and the caiman (Sect. 12.5), the tuning of primary auditory fibres of the pigeon has been shown to be temperature sensitive

(Klinke and Smolders, 1984; Schermuly and Klinke, 1985). Primary-fibre tuning from cells in the cochlear ganglion was examined in the pigeon using head temperatures between 27 °C and 39 °C. As in the reptile species, the CF of single units shifted up with raised temperature and down with lowered temperature, the shifts ranging from 0.14 to 0.016 octaves/ °C in the low- and high-temperature ranges, respectively. These values are comparable to those found in the gecko and the caiman. In addition, in birds the thresholds became poorer for lower temperatures. Thus, the temperature effect is not restricted to ectotherms.

Chapter 14

Overview and Outlook

Modern vertebrates display an immense variety of inner-ear structures and functions. While it is necessary to take the huge structural variety into account, it is also important to attempt to describe some unifying principles underlying the facts and concepts that have emerged from 20 years of research on the anatomy and the electrophysiology of the hearing organs of birds and reptiles, and to suggest which aspects are deserving of our attention in the near future. It is also important to consider the ways in which these comparative studies have modified our concepts of the function of the mammalian hearing organ. I will attempt to do this as concisely as possible in this chapter.

One of the central questions to be considered in comparative auditory physiology is that of the relationship between structure and function, especially in view of the fact that, despite large structural variations, the variation in function revealed to date is surprisingly small. What can the data tell us about the function of the diverse structures in the various parts of the ear?

I shall discuss the following conclusions:

1. The middle ear is partially responsible for the relatively low upper limit of hearing in non-mammals.
2. The hearing range of reptiles is almost independent of the development of the hearing organ.
3. There are different patterns in the spontaneous activity that are partly related to tuning mechanisms.
4. The tectorial membrane plays a role in the sharpening of frequency selectivity and in suppression.
5. There is a specialization of hair-cell populations *across* the papilla in the archosaur lineage but not in other reptile lines.
6. The functional consequences of variations in hair-cell polarity and innervational pattern in lizards are not yet clear.
7. All vertebrate hair-cell systems are frequency selective.
8. All vertebrate hearing organs show tonotopic organization.
9. There are four different mechanisms of hair-cell frequency selectivity, appearing in different combinations in the various groups.
10. There is a strong tendency towards a division of the hearing range into roughly 'below 1 kHz' and 'above 1 kHz'. In lizards. this division has an anatomical substrate and manifests itself in several characteristics of the physiological response patterns. It is also observable in the physiological data from both birds and, to a lesser extent, mammals.

14.1 The Middle Ear and the Hearing Range

As discussed in Chapter 3, land vertebrates have one of two fundamental types of middle ear, namely the single- or the three-ossicle type. The reptiles and birds do show significant variability in the details of their middle-ear structure and in the ossification of columella and extracolumella, but can still be described as possessing the single-ossicle, *second-order* lever system.

The joint between the extracolumella and the columella cannot be at the position where the greatest articulation takes place to transform the swinging motion of the inferior process into the piston-like motion of the columella, but is some way down the shaft towards the footplate. Thus the transformation to a piston-like motion must take place within the extracolumella itself, for which the extracolumella must be made of a flexible substance. This fact prohibits a full ossification of the extracolumella. In many reptiles, such an ossification is out of the question, as the extracolumella-columella complex is highly exposed to mechanical disturbance both on the body surface and within the buccal cavity. Anyone who has seen small lizards ingesting very large insect prey can understand the necessity of these animals retaining a flexible, non-rigid, middle-ear transmission system. Birds have isolated their middle ear from the buccal cavity to a much greater extent and have, on average, a deeper external auditory meatus than the reptiles. Thus in birds, the middle-ear ossicle is more highly ossified than in reptiles. A degree of flexibility must, however, be retained by the extracolumella in order to translate the rotary motion of the inferior process into a piston-like motion of the columella shaft. In general, all of these non-mammalian middle ears have, as far as their transfer function for displacement is concerned, a low-pass characteristic. The upper limits of this characteristic are significantly lower than in mammals (Ch. 3; Manley, 1981).

The upper frequency limit of the non-mammalian ear is strongly influenced by the flexibility of the middle ear (Manley, 1972 a,b,c, 1973). At high frequencies (>4 kHz), much of the acoustic energy is lost in a flexing motion within the inferior process and the efficiency of the middle ear deteriorates rapidly. A higher degree of ossification in birds has extended the limit of efficient transmission only slightly. In addition, however, the inner ear itself influences middle-ear transmission, especially at low levels. This fact has largely been ignored until it recently became possible to measure motion at much lower SPLs. Destruction of the basilar papilla and round window uncouples the middle ear from significant damping even at high sound levels (Manley, 1972 c).

14.2 The Hearing Range and Papillar Development

A glance at Fig. 14.1 makes the following fact obvious: regardless of whether a lizard has a very well-developed hearing organ with over a 1000 hair cells on a relatively long papilla (e.g. geckos and skinks) or 100 or 200 hair cells on a very

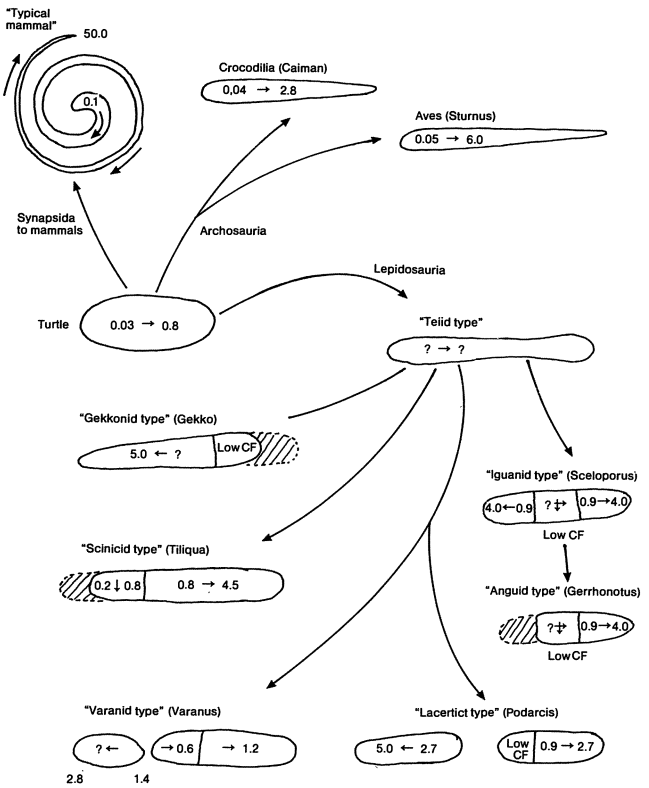

Fig. 14.1. Schematic diagram of the evolution of the structural and functional arrangement of the auditory papillae of amniotic vertebrates. The papilla of a turtle is taken as illustrative of the primitive state from which the different patterns of advanced papillae arose along several different lines. The *numbers* within the schematic papillae outlines are to indicate the known or suspected CFs of the cells of different regions (in kHz). The single hair-cell area with unidirectional orientation of the turtle-type papilla is retained by the lines leading to the mammals and the archosaurs. For the lizards, the "teiid type" of papilla is taken as primitive. Among the other lizard families, the fate of the putative primitive three hair-cell areas is indicated. The different area not present in the gekkonid, scincid and anguid papillae are *shaded* with *dotted outlines*. On the basis of this scheme, the "reversed" tonotopic organization of the gekkonid papilla can be easily explained. A question mark indicates that the direction of the tonotopic organization is not known. The different papillae are not drawn to scale

short papilla (iguanids, anguids, lacertids), the frequency range of hearing remains roughly the same. It appears that the (probably most primitive) low-frequency sensitivity is retained in all cases. At the high-frequency end, sensitivity developed up to the limit set by the middle ear.

One important difference between reptile and bird groups concerns the number of hair cells that carry out the analysis of stimulus information. Large and

systematic differences between, e.g., the frequency selectivity of individual nerve fibres emanating from these different papillae are less frequent than intuitively expected. The question as to the functional correlates of the extreme differences to be expected, e.g., in the 'potential' frequency resolution of the organ, is not easy to answer. Whereas there may be no systematic difference in the sharpness of tuning of individual nerve fibres, a papilla with 100 hair cells could code maximally for 100 different CFs, whereas a much larger papilla could have correspondingly more and, of course, finer frequency steps. The number of CF steps would be much smaller if neighbouring hair cells behave the same, or if they are combined into units by non-exclusive afferent innervation or by tectorial connections. It is interesting to note that in the Iguanidae, Agamidae and Anguidae, which have small papillae, the hair cells of the high-frequency, BDT area are not connected by a tectorial membrane. Their stereovillar bundles can thus move independently of each other, so that the frequency tuning of neighbouring hair cells can be different (see Sects. 7.1, 14.9). Our model of frequency tuning in the skink *Tiliqua*, which has a large papilla, assumes that hair cells linked together via sallets of the tectorial membrane vibrate as a unit. Although the latter mechanism involves linking many hair cells, the large number of hair cells in total permits the tuning quality still to be better than in species having hair cells without tectorial attachments (Sect. 11.3).

As individuals vary in their structure, and it is seldom possible to record from a large percentage of the nerve fibres of one individual, the possibility that a larger number of hair cells brings improved frequency resolution is virtually impossible to investigate adequately (see also Sect. 14.6, below). Sneary (1987) suggested for the red-eared turtle that higher-CF nerve fibres are more sharply tuned than low-CF fibres because, on average, they innervate fewer hair cells (1.3 vs. 1.8). However, higher-CF fibres of most species are generally more sharply tuned than low-CF fibres, a fact which is not correlated with innervation patterns. Also, Sneary suggested that the larger number of synapses (51 vs. 24) on high-CF fibres are responsible for their higher sensitivity. It is, however, very difficult to separate different factors potentially contributing to sensitivity (starting, for example, with the middle-ear transfer function). The investigation of the functional consequences of different innervation patterns is certainly one of the more important aspects for future work and requires detailed studies of the activity of fibres traced individually to the papilla.

In birds, most of the papillae code for roughly the same frequency range. The owls are an exception, and have much longer papillae and a somewhat higher upper frequency limit (Fig. 13.26). This upper limit is, however, still very much lower than that for mammals of equivalent size, indeed for virtually all mammals (see Sect. 14.1 above).

14.3 Patterns in Spontaneous Activity

The overall interval distribution in the spontaneous activity of primary auditory nerve fibres in reptiles and birds generally resembles that in mammals, where the

Poisson distribution is attributed to stochastic processes either in the hair cell or in the nerve-fibre terminal. At short intervals, however, these processes are modified at least by the absolute and relative refractory periods of the fibre (Manley, 1983). Preferred intervals represent a striking deviation from this pattern and have been described in the red-eared turtle (Sect. 6.1.5), in European lizards (seldom, Sect. 8.2.1), in the tokay gecko (Sect. 10.2.1) and in the pigeon and the starling (Sect. 13.4.1). They were not reported for the redwing blackbird (Sect. 13.4.1), for the caiman (Sect. 12.4), or the granite spiny lizard and alligator lizard (Sect. 7.3.1) and we did not find them in the bobtail skink (Sect. 11.2.3). It is an attractive hypothesis that preferred intervals are most easily seen in nerve fibres that only innervate one single hair cell, as it would seem unlikely that the hair-cell oscillations underlying this phenomenon would be coordinated between different hair cells. Some turtle hair cells and some hair cells of European lizards (*Podarcis*) are exclusively innervated, as are the low-CF hair cells of the tokay gecko and the tall hair cells of birds. However, the alligator and granite spiny lizards and the redwing blackbird and caiman also have, at least partly, exclusive innervation. It is, however, not clear in many cases whether they were really looked for in the data analysis. Perhaps these uncertainties will be removed through future research. It is not surprising that such intervals do not appear in skinks (where the hair cells are *not* exclusively innervated), although we looked carefully for them.

In the red-eared turtle, preferred intervals have been shown to result from the electrical tuning mechanism of the hair cells, which produces selective oscillations of the membrane potential. The transmitter release modulated by the membrane potential thus also shows a rhythm which is superimposed on the normal, random release pattern. The fact that this kind of spontaneous activity has never been observed in mammals may indicate that the mammals have largely abandoned the (undoubtedly ancient) electrical mechanism of frequency selectivity still found in other vertebrate groups (Sect. 14.9.1; Manley, 1986).

14.4 The Functions of the Tectorial Membrane

In lateral-line organs, there seems to be little doubt that the cupula serves as a 'sail' which increases the effective surface exposed to water motions. In detectors of linear acceleration, the otolithic membranes serve as carriers of particles of high specific gravity. However, the role played by the tectorial membrane in the hearing process is less well established. The large variation in structure of the tectorial membrane over the basilar papillae of lizards makes them ideal candidates for the investigation of the role of this structure.

Classically, the tectorial membrane of mammals has been regarded as a shearing partner for the hair cells. The hair-bundle motion was conceived of as being primarily produced by an up-and-down motion of the basilar membrane. If the tectorial membrane is stiff enough to deform all the local hair-cell stereovillar bundles, a shearing force should develop at the top of the hair cells during

stimulation. Recent measurements of the stiffness of the tectorial membrane in mammals have, however, shown that it is not stiff enough to shear the many hair-cell bundles attached to it (Zwislocki et al., 1988). Thus, it is more likely that the tectorial membrane in fact acts as a vibrating mass overlying the bundles. Such mechanical systems show a resonance frequency determined by this mass and the stiffness of the bundles.

Recent measurements in some non-mammals (see Sects. 7.4 and 11.3) have shown that the motion of the basilar membrane is smaller than in mammals, is not sharply tuned and also not tonotopically organized. A number of models and concepts of the function of non-mammal papillae (e.g. Weiss and Leong, 1985a for the alligator lizard; Manley et al, 1989 b for the bobtail skink) suggest that the motion of individual hair-cell bundles, or groups of hair cells together with part of the tectorial membrane, stimulates the hair cells. This can be produced by a more direct influence of columellar-driven fluid motion driving the hair bundles or tectorial membrane, rather than the basilar membrane being the 'prime mover'. Thus, the properties of the tectorial membrane would be expected to have a significant influence on the responses of the hair cells and their afferent fibres, depending on the actual structural configuration in the different papillae. Zwislocki et al. (1988) have proposed that in mammals also, the tectorial membrane functions as a mass in a mechanical resonance system. It also appears to be quite likely that the large, frequency-selective motions of the basilar membrane in mammals are not purely primary phenomena due to the properties of the basilar membrane, but partly secondary, deriving from a micromechanical input from large numbers of outer hair cells (Sect. 14.9.3). I have previously argued that this is only possible in an inner ear with a large number of hair cells, i.e., a significant amount of space, devoted to each frequency section (Manley, 1986).

In both the alligator lizard and the granite spiny lizard, the high-frequency population of nerve fibres is not very sharply tuned (Weiss et al., 1976) when compared to fibres of similar CF in other lizard species with similarly-sized papillae, e.g. the *Podarcis* species (Sect. 8.2.2; Köppl and Manley, in preparation) and also when compared to data from lizards with larger papillae. It seems likely that the absence of a tectorial membrane over this hair-cell group results in the shallower high-frequency flank of the tuning curves. The model we proposed for tuning in the papilla of the bobtail skink (Figs. 11.17, 11.18; Manley et al., 1988 d) suggests that the tectorial membrane plays a vital role in determining the resonance frequency of localized salletal hair-cell groups and in sharpening tuning curves.

A second, but related, aspect concerns the potential influence of the tectorial membrane in two-tone and primary suppression. Weiss et al. (1976) noted the absence of two-tone suppressive effects in nerve fibres of the alligator-lizard papilla emanating from the hair-cell region which is devoid of a tectorial membrane. It is possible that the tectorial membrane is necessary for mediating this effect, although there are many other differences between the two hair-cell regions. In the bobtail skink, however, a tectorial structure is present over both areas of the basilar papilla, yet only the low-frequency group of fibres shows two-tone suppression. Thus, it is possible that a tectorial structure is necessary but not sufficient to mediate two-tone suppression. The tectorial structure in the higher-

frequency area of the bobtail lizard papilla is very different from that of the apical area. The model we proposed for tuning in the higher-CF region of the papilla of this species indicates that more distant tectorial-membrane regions do not significantly affect the tuning of a hair-cell group (Manley et al. 1988 d). It may be that a long-distance effect is necessary for two-tone suppression. Thus, the presence of motion in a neighbouring region may induce the tectorial membrane to move in a direction unsuitable for hair-cell stimulation. The fact that in the low-frequency fibres in the bobtail lizard, the upper bounds of the suppressive areas of different CF cells are so similar (and frequently identical in individual animals) would also suggest one common stucture as the mediator of suppression. However, there is still no indication as to why two-tone suppression is not present (bobtail lizard) or is only weak (alligator lizard) on the *low*-frequency flank of cells showing suppression.

14.5 Specialization of Hair Cell Populations

Hair-cell populations are distinguished on the basis of cell position, structure and innervation pattern. The distinction between hair-cell types in lizards (which are found at different positions along the *length* of the papilla) will be dealt with in Section 14.6, below. In the hair-cell populations recognized in Crocodilia and in birds (found *across* the papilla), the differences in the position of the cells (neural or abneural part of the papilla, over the limbus or on the free basilar membrane), in their structure (e.g., form of the cell body, form and position of the stereovillar bundle) and in the pattern of the afferent and efferent innervation (see Chs. 12 and 13) are substantial.

These anatomical indicators of specialization correlate with recent findings of functional differentiation in the starling and the chick (Gleich, 1988; Manley et al., 1987 a, 1989 a) where the single fibres we characterized and stained only innervated single tall hair cells and even within the tall hair cells, there was a gradient in threshold from neurally- to centrally-lying hair cells (Sect. 13.4.3). This strengthens very much the notion that the division of the avian papilla into two or more sub-populations of hair cells parallels the division seen in the mammalian cochlea and raises the important question of the evolutionary origin of separate hair-cell populations.

The cochlea of the most primitive mammals (the monotreme platypus and spiny anteaters) bears both a resemblance to that of birds and Crocodilians and to that of the other mammalian groups. It is not coiled, but the hair-cell populations look something like a cross between bird and therian mammal cochleae (Chen and Anderson, 1985; Griffiths, 1968). However, mammalian and avian reptile lineages have at least 250 million years of separate evolution (Carroll, 1987), and they almost certainly stem from ancestors with a cochlear structure not showing separated hair-cell populations, for there is no indication of such different populations of hair cells in other reptilian groups which originated at about the same time (e.g., chelonians, rhynchocephalians and lepidosaurs). At this stage, it seems most likely that the resemblance between avian and

monotreme cochleae is due to convergent evolution. In other mammals, the number of hair-cell rows was reduced as compared to the monotremes. It is not inconceivable that, granted that hair cells have certain basic properties, the selection pressures acting on a large uniform population of hair cells in different vertebrate groups could produce sense organs of similar structure and function based on a 'division of labour' between hair-cell groups. The related question of interactions in space is further discussed below (Sect. 14.9).

The question might be asked as to why the specialization and reduction in hair-cell number across the papilla did not progress to such an extent in birds as it did in mammals, or even as it did in *Crocodilia*. The recent finding of infra-sound reception in abneural, apical hair cells of the pigeon and of similar cells in the starling (Sect. 13.4.3) may give us a clue. It is reasonable to speculate that the hair-cell specialization in birds, while tending strongly in the same direction to that of mammals, was hindered by the presence of an additional function. As flying animals, it is certainly important for birds to collect information about their position in space. The infrasound receptors described are in a position to respond to the slow air-pressure changes of winds and of slightly different flight altitudes. Such a function would be possible in hair cells over the free basilar membrane (abneurally-lying, intermediate or short hair cells). A specialization for this function could perhaps have hindered or reduced the appearance of the same specializations as shown by mammalian outer hair cells. This notion is strengthened by the finding that the hair-cell populations are more easily distinguished in crocodilians (ground-living) than in birds. The speculation could even go so far as to suggest that the specialization of hair-cell populations in crocodilians has progressed so far that they show a more similar pattern of spontaneous activity to that of mammals (a bimodal distribution of rates) than do the birds. Further study of the specializations of hair-cell populations will show whether these speculations have any real substance. Indeed, the investigation of the functional significance of distinct hair-cell populations will be one of the most fruitful future areas of auditory research.

14.6 Hair Cell Types and Innervation in Lizards

Although oppositely-oriented hair cell areas are the rule rather than the exception in the lateral-line and vestibular organs, they are found only in lizard auditory papillae and not in the other reptiles and birds. The observation of two different hair-cell orientation polarities in all auditory papillae of lizards intuitively suggests the presence of different hair-cell populations. However, we have no evidence that there is any physiological difference between the oppositely-oriented hair cells in bidirectionally-oriented hair-cell areas of the lizard inner ear, apart from their preferred polarity of response to sound. Therefore, there is no reason to regard them as different populations. In addition to at least one bidirectionally-oriented area, there is generally a unidirectionally-oriented area in lizard papillae. Even comparing bidirectionally – with unidirectionally-oriented areas, however, there are no aspects of the physiological responses

which can at this stage be clearly related to the *orientation* of single hair cells, except of course their phase of response.

In their study of the innervation patterns of auditory hair cells in lizards, Miller and Beck (1988) concluded that it is only on the basis of *cytological* features, such as relative cell size and innervation pattern, that it is consistently possible to recognize two hair-cell populations in different lizard papillae. Thus they described two hair-cell types which are, for historical reasons, termed the unidirectional type (UDT) and bidirectional type (BDT; Sect. 4.3.4), but which are sometimes not correlated with their orientation patterns. With this distinction, they have eliminated some of the confusion which has arisen through too great an emphasis on the directionality of different hair-cell areas. In the divergent bidirectional area of the skink papilla, for example, the hair cells are clearly of the UDT type.

The functional significance of bidirectionality is obscure. In earlier chapters I have described evidence that in the varanid (Sect. 9.2) and scincid (Sect. 11.1) papilla, single nerve fibres often innervate hair cells of both polarities. In order to assess the significance of this, we must compare nerve fibres known to innervate single hair cells or cells of the same polarity to fibres innervating hair cells of different polarities. In the bobtail skink *Tiliqua*, the phase histograms of the responses of single fibres to sinusoidal stimuli often show two peaks, 180 ° apart, per cycle (Sect. 11.2.3). This is a result of the fact that nerve fibres often innervate hair cells of opposite polarities, which has been confirmed in cobalt-stained fibres. It can also be speculated that, if the hair-cell-driven motion of the stereovillar bundle contributes to a rocking motion of the tectorial membrane over the hair cells, the energy transfer to the tectorial membrane would be more efficient if oppositely-oriented hair-cell groups were present.

Bidirectionality is unlikely to play a major role in determining the variety in the shape of peri-stimulus-time histograms (PSTH) of lizard auditory-nerve fibres. Similar trends in PSTH shape have been found in European lizards (Sect. 8.2.2), the monitor lizard (Sect. 9.2), tokay gecko (Sect. 10.2.2) and the bobtail lizard (Sect. 11.2.3). Low-CF cells tend to have a more tonic discharge pattern, whereas high-CF cells have a more phasic pattern. The low-CF area is sometimes unidirectionally-oriented (e.g., gecko, monitor) and sometimes bidirectionally-oriented (e.g., bobtail); thus the origin of these patterns is more likely to be traceable, for example, to the number of synapses made by fibres on hair cells in different areas and to the time constants of the nerve-fibre membranes (Oertel, 1985). Miller and Beck (1988) state that in lizards of all the 6 families they investigated, UDT hair cells were supplied with a larger number of synapses (from larger-diameter fibres) than BDT hair cells. Thus, as low-CF hair cells are always of the UDT type, the higher discharge rates seen in the tonic PSTH may result from the larger synaptic areas available for signal transmission. Ideally, such comparisons should be made using different fibres in the same species, but of known innervation pattern. So far, information in this detail is not available.

One interesting correlation between Miller and Beck's hair-cell types and physiological responses is that the UDT hair cells always respond to low frequencies (CFs up to maximally 1 kHz), whereas BDT hair cells respond to the higher frequencies. It seems that in the course of their early evolution, lizards added a

differently-structured, BDT high-CF area to the primitive low-CF, UDT hair-cell area. The UDT area is comparable to the entire papilla of turtles, *Sphenodon* and snakes. At least in some cases, the UDT-area hair cells are electrically tuned and the BDT-area cells are mechanically tuned. Future research should also be directed towards learning about the constraints on frequency analysis that underlie the division of the papillae into two separated frequency regions.

Miller and Beck (1988) describe variants in the pattern of afferent innervation that are potentially of value for neurophysiological investigation. Thus in the iguanids, all hair cells are exclusively innervated, but the number of synapses varies with the cell's location on the papilla, being greater in UDT hair cells than BDT hair cells. In the European lizard *Podarcis*, as in other lizards, UDT hair cells make up to 12 times as many synapses on afferent fibres as do BDT hair cells. Mulroy (1986) suggested for the alligator lizard that a greater number of synapses may be correlated with a better phase locking behaviour of the fibres. Evidence in support of this possibility is described by Rose and Weiss (1988). Similar results were found in the bobtail lizard (Sect. 11.2.3).

Miller's (1985) and Miller and Beck's (1988) study of innervational patterns in lizards show a definite tendency towards *exclusive* (one fibre only innervates one hair cell) innervation in small papillae and *nonexclusive* (branching) innervation in large papillae. However, there are also interesting differences between different large papillae. Thus, while UDT hair cells in geckos are exclusively innervated, all hair cells in skinks are non-exclusively innervated. This has important consequences for the study of the presence or absence of preferred intervals in the spontaneous activity of the fibres as indicators of electrical tuning of hair cells (Sect. 14.3).

Non-exclusive innervation reduces the potential gain, e.g., in frequency resolution possible through greater hair-cell numbers in the larger papillae. If we compare the ratio of the number of nerve fibres to the number of hair cells in a large papilla (e.g., 0.8 in a skink) and in a small papilla (5.3 in a European lizard, Miller, 1985), we have the enigmatic situation that a nerve supplying a small papilla with, say, 300 hair cells may be composed of the same number of nerve fibres as a nerve supplying a much larger papilla with over 1000 hair cells (Fig. 4.17). It becomes obvious that the potential increase in the degree of frequency resolution offered by an increase in papilla size and hair-cell number has played an insignificant or no role in the evolution of lizard papillae. It is more likely that any differences between these two innervation patterns will be seen in the threshold sensitivity, dynamic range, etc. of individual nerve fibres and in brain centres where, potentially, parallel processing can occur. More detailed comparisons of these aspects must await further research.

Whereas the difference between exclusive and non-exclusive innervational patterns is related to the size of the papilla, no consistent pattern with respect to the two hair-cell types has evolved in the various families of lizards. Whereas in skinks *all* hair cells are non-exclusively innervated, in geckos only the BDT hair cells show this pattern. In teiids, the pattern is the reverse of that shown in geckos; the BDT hair cells are exclusively innervated, the UDT hair cells are not. These details will become increasingly important as further physiological data from different lizard families become available.

Unlike in other lizards (Sect. 4.3.4), the papilla of the agamid lizard *Calotes versicolor* has no *efferent* innervation (Bagger-Sjöbäck, 1976). This observation has been confirmed (Miller and Beck, 1988) and extended to two other agamid lizards (*Agama agama* and *Acanthosaura crucigera*). Until more extensive studies of the fine anatomy are available, it will not be possible to adequately judge the extent of these variations within and between the lizard families, much less attempt to further assess their functional significance. However, as Miller and Beck (1988) point out, these species may be suitable for a comparative study of the function of the efferent fibres. As yet, no studies of the function of efferent fibres have been carried out on lizard or avian species.

In all the lizard auditory nerves that he investigated, Miller (1985) found that the nerve fibres (diameter range 0.8 to 6 μm) were unimodally distributed with regard to their diameter. However, almost all the larger fibres supplied only the UDT area of the papillae.

14.7 Frequency Selectivity of Vertebrate Auditory Receptors

Except where there is no tectorial membrane, the frequency selectivity of reptile and bird auditory-nerve fibres is as high as that in mammals in the same frequency range. There are differences in shape of the tuning curves, with some primary fibres showing asymmetrical tuning curves sharper on the high side (e.g., *Gekko, Caiman*), others showing no particular asymmetry (e.g., *Varanus*; Manley, 1981), while still others (e.g., the starling, have an asymmetry that varies with the CF of the fibre (Manley et al., 1985). There are no obvious structural candidates to explain these differences. It is interesting to note that in both the alligator lizard (Sect. 7.3) and the bobtail skink (Sect. 11.2.1), in spite of differences in the tip region, there are some similarities in the shape of the tuning curves. Thus for both high-CF populations, the low-frequency slopes of different-CF tuning curves run more-or-less parallel to each other. The high-frequency slopes, however, run closer and closer together at higher frequencies and SPL. This similarity is correlated with their shape being determined by the superimposition of the high-pass filter characteristics of the hair cells on the broad basilar-membrane tuning (Sects. 14.9.2, 14.9.3). With regard to the sharpness of the tuning-curve tip, it is interesting with respect to our model of frequency selectivity in the basal segment of the papilla of the bobtail lizard (Sect. 11.3), that in *Gekko,* there are about twice as many sallets (170 vs. 80) along the similarly-sized papilla, implying that the tuned units of tectorial membrane and hair cells are smaller. Correlated with this is the fact that the $Q_{10\ dB}$ of nerve fibres in *Gekko* are higher than in the bobtail lizard (cf. Sect. 10.2.2 and 11.2.1).

14.8 Tonotopic Organization and its Evolution in Lizards

Tonotopicity is one of the fundamental principles underlying the organization of vertebrate hearing organs (Fig. 14.1). Encoding a wide spectrum of frequencies is

always achieved by breaking up the spectrum into narrow ranges, each of which is coded for by a number of hair cells. As far as can be seen, there are no discrete frequency steps, due, among other reasons, to the fact that the frequency-response ranges of neighbouring cells overlap for stimuli just a few dB above threshold. This range of behaviours of an array of sensory cells is presumably achieved by the creation of gradients during ontogeny, as seen in other developing organs. These gradients manifest themselves in anatomical (e.g., cell morphology, length of stereovillar bundle) and electrophysiological properties (e.g., ion-channel characteristics) of the hair-cell array (Sect. 14.9).

From the study of the vast amount of data on the ear of mammals, we are accustomed to a polarity of the tonotopic organization such that the high frequencies are basal and the low frequencies are apical in the cochlear duct. To a very large extent, this pattern is also found in bird and reptile papillae. In lizards, however, the pattern is often more complex and some small papillae do not conform to this plan. Also, the tonotopic organization in the apical papillar segment in the bobtail lizard (and probably many other lizards) runs across, that is, from abneural to neural, rather than along the papilla. In many papillae, such as in the iguanid *Sceloporus*, the tonotopic organization is not monotonic. In others, for example in *Gekko*, it is probable that the polarity of the tonotopic organzation is even reversed (Fig. 14.1). As shown by Miller (1973 b) and Wever (1978), the basal end of the papilla of this gecko species is unidirectionally oriented. Based on the fact that all unidirectional areas of lizards so far studied respond to low frequencies, this would mean that the low frequencies would lie basally, instead of apically. A comparison of the cochlear-microphonic and neural threshold data at low frequencies in *Gekko* supports the idea that the low frequency responses are found in the unidirectionally-oriented hair-cell area (Sects. 1.3, 10.2.2). This reversed tonotopic organization is not surprising, however, if we consider the following scheme of the evolution of the lizard papilla.

As outlined in Chapter 4, Miller (personal communication) regards the teiid lizards as possessing relatively primitive basilar papillae which can most easily be derived from the putative primitive, unidirectional, ancestral type. From the starting point of a teiid papilla with BDT hair-cell areas which are differentiated out at both ends of the papilla and which flank the primitive UDT area, the different papillae of other families can be derived by loss of BDT areas at the one or the other end or by the separation of subpapillae via a limbic bridge (Fig. 14.1). In all cases, the BDT areas respond to high frequencies, the UDT area to low frequencies, although it remains to be clarified if the tonotopic organization of the UDT areas runs across or along the papilla. From the presumptive teiid starting point, I suggest the papilla evolved in three directions:

1. Loss of the basal bidirectional area, as in geckos, which results in a reversed tonotopic organization relative to the most common pattern (see Ch. 10).
2. Loss of the apical bidirectional area, as in the skinks. This results in the most common pattern of tonotopicity, where the high-frequency region continues the tonotopicity of the low-frequency area 'inherited' from the more primitive, exclusively unidirectional, reptile papillae (as in turtles). Although skinks have this kind of tonotopic organization, they have often modified the direc-

tionality of the low-frequency area, resulting in 'divergent' orientation. The hair cells of this region are UDT and still respond to low frequencies.

3. Retention of three hair-cell areas. In the granite spiny lizard, an iguanid, the mirror-image BDT areas respond to higher frequencies but their individual tonotopic organization *runs in opposite direction* resulting in a disjoint tonotopicity. In two other families, we see a diversification of the two BDT areas through the creation of a physical division within the papilla, producing sub-papillae. The result is a disjoint tonotopicity where the two separated BDT areas do not respond to the same frequency range. This is the path taken by the Lacertidae (Ch. 8) and to a lesser extent by the Varanidae (Ch. 9). It may be that the dividing bridge of limbic material isolates the sub-papillae mechanically from each other, so that the (presumably different) motions of one membrane do not influence hair cells in the other sub-papilla.

14.9 Mechanisms of Frequency Selectivity

It has been suggested for some years now that there is more than one mechanism of frequency analysis in the vertebrate inner ear (Klinke, 1979; Manley, 1979). More recently, fundamentally different mechanisms of frequency selectivity have been recognized in terrestrial vertebrates (Manley, 1986). Although it is not possible in any case to cleanly separate the different mechanisms (see, e.g., Sect. 6.1.4), for descriptive purposes they will be treated separately under the following headings:

a) Frequency selectivity in the electrical characteristics of the cell membrane,
b) Frequency selectivity resulting from the mechanical properties of the hair-cell stereovillar bundle,
c) Frequency selectivity dependent on an interaction between hair-cell bundles and the tectorial membrane, and
d) Frequency selectivity resulting from active processes in a large number of hair cells, resulting in mechanical interactions between the hair cells and the basilar membrane. This last mechanism is inextricably mixed with the passive selectivity of the basilar membrane itself.

As outlined in earlier chapters, there is evidence for the presence of all these mechanisms in reptiles and birds, but that no one species uses them all. In contrast to mammals, the fourth mechanism referred to above most probably does not operate in the inner ear of most reptiles. In birds and Crocodilia, however, it may indeed play an important role.

14.9.1 Electrical Tuning

As described in Chapters 2, 6 and 10, electrical tuning is likely to be a primordial property of hair cells and their derivatives, the electroreceptors and of all nerve-cell membranes which contain appropriate combinations of ion channels. In tonic electroreceptors, there is no additional electrical reaction of the cell to the

DC stimuli. In contrast, phasic receptors, some of which show a tuning like that of hair cells (Bennett and Clusin, 1979; Hopkins, 1976; Viancour, 1979), show a membrane tuning involving not only the passive membrane properties of the cell (especially the large capacitance), but also ion channels. As already noted, the presence of the combination of a voltage-sensitive Ca^{2+} conductance and a Ca^{2+} sensitive K^+ conductance can produce a resonance whose properties can explain the frequency selectivity of hair cells. The variations in the number and the kinetics of these channels are thought to be responsible for the different CFs of cells, at least in the frog sacculus and the turtle basilar papilla (Sect. 2.4.2; Art et al., 1986; Ashmore and Attwell, 1985; Crawford and Fettiplace, 1981 a; Fettiplace, 1987; Hudspeth, 1985, 1986). Recently, it has also been shown that such channels are found in low-CF hair cells of the alligator (Evans and Fuchs, 1987) and the chicken (Fuchs, 1988). In the latter, the channel kinetics also suggest a role of electrical tuning in the frequency selectivity of avian hair cells.

The presence of preferred intervals in spontaneous activity and of a temperature sensitivity in the tuning of primary auditory fibres provides strong evidence for the presence of electrical tuning in many nonmammalian hair cells, at least at low CF (Sect. 6.1.3, 6.1.5, 10.2.1 and 13.4.1; Eatock and Manley, 1981; Klinke, 1979; Manley, 1979, 1981, 1986; Manley and Gleich, 1984). At least in some cases, all or a major part of the peripheral tuning mechanism resides in the properties of individual cell membranes of the sensory cells. However, preferred intervals have not been reported in primary auditory afferents in a number of nonmammals, such as the alligator lizard (Ch. 7) the caiman (Ch. 12), and the bobtail lizard (Ch. 11), so this mechanism may not be universally present. In the caiman, however, there is evidence that the hair cells contain appropriate cell-membrane channels (Evans and Fuchs, 1987).

At least in the bobtail lizard, such preferred intervals may not be seen due to the fact that each nerve fibre innervates several hair cells, which are unlikely to have their membrane oscillations synchronized. In the papilla of the tokay gecko (Ch. 10), which is equally large, preferred intervals are found at CFs below 500 Hz. Assuming that these frequencies are localized in the unidirectional area and assuming the innervation pattern is the same as in the related gecko *Coleonyx*, then they are found in nerve fibres that innervate only one hair cell (exclusive innervation; Sect. 14.3).

In mammals, no evidence exists for electrical tuning of the kind described above. A temperature-dependent CF shift was not seen for any mammalian auditory units (Gummer and Klinke, 1983); there are no reports of preferred intervals in the spontaneous activity of primary auditory-nerve fibres or of 'ringing' responses in single mammalian hair cells (Russell et al., 1986). Thus it appears that electrical tuning is restricted to nonmammalian auditory organs and, even there, it may not be universally present. There are indications (see Sect. 14.10 below) that in representatives of each of the three groups: reptiles, birds and mammals, there is a difference between low-CF and high-CF frequency analysis. Even though it is a tempting idea, it is unlikely that this is always due to electrical tuning playing an important role at low frequencies.

One important feature of electrical tuning to be investigated in future research concerns the factors which might limit its frequency response. The

highest limits found for indicators of electrical tuning are in the preferred intervals in the spontaneous activity of primary auditory-nerve fibres in birds, where limits near 1.5 kHz (Manley et al., 1985) and 2.5 kHz (Temchin, 1988) have been found. It is certainly possible that the time 'jitter' of the hair-cell synapse degrades the transmission of hair-cell potentials, so that in avian *hair cells* the frequency limit may be higher. In the available hair-cell recordings from other species, the limit generally lies below 1 kHz (red-eared turtle, frog sacculus), a difference which is probably mainly related to these experiments being carried out at room temperature. As low-frequency tuning in non-mammals is temperature-dependent (up to one octave/10 °C; Sects. 10.3, 12.5, 13.4.5.4), the theoretical upper limit of electrical tuning in red-eared turtle hair cells at an avian temperature (40 °C) would be above 1.5 kHz. It remains to be investigated to what extent the basic phenomena underlying sharp electrical filtering (e.g., the kinetics of the K^+ channels and the increasing number of Ca^{2+} channels required at higher CFs; Fettiplace, 1987) provide built-in frequency limitations making it necessary for higher CFs to be analyzed using other, micromechanical phenomena.

14.9.2 Hair Cell Micromechanics

The situation with regard to mechanical tuning is much more complex than with electrical tuning, for there is a variety of mechanical structures that can play a role in tuning – the basilar and tectorial membranes and the hair-cell stereovillar bundles being the most obvious candidates. The presence of obvious gradients in the structural parameters of hair-cell stereovillar bundles in all species examined in this respect has led to the expectation that in all hair cells, the mechanical properties of the stereovillar bundle will play an important role in frequency selectivity. This would be true irrespective of the presence or absence of, e.g., a tectorial membrane. Thus many models attempt to explain both the frequency selectivity as such and the tonotopic organization of papillae partly on the basis of mathematical examination of the intuitive expectations resulting from the properties of mechanical resonances of these structures (e.g. Crawford and Fettiplace, 1985; Manley et al., 1988 d; Nielsen and Turner, 1983; Rosowski et al., 1985; Turner and Nielsen, 1983; Weiss and Leong, 1985 a,b; Weiss et al., 1985). In all cases, there are few data available on direct measurements of the stiffness of hair-cell bundles and other important parameters, so that some of the values used in calculations are little more than intelligent guesses. In some cases, motion of the stereovillar bundle is conceived as being brought about by fluid coupling of the bundle to the endolymph (alligator lizard; Weiss and Leong, 1985 a); for free-standing bundles, the degree of coupling would vary with the bundle length and its mechanical properties. In those cases where the motion of free-standing bundles of different cells in vitro has been found to correlate with the lengths of their stereovillar bundles (that is, the longer the bundle, the lower the CF), it has been assumed that the length-dependent mechanical tuning of the bundles partly or solely determines the frequency selectivity and tonotopic organization of that part of the papilla (Ch. 7; Frishkopf and DeRosier, 1983; Holton and Hudspeth, 1983).

In other cases, the mass of the tectorial membrane certainly strongly influences the resonant frequencies of hair cells or groups of hair cells. This can be seen in the very different height of stereovillar bundles in neighbouring regions of the alligator lizard papilla which respond to very similar frequencies near 1 kHz, depending on whether they are connected to a tectorial membrane (apical area, height about 7 μm) or not (apical end of basal area, height about 37 μm; see Sect. 7.3). It is worth noting that the absolute height of the stereovilli between different hair cells along an area without a tectorial membrane is substantially greater than for those under a tectorial membrane. Thus, the highest-CF and lowest-CF cells of the alligators lizard's BDT area ('free-standing') have 12-μm and 37-μm-long bundles, respectively: a prolongation of such an area to very low frequencies (and therefore substantially longer bundles) is hardly conceivable. The same frequency range in the bobtail lizard basal area (under a tectorial membrane) is coded by hair cells whose bundle heights range from 5.5 to 14 μm. In itself providing mass and in its ability to link the micromechanical responses of a number of hair cells, the tectorial membrane thus plays an vital role in reducing the absolute height of the bundles of hair cells responding to different frequencies, thus extending the total frequency spectrum able to be coded within the mechanically possible range of bundle heights.

It is probable, however, that there are usually influences from the cell body on the properties of the hair-cell bundle. For example, Crawford and Fettiplace (1985) produced evidence that the bundle resonance in the red-eared turtle is dependent on an active contribution of the cell body. Thus all frequency-selectivity mechanisms that are more or less dependent on the properties of the stereovillar bundles (Sect. 14.9.2–4) cannot be regarded as resulting from purely passive mechanical characteristics. Whether there are such large and fundamental differences between the red-eared turtle hair cells, which have a strong electrical resonance, and the alligator-lizard hair cells which apparently do not, remains to be seen. At the moment it is unclear to what extent the obvious correlation between stereovillar bundle length and CF can be regarded as the only causal relationship underlying the frequency response and the tonotopic organization. As noted in Section 7.4, however, the relationship between the range of stereovillar heights in the high-CF regions of the papillae of the alligator lizard *Gerrhonotus* and granite spiny lizard *Sceloporus* are not the same, although the CF ranges are identical. Thus, there are certainly subtle, species-specific factors involved in the mechanical resonances of the bundles.

14.9.3 Interaction of Hair Cell Groups with the Tectorial Membrane

The role of the tectorial membrane has, in part, been discussed above (see Sect. 14.4). In the bobtail lizard, we (Manley et al., 1988 d) suggested an important role of groups of hair cells together with the salletal units of the tectorial membrane in neural sharpening (Ch. 11, Figs. 11.17, 11.18). In this animal, structural parameters such as the mass of the tectorial membrane sallets and of the bundle length are strongly correlated with the CF of different locations on the basal papilla area. Details of these morphological variations, such as the number of hair cells per sallet, the number of stereovilli in their bundles and the mass of

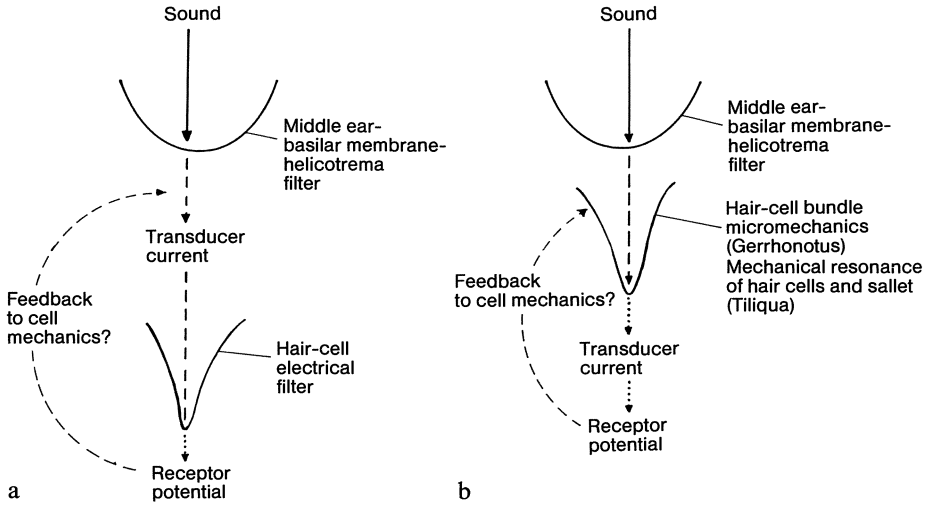

Fig. 14.2. Diagram to illustrate current thinking about the differences between the sites of frequency selectivity in *a* the turtle and *b* the high-CF cells in the alligator lizard (*Gerrhonotus*) and the bobtail lizard (*Tiliqua*). The sound input is first broadly filtered by the mechanics of the middle ear, basilar membrane and, possibly, the connection between scala vestibuli and tympani (helicotrema). In *b*, there is a narrower mechanical filter *before*, in *a*, the narrow filter is *after* the production of transducer current. There may, however, be feedback from the resulting receptor potential into the hair cell's micromechanics

the associated sallet were used in a calculation of the resonant frequency of individual locations along the salletal chain. For this purpose, estimates of the bundle stiffness were derived from measured values from the red-eared turtle. Using these data and assuming the resonant frequency to be only dependent on the mass and the stiffness, we were successful in closely modelling the range and gradient of frequencies along the basal segment of the bobtail papilla (Manley et al., 1989 b. The actual form of individual tuning curves in the bobtail skink was only well matched when it was assumed that neighbouring hair cells were in some way linked; this linkage occurs via the tectorial membrane. As mentioned above, in *Gekko,* part of the tectorial structure has an even finer salletal structure (170 sallets along a similar length of papilla to that in *Tiliqua,* with 80 sallets). The $Q_{10\ dB}$ of *Gekko* primary auditory nerve fibres are on average substantially higher than those of *Tiliqua* (see Sect. 11.2.1 and 10.2.2).

It is not possible at the present time to present a fully integrated explanation of the relative importance of active mechanical input from the hair cells (how much does this influence the stiffness of the stereovilli?), passive resonances of the stereovillar bundles alone or resonances together with the tectorial membrane. In the assumptions behind the bobtail-lizard model at least, although the mass of the tectorial structures varies along the basal segment to which the model applies, the *presence* of the mass over the hair cells is necessary to bring the entire spectrum of resonance frequencies into a reasonable range. In that model, the stereovillar-bundle stiffness was assumed to be as in the red-eared turtle, where its resonance is known to depend on influences from the cell body.

As is evident above, the mixture of tuning mechanisms in the various reptile groups is not the same. In Fig. 14.2, an attempt has been made to compare and contrast the location of the origin of tuning in three reptile species, the red-eared turtle and the high-CF areas of both the alligator lizard and the bobtail skink. In the first case, electrical tuning directly or indirectly (via control of cell mechanical properties) dominates the tuning. In the latter two species, the tuning is mechanical, determined either almost exclusively by the stereovillar bundle (alligator lizard) or by the resonance of a group of bundles and a tectorial mass (bobtail lizard). Again, bundle stiffness may well be under the active control of the cell. One very important difference is that in the turtle, the transduction current arises *before* the tuning; in the other species, it arises *after* the tuning mechanism has been effective.

14.9.4 Interactions Between Hair Cells and Basilar Membrane

The early observations of von Békésy (1960) that the basilar membrane of mammals and of the chicken support a travelling wave have had a powerful influence on thinking about frequency analysis in the cochlea. There is, however, increasing evidence that in mammals, the normal motion of the basilar membrane-organ of Corti complex is strongly influenced by rapid active processes in the hair cells – at least in the outer hair cells – themselves (for references see e.g., Ashmore, 1986; Manley, 1986; Pickles, 1985). While it is not the purpose of this book to include a discussion of hearing processes in mammals, it is in regard to frequency selectivity that comparative auditory physiology can make its greatest contribution to our understanding of the mammalian hearing organ, for there is no doubt that at least some of the mechanisms of frequency selectivity are common to more than one vertebrate group.

It is not clear at the present time whether there is a relationship between the force-generating mechanism observed in turtle hair cells and those – fast and slow – observed in mammalian outer hair cells (Ashmore, 1986; Brownell, 1986; Crawford and Fettiplace, 1985; Zenner et al., 1985). It is, however, clear that hair-cell activity contributes much to the amplitude of motion of the normal mammalian basilar membrane. In the mammalian cochlea, this kind of interaction between the outer hair cells and the basilar membrane is one which requires a large number of hair cells (Manley, 1986). The question of the amount of space available per octave, and thus the number of hair cells per octave, has been briefly alluded to above and is discussed below (Sect. 14.10). In the typical mammal, about 2 mm are devoted to each octave (Fig. 14.3). This makes it possible for a relatively large number of hair cells, which have the same or similar frequency response, to act together and actually move, or affect the motion of, the relatively thin basilar membrane.

In most reptiles, the basilar membrane is thick and the number of hair cells responding at any one small frequency band is often extremely small, so that it would not be expected that they could actually move the basilar membrane in a similar frequency-selective motion pattern to that in mammals. It now seems likely that, contrary to the concept which has dominated auditory physiology since Békésy, the basilar membrane makes little contribution to the frequency selec-

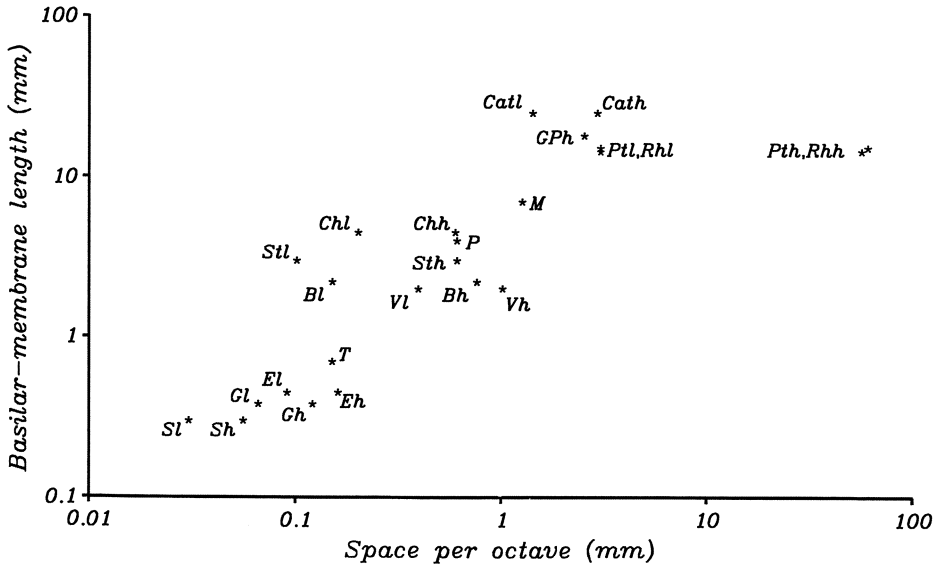

Fig. 14.3. The amount of space along the basilar papilla devoted to one octave for various vertebrates as a function of the total length of the papilla (*asterisks*). It is obvious that the amount of space is smallest in some reptiles, next largest in birds and in reptiles with well-developed papillae and largest in some mammals. In some species, the figures are given both for the low-frequency (suffix: *l*) and high-frequency areas (suffix: *h*) of the papilla. The abbreviations are as follows: *Catl, Cath* cat; *GPh* guinea pig; *Rhl, Rhh* Rhinolophus; *Ptl, Pth* Pteronotus (for the two constant-frequency bats; the "h" figure is for the specialized acoustic fovea area of the cochlea); *M* mouse; *Chl, Chh* chicken; *P* pigeon; *Stl, Sth* starling; *Bl, Bh* bobtail lizard; *Vl, Vh* monitor lizard; *T* red-eared turtle; *El, Eh* European lizards (*Podarcis*); *Gl, Gh* alligator lizard; *Sl, Sh* granite spiny lizard

tivity of hair-cell motion in, e.g., lizards (see Ch. 7 and 11), and in mammals the motion is a complex one involving feedback from hair cells which apparently substantially increases the displacement of the basilar membrane. In birds and in *Caiman*, the situation may be intermediate. Our newer experiments marking single avian nerve fibres (Gleich, 1988; Manley et al., 1989 a) indicate that it is not unreasonable to expect a similar hair-cell population interaction in birds as in mammals. Although there is a large number of hair cells across the papilla in birds (so that if they can also produce active movement there would be enough driving cells), the space/octave is less and the basilar membrane is thick. There is only a crude equivalent of the travelling wave of mammals (Sect. 13.2).

It seems that only the mammals have achieved the spacial prerequisites for perfecting to a high level this mechanism of tuning based on the influence of one hair-cell population on the motion of the basilar membrane-organ of Corti complex. In extreme cases, the amount of space devoted to a small frequency range is enormous – for example in some bats with cochlear regions specialized for the analysis of narrow frequency bands, the distribution of CFs can reach 60 mm/octave (Manley, 1986)! It is probable that the necessity of producing more space to accommodate this tuning mechanism led to the development of an

organ of Corti of disproportionate length as compared to the papillae of non-mammals.

14.10 Below and Above 1 kHz

The scheme outlined above in Section 14.8 helps to explain the great diversity in tonotopic arrangements seen in the lizards. Given that all lizard papillae respond roughly to the same range of frequencies, but there is great variation in papillar length, there may be great variation in frequency resolution. If we calculate how much space (and therefore, how many hair cells) is devoted to one octave on each papilla, we find that there are very substantial differences between species (Fig. 14.3). Thus in the granite spiny lizard, less than 0.05 mm are devoted to one octave; this represents a row of fewer than 5 hair cells! Corresponding figures for the alligator lizard and the turtle are 0.1 and 0.13 mm, respectively (Manley, 1986). In some more advanced reptilian papillae, the length of the papilla devoted to one octave is closer to the values known for birds. Thus in the bobtail skink, 0.5 mm code on average a one-octave frequency range. Corresponding values for the pigeon, starling and chicken (high-CF area) are only slightly higher (Ch. 13). Typical values for mammals are nearer 2 mm/octave.

The amount of space devoted to one octave is not, however, constant along the entire papilla. Although we have relatively little data for reptiles, it appears as if less space is devoted to octaves below about 1 kHz than to those above 1 kHz. Thus, data on various reptile papillae indicate the following approximate mapping constants:

Species	CFs < 1 kHz	CFs > 1 kHz
Sceloporus (granite spiny lizard)	30 μm/oct.	55 μm/oct.
Gerrhonotus (alligator lizard)	65 μm/oct.	120 μm/oct.
Podarcis (European lizards)	100 μm/oct.	250 μm/oct.
Chrysemys (red-eared turtle)	135 μm/oct.	–
Tiliqua (bobtail skink)	150 μm/oct.	750 μm/oct.
Varanus (monitor lizard)	390 μm/oct.	1000 μm/oct.

In no case is it clear to what extent the slopes change sharply at the border of morphologically-distinct areas, whether a more gradual change is present or whether there is even overlap of frequency ranges. It is even likely that in most lizards, as in *Tiliqua,* the low frequencies are mapped *across* the papilla, as there is evidence in some lizard species that morphological properties of the stereovillar bundle also change across (instead of along) the papilla in the low-CF area. Definitive statements will have to await more exact mapping of the papillae.

The same phenomenon is seen in maps of the chick papilla (Manley et al., 1987 a), the starling papilla (Gleich, 1988) and the cat organ of Corti (Liberman, 1982 b). This is true even though in these species there is no obvious anatomical break between low- and high-frequency areas as there is in the lizards (see Ch. 13;

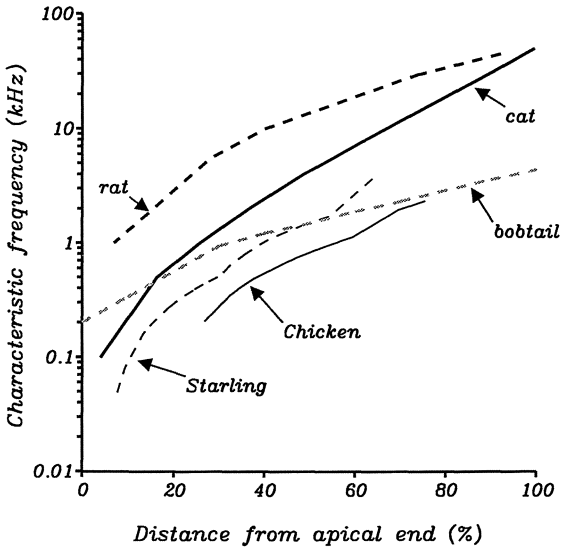

Fig. 14.4. A comparison of the tonotopic organization of the hearing organs of various vertebrates, expressed as the distribution of CFs of primary auditory nerve fibres from apex to base of the auditory papilla. Data for the chick and the starling (see Ch. 13) and the bobtail lizard (see Ch. 11), but also for the cat (Sect. 14.10) are derived from direct mapping techniques using single-fibre staining. In order to more easily compare papillae of different lengths, the values are given as a percentage of each papillar length. In all cases, less space is devoted to low-frequency octaves (After various authors)

Fig. 14.4). This remarkable parallel across vertebrate groups reinforces the impression gained from other data (e.g. pattern of $Q_{10\,dB}$ across frequencies, presence of preferred intervals at low freguencies) that the collection of mechanisms responsible for frequency selectivity in low-CF cells is different from the mechanisms in high-CF cells (Manley et al., 1988 a).

In the red-eared turtle, the function relating the CF of nerve fibres to their sharpness of tuning (Sect. 6.1.5) indicates that the tuning curves have an approximately constant 10 dB bandwidth of near 125 Hz. The rate of increase of $Q_{10\,dB}$ with CF is thus much steeper than on average in other reptiles. However, it appears that in the bobtail lizard and perhaps other species, the rate of increase of tuning sharpness with CF is also steeper at CFs below 1 kHz, becoming much slower at higher CFs (Fig. 11.9). The possibility of an intrinsic upper frequency limitation in electrical tuning mechanisms and the resulting necessity of switching to micromechanical mechanisms for the analysis of higher CFs has been mentioned in Section 14.9.1. In contrast to the reptiles and birds, the mechanisms underlying this putative difference in mammals are, however, unknown. As recently shown in the bobtail and the alligator lizard, phase-locked timing information is present in low-CF fibres. The usage of this information in low-CF fibres would provide an adequate explanation for the small amount of space devoted to low-frequency octaves in the vertebrate cochlea. This concept was fundamental to the early 'volley' theory of hearing, which was thought of as an alternative to the 'place' theory of von Békésy.

References

Anastasio TJ, Correia MJ, Perachio AA (1985) Spontaneous and driven responses of semicircular canal primary afferents in the unanaesthetized pigeon. J Neurophysiol 54:335–347

Anderson DJ, Rose JE, Brugge JF (1971) Temporal position of discharges in single auditory nerve fibers within the cycle of a sine-wave stimulus: frequency and intensity effects. J Acoust Soc Amer 49:1131–1139

Art JJ, Fettiplace R (1984) Efferent desensitization of auditory nerve fibre responses in the cochlea of the turtle *Pseudemys scripta elegans*. J Physiol 356:507–523

Art JJ, Fettiplace R (1987) Variation in membrane properties in hair cells isolated from the turtle cochlea. J Physiol 385:207–242

Art JJ, Crawford AC, Fettiplace R, Fuchs PA (1982) Efferent regulation of hair cells in the turtle cochlea. Proc R Soc Lond B 216:377–384

Art JJ, Fettiplace R, Fuchs PA (1984) Synaptic hyperpolarization and inhibition of turtle cochlear hair cells. J Physiol 356:525–550

Art JJ, Crawford AC, Fettiplace R, Fuchs PA (1985) Efferent modulation of hair cell tuning in the cochlea of the turtle. J Physiol 360:397–421

Art JJ, Crawford AC, Fettiplace R (1986) Electrical resonance and membrane currents in turtle cochlear hair cells. Hearing Res 22:31–36

Ashmore JF (1983) Frequency tuning in a frog vestibular organ. Nature 304:536–538

Ashmore JF (1986) The cellular physiology of isolated outer hair cells: implications for cochlear frequency selectivity. In: Moore B C J, Patterson R D (eds) Auditory frequency selectivity. Plenum, New York, pp 103–108

Ashmore JF, Attwell, D (1985) Models for electrical tuning in hair cells. Proc R Soc B 226:325–344

Ashmore JF, Russell IJ (1983) The physiology of hair cells. In: Lewis B (ed) Bioacoustics, a comparative approach. Academic Press, London, pp 149–180

Baden-Kristensen K, Weiss TF (1983) Receptor potentials of lizard hair cells with free-standing stereocilia. J Physiol 335:699–721

Bagger-Sjöbäck D (1976) The cellular organization and nervous supply of the basilar papilla in the lizard, *Calotes versicolor*. Cell Tiss Res 165:141–156

Bagger-Sjöbäck D, Wersäll J (1973) The sensory hairs and tectorial membrane of the basilar papilla in the lizard *Calotes versicolor*. J Neurocytol 2:329–350

Bagger-Sjöbäck D, Wersäll J (1976) Toxic effects of gentamicin on the basilar papilla in the lizard *Calotes versicolor*. Acta Otolaryngol 81:57–65

Baird IL (1960) A survey of the periotic labyrinth in some representative recent reptiles. Univ Kansas Sci Bull 41:895–981

Baird IL (1970) The anatomy of the reptilian ear. In: Gans C, Parsons TS (eds) Biology of the Reptilia Vol 2. Academic Press, New York, London, pp 193–275

Baird IL (1974) Anatomical features of the inner ear in submammalian vertebrates. In: Keidel W D, Neff W D (eds) Handbook of Sensory Physiology Vol V/1. Springer, Berlin Heidelberg New York, pp 159–212

Beagley HA (1979) Auditory Investigation: the Scientific and Technological Basis. Clarendon Press, Oxford

Békésy G von (1960) Experiments in Hearing. (Wever E G, trans) McGraw-Hill, New York

Bennett MVL (1970) Comparative physiology: electric organs. Ann Rev Physiol 32:471–528

Bennett MVL (1971) Electrolocation in fish. Ann N Y Acad Sci 188:242–269

Bennett MVL, Clusin WT (1979) Transduction at electroreceptors: origins of sensitivity. In: Cone RA, Dowling JE (eds) Membrane transduction mechanisms, Raven, New York, pp 91–116
Berger K (1924) Experimentelle Studien über Schallperzeption bei Reptilien. Z Vgl Physiol 1:517–540
Boord RL, Rasmussen GL (1963) Projection of the cochlear and lagenar nerves on the cochlear nuclei of the pigeon. J Comp Neurol 120:463–471
Brix J, Kaiser A (1988) Peripheral hearing properties in chicks do not change during post-hatching development. In: Elsner N, Barth FG (eds) Sense Organs: Interfaces between Environment and Behaviour. Thieme, Stuttgart, p 180
Brownell WE (1986) Outer hair cell motility and cochlear frequency selectivity. In: Moore BCJ, Patterson RD (eds) Auditory frequency selectivity. Plenum, New York, pp 109–118
Campbell HW (1969) The effects of temperature on the auditory sensitivity of lizards. Physiol Zool 42:183–210
Carroll RL (1977) The origin of lizards. In: Andrews SM, Miles RS and Walker AD (eds) Problems in Vertebrate Evolution. Linnean Soc. Symp. Series No. 4, pp 359–396
Carroll RL (1987) Vertebrate Palaeontology and Evolution. Freeman, New York
Chandler JP (1984) Light and electron microscopic studies of the basilar papilla in the duck, *Anas platyrhynchos*: I. The hatchling. J Comp Neurol 222:506–522
Chen CS, Anderson LM (1985) The inner ear structures of the echidna – an SEM study. Experientia 41 : 1324-1326
Coles RB, Guppy A (1988) Directional hearing in the barn owl (*Tyto alba*). J Comp Physiol A 163:117–133
Coles RB, Lewis DB, Hill KG, Hutchings ME, Gower DM (1980) Directional hearing in the Japanese quail (*Coturnix coturnix japonica*) II. Cochlear physiology. J Exp Biol 86:153–170
Corey DP, Hudspeth AJ (1979 a) Ionic basis of the receptor potential in a vertebrate hair cell. Nature 281:675–677
Corey DP, Hudspeth AJ (1979 b) Response latency of vertebrate hair cell. Biophys J 26:499–506
Corey DP, Hudspeth AJ (1983) Analysis of the microphonic potential of the bullfrog's sacculus. J Neurosci 3:942–961
Cotanche DA, Saunders JC, Tilney LG (1987) Hair cell damage produced by acoustic trauma in the chick cochlea. Hearing Res 25:267–286
Counter SA, Tsao P (1986) Morphology of the seagull's inner ear. Acta Otolaryngol 101:34–42
Cousillas H, Rebillard G (1985) Age-dependent effects of a pure tone trauma in the chick basilar papilla: evidence for a development of the tonotopic organization. Hearing Res 19:217–226
Crawford AC, Fettiplace R (1978) Ringing responses in cochlear hair cells of the turtle. J Physiol 284:135P
Crawford AC, Fettiplace R (1980) The frequency selectivity of auditory nerve fibres and hair cells in the cochlea of the turtle. J Physiol 306:79–125
Crawford AC, Fettiplace R (1981 a) An electrical tuning mechanism in turtle cochlear hair cells. J Physiol 312:377–412
Crawford AC, Fettiplace R (1981 b) Non-linearities in the responses of turtle hair cells. J Physiol 315:317–338
Crawford AC, Fettiplace R (1983) Auditory nerve responses to imposed displacements of the turtle basilar membrane. Hearing Res 12:199–208
Crawford AC, Fettiplace R (1985) The mechanical properties of ciliary bundles of turtle cochlear hair cells. J Physiol 364:359–379
Davis H (1968) Mechanisms of the inner ear. Ann Otol Rhinol Laryngol 77:644–656
Denison RH (1966) The origin of the lateral-line sensory system. Amer Zool 6:369–370
Duifhuis H, Horst JW, Wit HP (1988) Basic Issues in Hearing. Academic Press, London
Eatock RA, Manley GA (1976) Temperature effects on single auditory nerve fiber responses. J Acoust Soc Amer 60:S80

Eatock RA, Manley GA (1981) Auditory nerve fibre activity in the tokay gecko: II, temperature effect on tuning. J Comp Physiol A 142:219–226
Eatock RA, Weiss TF (1986) Relation of discharge rate to sound-pressure level for cochlear nerve fibres in the alligator lizard. Abstracts 9th Mtg. Assoc Res Otolaryngol, pp 63–64
Eatock RA, Corey DP, Hudspeth AJ (1979) Adaptation in a vertebrate hair cell: stimulus-induced shift of the operating range. Soc Neurosci Abstr 5:19
Eatock RA, Manley GA, Pawson L (1981) Auditory nerve fibre activity in the tokay gecko: I, implications for cochlear processing. J Comp Physiol A 142:203–218
Eatock RA, Corey DP, Hudspeth AJ (1987) Adaptation of mechanoelectrical transduction in hair cells of the bullfrog's sacculus. J Neurosci 7:2821–2836
Estes R, Pregill G (eds) (1988) Phylogenetic relationships of the lizard families. Stanford University Press, Stanford, CA
Evans MG, Fuchs PA (1987) Tetrodotoxin-sensitive, voltage-dependent sodium currents in hair cells from the alligator cochlea. Biophys J 52: 649–652
Fay RR, Popper, AN (1980) Structure and function in teleost auditory systems. In: Popper AN and Fay RR (eds) Comparative studies of hearing in vertebrates. Springer, Berlin Heidelberg New York, pp 3–42
Fengler R, Klinke R, Pause M, Smolders J (1978) Reverse correlation in primary auditory fibres of the caiman. Pflügers Archiv 373:R85
Fettiplace R (1987) Electrical tuning of hair cells in the inner ear. Trends Neurosci 10:421–425
Fettiplace R, Crawford AC (1978) The coding of sound pressure and frequency in cochlear hair cells of the terrapin. Proc R Soc Lond B 203:209–218
Fettiplace R, Crawford AC (1980) The origin of tuning in turtle cochlear hair cells. Hearing Res 2:447–454
Firbas W, Müller G (1983) The efferent innervation of the avian cochlea. Hearing Res 10:109–116
Fischer FP, Köppl C, Manley, G (1988) The basilar papilla of the barn owl *Tyto alba*: A quantitative morphological SEM analysis. Hearing Res 34:87–101
Fleischer, G (1978) Evolutionary principles of the mammalian middle ear. Adv Anat Embryol Cell Biol 55:6–70
Flock A (1965) Transducing mechanisms in the lateral line canal organ receptors. Cold Spring Harbor Symp Quant Biol 30:133–145
Flock A (1967) Ultrastructure and function in the lateral line organs. In: Cahn P (ed) Lateral line detectors. Indiana University Press, Bloomington, pp 163–197
Flock A (1971) The lateral-line organ mechanoreceptors. In: Hoar WS, Randall DJ (eds) Fish physiology Vol. 5, Academic Press, New York, pp 241–263
Flock A, Russell IJ (1976) Inhibition by efferent nerve fibres: action on hair cells and afferent synaptic transmission in the lateral-line canal organ of the burbot, *Lota lota*. J Physiol Lond 257:45–62
Flock A, Jorgensen M, Russell I (1973) The physiology of individual hair cells and their synapses. In: Moller A R (ed) Basic mechanisms in hearing. Academic Press, New York, pp 273–302
Flock A, Flock B, Murray E (1977) Studies on the sensory hairs of receptor cells in the inner ear. Acta Otolaryngol 83:85–91
Flock A, Cheung HC, Flock B, Utter G (1981) Three sets of actin filaments in sensory cells of the inner ear: Identification and functional orientation determined by gel electrophoresis, immunofluorescence and electron microscopy. J Neurocytol 10:133–147
Frankenberg E (1975) Distress calls of gekkonid lizards from Israel and Sanai. Isr J Zool 24:43–53
Frezza WA (1976) Spontaneous activity in the auditory nerve of the alligator lizard. B. Sc. thesis, Dept Electr Eng, Mass Inst Technology
Frishkopf LS, DeRosier DJ (1983) Mechanical tuning of free-standing stereociliary bundles and frequency analysis in the alligator lizard cochlea. Hearing Res 12:393–404
Fritzsch B (1987) Inner ear of the coelacanth fish *Latimeria* has tetrapod affinities. Nature 327:153–154

Fritzsch B, Wake MH (1988) The inner ear of gymnophione amphibians and its nerve supply: A comparative study of regressive events in a complex sensory system (Amphibia, Gymnophiona). Zoomorphol 108:201–217
Fuchs PA, Mann AC (1986) Voltage oscillations and ionic currents in hair cells isolated from the apex of the chick cochlea. J Physiol 371:31P
Fuchs PA, Fettiplace R, Crawford AC (1983) Synaptic hyperpolarization and loss of tuning in turtle cochlear hair cells. In: Klinke R, Hartmann R (eds) Hearing – Physiological Bases and Psychophysics. Springer, Berlin Heidelberg New York Tokyo, pp. 25–31
Fuchs PA, Nagai T, Evans MG (1988) Electrical tuning in hair cells isolated from the chick cochlea. J. Neurosci 8:2460–2467
Furukawa T (1978) Quantal analysis of the size of excitatory post-synaptic potentials at synapses between hair cells and afferent nerve fibres in goldfish. J Physiol 276:211–226
Garrick LD, Lang JW, Herzog HA (1978) Social signals of adult American alligators. Bull Amer Mus Nat Hist 160:153–192
Gaudin EP (1968) On the middle ear of birds. Acta Otolaryngol 65:316–326
Geisler CD (1981) A model for discharge patterns of primary auditory-nerve fibers. Brain Res 212:198–201
Gleich O (1987 a) Evidence for electrical tuning in the starling inner ear. In: Elsner N, Creutzfeldt O (eds) New Frontiers in Brain Research. Thieme, Stuttgart, p 101
Gleich O (1987 b) Electrical tuning in the avian inner ear. Abstracts 10th Mtg. Assoc Res Otolaryngol, p. 22
Gleich O (1988) Untersuchungen zur funktionellen Bedeutung der Haarzelltypen und ihrer Innervationsmuster im Hörorgan des Staren. Thesis, Institut für Zoologie, Technische Universität München
Gleich O, Manley GA (1987) Peripheral origin of functionally-characterized cochlear ganglion cells in the starling. Inner Ear Biology, Nijmegen, p 84
Gleich O, Manley GA (1988) Quantitative morphological analysis of the sensory epithelium of the starling and pigeon basilar papilla. Hearing Res, 34:69–86
Gleich O, Narins PM (1988) The phase response of primary auditory afferents in a songbird (*Sturnus vulgaris L.*). Hearing Res. 32:81–91
Griffiths M (1 968) Echidnas. Pergamon, Oxford
Gross NB, Anderson DJ (1976) Single unit responses recorded from the first order neuron of the pigeon auditory system. Brain Res 101:209–222
Gummer A, Klinke R (1983) Influence of temperature on tuning of primary-like units in the guinea pig cochlear nucleus. Hearing Res 12:367–380
Gummer A, Smolders JWTh, Klinke R (1986) The mechanics of the basilar membrane and middle ear in the pigeon. In: Allen JB, Hall JL, Hubbard A, Neely ST, Tubis A (eds) Peripheral auditory mechanisms, Springer, Berlin Heidelberg New York Tokyo, pp 81–88
Hamilton DW (1964) The inner ear of lizards I. Gross structure. J Morphol 115:255–271
Harris GG, Frishkopf L, Flock A (1970) Receptor potentials from hair cells of the lateral line. Science 167:76–79
Hartline PH (1971 a) Physiological basis for detection of sound and vibration in snakes. J Exp Biol 54:349–371
Hartline PH (1971 b) Mid-brain responses of the auditory and somatic vibration systems in snakes. J Exp Biol 54:373–390
Hartline PH, Campbell HW (1969) Auditory and vibratory responses in the midbrains of snakes. Science 163:1221–1223
Held H (1926) Die Cochlea der Säuger und der Vögel, ihre Entwicklung und ihr Bau. In: Bette A, von Bergmann G, Embden G, Ellinger A (eds) Handbuch der nomalen und pathologischen Physiologie mit Berücksichtigung der experimentellen Pharmakologie. Springer, Berlin, pp 467–534
Hepp-Reymond M-L, Palin J (1968) Patterns in the cochlear potentials of the tokay gecko (*Gekko gecko*). Acta Otolaryngol 65:270–292
Hildebrand, M (1974) Analysis of Vertebrate Structure. Wiley, New York

Hillery CM, Narins PM (1984) Neurophysiological evidence for a traveling wave in the amphibian inner ear. Science 225:1037–1039
Holmes RM, Johnstone BM (1984) Gross potentials recorded from the cochlea of the skink *Tiliqua rugosa*. II. Increases in metabolic rate and hearing responsiveness during austral spring. J Comp Physiol A 154:729–738
Holton T (1980) Relations between frequency selectivity and two-tone rate suppression in lizard cochlear-nerve fibres. Hearing Res 2:21:38
Holton T, Hudspeth AJ (1983) A micromechanical contribution to cochlear tuning and tonotopic organization. Science 222:508–510
Holton T, Weiss TF (1978) Two-tone rate suppression in lizard cochlear nerve fibres, relation to receptor organ morphology. Brain Res 159:219–222
Holton T, Weiss TF (1983 a) Receptor potentials of lizard cochlear hair cells with free-standing stereocilia in response to tones. J Physiol 345:205–240
Holton T, Weiss TF (1983 b) Frequency selectivity of hair cells and nerve fibres in the alligator lizard cochlea. J Physiol 345:241–260
Hopkins CD (1976) Stimulus filtering and electroreception: tuberous electroreceptors in three species of gymnotid fish. J Comp Physiol A 111:171–207
Hopson JA (1966) The origin of the mammalian middle ear. Amer Zool 6:437–450
Hotton N (1959) The pelycosaur tympanum and early evolution of the middle ear. Evolution 13:99–121
Hudspeth AJ (1982) Extracellular current flow and the site of transduction by vertebrate hair cells. J Neurosci 2:1-10
Hudspeth AJ (1985) The cellular basis of hearing: the biophysics of hair cells. Science 230:745–752
Hudspeth AJ (1986) The ionic channels of a vertebrate hair cell. Hearing Res 22:21–27
Hudspeth AJ, Corey DP (1977) Sensitivity, polarity and conductance change in the response of vertebrate hair cells to controlled mechanical stimuli. Proc Natl Acad Sci USA 74:2407–2411
Hudspeth AJ, Holton T (1986) Ensemble-variance analysis of transduction in saccular hair cells. Hearing Res 22:30
Hudspeth AJ, Jacobs R (1979) Stereocilia mediate transduction in vertebrate hair cells. Proc Natl Acad Sci USA 76:1506–1509
Hudspeth AJ, Lewis RS (1986) The ionic basis of electrical resonance in hair cells of the bullfrog's sacculus. Hearing Res 22:37
Jahnke V, Lundquist P-G, Wersäll J (1969) Some morphological aspects of sound perception in birds. Acta Otolaryngol 67:583–601
Johnstone JR, Johnstone BM (1969 a) Electrophysiology of the lizard cochlea. Exp Neurol 24:99–109
Johnstone JR, Johnstone BM (1969 b) Unit responses from the lizard auditory nerve. Exp Neurol 24:528–537
Johnstone BM, Taylor KJ (1971) Physiology of the middle-ear transmission system. J Otolaryngol Soc Aust 3:226–228
Johnstone BM, Taylor, KJ, Boyle AJ (1970) Mechanics of the guinea pig cochlea. J Acoust Soc Amer 47:504–509
Kämpfe L, Kittel R, Klapperstück J (1970) Leitfaden der Anatomie der Wirbeltiere. G. Fischer, Stuttgart
Kemp DT (1978) Stimulated acoustic emissions from the human auditory system. J Acoust Soc Amer 64:1386–1391
Khanna SM, Tonndorf J (1972) Tympanic membrane vibrations in cats studied by time-averaged holography. J Acoust Soc Amer 51:1904–1920
Kiang NYS, Watanabe T, Thomas EC, Clark LF (1965) Discharge patterns of single fibers in the cat's auditory nerve. Cambridge, Mass., MIT Press
Klinke R (1979) Comparative physiology of primary auditory neurones. In: Hoke M, de Boer E (eds) Models of the auditory system and related signal processing techniques. Scand Audiol Suppl 9:49–61
Klinke R (1986) Neurotransmission in the inner ear. Hearing Res 22:235–243

Klinke R, Hartmann R (1983) Hearing – Physiological Bases and Psychophysics. Springer, Berlin Heidelberg New York Tokyo
Klinke R, Pause M (1980) Discharge properties of primary auditory fibres in *Caiman crocodilus*; comparisons and contrasts to the mammalian auditory nerve. Exp Brain Res 38:137–150
Klinke R, Schermuly L (1986) Inner ear mechanics of the crocodilian and avian basilar papillae in comparison to neuronal data. Hearing Res 22:183–184
Klinke R, Smolders J (1984) Hearing mechanisms in caiman and pigeon. In: Bolis L, Keynes RD, Maddrell SHP (eds) Comparative physiology of sensory systems. Cambridge Univ. Press, pp 195–211
Klinke R, Drenckhahn, Smolders J (1987) Supporting cells of the caiman inner ear contain contractile proteins. Abstracts 10th Mtg Assoc Res Otolaryngol, p 186
Klump GM, Kretzschmar E, Curio E (1986) The hearing of an avian predator and its avian prey. Behav Ecol Sociobiol 18:317–323
Konishi M (1970) Comparative neurophysiological studies of hearing and vocalizations in songbirds. Z Vgl Physiol 66:257–272
Konishi M (1973 a) Development of auditory neuronal responses in avian embryos. Proc Natl Acad Sci 70:1795–1798
Konishi M (1973 b) How the owl tracks its prey. Amer Sci 61:414–424
Konishi M (1986) How auditory space is encoded in the owl's brain. In: Cohen MJ, Strumwasser F (eds) Comparative neurobiology: modes of communication in the nervous system. John Wiley, New York, pp 335–349
Köppl C (1988) Morphology of the basilar papilla of the bobtail skink *Tiliqua rugosa*. Hearing Res 35:209–228
Köppl C, Gleich O (1988) Cobalt labelling of single primary auditory neurons – an alternative to HRP. Hearing Res 32:111–116
Köppl C, Manley GA (1987) Tonotopic organization of the basilar papilla of the bobtail skink *Tiliqua rugosa*. Abstracts 10th Mtg Assoc Res Otolaryngol, p 229
Köppl C, Manley GA, Johnstone BM (1988) Seasonal changes in the hearing of the Australian bobtail lizard *Tuliqua* – an artefact of anaesthesia level? Abstracts 11th Mtg. Assoc Res Otolaryngol, p 236
Kreithen ML, Quine DB (1979) Infrasound detection by the homing pigeon: a behavioural audiogram. J Comp Physiol 129:1–4
Kronester-Frei A (1979) The effect of changes in endolymphatic ion concentrations on the tectorial membrane. Hear Res 1:81–94
Kuhn A, Müller CM, Leppelsack H-J, Schwartzkopff J (1982) Heart rate conditioning used for determination of auditory threshold in the starling. Naturwissenschaften 69:245–246
Leake PA (1976) Scanning electron microscopy of labyrinthine sensory organs in *Caiman crocodilus*. Scaning Electron Microsc 1976:277–284
Leake PA (1977) SEM observations of the cochlear duct in *Caiman crocodilus*. Scaning Electron Microsc 2:437–444
Leppelsack H-J (1978) Unit responses to species-specific sounds in auditory forebrain centers of birds. Fed Proc 37:2336–2341
Lewis DB (1983) Directional cues for auditory localization. In: Lewis DB (ed) Bioacoustics, a comparative approach. Academic Press, London, pp 233–257
Lewis DB, Coles RB (1980) Sound localization in birds. Trends in Neurosci 3:102–105
Lewis ER, Leverenz EL, Bialek WS (1985) The vertebrate inner ear. CRC Press, Boca Raton
Lewis RS, Hudspeth AJ (1983 a) Voltage- and ion-dependent conductances in solitary vertebrate hair cells. Nature 304:538–541
Lewis RS, Hudspeth AJ (1983 b) Frequency tuning and ionic conductances in hair cells of the bullfrog's sacculus. In: Klinke R, Hartmam R (eds) Hearing – physiological bases and psychophysics. Springer, Berlin Heidelberg New York, pp 17–22
Liberman MC (1982 a) Single-neuron labeling in the cat auditory nerve. Science 216:1239–1241

Liberman MC (1982 b) The cochlear frequency map for the cat: labeling auditory-nerve fibers of known characteristic frequency. J Acoust Soc Amer 72:1441–1449
Lombard RE (1980) The structure of the amphibian auditory periphery: a unique experiment in terrestrial hearing. In: Popper AN, Fay RR (eds) Comparative studies of hearing in vertebrates. Springer, Berlin Heidelberg New York, pp 121–138
Lombard RE, Bolt JR (1979) Evolution of the tetrapod ear: an analysis and reinterpretation. Biol J Linn Soc 11:19–76
Lutz PL, Rosenthal M, Sick TJ (1985) Living without oxygen: turtle brain as a model of anaerobic metabolism. Mol Physiol 8:411–425
Manley GA (1972 a) Frequency response of the ear of the tokay gecko. J Exp Zool 181:159–168
Manley G A (1972 b) The middle ear of the tokay gecko. J Comp Physiol 81:239–250
Manley GA (1972 c) Frequency response of the middle ear of geckos. J Comp Physiol 81:251–258
Manley GA (1973) A review of some current concepts of the functional evolution of the ear in terrestrial vertebrates. Evolution 26:608–621
Manley GA (1976) Auditory responses from the medulla of the monitor lizard *Varanus bengalensis*. Brain Res 102:329–324
Manley GA (1977) Response patterns and peripheral origin of auditory nerve fibres in the monitor lizard, *Varanus bengalensis*. J Comp Physiol A 118:249–260
Manley GA (1979) Preferred intervals in the spontaneous activity of primary auditory neurones. Naturwissenschaften 66:582
Manley GA (1981) A review of the auditory physiology of the reptiles. Progr Sens Physiol 2:49–134
Manley GA (1983) Auditory nerve fibre activity in mammals. In: Lewis B (ed) Bioacoustics. Academic Press, London, pp 207–232
Manley GA (1986) The evolution of the mechanisms of frequency selectivity in vertebrates. In: Moore BCJ, Patterson RD (eds) Auditory frequency selectivity. Plenum, New York, pp 63–72
Manley GA, Johnstone BM (1974) Middle-ear function in the guinea pig. J Acoust Soc Amer 56:571–576
Manley GA, Leppelsack H-J (1977) Preliminary data on activity patterns of cochlear ganglion neurones in the starling. In: Portmann M, Aaron J-M (eds) Inner ear biology XIVth workshop. INSERM, Paris, pp 127–136
Manley GA, Gleich O (1984) Avian primary auditory neurones: the relationship between characteristic frequency and preferred intervals. Naturwissenschaften 71:592–594
Manley GA, Gleich O, Leppelsack H-J, Oeckinghaus H (1985) Activity patterns of cochlear ganglion neurones in the starling. J Comp Physiol A 157:161–181
Manley GA, Brix J, Kaiser A (1987 a) Developmental stability of the tonotopic organization of the chick's basilar papilla. Science 237:655–656
Manley GA, Schulze M, Oeckinghaus H (1987b) Otoacoustic emissions in a song bird. Hearing Res 26:257–266
Manley GA, Brix J, Gleich O, Kaiser A, Köppl C, Yates G (1988 a) New aspects of comparative peripheral auditory physiology. In: Syka J, Masterton RB (eds) Auditory Pathway – Structure and Function. Plenum, London, pp 3–12
Manley GA, Gleich O, Brix J, Kaiser A (1988 b) Functional parallels between hair-cell populations of birds and mammals. In: Duifhuis H, Horst JW, Witt HP (eds) Basic Issues in Hearing. Academic Press, London, pp 64–71
Manley GA, Köppl C, Konishi M (1988 c) A neural map of interaural intensity difference in the brainstem of the barn owl *Tyto alba*. J Neurosci 8:2665–2676
Manley GA, Yates G, Köppl C (1988 d) Auditory peripheral tuning: evidence for a simple resonance phenomenon in the lizard *Tiliqua*. Hearing Res 33:181–190
Manley GA, Yates G, Köppl C, Johnstone B M (1988 e) Response delays in auditory-nerve fibres of the bobtail lizard in the absence of a travelling wave. Abstracts 11th Mtg. Assoc Res Otolaryngol, p 241
Manley GA, Gleich O, Kaiser A, Brix J (1989 a) Functional differentiation of sensory cells in the avian auditory periphery. J Comp Physiol A, 164:289–296

Manley GA, Köppl C, Yates G K (1989 b) Micromechanical basis of highfrequency tuning in the bobtail lizard. In: Wilson JP, Kemp D (eds) Cochlear mechanisms-structure, function and models. Plenum, New York, in press
Marcellini D (1977) Acoustic and visual display behavior of gekkonid lizards. Amer Zool 17:251–260
Miller MR (1966) The cochlear duct of lizards. Proc Calif Acad Sci 33:255–359
Miller MR (1968) The cochlear duct of snakes. Proc Calif Acad Sci 35:425–476
Miller MR (1973 a) Scanning electron microscope studies of some lizard basilar papillae. Am J Anat 138:301–330
Miller MR (1973 b) A scanning electron microscope study of the papilla basilaris of *Gekko gecko*. Z Zellforsch 136:307–328
Miller MR (1978a) Scanning electron microscope studies of the papilla basilaris of some turtles and snakes. Am J Anat 151:409–435
Miller MR (1978 b) Further scanning electron microscope studies of lizard auditory papillae. J Morphol 156:381–418
Miller MR (1980) The reptilian cochlear duct. In: Popper A N, Fay R R (eds) Comparative studies of hearing in vertebrates. Springer, Berlin, Heidelberg, New York, pp 169–204
Miller MR (1981) Scanning electron microscope studies of the auditory papillae of some iguanid lizards. Am J Anat 162:55–72
Miller MR (1985) Quantitative studies of auditory hair cells and nerves in lizards. J Comp Neurol 232:1–24
Miller MR, Beck J (1988) Auditory hair cell innervational patterns in lizards. J Comp Neurol, 271:604–628
Moffat AJM, Capranica RR (1976) Effects of temperature on the response properties of auditory nerve fibres in the American toad (*Bufo americanus*). J Acoust Soc Amer 60:S80
Moffat AJM, Capranica RR (1978) Middle ear sensitivity in anurans and reptiles measured by light scattering spectroscopy. J Comp Physiol 127:97–107
Moiseff A, Konishi M (1981) The owl's interaural pathway is not involved in sound localization. J Comp Physiol 144:299–304
Moore BCJ, Patterson RD (1986) Auditory frequency selectivity. Plenum, New York
Mulroy MJ (1974) Cochlear anatomy of the alligator lizard. Brain Beh Evol 10:69–87
Mulroy MJ (1986) Patterns of afferent synaptic contacts in the alligator lizard's cochlea. J Comp Neurol 248:263–271
Mulroy MJ, Oblak TG (1985) Cochlear nerve of the alligator lizard. J Comp Neurol 233:463–472
Mulroy MJ, Williams RS (1987) Auditory stereocilia in the alligator lizard. Hearing Res 25:11–21
Mulroy MJ, Altmann DW, Weiss TF, Peake WT (1974) Intracellular electric responses to sound in a vertebrate cochlea. Nature 249:482–485
Münz H, Claas B, Fritzsch B (1984) Electroreceptive and mechanoreceptive units in the lateral line of the axolotl *Ambystoma mexicanum*. J Comp Physiol A 154:33–44
Nielsen DW, Turner RG (1983) Micromechanics of the reptilian ear. Audiology 22:530–544
Northcutt RG (1978) Forebrain and midbrain organization in lizards and its phylogenetic significance. In: Greenberg N, MacLean PD (eds) Behavior and Neurology of lizards. Bethesda, NIMH
Northcutt RG (1980) Central auditory pathways in amniotic vertebrates. In: Popper AN, Fay RR (eds) Comparative Studies of Hearing in Vertebrates. Springer, Berlin Heidelberg New York, pp 79–118
Oeckinghaus H (1985) Modulation of activity in starling cochlear ganglion units by middle-ear muscle contractions, perilymph movements and lagena stimuli. J Comp Physiol A 157:643–655
Oeckinghaus H, Schwartzkopff J (1983) Electrical and acoustical activation of the middle ear muscle in a songbird. J Comp Physiol 150:61–67

Oertel D (1985) Use of brain slices in the study of the auditory system: Spatial and temporal summation of synaptic inputs in cells in the anteroventral cochlear nucleus of the mouse. J Acoust Soc Am 78:328–333
Ohmori H (1984) Studies of ionic currents in the isolated vestibular hair cell of the chick. J Physiol 350:561–581
Ohmori H (1985) Mechano-electrical transduction currents in isolated vestibular hair cells of the chick. J Physiol 359:189–217
Olson EC (1966) The middle ear – morphological types in amphibians and reptiles. Amer Zool 6:399–419
Osborne MP, Comis SD, Pickles JO (1984) Morphology and cross-linkage of stereocilia in the guinea pig labyrinth examined without the use of osmium as a fixative. Cell Tiss Res 237:43–48
Palmer AR, Russell IJ (1986) Phase-locking in the cochlear nerve of the guinea pig and its relation to the receptor potential of inner hair cells. Hearing Res 24:1–15
Paton JA, Moffat AJM, Capranica R R (1976) Electrophysiological correlates of basilar membrane motion in the turtle. J Acoust Soc Amer 59:S46
Patterson WC (1966) Hearing in the turtle. J Aud Res 6:453–464
Peake WT, Ling A (1980) Basilar-membrane motion in the alligator lizard: its relation to tonotopic organization and frequency selectivity. J Acoust Soc Amer 67:1736–1745
Peterson SK, Frishkopf LS, Lechène C, Oman CM, Weiss TF (1978) Element composition of inner ear lymphs in cats, lizards and skates determined by electron probe microanalysis of liquid samples. J Comp Physiol 126:1–14
Pickles JO (1982) An Introduction to the Physiology of Hearing. Academic Press, London
Pickles JO (1985) Recent advances in cochlear physiology. Prog Neurobiol 24:1–42
Pickles JO, Comis SD, Osborne MP (1984) Cross-links between stereocilia in the guinea pig organ of Corti and their possible relation to sensory transduction. Hearing Res 15:103–112
Pickles JO, Brix J, Gleich O, Köppl C, Manley GA, Osborne MP, Comis SD (1988 a) The fine structure and organization of tip links on hair cell stereovilli. In: Duifhuis H, Horst JW, Witt HP (eds) Basic Issues in Hearing. Academic Press, London, pp 56–63
Pickles JO, Osborne MP, Comis SD, Köppl C, Gleich O, Brix J, Manley GA (1988 b) Tip-link organization in relation to the structure and orientation of stereovillar bundles. In: Wilson JP, Kemp D (eds) Cochlear mechanisms: structure, function and models. Plenum, New York pp 37–44
Pitchford S, Ashmore JF (1987) An electrical resonance in hair cells of the amphibian papilla of the frog *Rana temporaria*. Hearing Res. 27:75–83
Popper AN, Fay RR (1980) Comparative studies of hearing in vertebrates Springer, Berlin Heidelberg New York
Pumphrey RJ (1961) Sensory organs: hearing. In: Marshall AJ (ed) Biology and comparative physiology of birds Vol. II. Academic Press, New York, pp 69–86
Rebillard M, Pujol R (1983) Innervation of the chicken basilar papilla during its development. Acta Otolaryngol 96:379–388
Rebillard G, Rubel EW (1981) Electrophysiological study of the maturation of auditory responses from the inner ear of the chick. Brain Res 229:15–23
Reisz R (1975) *Petrolacosaurus kansensis* Lane, the oldest known diapsid reptile. Ph.D. thesis, McGill University, Montreal
Reisz R (1977) *Petrolacosaurus*, the oldest known diapsid reptile. Science 196:1091–1093
Remane A, Storch V, Welsch U (1985) Kurzes Lehrbuch der Zoologie. G. Fischer, Stuttgart
Retzius G (1884) Das Gehörorgan der Wirbeltiere II Das Gehörorgan der Reptilien, der Vögel und der Säugethiere. Samson and Wallin, Stockholm
Roberts WM, Robles L, Hudspeth AJ (1986) Correlation between the kinetic properties of ionic channels and the frequency of membranepotential resonance in hair cells of the bullfrog. In: Moore BCJ, Patterson RD (eds) Auditory frequency selectivity. Plenum, New York, pp 89–95
Robertson D (1984) Horseradish peroxidase injection of physiologically characterized afferent and efferent neurones in the guinea pig spiral ganglion. Hearing Res 15:113–121

Romer AS, Parsons TS (1977) The vertebrate body. Saunders, Philadelphia
Rose C, Weiss TF (1988) Frequency dependence of synchronization of cochlear nerve fibres in the alligator lizard: Evidence for a cochlear origin of timing and non-timing neural pathways. Hearing Res 33: 151–166
Rosowski JJ, Saunders JC (1980) Sound transmission through the avian interaural pathway. J Comp Physiol 136:183–190
Rosowski JJ, Peake WT, Lynch TJ (1984) Acoustic input-admittance of the alligator-lizard ear: nonlinear features. Hearing Res 16:205–223
Rosowski JJ, Peake WT, Lynch TJ, Leong R, Weiss TF (1985) A model for signal transmission in an ear having hair cells with free-standing stereocilia. II. Macromechanical stage. Hearing Res 20:139–155
Rosowski JJ, Carney LH, Lynch TJ, Peake, WT (1986) The effectiveness of external and middle ears in coupling acoustic power to the cochlea. In: Allen JB, Hall JL, Hubbard A, Neely ST, Tubis A (eds) Peripheral auditory mechanisms. Springer, Berlin Heidelberg New York Tokyo, pp 3–12
Rubel EW, Ryals BM (1982) Patterns of hair-cell loss in chick basilar papilla after intense auditory stimulation – expose duration and survival time. Acta Otolaryngol 93:31–41
Rubel EW, Ryals BM (1983) Development of the place principle; acoustic trauma. Science 219:512–514
Runhaar G (1988) The surface morphology of the avian tectorial membrane. Hearing Res, in press
Runhaar G, Schedler J (1988) The potassium concentration in the cochlear fluids of the chick. In: Elsner N, Barth FG (eds) Sense Organs: Interfaces between Environment and Behaviour. Thieme, Stuttgart. p 179
Rüsch A, Thurm U (1986) Passive and active deflections of ampullary kinocilia correlated with changes in transepithelial voltage. Otorhinolaryngol 48:76–80
Russell IJ, Lowe DA (1983) The effect of efferent stimulation on the phase and amplitude of extracellular receptor potentials in the lateral line system of the perch (*Perca fluviatilis*). J Exp Biol 102:223–238
Russell IJ, Sellick PM (1976) Measurement of potassium and chloride ion concentrations in the cupulae of the lateral lines of *Xenopus laevis*. J Physiol 257:245–255
Russell IJ, Richardson GP, Cody AR (1986) Mechano-sensitivity of mammalian auditory hair cells in vitro. Nature 321:517–519
Ryals BM, Rubel EW (1982) Patterns of hair-cell loss in chick basilar papilla after intense auditory stimulation – frequency organization. Acta Otolaryngol 93:205–210
Sachs MB, Kiang NY-S (1968) Two-tone inhibition in auditory-nerve fibres. J Acoust Soc Amer 43:1120–1128
Sachs MB, Lewis RH, Young ED (1974) Discharge patterns of single fibers in the pigeon auditory nerve. Brain Res 70:431–447
Sachs MB, Sinnott JM, Hienz RD (1978) Behavioral and physiological studies of hearing in birds. Fed Proc 37:2329–2335
Sachs MB, Woolf NK, Sinnott JM (1980) Response properties of neurons in the avian auditory system: comparisons with mammalian homologues and consideration of the neural encoding of complex stimuli. In: Popper AN, Fay RR (eds) Comparative studies of hearing in vertebrates. Springer, Berlin Heidelberg New York, pp 323–353
Saito N (1980) Structure and function of the avian ear. In: Popper AN, Fay RR (eds) Comparative studies of hearing in vertebrates. Springer, Berlin Heidelberg New York, pp 241–260
Sakaluk SK, Belwood JJ (1984) Gecko phonotaxis to cricket calling song: a case of satellite predation. Anim Behav 32:659–662
Sand O, Ozawa S, Magiwara S (1975) Electrical and mechanical stimulation of hair cells on the mud puppy. J Comp Physiol 102:13–26
Saunders JC (1985) Auditory structure and function in the bird middle ear: an evaluation by SEM and capacitative probe. Hear Res 18:253–268
Saunders JC, Johnstone BM (1972) A comparative analysis of middle-ear function in non-mammalian vertebrates. Acta Otolaryngol 73:353–361

Saunders JC, Coles RB, Gates R (1973) The development of auditory evoked responses in the cochlea and cochlear nuclei of the chick. Brain Res 63:59–74
Scheich H (1983) Biophysics of electroreception. In: Hoppe W, Lohmann W, Markl H, Ziegler H (eds) Biophysics. Springer, Berlin Heidelberg New York Tokyo, pp 764–776
Schermuly L, Klinke R (1985) Change of characteristic frequencies of pigeon primary auditory afferents with temperature. J Comp Physiol A 156:209–211
Schermuly L, Klinke R (1988) Single-fibre staining of infrasound-sensitive neurones in the pigeon inner ear. Syka J (ed) Pflüger's Archiv Suppl 411:R168
Schmidt B, Thurm U (1984) Structures transmitting stimulatory force to the sensory hairs (stereovilli) of the frog sacculus. Verh Dtsch Zool Ges 77:326
Schmidt RS (1963) Types of endolymphatic potentials. Comp Biochem Physiol 10:83–87
Schmidt RS, Fernandez C (1962) Labyrinthine d.c. potentials in representative vertebrates. J Cell Comp Physiol 59:311–322
Schwartzkopff J (1968) Structure and function of the ear and of the auditory brain areas in birds. In: deReuck AVS, Knight J (eds) Hearing Mechanisms in vertebrates. Little, Brown, Boston, pp 41–58
Schwartzkopff J, Winter P (1960) Zur Anatomie der Vogel-Cochlea unter natürlichen Bedingungen. Biol Zentralbl 79:607–625
Shotwell SL, Jacobs R, Hudspeth AJ (1981) Directional sensitivity of individual vertebrate hair cells to controlled deflections of hair bundles. Am N Y Acad Sci 374:1–10
Smith CA (1981) Recent advances in structural correlates of auditory receptors. Prog Sens Physiol 2:135–187
Smith CA (1985) Inner ear In: King AS, McLeland J (eds) Form and function in birds, Vol 3. Academic Press, London, pp 273–310
Smith CA, Konishi M, Schull N (1985) Structure of the bam owl's (*Tyto alba*) inner ear. Hearing Res 17:237–247
Smith HM (1960) Evolution of Chordate Structure. Holt, Rinehart, Winston, New York
Smolders JWT, Klinke R (1977) Effect of temperature changes on tuning properties of primary auditory fibres in caiman and cat. INSERM 68:125–126
Smolders JWT, Klinke R (1984) Effects of temperature on the properties of primary auditory fibres of the spectacled caiman, *Caiman crocodilus* (L.). J Comp Physiol 155:19–30
Smolders JWT, Klinke R (1986) Synchronized responses of primary auditory fibre populations in *Caiman crocodilus* (L.) to single tones and clicks. Hearing Res 24:89–103
Sneary MG (1986) The fine structure and innervational pattern of the basilar papilla in the red-eared turtle, *Chrysemys scripta elegans*. Doctoral thesis, University of California, San Francisco
Sneary MG (1987) Structural basis of auditory afferent fiber sensitivity and tuning. Abstracts 10th Mtg. Assoc Res Otolaryngol, pp 199–200
Spoendlin H (1978) The afferent innervation of the cochlea. In: Naunton RF, Fernandez C (eds) Evoked electrical activity in the auditory nervous system. Academic Press, New York, pp 3–19
Starck D (1978) Vergleichende Anatomie der Wirbeltiere, Band 1. Springer, Berlin Heidelberg New York
Starck D (1979) Vergleichende Anatomie der Wirbeltiere, Band 2. Springer, Berlin Heidelberg New York
Starck D (1982) Vergleichende Anatomie der Wirbeltiere, Band 3. Springer, Berlin Heidelberg New York
Strack G, Klinke R, Wilson JP (1981) Evoked cochlear response in Caiman crocodilus. Pflüger's Arch Suppl 391, R43
Strelioff D, Honrubia V (1978) Neural transduction in *Xenopus laevis* lateral line system. J Neurophysiol 41:432–444
Strelioff D, Flock A, Minser KE (1985) Role of inner and outer hair cells in mechanical frequency selectivity of the cochlea. Hearing Res 18:169–175
Suga N (1967) Electrosensitivity of specialized and ordinary lateral-line organs of the electric fish *Gymnotus carapo*. In: Cahn P (ed) Lateral line detectors. Indiana University Press, Bloomington, pp 395–409

Sullivan WE, Konishi M (1984) Segregation of stimulus phase and intensity coding in the cochlear nucleus of the barn owl. J Neurosci 4:1787–1799
Syka J (1988) Auditory System – Structure and Function. Plenum, London
Takasaka T, Smith CA (1971) The structure and innervation of the pigeon's basilar papilla. J Ultrastruct Res 35:20–65
Tanaka K, Smith CA (1975) Structure of the avian tectorial membrane. Ann Otol Rhinol Laryngol 84:287–297
Tanaka K, Smith CA (1978) Structure of the chicken's inner ear. Am J Anat 153:251–271
Temchin AN (1982) Acoustical reception in birds. In: Ilyichev VD, Gavrilov VM (eds) Acta XVIII Congressus Internat Ornithologicus, Moscow, August 1982
Temchin AN (1988) Discharge patterns of single fibres in the pigeon's auditory nerve. J Comp Physiol A 163:99–115
Teresi PV (1985) Hair cell innervation patterns in the papilla basilaris of the fence lizard *Sceloporus occidentalis*. Dissertation, University of California, San Francisco
Thompson KS (1966) The evolution of the tetrapod middle ear in the Rhipidistian-Amphibian transition. Amer Zool 6:379–397
Tilney LG, Saunders JC (1983) Actin filaments, stereocilia, and hair cells of the bird cochlea. I. Length, number, width, and distribution of stereocilia of each hair cell are related to the position of the hair cell on the cochlea. J Cell Biol 96:807–821
Tilney LG, Tilney MS (1986) Functional organization of the cytoskeleton. Hearing Res 22:55–77
Tilney MS, Tilney LG, DeRosier DJ (1987) The distribution of hair cell bundle lengths and orientations suggests an unexpected pattern of hair cell stimulation in the chick cochlea. Hearing Res 25:141–151
Tonndorf J, Khanna SM (1970) The role of the tympanic membrane in middle ear transmission. Ann Otol Rhinol Laryngol 79:743–754
Turner RG (1980) Physiology and bioacoustics in reptiles. In: Popper AN, Fay RR (eds) Comparative studies of hearing in vertebrates. Springer, Berlin Heidelberg New York, pp 205–237
Turner RG (1987) Neural tuning in the granite spiny lizard. Hearing Res 26:287–299
Turner RG, Nielsen DW (1983) A simple model of cochlear micromechanics in the mammal and lizard. Audiology 22:545-559
Turner RG, Shepard NT (1986) Compound action potential thresholds and tuning curves in the alligator lizard. J Acoust Soc Amer 79:1873–1882
Turner RG, Muraski AA, Nielsen DW (1981) Cilium length: Influence on neural tonotopic organization. Science 213:1519–1521.
Van Bergeijk WA (1966) Evolution of the sense of hearing in vertebrates. Amer Zool 6:371–377
Viancour TA (1979) Peripheral electrosense physiology: a review of recent findings. J Physiol Paris 75:321–333
Von Düring M, Karduck A, Richter HG (1974) The fine structure of the inner ear in *Caiman crocodilus*. Z Anat Entwicklungsgesch 145:41–65
Von Düring M, Andres KH, Simon K (1985) The comparative anatomy of the basilar papillae in birds. Fortschr Zool 30:681–685
Warchol ME, Dallos P (1987) Single unit response to very low frequency sound in the avian auditory brainstem. Abstracts 10th Mtg. Assoc Res Otolaryngol, pp 38–39
Watson DMS (1953) The evolution of the mammalian ear. Evolution 7:159–177
Weiss TF, Leong R (1985 a) A model for signal transmission in an ear having hair cells with free-standing stereocilia. III. Micromechanical stage. Hearing Res 20:157–174
Weiss TF, Leong R (1985 b) A model for signal transmission in an ear having hair cells with free-standing stereocilia. IV. Mechanoelectric transduction stage. Hearing Res. 20:175–195
Weiss TF, Rose C (1988) Stages of degradation of timing information in the cochlea: a comparison of hair-cell and nerve-fibre responses in the alligator lizard. Hearing Res 33:167–174
Weiss TF, Mulroy MJ, Altmann DW (1974) Intracellular responses to acoustic clicks in the inner ear of the alligator lizard. J Acoust Soc Amer 55: 606–619

Weiss TF, Mulroy MJ, Turner RG, Pike CL (1976) Tuning of single fibres in the cochlear nerve of the alligator lizard: relation to receptor morphology. Brain Res 115:71–90
Weiss TF, Altmann DW, Mulroy MJ (1978 a) Endolymphatic and intracellular resting potential in the alligator lizard cochlea. Pflügers Arch 373:77–84
Weiss TF, Peake TP, Ling A, Holton T (1978 b) Which structures determine frequency selectivity and tonotopic organization of vertebrate cochlear nerve fibers? Evidence from the alligator lizard. In Naunton RF, Fernandez C (eds) Evoked Electrical Activity in the Auditory Nervous System. Academic Press, New York pp 91–112
Weiss TF, Peake WT, Rosowski JJ (1985) A model for signal transmission in an ear having hair cells with free-standing stereocilia. I. Empirical basis for model structure. Hearing Res 20:131–138
Werner YL (1972) Temperature effects on inner-ear sensitivity in six species of iguanid lizards. J Herpetol 6:147–177
Werner YL (1976) Optimal temperatures for inner-ear performance in gekkonid lizards. J Exp Zool 195:319–352
Werner YL, Wever EG (1972) The function of the middle ear in lizards: *Gekko gecko* and *Eublepharis macularius* (Gekkonoidea). J Exp Zool 179:1–16
Werner YL, Frankenberg E, Adar O (1978) Further observations on the distinctive vocal repertoire of *Ptyodactylus hasselquistii* CF. *hasselquistii* (Reptilia: Gekkonidae). Isr J Zool 27:176–188
Wever EG (1967 a) The tectorial membrane of the lizard ear: types of structure. J Morphol 122:307–320
Wever EG (1967 b) The tectorial membrane of the lizard ear: species variations. J Morphol 123:355–372
Wever EG (1978) The Reptile Ear. Princeton Univ Press, Princeton N.J.
Wever EG, Vernon JA (1960) The problem of hearing in snakes. J Aud Res 1:77–83
Wever EG, Werner YL (1970) The function of the middle ear in lizards: *Crotaphytus collaris* (Iguanidae). J Exp Zool 175:327–342
Whitehead MC, Morest DK (1985 a) The development of innervation patterns in the avian cochlea. Neuroscience 14:255–276
Whitehead MC, Morest DK (1985 b) The growth of cochlear fibers and the formation of their synaptic endings in the avian inner ear: a study with the electron microscope. Neuroscience 14:277–300
Wilson JP, Johnstone JR (1975) Basilar membrane and middle ear vibration in guinea pig measured by capacitative probes. J Acoust Soc Amer 57:705–723
Wilson JP, Smolders JWT, Klinke R (1985) Mechanics of the basilar membrane in *Caiman crocodilus*. Hearing Res 18:1–24
Yates GK (1982) A sensitive opto-electronic displacement transducer for the neurophysiological laboratory. J Neurosci Meth 6:103–111
Yates GK, Johnstone BM (1979) Measurement of basilar-membrane movement. In: Beagley HA (ed) Auditory Investigation: the Scientific and Technological Basis, Clarendon, Oxford, pp 418–430
Young JZ (1981) The life of vertebrates. Clarendon Press, Oxford
Zenner HP, Zimmermann U, Schmitt U (1985) Reversible contraction of isolated mammalian cochlear hair cells. Hearing Res 18:127–134
Zwicker E, Manley GA (1981) Acoustical responses and suppression-period patterns in guinea pigs. Hearing Res 4:43–52
Zwislocki J, Slepecky N, Cefaratti L (1988) Tectorial-membrane stiffness and hair-cell stimulation. Abstracts 11th Mtg. Assoc Res Otolaryngol, p 170

Subject Index